Technische Universität Berlin

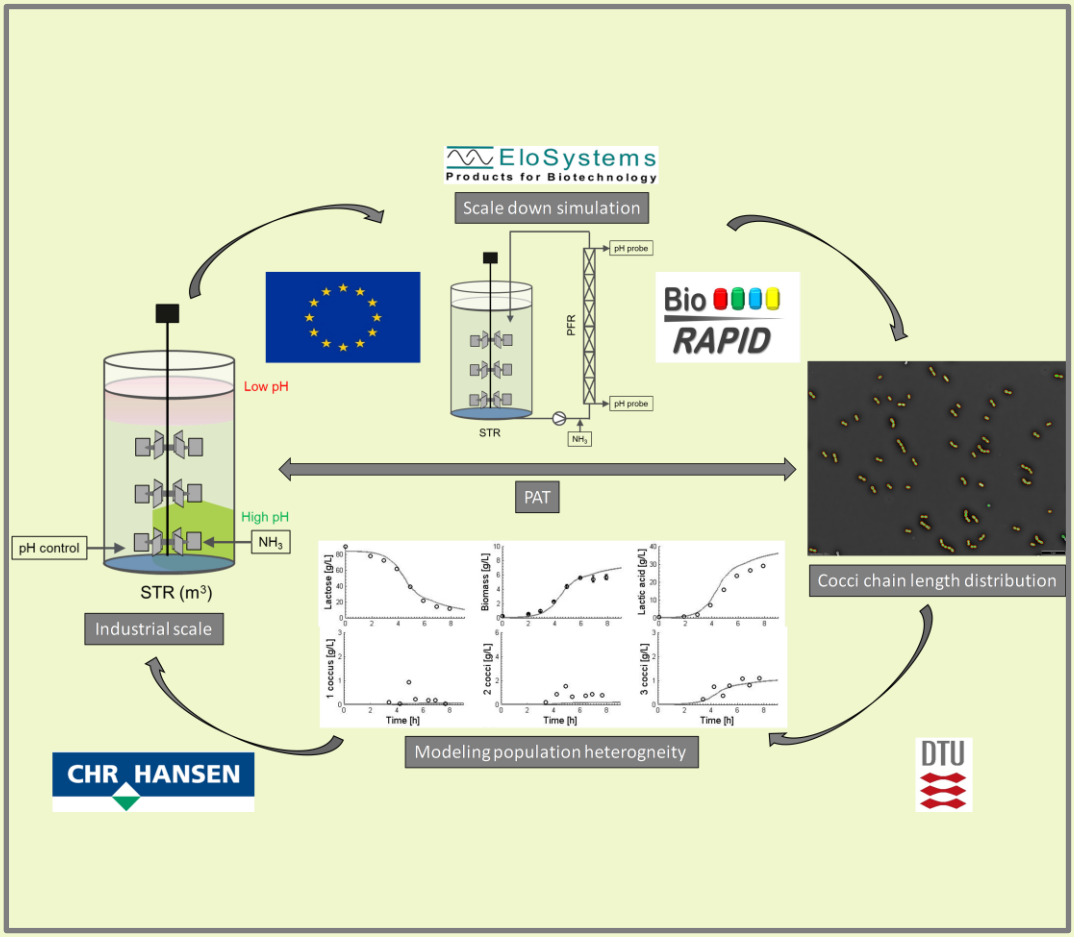

Cocci chain length distribution as control parameter in scaling lactic acid fermentations

Klaus Pellicer Alborch - Dissertation

Institute of Biotechnology
Technische Universität Berlin
Bioprocess Engineering

Cocci chain length distribution as control parameter in scaling lactic acid fermentations

vorgelegt von
M. Sc. Eng.
Klaus Pellicer Alborch
ORCID: 0000-0002-2207-6052

an der Fakultät III-Prozesswissenschaften
der Technischen Universität Berlin
zur Erlangung des akademischen Grades

Doktor der Ingenieurwissenschaften
-Dr.-Ing.-
genehmigte Dissertation

Promotionsausschuss:

Vorsitzender:	Prof. Dr. Eng. habil. Rudibert King, School of Process Sciences and Engineering, Technische Universität Berlin
Gutachter:	Prof. Dr. Eng. Frank Delvigne, Gembloux Agro-Bio Tech, University of Liège
Gutachter:	Dr. Eng. Alain M. Sourabié, Science Technology & Innovation, Lessafre BU Procelys
Gutachter:	Prof. Dr. rer. nat. Peter Neubauer, Institute of Biotechnology, Technische Universität Berlin

Tag der wissenschaftlichen Aussprache: 23. Juli 2020

Berlin 2020

Abstract

The world population is projected to reach 9.7 billion in 2050, which means that the Food and Feed industry is supposed to keep improving its productivity in order to provide all these people with enough food at the same pace. The current trend of regulatory authorities toward application of new process analytical technology tools to improve process understanding as well as reliability and ensure product quality during the production, has awakened the need of investing in novel analytics, especially in (bio)pharmaceutical industries, but is being extended to other fields. Moreover, the increasing acceptance of industrial companies that relevant concentration gradients affecting process performance as well as product quality appear in production vessels, is turning the scale down representation of conditions of the large scale in the lab indispensable. Furthermore, the actual digitalization transformation experienced in everyone´s life is becoming more and more relevant in industrial manufacturing, with the current tendency to develop a so-called digital twin, which simulates the (bio)process running in the plant in silico, thus minimizing out-of-specification batches and allowing near future personnel as well as materials/consumables planning.

In this work, (i) electrooptical measurements of cell polarizability as well as size, (ii) single- and multi-compartment scale down strategies and (iii) mechanistic modeling of macroscopic variables as well as population heterogeneity were applied to *Streptococcus thermophilus* fermentations for the first time. Firstly, the at-line determination of bacterial polarizability (i.e. orientation under the application of an electrical field) allowed the elucidation of different growth phases and resulted to be an early indicator of nutrient imbalance as well as growth cessation. Moreover, the analysis of the mean cell size without sample preparation with the same device also allowed the monitoring of qualitative morphological changes during growth. These were verified with parallel flow cytometric analyses, which revealed calibration issues in the equipment preparation, which should be addressed in future experiments. Secondly, pH shifts in the range from 5.5 until pH 8.0 (i.e. ΔpH = +2.0;-0.5) were induced in single-compartment reactor cultivations leading to a 48.5 % biomass productivity loss in the worst case scenario, while repeated pH pulses in a similar region were performed through ammonia addition in the plug-flow reactor of multi-compartment reactor experiments which yielded a 20 % less cell concentration at the end. Importantly, relevant morphologic changes under the different cultivation conditions were detected: increased chain length under alkali conditions and more homogenous cocci chain length distribution with shorter chains at low pH values. Nevertheless, computational fluid dynamic studies of a 700 L pilot scale fermenter revealed that those scale down conditions were exaggerated in terms of pH-gradients induced: only pH pulses up to 6.3 were monitored throughout a *S. thermophilus* fermentation under optimal growth conditions, while the pH never dropped below 5.8 far away from the base addition zone. However, extended mixing times and limited power input in the industrial scale may lead to higher ΔpH, so that their effect on process performance and product quality was further assessed. Thirdly, a population balance model based on a mechanistic description of typical growth metabolites (namely biomass, lactose, lactic acid and galactose concentrations) was developed, being able to predict the evolution of certain populations (namely 1-coccus, 2-, 3-, 4- and 5 or more cocci chains) during *S. thermophilus* cultivation under optimal growth conditions and variable pH-gradients.

The application of the first device (EloTrace, EloSystems GmbH, Berlin, Germany) in lactic acid bacteria large scale production would change the current quality by testing mindset to a quality by design/control approach, where the polarizability could be defined as a new critical quality attribute to be maintained inside a certain window by changing critical process parameters during the fermentation. The different scale down concepts applied in this study improved current process understanding of the industrial partner and should encourage the consideration of such lab scale simulators in early process development of new products or in optimization of existing bioprocesses. Finally, the hydrodynamic as well as population balance models developed in this work, if coupled to in situ microscopy technologies to determine cell size distribution in real-time, would enable the implementation of a model-based soft sensor strategy, where population heterogeneity could be minimized by changing critical process parameters, like the tip speed or base addition point.

Zusammenfassung

Die prognostizierte Weltbevölkerung im Jahr 2050 beträgt 9,7 Milliarden, was bedeutet, dass die Lebens- und Futtermittelindustrien ihre Produktivität weiter erhöhen müssen, um der gesamten Bevölkerung genügend Lebensmittel zur Verfügung stellen zu können. Regulierungsbehörden tendieren immer mehr zur Anwendung neuer Werkzeuge der Prozessanalysetechnologie, um das Prozessverständnis sowie die Zuverlässigkeit zu verbessern und die Produktqualität während der Produktion sicherzustellen. Dies geht einher mit der Notwendigkeit in neuartige Analytik zu investieren, insbesondere in der (bio-) pharmazeutischen Industrie, aber auch in anderen Gebieten. Außerdem, die zunehmende Anerkennung von Industrieunternehmen, dass relevante Konzentrationsgradienten, die die Prozessleistung sowie die Produktqualität beeinflussen, in Produktionsbehältern auftreten, macht eine Verkleinerung der Darstellung von Bedingungen im großen Maßstab im Labor unverzichtbar. Darüber hinaus gewinnt die Digitalisierung in der industriellen Fertigung immer mehr an Relevanz. Insbesondere die Entwicklung sogenannter digital twins ermöglicht, den (Bio-) Prozess zu simulieren und die Anlage in silico ablaufen zu lassen. Dies minimiert die Anzahl der Chargen, die außerhalb der Spezifikation liegen, und ermöglicht eine zeitnahe Personal- und Materialplanung.

In dieser Arbeit wurden (i) elektrooptische Messungen der Zellpolarisierbarkeit sowie der Größe, (ii) Einzel- und Multikompartiment- scale down Strategien und (iii) mechanistische Modellierung makroskopischer Variablen sowie der Populationsheterogenität während *Streptococcus thermophilus* Fermentationen zum ersten Mal angewandt. Erstens ermöglichte die Bestimmung der bakteriellen Polarisierbarkeit (d. h. Zellorientierung unter Einfluss eines elektrischen Feldes) die Aufklärung verschiedener Wachstumsphasen und war damit ein früher Indikator für ein Nährstoffungleichgewicht sowie eine Wachstumsverzögerung. Darüber hinaus ermöglichte die Analyse der durchschnittlichen Zellgröße ohne Probenvorbereitung mit demselben Gerät auch die Überwachung qualitativer morphologischer Veränderungen während des Wachstums. Diese wurden mit parallel durchgeführten durchflusszytometrischen Analysen verifiziert, welche Kalibrierungsprobleme bei der Gerätvorbereitung offenbarten, die in zukünftigen Experimenten behoben werden sollten. Zweitens wurden pH-Verschiebungen im Bereich von 5.5 bis 8.0 (d. h. ΔpH = +2.0; -0.5) in Einzelkompartiment-Reaktorkultivierungen induziert, was im schlechtesten Fall zu einem Biomasse-Produktivitätsverlust von 48.5 % führte. Wiederholte pH-Pulse in einem ähnlichen pH-Bereich durch Ammoniakzugabe in den Pfropfenströmungsreaktor während Mehrerekompartiment-Reaktorexperimenten ergaben am Ende eine 20 % geringere Zellkonzentration. Bemerkenswerterweise wurden relevante morphologische Veränderungen unter den verschiedenen Kultivierungsbedingungen festgestellt: längere Kettenlänge unter alkalischen Bedingungen und homogenere Verteilung der Kokkenkettenlänge mit kürzeren Ketten bei niedrigen pH-Werten. Dennoch ergaben fluiddynamische Betrachtungen eines 700 L-Fermenters im Pilotmaßstab, dass die Laborbedingungen in Bezug auf die induzierten pH-Gradienten übertrieben waren: während einer *S. thermophilus* Fermentation unter optimalen Wachstumsbedingungen wurden nur pH-Pulse bis zu 6.3 festgestellt während der pH-Wert weit entfernt von der Basenzugabezone nie unter 5.8 fiel. Verlängerte Mischzeiten und eine begrenzte Leistungsaufnahme im industriellen Maßstab können jedoch zu einem höheren ΔpH führen, sodass der Einfluss auf die Prozessleistung und die Produktqualität weiter untersucht wurde. Drittens wurde ein Populationsmodell entwickelt, das auf einer mechanistischen Beschreibung typischer Wachstumsmetaboliten (Biomasse-, Laktose-, Milchsäure- und Galaktosekonzentration) basierte und

die Entwicklung bestimmter Populationen (1-Coccus, 2-, 3-, 4 und 5 oder mehr Kokkenketten) während *S. thermophilus* Kultivierungen sowohl unter optimalen Wachstumsbedingungen als auch unter variablen pH-Gradienten vorhersagen konnte.

Die Anwendung des ersten Geräts (EloTrace, EloSystems GmbH, Berlin, Deutschland) in der industrielle Produktion von Milchsäurebakterien würde die aktuelle quality by testing Denkweise auf einen quality by design/control Ansatz ändern. Hierbei könnte die Polarisierbarkeit als neues kritisches Qualitätsattribut definiert werden, das innerhalb eines bestimmten Rahmens gehalten werden soll, indem kritische Prozessparameter während der Fermentation angepasst werden. Die in dieser Studie angewandten unterschiedlichen scale down-Konzepte verbesserten das aktuelle Prozessverständnis des Industriepartners und sollten die Berücksichtigung solcher Laborsimulatoren bei der frühen Prozessentwicklung neuer Produkte oder bei der Optimierung bestehender Bioprozesse fördern. Schließlich könnten die in dieser Arbeit entwickelten hydrodynamischen- und Populationsmodelle, in Verbindung mit in situ Mikroskopietechnologien zur Bestimmung der Zellgrößenverteilung in Echtzeit, die Implementierung einer modellbasierten Soft-Sensor-Strategie ermöglichen. Schlussendlich könnte damit eine minimale Populationsheterogenität durch die Änderung kritischer Prozessparameter (z.B. der Rührgeschwindigkeit oder des Basenzugabepunkts) sichergestellt werden.

List of Contents

Acknowledgements

I would like to express my sincere gratitude to a number of people who contributed in various ways to the success of this work.

Firstly, I would like to specially thank Dr. Stefan Junne, as the group leader of the Scale Up&Down and PAT group, not only for his constant support in the preparation of experiments, manuscripts and this thesis, but also for his personal support in preparing talks for conferences as well as giving advice to make my next career move.

Secondly, I would also like to thank Prof. Peter Neubauer, who gave me the opportunity to perform my PhD in his lab and improved my knowledge in bioprocesses, specially cell biology. I appreciate his enthusiasm, as well as all the suggestions and fruitful discussions during seminars to keep advancing my research work.

Furthermore, I would like to thank the rest of my thesis committee: Prof. Frank Delvigne and Dr. Alain Sourabié, for having the patience of reading my work and for the useful discussions.

My gratitude goes to the EloSystems GmbH employees, who made the equipment maintenance of EloTrace between experiments and were always open to use the device in my work. A special mention to Dr. Alexander Angersbach, who supported me in the installation of the equipment in all fermentations carried out, even in Copenhagen, Denmark. He was always open for discussion and arranged all the logistics for the measurements.

Many thanks for the support of the students Peter Unger, Adriana Mora Barrabés, Lucas Kaspersetz and Verena Tiede for the effort made during your work. Without you, this thesis and my research work would not have been possible. Additionally, I would like to thank Brigitte Burckhardt, Irmgard Maue-Mohn and Thomas Högl for their support regarding the practical work during all the experiments. Again, without your commitment and daily work, I would not be where I am and this work would not have been doable. And of course, thanks to all colleagues from the Chair of Bioprocess Engineering especially Dr. Emmanuel Anane: it was a pleasure spending time with you trying to overcome the barriers encountered throughout your professional as well as private life in Berlin. I would like to thank also Dr. Anna-Maria Marbà-Ardébol and Dr. Anja Lemoine, you were always prepared to lend a hand; Dr. Anika Bockisch, for the perfect organization at every event in the Chair and for your support regarding flow cytometric analysis; the Latin colleagues (Prof. Howard Diego Ramírez Malule, Dr. Carlos Enrique Gómez Camacho and Dr. David Andrés Gómez Ríos) for being so friendly and cheering up the atmosphere every time you visited us.

This project has received funding from the European Union's Horizon 2020 research and innovation program under the Marie Skłodowska-Curie actions grant agreement No. 643056 (project Biorapid). I would like to thank the EU not only for the financial support, but also for funding such multi-cultural as well as multi-disciplinar projects, where one can attend conferences, seminars and workshops. I had a lot of fun being the early-stage researchers' representative and I would like to thank all the colleagues in the project. The industrial partner of this work was Chr. Hansen A/S and I would also like to thank the employees supporting the collaboration and allowing me to be three months in the company (Dr. Anders Clausen, Dr. Christophe Roca and Dr. David Kold), especially Dr. Robert Spann for being the perfect partner in the lab: we understood each other really well and we helped each other, ending up with really nice joint publications. You were always my professional reference inside and outside the

laboratory. People from DTU (Prof. Krist Gernaey, Dr. Pedram Ramin, Dr. Teresa-Melo de Carvalho, Dr. Tannaz Tajsoleiman, Dr. Frederico Montinho, Gisela Nadal-Rey, Dr. Merve Öner), thank you for being so friendly and welcoming me warmly when I stayed there one month and every time I visited you. Also, thanks to the BASF SE colleagues that were making pressure on me during this first year of industrial experience, especially Dr. Max-Ulrich Becker, for being so friendly and positively competing against me to see who defends first.

Finally, I thank my parents (Albert and Silvia), my Oma (Monika), my family in Mallorca (Jordi, Marilén, Gemma, Marc and Gerard) as well as my brothers (Aleix and Eric), because they were always there encouraging me and believing in me, although they were more than 1,800 km away. I thank specially and enormously Nuria for always (once a month physically, but daily through skype) being by my side, even developing the CellProfiler pipeline for microscopic analysis when “experts” were not able to do it. Thanks also for giving me advice, for your unconditional support and for being the light guiding my life. I love you!

List of Abbreviations

General

ANN	Artificial neural network
ATR	Acid tolerance response
CFD	Computational fluid dynamics
CFU	Colony forming units
cGMP	Current good manufacturing practices
CHO	Chinese hamster ovary
CPP	Critical process parameter
CQA	Critical quality attribute
CR	Cascade reactor
CSDR	Compartment scale down reactor
DAPI	4', 6-diamidino-2-phenylindol
DCW	Dried cell weigth
DoE	Design of experiments
DSP	Down-stream processing
DVS	Direct vat set
e.g.	exempli gratia
EMA	European medicines agency
etc.	et cetera
EPS	Extracellular polymeric substances
FACS	Fluorescence-activated cell sorting
FALS	Forward angle light scatter
FCM	Flow cytometry
FDA	Unitated States food and drug administration
FDAP	Frequency-dependent anisotropy of polarizability
FSC	Forward-scattered light
GFP	Green fluorescent protein
GIT	Gastrointestinal tract
GMO	Genetically modified organism
GMP	Good manufacturing practices
HPLC	High-performance liquid chromatography
HTS	High-trhoughouput screening
i.e.	id est
ICH	International conference on harmonisation
KPI	Key performance indicator
LAB	Lactic acid bacteria
LDH	Lactate dehydrogenase
M^3C	Measuring, monitoring, modeling and control
MS	Mass spectrometry
MVDA	Multi-variate data analysis
NADH	Nicotinamide adenine dinucleotide
OD	Optical density

ODE	Ordinary differential equation
PAT	Process analytical technology
PBE	Population balance equation
PBM	Population balance modeling
PCA	Principal component analysis
pCO_2	Dissolved carbon dioxide concentration
PCR	Polymerase chain reaction
PFR	Plug-flow reactor
PI	Propidium iodide
PLS-R	Partial least squares regression
pO_2	Dissolved oxygen concentration
QbC	Quality by control
QbD	Quality by design
QbT	Quality by testing
RALS	Right angle light scatter
RMSSE	Root-mean-square of standardized effects
ROI	Return of investment
SSC	Side-scattered light
STR	Stirred-tank reactor
STY	Space-to-time yield
USP	Up-stream processing
VCC	Viable cell count
VCD	Viable cell density
WCW	Wet cell weigth

Symbols

μ	Specific growth rate (in h^{-1})
$Y_{X/S}$	Yield of biomass produced per substrate (i.e. lactose) consumed (in $gX \cdot (gS)^{-1}$)
$Y_{P/S}$	Yield of product (i.e. lactic acid) produced per substrate consumed (in $gP \cdot (gS)^{-1}$)
$Y_{P/X}$	Yield of product produced per biomass formed (in $gP \cdot (gX)^{-1}$)

List of publications

I. **Pellicer-Alborch, K.**, Angersbach, A., Neubauer, P., Junne S. *Electrooptical Determination of Polarizability for On-Line Viability and Vitality Quantification of Lactobacillus plantarum Cultures*. Front. Bioeng. Biotechnol. 2018; 6:188. DOI: 10.3389/fbioe.2018.00188

II. **Pellicer-Alborch, K.**, Spann, R., Sin, G., Gernaey, K. V., Neubauer, P., Junne, S. *Mechanistic model validation and electrooptical monitoring of Streptococcus thermophilus growth in lactose-limited acceleration stat (A-stat) fermentations*. In preparation.

III. Spann, R., Glibstrup, J., **Pellicer-Alborch, K.**, Junne, S., Neubauer, P., Roca, C., Kold, D., Lantz, A. E., Sin, G., Gernaey, K. V., Krühne, U. *CFD predicted pH gradients in lactic acid bacteria cultivations*. Biotechnol. Bioeng. 2018; 1-12. DOI: 10.1002/bit.26868

IV. **Pellicer-Alborch, K.**, Kaspersetz, L., Paulick, K., Neubauer, P., Junne, S. *Response of Streptococcus thermophilus exposed to pH gradients in Two- and Three-Compartment Scale down Cultivations*. Submitted in MDPI, Bioengineering. (2020)

V. **Pellicer-Alborch, K.**, Spann, R., Cristino-Falco, F., Ramin, P., Gernaey, K. V., Neubauer, P., Junne, S. *Population Balance Modelling of Streptococcus thermophilus Based on the Cocci Chain Length Distribution for Optimization of Starter Cultures Production*. In preparation.

Author Contributions to the Publications

Paper	Co-author	Contribution
I	**Klaus Pellicer Alborch**	Writing publication, helping by *L. plantarum* fermentations and interpretation of results
	Alexander Angersbach	Running the *L. plantarum* fermentations, interpretation of results and revision of text
	Peter Neubauer	Supervision, interpretation of results and revision of text
	Stefan Junne	Supervision, interpretation of results and revision of text
II	**Klaus Pellicer Alborch**	Writing publication, running *S. thermophilus* fermentations and interpretation of results
	Robert Spann	Writing the model, helping by *S. thermophilus* fermentations and interpretation of results
	Gürkan Sin	Supervision of model
	Krist V. Gernaey	Supervision of model, interpretation of results and revision of text
	Peter Neubauer	Supervision, interpretation of results and revision of text
	Stefan Junne	Supervision, interpretation of results and revision of text
III	Robert Spann	Writing publication, developing mechanistic model, supervision of CFD model, running *S. thermophilus* fermentations and interpretation of results
	Jens Glibstrup	Developing CFD model
	Klaus Pellicer Alborch	Running *S. thermophilus* fermentations, interpretation of results and revision of text
	Stefan Junne	Supervision, interpretation of results and revision of text
	Peter Neubauer	Supervision, interpretation of results and revision of text
	Christophe Roca	Supervision from industrial partner
	David Kold	Supervision from industrial partner
	Anna Eliasson Lantz	Supervision of model
	Gürkan Sin	Supervision of model
	Krist V. Gernaey	Supervision, interpretation of results and revision of text
	Ulrich Krühne	Supervision, interpretation of results and revision of text
IV	**Klaus Pellicer Alborch**	Writing publication, running *S. thermophilus* fermentations and interpretation of results
	Lucas Kaspersetz	Running *S. thermophilus* fermentations and interpretation of results
	Katharina Paulick	Performing image analysis
	Stefan Junne	Supervision, interpretation of results and revision of text
	Peter Neubauer	Supervision, interpretation of results and revision of text
V	**Klaus Pellicer Alborch**	Writing publication, running *S. thermophilus* fermentations, developing population balance model and interpretation of results
	Robert Spann	Helping by developing model and interpretation of results
	Francesco Cristino F.	Supervision of model and interpretation of results
	Pedram Ramin	Supervision of model and interpretation of results
	Krist V. Gernaey	Supervision of model and interpretation of results
	Peter Neubauer	Supervision, interpretation of results and revision of text
	Stefan Junne	Supervision, interpretation of results and revision of text

1. Introduction

Conversion of carbohydrates to lactic acid is one of the most employed fermentation processes in food industry today. Applications of lactic acid fermentation are found in the dairy industry, production of wine and cider, production of fermented vegetable products and in the meat industry (Nagpal et al., 2012). Biopharmaceuticals, enzymes, biological cell materials or food supplements, among others, are all derived from the cultivation of bacteria, fungi or animal cells in bioreactors. These bioprocesses are usually developed at laboratory scale. Later, the established processes are stepwise transferred to larger volumes until the final industrial production scale is reached. This procedure is known as scale up, which is influenced by several factors. Kinetics and thermodynamics are virtually unaffected by the reaction volume. However, the mass transfer within a process is highly dependent on the scale. The geometries of the stirred-tank reactor (STR) and the impeller influence the mixing time and as such the oxygen uptake, substrate supply of a culture and the reagents addition for e.g. pH-control just as the agitation speed and gassing rate do (Garcia-Ochoa & Gomez, 2009; Rosseburg et al., 2018).

Engineering parameters such as the vessel (e.g. height-to-diameter ratio) and impeller geometry, tip speed, mixing time, oxygen transfer rate, volumetric mass transfer coefficient (kLa), or power number can be used as scale up criteria (Takors, 2012). The general strategy is to keep a specific process parameter constant throughout the scale up process. In this way, negative effects caused by changing environmental cultivation conditions during scale up are minimized. Geometric similarity is probably the most widely applied method, which basically aims at maintaining the aspect ratio (i.e. the liquid height-to-diameter ratio) constant across scales (Palomares & Ramírez, 2009). Another option is to maintain the mixing times between larger and smaller bioreactors to ensure a proper and uniform supply of nutrients, gasses, and heat to the culture (Tissot et al., 2010). Nevertheless, one of the most widely accepted scale up strategies consist of maintaining a constant impeller power consumption per liquid volume (P/V). This is carried out by adapting the impeller size and shape to the different working volumes (Flickinger & Nienow, 2010; Hewitt & Nienow, 2007). (Xu et al., 2017) recently applied a combination of these strategies in scaling up the production of five monoclonal antibodies (MAbs) from 3 to 2,000 L fermenters, concluding that the best scale up criterion was a combination of a minimum constant air flow rate per reactor volume (vvm) with a similar specific power input (P/V).

Already two decades ago, gradient formation mainly because of limited power input and increased mixing times in industrial scale fermenters was described (Bylund et al., 1998). Limitations inherent to traditional scale up methods and practical constraints during large scale bioreactor design and operation lead to a deficient mixing and a concominant appearance of spatial gradients in fundamental culture parameters, such as dissolved gases, pH, concentration of substrates, and shear rate, among others. When cultured in a heterogeneous environment, cells are continuously exposed to fluctuating conditions as they travel through the various zones of a bioreactor. Such fluctuations can affect cell metabolism, yields, and quality of the products of interest (Lara, Galindo, et al., 2006). In this thesis, pH-gradient formation during *Streptococcus thermophilus* fermentations was quantified and modelled by means of computational fluid dynamics (CFD) for the first time.

As described above, conventional scale up is mainly based on the principle of similarity and dimensional analysis. Biological properties are usually not considered. The main aim in this work, was to make a step forward by identifying a characteristic property of cells to be included in scale up and down. Usually, volumetric macroscopic variables are considered, e.g. biomass concentration, but the

heterogeneity among the individual cells is not taken into account. Nevertheless, it has been shown that the population heterogeneity can be notably affected by scale up effects (Delvigne et al., 2014). Therefore, the consideration of the single-cell level has the potential to reduce scale up effects, while population heterogeneity is considered. In fact, the morphologic analysis of the biomass allowed the identification of a new critical quality attribute (CQA), cell size, which resulted to be sensible to the induced oscillating conditions. Moreover, cell macromorphology is a feature of microorganisms that is often related to physiologic properties. Hence, the consideration of individual macromorphologies of cells may be related to their contribution to the overall process goals. If coupled to automatic cell size distribution quantification, a rapid evaluation of the effect of various process conditions on population heterogeneity may be possible.

Scale down experiments can give insight into bioprocess phenomena that are otherwise seen only in industrial scale. Multi-compartment bioreactors or oscillating cultivation conditions induced in one reactor are suitable tools to mimic the heterogeneities of industrial scale bioreactors in the lab (Neubauer & Junne, 2010). By this, the prediction of potential quality losses during scale up becomes possible at the process development stage. When pulses of a certain nature are introduced in a single vessel, the whole cell population is opposed to the same stress at the same time. In the case of multi-compartment bioreactors, each of the compartments has a specific cultivation environment with its own parameter settings, representing one of the zones of an industrial scale bioreactor, and microorganisms are intermittently exposed to the different simulated conditions. Here, the concept of residence time appears, which represents the time during which the cells are in contact with the gradient(s) induced. By connecting two or more vessels (the so called STR-STR system), the residence time in each compartment is defined by the liquid volume in each reactor and the pump rate of the fermentation broth from one zone to the other. In order to avoid the vigorous mixing in STRs, the main fermenter can be connected to a plug-flow loop (PFR), with typically a liquid volume of 10 % of the total fermentation broth volume, equipped with static mixers. In this scale down system (generally named STR-PFR), the residence time is defined only by the pump rate, with the additional advantage of sampling and monitoring critical process parameters (CPPs; e.g. pH, pO_2) at different points along the height of the PFR (Enfors et al., 2001b). In this work, both scale down approaches were used for the first time in lactic acid bacteria (LAB) processes.

In recent years, parameters including cell-to-cell variation as well as the detection of many parameters at the same time are becoming more important in industrial fermenters in pharmaceutical bioprocesses (Glassey et al., 2011; Rathore et al., 2010). A similar development has not yet been started in many areas of food bioprocesses: in the actual up-stream processing (USP) of starter cultures, the most important CQA is the biomass concentration before harvesting, but usually no measurement of cell activity is performed throughout the fermentation.

In order to increase the understanding of scale up effects and, in general, the influence of population heterogeneity on process performance in real-time, single-cell based monitoring methods, coupled to novel process analytical technology (PAT) for the assessment of cell viability, were adjusted and applied for LAB for the first time. Firstly, multi-parameter flow cytometry was used to study cell viability and distinguish dead from living cells by staining depolarized cells with propidium iodide (PI). Secondly, electrooptical measurements of cell polarizability (i.e. orientation of microorganisms to an applied electrical field of a certain frequency) were performed, thus enabling the at-line monitoring of cell activity.

Cell-to-cell variations in terms of morphological heterogeneity were quantified under different growth conditions. Finally, the consideration of single cells by developing a population balance model (PBM) based on cocci chain lengths was used to better understand, predict and optimize the bioprocess. In this context, the cell size distribution was chosen as new CQA and as potential scale up&down criterion to mimic the industrial scale conditions in the lab.

2. Scientific Background

2.1. Industrial LAB Production for Probiotics

LAB fermentation is the simplest and safest way of preserving food. As traditional strains in food fermentation, especially in dairy, fermented meat and vegetable products (Kleerebezemab et al., 2000), LAB can produce lactic acid to extend the shelf life of food and provide beneficial effects to human beings by improving the body's natural defense system and regulating the gastrointestinal tract's (GIT) micro-ecological balance (Wang, He, et al., 2018). These microorganisms are consumed world-wide in the industrial manufacture of fermented food products, but their most important application in this respect is undoubtedly in the dairy industry, where these bacteria are used to convert milk or milk-derived products to an enormous variety of fermented dairy products.

LAB are a group of Gram-positive bacteria belonging to genera *Aerococcus*, *Alloiococcus*, *Atopobium*, *Bifidobacterium*, *Carnobacterium*, *Enterococcus*, *Lactobacillus*, *Lactococcus*, *Leuconostoc*, *Oenococcus*, *Pediococcus*, *Streptococcus*, *Tetragenococcus*, *Vagococcus* and *Weissella*. They are nonsporulating rods or cocci which produce lactic acid as the main fermentation product under suitable substrate availability and cultivation conditions. Additionally, they are oxidase and benzidine negative, lack cytochromes and do not reduce nitrates to nitrite (Carr et al., 2002). Most of the LAB are anaerobic, but some of them can shift to oxygen-dependent metabolism in aerobic conditions (Murphy & Condon, 1984; Sedewitz et al., 1984). LAB have complex nutrient requirements, including specific minerals, B vitamins, several amino acids, and purine and pyrimidine bases. What is more, this bacteria ferment sugars via homo-, hetero-, or mixed acid fermentation. Homofermentative LAB produce lactic acid as main product from sugar oxidation, while hetero- or mixed acid fermentations produce also ethanol and/or acetic acid, formic acid and carbon dioxide. Although it is a common practice to divide LAB into homo- and heterofermentative strains, the division is not that straightforward as the actual metabolism is dependent on both, the nature of the C-source (e.g. hexose vs. pentose sugars) and the fermentation conditions (e.g. growth rate and availability of the C-source). Importantly, LAB used for probiotics production are commonly classified as homofermentative (*Lactococcus*, *Enterococcus*, *Streptococcus* and some Lactobacilli) since their hexose metabolism under non-limiting conditions follows entirely the Embden-Meyerhof pathway to pyruvate, which is then used to regenerate the reducing power (NADH) in the lactate dehydrogenase (LDH) catalyzed reaction to lactic acid. Nevertheless, at slow growth rates and low glycolytic fluxes, mixed acid fermentation may take place and acetic acid, formic acid and ethanol may be formed in addition to lactic acid (Zaunmüller et al., 2006). In milk, these bacteria encounter lactose as the major C-source, but they have the capacity to use a number of other mono- and disaccharide substrates. The major product of these fermentations is lactic acid, which plays a crucial role in protection of the final fermented product against spoilage. Besides this acidification that acts as a natural preservative effect, the LAB main carbon metabolism is essential for development of desired product properties like flavor, shelf-life and texture.

In this work, the strain *Lactobacillus plantarum* ATCC 2014 and a *Streptococcus thermophilus* strain provided by Chr. Hansen A/S (Hoersholm, Denmark) were used. The first one was employed as LAB in initial, proof-of-concept experiments, while the *S. thermophilus* strain was used for all scale down studies and for the development of the process and population balance model. Lactobacilli are unusual in that they can respire oxygen, without possessing a respiratory chain or cytochromes. Instead, the

consumed oxygen ultimately ends up as hydrogen peroxide (Brooijmans et al., 2009). In fact, *L. plantarum* are aerotolerant bacteria, while *S. thermophilus* are facultative anaerobes. This means that the latter can grow with or without oxygen, because it can metabolize energy aerobically or anaerobically.

2.2. PAT in Industrial LAB Fermentation

The industrial production of these LAB is performed in a batch mode with complex media in the scale of tens of cubicmeters. The pH value is allowed to drop, due to acidification (initial production of lactic acid from the bacteria) until pH 6, from which it is controlled with addition of concentrated base (i.e. 24 % v/v NH_3). The end of fermentation (i.e. the harvesting point) is decided by means of growth reduction, more precisely the decrease of the acidification rate (monitored on-line by the base addition rate to compensate the lactic acid production). The bioreactor is then cooled down to 4 ºC and the fermentation broth is further processed (DSP), depending on the product to be prepared:

- ✓ Frozen-direct vat set (F-DVS): simple centrifugation step to concentrate the biomass and directly sell as starter culture solution.
- ✓ Pre-freeze dried DVS: more concentrated biomass than obtained in the previous method, even with a cryoprotectant and ready to be freeze dried.
- ✓ Freeze dried DVS: freeze dried suspension after the concentration step, to sell as stabilized powder biomass, with a longer shelf-life than the two previous products.

This work focused on the optimization of the fermentation part (i.e. USP). Nowadays, the application of PAT to industrial LAB production is quite limited: although the biomass is sold as starter culture for different food and feed industries, the only way of controlling cell viability currently available in production is the acid production rate of the culture. This is definitely an important parameter in yogurt and probiotic fermented milk manufacturing, since the acidification generally correlates with the growth rate of LAB (Turner & Thomas, 1975). Nevertheless, measuring the pH decrease over time in LAB production has some disadvantatges: a limited physiological information that can be extracted from the culture broth and a dependency on the buffering capacity of the media (Zare et al., 2011, 2012). In this context, the analysis of multiple metabolites (e.g. with Raman technology and applying MVDA tools for correlation) and of cell viability (by means of polarizability and morphological changes, for example), specially in the single-cell level (accounting for population heterogeneity), would significantly improve process monitoring.

The fact that this process is ran without aeration (nitrogen is introduced in the head space, basically to maintain an anaerobic backpressure) eliminates operational challenges in such an industrial scale, but still real-time process understanding could be improved. For example, O_2 and CO_2 in the offgas are currently not analyzed, which could enable a fast and easy contamination detection or allow the monitoring of the CO_2 production rate with an already commercially available on-line measuring tool.

Usually, at the end of a fermentation, some CQAs from the biomass are measured off-line, which include (i) % solids, (ii) dry matter and (iii) acidification activity, apart from typical metabolites quantified with HPLC. These analyses require well established methods as well as equipments: 10 mL biomass tubes with a benchtop centrifuge, a Smart Turbo (CEM Corporation, NC, USA) device and a pH sensor that monitors the pH development over time in pre-boiled milk inoculated with the fresh LAB, respectively.

It is obvious that there is gap for improvement regarding PAT in the industrial fermentation of LAB, specially toward Quality by Design (QbD) strategy and product quality analysis. Nowadays, the biomass is tested after harvesting if it meets product specifications and only the amount of LAB and the unconsumed C-source are determined during the fermentation.

Classic microbiology states that a cell is viable when it has been shown to reproduce itself, e.g. on agar plates. However, such a definition does not consider the different physiological states of a cell in between active growth and death. Therefore, stressed, injured or otherwise "viable but non-culturable" cells can remain undetected. Moreover, traditional techniques tend to underestimate the viability of the culture, just quantifying the dividing cells (CFU/mL), but not all the living cells. Flow cytometry (FCM) has a number of advantages over the more traditional techniques (Diaz et al., 2010) and was initially used for studying animal cell culture where it became a powerful technique for the rapid characterization of cell populations using scattered light (Mohamed Al-Rubeai, 1995). Cells pass individually through a laser beam and scattered light is detected in two planes. On the one hand, forward angle light scatter (FALS or FSC) is measured in the plane of the beam and provides relative information on the cell size. On the other hand, the right angle light scatter (RALS or SSC) is measured at 90° to the beam and can provide an information on cell granularity. Emitted light from fluorescent stains, which have specific intracellular or extracellular binding sites, are also measured at a 90° angle. This information, coupled with the rapid throughput of thousands of cells per second, provides real-time, statistically reliable information on cell physiology, including viability, which allows FCM to be used in order to make informed decisions on process control (Hewitt & Nebe-von-Caron, 2004). All microbial cells are bound by the cytoplasmic membrane, allowing the cell to communicate selectively with its immediate environment. Passive and active transport systems across the membrane exist and generate an electrochemical gradient. The presence of both, an intact polarized cytoplasmic membrane and active transport systems across it, are essential for a fully functional healthy cell. Fluorescent dyes used in flow cytometry differ in their ability to cross fully functional cell membranes. Therefore, dyes that are normally impermeable to cell membranes and that have specific intracellular or periplasmic binding sites can be used to measure cell membrane integrity. Using multi-parameter flow cytometry, it becomes possible to classify the physiological state of individual bacterial cells beyond culturability, based on the presence or absence of an intact polarized cytoplasmic membrane. The most established dye to stain dead cells is propidium iodide (PI), which binds to DNA, but cannot cross an intact cytoplasmic membrane (Looser et al., 2005). Fluorescent dyes can also interact with particles, which are not cells and, consequently, provide false positive results. Therefore, it is important to be able to discriminate between the target cells and debris or other particles, e.g. from media. DAPI (Otto, 1990) or SYTO13 (Taimur Khan et al., 2010) can be used for this purpose, since both stain DNA. Flow cytometry is typically regarded as a tool to determine population heterogeneity, but this is based on the amount of dyes used to stain the different cell stages of interest. Therefore, a huge effort needs to be invested to fully develop an optimized protocol for the microorganism under study. Every staining procedure depends, at least, on (i) the staining temperature, (ii) the staining time and (iii) the cells:dye ratio. Additionally, some dyes are light-sensitive, for instance. This means, that for each dye to be employed (i.e. cell stage to be investigated) a directed Design of Experiments (DoE) should be conducted (Marba-Ardebol et al., 2016). (Ou et al., 2017) recently demonstrated the absolute *E. coli* cell enumeration using flow cytometry, which would be interesting to apply, but the technology may be too expensive for the information provided. In case of LAB, as an example, (Bensch et al., 2014) applied flow cytometry to assess viability of *Lactobacillus plantarum* starter cultures by membrane integrity analysis using SYBR®Green I and PI staining. The enumeration method allowed for rapid,

precise and sensitive determination of the viable cell count (VCC) and was used to investigate effects of fluidized bed drying and storage on LAB viability. In a recent study, (Robertson et al., 2019) simplified the process of staining live and dead *E. coli* cells, by using the commercially available dyes SYTO9 and PI: the authors minimised the steps involved and determined the optimal analytical parameters for fluorescence measurements. (Ou et al., 2019) used the same kit protocol, but measured the fuorescence spectra with a fibre-based spectroscopic device (the optrode system). Together with principal component regression for spectral processing, this methodology may be of interest for the rapid, on-site measurement and analysis of LAB. Nevertheless, each additional dye included increases the sample preparation time and further delays the measurement from the sampling time. Another relevant drawback of this technology is its price, when compared to other possible analyses.

Although FCM analysis is applied in some industrial bioprocesses, its implementation in the production of bulk products is challenging due to the limitations described above. As previously mentioned, there is no on-line determination of cell activity during the actual process and this would be a crucial step for moving toward QbD. There are a few technologies commercially available that can provide similar information than FCM without the need of sample staining. The electrooptical analysis of the anisotropy of polarizability (AP) relies on the cell orientation under the effect of an electrical field, measured by the change of extinction from two orthogonal light sources: it decreases in the direction of orientation, while it increases in the orthogonal direction. The time, which is needed for re-orientation depends directly on the cells' polarizability (A. Angersbach, V. Bunin, 2006; Bunin, 2002) and has been related to the metabolic activity of a variety of microorganisms (Bunin et al., 2004; Junne et al., 2008, 2010; Lemoine et al., 2015). This principle, combined with a continuous and automated sampling and sample preparation device, represents a fully automated methodology that could be used to monitor the viability of LAB during their fermentation. Importantly, this option would be preferred to the already available tools for cell physiology determination (namely multi-parameter flow cytometry, quantitative real-time PCR or viable cell counting), since these are slower and require manual off-line sample pre-treatment. Nevertheless, currently, the device provides the mean contribution of all individual cells in the sample, so that it would only give a single-cell analysis if coupled to microscopy and automated image detection to track the orientation of every singe cell.

Additionally, microscopic analysis for the investigation of macromorphological changes over culture time might be a suitable alternative for determining cell-to-cell variations. Changes in cell size are linked to physiological responses to the surrounding environment (e.g. cell shrinkage under osmotic pressure) and can thus provide insights in the actual metabolic state of microorganisms and their viability (Gonzalez & Barrett, 2010; Syed et al., 2016). This has been a special focus in filamentous fungi in recent years (Ehgartner et al., 2017; Posch et al., 2013; Veiter et al., 2018), but it has been demonstrated for yeast (Marbà-Ardébol, Bockisch, et al., 2018) and bacteria (Alvarez et al., 2004; Mañas & Mackey, 2004; Shi et al., 2017; Wang, Chen, et al., 2019), as well. Just recently, in situ microscopy (ISM) techniques providing cell-to-cell variations in real-time have been developed and will be further discussed in 2.3.3.

2.3. Liquid Phase Inhomogeneity in Large Scale Processes

The vast majority of economical bioprocesses use cell factories cultivated in submerged fermentation systems, although some cell-free synthesis platforms have been reported recently (Ogonah et al., 2017). It is important to understand how differences in the internal bioreactor environment influence cells' growth, especially when there is a change of scale. The first step of a typical bioprocess development strategy consists of screening large strain libraries to select the best candidates in terms of growth (and recombinant protein production, if applicable). This is usually carried out in shaken cultures in (i) parallel microwell plates where normally only endpoint measurements are possible because of sample limitation (Lattermann & Büchs, 2015), or (ii) recently in parallel minibioreactors (Back et al., 2016), or (iii) even in Erlenmeyer flasks (0.1 - 1 L). Following screening, the process is developed further in laboratory scale bioreactors, usually with operating volumes between 1 and 20 L where control strategies and process characterisation are applied. The next step is to scale up the bioprocess to pilot plant bioreactors (from hundreds of liters up to some cubicmeters). If regulatory clearance is obtained for commercial use of the product, the process is then scaled-up to large scale bioreactors (10 to larger than 300 m^3) for mass production. The critical point at this level is to ensure the same process performance than the one seen in smaller scales and to make sure that this industrial production is economically feasible considering ROI and market analysis.

The inevitable limitation in the power input in large scale bioreactors ends up with increased mixing times and thus the appearance of liquid heterogeneities in the culture broth (Lara, Galindo, et al., 2006). This means that, independently from the bioprocess, to ensure the same (or acceptably similar) process conditions in such scales when compared to development vessels is a real challenge.

2.3.1. Consideration of Large Scale Mixing Effects in Process Development

Production volumes are in scales between 20 and 200 m^3 (Wittmann & Liao, 2016), but they can be as huge as 500 m^3 like some beer fermenters (Nienow et al., 2011) or lysine production vessels (Eggeling & Bott, 2015), or even bigger (Gradov et al., 2018). If the characteristic time of relevant biochemical reactions taking place inside bacteria (i.e. translation, cell division, etc.) is similar to the mixing time in such bioreactors, there is a potential influence caused by gradients on the growth and metabolic activity of the culture (Lara, Galindo, et al., 2006; Sweere et al., 1987). Generally, transport phenomena are difficult to scale up in a bioprocess, since they perform in a non-linear manner. Moreover, mixing times in the lab scale are lower than 5 seconds, but increase with scale (Dreher et al., 2014; Schirmer et al., 2017) and, at least, by one order of magnitude in industrial scale bioreactors (Delvigne et al., 2006; Hewitt & Nebe-Von-Caron, 2001; Vrábel et al., 2000). For instance, mixing times in the range of several minutes were detected in bioreactors at a scale of 120 and 150 m^3 (Junker, 2004; Namdev et al., 1992). Therefore, the inefficient mixing in such bioreactors typically leads to the appearance of spatial concentration zones of important process parameters, such as substrate, dissolved gases (O_2, CO_2), pH and temperature. As a result, biomass and product yields are often lower at larger scales than at the lab scale (Bylund et al., 1998; de Jonge et al., 2011; Enfors et al., 2001b; George et al., 1998; Xu et al., 1999; Zhou et al., 2018; Zou et al., 2012).

Gradients occur at all scales, but specially in industrial vessels, because certain components (e.g. substrate, oxygen, base or acid, among others) are introduced at one (or sometimes several) positions of the fermenter during almost all bioprocesses. Additionally, it takes several seconds up to minutes to distribute them homogeneously throughout the bioreactor (Delvigne et al., 2006). In fact, the specific power input in such production scales is often the bottleneck to keep mixing times sufficiently low so that gradient formation of concentrations of additives is in most cases inevitable (Lemoine et al., 2017). This leads to a heterogeneous distribution of CPPs, such as substrate, oxygen, carbon dioxide concentration, pH, and temperature (**Figure 1**). Additionally, pressure gradients also exist in production bioreactors owing to their height (Neubauer & Junne, 2016), and cells are exposed to changing flow conditions throughout the cultivation (Nienow, 2006, 2014). Particularly, microorganisms are continuously subjected to changing environmental conditions, thus inducing cell stress or so-called stress responses, characteristic for each organism. It is therefore necessary to study the strain-specific response in what is known as scale down experiments, where large scale conditions are mimicked in lab scale experiments, so that a hopefully comparable microbial response can be investigated in a smaller volume, thus opening the possibility of performing high throughput screening (HTS) experiments (Neubauer & Junne, 2010; Wang et al., 2014).

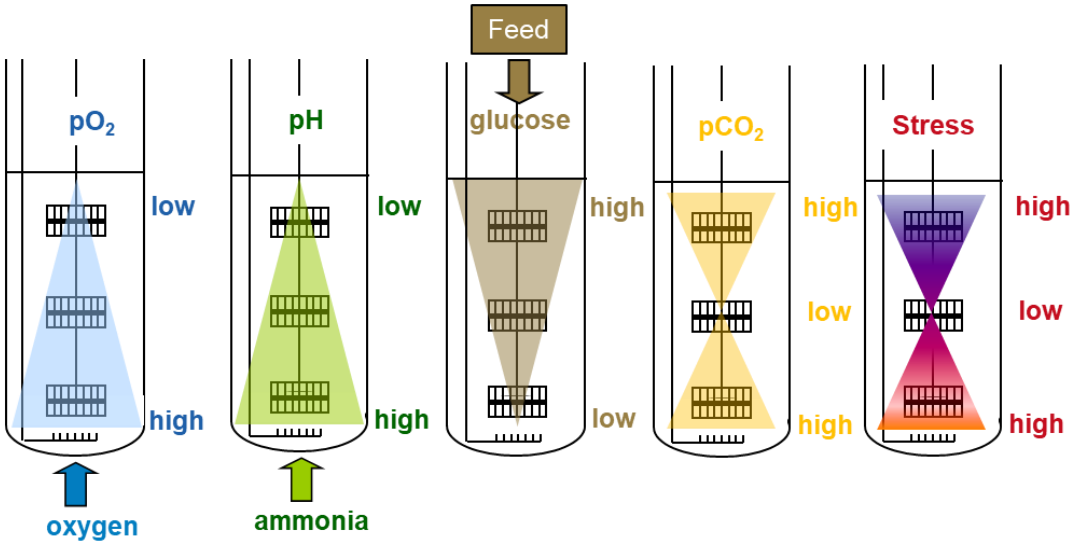

Figure 1. Possible concentration gradients (among others) encountered in industrial scale bioreactors. Adapted from Dr. Arne Matzen, Laboratory Head QC Monoclonal Antibody, Sanofi-Aventis Deutschland GmbH.

Unfortunately, data of gradients measured in large scale bioreactors are found in literature only rarely, probably because of lack of suitable tools. A possible explanation for this may be that manufacturing processes are typically rigid due to legislation requirements and cost restrictions. Another reason might involve the fact that bioreactors in the production scale have hardly changed over time, so the feasibility of applying new technologies may be difficult. As an example toward investigating heterogeneities in relevant manufacturing scales, multi-position and multi-parameter sensors installed on movable lances within the bioreactor have been used to measure spatial gradients in industrial scale brewery as well as biogas processes (Bockisch et al., 2014; Kielhorn et al., 2015). The scenario looks completely different in processes under good manufacturing practices (GMP), where techniques such as CFD modeling and regime analysis based on mixing time calculations are used to determine the existence of gradients in large scale bioreactors (Nørregaard et al., 2019). Finally, just recently, movable, free floating balls with embedded sensors have been developed to enhance the

measurement of variable process parameters in different known zones of large scale bioreactors and are currently being tested by various industrial companies (Lauterbach et al., 2017; Petersen, 2018).

Additionally, recent publications are emphasizing the importance to perform a consistent analysis of cells' physiological state under production scale environmental conditions for developing a proper scale up (or scale down) methodology (Neubauer & Junne, 2016; Olughu, Deepika, et al., 2019; Xia et al., 2016). Nevertheless, gradient formation and other scale-related stresses are often not considered appropriately during scale up, and thus the sensitivity of the physiological state of the microorganisms to these oscillating conditions remains unknown. In order to predict spatial gradients, CFD simulations are usually applied, where the liquid volume is divided into many (up to a few million) small elements (forming the so called mesh) for the simulation, and the fluid dynamic equations (based on the conservation of mass, momentum and energy) are solved for each element. These can, for instance, simulate the fluid dynamics as well as the mixing time (time needed to accomplish a certain homogeneity in the reactor, typically 90 or 95%, after performing a pulse of a pre-defined tracer element) when different impeller designs are tested for a bioreactor (Yang et al., 2012; Zou et al., 2012) or when the kLa is predicted for consistent bioprocess development of aerated bioreactors (Bach et al., 2017). CFD supports an estimation of the liquid flow: mass transfer (e.g. mixing of fed streams or gas-liquid transfer), shear rates and transport of microorganisms through the liquid phase of a bioreactor (Delvigne, Takors, et al., 2017; Schmalzriedt et al., 2003) can be simulated. Importantly, year after year, CFD studies of bigger reactors and more industrially relevant bioprocesses have been performed (Gradov et al., 2018; Wright et al., 2018; Zhu et al., 2018). To investigate the effects of theses simulated spatial gradients on cell physiology, CFD simulations can be combined with kinetic models, which typicall describe cell metabolism mathematically (Chassagnole et al., 2002; Papapostolou et al., 2019; Robitaille et al., 2015; Tang et al., 2017). This means that the set of biological kinetic equations are solved under the consideration of fluid flow (itself derived from mass balances) within the CFD simulations. The entire simulation describes concentration gradients (e.g. substrate, pO_2, pCO_2, etc.), gradients of physical parameters (e.g. pH, mass transfer coefficients, gas hold-up, etc.) as well as temporal and spatial performance of the microorganisms (e.g. substrate uptake, product formation, by-product accumulation, growth, etc.). There are two main approaches to model microorganisms in the CFD simulation, which are applied depending on the purpose of the simulation:

- ✓ The Euler-Euler approach (Azargoshasb et al., 2016; Bannari et al., 2012; Elqotbi et al., 2013; Morchain et al., 2014): the microorganisms are treated as a continuum (i.e. all cells are treated in the same way). It is computationally less demanding, but it loses the individual history of the cells (Lapin et al., 2004).
- ✓ The Euler-Lagrange approach (Haringa et al., 2016; Haringa, Deshmukh, et al., 2017; Haringa, Noorman, et al., 2017; Haringa, Tang, et al., 2018; Kuschel et al., 2017; Lapin et al., 2004, 2006; Morchain et al., 2012): the fluid is treated as a continuum, while microorganisms are considered as individual particles (i.e. individual cells travelling through the bioreactor are tracked). It needs a longer computational time, but accounts for population heterogeneity (see 2.3.3)

The purpose of these studies is usually to predict the oscillating culture conditions in the industrial scale and design controlled scale down experiments at the lab scale that mimic large scale conditions as closely as possible (Haringa, Mudde, et al., 2018). Nevertheless, the major drawback of CFD simulations is their high computational demand (hours or even days) and therefore, some authors decide to simplify them to so-called compartment models, which can still simulate the most relevant

spatial distribution of gradients in the bioreactor with a faster computational speed, thus enabling its application as a real-time PAT tool (Spann et al., 2019; Tajsoleiman, Spann, et al., 2019).

Microbial responses to all kind of environmental stresses have been reviewed elsewhere (Guan et al., 2017; Spadiut et al., 2013) and are commonly influenced by certain reactor geometry limitations (Garcia-Ochoa & Gomez, 2009; Nienow, 2006). The effects of substrate, oxygen, and other gradients have been studied in detail for many microorganisms and the most relevant specific literature is summarized in **Table 1**. Generally, these studies aim to answer (i) how microorganisms respond to shifts in different heterogeneous conditions (or combinations of them), (ii) how fast the organisms react to changes at the -omics level (genomic, transcriptomic, proteomic, and metabolomic) and (iii) what are the long-term effects of oscillating conditions. Interestingly, ensuring the correct O_2 concentration to microorganisms seems challenging: in cultures, in which the air is enriched with pure oxygen due to high cell densities, too high oxygen concentrations can lead to leakage of reactive oxygen species from metabolic routes, which may affect both DNA synthesis and the activity of relevant intracellular enzymes, thus resulting in poor growth (Baez & Shiloach, 2014). Even dynamic *S. cerevisiae* responses to increasing ethanol stresses have been investigated to monitor yeast viability and to optimize bioprocess performance (Sanchez-Gonzalez et al., 2009). Another study described the investigation of physiological effects of nutrient-enriched media (i.e. addition of complex components as well as variable aminoacids cocktails to minimal media) throughout *C. glutamicum* cultures (Graf et al., 2018).

This work, as described previously, focuses on the effect of pH-gradients on *S. thermophilus* cultures and therefore only a detailed overview on the state of the art regarding the heterogeneities of this nature in different bioprocesses is given. On the one hand, the production process of these LAB consists of a simple batch culture, thus making substrate gradients irrelevant. On the other hand, the fermentation is run under microaerobic conditions, so that no oxygen is sparged into the bioreactor. Simply a positive pressure inside the fermenter is maintained by introducing N_2 in the head space, leading to an irrelevance of oxygen gradients as well.

Table 1. Publications which describe the impact of certain gradients throughout the cultivation of various microorganisms.

Gradient	Microogranism	Literature
Substrate	*E. coli*	(Anane, García, et al., 2019; Anane, Sawatzki, et al., 2019; Brand et al., 2018; Brognaux et al., 2014; Bylund et al., 1998; Delvigne et al., 2005, 2006, 2009, 2010, 2011; Enfors et al., 2001b; Hewitt & Nienow, 2007; Hewitt et al., 2000, 2006; Li et al., 2015; Lin & Neubauer, 2000; Lin et al., 2001; Löffler et al., 2016, 2017; Neubauer et al., 1995; Nieß, Löffler, et al., 2017; Philip et al., 2017; Schweder et al., 1999; Simen et al., 2017; Soini et al., 2011; Sunya et al., 2013; Taymaz-Nikerel et al., 2011; Ukkonen et al., 2013; Xu et al., 1999)
	S. cerevisiae	(Aboka et al., 2012; George et al., 1993, 1998; Hakkaart et al., 2019; Larsson et al., 1996; Marbà-Ardébol, Bockisch, et al., 2018; Mashego et al., 2006; McClure et al., 2016; Visser et al., 2004; Wu et al., 2006)
	C. glutamicum	(Käß et al., 2013, 2014; Lemoine et al., 2015, 2016; Lindemann et al., 2019; Olughu, Nienow, et al., 2019)
	B. subtilis	(Junne et al., 2011; Lyubenova et al., 2013)
	P. chrysogenum	(de Jonge et al., 2011, 2014; Nasution, van Gulik, Kleijn, et al., 2006; Nasution, van Gulik, Proell, et al., 2006; Wang, Chu, et al., 2019; Wang, Wang, et al., 2019; Wang, Zhao, et al., 2018, 2019)
	A. niger	(Li et al., 2018; Torres et al., 1996; Wang, Liu, et al., 2019)
O_2	*L. lactis*	(Azizan et al., 2017)
	E. coli	(Anane, García, et al., 2019; Baert et al., 2016; Bylund et al., 1998; Hewitt et al., 2000, 2006; Lara, Leal, et al., 2006; Li et al., 2015; Philip et al., 2017; Sandoval-Basurto et al., 2005; Soini et al., 2008; Ukkonen et al., 2013; Xu et al., 1999)
	S. cerevisiae	(Aon et al., 2018; Marbà-Ardébol, Bockisch, et al., 2018)
	C. glutamicum	(Conrady et al., 2019; Kaboré et al., 2015, 2017, 2019; Käß et al., 2013, 2014; Lange et al., 2018; Lemoine et al., 2015, 2016; Limberg, Schulte, et al., 2017; Olughu, Nienow, et al., 2019)
	B. subtilis	(Junne et al., 2011; Lyubenova et al., 2013)
	S. aureofacies	(Manfredini et al., 1983)
	Y. lipolityca	(Kar et al., 2008, 2012)
	P. putida	(Lieder et al., 2016)
	CHO cells	(Gao et al., 2016)
CO_2	*E. coli*	(Baez et al., 2009, 2011)
	S. cerevisiae	(Eigenstetter & Takors, 2017; Hakkaart et al., 2019; Richard et al., 2014)
	C. glutamicum	(Blombach et al., 2013; Buchholz et al., 2014)
	CHO cells	(Brunner et al., 2018; Xu et al., 2018)
Temperature	*Rhodococcus sp.*	(Wang, Chen, et al., 2019)
	L. lactis	(Azizan et al., 2017)
	E. coli	(LeThanh et al., 2005; Yamamori & Yura, 1980)
	S. aureofacies	(Manfredini et al., 1983)
	CHO cells	(Tsao et al., 1992)
Mechanical (shear stress)	*A. niger*	(Fujita et al., 1994; Grimm et al., 2005)
	Mammalian	(Chalmers, 2015; Sieck et al., 2014)

Compared to these classical stimuli, the consequences of changing the pH value are rarely studied so far and almost none of such studies were performed with LAB. pH-gradients appear in bioreactors due to the pH control of the fermentation broth by the addition of either a base or an acid, depending on (i) the pH setpoint, (ii) the microorganism metabolism and (iii) the growth phase. Additionally, pH control is based on one (maximum two) point measurements. On the one hand, in aerated cultivations the pH controlling agent is often introduced together with the incoming aeration gas, thus ensuring a fast distribution of the acid or base. On the other hand, in non-aerated fermentations the acid or base is usually added to the bioreactor in a liquid form, either at the top or at another position (e.g. close to the impeller blades to maximize liquid mixing with the cultivation broth). This leads to the appearance of a zone with suboptimal pH conditions in close vicinity of the dosage point. Microorganisms circulating throughout this zone are prone to cell damage or, at least, to manifest cell stress responses to changing pH. As far as LAB are concerned, stress responses to a wide range of parameters have been reviewed elsewhere (Guchte & Serror, 2002; Hosseini Nezhad et al., 2015; Hussain et al., 2013; Papadimitriou et al., 2016), but pH-stress responses are of particular interest for this work. (Rhee & Pack, 1980) tried to explain the shift of *Lactobacillus bulgaricus* fermentation pattern from homofermentative to heterofermentative with the change in environmental pH from acidic to alkaline, by means of high lactate dehydrogenase (LDH) synthesis under acidic culture conditions, together with the alkaline preference of enzymes related to the phosphoroclastic split. Jin et al. improved the acid resistance of *Bifidobacteria* to subsequent acid stress by pre-stressing them (Jin et al., 2015). Shoug et al. showed that basic (pH 6.5) as well as acidic (pH 4.5) fermentation pH values significantly reduced freeze-drying survival rates of *Lactobacillus coryniformis* Si3 (Schoug et al., 2008). In a similar study, an acidic pH (pH 4.7) during fermentation significantly reduced *Lactobacillus reuteri* I5007 survival following freeze-drying, whilst growth at a neutral pH (pH 6.7) significantly increased it (Liu et al., 2014). In a recent publication, acid acclimation has been proven to be useful for enhancing the viability of lyophilized *Oenococcus oeni*: after lyophilization, improvement of cell integrity and more extracellular polymeric substances (EPS) were observed in acid acclimated cells, thus linking them to deal with the induced pH-stresses. In fact, different abundant proteins were noticeably enriched in the carbohydrate metabolism process, especially in the amino sugar and nucleotide sugar metabolism (mainly UDP-sugar metabolism). The most significant result was the over-expression of proteins participating in cell wall biosynthesis (formation of dTDP-L-rhamnose), EPS production, ATP binding and the bacterial secretion system (Yang et al., 2019). (Narayana et al., 2020) showed that decreased pH (from the optimal 5.5 to 4.5) caused a shift in *Lactobacillus acidophilus* size distribution from a heterogeneous mix of elongated and short cells to a homogenous population of short cells, by means of flow cytometric as well as microscopic studies. Some authors determined the impact of acidic pH on growth rate (more than a 50 % reduction) of *Lactobacillus casei* fermentations, concluding to have identified clear disturbances of the cell surface at pH 4 (i.e. appearance of granular material at the cell envelope-environment interface), when compared to cultures at optimum pH 6.5 (Hossein Nezhad et al., 2010). Two years later, the same research group performed a deeper study on this topic, stating that these LAB are able to develop an adaptive strategy corresponding to slower growth at low pH (Nezhad et al., 2012). Importantly, extracellular pH has a direct effect on cell physiology as it affects intracellular pH (pH_i), which is crucial for enzymatic activity during biochemical reactions and is controlled by proton pumps (Hansen et al., 2016). Ramos et al. developed an *in vitro* model of the gastrointestinal tract and investigated the influence of passing different juices on pH homeostasis of *Lactobacillus spp.* (Ramos et al., 2014). Hansen et al. studied the effect of variable extracellular pH values on growth, viability, cell size, acidification activity in milk and pH_i of *Lactococcus lactis* during batch fermentations (Hansen et al., 2016). (Azizan et al., 2017) suggested intracellular acid

tolerance response (ATR) of these LAB in response to pH stress based on higher flux ratios through oxalacetate from pyruvate cultivating them at different temperatures and agitation rates. The gathered literature indicates that even short-term exposure of cells to elevated pH values during large scale processes can affect cell physiology and overall process performance. However, no publication with *Streptoccocus spp.* has been mentioned so far. This is because there is simply no recent literature available for stress responses of these LAB to changing pH. (Siegumfeldt et al., 2000) showed that when the extracellular pH is decreased (from pH 7 to pH 5), the pH_i of four *S. thermophilus* strains (among other LAB) also decreased until pH 5.5 after 5-10 min of the pH shift, thus emphasizing the adaptability of LAB to a low external pH. (Adamberg et al., 2003) investigated the effect of low media pH on a wide variety of LAB (including one *Streptococcus* strain). With decreasing pH, both the growth yield as well as the specific lactate production rate decreased in all cases. *S. thermophilus* St20 showed the highest maximum specific growth rate of 2.2 h^{-1}, but was the most acid sensitive strain. This means, that although this strain may divide rapidly, its capacity to lower pH_i when the extracellular pH becomes acidic is low, although this adaptation mechanism is partly achieved at the expense of ATP using H^+-ATPase pump. The direct consequence of this is, that those bacteria become more sensitive to potential pH-gradients, specially far away from the base addition zone (where the pH is in principle lower), thus lowering the overall biomass yield.

Adaptation to acid stress is essential for survival of *S. thermophilus*, since these LAB produce acidic end products (i.e. lactic acid) during fermentation, which accumulate extracellularly, thus creating an unfavourable environment for many other bacteria (Guchte & Serror, 2002; Papadimitriou et al., 2016) to prevent their proliferation. At low pH, these acidic end products are predominant in their non-dissociated form (Hansen et al., 2016), which can diffuse trough the membrane and dissociate into H^+ and its charged derivate to which the membrane is impermeable (Presser et al., 1997). Hence, the pH_i is lowered, which may affect biochemical reactions by damaging intracellular enzymes and DNA. Stress responses to a low pH in the environment could include:

- ✓ The F_0F_1-ATPase either produces ATP using protons or expulses protons out of the cell at the expense of energy consumption. At low pH the proton expulsion activity increases in order to maintain the homeostatic pH_i (Nannen & Hutkins, 1991). This reaction requires ATP as an energy source, because the expulsion of protons to the cytoplasm takes place against an increasing proton gradient in the media (Papadimitriou et al., 2016).
- ✓ Another adaptation mechanism to acid stress is the production of basic compounds, which can help to alkalize the environment as well as the cytoplasm. The nickel metalloenzyme urease in *S. thermophilus* hydrolyses urea to carbon dioxide and ammonia, which can take up a proton and maintain the intracellular pH (Guchte & Serror, 2002).
- ✓ The arginine deaminase pathway is present in different *Streptococcus spp.* (Griswold et al., 2004; Liu et al., 2008), although the physiological role and especially the mode of regulations can be different (Griswold et al., 2004). The system consists of arginine deaminase, ornithine carbamalytransferase and carbamate kinase, which catalyse the conversion of arginine to ornithine, ammonia, carbon dioxide and the formation of ATP (Cunin et al., 1986). The resulting NH_3 can help to alkalize the intracellular environment, while the generated ATP can be additionally used to expulse protons through the F_0F_1-ATPase mechanism described before (Guchte & Serror, 2002). The importance of this pathway in LAB for the adaptation to acidic conditions is highlighted in the most recent publication mentioned before (Yang et al., 2019).

- ✓ Moreover, the arginine/ornithine antiporter can exchange these molecules without energetic costs (Papadimitriou et al., 2016). Nevertheless, the factors involved in this respsonse are rather a combination of starvation, arginine availability and low pH than low pH by itself (Cunin et al., 1986; Guchte & Serror, 2002). (Marquis et al., 1987) highlighted that *Streptococcus* having the arginine deaminase system are adapted to the effects of an acidic environment, emphasising that arginine can be catabolized below the pH threshold for glycolysis. Hence, energy trough the generated ATP is still available, although glycolysis may be affected.

Secondly, LAB seem to have considerably few mechanisms to support alkali tolerance. The portion of the dissociated form of lactic acid, which does not cross the cytoplasmic membrane by simple diffusion, is increased at a high pH-value (Revilla-Guarinos et al., 2014). Under these conditions, less lactic acid may dissolve into the medium, because the chemical equilibrium is displaced toward stabilizing lactate, the dissociated form. Hence, a higher intracellular concentration of lactate might have a negative effect on the cells' viability and growth activity. If lactate accumulates intracellularly due to a high portion of dissociated lactate in the media (at alkali pH), several mechanisms are activated (Nyanga-Koumou et al., 2012). They facilitate survival and growth of LAB under such conditions, and include (i) the ATP-driven K^+ extrusion and the K^+/H^+ antiport system, (ii) the sodium-proton antiport system, (iii) the proton-translocating adenosine triphosphatase (ATPase), (iv) the formation of transmembrane proton gradients (ΔpH) in a reversed direction, and (v) the adaptation of protein synthesis. As an example, cation transport ATPases, such as Na^+ $(K^+)/H^+$ antiporters described for *Lactobacilli* by (Sawatari & Yokota, 2007), can contribute to pH homeostasis under basic conditions by exchanging a cation by one H^+ and converting the transmembrane potential into a pH gradient (Guchte & Serror, 2002), thus stabilizing the intracellular pH.

LAB are able to maintain a homeostatic cytoplasmic or pH_i, typically at a neutral or near neutral value (Hutkins & Nannen, 1993), when the external pH varies. This requires additional resources of carbon, amino acids and energy. The aforementioned mechanisms might, however, also have a growth reducing effect. As their name describes, LAB are obviously more used to deal with acidic conditions rather than with basic ones, thus emphasizing the relevance of investigating the responses of these microorganisms to a high alkali environment, possibly encountered next to the base addition zone during their production process. In fact, literature where basic pH shifts are induced during LAB fermentations can be hardly found. One of the relevant responses to physicochemical stress still to be mentioned is a change in the fatty acid composition of the membrane. For instance, the adaptation of *Streptococcus mutans* includes an accumulation of longer mono-unsaturated fatty acids in the membrane (Fozo & Quivey Jr., 2004; Quivey Jr. et al., 2000). As a consequence, the permeability for protons was reduced like it has been observed for acid adapted cells by (Ma & Marquis, 1997). Furthermore, extreme environmental stress conditions like acidic or alkali pH can trigger additional responses, besides their influence on the cell's constitution. Indirectly the substrate availability can be reduced by decreasing the activity of transporters for sugar uptake (Guchte & Serror, 2002). Therefore, starvation and energy depletion can occur independent from extracellular concentrations of nutrients (Poolman et al., 1987). At the beginning of carbohydrate starvation, LAB tend to accumulate glycolytic intermediates (Papadimitriou et al., 2016) in order to maintain an active metabolic state (Guchte & Serror, 2002). Proteomic studies have highlighted that under acid, thermal or osmotic stress many LAB increase their level of glycolytic enzymes (Heunis et al., 2014), although the specific rate of glucose consumption can be diminished at low pH values (Mercade et al., 2000). Importantly to remember at this point is, that the pH-value is generally not allowed to drop below 5.2 prior to the onset of base addition so that growth reducing conditions are avoided (Hetényi et al., 2011). Hence, the growth

phase of LAB is typically limited by the amount of lactic acid produced by themselves, as long as pH is controlled, and any inhibiting effect is directly caused by a high lactic acid concentration. If lactic acid is accumulated in the medium, less lactic acid can diffuse from the inside to the outside of the cell due to a lower gradient. As a consequence, the pH_i decreases while lactic acid dissociates inside the cell (Hansen et al., 2016). In the literature, it is commonly accepted, that both, the dissociated and non-dissociated forms of lactic acid can inhibit growth of LAB (Åkerberg et al., 1998; Hetényi et al., 2011). While (Amrane & Prigent, 1999; Even et al., 2002) stated that the non-dissociated form of lactic acid was the main inhibitory compound for growth of *Lactobacillus helveticus* and of *Lactococcus lactis*, respectively, a loss of cell viability and membrane integrity by high lactate concentrations was examined *in Lactobacillus bulgaricus* cultures (Rault et al., 2009). The authors concluded that the higher the lactate concentration, the higher the cellular mortality (which was more than one order of magnitude higher in cultures conducted at a higher pH value). They observed that the dissociated form accumulated more under fermentations controlled at pH 6, than at pH 5, which is in accordance with the chemical equilibrium between the species involved. What is more, (Gonçalves et al., 1997) already concluded that the non-dissociated form of lactic acid is not solely responsible for growth inhibition and stated that the total acid concentration is the main cause.

In the case of other microbes, Onyeaka, et al. were the first resarchers including oscillating exposure of *E. coli* to high pH zones (apart from substrate as well as O_2 gradients), which led to a negative effect on the viability and cell growth throughout fed-batch cultivations (Onyeaka et al., 2003). Cortés et al. reported decreases in the plasmid DNA and biomass yields, as well as an increased accumulation of organic acids, apart from a clear influence at the transcriptomic level as the residence time of *E. coli* in an alkali compartment was increased (Cortés et al., 2016). Simen et al. investigated the effect of ammonia pulses on the same bacteria and observed a higher maintenance (15 % increase, compared to optimal pH conditions) and the activation of over 400 genes in response to the induced pH-gradients (Simen et al., 2017). Moreover, only one pH unit in acidic as well as alkaline direction reduced the biomass and product formation and induced phenotypic changes in *C. glutamicum* scale down experiments (Limberg, Joachim, et al., 2017). (Olughu, Nienow, et al., 2019) just recently concluded an expenditure of energy toward maintenance of intracellular homoeostasis of these microorganisms at the detriment of cadaverine productivity, after inducing ΔpH of +0.3 and -1.0 respect the optimal value under scale down conditions. Additionally, an old study of Amanullah et al. indicates that although *B. subtilis* biomass concentration remained unaffected by pH variations, product formation was influenced by residence times of one minute or longer in a high-pH compartment, attributed to the sensitivity of certain enzymes to varying pH and increasing dissociated acetate concentrations (Amanullah et al., 2001). Also, the decrease of the optimal pH of 5.0 to pH 3.0 predominantly increased maintenance-energy requirements and death rates in aerobic, glucose-limited *S. cerevisiae* cultures, veryfied by transcriptional analyses (Hakkaart et al., 2019). The influence of the pH level on the physico-chemical properties of the cultivation medium (i.e. foam formation) and on cell physiology during *Y. lipolytica* cultivations has even been investigated (Bouchedja et al., 2018), resulting in an optimum pH of 6 for maximum cell growth and intracellular lipid accumulation. Nevertheless, pH fluctuating conditions have mostly been investigated during mammalian cell culture. For instance, some years ago, a cell viability decrease was observed with increasing pH perturbation time: a 90-minute exposure to basic pH environment induced a 100 % cell viability loss (Osman et al., 2002). Additionally, pH shifts of almost one pH unit have been measured before close to the alkali addition point in an $8m^3$ bioreactor during mammalian cell cultures (Langheinrich & Nienow, 1999). Growth of CHO cells exposed to pH 9, especially during the exponential growth phase, was strongly

affected resulting in a 37 and 25 % decreased maximum viable cell density and final product titer, respectively (Brunner et al., 2017). Interestingly, three mAb-producing CHO cell lines were sensitive to pH excursions, since base addition led to increase in osmolality, pCO_2, and lactate production, with a concominant antibody galactosylation increase with increasing cultivation pH, correlating to the decrease in cell-specific productivity (Jiang et al., 2018). Recently, Lee et al. were able to analyze the Golgi pH of such cells by using a pH-sensitive fluorescent protein (Lee et al., 2019).

Finally, other gradients may appear during the *S. thermophilus* production process, like CO_2 and temperature inhomogeneities. On the one hand, LAB are fast growing microorganisms and thus produce CO_2 at high local concentrations. What is more, not only microorganisms can change the composition of the media and hence gas solubility, but the hydrostatic pressure in large bioreactors caused by their height becomes also critical when it comes to gas solubility. Thus, elevated regions of pCO_2 may be present in the lower parts of industrial scale bioreactors. The effects of elevated CO_2 concentrations on microbes and its mechanisms have been reviewed elsewhere (Yu & Chen, 2019). As an example from **Table 1**, (Baez et al., 2011) investigated the influence of increasing pCO_2 concentration on growth as well as recombinant protein production during scale down experiments of *E. coli* cultivations. The authors observed a decrease of the specific growth rate of 11 % and an increase of the acetate concentration of 23 % at the highest circulation time compared to reference cultures, but they also noticed a short time of metabolism recovery from high-low CO_2 interminent pulses. Moreover, high concentrations of pCO_2 may cause acidification and concomitant acid stress responses from microorganisms, which is the usual observation described in the literature. For example, (Román et al., 2018) demonstrated the existence of an interaction between pCO_2 and pH in cell density as well as recombinant protein production using mammalian cells. On the other hand, heat exchange surface may sometimes become the limiting factor in high-cell density processes (Hewitt & Nienow, 2007) and specially during LAB production, where the optimal growth temperature is considerably higher than that of the majority of bioprocesses (40 ºC or even higher). When scaling-up, heat release scales with the reactor volume, whereas the relation between surface area to volume is dramatically reduced, and thus the cooling capacity. So far, (Caspeta et al., 2009) investigated the production of a recombinant protein with *E. coli* using a thermo-inducible expression system and gave a positive consequence of this scale up phenomenon. The authors obtained a correlation between by-products accumulation and heating rate: the highest yield and productivity were achieved with the lowest heating rate, such those likely to encounter in conventional large scale fermenters.

2.3.2. Scale Down for Reliable Simulation of Industrial Scale Conditions

In order to consider the effect of large scale oscillating conditions discussed above on cell physiology during bioprocess development and/or optimization, scale down simulators are usually applied. These are smaller bioreactors (than the one being studied) that have been configured to reproduce the environmental conditions of the bigger bioreactor, thus enabling the study of the cell stress responses to the induced oscillations. The main reason for this is clear: large industrial scale bioreactors can seldomly be used for experimental investigation due to costs, cGMP, regulatory, handling and time limitations. The smaller scale abstraction of the industrial scale bioreactor provides the flexibility of laboratory cultivations with smaller inventory (media and energy costs) in dedicated research facilities. This topic has been reviewed several times in recent years (Delvigne & Noorman, 2017; Delvigne, Takors, et al., 2017; Neubauer & Junne, 2010, 2016; Olughu, Deepika, et al., 2019; Takors, 2012; Wehrs et al., 2019) and its strategies are already being applied in academic as well as industrial research

projects. Some recent examples in industrially relevant fields include the use of scale down devices combined with fast sampling and quenching protocols for scale up of penicillin production (Wang et al., 2014), taking into account this concept for optimization of the fermentation of filamentous fungi (Hardy et al., 2017) and the consideration of such studies for the successful implementation of gas fermentation technologies (CO and CO_2/H_2 mixtures) in the industrial scale to reduce CO_2 emissions (Takors et al., 2018). Importantly, the study of the influence of gradient formation encountered in large scale bioreactors in the lab, can be performed empirically, through mathematical models or a combination thereof. Already more than ten years ago, the use of stochastic models to investigate the effect of scale up on bioreactors' hydrodynamics was proposed. As an example, (Villiger et al., 2018) characterized bioreactors with working volumes ranging from 15 mL up to 15 m^3 using a combination of computational and experimental methods for transferring mammalian cell culture processes from the lab to the industrial scale. With the rapid improvement of computational devices, the integration of mathematically modelled microbial kinetics and fluid dynamics toward model-driven scale up of industrial bioprocesses has been a common trend in recent years (Delvigne et al., 2006; Siebler et al., 2019; Wang et al., 2015; Xia et al., 2016; Zieringer & Takors, 2018). In almost all these publications scale down experiments that resemble large scale conditions were designed based on CFD simulations discussed in 2.3.1. Nowadays, even bioreactors in the scale of milliliters are suggested for performing scale down studies of industrial fermenters (Sandner et al., 2019; Tajsoleiman, Mears, et al., 2019). The main advantage of this approach is the HTS of experiments that can be carried out in such a small scale, but the main limitation is the proper transfer of fluid dynamics and gradient formation from a cubicmeter scale to such a small scale, typically using single-use bioreactors. Finally, even microliter scale bioreactors can be used to simulate conditions in a bigger scale and further increase the throughput of experiments (Ukkonen et al., 2013).

Scale down bioreactors can be broadly categorized into single-compartment and multi-compartment reactors. The first scale down systems developed were mainly as single-compartment bioreactors, either shaped in the form of a tubular closed-loop toroid (Gschwend et al., 1983) or single STRs with pulse-based inputs or internal horizontal discs for increased mixing times (Schilling et al., 1999). Later, the multi-compartment scale down systems were developed, comprising either two connected STRs or a STR connected to a so called plug flow reactor (PFR) (Limberg et al., 2016).

- ✓ Cyclic oscillations can be induced by applying pulse feed of some growth-related parameters (i.e. aeration, substrate) into the bioreactor to investigate metabolic shifts of all cells to a certain perturbation. During operation of single-compartment scale down bioreactor with pulse feeding, the stress inducing agent (usually in the form of a highly concentrated substrate feed or a base or acid) is intermittently injected into the bioreactor, at specified intervals (Neubauer et al., 1995) or randomly (Sunya et al., 2013). One important question to be answered when using this approach is how relevant the response after single pulses is for large scale operation, where the cells are exposed to continuous changes during the full process duration. It has been shown before (de Jonge et al., 2014; Tang et al., 2017; Wang, Zhao, et al., 2018) that under such conditions, the average metabolic state can be very different from steady-state chemostat conditions.
- ✓ Stochastic extracellular fluctuations can be achieved by the compartmentalization of the reactor, where not only spatial, but also temporal gradients are created, thus resembling large scale bioreactors. In multi-compartment scale down bioreactors, one of the compartments is usually an assumed perfectly mixed STR, whereas the other STR or PFR is used to induce the required gradient(s). The culture is circulated between the perfectly mixed zone and the stress

inducing zone, at a rate equivalent to a specified residence time (established with the pump rate). The stress inducing agent is injected into the heterogenous part (PFR or second STR), from where it is eventually mixed with the bulk of the culture in the other section(s). Recent improvements in the construction of the plug-flow reactor section include the use of static mixers, which prevent back mixing of the liquid fed and helps to achieve a higher degree of plug flow behaviour upon aeration than previous hollow tube versions (Junne et al., 2011). Additionally, (Lemoine et al., 2015, 2016; Marba-Ardebol et al., 2016; Marbà-Ardébol, Bockisch, et al., 2018) used a scale down bioreactor consisting of one STR connected to two PFRs to simultaneously study the influence of excess substrate and oxygen limitation on the metabolic behaviour of different microorganisms, which are the only three-compartment scale down reactor studies involving two plug-flow reactors and a STR reported in the literature so far.

Both operation mechanisms simulate zones that are similar to feeding and starvation zones in large scale bioreactors. The resulting periodic exposure of the culture to varying stresses induces stress responses that are also observed in industrial scale bioreactors (Enfors et al., 2001b). Scale down techniques have been applied for the successful study of the impact of large scale gradients for most industrially relevant organisms (Neubauer & Junne, 2016) and are summarized in **Table 2**. The vast majority of scale down techniques found in literature aim at mimicking substrate and/or oxygen gradients, since typical industrial bioprocesses are performed in fed-batch mode and use aerobic microorganisms. Nevertheless, in this work, the process under study is carried out in batch mode and uses aerotolerant bacteria, but without sparging air during the production.

Table 2. List of scale down systems used with various microorganisms. SCSDR: single-compartment scale down reactor; TwoCSDR: two-compartment scale down reactor; ThreeCSDR: three-compartment scale down reactor.

Scale down setup	Microorganism	Literature
SCSDR with intermitent feeding	*E. coli*	(Anane, García, et al., 2019; Anane, Sawatzki, et al., 2019; Baert et al., 2016; Delvigne et al., 2009, 2010; Neubauer et al., 1995)
	S. cerevisiae	(Aboka et al., 2006, 2012; Mashego et al., 2006; Sweere et al., 1988; Visser et al., 2002, 2004; Wu et al., 2006)
	P. chrysogenum	(de Jonge et al., 2011, 2014; Nasution, van Gulik, Proell, et al., 2006; Wang, Chu, et al., 2019; Wang, Zhao, et al., 2018)
	A. niger	(Wang, Liu, et al., 2019)
	G. oxydans	(Oosterhuis et al., 1985)
	Plant cells	(Cheung et al., 2018)
TwoCSDR STR-STR configuration	*E. coli*	(Baert et al., 2016; Baez et al., 2011; Lara, Leal, et al., 2006; Sandoval-Basurto et al., 2005)
	S. cerevisiae	(Heins et al., 2015; Sweere et al., 1988)
	C. glutamicum	(Kaboré et al., 2019)
	G. oxydans	(Oosterhuis et al., 1985)
	Mammalian	(Brunner et al., 2017; Osman et al., 2002)
TwoCSDR STR-PFR configuration	*E. coli*	(Brognaux et al., 2014; Delvigne et al., 2005, 2009, 2010, 2011; Hewitt & Nebe-Von-Caron, 2001; Hewitt et al., 2000, 2006; Li et al., 2015; Löffler et al., 2016; Marba-Ardebol et al., 2016; Neubauer et al., 1995; Nieß, Löffler, et al., 2017; Schweder et al., 1999; Simen et al., 2017; Xu et al., 1999)
	S. cerevisiae	(George et al., 1993, 1998; Marbà-Ardébol, Bockisch, et al., 2018)
	Y. lipolytica	(Kar et al., 2008, 2012)
	C. glutamicum	(Käß et al., 2013, 2014; Lemoine et al., 2015; Limberg et al., 2016; Olughu, Nienow, et al., 2019)
	B. subtilis	(Junne et al., 2011; Lyubenova et al., 2013)
	Mammalian	(Nienow et al., 2013)
ThreeCSDR STR-CR-CR configuration	*C. glutamicum*	(Buchholz et al., 2014)
ThreeCSDR PFR-STR-PFR configuration	*E. coli*	(Marba-Ardebol et al., 2016)
	S. cerevisiae	(Marbà-Ardébol, Bockisch, et al., 2018)
	C. glutamicum	(Lemoine et al., 2015, 2016)

Research aims at simulating gradients of substrate (normally glucose) and/or oxygen concentrations. Compared to these classical stimuli, the consequences of changing the pH value throughout cultivations are not commonly studied. No literuature about applying scale down strategies during LAB fermentation for studying the impact of pH-gradients on cell physiology can be found. Generally, the range of values to be chosen for the amplitude, duration, frequency and number of pH perturbations prior to lab experiments should be estimated from published measurements with the microorganism under study. Nevertheless, this work was performed without any previous knowledge on pH oscillations simulated in scale down *S. thermophilus* bioreactors. (Hewitt et al., 2006; Onyeaka et al., 2003) were the first researchers including the influence of pH disturbances during *E. coli* two-compartment scale down experiments (STR-PFR setup). It was demonstrated that oscillating conditions in a 20 m^3 industrial fed-batch fermentation, induced a lower biomass yield than that found in the equivalent well-mixed, 5L laboratory scale case. However, by using a combination of the well-mixed 5L STR with a suitable PFR to mimic the changing microenvironment at the large scale, very similar results to those in the 20 m^3 reactor may be obtained. In fact, the similarity was greatest when the PFR was operated with a mean residence time of 50 seconds with a low level of pO_2 and a high glucose concentration with either a pH of 7 throughout the two reactors or with pH controlled at 7 in the STR by addition of base into the PFR (where the pH was higher than 7). Additionally, (Cortés et al., 2016) applied a STR-STR approach with the same purpose and detected the activation of a series of mechanisms to cope with alkaline pH: decrease of plasmid DNA and biomass yields, as well as decrease of plasmid DNA final titer, but accumulation of organic acids, accompanied by a transcriptional response, coding for ion transporters, amino acids catabolism enzymes and transcriptional regulators. These results were confirmed in a similar study using a STR-PFR setup, where about 400 genes were repeatedly switched on/off when *E. coli* circulated between both compartments. More importantly, cellular ATP demands for coping with fluctuating ammonia supply were found to increase maintenance by 15 % (Simen et al., 2017). (Olughu, Nienow, et al., 2019) just recently published STR vs. STR-PFR scale down studies performing *C. glutamicum* cultivations, concluding an expenditure of energy toward maintenance of intracellular homoeostasis with a decreased productivity of cadaverine, after inducing a ΔpH of +0.3 and -1.0 along the height of the PFR with a residence time of 5 min. Amanullah studied the effect of pH on *B. subtilis* by comparing the STR-STR and STR-PFR scale down models. In the first setup, the author maintained the large vessel at pH 6.5 with acid additions and the small bioreactor at pH 7.2 by feeding alkali, thus representing the homogenous bulk zone and the base addition point in an industrial reactor, respectively. The pump rate as well as vessel sizes were carefully chosen to obtain circulation times through the high pH compartment, similar to that found at large scale, resulting in a decreased biomass and product formation. Importantly, it was commented that almost a continuous addition of both, alkali and base, to the corresponding vessels was required in order to maintain both reactors at different pH values, which caused the formation of salt, with a subsequent increase of the osmolality and a concominant slight decrease in culture growth. For the second approach, the author used a glass mixing bulb positioned upstream of the PFR to mix 5M NaOH with the culture before it entered the PFR, thus producing a high pH zone. These were the first studies suggesting that the PFR represented the alkali addition point and the STR the well mixed bulk liquid of an industrial fermenter. Later on, these results were published, which indicate that although biomass concentration remained unaffected by pH variations, product formation was influenced by residence times in the PFR of one minute or longer (Amanullah et al., 2001). Moreover, (Kar et al., 2008) investigated the effect of extracellular pH on microbial growth, extracellular lipase production as well as gene expression by *Yarrowia lipolityca* on the basis of a STR-PFR scale down approach. The authors concluded that pH-gradients impacted biomass growth and the specific rate of lipase production, but

not the gene expression. Nevertheless, a morphological modification of the cells was observed when maintaining them during 2-5 minutes under pH-gradients, which is in accordance with previously reported dimorphism manifestation of these yeast cells exposed to pH fluctuations (Ruiz-Herrera & Sentandreu, 2002; Szabo & Štofaníková, 2002). (Brunner et al., 2017; Nienow et al., 2013; Osman et al., 2002) used two-compartment systems (STR-STR, STR-PFR and STR-STR configurations, respectively) to simulate pH inhomogeneities of 10-20 m^3 bioreactors during mammalian cell cultures. The specific growth rate, specially during the exponential growth phase, was strongly affected when inducing temporary pH zones of pH 9, thus resulting in a decreased viable cell density (VCD) and final product titer. The gathered results indicate that even short-term exposure of cells to elevated pH values during large scale processes can affect cell physiology and overall process performance.

As described by (Noorman, 2011) any type of scale down simulator based on ideal lab reactors has a total of five degrees of freedom: number of compartments, vessel volumes, flow patterns, circulation rates and feed rates. The key question is typically: do we really know (i) the fluid dynamics, (ii) the mixing times, (iii) the gradient formation, (iv) the resulting compartmentalization and (v) the residence times on those zones at the industrial scale that should be mimicked? Although it has been demonstrated that scale down systems are reliable for studying large scale conditions (examples presented in **Table 2**), their application is not yet a standard step in bioprocess optimization and development in the biopharmaceutical industry. As stated some years ago, one of the difficulties in the design and operation of scale down bioreactors is the lack of data on the heterogeneities in large scale bioreactors (Formenti et al., 2014). A huge variability of the conditions in the large scale along with confidential issues have let to this scenario. This is further attributed to the lack of spatially distributed sensors, as well as the rigidity of industrial scale cultivations/bioreactors in terms of reactor modifications and retrofitting that would enable the measurement of gradient profiles. Thus, some researchers decide to apply the reversed approach to overcome this limitation: keep changing the conditions (and CPPs) during scale down experiments in the lab until similar performance (i.e. CQAs, KPIs) to measurements in the industrial scale are obtained, so that a suitable scale down model is achieved. Still, in industrial practice, investments of time, capital and resources often prohibit systematic effort toward scale down studies prior to scale up or for its optimization, although, in the end, savings obtained in this way are trivial compared to the expenses that result from real process disturbances and batch failures with loss of business opportunity.

2.3.3. Monitoring of Population Heterogeneity for Scale Up&Down

In most bioprocesses, the assessment of the physiological response of microbial cells to the changes in environmental conditions associated with large scale operation is limited to the indirect measurement of external variables outside of the cell; or directly by analysis of internal variables such as the concentration of key cellular metabolites (e.g. ATP, NAD(P)H or ppGpp) within the cell and via the quantification of mRNA levels of all genes in a microbial genome at a specific moment in time using microarray technology. However, these studies, using the techniques described, typically take the "bulk approach", that is it is assumed that all cells in a population behave in the same way. Therefore, any results thereof represent only a population average contribution to the measured variable or parameter. Already some years ago (Hewitt & Nebe-Von-Caron, 2004; Hewitt et al., 2006), it was suggested that this assumption is inappropriate and that both environmental and cell physiological heterogeneity exist. This means that, in order to fully understand a cell's metabolic response to the process environment at large scale, physiological heterogeneity should be taken into account and,

where heterogeneity is shown to exist, sub-populations of cells should be separated, sorted and collected for further microarray analysis. In this way, it should be possible to identify genes which are being differentially expressed in each sub-population, allowing a deeper level of understanding of the physiological responses of cells to the differing fluctuating microenvironments found at the different scales of bioprocess operation. Also, in recent years, literature emphasizing the importance of considering individual cells rather than a whole cell population during optimization and scale up of a wide variety of bioprocesses has been published (Delvigne & Noorman, 2017; Delvigne et al., 2014, 2018; Delvigne, Baert, et al., 2017; Delvigne, Takors, et al., 2017; Heins & Weuster-Botz, 2018; Müller et al., 2010; Zacchetti et al., 2018). In nature, microbes face rapidly changing and highly competitive environments, where phenotypic heterogeneity has evolved as an innate survival strategy to gain an overall fitness advantage over cohabiting competitors. However, in defined artificial environments such as monocultures in small to large scale bioreactors, cell-to-cell variations are presumed to cause reduced production yields as well as process instability. Although emerging strategies and tools to reduce phenotypic heterogeneity in biotechnological expression setups have been proposed (Binder et al., 2017), this is not the focus of this work, since wild type (non-GMO) strains were used.

Interestingly, population heterogeneity can have a positive impact on the process (Grote et al., 2015). The most important question is how and with which tools can cell-to-cell variations be determined and monitored. These have been intensively reviewed for different bioprocesses and microorganisms in recent years (Croop et al., 2019; González-Cabaleiro et al., 2017; Huys & Raes, 2018; Lemoine et al., 2017; Schmitz et al., 2019; Theron et al., 2018), but can basically be separated into flow cytometric or microscopic analysis, with or without the use of microfluidic systems:

- ✓ Already at the beginning of the 21st century, the advantages of multi-parameter flow cytometry over the more conventional microbiological techniques such as dilution plating (CFU/mL) were shown (Davey & Kell, 1996; Davey & Winson, 2003; Shapiro & Nebe-von-Caron, 2004). Using various mixtures of fluorescent dyes, it is possible to resolve an individual microbial cell's physiological state beyond culturability, based on the presence or absence of an intact polarized cytoplasmic membrane and the transport mechanisms across it, enabling assessment of population heterogeneity (Díaz et al., 2010). Moreover, by offering high-throughput, quantitative and multi-parameter analysis at the single-cell level, this technique has gained an increased popularity in microbiological research, food safety monitoring, water quality control and clinical diagnosis (Ambriz-Aviña et al., 2014; Wu et al., 2016). When the cells pass through the detection volume via hydrodynamic focusing by a sheathed flow, rapid, multi-parameter and quantitative measurement can be achieved through simultaneous light-scattering and multicolor fluorescence detection of single cells at a speed up to 50,000 s^{-1} (Cram, 2003). With this technology, structural as well as functional diversity of bacterial populations can be characterized in a rapid and statistically representative manner. The new development of high sensitivity flow cytometry overcomes the main limitation of conventional flow cytometers by adopting strategies for single molecule fluorescence detection in a sheathed flow. To date, using label-free side scattering detection, a single bacterial cell can be well discriminated from the instrumentation background.
- ✓ Since modern image analysis allows fast, accurate and reliable quantitative analysis, it is widely used at present in many areas of research and development (Jung, 2019). Generally, images captured by imaging hardware, which is not limited to digital cameras, are processed in multiple steps by applying various image processing algorithms to extract quantitative

features. On-line image analysis has been used in the bioprocessing community to count cell numbers, to quantify cell morphology and to measure cell concentrations in the lab only in recent years (Bluma et al., 2010; Marquard et al., 2016, 2017). What is more, late advances in photo-optics already enable to monitor particle size distribution, aspect ratio and particle concentration with advanced image analysis in real time in multiphase systems (Emmerich et al., 2019). Nevertheless, several challenges appear when measuring directly in the culture broth: liquid (media), solid (cells) and air bubbles in aerated systems have to be distinguished from each other. Besides, particular cell features, which are of interest, have a size smaller than 1 μm, which makes monitoring complicated. Furthermore, the usually applied complex media possess many insoluble particles, which demands a sophisticated image analysis and absorbs much light. Finally, the high cell densities obtained today create many overlapping particles, which cannot be easily identified. Despite all these challenges, monitoring of life cells has a great potential and is therefore already conducted for many applications, although not often in-line due to a lack of suitable devices.

- ✓ Single-cell analysis in microfluidic cultivation devices bears a great potential for the development and optimization of industrial bioprocesses since large scale dynamics might be emulated in such systems (Grünberger et al., 2014; Haringa, Mudde, et al., 2018). Low volumes together with high parallelization allows to increase the throughput, thus running a larger number of cultivation experiments simultaneously even under quick alteration of environmental conditions than with lab bioreactors. For example, the impact of changes in media composition on cell growth during classical batch cultivation can be easily resolved (Demling et al., 2018). Until now, microfluidic devices and bulk measurement techniques have been more frequently used to determine microbial growth via biomass, biovolume or OD. Meanwhile, growth rates acquired in the microfluidic single-cell cultivation can be based on doubling times measured with time-lapse microscopy. By using this technology together with fluorescence-based biosensors, specific growth rates of micro-colonies, morphological changes of single cells and cell population heterogeneities can be precisely determined (Mustafi et al., 2014). The additional information gained on a single-cell level allows to determine not only μ_{max} very precisely but also gives information on cell-to-cell heterogeneity.

In-situ microscopy (ISM) has been developed in recent years to bring this concept of measuring population heterogeneity to the industrial scale (Belini et al., 2013; Beutel & Henkel, 2011). (Marbà-Ardébol et al., 2019) just summarized the ISM methodology followed to study the morphologic dynamics of fungi, microalgae and yeast cells, which enabled the determination of growth activity as well as intracellular product accumulation. The sensor has no movable parts and can be directly connected to any standard STR, either through a standard port (in-line measurement) or in a sterilizable by-pass (on-line approach).

The use of fluorescent probes to assess physiological functions of bacteria at the single-cell level was developed some years ago (Joux & Lebaron, 2000), but it is a smart way to make physiological heterogeneity visible, when combined with flow cytometry or microscopy. For instance, propidium iodide (PI) is a fluorescent marker broadly used for the assessment of cell viability on the basis of membrane permeability, since, in principle, it can only be taken up by microbial cells exhibiting compromised membranes (Davey & Hexley, 2011; Shi et al., 2007). In a similar direction, the genetic modification of introducing a fluorescent transcriptional reporter into the DNA of the strain under study is a novel biotechnological approach for studing population heterogeneity, but does not allow

to study the original strain, since the GMO may show some different properties when compared to microorganisms without fluorescent biomarker (Díaz et al., 2010). As examples, (Delvigne et al., 2009, 2010, 2011) used flow cytometric analysis to study changes on the expression of different transcriptional reporter genes, based on the green fluorescent protein (GFP), on a single-cell basis during cultivations performed under well mixed and heterogenous conditions. Results show a significant drop of the GFP content in *E. coli*, as stress response under scale down conditions (excess, limitation and starvation of glucose and exhaustion of oxygen). This reduction was associated with a segregation in the population heterogeneity. The same authors applied *S. cerevisiae* reporter strains for investigating the cell robustness against freeze-thaw stress and growth on ethanol in a continuous STR-STR scale down cultivation, where sugar concentration and dissolved oxygen oscillations were encountered. Flow cytometry measurements evaluating freeze-thaw stress revealed that the membranes of cells growing with higher dilution rate appeared to be more robust toward freeze–thaw stress, in comparison to cells growing at lower dilution rate. In terms of ethanol consumption, cells cultivated in SingleCR showed no growth on ethanol, whereas 64 % higher fluorescence was detected in TwoCR cultivations, where the population heterogeneity increased as well (Heins et al., 2015). Additional relevant literature already published regarding investigation of population heterogeneity in the single-cell level using the tools described above in different bioprocesses can be found in **Table 3**.

Table 3. List of the most relevant and recent research articles applying the tools previously described for monitoring population heterogenetiy throughout cultivations using different microorganisms.

Tool/strategy	Microorganism	Literature
Flow cytometry	*L. acidophilus*	(Narayana et al., 2020)
	E. coli	(Brognaux et al., 2013; Heins, Johanson, et al., 2019; Heins, Lundin, et al., 2019; Hewitt & Nebe-Von-Caron, 2001; Hewitt et al., 2006)
	S. cerevisiae	(Heins, Johanson, et al., 2019; Hewitt & Nebe-Von-Caron, 2001)
	C. glutamicum	(Neumeyer et al., 2013)
	P. pastoris	(Raschmanová et al., 2019)
	CHO cells	(Möller et al., 2019)
Microscopy	*L. acidophilus*	(Narayana et al., 2020)
	E. coli	(Panckow et al., 2017)
	S. cerevisiae	(Ginovart et al., 2018; Marbà-Ardébol, Bockisch, et al., 2018; Marbà-Ardébol, Emmerich, et al., 2018; Suhr & Herkommer, 2015)
	H. anomala	(Camisard et al., 2002)
	B. amyloliquefaciens	(Ziegler et al., 2015)
	C. cohnii	(Marbà-Ardébol et al., 2017)
	C. reinhardtii + C. vulgaris	(Havlik et al., 2013)
	Mammalian	(Guez et al., 2004; Suhr & Herkommer, 2015)
Reporter strains + flow cytometry	*E. coli*	(Baert et al., 2015; Heins, Johanson, et al., 2019; Heins, Lundin, et al., 2019)
	S. cerevisiae	(Carlquist et al., 2012; Delvigne et al., 2015; Heins et al., 2015)
Microfluidics + microscopy	*E. coli*	(Binder et al., 2016; Fragoso-Jiménez et al., 2019; Hashimoto et al., 2016)
	C. glutamicum	(Grünberger et al., 2015; Lindemann et al., 2019)
	S. lividans	(Koepff et al., 2018)
	S. mycelium	(Sachs et al., 2019)

Additionally, innovative strategies for analyzing population heterogeneity during cultivation of industrially relevant microorganisms have been proposed in recent years. (Wang & Dunlop, 2019) just recently reviewed the origins of cell-to-cell variation in metabolic engineering and strategies to control variability in such scenarios. While (Li, Tang, et al., 2019) suggest a novel mass spectrometry (MS) strategy to eliminate matrix effects and thus obtain information of mammalian cells on a single cell in their native state, (Vasdekis et al., 2019) used MS together with high-throughput quantitative-phase imaging for quantifying the tradeoffs between triacylglycerol production and growth in the oleaginous microorganism *Y. lipolytica*. (Sassi et al., 2019) propose the use of a so called segregostat to control phenotypic diversification dynamics of *E. coli* as well as *P. putida* cells. This cultivation mode, in contrast to a traditional chemostat, allows the control of phenotypic diversification of microbial populations over time. Results show that, upon nutrient limitation, cell population tends to diversify into several subpopulations exhibiting distinct phenotypic features (non-permeabilized vs. permeabilized cells). On-line flow cytometry analysis leads to the determination of the ratio between cells in these two states, which in turn triggers the addition of glucose pulses to maintain a predefined diversification ratio. Literature work found toward quantification of population heterogeneity in LAB cultivations, proposes the use of single cell Raman spectroscopy, coupled to chemometrics, for real-time analysis and prediction of cells in different growth phases during batch culture of *Lactobacillus casei*. Spectral shifts were identified in different states of cell growth that reflect biochemical changes specific to each cell growth phase (Ren et al., 2017). The authors conclude that Raman spectroscopy allows label-free, continuous monitoring of cell growth, which may facilitate more accurate estimates of growth states of LAB populations during fermented batch culture in industry.

Due to the continuous development, in the last decades, of analytical techniques providing complex information at the single cell level, the study of cell heterogeneity has been the focus of several research projects within analytical biotechnology (**Table 3**). Nonetheless, the complex interplay between environmental changes and cellular responses to them is still not fully understood, and the integration of this new knowledge into the strategies for design, operation and control of bioprocesses is far from being an established reality. Indeed, the impact of cell heterogeneity on productivity of large scale cultivations is acknowledged but seldom accounted for. In order to include population heterogeneity mechanisms in the development of novel bioprocess control strategies, authors have developed a reliable mathematical description of such phenomena (Lencastre Fernandes et al., 2011). Multiple modeling frameworks have been proposed to describe and simulate the dynamics of heterogeneous populations. Measurement data are used to adjust computational models, which results in parameter and state estimation problems. Then, methods to solve these estimation problems need to take the specific properties of data and models into account (Waldherr, 2018):

- ✓ In a stochastic approach, cell heterogeneity can be described by looking at a probability distribution over the cellular variables (Wilkinson, 2009). (Delvigne et al., 2005, 2006, 2011) published a stochastic model enabling the simulation of the mixing and the circulation of *E. coli* in a TwoCSDR system (STR-PFR). The superimposition of mixing and circulation processes determines the (glucose) concentration profile experienced by a microorganism in the bioreactor during fed-batch cultures. Such methodology as part of an Euler-Lagrange approach has also been applied to *P. chrysogenum* cultures in recent years (Haringa et al., 2016).
- ✓ In the concept of population balance modeling (PBM), so-called population balance equations (PBEs) are defined, thus formulating a density function over the heterogeneous cellular variables. Changes of this density function over time describe population dynamics

(Ramkrishna, 2000). Mathematically, PBEs are partial differential (or integro-differential) equations, with time and heterogeneous cellular variables as independent variables. These models contain distinct elements for several processes which, together, shape the population heterogeneity and are thus useful, for instance, to distinguish the effects of different parts of the system including intracellular dynamics, cell division and death rates or cell partition at division, on the overall population state and dynamics. Different applications of these models to biological systems were reviewed some years ago (Ramkrishna & Singh, 2014).

- ✓ Another option to model cell population behaviour are individual-based or cell ensemble models (Henson, 2003). These models simulate a large number of individual cells which are representative for the full population. Population characteristics can then be inferred from gathering the individual cells' properties. While individual cells are sometimes modelled stochastically in ensemble models, the statistical properties of the overall population do still deterministically depend on the single-cell dynamics. (Nieß, Löffler, et al., 2017) recently published a transcriptomic model to predict the influence of varying substrate levels on the transcriptional and translational response of *E. coli*. In summary, the resulting model is not only able to anticipate the experimentally observed short-term and long-term transcriptional response, it further allows envision of altered protein levels. The model shows that locally induced stress responses propagate throughout the bioreactor, resulting in temporal and spatial population heterogeneity.

Although all these modeling tools try to predict the occurrence of population heterogeneity in large industrial scale bioreactors, the PBM approach solving the PBEs is the most frequently reported strategy in literature. As discussed earlier in this work, microorganisms can either be regarded as a continuum or treated individually and tracked inside the bioreactor. (Morchain et al., 2014), for example, simulated lab scale (70 L) and industrial scale (70 m^3) aerated fermenters combining an Euler-Euler approach for the two-phase flow: a PBM for biological adaptation of *E. coli* to concentration gradients and a kinetic model for biological reactions. Similar studies for *E. coli*, *T. reesei* and *A. niger* have been published elsewhere (Azargoshasb et al., 2016; Bannari et al., 2012; Elqotbi et al., 2013), respectively. On parallel, the Euler-Lagrange approach has also played a relevant role in investigating population heterogeneity during *E. coli* (Lapin et al., 2006; Pigou & Morchain, 2015), *S. cerevisiae* (Haringa, Deshmukh, et al., 2017; Lapin et al., 2004), *P. chrysogenum* (Tang et al., 2017) and *C. tropicalis* (Morchain et al., 2012) cultivations, for instance. As stated by (Henson et al., 2002) more than fifteen years ago, an inherent limitation of the PBE approach, however, is that the incorporation of a detailed intracellular reaction network leads to a computationally intractable model already for ideally mixed systems because a high dimensional distribution function must be computed. Nevertheless, with the fast evolution of computers in the last decades, research including a broader spectrum of cellular responses has been published: key metabolic enzymes (Haringa, Tang, et al., 2018), transcription and translation dynamics (Löffler et al., 2016; Simen et al., 2017), protein formation (Nieß, Failmezger, et al., 2017) and cell cycles (Kuschel et al., 2017), among others. A typical PBE contains terms for spatial transport, loss/growth and breakage/coalescence source terms. The method of moments, its derivates and further challenging matematical solutions are currently being proposed (Li, Li, et al., 2019; Müller et al., 2019; Pigou et al., 2017, 2018; Wang, Yu, et al., 2019) to solve analytically and numerically these complex terms. So far, no reported studies accounting for population heterogeneity (its measurement or model-based prediction) have been published in industrially relevant LAB processes.

3. Research Questions and Aim of the Project

One focus of this project is to study the feasibility and meaning of polarizability measurements to determine the viability of LAB at-line in comparison to other methods, like flow cytometry and lactic acid (pH coupled to base addition rate) measurements. The second aim of this work is to apply, for the first time, pH-oscillations in multi-compartment scale down bioreactors in LAB cultivations and try to assess their impact on population heterogeneity by monitoring the micromorphology, in case of *S. thermophilus*, the cocci chain length formation in a stirred tank reactor shear force environment. Finally, the third aim, is to apply a PBM-based approach to predict population heterogeneity inside a bioreactor as a function of pH-gradient formation and relate the macromoprpholgy to viability features of the culture.

RQ1. *Is the automated polarizability measurement feasible to be applied across scales as indicative of cell activity?*

Metabolic activity is a key CQA, specially in the production of biomass to be applied as starter culture. This bacterial attribute is currently quantified as acidification activity (i.e. time needed to decrease about 0.1 units the pH value of milk), but is taking place after harvesting the bioreactor. This means that this procedure is rather following the Quality by Testing (QbT) than the QbD approach. Product quality should be quantified and monitored during the whole process to be able to ensure product specifications until delivery. In different research publications, it has been concluded that the electrooptical measurement of cell polarizability is a suitable indicator of population activity and, together with the automated sampling and sample preparation unit EloTrace (EloSystems GmbH, Berlin, Germany), could constitute a future at-line quality check during LAB fermentations. The key question is whether this methodology can be applied across scales, providing meaningful information of the metabolic activity and viability, including the status after downstream processing and confection.

RQ2. *Is it possible to automatically and with 100 % reliability perform microscopic image analysis to get morphologic heterogeneity of bacteria in real-time?*

Microscopy is one of the most established methods to observe cellular macromorphology, but usually takes a considerable amount of time and effort. Advances in on-line microscopy application for bioprocesses together with automated image recognition can resolve such problems. Therefore, the question shall be solved whether the consideration of macromorphology in combination with microscopy can lead to a fast capture of the physiological cell status, including population heterogeneity.

RQ3. *How does the division cycle of streptococci work and how can it be mathematically described? Is there a real relationship between population heterogeneity and pH-gradients? Can this knowledge improve the industrial production of LAB starter cultures?*

As stated in the literature, the division of streptococci is a poorly understood process and still more research is needed on that direction. However, with the actual state of the art and the experience acquired in this work, a simplified mathematical description of the cell separation/elongation was proposed. To which extend is this in silico model describing the actual division cycle?

RQ4. *Can industrial pH-gradients better be simulated in single- or multi-compartment scale down models?*

Assuming that pH-gradients are the most relevant inhomogeneities in the industrial production of starter cultures, which is their influence on process performance (i.e. biomass quantity and quality)? Can those heterogeneities be simulated in lab scale down experiments? More importantly, among all scale down simulators described in literature, which is the one that better mimics the conditions in the industrial scale? Obviously, this is difficult to answer without the exact knowledge of the fluidodynamics and gradient formation in the production fermenter/s. Also, are pH-gradients the main or only heterogeneity faced by LAB in the large scale? With our actual knowledge it may be, but the potential influence on product quantity as well as quality of further inhomogeneities (e.g. pCO_2, temperature, shear forces, etc.) should be discussed.

RQ5. *The consideration of individual cells (i.e. population heterogeneity) can really improve the actual process understanding of LAB fermentations?*

Nowadays, in the vast majority of bioprocesses, the end of USP is determined by analysis of macroscopic variables (e.g. concentration of C-source, biomass concentration, VCC, OD, pO_2, pH, etc.). The production of LAB starter cultures is not an exception, since the end of fermentation point is determined based on the base addition rate. Importantly, the product in this bioprocess is the biomass generated, which can be macroscopically easily quantified by well established methods (i.e. OD, DCW, WCW, % solids, among others). Nevertheless, the product quality in this case is measured by acidification activity tests, which provide a volumetric value of the metabolic activity. This means that, actually, there is no single-cell level analysis of the biomass, while its adequate function in the final customer depends on the performance of each individual bacterium. Since this project focused on population heterogeneity determination in this industrial bioprocess, an answer needs to be given on whether it is advantageous to consider the characteristics of individual cells or not, compared to the macroscopic analysis of CQAs. Therefore, how can the industrial production of LAB benefit from studying this population heterogeneity?

4. Results

Firstly, as discussed in the introduction and described in literature in the last decade (Faassen & Hitzmann, 2015; Glassey et al., 2011; Luttmann et al., 2012), there is an increasing interest by regulatory authorities (mainly, FDA as well as EMA) for applying PAT to move from the QbT to the QbD approach in (bio-) pharmaceutical industries. The main objective consists of monitoring and controlling the CPPs in order to ensure the CQAs of the product of interest during the entire production process. In this context, the concept of the so called measurement, monitoring, modeling and control (M^3C) methodology (Bracewell et al., 2010; Carrondo et al., 2012) appeared with a "Pharmaceutical Current Good Manufacturing Practices (cGMPs) for the 21st century—a Risk Based Approach" initiative announced by the FDA some time ago to improve and modernize pharmaceutical manufacturing (Rathore et al., 2010). This is why, a relevant focus was put on applying novel process analytical tools throughout the LAB fermentations performed in this work, aiming at suggesting new devices for the food industry to improve the measurement of existing CQAs or even propose the analysis of, until now, unknown properties of the biomass. This part of the results contains three publications, one already published, one submitted and one prepared for submission.

Secondly, it was extensively emphasized that knowing and simulating in the lab the fluid dynamics of the large scale fermenter is key for a future successful process optimization and scale up. Therefore, two published research articles aimed at characterizing the industrial environmental conditions encountered by LAB in the production scale by using CFD and applying scale down.

Thirdly, mechanistic modeling was applied to describe the process performance by means of cell division indicators. This was then used to couple growth to population balances in order to predict the process performance under the appearance of pH-gradient formation in another publication.

4.1. At-line Physiology and Morphology Analysis in LAB Cultivations using Electrooptic Methods

In the industrial production of biomass (where no commercial product is synthesized by the cells) to be manufactured as its whole (e.g. starter cultures, plant growth promoters, etc.), the key CQA is obviously the concentration of microorganisms at the "end" of the batch (or time of harvest). This point is typically selected based on the usual exponential growth profile of the vast majority of cells, but a rule that applies to all microorganisms is unfortunately not available. The decision on when to harvest the biomass is generally a trade-off between the maximum cell concentration possible (under optimal growth conditions: temperature, pH, initial C-source concentration, reactor volume, aeration flow, stirring speed, among others), minimum cell damage and maximum overall throughput to release as much final product as possible (CIP, SIP, cultivation, harvest, DSP, formulation and packaging).

The limitation of this established philosophy is that in most cases at no point during the decision of when to harvest the biomass, emphasis is put on cells' activity. In this scenario, the performance of the product (i.e. living microorganisms) depends on its activity in the final application and thus, the manufacturing company ends up selling a lot of biomass (product), but which is performing with a

considerably high variation when the customers use it, thus leading to reclamations and confrontations between seller and buyer. What is more, biomass activity, if determined, is typically measured after having harvested the bioreactor and this strategy corresponds to QbT, which has been discussed previously that is the wrong decision if one aims at complying with evolving regulatory specifications going toward QbD and/or Quality by Control (QbC) by using novel PAT.

In this work, a new device able to assess the metabolic activity of bacteria is suggested to improve the current QbT approach during the production of LAB cultures to be sold as starter cultures for the yogurt, cheese and probiotics industries. As previously explained in more detail, the measurement principle relies on the orientation of cells under the application of an electrical field of a certain frequency as a function of their ionic load (i.e. difference between ions inside and outside the membrane). Moreover, the equipment is sold with an automated sampling as well as sample preparation system (filtration of complex media, rinsing with distilled water and OD adjustment) and thus, can be directly connected to the fermenter. With this, the determination of microorganisms' activity inside the bioreactor becomes feasible in an at-line setup, obtaining a result in less than 15 minutes. Additionally, since this property has barely been measured during the fermentation of LAB, it could be proposed as novel CQA and be also used to contribute to the decision on when no stop one batch.

In this section, this measuring device is applied to *L. plantarum* (Paper I) and *S. thermophilus* (Paper II) fermentations in different setups in order to generate the proof-of-concept results that may hopefully approximate industrial companies to move from the actual QbT to the QbD strategy, when it comes to determination of cells' metabolic activity. Finally, results are compared with flow cytometry analyses throughout some of the experiments, which is the established method to differentiate between living and dead cells.

4.1.1. Polarizability Analysis throughout *Lactobacillus plantarum* Cultivations (Paper I)

The measurement of cells' metabolic activity is scarcely included in bioprocess development and is typically determined off-line and after the biomass has been harvested. In this first paper, the application of electrooptical measurements of cell polarizability in LAB was published for the first time. The aim was to investigate the time course of polarizability of *L. plantarum* ATCC 2014 in batch and fed-batch fermentations in complex, industrially relevant media, assessing the response of this parameter to certain disturbances of the CPPs.

Firstly, the following experiments were carried out (**Figure 2**):

- ✓ The initial amount of C-source (glucose) was doubled in comparison to the control experiment.
- ✓ Fermentations without pH control were performed to investigate the influence of acidic conditions on the anisotropy of polarizability (AP).
- ✓ A nitrogen-sparged cultivation was compared to an aerated one.
- ✓ The impact of a lower cultivation temperature, and thus a lower metabolic activity, on the AP was investigated.

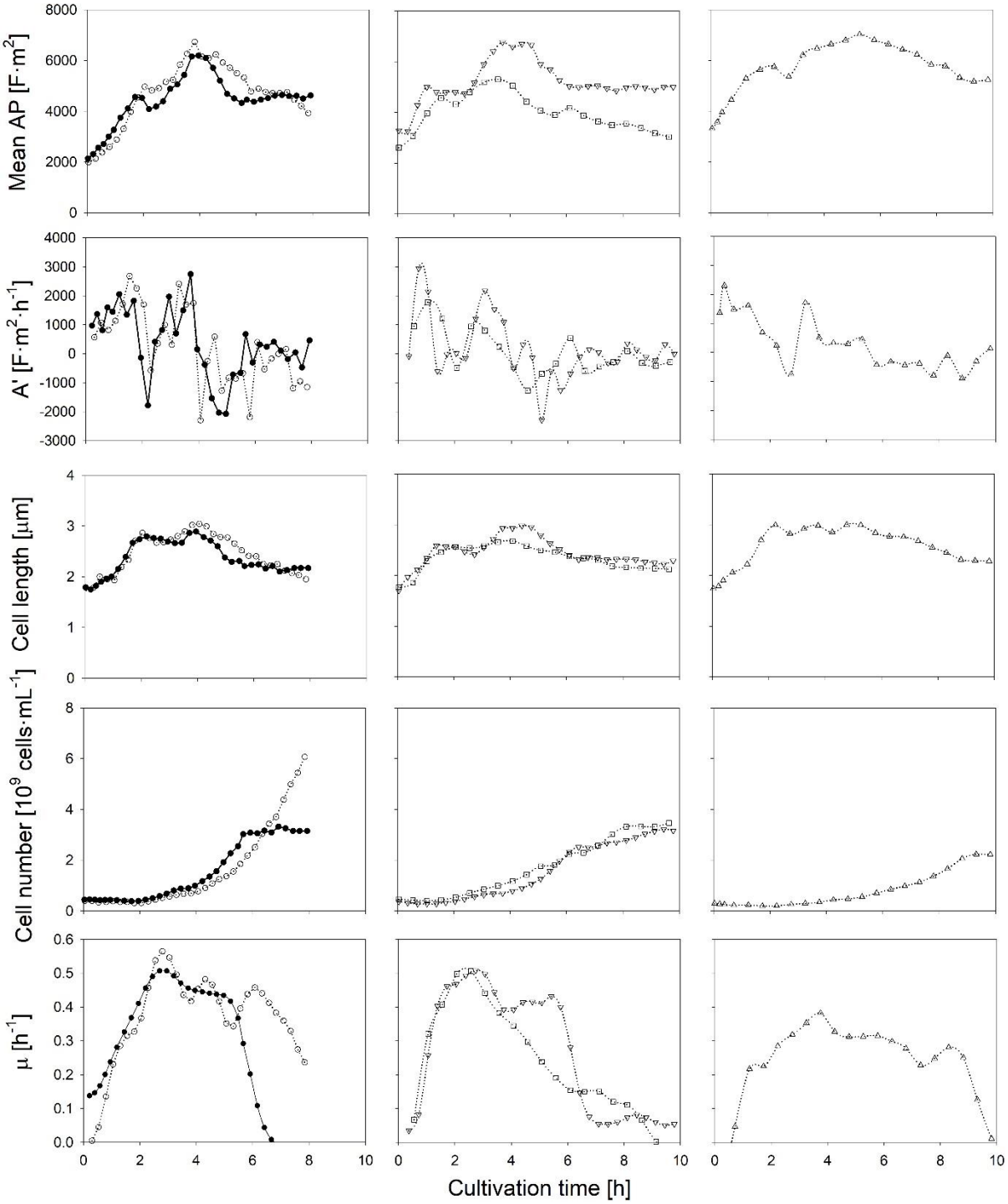

Figure 2. Time course of the mean AP (scaling factor $5 \cdot 10^{-31}$), its first derivative, cell size, the amount of cells and the specific growth rate throughout six *L. plantarum* batch cultivations: at standard conditions (●), with additionally 1 % of glucose in the medium (○), without pH control (□), with aeration (▽) and at a reduced temperature of 25 ºC (△). Taken directly from Paper I.

The results obtained indicated that:

- ✓ Although more glucose was available before inoculation, the development of the AP level during the first two hours of cultivation was almost the same than under standard initial C-source concentration. What is more, the local as well as global maximum of the AP is also reproduced under a higher initial glucose concentration. Nevertheless, the evolution of this

parameter after the peak at 5,000 F·m² was more retarded when more glucose was available, probably because of an earlier substrate limitation under standard conditions.

- ✓ When the pH-value was not controlled throughout the cultivation, a sudden drop of the AP was observed after 3 hours, after reaching the maximum level commented before, compared to the standard polarizability profile. The external pH was 4.5 at that time and from then on, the AP level decreased in parallel with the pH, thus indicating unfavourable cultivation conditions at extremely acidic conditions, being in accordance with the literature.
- ✓ Aerobic conditions retarded growth only slightly but had no negative impact on the cells' physiological state, since the time course of the AP and mean cell length was rather the same as in the control cultivation.
- ✓ At a lower fermentation temperature, the rate of chemical reactions is naturally lower, which yields an expected lower specific growth rate as well as final cell number when compared with the cultivation at the optimal temperature. Interestingly, cells were larger when cultivated at a lower temperature, which may be attributable at an intracellular accumulation of intermediates during a slower cell metabolism under these growth conditions. Nevertheless, this temperature shift did not alter notably the physiological conditions of cells.

The at-line monitoring of the AP enabled the identification of suitable cultivation conditions in all cases: an optimal range of the AP and cell length can be assumed, in which the cell reaches an optimal physiologic and morphologic state: an AP level of above 4,500 F·m² and a cell length of about 2.5 µm. Moreover, the experiment without pH control allowed the elucidation of the development of the AP level as a function of pH (**Figure 3**), thus determining the sensitivity and adaptation capacity of *L. plantarum* activity to changing external pH. Additionally, the AP measurement was identified as an early indicator for growth retardation, since it decreased earlier than the growth rate in all cultivation conditions (**Figure 2**).

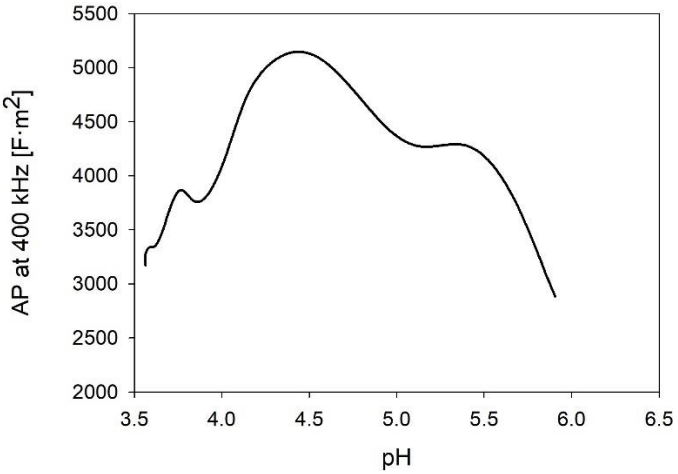

Figure 3. Development of the mean AP level (scaling factor $5 \cdot 10^{-31}$) over a *L. plantarum* cultivation without pH control. Taken directly from Paper I.

In **Figure 4** a sudden glucose pulse addition in the stationary phase was performed to investigate the response time of the AP to a changed nutrient supply and to prove the dependency between cells' metabolic activity and their polarizability: the glucose pulse led to an immediate response of growth with a concomitant increase of the AP level. Again, the polarizability decreased half an hour before the growth rate did so (9h after the pulse).

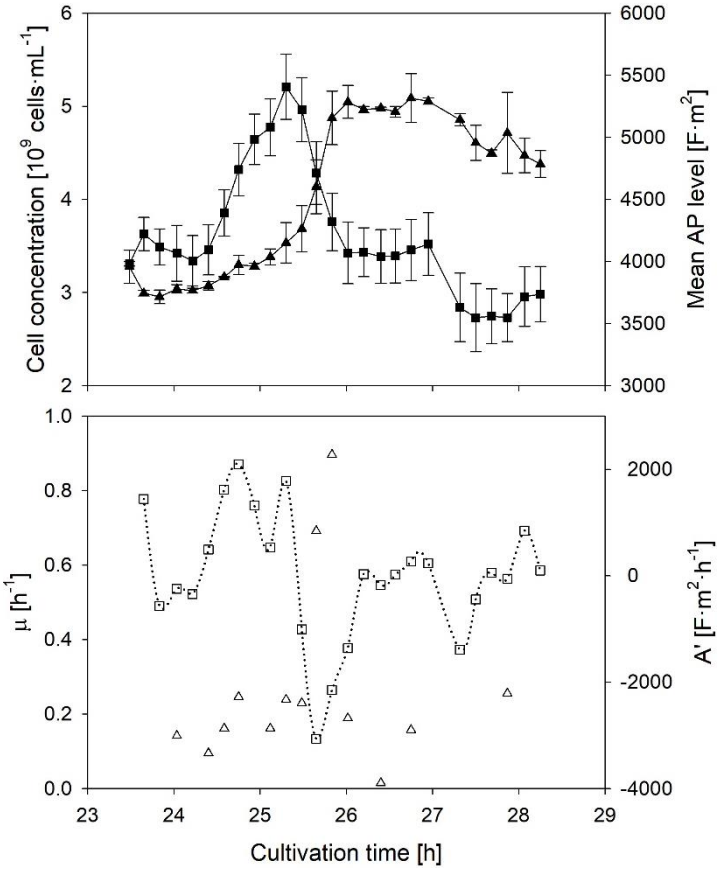

Figure 4. Time course of the mean anisotropy of polarizability (■), its first derivative (□), cell concentration (▲) and specific growth rate (Δ) after a sudden substrate pulse after cells suffered 17 h of starvation. Error bars represent the technical reproducibility of EloTrace with two biological replicates. Taken directly from Paper I.

Subsequently, the course of the AP was monitoried during a prolonged nutrient-limited *L. plantarum* cultivation (**Figure 5**) to study the development of cell polarizability with different nutrient supply. During a first fed-batch phase with a constant feed, where substrate availability per cell is declining, the mean cell size remained almost constant, whereas the AP and the specific growth rate decreased in parallel. Nevertheless, once the feed rate was doubled, a clear response of the AP level was observed, thus confirming that the AP depends on the nutrient availability under nutrient-limited conditions, although the dependencies were not as clear as in the batch experiments: here the AP showed a rather decoupled development compared to the growth rate. Importantly, a depletion of three amino acids was detected during the feed phases (firstly serine, then aspartate and finally glycine), accompanied by changes on the slope of the AP level at the corresponding time points.

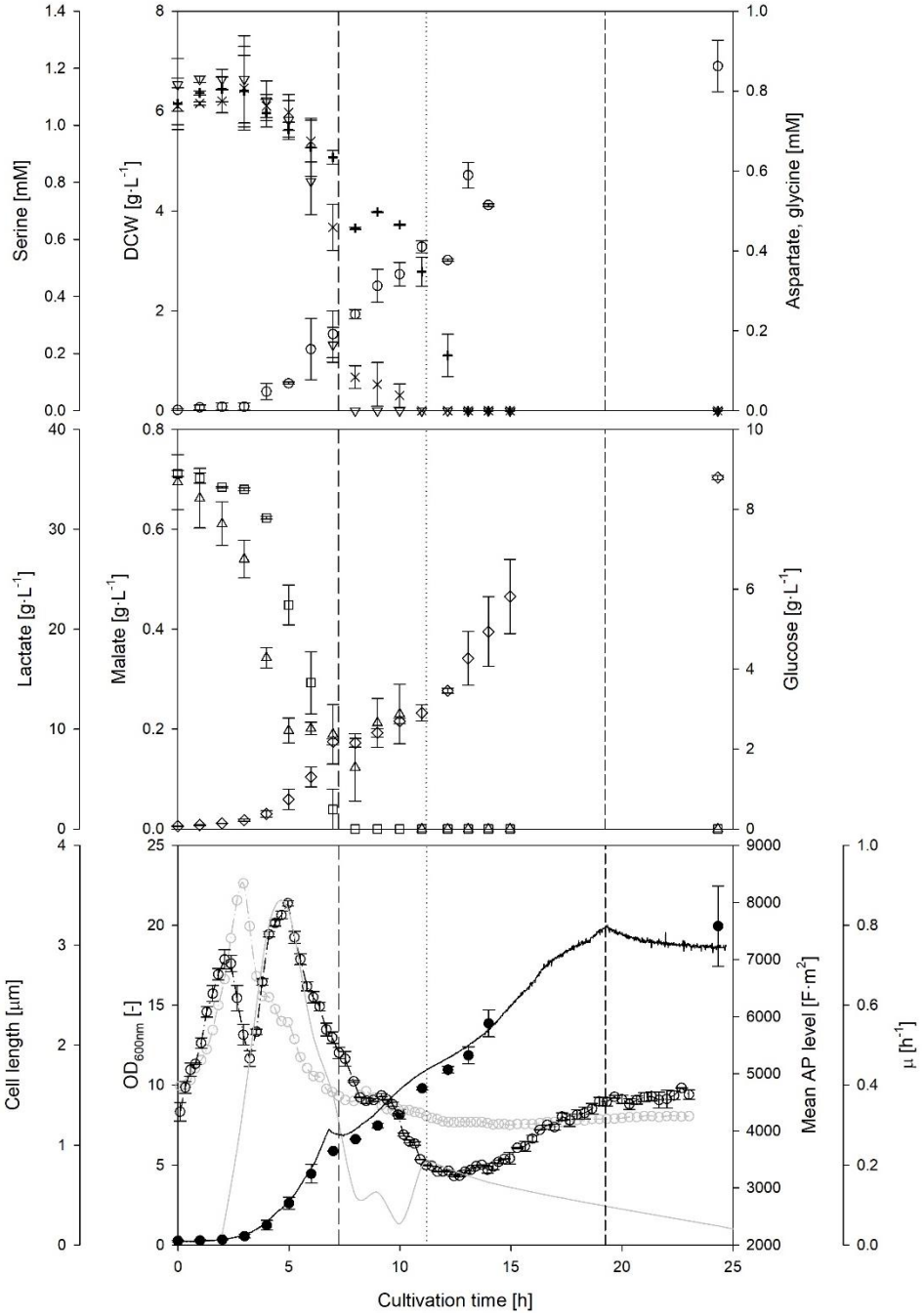

Figure 5. Course of on-line and off-line cultivation parameters, as well as main metabolites and amino acids throughout a *L. plantarum* fed-batch cultivation under standard conditions. Off-line monitoring of DCW (○), aspartate (×), serine (▽), glycine (+), glucose (□), lactate (◊) and malate (△) concentrations over time. At-line optical density (—●—), cell size (—⊖—), mean polarizability (—·⊖·—) and growth rate (——) measurements. During the fed-batch phase, the feed start (— — —), doubling of feed rate (·····) and feed stop (- - - -) are highlighted with vertical lines. Error bars denote standard deviation of two biological replicates. Taken directly from Paper I.

Finally, the behaviour of the AP of *L. plantarum* after revitalization (i.e. resuspension in fresh media) of freeze-dried cell pellets taken at different phases of a batch cultivation was investigated (**Figure 6**):

a) During the growth phase.
b) At strong retardation/growth cessation.
c) In the early stationary phase two hours after growth cessation.
d) In the late stationary phase 13 hours later.

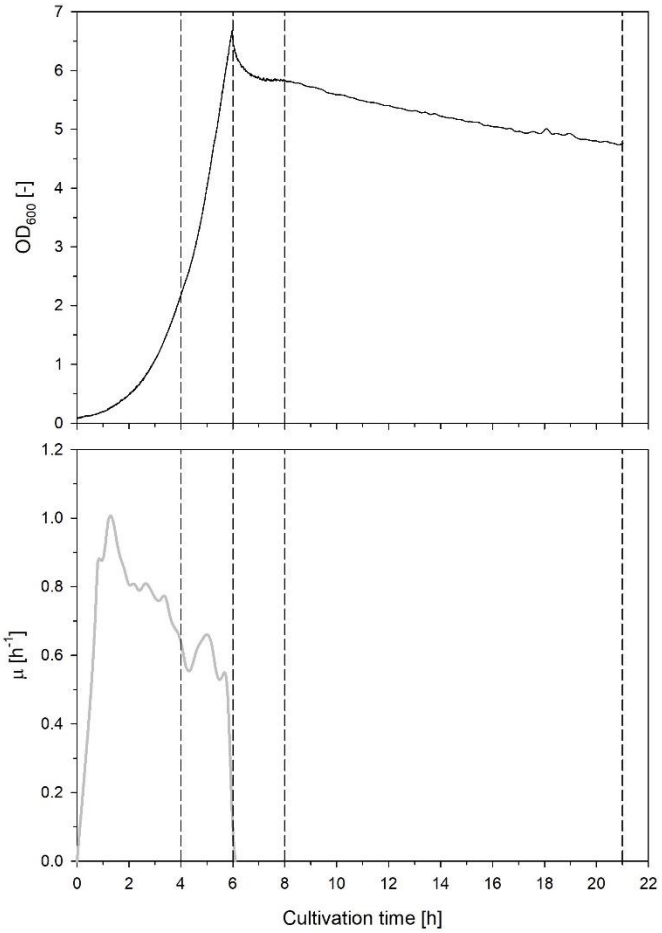

Figure 6. *L. plantarum* batch fermentation under optimal conditions. OD (black line) and specific growth rate (grey line) development over time with sampling points depicted with vertical dotted lines. Samples were directly frozen and subsequently freeze-dried. Taken directly from Paper I.

As seen in **Figure 7**, the growth after resuspension in fresh media varied depending on at which growth phase had the biomass been freeze-dried. Interestingly, the highest acidification activity (i.e. decrease of the pH over time) as well as growth rate was observed in samples taken at strong retardation/growth cessation and at the late stationary phase. These were indeed the samples that showed the highest and fastest increase of AP after revitalization. Apparently, the polarizability at a higher frequency (2,100 kHz), is more suitable to distinguish between the different states of revitalization, e.g. the reconstitution of ion transport and functional cell structures.

With this publication it was shown that the consideration of cells' polarizability during LAB cultures may be of special interest for the food industry, since it can provide new insights in cell's metabolism, unknown until now. The use of a commercial device with automated sampling and sample preparation allows its measurement in minutes, thus being a potential new PAT to move toward QbD.

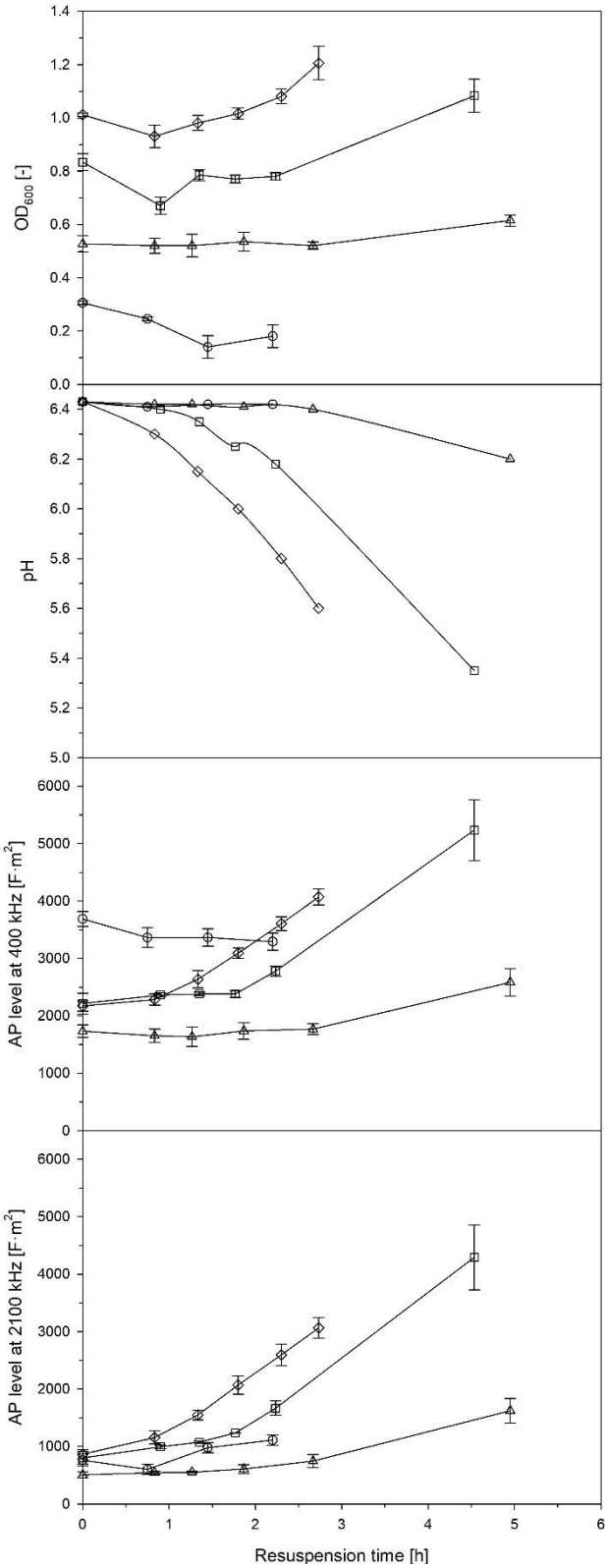

Figure 7. OD_{600nm}, pH and AP level at a frequency of 400 kHz and 1,200 kHz of formerly freeze-dried and resuspended *L. plantarum* culture broth in 50 % MRS media collected after 4 h (○), 6 h (□), 8 h (△) and 21 h of batch cultivation (◊). Error bars: Mean ± SD (n = 2). Taken directly from Paper I.

4.1.2. Polarizability Determination in *Streptococcus thermophilus* Fermentations (Paper II)

After the successful application of the cell polarizability measurement tool to *L. plantarum* as proof-of-concept study in LAB, the same approach was used throughout the cultivation of the bacteria of the industrial partner in the project (i.e. *Streptococcus thermophilus*). Importantly, in the large scale production of these LAB, the pH of the media is neither adjusted after preparation nor after sterilization. Instead, the bioreactor is inoculated at the media pH and it is allowed to decrease (through media acidification because of the fermentation product lactic acid) until pH 6, where it is controlled with ammonia addition. Generally, from a physioloigical point of view, cells have two options, they either use ATP to improve their individual energy household to adapt to the surrounding environment or they divide themselves and grow. This trade-off is supposed to be always present in the cultures, so that external oscillations of the extracellular media are obiviously going to affect cells' polarizability (see results obtained in Paper I in 4.1.1). Additionally, the equipment is also capable of determining a further cell viability indicator: the membrane status. A lower value is a good indicator for cells with intact membrane and good defined semi-permeable properties (i.e. intact and active ion exchange), while a higher value of this parameter correlates with an affected cell membrane: *E. coli* treated with ethanol and a bacteriocid showed a membrane status higher than 0.5 (data not shown).

For the initial cultivations with the industrial strain, some batch experiments at 40 ºC and controlling the pH as just described with NH_3 5 % v/v (Carl Roth, Karlsruhe, Germany) were performed in 300 mL EloFerm bioreactors (EloSystems GmbH, Berlin, Germany). Throughout one of these cultivations, EloTrace (EloSystems GmbH, Berlin, Germany) was also connected to the fermenter. The results are summarized in **Figure 8** and some similarities with the development of electrooptical measurements during previous *L. plantarum* fermentations were identified:

- ✓ During lag and early exponential phases, an increase of mean polarizability over time of the small number of cells available in the culture, with almost no biomass growth, was observed.
- ✓ Both, the AP level at 400 kHz as well as the cell size reached maximum values at the maximum specific growth rate. Nevertheless, these were notably different (around 3,000 $F \cdot m^2$ and 5.5 μm, respectively) despite of both strains presenting similar maximum growth rates during batch cultivations (around 0.8 h^{-1}). On the one hand, here completely different LAB are compared and the media employed for their fermentation were also not the same (see corresponding publications), thus obtaining a completely distinct polarizability profile over time. On the other hand, *S. thermophilus* form chains of variable cocci length (as explained in the Scientific Background) and can therefore be notably larger than bacilli.
- ✓ The polarizability decreased about one hour before the growth rate did, thus being a potential indicator of growth reduction due to depletion of key nutrients, before decrease of □ with a subsequent entrance into the stationary phase.
- ✓ The AP level at 400 kHz remained almost constant once entering the stationary phase.

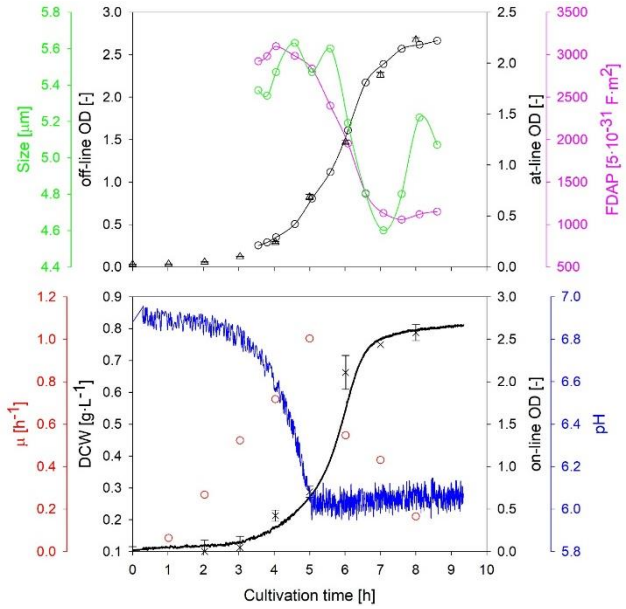

Figure 8. Development over time of CPPs and CQAs during a *S. thermophilus* batch cultivation. On-line (lines), at-line (symbols with lines) and off-line (symbols) acquired data. Error bars: Mean ± SD (n = 2).

This preliminary comparison between LAB grown at different days was extended by performing fermentations of *L. plantarum* and *S. thermophilus* under optimal growth conditions in parallel 300 mL bioreactors, sampling at different intervals for (i) at-line determination of growth related parameters, (ii) electrooptical measurement of cell polarizability and size as well as (iii) microscopic analysis of morphological changes over cultivation time (**Figure 9**). Growth of both LAB was similar under the correspondent optimal pH conditions: biomass concentration (DCW and OD) increased exponentially over time, while the mean cell polarizability steadily declined with a concomitant increase of the membrane status, because of the specific use of energy for cell division in the absence of oscillating conditions, but also due to an increasing amount of daughter cells typically possesing a lower ionic activity. Nevertheless, both LAB were considerably different in terms of morphological characteristics: *L. plantarum* are rod-shaped bacteria with typically 1-2 rods per cell throughout the whole fermentation, whilst *S. thermophilus* are cocci chains of varying length depending on the growth stage (**Figure 9**). In fact, chain length tended to increase turning the cocci chain length distribution more heterogeneous, specially when the *S. thermophilus* culture entered the stationary phase. Theses differences on morphology were in accordance with electrooptical measurement of mean cell size with EloTrace (EloSystems GmbH, Berlin, Germany). It is worth mentioning, that a magnetic flea was used to maintain a relative homogeneous mixing of the base fed throughout the experiments presented here, so comparison of the cell size distribution results with following cultivations using STRs might be meaningless, because of the notably higher shear stress induced with a rotating impeller.

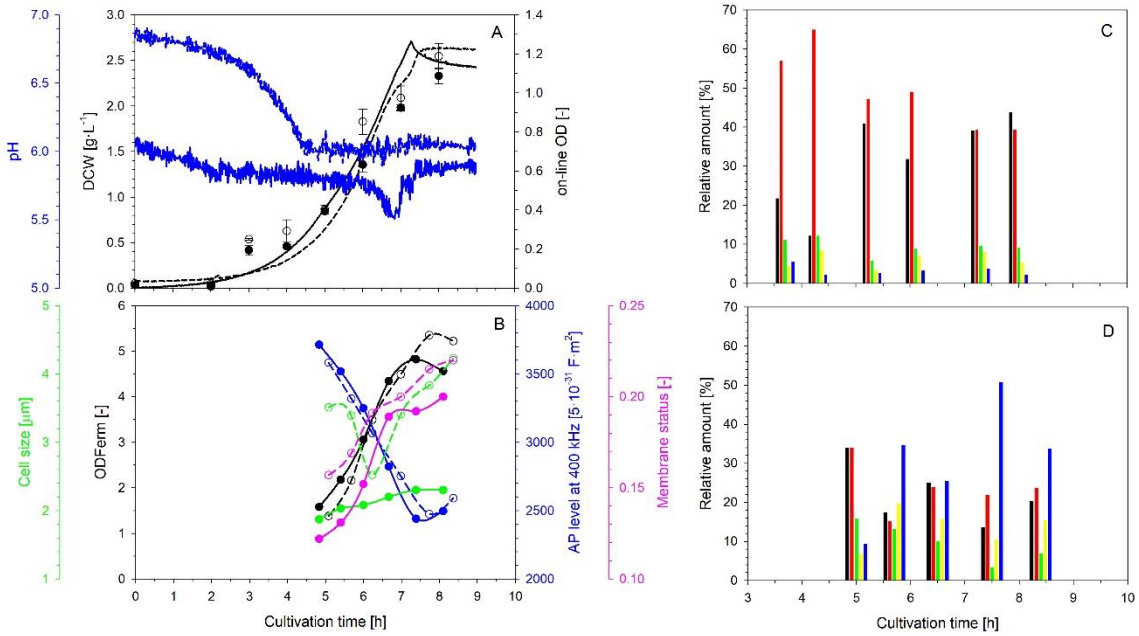

Figure 9. Cultivations of *L. plantarum* (pH control at 5.8, solid lines) and *S. thermophilus* (dotted lines) under optimal conditions in 300 mL EloFerm bioreactors. Development of growth-related indicators (A), electrooptical measurements (B) and microscopic analysis of morphological changes (C and D) over fermentation time. The cell size distribution (C; rods for *L. plantarum* or D; cocci for *S. thermophilus*) is described in vertical bars of different colors: populations of 1, 2, 3, 4 and 5 or more units per cell in black, red, green, yellow and blue, respectively.

For the publication arisen from this section, it was decided to characterize the strain in terms of maximum specific growth rate. An accelerostat (A-stat) cultivation was performed in duplicates, where the batch phase is followed by stabilization of the culture at a fixed specific growth rate to obtain an initial steady state. Subsequently, the dilution rate (D), which equals to the specific growth rate (μ), is increased with a constant speed at a certain slope until the culture cannot keep up with the rising D, resulting in the so called wash-out (cells can no longer consume the amount of C-source introduced and this starts to accumulate extracellularly, in parallel with a decrease of the cells as well as byproduct/s, which are "washed-out" from the bioreactor). Under such cultivation conditions, the culture is in a quasi-steady state, which is a physiological state of a microorganism where every point represents the corresponding steady state value. Great advantages of A-stat experiments are (i) the possibility to monitor bacterial growth in real time to study cell physiology in a large variety of specific growth rates (each time point where sample is taken is like a snapshot at that specific D, i.e. μ), (ii) while reducing the duration of the experiment at the same time.

As explained, the cultivations began with a batch phase, followed by a chemostat at a dilution rate of first 0.3 h^{-1} and then 0.1 h^{-1} for ca. 50 h each. Subsequently, the accelerostat was started with an acceleration rate of the feed of 0.005 h^{-2}. Later on, the acceleration rate was increased stepwise to 0.008 h^{-2} (**Figure 10**).

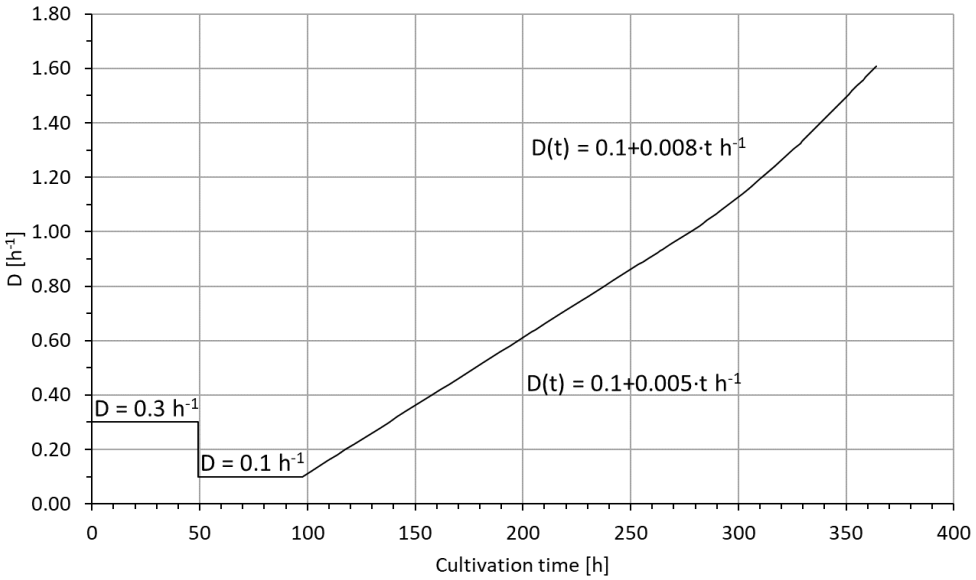

Figure 10. Dilution rate throughout duplicates of a *S. thermophilus* continuous cultivation. The cultivation started with a batch phase (data not shown), followed by two chemostat and an accelerostat. Taken directly from Paper II.

The EloTrace (EloSystems GmbH, Berlin, Germany) device was connected to one of the two fermenters throughout the whole experiment, performing an equipment maintenance (i.e. system washing and filter renovation) once every day. Temperature and pH in the bioreactors were always controlled at 40ºC and 6, respectively, taking sample for off-line analysis, at least, four times a day. Further details regarding the experimental setup may be found in the prepared manuscript with joint authorship together with Dr. Robert Spann (Denmark Techical University). The batch cultivations were initated with 20 $g \cdot L^{-1}$ of lactose, which is equivalent to a molecule of glucose plus one of galactose. As already explained, the first is used by the bacteria to generate biomass through glycolysis and lactic acid fermentation, while the latter is excreated into the media. Importantly, as seen in **Figure 11**:

a) At the beginning of the A-stat experiment (i.e. steady increase of D/μ over time), lactose was measured in residual concentrations, while lactic acid concentration, OD_{600} and DCW remained almost unchanged as the continuous cultivations evolved over time (i.e. over D or μ). These observations confirmed the quasi-steady state metabolism of the bacteria inside both bioreactors.
b) Just before D = 0.6 h^{-1}, the feed bottle of one of the experiments fell overnight, thus influencing the whole cell metabolism: surprinsingly, the galactose (which is in principle not metabolized by this *S. thermophilus* strain) was depleted and lactic acid, OD_{600} and DCW values had increased just in the next measuring point after the accident (data not shown). This indicated that the LAB had been adapting to a limiting lactose concentration and galactose excess in the media throughout the whole experiment (i.e. batch, two chemostats and A-stat), so that once the preferred C-source (lactose) ceased to be introduced, cells consumed the next C-source available (i.e. galactose). For that reason, from then on, off-line data related to this replicate was no longer plotted in the graphs. Also, luckily the EloTrace device was connected to the other fermenter.
c) Around D = 0.6 - 0.7 h^{-1}, the lactose started to accumulate extracellularly, but lactic acid, OD_{600} and DCW still remained statistically constant (see manuscript) over time or D.
d) It was at D = 1.3 h^{-1} where the lactose concentration increased and the fermentation product, OD_{600} as well as DCW decreased in parallel notably, thus indicating a clear wash-out.

e) The mean cell size (if the washing steps are ignored) as well as the AP level at 400 kHz measured at-line electrooptically were steadily increasing, reaching their maxima during the detected region of D between 0.9 and 1.3 h^{-1} (**Figure 12**). The morphology changes were verified under the microscope, detecting the longest cocci chains around D = 0.8 h^{-1}. It is worth mentioning, that a certain correlation between the polarizability and the yield biomass/substrate ($Y_{X/S}$) during the continuous cultivation of *S. thermophilus* was found (data not shown): the higher the AP level at 400 kHz, the higher the $Y_{X/S}$.

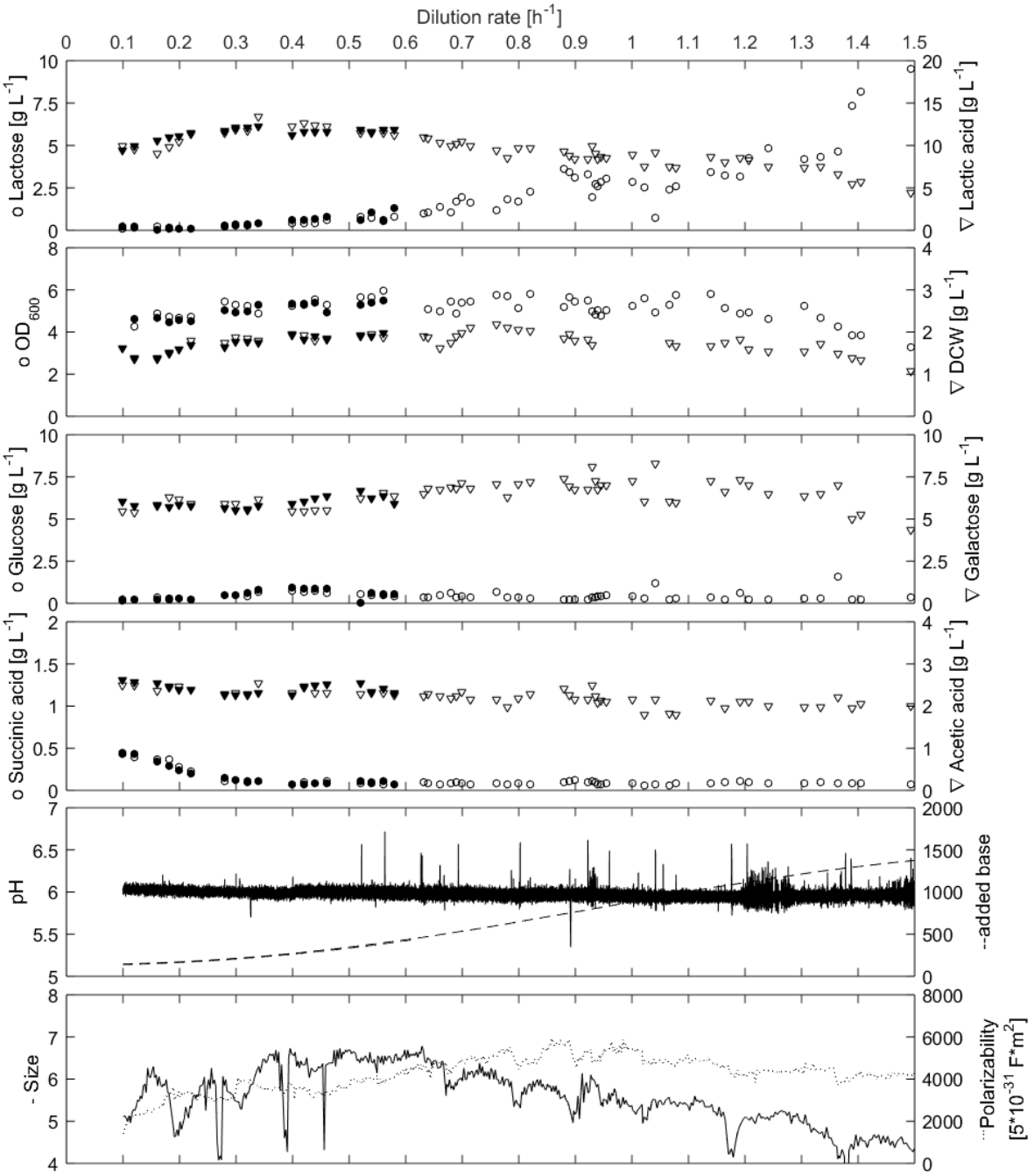

Figure 11. CPPs monitored throughout two (flled and unfilled symbols) A-stat cultivations of *S. thermophilus*. Off-line analyses of OD_{600nm}, DCW and metabolites performed with HPLC are represented by symbols, while in-line measurement of pH as well as at-line determination of base addition, cell size and polarizability at 400 kHz are plotted with lines. Taken directly from Paper II.

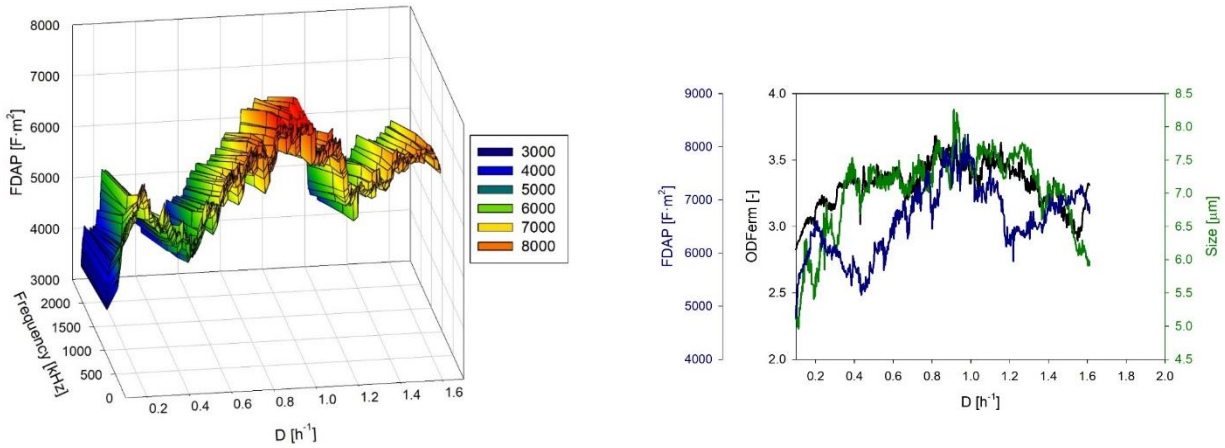

Figure 12. At-line electrooptical measurement of cell polarizability and size during a *S. thermophilus* A-stat fermentation. AP development over D at different frequencies (left) and comparison with on-line measurement of OD (black line right) with EloFerm (EloSystems GmbH, Berlin, Germany). AP level at 400 kHz (blue line right) and cell size (green line right). Taken directly from Paper II.

With this second publication using the EloTrace device, it was demonstrated that the electrooptical measurement of cell polarizability in LAB cultures may be of special interest for future improvement of the current QbT strategy used in the industrial scale. The consideration of a new CQA (namely bacterial ionic activity under the application of a certain electrical field or even the mean chain length) is suggested, which could be measured at-line, thus allowing the move toward a QbD or QbC approach (e.g. ensuring these new CQAs by changing the CPPs, like stirring speed or base addition rate, during the production process in the industry).

Importantly, a clear influence of pH on this parameter was identified when a *S. thermophilus* cultivation under an optimal pH was compared to a fermentation without pH control (**Figure 13**). The extreme acidification because of steady lactic acid production lead to a 66 % biomass productivity loss, while more energy was available to increase the energy household (i.e. polarizability), leading to a higher AP level than under optimal pH conditions. Furthermore, cell morphology was almost not varied with an optimal pH, but a tendency toward higher cell sizes was observed with a continuous media acidification, both observations verified by microscopic analysis. In fact, at the beginning of the suboptimal pH conditions, rather shorter chains were detected, but the distribution evolved toward increasing chain length probably as an effort to decrease the specific surface area in contact with the unfavorable ambient.

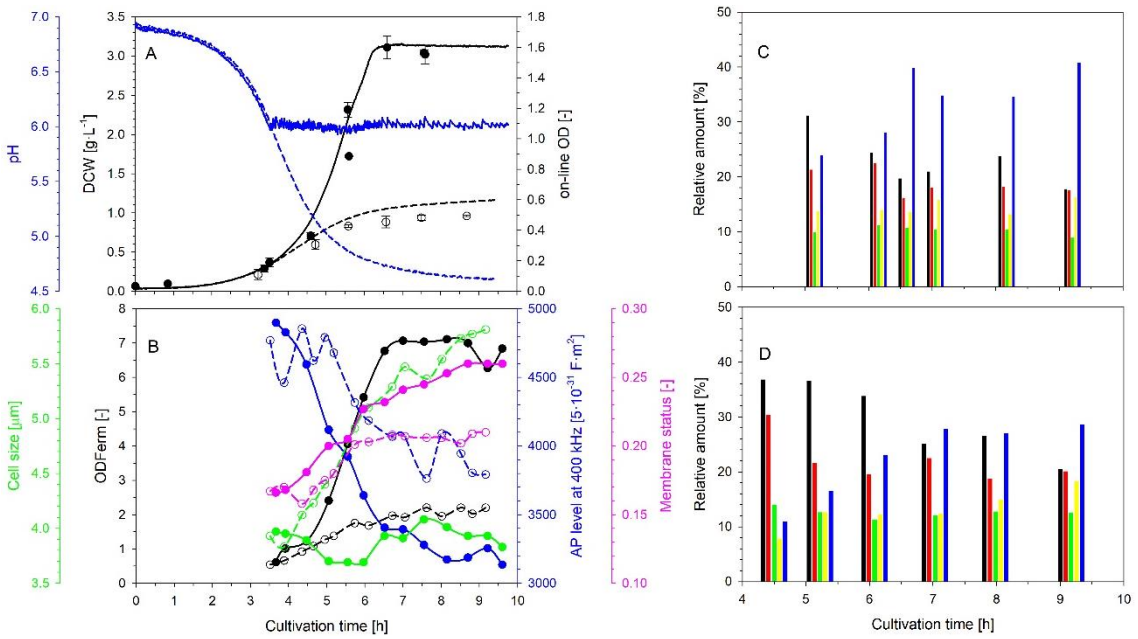

Figure 13. Development of growth-related parameters (A), electrooptical measurements (B) and microscopic analysis of morphological changes (C and D) throughout *S. thermophilus* fermentations under optimal pH contiditions (solid lines and C) and without pH control (dotted lines and D). The cell size distribution is described in vertical bars of different colors: populations of 1, 2, 3, 4 and 5 or more cocci per chain in black, red, green, yellow and blue, respectively.

The cell polarizability of *S. thermophilus* also confirmed the detection of a limitation in glass bioreactors. Fermentations were run in 300 mL EloFerm glass vessels (EloSystems GmbH, Berlin, Germany) and in a 10 L stainless-steel STR (Techfors S, Infors HT, Bottmingen, Switzerland) and the former lead to a lower biomass productivity and a hardly seen polarizability drop until 1000 x5·10^{-31} F·m^2 (**Figure 14**), thus indicating a clear growth imbalance despite of the fact of having used the same media and incoculum. Furthermore, the decreased mean cell size in the 10 L stainless-steel vessel was probably due to an increased shear rate from the rotating impeller, compared to the magnetic flea.

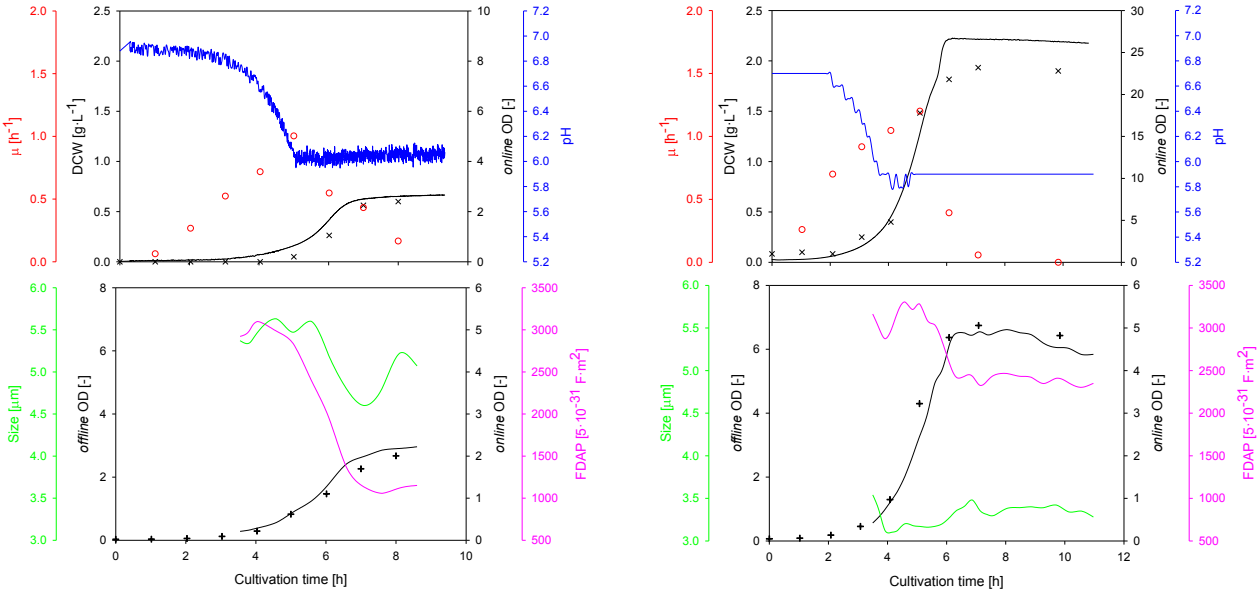

Figure 14. Development of growth-related parameters (top) and electrooptical measurements (bottom) during *S. thermophilus* fermentations in 300 mL glass (left) and 10 L stainless-steel (right) bioreactors.

These observations were verified with HPLC analyses of key metabolites, identifying a notorious glucose accumulation in the media when the glass bioreactors were used, which was never observed when cultivating in stainless-steel fermenters (**Figure 15**). Additionally, a media pulse was performed after the typical cultivation time of 10 hours and the culture was left overnight until next day, when sampling was restarted (**Figure 16**). Results showed a clear limitation in the media when using glass fermenters, because the accumulated glucose of the previous day had been almost depleted overnight (i.e. after 15 hours of the pulse). A final media addition made the cells consume the glucose left in about 6 additional hours.

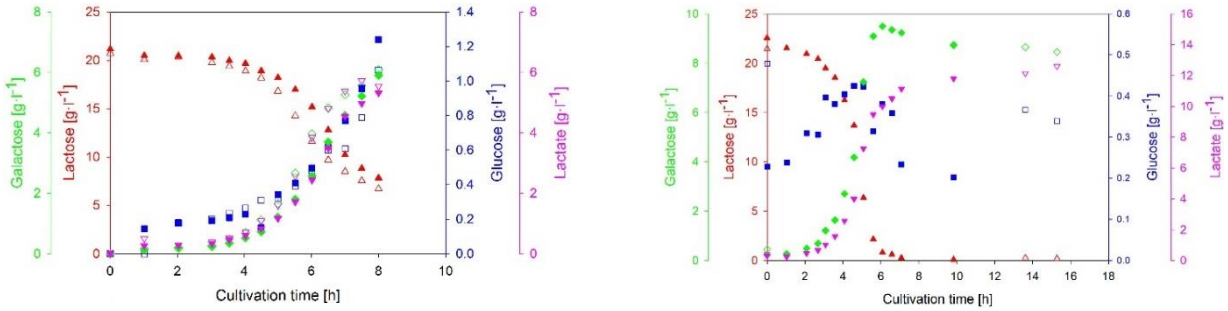

Figure 15. Evolution of key metabolites over duplicate (filled and empty symbols) *S. thermophilus* fermentations in 300 mL glass (left) and 10 L stainless-steel (right) vessels.

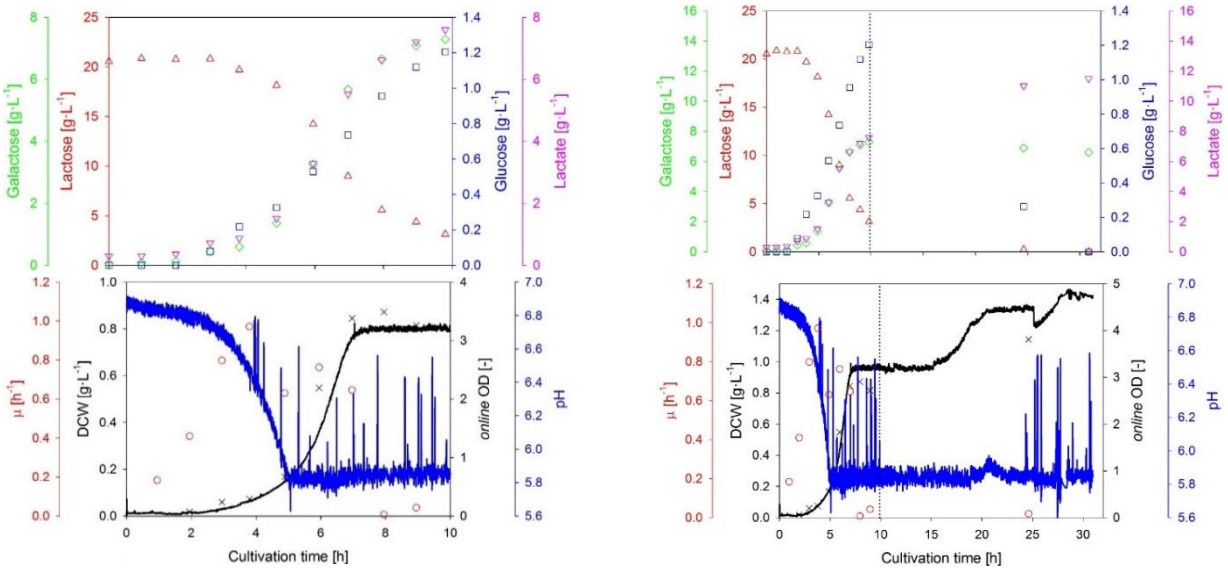

Figure 16. Development of key metabolites (top) and growth-related parameters (bottom) during a *S. thermophilus* fermentation in a 300 mL glass bioreactor before (left) and after (right) a pulse of media.

4.1.3. Comparison of Automated Sampling and Sample Preparation with Flow Cytometry

Always when a new PAT or analysis is suggested, it needs to be compared with the "established method" performing the "same" analysis (i.e. giving the same information or providing the same result/response, maybe in a different manner or in another time scale). In the case of the electrooptical determination of cell polarizability and size with EloTrace (EloSystems GmbH, Berlin, Germany), somehow changes on bacterial viability as well as morphology are obtained. In that sense, the well-established method of analysis of both CQAs at the same time is multi-parameter flow cytometry:

a) As unstained cells pass individually through a laser beam and scattered light is detected in two planes; FSC provides relative information on the cell size, while SSC is measured at 90° to the beam and can provide information on cell granularity.
b) Staining the sample with specific dyes for viable and/or non-viable/permeabilized cells, coupled to the high-throughput flow of particles, a percentage of death cells ressembling something like the VCC can be obtained.

Firstly, some general advantages and disadvantatges of both measuring principles are listed in **Table 4**. Importantly, when developing the flow cytometry analysis protocol, at least, three factors have to be taken into account: the cells:dye ratio, the staining temperature and the staining time. What is more, interactions between those factors should also be considered when developing a staining protocol. Additionally, the majority of dyes are light-sensitive and some are dangerous for human health, apart from every microorganism and even strain needing a specific protocol. This means that, although dye manufacturers typically include an SOP for staining any biological sample, the reality is that an individual and meticulous DoE should be performed for each microorganism.

Table 4. Summary of advantages and disadvantages of the electrooptical measurement of cell activity as well as size compared to multi-parameter flow cytometry.

	Electrooptical method (EloTrace)	**Multi-parameter flow cytometry**
Advantages	+ At-line measurement + Automated sampling + Automated sample preparation + Easy to handle + Quantitative	+ Population heterogeneity + "Automated" washing
Disadvantatges	- Mean contribution of whole population - Manual washing (once a day) - Destructive	- Off-line measurement - Manual sampling - Manual sample preparation - Laborious - "Qualitative" - Destructive

In this work, DAPI and SYBR Green were used to stain *S. thermophilus* cells during flow cytometric analysis at TU Berlin and at Chr. Hansen A/S, respectively. PI was used to stain permeabilized bacteria throughout the whole study and in all institutions. The staining protocols used are summarized in the Flow cytometry analysis, where also the correct staining of the dyes was verified (e.g. positive control of PI performed by staining a sample of the bacteria treated at 80 ºC for 10 minutes). Moreover, negative controls (i.e. unstained cells) were also done in each flow cytometry experiment. Additionally, BOX was also tried, which has been used for monitoring changes in the plasma membrane potential of

other microorganisms, but the protocol was staining almost all cells (**Figure 17**), so it was no longer used for further studies.

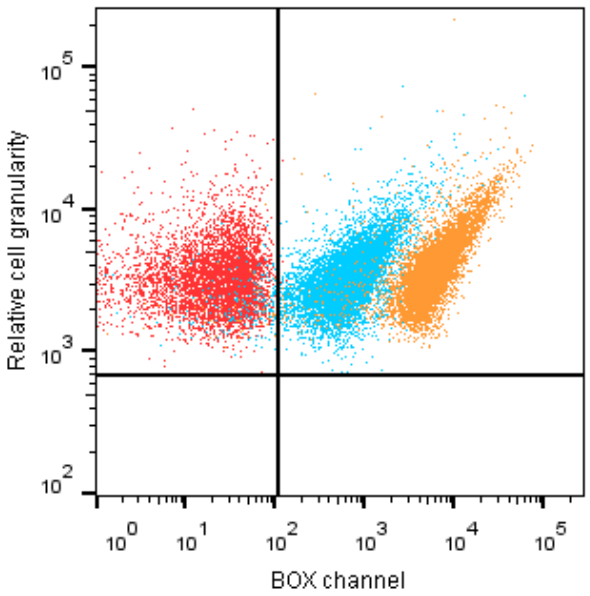

Figure 17. Flow cytometry analysis of an unstained sample of *S. thermophilus* (red), a BOX-stained sample (blue) and a sample incubated at 80 ºC for ten minutes (positive control - orange).

In this section, a pilot scale (700 L) cultivation of *S. thermophilus* will be compared to lab scale (2 L) fermentations, all performed at Chr. Hansen A/S. During all experiments both PAT (electrooptical measurement of cell polarizability as well as size with EloTrace and multi-parameter flow cytometry) were applied to monitor cell activity/viability, apart from the usual in-line and off-line analyses. The results obtained throughout the pilot scale fermentation (**Figure 18**) show a similar development over time of the CQAs (biomass, pH as well as base addition rate) when compared to previous results in the lab scale. More detailed information about the culture conditions can be found in Paper III, but the most relevant milestone is the at-line measurement of cells' polarizability and size with EloTrace (EloSystems GmbH, Berlin, Germany) in such a fermenter. Firstly, the OD determined at-line with the device over time correlates with the rest of biomass growth indicators. Moreover, the relative frequency-dependent anisotropy of polarizability (FDAP) and the so-called membrane status provided information on cellular ionic activity: the relative FDAP relates to the polarizability at 400 kHz, if not otherwise stated, and the membrane status indicates the integrity of the cell membrane based on the measured relative polarizability at 900 kHz and 2.1 MHz. Importantly, different growth phases were identified:

a) An initial lag-phase where cells show an active metabolism (increase of the relative FDAP and decrease of membrane status) taking substrates up and increasing their size.
b) An acceleration phase where cells reach a maximum mean polarizability and size as well as a minimum membrane status, while the biomass concentration has not really started to increase linearly over time, clearly showing the trade-off between cell division and maintenance.
c) An exponential growth phase where DCW and OD increase linearly over time, while the relative FDAP and cell size steadily decline and the membrane status increases.
d) A deceleration phase where the sudden increase of the mean bacterial size without further biomass growth after 5 hours of cultivation clearly correlates with a final increase of the at-

line measured OD, while the DCW remains constant. The relative FDAP decreases to a stable value, whilst the membrane status experiences a last increase.

e) A final stationary phase, where all CQAs (DCW, OD, relative FDAP, cell size and membrane status) remain unchanged.

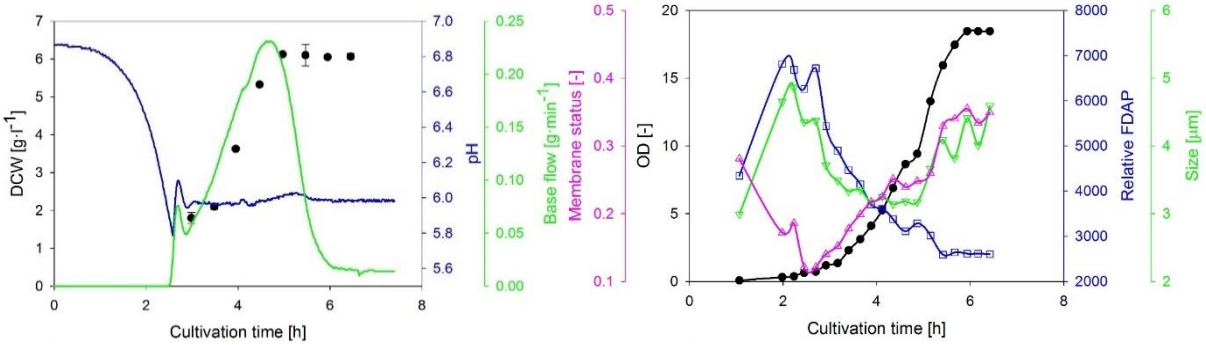

Figure 18. Pilot scale (700 L) cultivation of *S. thermophilus* at the industrial partner. Development over time of relevant CPPs (pH and base addition rate) and CQAs (off-line DCW and at-line OD, relative FDAP, cell size as well as membrane status). The relative FDAP refers to the polarizability at 400 kHz. Error bars: Mean ± SD (n = 2).

As already mentioned, SYBR Green and PI were used during this fermentation to analyze all the bacteria and the permeabilized ones, respectively. Nevertheless, the investigation of the evolution of the unstained samples over time with flow cytometry can already provide relevant information (**Figure 19**). Interestingly, after 2.5 hours cells showed the biggest size as well as granularity (in accordance with the electrooptical results in **Figure 18**) and from then on, their morphology remained moreorless unchanged. The overall trend correlates with the morphological changes observed with the at-line electrooptical measurement (**Figure 18**), but apparently the resolution of the flow cytometric analysis is not enough to monitor the small changes (1-2 µm observed during growth in **Figure 18**) experienced by *S. thermophilus* during exponential growth under optimal conditions in a 700 L bioreactor. With these results, EloTrace seems to be more sensitive to small size changes, thus allowing the at-line monitoring of cell morphology of these bacteria over time, faster, simplier and without sampling nor sample preparation.

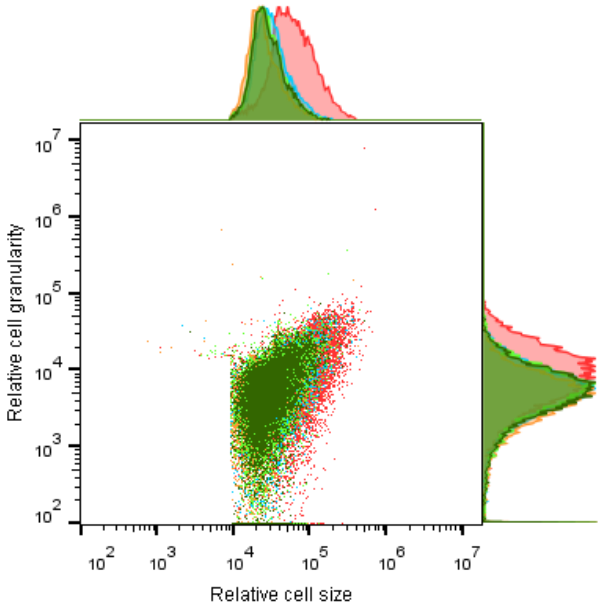

Figure 19. Flow cytometry analysis of unstained samples of *S. thermophilus* growth over time in a 700 L fermenter under optimal conditions. Samples after 2.5 (red), 3.5 (blue), 4.5 (orange), 6 (light green) and 6.5 (darw green) hours of cultivation.

This cultivation in the pilot scale was compared with three fermentations performed in 2 L bioreactors also under optimal conditions (**Figure 20** and **Figure 21**). For more detailed information about the cultivation conditions in lab scale fermenters see (Spann, Roca, et al., 2018). Both, off-line biomass and off-line cell concentration (determined with flow cytometry) throughout all experiments show no differences on growth profile between scales. Furthermore, the development of the relative FDAP between cultivations is also comparable, although different cryovials were used as inocula (initial values of polarizability are not available, because EloTrace needs a minimum of OD 0.1 to be able to perform the electrooptical measurement). The growth rate evolution over time is also similar between scales and, more importantly, here again, cells' polarizability seems to be an early indicator of growth reduction, since it decreased about one hour before than the growth rate did in 2 and 700 L fermenters. Finally, flow cytometric analyses of samples throughout the different cultivations provide relevant but limited information: apart from obtaining the cell concentration (cells·L^{-1}), the percentage of permeabilized bacteria was calculated as the proportion of PI-stained cells respect all SYBR Green-stained particles (i.e. cells). A different and relatively high proportion of cells (> 5 %) were permeabilized after 2 hours of cultivation if both scales are compared, but this is probably a result of the different inocula used and that both cultures were still in the lag-phase, thus adapting to the extracellular environment (as commented above). Importantly, the further development of the dead cells over time is statistically equal across scales and the percentage of permeabilized bacteria remains always below 2-3 % toward the end of all cultivations, possibly because they were performed under optimal growth conditions.

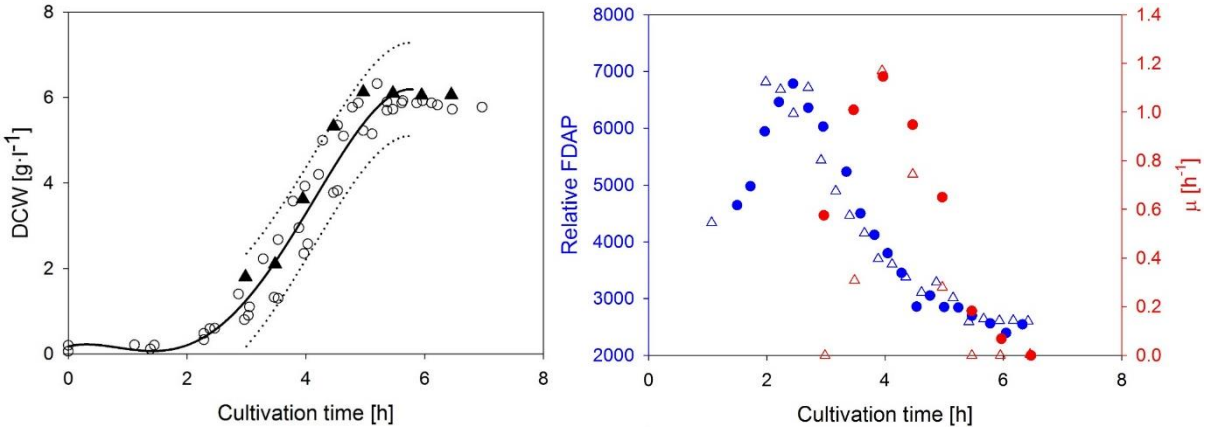

Figure 20. Development over time of *S. thermophilus* cultivations in 2 L (circles) and 700 L (triangles) fermenters. Biomass (left), polarizability at 400 kHz (right blue) and growth rate (right red) evolution throughout the experiments. Confidence interval for DCW during three independent replicates of 2 L cultivations: Mean ± 5 %. The CV% of the DCW determination for all experiments was always below a 10 %, performed in duplicates, and error bars were not included for a better interpretation of the results.

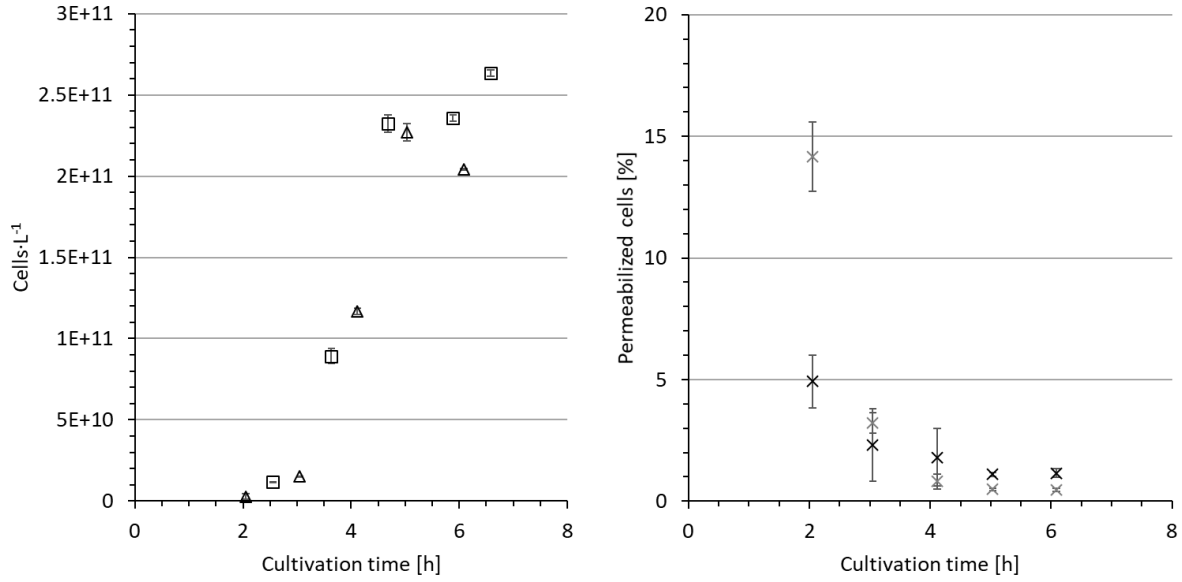

Figure 21. Flow cytometry analysis of *S. thermophilus* fermentations in 2 L (triangles and grey crosses) and 700 L (squares and black crosses) bioreactors. Biomass concentration (left) and percentage of dead cells (right) over cultivation time. Error bars for cell concentration: Mean ± t-Student distribution (α = 0.05, n = 2). Error bars for PI staining: Mean ± SD (n = 2).

Figure 22 confirmed that the *S. thermophilus* population evolves toward diplococcal morphologies during growth in STR under optimal conditions across scales. What is more, a second division cycle could be expected under high growth rates, thus leading to 4-cocci chains, which resulted to be the second most relevant population in 2 L as well as 700 L *S. thermophilus* fermentations (**Figure 22**). Importantly, throughout these experiments flow cytometric analysis (more specifically, the mean between replicates of the FSC-median) correlated (R^2 > 0.91) with the correspondent median of the cocci chain length distributions. Generally, the median and quartile range were used in this study because these statistics are less sensitive to outliers than the mean and mode of a distribution (Kwak & Kim, 2017).

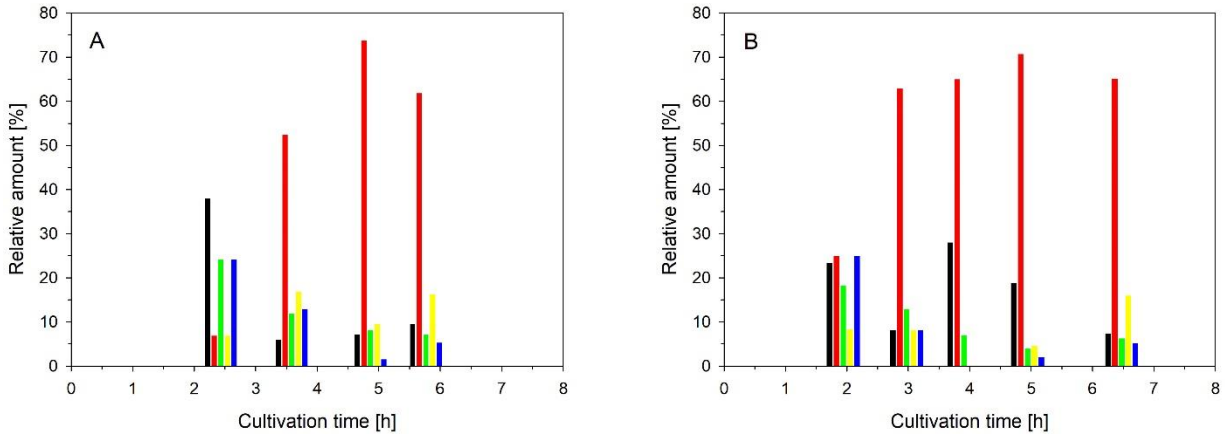

Figure 22. Cocci chain length distribution during *S. thermophilus* cultivations under optimal growth conditions in 2 L lab (A) as well as 700 L pilot (B) bioreactors. 1-coccus, 2-, 3-, 4- and 5 or more cocci chains in black, red, green, yellow and blue bars, respectively.

Interestingly, the development over cultivation time of the cell size determined with electrooptical measurements (i.e. with the EloTrace device) was in accordance with the median FSC that resulted from flow cytometrical analyses in lab as well as pilot scale fermentations (**Figure 23**). It is worth mentioning, that the most similar tendency between the two parameters was detected during growth, while a certain deviation was observed when the cultures were entering the stationary phase in both scales. Changes in the bacterial cell size at the late growth and/or early stationary phase have been reported since many years ago (Akerlund 1995) and have been a limitation when determining biomass concentration at those cultivation times with in-line probes, since the final change in cell size, but without cellular division, triggers an increase of the OD before entering the apparent stationary phase (Ude 2014). Therefore, this fermentation point where bacteria are decreasing their growth rate needs special attention and individual (microorganism as well as media dependent) calibration is necessary.

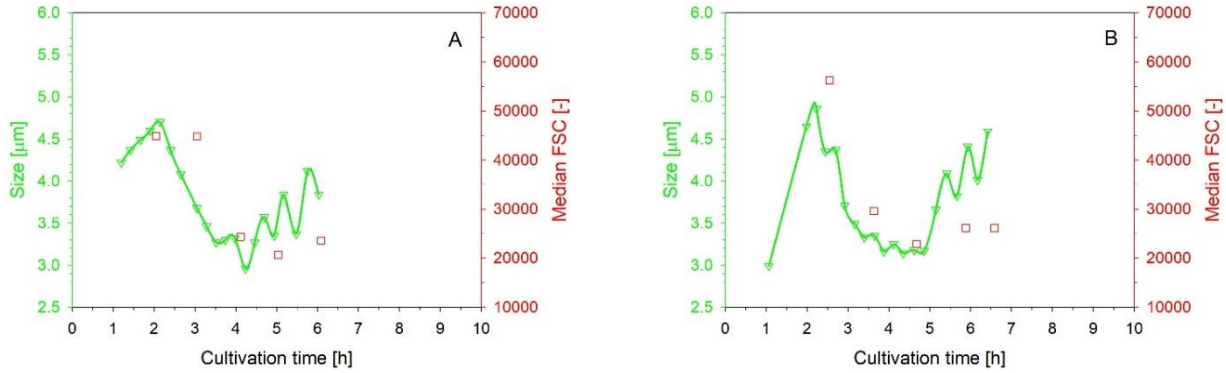

Figure 23. Electrooptical monitoring of the mean cell size (green) and flow cytometric analysis of bacterial morphology (red) throughout *S. thermophilus* cultivations under optimal growth conditions in 2 L lab (A) as well as 700 L pilot (B) bioreactors.

Nevertheless, the correlation between the two morphological indicators compared in this section was not following a linear regression, thus suggesting a possible calibration error. Based on supplier's information, the EloTrace device (EloSystems GmbH, Berlin, Germany) was originally calibrated with freeze-dried *L. plantarum* bacteria (≈ 2 µm), which means that the quantitative cell size provided by the equipment is an equivalent to a rod-shaped form, which indeed is notably different from the cocci chains of *S. thermophilus*. Therefore, the device output (i.e. relaxation time after application of the electrical field) should be newly correlated to the morphological characteristics of the bacteria used in

this study. Additionally, because of the ability of *S. thermophilus* chains to elongate and become relatively flexible (e.g. **Figure 24**), their orientation under the influence of an electrical field is surely different from that of rod-shape bacteria and may also influence the calculated polarizability.

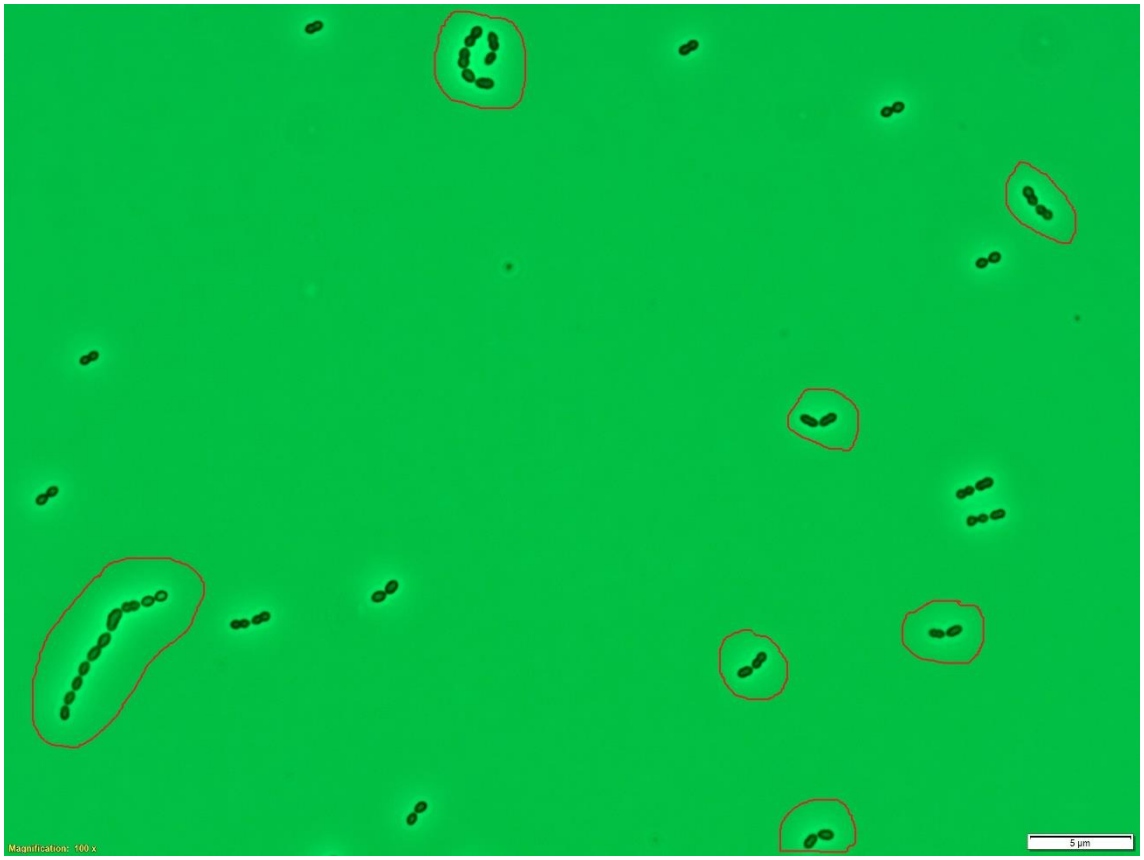

Figure 24. Microscopic analysis of *S. thermophilus* morphology during a 700 L pilot scale fermentation under optimal conditions. Chains with a relative flexibility are marked with red.

In summary, the dynamics of cells' metabolic activity were monitored with a higher resolution using at-line electrooptical methods than with off-line multi-parameter flow cytometry. Indeed, both technologies are not directly comparable and they rather provide complimentary information about cell status. It is worth mentioning that both tools presented in the last sections (namely electrooptical measurement of cell polarizability and size, and multi-parameter flow cytometry) were used throughout the vast majority of fermentations carried out in this work and will be appearing also in the next sections, whenever they are relevant to be mentioned.

4.2. Scale down of *S. thermophilus* Cultivations Based on pH-Gradients

4.2.1. Computational Fluid Dynamics (CFD) Predicted pH-Gradients (Paper III)

As discussed in the Scientific Background, the first step to achieve a representative scale down model in the lab from a bigger fermenter consists of characterizing the fluid dynamics of the largest bioreactor. For this purpose and as a business case study, the pilot scale fermentation explained in 4.1.3 was used to characterize the pH fluctuations encountered by *S. thermophilus* throughout a cultivation in a 700 L fermenter, due to 24 % (w/v) ammonia addition at a position 5.2 % of the liquid height once the pH was controlled through a pH sensor located at 15.6 % of the liquid height. A lance with four pH sensors (located at 5.2, 31.3, 65.1 and 83.3 % of the liquid height) was introduced into the bioreactor prior to inoculation, so that the pH development over time was monitored at five positions of the liquid (**Figure 25**). In 4.1.3, it was already concluded that the growth profile in this pilot scale bioreactor was almost identical as in 2 L scale vessels and therefore it was not surprising that the pH-gradients encountered by bacteria at such a pilot scale fermenter were not that high and were apparently not affecting cell metabolism. A minimum pH value of 5.9 was detected in the upper part of the bioreactor (i.e. far away from the base addition point), but some pH shifts above 6.5 were measured next to the ammonia addition zone.

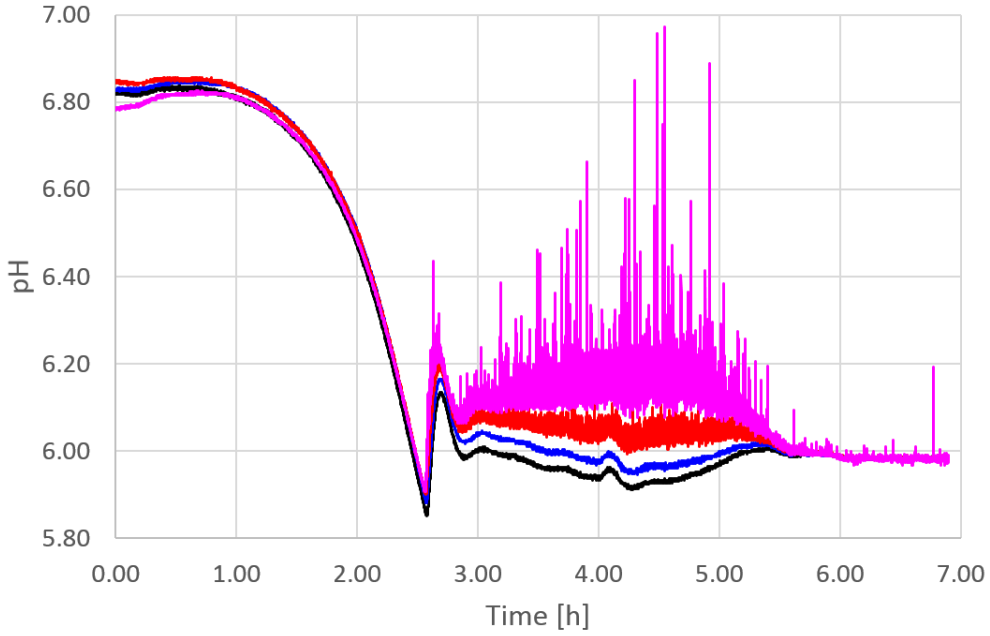

Figure 25. Development of the pH value at four liquid heights during a *S. thermophilus* cultivation in a 700 L pilot scale fermenter. pH sensors located at 5.2 % (magenta), 31.3 % (red), 65.1 % (blue) and 83.3 % (black) of the liquid height. The fifth pH sensor, used for pH control and therefore always around 6.00, was not included for a better representation of the pH-gradients along the fermenter. Taken directly from Paper III.

At this point, the objective was to validate a mechanistic model developed and calibrated with 2 L scale fermentations by the Denmark Technical University (DTU) partners in the project. The model (Spann, Roca, et al., 2018) was predicting the macroscopic variables biomass, lactose, lactate and galactose concentrations based on prediction of the pH as a function of the lactic acid and ammonia concentrations. As seen in **Figure 26**, the model successfully predicted all macroscopic variables in the pilot scale experiment (galactose used to close the C-balance and also less relevant for the process).

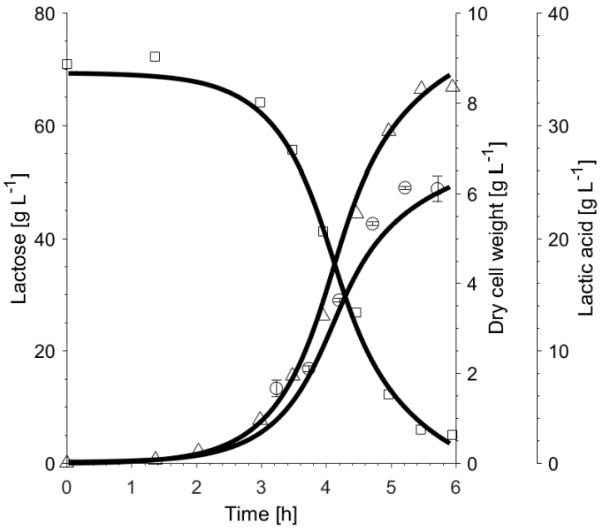

Figure 26. Develoment over time of DCW (circles), lactose (squares) and lactic acid (triangles) during a *S. thermophilus* fermentation in a 700 L scale bioreactor. Error bars: Mean ± SD (n = 2). Model predictions of the different variables are simply represented by the black lines. Taken directly from Paper III.

A CFD model of the bioreactor describing the fluid dynamics was developed on parallel by the DTU partners, thus being able to predict accurately the mixing times based on tracer pulse experiments performed from the top of the vessel (more information in Paper III). Additionally, the CFD model was coupled to the biokinetic model describing the macroscopic variables commented before and the pilot scale fermentation over time was predicted again (now considering fluid dynamics, included in the newly developed CFD model). As seen in the supplementary material of the publication, the fact of including the fluid dynamics in the model prediction was not notably influencing the overall prediction of the macroscopic variables, basically because the fluid oscillations encountered during 2 L as well as 700 L scale cultivations under optimal conditions are not affecting cell growth of *S. thermophilus*. Nevertheless, the pH oscillations measured during the experiment were successfully predicted by the CFD model developed (**Figure 27**). What is more, dynamic simulations of biokinetic models integrated in the fluidic profile simulated by a CFD model can pave the way for an enhanced understanding of microbial behavior in larger scale bioreactors.

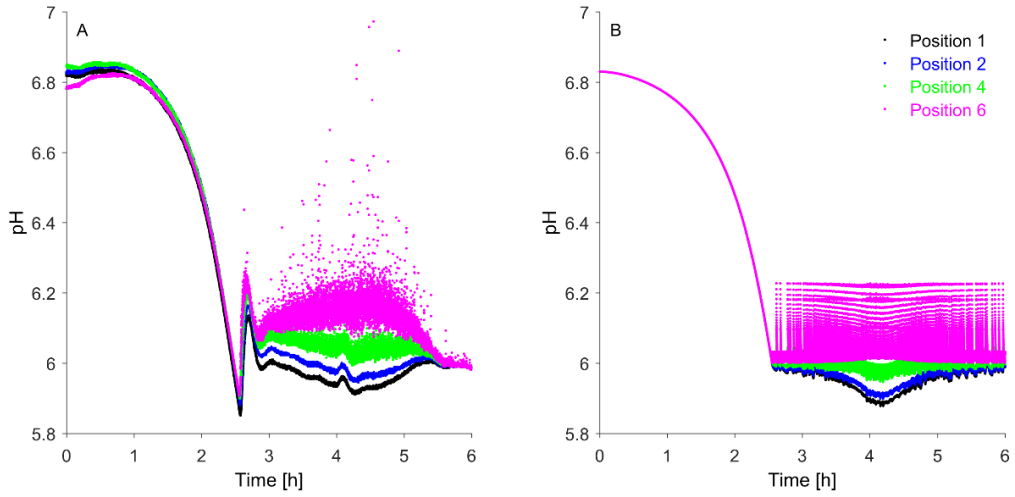

Figure 27. CFD-model prediction (right) and actual measurements (left) of the pH value at four reactor heights during a *S. thermophilus* cultivation in a 700 L pilot scale fermenter. pH sensors located at 5.2 % (magenta), 31.3 % (red), 65.1 % (blue) and 83.3 % (black) of the liquid height. Taken directly from Paper III.

4.2.2. Single- and Multi-CSD Approaches to mimic pH-Gradients (Paper IV)

The industrial production of *S. thermophilus* biomass is performed in a similar bioreactor than the one described in the two previous sections, but in the scale of several tens of cubicmeters. During the batch process, the base to compensate the lactic acid production by bacteria is introduced from the bottom of the fermenter once the pH has reached a value of 6. Taking into account the limitation on the power input in such a scale, the presence of only one pH measurement point in the whole reactor and the position of the base addition, cells are likely to face oscillating environmental conditions once the pH control starts. Moreover, insufficient mixing probably leads to extended mixing times and gradient formation, thus favoring the appearance of compartments with different pH values in the bioreactor, so that the residence times in those zones also become relevant. Therefore, it was of special interest to study the impact of liquid heterogeneities (basically pH) on the microbial cells under laboratory conditions in scale down approaches that mimicked the industrial (large scale) conditions as closely as possible. The challenge here was that those heterogeneities in the production fermenter were unknown and no CFD model had been developed for the industrial scale bioreactor. Thus, this part of the work aimed at investigating and understanding the influence of certain pH-gradients on *S. thermophilus* growth as well as morphological changes (i.e. cocci chain length distribution).

Among the scale down reactor designs commented in the Scientific Background, firstly the influence of certain pH perturbations on the whole cell population were investigated, thus single-compartment scale down experiments were performed and compared to cultivations under optimal pH conditions. In initial experiments carried out at Chr. Hansen A/S in 2 L bioreactors, basic as well as acidic gradients were induced both, individually and combined after 1.5 hours of pH control at 6 (**Figure 28** and **Figure 29**). To perform a basic pulse, for example, the pH was increased with ammonia addition using a syringe through a septum until the desired pH value was accomplished and the pH was subsequently decreased with phosphoric acid until pH 6.

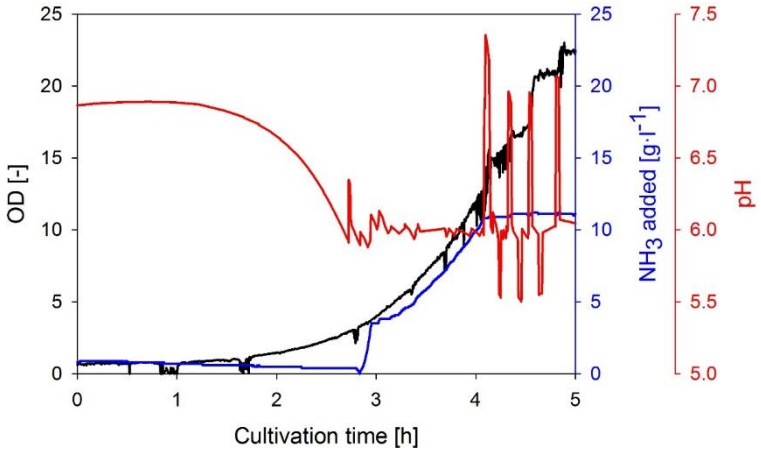

Figure 28. CPPs during a sigle-compartment scale down experiment of *S. thermophilus* in a 2 L bioreactor with combined acidic as well as basic pH shifts.

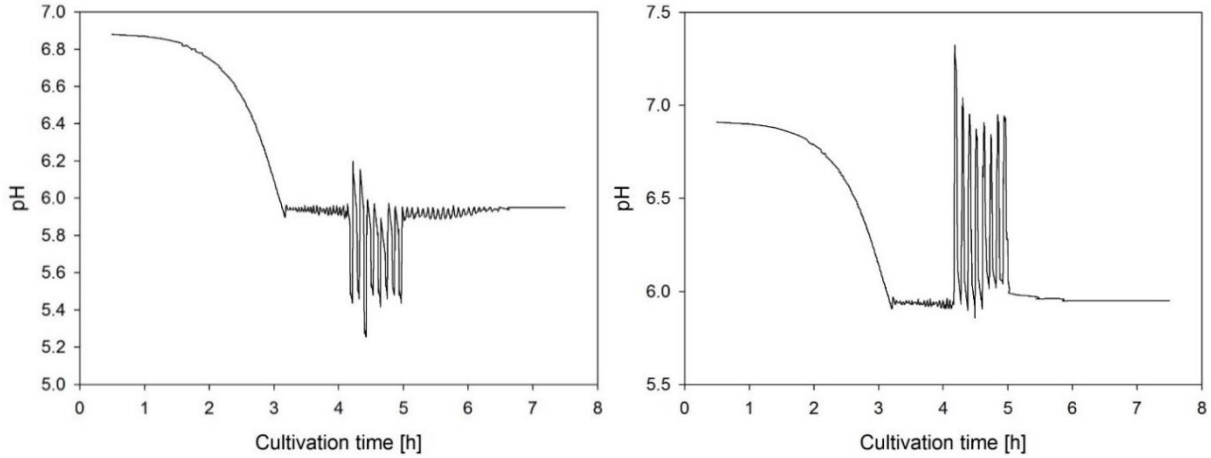

Figure 29. Evolution of pH over time during two sigle-compartment scale down experiments of *S. thermophilus* in a 2 L bioreactor inducing independent acidic (left) and basic (right) pH shifts.

The growth development over time of these three initial scale down experiments was then compared with optimal pH conditions in the same fermenter (**Figure 30** and **Table 5**). It is worth mentioning that the lag-phases of these experiments were not normalized, which means that the small retardation on starting the exponential growth phase (i.e. pH control initiation) was fundamentally due to variations in the inocula and the freshly prepared cultivation media. While basic pH conditions had a severe impact on cell growth, acidic pH shifts did not influence cell growth that drastically. Consequently, the combination of both pH excursions also resulted in a reduced biomass formation and heavily affected growth. Variation of the pH only toward acidic values resulted in a moderate 8 % less amount of C-soruce consumed during growth, whilst independent basic pH pulses and a combination of both acidic and basic pH oscillations, yielded a 42 % reduction of the total lactose consumed after 7 hours of growth. Similar effects were observed in terms of final biomass production: reduction of 5 %, 39 % and 42 % of the final DCW was achieved during cultivations with only acidic pH pulses, with combined basic and acidic pH shifts and with basic pH excursions, respectively, when compared with a fermentation under optimal conditions (i.e. pH controlled at 6 the whole cultivation time). Only small differences were observed in terms of overall yields of the different experiments performed: the $Y_{X/S}$ remained unaffected, but the $Y_{P/S}$ was slightly reduced when inducing basic pH shifts, thus also moderately decreasing the $Y_{P/X}$ under such conditions compared to optimal and only acidic environments. Since *S. thermophilus* are LAB, it is not surprising that they can better adapt to acidic pH environments than to high pH ambients.

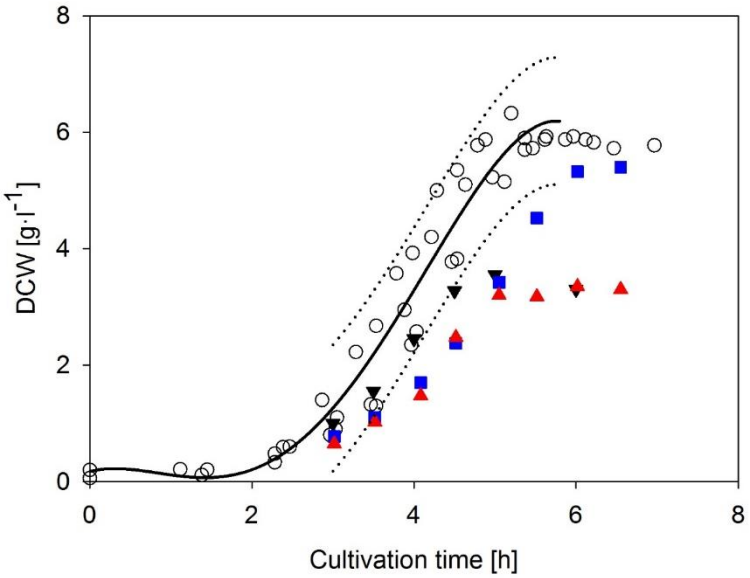

Figure 30. Biomass development over time of *S. thermophilus* cultivations in 2 L bioreactors under optimal conditions (black circles), under combined acidic and basic pH pulses (black triangles), under acidic pH shifts (blue squares) and under basic pH oscillations (red triangles). Confidence interval for DCW during three independent replicates of 2 L cultivations: Mean ± 5 %. The CV% of the DCW determination for all experiments was always below a 10 %, performed in duplicates, and error bars were not included for a better interpretation of the results.

Table 5. Total lactose consumed, final biomass concentration and growth yields of *S. thermophilus* cultivations in 2 L bioreactors under optimal conditions, under combined acidic and basic pH pulses, under acidic pH shifts and under basic pH oscillations.

Experiment pH shifts	**Lactose consumed** $g \cdot L^{-1}$	**Final DCW** $g \cdot L^{-1}$	$Y_{X/S}$ $g \cdot g^{-1}$	$Y_{P/S}$ $g \cdot g^{-1}$	$Y_{P/X}$ $g \cdot g^{-1}$
None	64.6	5.7 ± 0.10	0.089	0.49	5.56
Acidic	59.5	5.4 ± 0.21	0.091	0.50	5.52
Basic and acidic	37.1	3.5 ± 0.07	0.094	0.48	5.17
Basic	37.0	3.3 ± 0.14	0.089	0.41	4.64

Then, a completely different single-compartment scale down (SCSD) approach was tested in TU Berlin, where basic pulses were induced with the automatic addition of 24 % (w/v) ammonia changing the pH set-point to the desired value and pH was allowed to decrease due to the own production of lactic acid from *S. thermophilus* (here no phosphoric acid was added to compensate for the ammonia previously introduced). This is a more realistic scenario compared to the industrial scale production of LAB, where no acid, but base is added during the process (acidification solely due to cell metabolism of LAB). The experiments presented in the next lines were fundamentally used for Paper V.

Variable ΔpH, calculated as (pH_{max} – pH_{min}) during the pulse experiment, were induced after the pH control had started in *S. thermophilus* fermentations performed in 1L STR bioreactors (**Figure 31**). Importantly, the growth rate development until the pH control started was similar in all experiments, always achieving a maximum specific growth rate of around 1.2 h^{-1}. Thereafter, μ was specially affected once the ΔpH was equal or above 2: the growth rate was low at pH < 5.5 and at pH > 7.5, but it slightly increased everytime a base pulse came when the pH was below 6. Since the optimum growth pH is 6 for this strain, anytime the whole culture has a pH environment next to this value, cell growth can be observed. Also, the base introduced after a pulse favors the dissociation of lactic acid, thus increasing growth, since only the non-dissociated form can diffuse across the cell membrane and stop growth, as commented in the Scientific Background. Moreover, the cell size distribution with microscopic images

was analyzed developing a CellProfiler pipeline (see CellProfiler pipeline for quantification of microscopic pictures) to agilize the image processing and reduce human error by counting the cocci number per chain. *S. thermophilus* population evolved to a more homogenous distribution under optimal growth conditions: a higher proportion of shorter cocci chains was analyzed, remaining two cocci-chains the most relevant, toward the end of the cultivation. Initially longer chains (3 and 4 cocci chains) evolved to single and two cocci chains, possibly because of a higher activity of the endopeptidase enzyme responsible for cell separation in *S. thermophilus* (Layec et al., 2009). Additionally, already a ΔpH = 1.8 was undoubtedly affecting the cell size distribution (moving toward longer cocci chains, becoming the longest chains the most important population). A more pronounced influence in the same direction was observed with ΔpH = 2.5, where the pH reached 8. Interestingly, when a rather acidic environment was induced during the fermentation (i.e. ΔpH = 2.0 with pH_{min} = 5 and pH_{max} = 7), the chain length did not elongate as much as under rather basic conditions. On the one hand, the cell size increase at high pH may be a consequence of bacteria trying to decrease the specific surface area in contact with the high ammonia concentration. On the other hand, a chain length decrease at low pH could come from cell shrinkage because of secreation of non-dissociated lactic acid (harmful for the cells) or because the Cse protein (i.e. endopeptidase cleaving the septum in a cocci chain) is apparently more active under acidic conditions (Layec et al., 2009).

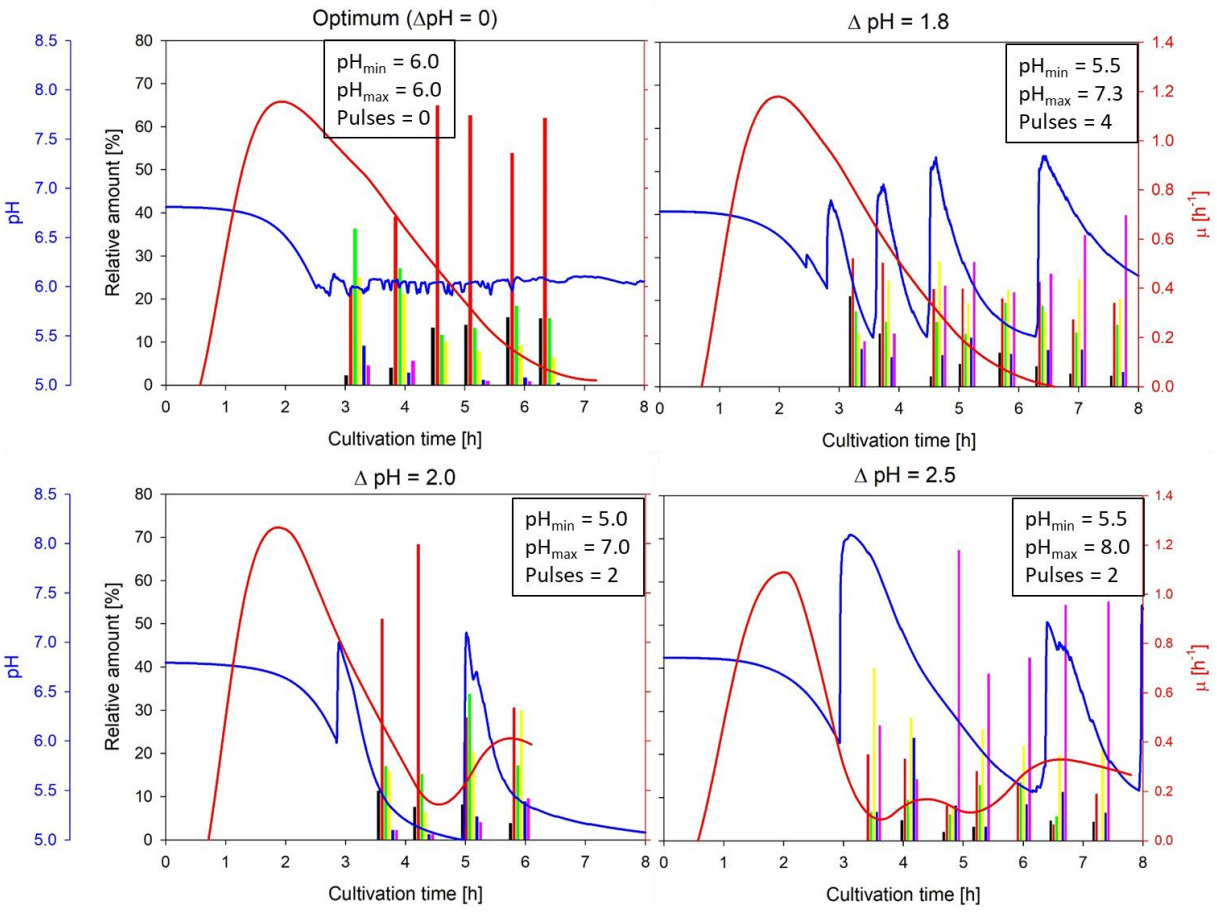

Figure 31. Development of the pH (blue line), the growth rate (red line) and the cocci chain length distribution (bars of different colors) over time in *S. thermophilus* fermentations under optimal conditions (upper left) and inducing a ΔpH of 1.8 (upper right), 2.0 (lower left) and 2.5 (lower right). One coccus (black), two cocci (red), three cocci (green), four cocci (yellow), five cocci (blue) and six or more cocci (magenta) chains. Inside the boxes the minimum as well as maximum pH values achieved during the experiments and the total pH pulses are summarized. Adapted from Paper V.

The biomass development throughout the course of these cultivations (**Figure 32**) showed that the higher the ΔpH, the higher the biomass producitivity loss. The worst-case scenario with the lower final DCW compared to the optimal conditions, resulting in a 48.5 % biomass loss, was obtained with a ΔpH of 2.5. Additionally, ΔpH = 1.5 influenced the maximum specific growth rate, but did not the slope of the growth rate decrease over time. From there on, the higher the ΔpH, the more sudden the growth rate decrease over time. Stress responses from LAB to maintain the homeostatic pH intracellularly under oscillating conditions have been extensively reviewed in the Scientific Background and, probably, a combination of two or more responses caused the observed growth decrease (**Figure 32**) and cell size distribution heterogenetiy (**Figure 31**). Moreover, the higher the pH shift, the more lactose remained unconsumed in the medium at the end of the fermentation (see Paper V). Galactose and lactate accumulated almost on parallel, with more lactate production as well as a higher galactose excreation with a lower pH gradient. Importantly, glucose accumulated under strong ΔpH (> 1.5), when compared to the glucose concentration over time throughout fermentations under optimal conditions, thus indicating an influence of oscillating pH on the glycolysis.

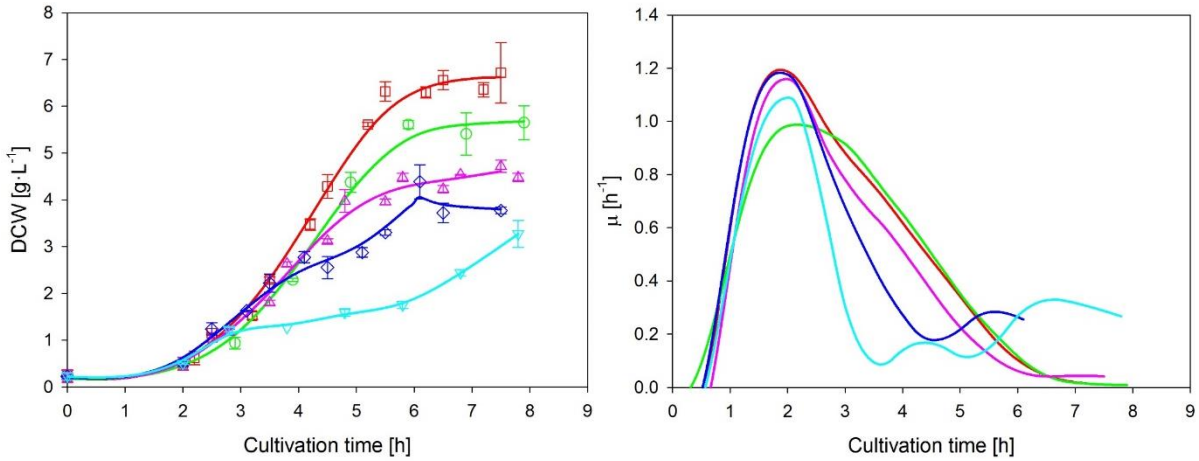

Figure 32. Biomass (left) and specific growth rate (right) development over time during *S. thermophilus* fermentations under optimal conditions (red) and inducing a ΔpH of 1.5 (green), 1.8 (magenta), 2.0 (blue) and 2.5 (cyan). Error bars: Mean ± SD (n = 2). Adapted from Paper V.

Until now, it has been seen, that not only the size of the pH pulses, but also their frequency (amount of pH pulses) and their application method during the relatively short cultivation time have similar influences on *S. thermophilus* growth, but because of completely different reasons, in a single-compartment bioreactor (i.e. 100 % of the population subjected to the stress induced). While independent repeated basic pulses (pH up to 7 and then compensated with phosphoric acid addition to pH 6 in eight occasions) reduced the biomass yield by ≈ 40 % (**Figure 28**, **Figure 29** and **Figure 30**), a prolonged slow acidification of the media after a comparable basic pH pulse (pH of the culture up to 7 and then allowed to decrease to 5 alone in two occasions) can also lead to a similar reduced STY (**Figure 31** and **Figure 32**), when compared to the biomass production under optimal conditions. Nevertheless, the cellular stress responses of *S. thermophilus* to those variable pH oscillations are definitely incomparable: on the one hand, these bacteria stop growing under short repeated basich pH values (ΔpH = +1 x8 pulses), but can survive with almost no influence on growth to ΔpH = -0.5 x8 pulses without the accumulation of the fermentation end product (**Figure 28**, **Figure 29** and **Figure 30**). On the other hand, steadily decline of the media pH because of lactic acid accumulation has a detrimental effect on cell growth, but sudden ammonia addition seems to reactivate cell metabolism for a short time (**Figure 31** and **Figure 32**).

As commented at the beginning of this section, large scale bioreactors are prone to compartmentalization and appearance of zones with variable oscillating conditions. To compartmentalize the fermentation broth is also a well-known strategy in the lab to try to mimick conditions of the industrial scale and this was also tried at Chr. Hansen A/S. Firstly, the acidification of the culture broth by *S. thermophilus* was investigated by connecting two stirred tank bioreactors (one with and the other one without pH control) and pumping the cells through both compartments with a peristaltic pump. This system (**Figure 33**) was then compared with a fermentation in a single bioreactor under optimal conditions. 2 L vessels were available in the lab and a residence time of two minutes was setup, considering that this is a rather pessimistic yield of mixing of a bioreactor. Importantly, the base was added in the same compartment where the pH was controlled at 6.

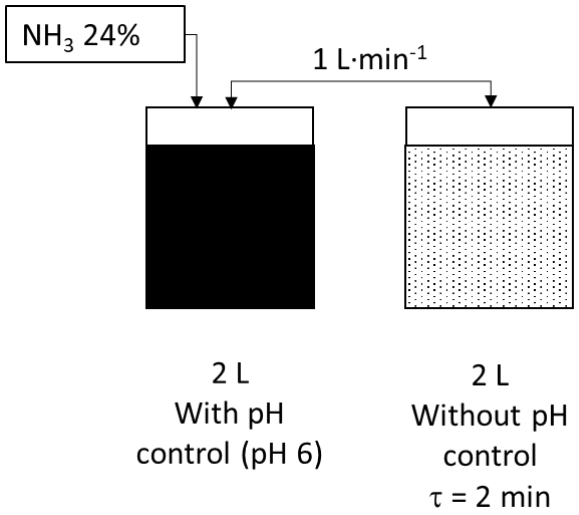

Figure 33. STR-STR two-compartment scale down approach to investigate the acidification of *S. thermophilus* when cells are far away from the base addition zone.

Under these scale down conditions, the growth was only slightly retarded (**Figure 34** and **Table 6**) and differences when compared to optimal growth conditions were hardly seen. Considering the adaptation capacity of *S. thermophilus* to acidic pH environments observed previously, it can be concluded that the moderated probable pH excursions toward lower pH values than the optimum, like 5.8-5.9 (observed in this experiment and in the pilot scale fermentation previously exposed), should not have an effect on cell growth, biomass formation and space-to-time yield (STY).

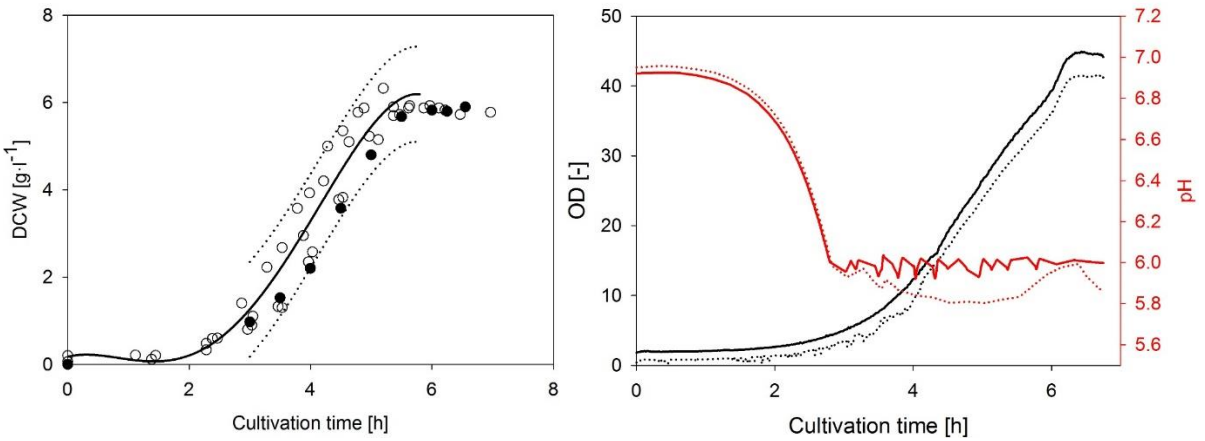

Figure 34. Biomass development over time (left) of *S. thermophilus* cultivations under optimal conditions (open circles) and under STR-STR two-compartment scale down conditions (filled circles). Evolution of the OD (right black) and pH (right red) over cultivation time in the STR with (solid line) and without (dotted line) pH control

during the STR-STR two-compartment scale down experiment. Confidence interval for DCW during three independent replicates of 2 L cultivations: Mean ± 5 %. The CV% of the DCW determination for all experiments was always below a 10 %, performed in duplicates, and error bars were not included for a better interpretation of the results.

Table 6. Total lactose consumed, final biomass concentration and growth yields of *S. thermophilus* cultivations in 2 L bioreactors under optimal and STR-STR scale down conditions.

Experiment Conditions	**Lactose consumed** $g \cdot L^{-1}$	**Final DCW** $g \cdot L^{-1}$	$Y_{X/S}$ $g \cdot g^{-1}$	$Y_{P/S}$ $g \cdot g^{-1}$	$Y_{P/X}$ $g \cdot g^{-1}$
Optimal	64.6	5.7 ± 0.10	0.089	0.49	5.56
STR-STR scale down	59.9	5.9 ± 0.15	0.098	0.50	5.12

For a more realistic scale down system that mimicked the industrial scale process, a third compartment was introduced, where the base addition for the whole fermentation broth was connected (**Figure 35**). The zone where the pH was controlled and therefore assumed to be 6 was reduced to 1 L, while the compartment where the pH is rather lower than 6 because of high lactic acid production from the bacteria was considered to be the bulk zone with 2 L and a residence time again of two minutes. Additionally, only 200 mL bioreactors were available in the lab and the base addition vessel cannot be completely filled at the beginning, because base will continuously be added when the pH control starts. Without the exact knowledge of the mixing times, compartmentalization and residence times in the industrial fermenter, four setups were suggested here: the pump rate between the 1 L and the 180 mL vessels was setup to ensure a residence time of *S. thermophilus* in the base addition compartment of 25, 38, 64 or 108 seconds (limited by the pump rate: 429, 282, 169 and 100 $mL \cdot min^{-1}$, respectively).

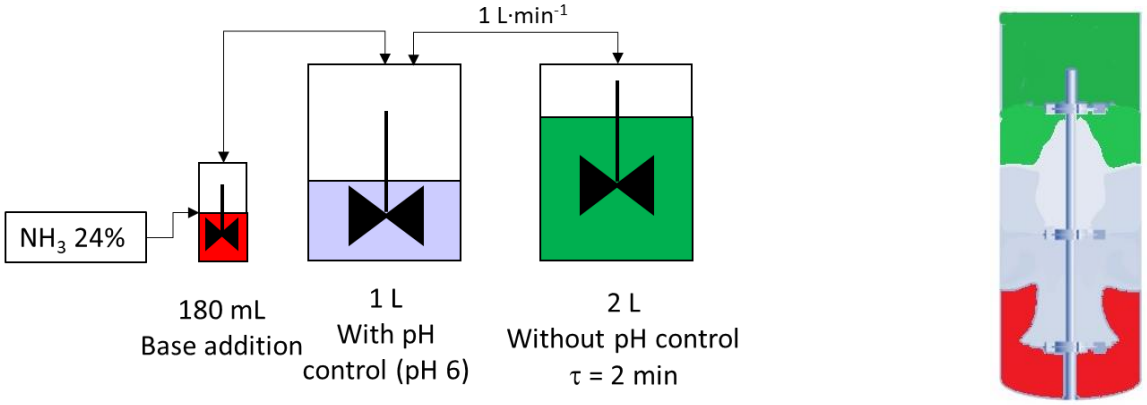

Figure 35. STR-STR-STR three-compartment scale down approach (left) to investigate the assumed fluid dynamics during *S. thermophilus* cultivation in the industrial scale (right). Four experiments were carried out with this system, where the pump rate between the 1 L and the 180 mL vessels was setup in such a way that the residence time of the bacteria in the base addition compartment was 25, 38, 64 or 108 seconds.

The pH profiles throughout the four cultivation conditions investigated are summarized in **Figure 36**. The pH in the 1 L vessel was noted manually because there was a problem retrieving the in-line data from the Biostat® B (Sartorius AG, Waldbronn, Germany) bioreactors and therefore pH values in that bioreactor are plotted with points. In each of the other bioreactors, a CPS471D pH sensor (Endress+Hauser AG, Reinach BL, Switzerland) was introduced only to monitor the pH during the experiments and this is why in-line data was available. It is worth mentioning, that after about 5.5 hours of cultivation in the third experiment (i.e. with 64 seconds of residence time in the base addition vessel), the 200 mL fermenter was almost overflowed and the pump rate to the 1 L vessel had to be

increased for half an hour. This is the explanation for the sudden decrease of the pH in the base addition vessel, but after 6 hours, the pH profile is in accordance with the profile before the problem occurred. It is also important to bear also in mind that the pH-axis for the last scale down experiment is different from the rest, due to the high pH induced with the longer residence time in the base addition vessel.

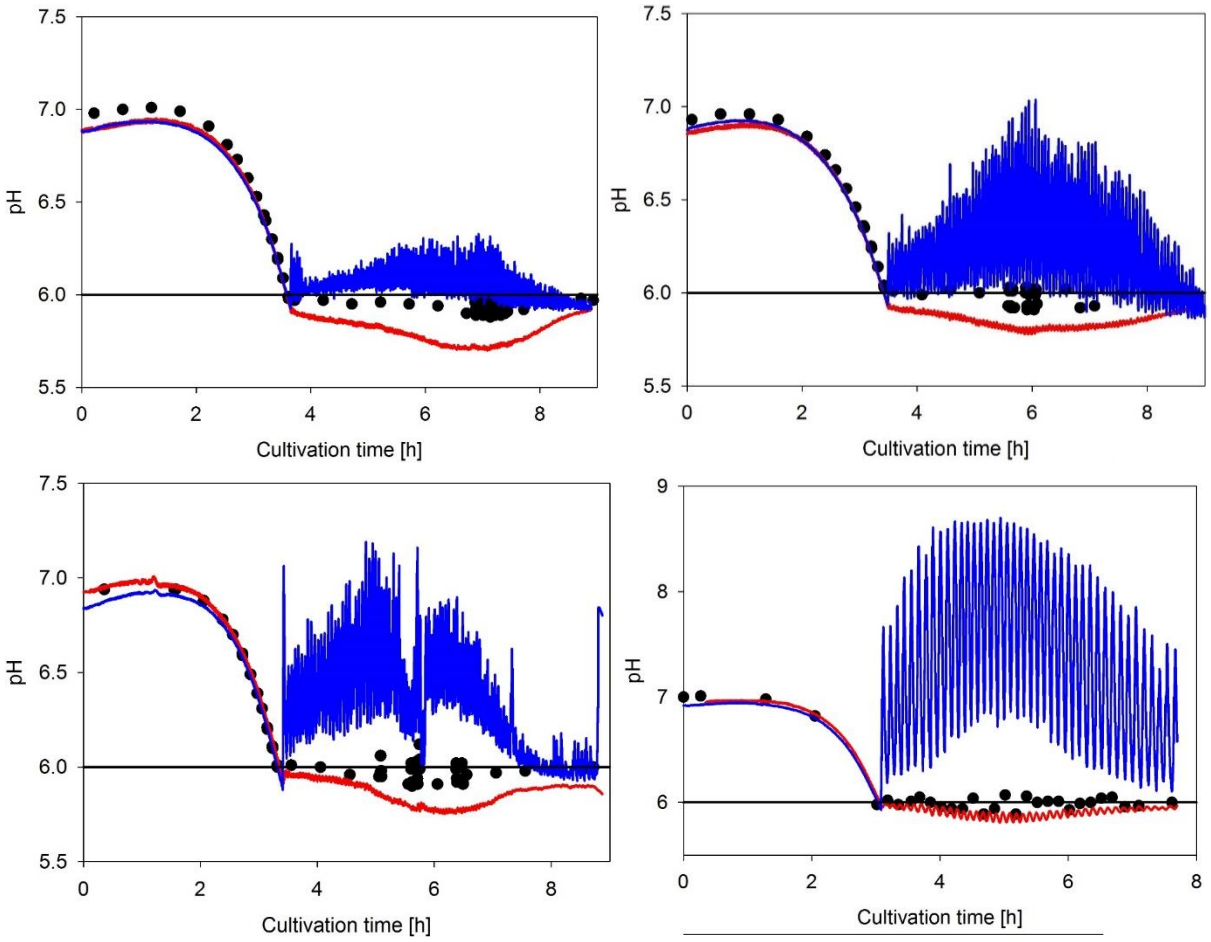

Figure 36. pH profiles during STR-STR-STR three-compartment scale down experiments with a residence time of *S. thermophilus* in the base addition compartment of 180 mL of 25 (upper left), 38 (upper right), 64 (lower left) and 108 (lower right) seconds. Development of the pH over time inside the 1 L bioreactor with pH control at 6 (black dots), the 2 L fermenter without pH control (red line) and the 180 mL base addition vessel (blue line).

The results obtained with the four STR-STR-STR three-compartment scale down expteriments were compared to the previously presented fermentation in the pilot scale (700 L) bioreactor, which is the largest bioreactor in the industrial partner from which the pH-gradients were known (**Figure 37**, **Figure 38** and **Table 7**). At this point, EloTrace (EloSystems GmbH, Berlin, Germany) as well as multi-parameter flow cytometry were used to monitor cells' metabolic activity, size and permeabilization. The growth profile was clearly affected with a specific growth rate as well as biomass productivity reduction under STR-STR-STR three-compartment scale down (3CSD) conditions compared to the cultivation in the pilot scale, but no clear tendency as a function of the residence time in the base addition compartment was identified. One important observation made during scale down experiments was the heavy foam formation, probably due to the level controlled pumping between bioreactors (the outlet tube in each vessel was placed at the specific height to maintain a pre-defined volume, but the inlet tube in each compartment was entering the liquid, thus sparging it when air was being pumped, i.e. the liquid level

coming from the other vessel was not high enough). This phenomenon could have influenced the response of *S. thermophilus* to the supposed induced stress (pH oscillations, rather than foaming) and therefore affected growth performance, thus making the interpretation of the results challenging. Nevertheless, the electrooptical measurement of cell polarizability provided additional information: as commented before, cells invested less energy in cell division and biomass production to rather improve their internal biochemical reactions to adapt to the stressful conditions under 3CSD conditions and therefore showed a lower maximum relative FDAP than in the 700 L fermentation, but a higher polarizability during the growth phase and toward the stationary phase. With the proportion of PI-stained bacteria a similar conclusion can be drawn: at the beginning of all 3CSD experiments (once pH control started), i.e. between 3 and 4 hours of cultivation time, the percentage of permeabilized cells was higher than 10 %, while it was already lower than 5 % in the 700 L fermentation. What is more, thereafter, all cultures adapted to the oscillating conditions and the proportion of dead cells steadily declined during all scale down experiments, reaching the same level as in the pilot scale cultivation toward the end of the fermentations (< 2 %). Although, again, there is no clear tendency with the increasing residence time in the ammonia addition vessel, the $Y_{X/S}$ was clearly lowered in 3CSD experiments respect the 700 L scale under optimal conditions, while the $Y_{P/S}$ remained basically unchanged across experiments, which ended up with slightly higher $Y_{P/X}$ under 3CSD conditions than under ideal growth environment in the pilot scale. In summary, the lactose being consumed under 3CSD conditions was less directed to biomass formation, but still produced similar lactic acid amounts, thus indicating a higher use of the energy produced (2 ATP·glucose^{-1} with glycolysis plus fermentation) for cell maintenance (i.e. increased mean polarizability, but decreased DCW production). Therefore, *S. thermophilus* successfully adapted to the induced stress by decreasing biomass production and increasing intracellular metabolism, but it could not be ensured that the main stress-inducing agent was the high pH value in the base addition compartment, and it may have been the foam formation due to pumping at relatively high speeds (to ensure moderate residence times in the vessels).

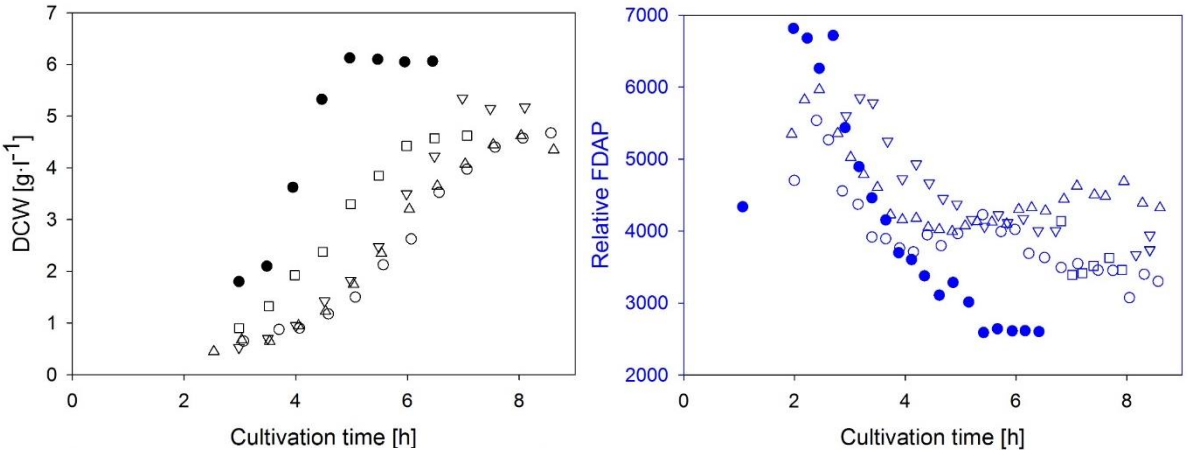

Figure 37. Development over time of *S. thermophilus* cultivations in 700 L pilot scale fermenter (filled circles) and STR-STR-STR three-compartment scale down experiments with 25 (empty circles), 38 (upper triangles), 64 (lower triangles) and 108 (squares) seconds of residence time in the 180 mL base addition vessel. Biomass (left) and polarizability at 400 kHz (right) evolution throughout the experiments. The CV% of the DCW determination for all experiments was always below a 10 %, performed in duplicates, and error bars were not included for a better interpretation of the results.

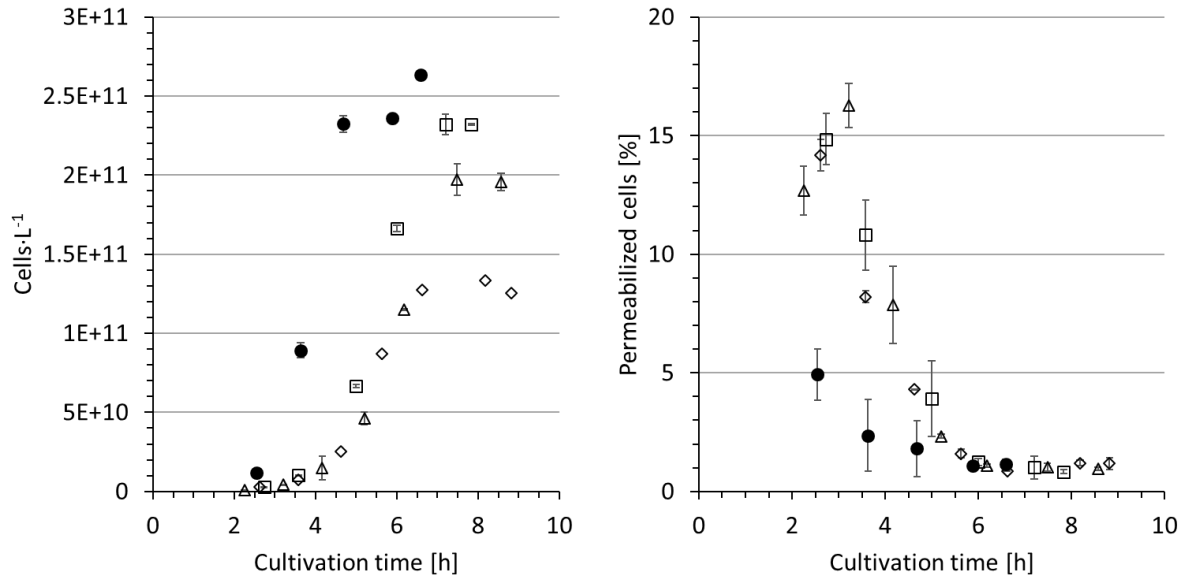

Figure 38. Flow cytometry analysis of *S. thermophilus* fermentations in a 700 L pilot scale bioreactor (circles) and in STR-STR-STR three-compartment scale down experiments with 25 (triangles), 38 (diamonds) and 64 (squares) seconds of residence time in the 180 mL base addition vessel. Biomass concentration (left) and percentage of dead cells (right) over cultivation time. Error bars for cell concentration: Mean ± t-Student distribution (α = 0.05, n = 2). Error bars for PI staining: Mean ± SD (n = 2).

Table 7. Total lactose consumed, final biomass concentration and growth yields of *S. thermophilus* cultivations in 700 L pilot scale fermenter and under STR-STR-STR three-compartment scale down reactor (3CSDR) conditions with variable residence times in the 180 mL base addition vessel.

Experiment	Lactose consumed	Final DCW	$Y_{X/S}$	$Y_{P/S}$	$Y_{P/X}$
	$g \cdot L^{-1}$	$g \cdot L^{-1}$	$g \cdot g^{-1}$	$g \cdot g^{-1}$	$g \cdot g^{-1}$
700 L	66.3	6.1 ± 0.12	0.092	0.52	5.64
3CSDR 25 s	60.2	4.4 ± 0.21	0.072	0.49	6.81
3CSDR 38 s	63.1	4.7 ± 0.25	0.074	0.51	6.88
3CSDR 64 s	60.2	5.2 ± 0.05	0.086	0.52	6.10
3CSDR 108 s	53.9	4.6 ± 0.06	0.086	0.50	5.86

The electrooptical measurements in these 2 L scale experiments (**Figure 39**) were further analyzed:

- ✓ Under optimal growth conditions: a higher biomass productivity was confirmed, a maximum polarizability during acceleration phase with minimal membrane status was detected and a lower polarizability toward the end of cultivation (because of high biomass production) was observed. In morphological terms, smaller cell size variability throughout the cultivation was measured.
- ✓ Between the STR-STR-STR scale down conditions, a relatively similar behavior was detected: a clear, but moreorless equal biomass productivity loss, a lower maximum polarizability and higher minimum membrane status (worse cell vitality than under optimal conditions), a higher polarizability toward the end (more energy spend on maintenance for dealing with pH-gradients). Slightly longer chains, but definitely more cell size variation during growth were additionally detected, probably aiming at diminishing the specific surface area in contact with oscillating conditions (i.e. pH-gradients and/or shear stress due to tubing/foaming).
- ✓ No clear tendency as a function of ΔpH, mainly because of foam formation.

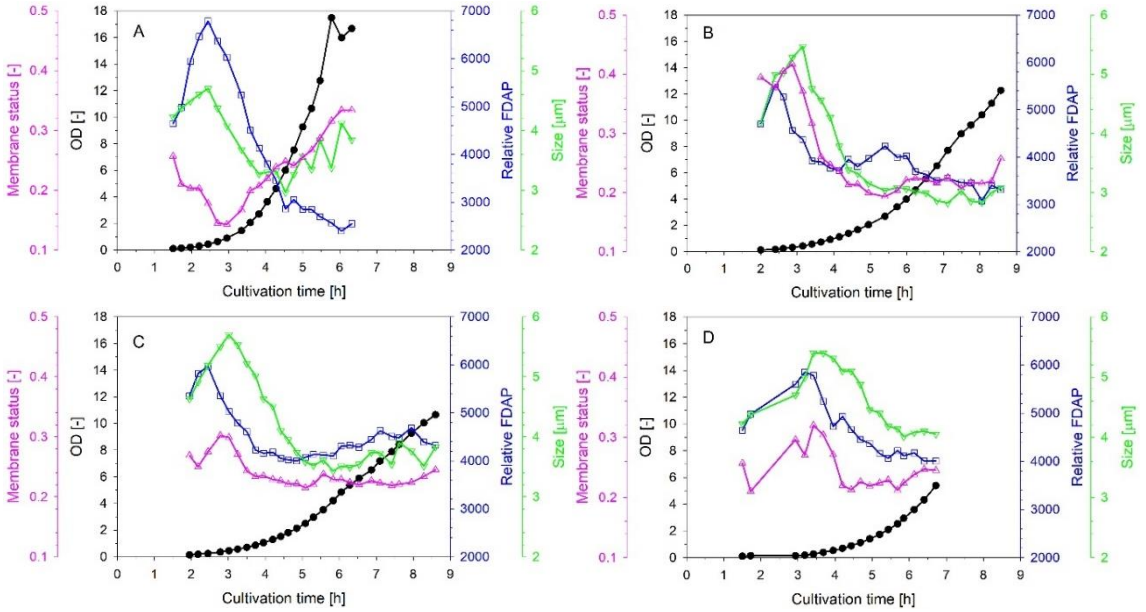

Figure 39. Electrooptical measurement of OD, AP level at 400 kHz, cell size as well as membrane status throughout 2 L *S. thermophilus* fermentations under optimal pH conditions (A) and under STR-STR-STR three-compartment scale down experiments with 25 (B), 38 (C) and 64 (D) seconds of residence time in the 180 mL base addition vessel.

Again, the development over time of the median FSC obtained from flow cytometry analysis of unstained samples followed the same trend as the electrooptical measurement of the mean cell size with EloTrace (**Figure 40**), but the absolute values were notably shifted. As commented before, the problem may lie in the calibration of the morphological parameter of the at-line device.

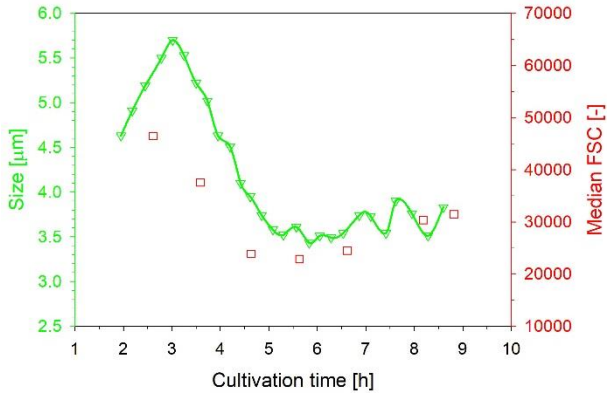

Figure 40. Electrooptical monitoring of the mean cell size (green) and flow cytometric analysis of bacterial morphology (red) throughout a Three-CSDR experiment with 38 s residence time in the base addition vessel.

In order to avoid the foaming problems encountered connecting STRs to run multi-compartment scale down experiments, two- and three-compartment scale down reactors (Two- and Three-CSDR, respectively) connecting one STR to one or two plug flow reators (PFR), respectively, were also used in this study (**Figure 41**). In fact, these scale down experiments conform the basics for Paper IV, but were also used for parameter estimation in Paper V. In this fourth publication, a single-compartment reactor (Single-CR) cultivation in a STR was compared with fermentations run in the two different scale down reactor designs: the Two-CSDR consisted of a STR combined with one PFR (PFR 1, at the bottom of which the ammonia for pH control was introduced), while the Three-CSDR consisted of the STR and

PFR 1 together with an additional PFR module (PFR 2, into which phosphoric acid was regularly added). As seen in **Figure 41**, pH probes along the height of each PFR module were installed to monitor the induced pH-gradients throughout the experiments. Importantly, the pH probe to control the pH during the fermentations in this setup was in the main fermenter (STR), but the base was fed at the bottom of PFR1.

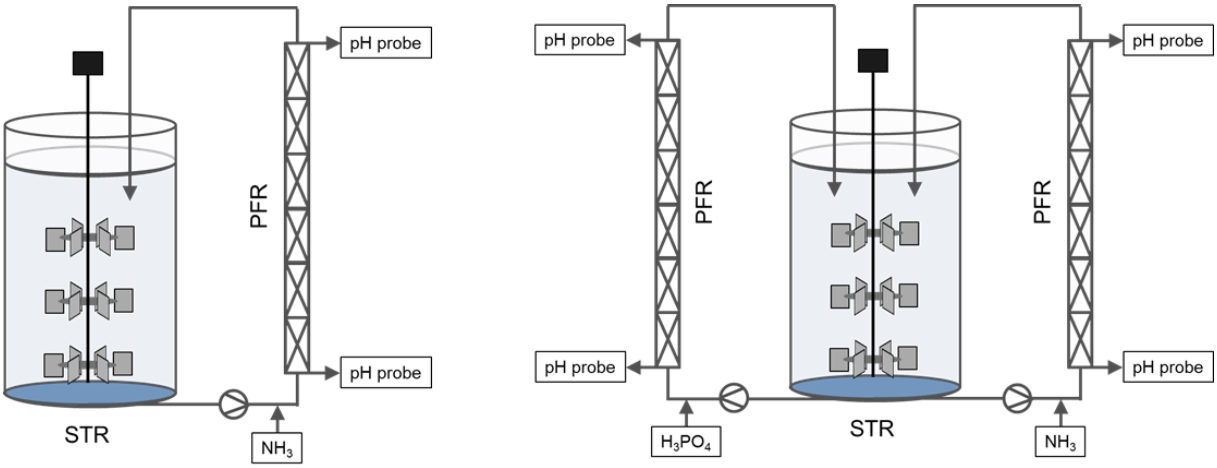

Figure 41. Multi-compartment scale down setups used during experiments in TU Berlin. Two-compartment scale down reactor (Two-CSDR – left) and Three-compartment scale down reactor (Three-CSDR – right). The PFR had a 10 % volume from the culture broth in the STR (total volume of 10 L) and the residence time in each PFR was of around 2 minutes (Junne et al., 2011; Lemoine et al., 2015). Importantly, the pH control sensor was situated in the main fermenter (STR) and the base addition was no longer performed in the STR, but at the bottom of the first PFR. Bacteria were continuously circulating trough the different compartments once the pH control (and subsequent ammonia addition) started.

The pH development over time in the different compartments of Two- and Three-CSDR experiments in duplicates is plotted in **Figure 42**. Importantly, 20 and 70 $g \cdot L^{-1}$ initial lactose concentration was used in the former and latter experiments, respectively. This was mainly to achieve a higher frequency of ammonia addition (higher carbon source yields higher lactic acid concentrations and therefore faster acidification of the media if pH is not controlled, with a concomitant increased base addition rate). Therefore, respective duplicates of the Single-CR experiments were carried out to compare the pH oscillating conditions with an optimal environment using both initial lactose concentrations. Additionally, the residence time of cells in the PFRs was set to two minutes, which is considerably longer than the mixing time of 45 seconds (for 95 % of homogeneity) obtained in Paper III, with pH-gradients during the fermentation ranging from 5.9 in the upper zone to 6.3 in the lower part of the 700 L pilot scale bioreactor, next to the base addition point. Nevertheless, the production fermenter of Chr. Hansen A/S is about a hundred times larger, which means that the power input applied is considerably lower because of economical as well as technical limitations. Without the exact knowledge of conditions in the industrial scale bioreactor (e.g. mixing and residence times, CFD studies, etc.), the slowest pumping rate (i.e. longest residence time = 120 seconds) was selected in the lab to really see an impact of pH oscillating conditions on cell morphology as well as physiology, but this could perfectly be in the order of magnitude of the actual residence time in the production scale. Maximum pH-values of 8.2 were created in PFR 1 during Two-CSDR fermentations, while acidic pulses where induced manually in PFR 2 of the Three-CR cultivations two hours after pH control had started, leading to minimum pH values of about 4.2. Here, it is worth mentioning, that a technical problem occurred just at the moment of connection of the PFR 1 (i.e. start of pH control at 6) during Two-CSDR

experiments and this is why a pH decrease until pH 5.2 in the main fermenter was measured. At the end, this resulted in the connection of PFR 1 almost one hour later, which definitely affected cell culture. Learning from the experience, in future experiments, the pH value in the STR was controlled manually with injecting 24 % (w/v) NH_3 through a septum while the problems with sterilization of the PFR were being solved, thus minimizing the effect of technical problems on the fermentation and interpretation of results.

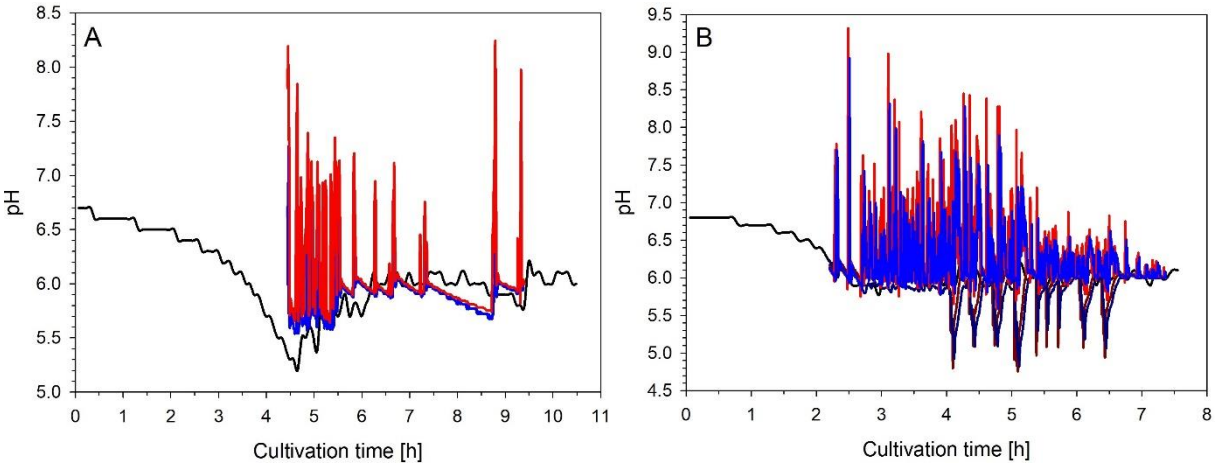

Figure 42. Development of the pH over time in different compartments during multi-compartment scale down experiments in TU Berlin. Monitoring of the pH value in the STR (black) as well as in the PFR modules during Two-CSDR fermentations (A) and Three-CSDR cultivations (B), measured with two probes located at the top and bottom of the PFR modules (blue and red, respectively). The pH in the PFR 1 (A - light blue and light red) during Two-CSDR experiments ranged from 5.6 to 8.2. pH-gradients throughout Three-CSDR cultures, considering also the pH shifts on top and bottom of PFR 2 (dark blue and dark red, respectively), were between 4.7 and 9.4. Taken directly from Paper IV.

The pH-gradients, as induced in the Two-CSDR cultivations, did not alter the final biomass concentration, so that the same biomass yield was obtained as under gradient-free conditions, but after more time, thus with a lower STY (**Figure 43** A, B and **Table 8**). Additionally, cell division and metabolic activity was considerably retarded under scale down conditions since lower specific growth (μ), lactose uptake (q_S) and lactate production (q_P) rates were obtained during growth. What is more, while all substrate was consumed under both conditions, a lower yield of lactate was determined in Two-CR cultivations (**Figure 44** A, B). It is clear, that the fact of retarding the connection of PFR 1 (and therefore of not controlling the pH at 6), already had influenced growth of *S. thermophilus*, but it should have recovered the optimal growth rate once the pH control actually started (and base addition through the bottom of PFR 1 was initiated). The stress responses to local high pH values described in the Scientific Background probably explain the growth reducing effect: under alkaline conditions LAB divert more energy to cell maintenance to cope with the pH-gradients induced (e.g. the ATP-driven potassium extrusion and the potassium-proton antiport system), thus remaining less energy for cell division while bacteria are adapting to the “new” environment, but if enough nutrients are available, the culture can reach comparable biomass production later on when compared to optimal growth conditions. In contrast to the Two-CSDR fermentations, a considerable reduction of biomass formation was observed in the Three-CSDR experiments (**Figure 43** C, D and **Table 8**). These experiments were performed with a higher concentration of lactose so that lactic acid inhibition occurred at about 30 $g \cdot L^{-1}$, which led to unconsumed lactose. Moreover, q_S as well as q_P remained high and reached maximum values when pH control started under optimal growth conditions, but both steadily declined while pH shifts in PFR 1 were induced (i.e. between 2 and 4 hours of experiment), thus detecting an influence

of the pH-gradients induced, which was also translated in a growth rate reduction after 1 hour of pH control (i.e. 3 hours of cultivation). Right after the phosphoric acid feed was connected to PFR 2, the substrate consumption and product formation were drastically affected compared to Single-CR cultivations. Furthermore, 10.5 % less lactose was consumed and 29 % less lactic acid was produced during Three-CSDR compared to Single-CR fermentations (**Figure 44** C, D). Interestingly, glucose tend to accumulate extracellularly once the acid pulses were applied, thus indicating a clear disturbance of the glycolytic pathway for glucose consumption with a concomitant growth cessation.

The $Y_{X/S}$ remained unchanged in all cultivation conditions, while the $Y_{P/S}$ slightly decreased (and as a cosequence $Y_{P/X}$ also did) under multi-compartment scale down conditions. Nevertheless, the solely fermentation product is generally considered to be lactic acid, but if the accumulated glucose concentration as well as the error of the HPLC method to quantify the metabolites are considered, similar yields are calculated. Finally, no remarkable differences in the amino acids' consumption and synthesis between Single-CR and scale down experiments were identified (see Paper IV).

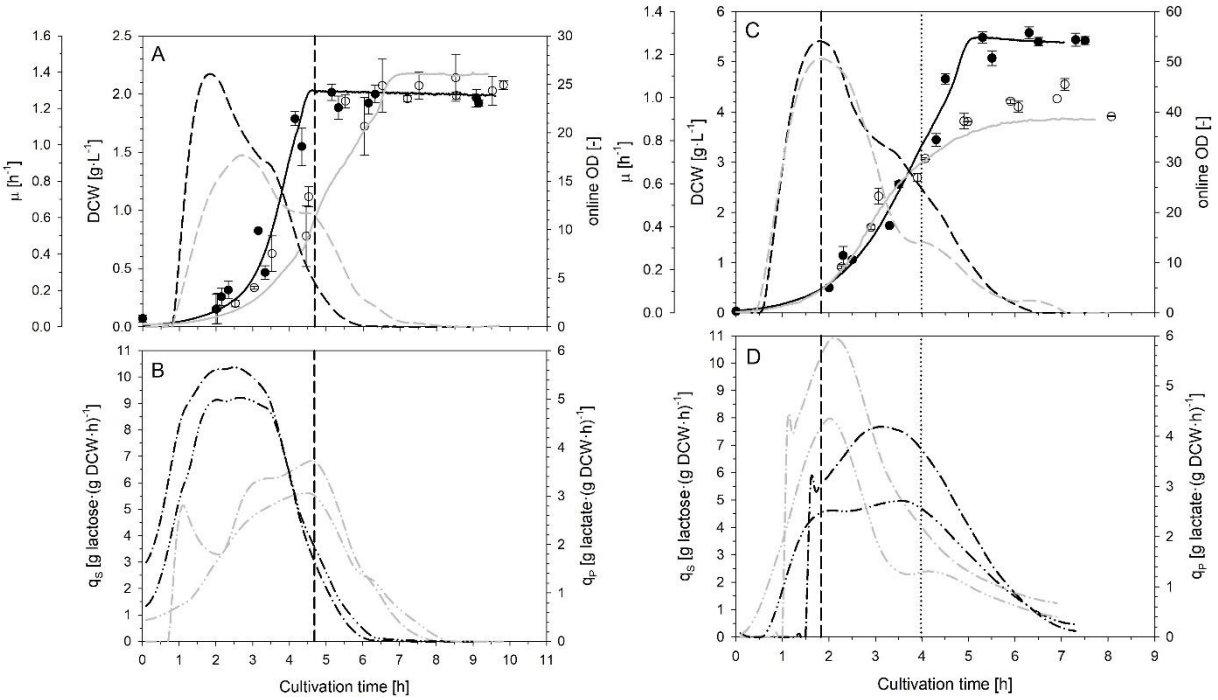

Figure 43. Biomass development throughout Single-CR (filled circles), Two-CSDR (empty circles, A) and Three-CSDR (empty circles, C) experiments. Error bars: Mean ± SD (n = 2). In-line optical density (OD, solid line in A and C), growth rate (μ, dashed line in A and C), specific lactose consumption rate (q_S, dashed-dotted line in B and D) and specific lactic acid production rate (q_P, dashed-dotted-dotted line in B and D) during Single-CR (black), Two-CSDR (grey, A and B) and Three-CSDR (grey, C and D) fermentations. The vertical dashed line indicates the start of pH control and connection of PFR 1 in scale down experiments (Two-CSDR in A and B, and Three-CSDR in C and D), while the vertical dotted line designates the start of manual acidic pulses at the bottom of PFR 2 (Three-CSDR in C and D). Taken directly from Paper IV.

Table 8. Mean value, standard deviation (SD) of biological duplicates (n = 2) and coefficient of variation (CV%) of the final biomass, the biomass yield ($Y_{X/S}$), lactate yield ($Y_{P/S}$) and biomass specific lactate yield ($Y_{P/X}$) in Single-CR (STR), Two- and Three-CSDR experiments with 20 or 70 g·L^{-1} initial lactose concentration. Mean (SD / CV%). Taken directly from Paper IV.

	STR	Two-CSDR	Three-CSDR
Final biomass (20 g·L^{-1} lactose)	1.94 (0.03 / 1.57)	2.05 (0.04 / 1.69)	-
$Y_{X/S}$ (20 g·L^{-1} lactose)	0.095 (0.000 / 0.479)	0.095 (0.002 / 1.66)	-
$Y_{P/S}$ (20 g·L^{-1} lactose)	0.616 (0.059 / 9.60)	0.485 (0.015 / 3.08)	-
$Y_{P/X}$ (20 g·L^{-1} lactose)	6.50 (0.66 / 10.08)	5.13 (0.24 / 4.74)	-
Final biomass (70 g·L^{-1} lactose)	5.43 (0.01 / 0.20)	-	4.41 (0.20 / 4.61)
$Y_{X/S}$ (70 g·L^{-1} lactose)	0.075 (0.001 / 1.11)	-	0.076 (0.001 / 1.25)
$Y_{P/S}$ (70 g·L^{-1} lactose)	0.383 (0.014 / 3.56)	-	0.317 (0.006 / 1.75)
$Y_{P/X}$ (70 g·L^{-1} lactose)	5.14 (0.13 / 2.46)	-	4.18 (0.02 / 0.50)

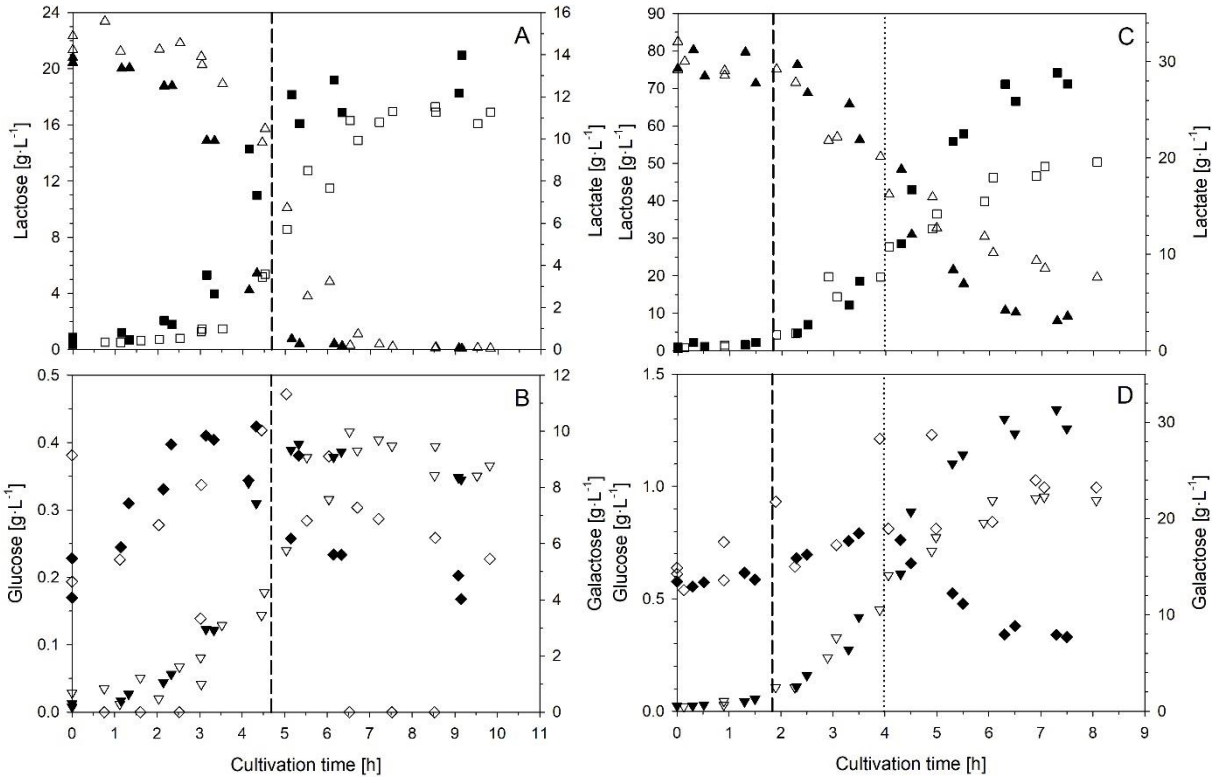

Figure 44. Lactose (upward triangles), lactic acid (squares), glucose (diamonds) and galactose (downward triangles) concentration course throughout duplicates of Single-CR (filled symbols in A and B with 20 g·L^{-1}, and in C and D with 70 g·L^{-1} initial lactose concentration), Two-CSDR (A and B with empty symbols) and Three-CSDR (C and D with empty symbols) experiments. Taken directly from Paper IV.

Again, the diplococcal morphology was found to be the dominant cocci chain length in *S. thermophilus* cultivations, which were conducted under optimal conditions (**Figure 45**). At the very late step of cell division, the septum formed is cleaved and converted into the new pole of each daughter cell by the action of cell wall hydrolases (Chapot-Chartier & Kulakauskas, 2014; Layec et al., 2009). Nevertheless, at high growth rates, a second round of cell division may start before closure of the septum, therefore longer chains might be detected. Indeed, base pulses, which were induced in Two-CSDR fermentations, shifted the population distribution toward longer chains. What is more, five or more cocci chains were the dominant chain lengths under pH oscillating conditions, while such chain lengths were hardly detected under gradient-free growth. Under the pH stress induced in the Three-CSDR system, the cocci chain length distribution was also broader, including a large portion of single cocci beside longer chains of an uneven number of cocci. Already 1.5 hours after starting the pH control (that is after connecting the PFRs and inducing base pH shifts), a 22 % lower number of diplococcal cells and more than twice the amount of single cells were identified under Three-CR conditions compared to Single-CR results.

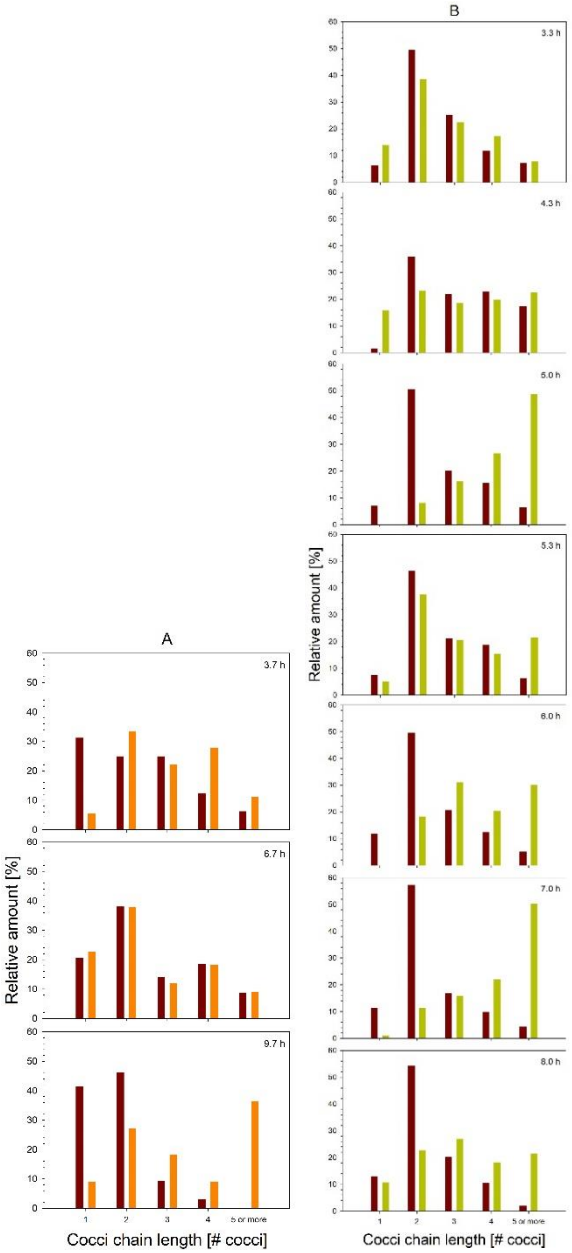

Figure 45. Cocci chain length distribution during Single-CR (dark red bars), Two-CSDR (orange bars) and Three-CSDR (yellow bars) fermentations. Adapted from Paper IV.

Electrooptical measurements throughout the scale down experiments presented here were also performed (**Figure 46**) and interesting behaviors were observed:

- ✓ Comparing optimal pH conditions with 20 and 70 g·L^{-1} initial lactose concentration: less lactic acid was produced with a lower starting C-source concentration, so polarizability could keep increasing, while a higher concentration of lactose led to an increased lactic acid production, thus decreasing mean polarizability over time. Additionally, toward the end of cultivation a lower drop of the AP level was detected with less initial lactose concentration.
- ✓ Under Multi-CSD conditions: generally, a lower polarizability and an increased mean cell size was observed compared to optimal conditions. When dealing with initial pH-oscillations, AP stayed stable or slightly decreased over time. After the acidic pulses started, activity stopped, while under alkali environments polarizability increased. Moreover, the mean size at basic pH pulses rather increased, but additional acidic pulses flattened morphology changes over time.
- ✓ Overall polarizability development throughout a fermentation is highly dependent on inoculum's activity. Since cryo-tubes were directly thawn from a -80 ºC freezer, heat shock prior to inoculation may be determining. Unfortunately, the small amount of cells at the beginning of LAB cultivations (0.03-0.1 % v/v) makes the EloTrace measurement not feasible, because it needs a minimum OD of 0.4 in the bioreactor. The industrial partner is thawing the pre-culture in a water bath near the fermentation temperature, but at TU Berlin the inoculum was thawn at room temperature. In fact, experiments under optimal growth conditions as well as inducing pH-gradients in Three-CSDR were performed in triplicates, but the media for the last replicate of both conditions was prepared with a different yeast extract, which influenced all the comparisons (DCW, polarizability, etc.) with previous cultivations (data not shown).

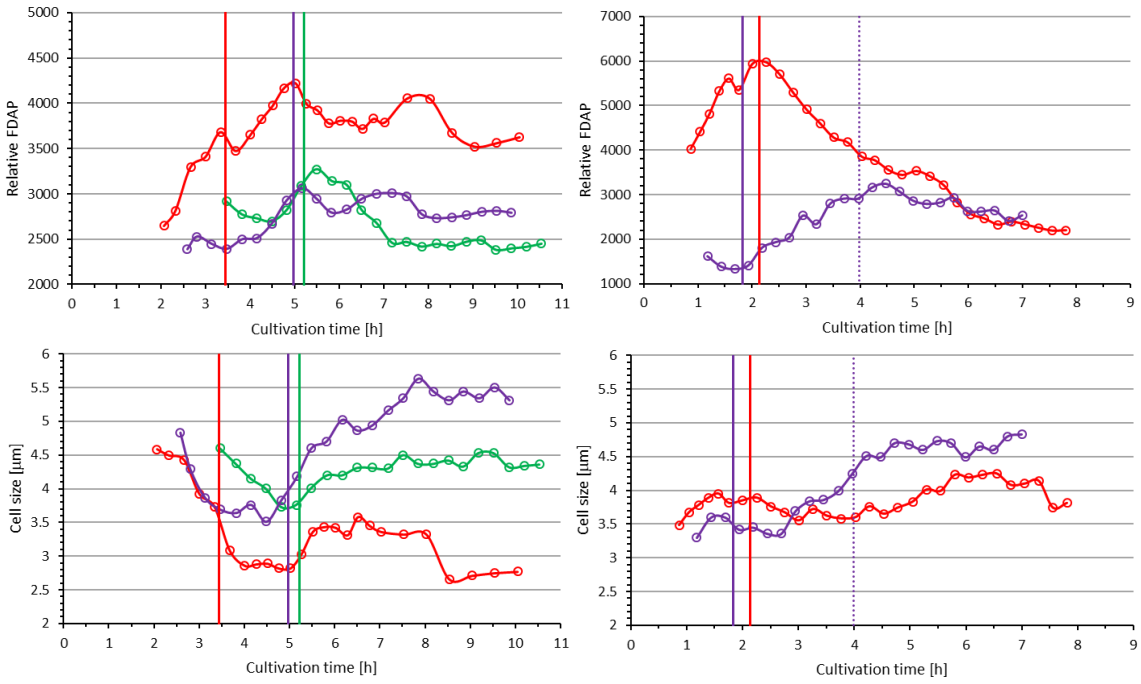

Figure 46. Development of the AP level (top) and the mean cell size (bottom) determined with electrooptical methods during *S. thermophilus* cultivations under optimal growth conditions (red) as well as pH oscillating environments induced in Multi-CSDR (green and lila). Two-CSDR (left) and Three-CSDR (right) experiments were conducted with 20 and 70 g·L^{-1} initial lactose concentration, respectively. Vertical lines correspond to the beginning of pH control (i.e. connection of the PFR with base pulses in scale down fermentations) in the different experiments, while dotted vertical lines denote initiation of additional H_3PO_4 pulses in Three-CSDR experiments.

Multi-parameter flow cytometric analysis during a Two-CSDR experiment was additionally compared to results during optimal growth conditions (**Figure 47** and **Figure 48**). On the one hand, when no pH-gradients were induced throughout a *S. thermophilus* cultivation, the initial relative cell size increased notably during the exponential growth phase, but decreased again toward the end of the fermentation. On the other hand, during the Two-CSDR experiments, the initial chains also elongated during cell division, but bacteria remained rather long under basic pH conditions induced in this setup. Additionally, in accordance with cultivations performed at the industrial partner (**Figure 21**), the amount of permeabilized cells increased during the lag phase, but disminished once the growth evolved, remaining below a 3 % toward the end of the fermentation. In contrast, the percentage of dead cells stayed above 4 % under the pH-gradients induced during Two-CSDR conditions once the pH control started.

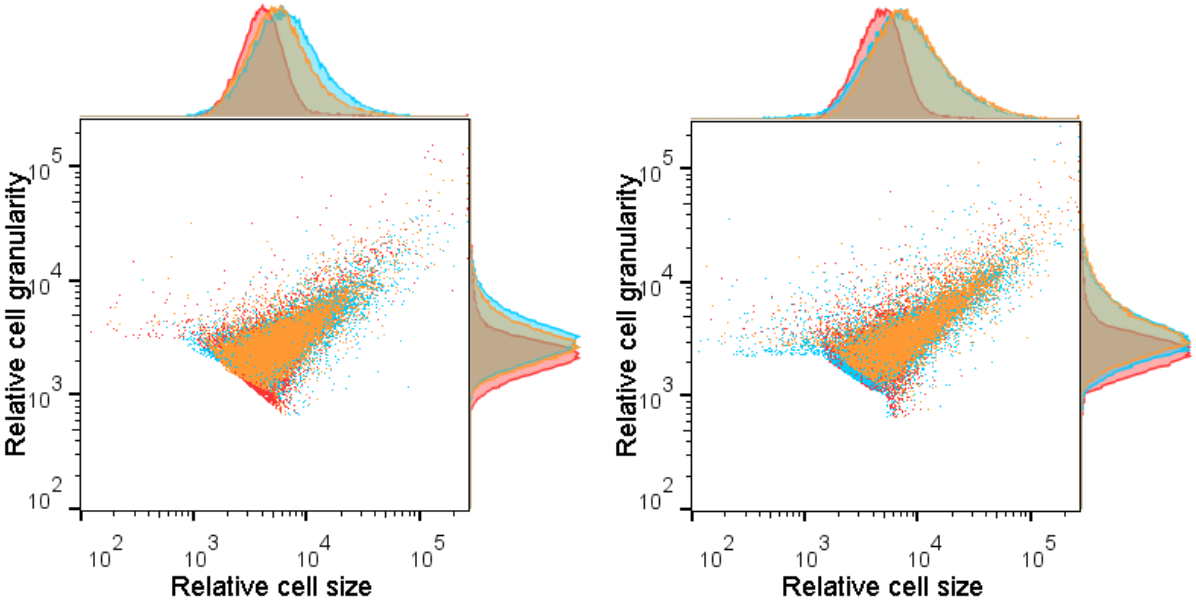

Figure 47. Flow cytometry analysis of unstained samples of *S. thermophilus* throughout a cultivation under optimal conditions (left) and under Two-CSDR (right) in 10 L STR bioreactors. Samples at the lag (red), exponential (blue) and stationary (orange) phases.

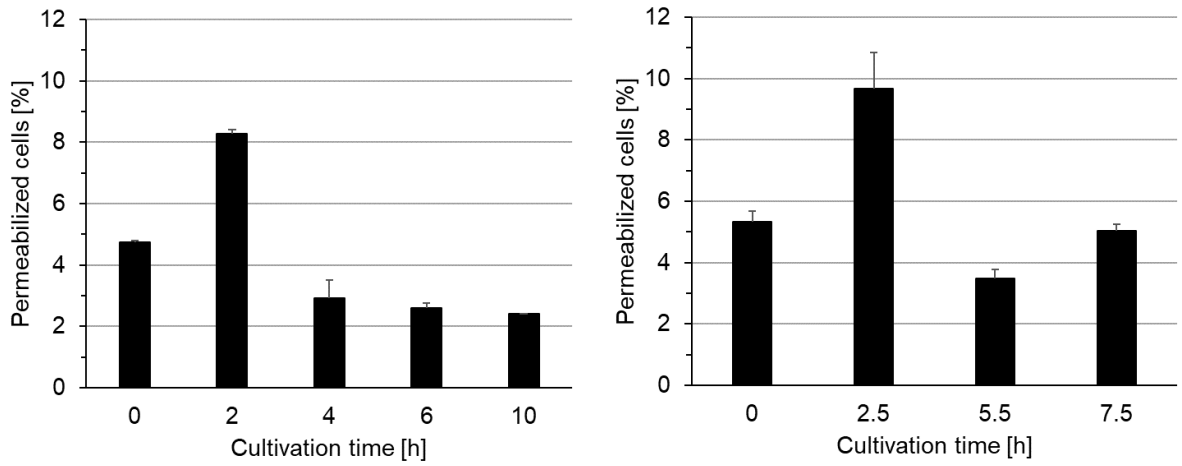

Figure 48. Percentage of dead cells (i.e. stained with PI, respect all DAPI-stained particles) during *S. thermophilus* fermentations under optimal conditions (left) and in a Two-CSDR experiment (right). Error bars: Mean ± SD (n = 2).

Since flow cytometry analysis was also performed in these experiments, it was interesting to see again a certain correlation between the median in FSC and the at-line cell size measured with EloTrace during 10 L STR and STR-PFR fermentations (**Figure 49**). Importantly, a sample of the cryo-tube used to inoculate both bioreactors in different days showed a comparable cell size distribution, so that similar initial culture conditions could be ensured.

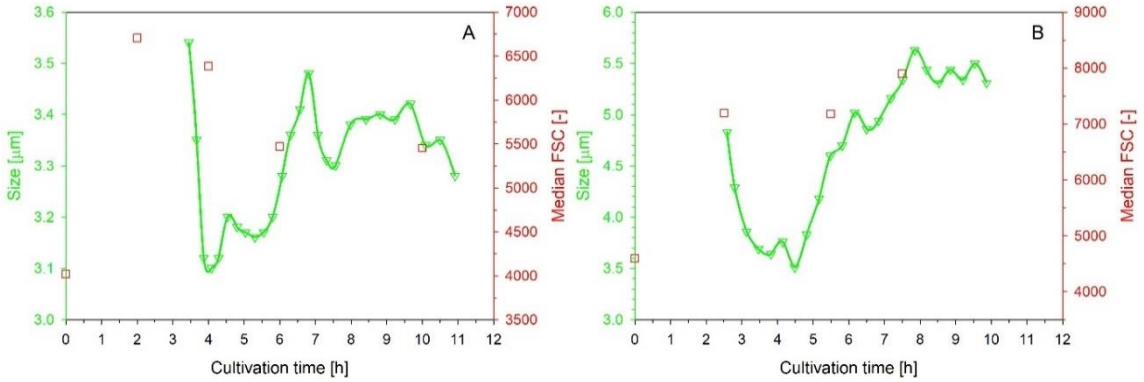

Figure 49. Electrooptical monitoring of the mean cell size (green) and flow cytometric analysis of bacterial morphology (red) throughout a 10 L *S. thermophilus* cultivation under optimal conditions (left) and during a Two-CSDR (STR-PFR setup) experiment (right). Note the different scales, specially for the mean cell size.

After all the scale down experiments performed in this work, the following key performance indicators (KPIs) were identified:

a) Under optimal growth conditions using 70 $g \cdot L^{-1}$ of initial lactose concentration, the stationary phase was entered after 6-7 h reaching a final DCW of ≈ 6 $g \cdot L^{-1}$ in 1 L, 2 L, 10 L as well as 700 L scale bioreactors (**Figure 20**, **Figure 32** and **Figure 43** C as well as **Table 5** - **Table 8**). Furthermore, a maximum growth rate (μ_{max}) of around 1.2 h^{-1} was reproducibly obtained in all experiments under such optimal conditions.

b) This initial carbon source was not completely consumed, even under optimal conditions, because of by-product accumulation, i.e. high lactic acid concentration in the media (**Figure 44** C as well as **Table 5** and **Table 7**). With an initial lactose concentration of 20 $g \cdot L^{-1}$, such product inhibition was not observed and the C-source was depleted at the end of the cultivation (**Figure 44** A). What is more, certain harsh pH-gradients (ΔpH > 1.5) induced the accumulation of glucose in the media and therefore had a clear influence on the glycolytic pathway (**Figure 44** D and Paper V), probably on the first step of phosphorylation of the glucose moiety (Jin et al., 2015).

c) In summary, high pH pulses resulted in rather longer chains, while at a lower pH a trend toward smaller chains was detected (**Figure 31** and **Figure 45**) if the cell size distribution is compared to optimal conditions. More precisely, the amount of one coccus chains as well as cells of five or more cocci seemed to be good indicators of the influence of pH shifts, when compared to optimal conditions.

d) The microscopic analysis observations were confirmed by means of electrooptical measurments of the mean cell size with the EloTrace device (**Figure 13**, **Figure 46** and **Figure 49**).

4.3. Model-based Process Monitoring and Control of *S. thermophilus* Fermentations

The basic idea behind the current trend on developing a digital twin in bioprocessing is the opportunity of predicting cell growth in silico, thus allowing the prediction of the harvesting point and, consequently, optimizing the planification of the DSP. Additionally, model-based bioprocess monitoring and/or control should improve the reproducibility of biomass production, leading to minimization of out-of-spec batches and improvement of process consistency. In this context, the EU project in which this work was involved aimed at developing a model network for different microorganisms, so that one could select the best modeling approach to its interest.

The project partners form DTU (Spann, Roca, et al., 2018) developed a model that consists of the prediction of the main CQA (i.e. biomass concentration) as well as the main metabolites (i.e. lactose, lactic acid and galactose) during the *S. thermophilus* fermentation under optimal growth conditions. The publication in this section takes this mathematical description of the macroscopic variables and tries to predict the population heterogeneity described in 4.3.2, in order to simulate the influence of certain pH-gradients, not only on total biomass production, but also on the single-cell level.

4.3.1. A Probabilistic Soft Sensor to monitor LAB Fermentations

The project partners from DTU developed a probabilistic model-based soft-sensor for predicting *S. thermophilus* cultivations (Spann, Roca, et al., 2018). The main goal consisted of using the available in-line and on-line measurements (such as the pH and the base addition rate) to predict the unknown (typically off-line determined) state variables and monitor the fermentation process in real time. For this purpose, a mechanistic model was first developed and validated, and then used as soft-sensor for monitoring cultivations at the lab scale. The dynamic model consisted of a biokinetic and a chemical model. The former described substrate consumption, biomass growth and lactic acid secretion while the latter comprised a mixed weak acid/base system to predict the pH. Additionally, Monte Carlo simulations of the dynamic model were performed within the monitoring system to account for uncertainties in the lactose (i.e. substrate) concentration, ammonia addition rate and model parameters. The output of the monitoring system was consequently a probability distribution of the state variables.

The model was based on the global stoichiometric process equation described in Eq. 1 and 2. Importantly, the biomass growth rate was modelled as a function depending on the lag-time (f_{lag}), lactose inhibition and limitation (f_S), lactate inhibition (f_P), and the pH (f_{pH}) (Eq. 3). The model was implemented and solved in MATLAB® (The MathWorks®, Natick, MA) using the ode15s solver (for more details on the model development see (Spann, Roca, et al., 2018)).

$$\text{Lactose} + \text{Ammonia} + \text{Phosphoric acid} \rightarrow \text{Biomass} + \text{Lactic acid} + \text{Galactose} \qquad \text{(Eq. 1)}$$

$$q_S \cdot CH_2O + q_{NH3} \cdot NH_3 + q_{Fos} \cdot H_3PO_4 \rightarrow q_X \cdot CH_{1.95}O_{0.63}N_{0.22}P_{0.02} + q_P \cdot CH_2O + q_{Gal} \cdot CH_2O \qquad \text{(Eq. 2)}$$

$$\frac{dX}{dt} = \mu = \mu_{max} \cdot f_{lag} \cdot f_S \cdot f_P \cdot f_{pH} \cdot X =$$

$$= \mu_{max} \cdot \left(1 - e^{-\frac{t}{t_{lag}}}\right) \cdot \left(\frac{S}{S + K_S + \frac{S^2}{K_I}}\right) \cdot \left(\frac{1}{1 + e^{K_P \cdot (P - K_{P1})}}\right) \cdot \left(e^{-\left(\frac{\left(pH_{opt} - pH\right)^2}{\sigma_{pH}^2}\right)}\right) \cdot X \quad \text{(Eq. 3)}$$

An amended Luedeking and Piret equation that considers only the growth dependent lactic acid synthesis was used (Eq. 4):

$$\frac{dP}{dt} = \alpha \cdot \frac{dX}{dt} \quad \text{(Eq. 4)}$$

Then, the lactose consumption was the sum of the biomass growth and the lactic acid synthesis rate considering the secretion of galactose (Eq. 5):

$$\frac{dS}{dt} = -(1 + Y_{Gal}) \cdot \left(\frac{dX}{dt} + \frac{dP}{dt}\right) \quad \text{(Eq. 5)}$$

The purpose of the mixed weak acid/base model was to predict the pH during the fermentation. The dissociation reactions of ammonia, phosphoric acid, lactic acid, carbonic acid, water, and an unspecified compound Z were considered. Importantly, Z accounted for the unknown compounds in the fermentation broth due to the use of complex media in the production of LAB, such as amino acids. The parameter estimation was performed to fit the experimental lactose, biomass, and lactic acid concentration measurements leaving the galactose to close the carbon balance.

For calibration, validation and monitoring several cultivations were performed in 2 L STR bioreactors with stirring at 300 rpm, a temperature of 40 °C, an initial lactose concentration of 20, 70 or 100 $g \cdot L^{-1}$ and the pH controlled at 5.0, 5.5, 6.0, 6.5, 7.0 and 7.5. Relevant for this work was the successful prediction of the growth performance at different pH control values (e.g. **Figure 50**). The root-mean-square of standardized effects (RMSSE) for biomass was around 0.4 $g \cdot L^{-1}$ for the vast majority of the fermentations, corresponding to a discrepancy of less than 10 %, giving evidence of an acceptable fit in the different calibration sets (pH 5.5, 6.0 and 6.5), apart from a cultivation at pH = 7.0, which had an error of biomass production of 30 %.

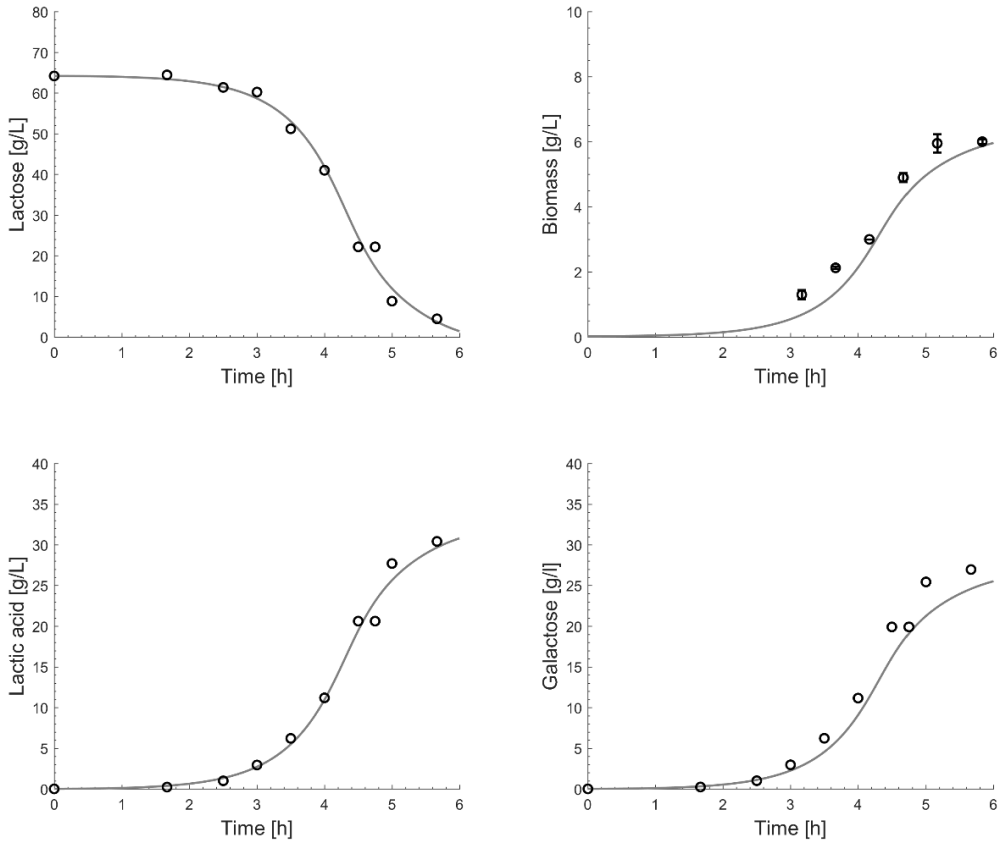

Figure 50. Model prediction (lines) and off-line measured variables (circles) during a *S. thermophilus* 2 L lab scale batch fermentation at pH = 6.0 with 70 $g \cdot L^{-1}$ initial lactose concentration. Error bars: Mean ± SD. Taken directly from (Spann, Roca, et al., 2018) with permission.

The evaluation of the pH function (f_{pH}) showed a clear maximum at pH = 6.4: growth was already reduced by 25 % when pH was controlled at 5.5 and 7.0 (**Figure 51** A). Furthermore, the growth inhibition by lactate was pH dependent: 20 $g \cdot L^{-1}$ lactate inhibited growth by 50 % in the pH range from 5.5 to 6.5, whereas at pH = 7 already 10 $g \cdot L^{-1}$ lactate inhibited growth by 50 % (**Figure 51** B).

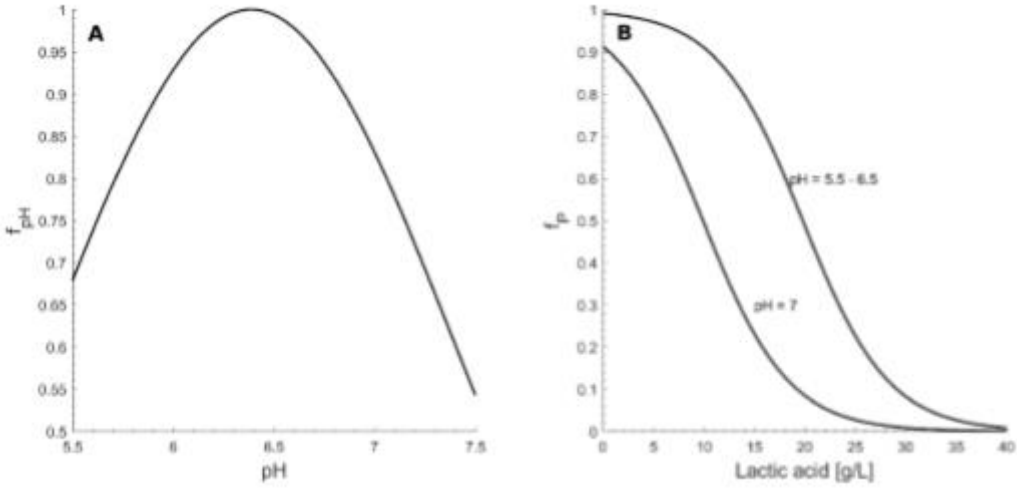

Figure 51. Growth affecting functions of pH and lactate inhibition. pH function vs. pH (A) and lactate inhibition function vs. lactic acid concentration (B). Taken directly from (Spann, Roca, et al., 2018) with permission.

The model was then validated against two independent fermentation data sets, which were performed at pH = 6.0 and with an initial lactose concentration of 20 $g \cdot L^{-1}$ (**Figure 52**). The model successfully predicted the measured lactose, biomass (RMSSE of 0.2 $g \cdot L^{-1}$), lactic acid and galactose concentrations. In the beginning of the fermentation, the pH dropped from 6.3 to 6.0 before the controller started to add ammonia. This drop was predicted to be faster than actually measured, which could be attributed to a slightly different buffer capacity of the media in reality compared to the mixed weak acid/base model. Nevertheless, the pH prediction was very accurate with a discrepancy of less than ± 0.1 pH units, once the pH overshoot was over. This was deemed sufficiently accurate for monitoring purposes, since pH measurement errors were expected to be in the same range. Finally, the validity of the mixed weak acid/base model was demonstrated by a correct prediction of the added ammonia, as the pH is controlled by base addition

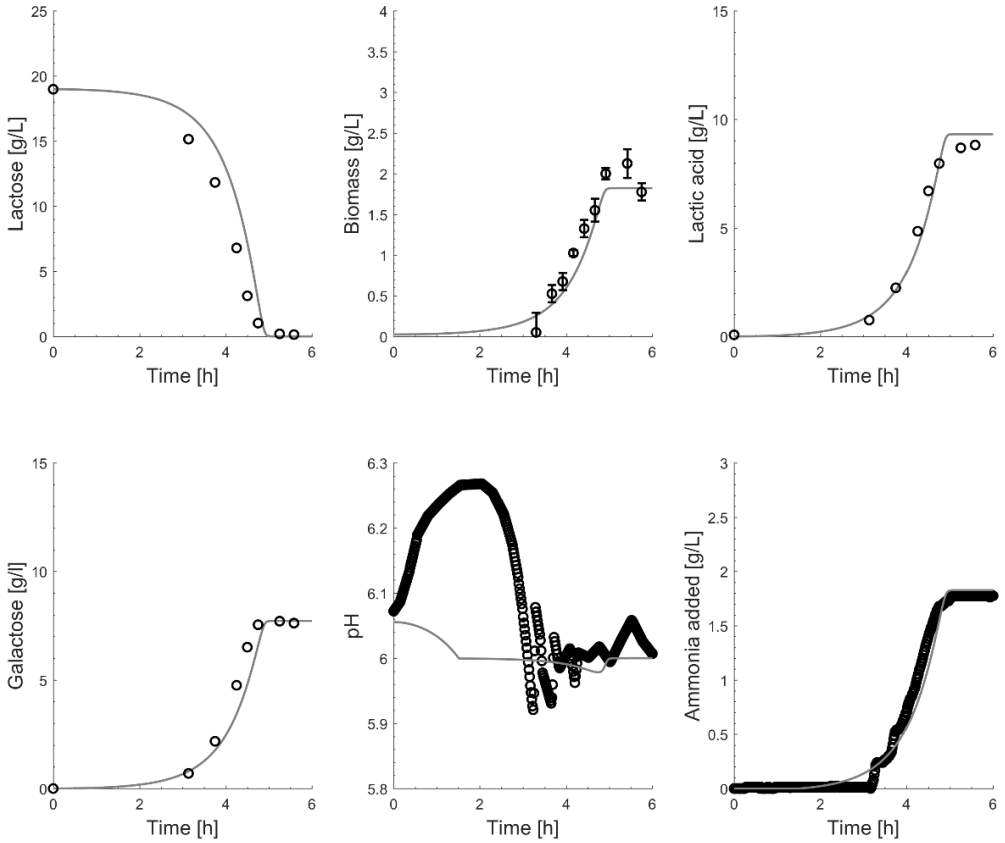

Figure 52. Model prediction (lines) and off-line measured variables (circles) during a *S. thermophilus* 2 L lab scale batch fermentation at pH = 6.0 with 20 $g \cdot L^{-1}$ initial lactose concentration. Error bars: Mean ± SD. Taken directly from (Spann, Roca, et al., 2018) with permission.

The probabilistic model-based soft sensor was applied to the data sets of three historical fermentations and successfully monitored the macroscopic state variables (see (Spann, Roca, et al., 2018)). The RMSSE for biomass was 0.8 $g \cdot L^{-1}$ when the fermentation started and improved to 0.5 $g \cdot L^{-1}$ at the end of the cultivation (both with a standard deviation of 0.1 $g \cdot L^{-1}$), mainly due to updating the t_{lag} parameter after pH control had started, which improved prediction accuracy.

The monitoring system successfully predicted the most relevant macroscopic CQAs and forecasted the future course of the fermentation. This monitoring system, applied at industrial production sites, would provide plant operators with a PAT tool to monitor the biological variables in the fermentation process, such as biomass concentration, instead of relying on on-line base addition rate.

It is worth mentioning, that this mechanistic model was also used in Paper II and III. On the one hand, the model successfully predicted the A-stat fermentation presented in 4.1.2 (**Figure 53**). As commented before, this model was calibrated (i.e. parameters were estimated) using batch fermentations controlled at different pH values with 65 $g \cdot L^{-1}$ initial lactose concentration and, eventhough, the model accurately simulated the dynamics during the continuous cultivation with 20 $g \cdot L^{-1}$ lactose initially and in the feed. On the other hand, the same mechanistic model developed by the DTU project partners also successfully predicted the development over time of macroscopic variables (namely biomass, lactose, lactic acid and galactose concentrations) during a fermentation in a 700 L bioreactor (**Figure 26**). This model, when coupled to CFD studies, additionally accurately simulated the pH-gradients encountered by *S. thermophilus* along the height of the pilot scale fermenter (**Figure 27**). In summary, the biokinetic model was always applied to predict the evolution of macroscopic variables (mainly the biomass, which is the product in the industry of starter cultures), even in further independent studies of the DTU colleagues (Spann et al., 2017; Spann, Lantz, et al., 2018; Spann et al., 2019). Based on the knowledge acquired investigating the morphological changes undergone by the *S. thermophilus* strain from Chr. Hansen A/S under optimal conditions as well as under certain pH-gradients (**Figure 31** and **Figure 36**), the next question was if it was possible to model specific key cell populations, rather than the overall biomass development over time.

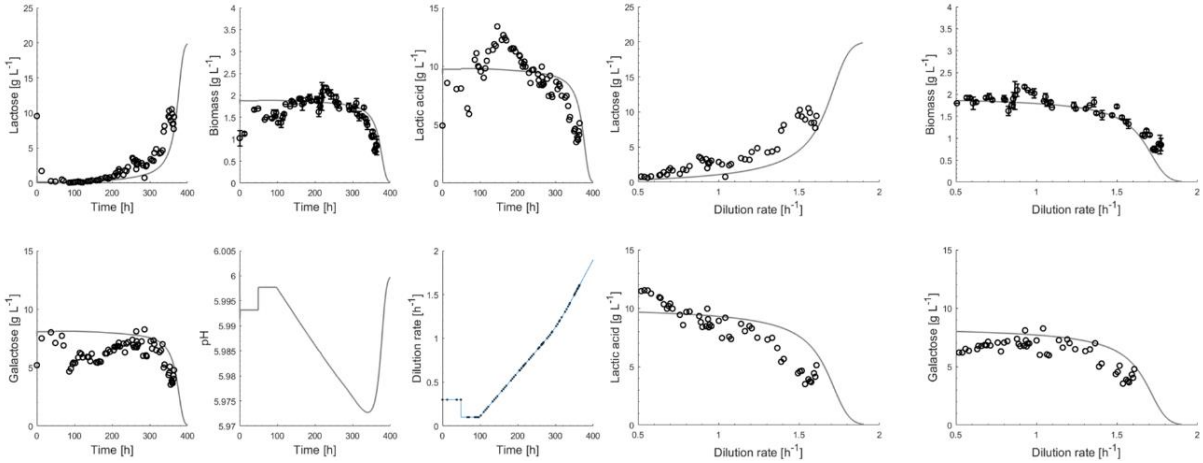

Figure 53. Experimental (circles) and modelled (lines) CPPs (pH, D) as well as CQAs (biomass, lactose, lactic acid and galactose concentrations) over time (left) and over dilution rate (D) during the A-stat experiment. Error bars: Mean ± SD (n = 2). Taken directly from Paper II.

4.3.2. Population Heterogeneity Analysis and PBM for Scale down (Paper V)

As a reminder, *S. thermophilus* under optimal growth conditions, i.e. without pH-gradients, showed the diplococcal morphology to be the dominant cocci chain length in stirred tank bioreactors (**Figure 22**, **Figure 31** and **Figure 45**). Nevertheless, once the pH environment turned acidic, the population tendencially shifted toward shorter chains (i.e. more homogenous distribution). What is more, under high pH values, bacteria elongated leading to chains with a larger number of cocci under the microscope. The possible explanations to these morphological observations have been discussed previously in this work and in the publications, but they emphasize the fact that the "biomass" is conformed by a mean contribution of distinct individual cells (i.e. the population is heterogenous).

Until this point of the work, the biomass concentration had been modelled as a whole (also because it is typically analyzed in this way, without accounting for cell heterogeneity), but it was also tried to predict the different populations detected microscopically under the different growth conditions presented here.

For this purpose, the model presented in 4.3.1 was adapted to predict population heterogeneity under certain pH-gradients:

- ✓ Since some morphological changes were induced under considerable acidic environments (pH < 5), an additional term accounting for the minimum pH value to ensure *S. thermophilus* growth was added to the equation describing cell growth over time (Eq. 6). Until now, only pH-shifts toward basic values had been performed and therefore this term was ignored (Eq. 3). This pH_{min} was determined experimentally carrying out a fermentation without pH control (see **Figure 13**), resulting in a value of 4.8.

$$f_{pHmin} = \left(1 - \frac{10^{pH_{min}}}{10^{pH}}\right) \quad \text{(Eq. 6)}$$

- ✓ The mixed weak acid/base model to predict the pH development during the fermentation (see (Spann, Roca, et al., 2018) for details) was ignored in this part of the work, since the pH inside the fermenters was always monitored in-line, so that it was used as an input variable to the population balance model, that aimed at predicting historical cultivations under sub-optimal growth conditions (i.e. not supposed to be used as soft-sensor, in this case).
- ✓ Based on the population heterogeneity detected in this work (e.g. **Figure 31** and **Figure 45**), *S. thermophilus* morphologies were differentiated between "natural" and "abnormal" cocci chain lengths: while 2- and 4-cocci chains were suggested as "natural" morphologies, 1-, 3-, 5-cocci and longer chains were proposed as "abnormal" cell sizes, because they predominated only when the culture broth was subjected to different pH oscillating environments. Additionally, as explained in the Scientific Background, chains are continuously being elongated and separated during growth of these LAB and, therefore, also a discretization between "natural" as well as "abnormal" events (i.e. elongation and separation) was taken into account. What is more, inside the abnormal elongation events, two categories were differentiated: light abnormal elongation was considered for events where a 2 or more cocci chain elongated simultaneously from both opposed poles (as described in the Scientific Background) and heavy abnormal elongation stands for events where only one of the extremes of the cell elongated. With these hypotheses, a scheme summarizing the rates of conversion between the different morphologies of all populations considered was proposed (**Figure 54**).

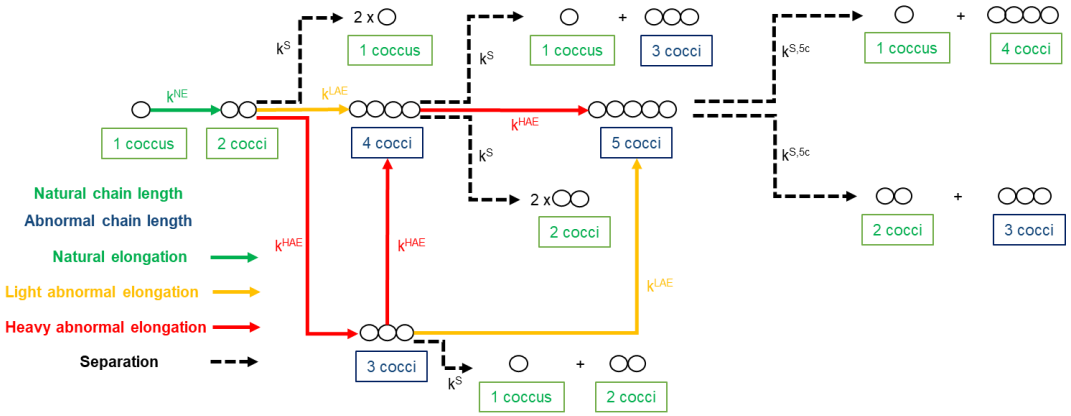

Figure 54. Scheme of the *S. thermophilus* populations and their conversion rates considered in the population balance model, based on microscopic observations throughout fermentations under optimal as well as oscillating pH conditions. Taken directly from Paper V.

✓ The event rates were then defined as follows (Eq. 7-11):

$$r^{NE,1c} = k^{NE} \cdot \mu \cdot C_{1c} \quad \text{(Eq. 7)}$$

$$r^{LAE,i} = k^{LAE} \cdot \mu \cdot C_i \qquad i \in 2c \text{ and } 3c \quad \text{(Eq. 8)}$$

$$r^{HAE,j} = k^{HAE} \cdot \mu \cdot C_j \qquad j \in 2c, 3c \text{ and } 4c \quad \text{(Eq. 9)}$$

$$r^{S,k} = k^{S} \cdot \mu \cdot C_k \qquad k \in 2c, 3c \text{ and } 4c \quad \text{(Eq. 10)}$$

$$r^{S,5+c} = k^{S,5+c} \cdot \mu \cdot C_{5+c} \quad \text{(Eq. 11)}$$

✓ The evolution over time of the populations considered depended on (i) the conversion of other cells to this chain length, (ii) its own evolution to the other morphologies and (iii) its own growth during the process. With this, the ordinary differential equations (ODEs) were defined for the system (Eq. 12-16), where the growth rate was calculated based on Eq. 17 (i.e. Eq. 6 incorporated into Eq. 3).

$$\frac{dC_{1c}}{dt} = r^{S,2c} + \frac{1}{3} \cdot r^{S,3c} + \frac{1}{4} \cdot r^{S,4c} + \frac{1}{5} \cdot r^{S,5+c} - r^{NE,1c} + \mu \cdot C_{1c} \quad \text{(Eq. 12)}$$

$$\frac{dC_{2c}}{dt} = \frac{2}{3} \cdot r^{S,3c} + r^{S,4c} + \frac{2}{5} \cdot r^{S,5+c} - r^{S,2c} + r^{NE,1c} - r^{LAE,2c} - r^{HAE,2c} + \mu \cdot C_{2c} \quad \text{(Eq. 13)}$$

$$\frac{dC_{3c}}{dt} = \frac{3}{4} \cdot r^{S,4c} + \frac{3}{5} \cdot r^{S,5+c} - r^{S,3c} + r^{HAE,2c} - r^{LAE,3c} - r^{HAE,3c} + \mu \cdot C_{3c} \quad \text{(Eq. 14)}$$

$$\frac{dC_{4c}}{dt} = \frac{4}{5} \cdot r^{S,5+c} - 2r^{S,4c} + r^{LAE,2c} + r^{HAE,3c} - r^{HAE,4c} + \mu \cdot C_{4c} \quad \text{(Eq. 15)}$$

$$\frac{dC_{5+c}}{dt} = -2r^{S,5+c} + r^{LAE,3c} + r^{HAE,4c} + \mu \cdot C_{5+c} \quad \text{(Eq. 16)}$$

$$\frac{dX}{dt} = \mu = \mu_{max} \cdot f_{lag} \cdot f_S \cdot f_P \cdot f_{pH} \cdot f_{pHmin} \cdot X =$$

$$= \mu_{max} \cdot \left(1 - e^{-\frac{t}{t_{lag}}}\right) \cdot \left(\frac{S}{S+K_S+\frac{S^2}{K_I}}\right) \cdot \left(\frac{1}{1+e^{K_P \cdot (P-K_{P1})}}\right) \cdot \left(e^{-\left(\frac{\left(pH_{opt}-pH\right)^2}{\sigma_{pH}^2}\right)}\right) \cdot \left(1 - \frac{10^{pH_{min}}}{10^{pH}}\right) \cdot X \quad \text{(Eq. 17)}$$

- ✓ The conversion rates constants (namely k^{NE}, k^{LAE}, k^{HAE}, k^{S} and $k^{S,5+c}$) were considered to be dependent on the pH oscillations encountered during growth and were the parameters to be estimated. The rest of parameters in Eq. 17 were taken from (Spann, Roca, et al., 2018).
- ✓ Since each initial data set (i.e. fermentation) possessed a different lag phase, the experimental data was normalized prior to be used as input for the model.

The parameter estimation was performed to fit the experimental cell size distribution (i.e. 1-, 2-, 3-, 4- and 5 or more cocci throughout the experiment or data set), with the initial conditions described in the publication (Paper V). The cocci chain length distribution during *S. thermophilus* cultivations under optimal growth conditions (i.e. without pH-gradients) was successfully predicted with the population balance model developed (**Figure 55** as an example). Moreover, substrate consumption, biomass production and the rest of off-line determined metabolites of the central carbon metabolism were also still accurately simulated (**Figure 56**). Additionally, the same parameter setup enabled the acceptable prediction of all variables when pH-gradients were induced, during both, single- and multi-compartment scale down experiments (Paper IV).

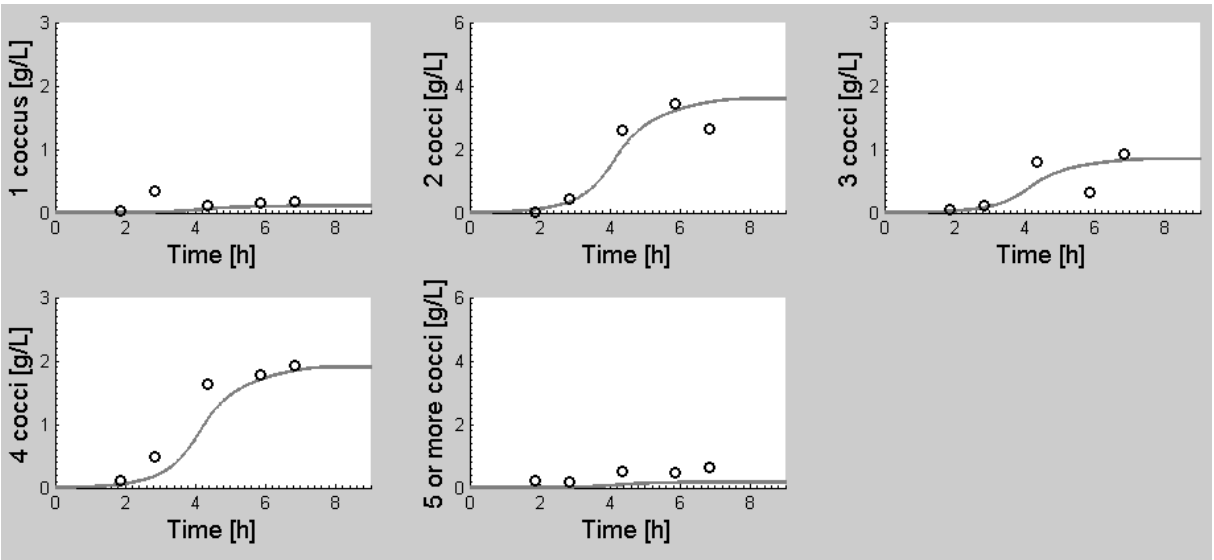

Figure 55. Experimental (empty circles) and predicted (lines) population heterogeneity (namely 1-, 2-, 3-, 4- and 5- or more cocci chains) throughout a *S. thermophilus* cultivation under optimal growth conditions in a 10 L STR with 70 $g \cdot L^{-1}$ initial C-source concentration.

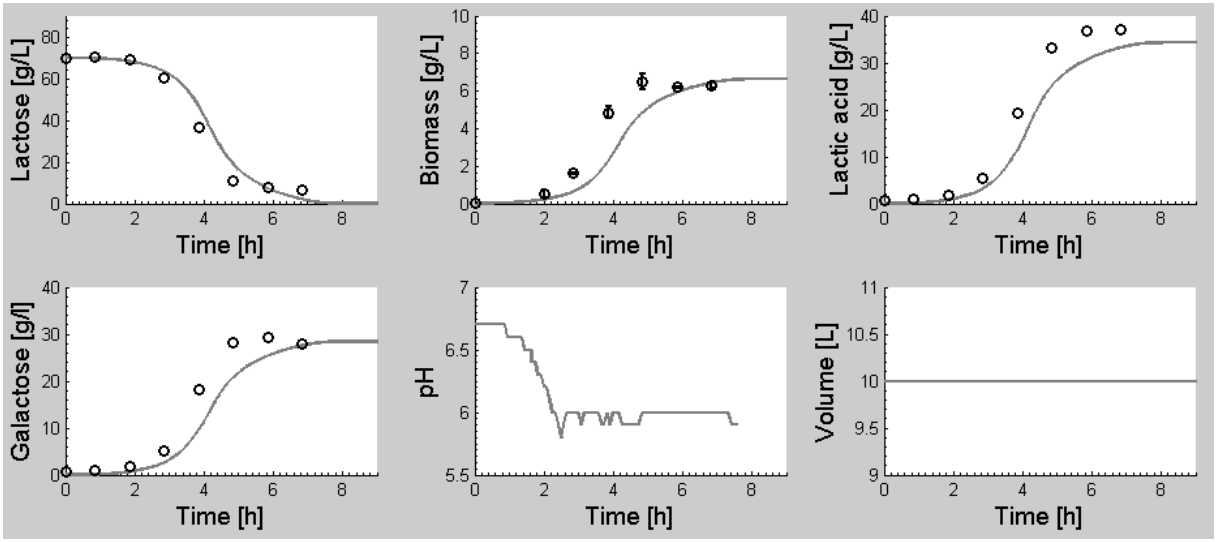

Figure 56. Experimental (empty circles) and predicted (lines) macroscopic variables (namely lactose, biomass, lactic acid and galactose concentrations as well as pH) throughout a *S. thermophilus* cultivation under optimal growth conditions in a 10 L STR with 70 $g \cdot L^{-1}$ initial C-source concentration.

The kinetic constants for the PBM under different pH-oscillations were obtained after modeling the four cultivation conditions (i.e. 1 L as well as 10 L STR under optimal growth conditions, 1 L Single-CSD and 10 L Multi-CSD with pH-gradients) at least in duplicates (**Table 9**), observing that:

- ✓ Both separation constants (i.e. k^{S} and $k^{S,\ 5c+}$) were 2x higher and k^{LAE} was 4x lower in 10 L STR fermentations than in 1 L STR experiments under optimal conditions, although a similar tip speed was used in both scales. Differences were rather attributed to a combination of factors of the rest of parameters.
- ✓ The rate of natural elongation (k^{NE}) reached its maximum value under optimal growth conditions (in both, 1 L as well as 10 L STR) mainly because 1-cocci chains were hardly detected under the microscope when no pH-gradients were induced. In the same direction, k^{HAE} took its minimum value under such gradient-free environments.
- ✓ Both, k^{S} and $k^{S,\ 5c+}$, were lower and k^{HAE} was noticeably higher under scale down conditions (in both, Single-CSD as well as Multi-CSD experiments) than under optimal STR conditions, basically because of the pH-gradients induced.
- ✓ k^{LAE} was almost not affected under Three-CSD experiments, but considerably influenced when base pulses were induced in Single-CSD reactors. Moreover, k^{HAE} was slightly higher in 1 L Single-CSD fermentations than during Multi-CSD cultivations. Both observations emphasize the fact that the whole population (i.e. 100 % of cells) were subjected to the gradients induced in Single-CSD experiments, while "only" a 20 % of the bacteria, and therefore less impacted on the cell division cycle, were in contact with pH-gradients during Three-CSD fermentations.

Table 9. Final biomass (i.e. DCW) and maximum pH gradient induced under optimal (1 L and 10 L STR) and scale down (Three-CSDR and Single-CSDR) fermentation conditions. Estimated kinetic parameters (k^{NE}, k^{LAE}, k^{HAE}, k^{S} and $k^{S,5+c}$) from the PBM after prediction of duplicates or triplicates of the different cultivation conditions. Taken directly from Paper V.

Experiment (replicates)	*Experimental*		*Population balance model*				
	DCW_{end}	**ΔpH_{max}**	**k^{NE}**	**k^{LAE}**	**k^{S}**	**k^{HAE}**	**$k^{S,5c+}$**
STR,10L,70g/L lac (n = 2)	5.4	+0;-0	1000.0	8.4	23.3	0.0	43.1
3CSDR,10L,70g/L lac (n = 2)	4.3	+2.0;-1.3	1000.0	5.6	9.2	288.2	31.9
STR,1L,70g/L lac (n = 2)	6.3	+0;-0	514.3	1.9	48.3	0.0	84.8
1CSDR,1L,70g/L lac (n = 3)	5.7	+1.3;-0.5	736.6	36.8	49.4	372.4	16.4

The rest of experimental data available from fermentations with Single-CSDR with larger pH-gradients (see **Figure 31**) was not used so far, since the central carbon metabolism was affected to such an extend, that the model with the highly disturbed measured pH as input, was no longer describing the growth kinetics. Importantly, the kinetic constants estimated within this PBM are completely arbitrary and it was impossible to compare the absolute values with any published literature. Nevertheless, the fitting of the experimental data available was satisfactory and the suggested parameters could allow the prediction of *S. thermophilus* growth under certain pH-gradients, if they would be measured throughout the fermentation with e.g. ISM techniques.

5. Discussion

5.1. Novel Process Analytical Tools applied to LAB Fermentations

The interest during the past decade in PAT and QbD from the regulatory authorities for (bio-) pharmaceuticals was clearly stated in the FDA and EMA guidance and recommendation documents, as well as in the quality guidelines from the International Conference on Harmonisation (ICH). In this context, on-line, in-line as well as at-line monitoring tools are considered to meet the specifications for product quality as well as process consistency (e.g. batch-to-batch reproducibility) during the entire production chain in the biotechnological, food and pharmaceutical industries and conform a relevant field in current research (Bockisch et al., 2019; Guerra et al., 2019). In this work (i) at-line electrooptical measurements of cell polarizability and size, (ii) off-line microscopic analysis followed by (iii) model-based population heterogeneity prediction were applied to LAB grown in complex, industrially relevant, media to assess cell viability characteristics for the first time.

5.1.1. Feasibility of Automated Polarizability Measurements in Industrial Scale (RQ1)

The application of electrooptical polarizability measurements to *L. plantarum* (**Figure 2** - **Figure 5** and **Figure 7**) as well as *S. thermophilus* (**Figure 8** - **Figure 14**, **Figure 20**, **Figure 37** and **Figure 46**) allowed a better insight into cells' integrity and viability during their cultivation across scales. Furthermore, the AP level seems to be an early indicator of limited nutrient availability and of the end of fermentation point. Similar observations had been previously published for *E. coli* (Bunin et al., 2004; Junne et al., 2010), *C. acetobutylicum* (Junne et al., 2008) and *C. glutamicum* (Lemoine et al., 2015). Nevertheless, for such a PAT tool to be applied in the industrial production of starter cultures, reliability across scales needs to be proven. The at-line electrooptical measurements in 2 L and 700 L fermenters was well reproducible (**Figure 20**). Moreover, the industrial partner allowed the application of electrooptical measurements in an industrial scale (several m^3) *S. thermophilus* fermentation with "similar" cultivation conditions than those performed in the lab and pilot scales. The results thereof are confidential and have not been disclosed in this work, but the experiment provided relevant data. Despite the fact that the media in production was slightly different than in the cultivations carried out in this thesis and thus (i) the lag-phase was considerably extended and (ii) the sample preparation had to be manually performed, the AP level at 400 kHz decreased regularly before the growth rate. The application of electrooptical monitoring steps allows to monitor and control a process easily based on the vitality of the culture without the measurement of secondary parameters: with further evidence that the AP level is a measure of the cellular physiology and, as such, one of the guiding parameters of cellular activity, cooling and harvesting preparation of the bioreactor could be scheduled according to this state. The current decision on the termination of fermentation is taken based on the base addition rate (i.e. a macroscopic chemical parameter linked to LAB growth), which actually represents the result of a performance loss. Similarly, on-line off-gas analysis of the CO_2 production rate also measures the consequence of an affected cell membrane, with lower ion transport and a concomitant physiological and transcriptional cell response (Abbott et al., 2008). Nevertheless, electrooptical measurements would provide a direct measurement on cells' metabolic activity at-line, also providing parameters causing a performance loss, like a low cell polarizability, but earlier, since it informs directly about cell

viability. In fact, this has been corroborated at own results. The cell polarizability could be even used as quality check in further processing steps (e.g. bioreactor cooling, biomass centrifugation and freeze-drying, etc.), so that biomass activity would be measured (and ideally maintained) in the whole production (Gomes et al., 2015). In fact, the last sample prior to bioreactor harvesting in the production scale was still analyzed by means of electrooptical measurements and resulted to show a 15 % polarizability reduction at 400 kHz compared to the previous sample (taken half an hour before). Growth rates are typically low at low temperature, which in turn increase the availability of essential metabolites (ATP included) for bacteriocin production, for instance (Abbasiliasi et al., 2017). Bacteriocins and bacteriocin-producing cultures have the potential to increase the shelf-life of foods and contribute toward decreasing the incidence of food-borne diseases. According to the authors, with a low growth rate there is a better utilization of energy resulting in enhanced bacteriocin production. The authors deduced from the reports reviewed that the most critical physiochemical factors which play a crucial role and exert a significant effect on bacteriocin production by bacteriocinogenic strains are pH and temperature:

- ✓ Since the synthesis of bacteriocin is enhanced at a relatively low growth rates, its production by some LAB is enhanced at non-optimal growth conditions. In fact, reduction in pH as well as temperature usually decrease enzymatic reactions, which in turn, reduce the growth rate of the bacterium. The positive effect is therefore on bacteriocin synthesis as a result of net increase of essential metabolites including ATP.

- ✓ An increased growth rate did not necessarily enhanced bacteriocin production. At high pH, bacteriocin production is lower because energy requirements for maintenance purposes are higher when pH increases.

- ✓ Maintenance operations, such as turnover of macromolecules (DNA, RNA) and maintenance of the potential along the membrane of cells are growth dependent and faster growth rates mean more energy is required for maintenance. In this context, evidence of this can be found throughout this work (e.g. **Figure 20**): the highest mean cell polarizability was detected at the highest growth rates under optimal growth conditions. Once the growth rate was affected (either by depletion of essential nutrients or by induced oscillating pH conditions), the AP level decreased in parallel with μ.

Furthermore, a typical freeze-drying process of LAB needs optimization of pressure, heating plate temperatures and frozen pellet bed thickness in order to obtain an appropriate water activity, cell count and shelf-life stability (Fenster et al., 2019; Fonseca et al., 2014; Passot et al., 2015). (Bensch et al., 2014) concluded that low temperature fluidized bed drying of *L. plantarum* caused membrane damages and high cell death: the VCC decreased a 50 % and the percentage of PI-stained cells was multiplied by five after drying. Additionally, (Shu et al., 2017) increased significantly the survival rate of *S. thermophilus* freeze-dried powder by the addition of a combination of sucrose, soluble starch and ascorbic acid as cryoprotectants (control = 4 %; optimized = 70 %). In Paper I, it was proven that the AP level at 400 kHz is a meaningful parameter to identify suitable harvesting stages prior to freeze-drying for the further use of *L. plantarum* biomass as a probiotic compound. Therefore, electrooptical measurements of LAB polarizability could be used as KPI during experiments for the optimization of freeze-drying conditions.

Interestingly, EloSystems GmbH (Berlin, Germany) has recently developed and patented a new equipment (named μCheck), which is capable of measuring OD, cell concentration and size without any sample preparation. Therefore, these attributes can be determined in a by-pass directly connected

to the fermenter through a glass measuring chamber (0.6 mm in diameter). This would then be an on-line approach for the analysis of bacterial morphology, which could potentially provide relevant information, without the need of off-line microscopic analysis.

5.1.2. Improvement on Microscopic Image Analysis (RQ2)

In this work, it has been demonstrated that microscopic analysis of LAB morphology can provide relevant information about the actual physiologic response to certain oscillations, mainly pH-gradients (**Figure 31** and **Figure 45**). Additionally, those observations were successfully predicted by means of population balance modeling with kinetic parameters describing cell division events (**Figure 55**). The current limitation of applying an in-line or on-line control strategy relies on the at-line analysis of bacterial cell size. Just in recent years, advances in microscopic technology have enabled the quantification of polyunsaturated fatty acid accumulation by microalgae (Marbà-Ardébol et al., 2017) and the real-time monitoring of the budding index in yeast cultivations (Marbà-Ardébol, Emmerich, et al., 2018). It is worth mentioning that, the ISM approach described by (Marbà-Ardébol et al., 2019) was applied in a sterilizable by-pass (on-line) during both, *L. plantarum* as well as *S. thermophilus* fermentations (**Figure 9**). Cultivations with and without pH control (**Figure 13**) were performed, while the aim was to compare the cell size distribution obtained on-line by ISM with conventional microscopy. The first results were promising as they proved the feasibility of the measurement of the cocci chain length distribution during *S. thermophilus* fermentations, although more data needs to be gathered to prove statistical validity. In-line acquired microscopic pictures are processed with artificial neural networks (ANNs). If coupled to the PBM developed, a QbC strategy in the industrial production of LAB may be possible: real-time measurement of population heterogeneity in the fermenter with PBM update after each analysis point, which would predict process performance in the next hours. This would lead to a soft-sensor for LAB cultivations (Spann, Roca, et al., 2018) or (Spann et al., 2019), but describing cocci chain length distribution, and thus considering population heterogeneity. The model output could then be connected to the stirring speed or the base addition rate (feedback loop control) to ensure a maximum population homogeneity throughout the cultivation, thus maximizing biomass yield, while maintaining product quality (Delvigne, Baert, et al., 2017; Pörtner et al., 2016; Randek & Mandenius, 2018; Simutis & Lübbert, 2015). As an example, (Lyubenova et al., 2013) designed a soft-sensor considering oscillating conditions during *B. subtilis* STR-PFR Two-CSDR experiments (to simulate industrial scale nutrient-limited fed-batch conditions) focusing on the substrate uptake rate and corresponding yield coefficients. Additionally, (Schaepe et al., 2014) developed a data-based modeling approach to find the specific growth rate profile of *E. coli* cultivations after induction that maximized the total amount of GFP. Moreover, software sensors were also applied for monitoring biomass concentration as well as kinetics during continuous yeast fermentation with immobilized cells (Kostov et al., 2015). (Craven et al., 2014) used an in situ Kaiser RXN2 Raman spectroscopy instrument to monitor the glucose concentration at 6 min intervals and update a non-linear model predictive controller, thus maintaining a fixed set-point of glucose concentration in a closed loop during a CHO mammalian cell fed-batch process. Special emphasis into model-based bioprocess control in mammalian cell culture has been put recently (Farzan & Ierapetritou, 2017, 2018; Narayanan et al., 2019; Paul et al., 2019; Sommeregger et al., 2017), probably because of the high-added value products typically manufactured thereof. Specially interesting literature has been found for fungi: a DO% control strategy for optimizing growth as well as enhancing the production of a phenolic compound (Wei et al., 2017) and (Wang, Chu, et al., 2019) published a dynamic model

describing *P. chrysogenum* growth and penicillin production based on quantitative metabolomics to simulate the fermentation process and design the fed-batch fermentation media, by cultivating the fungi in a fed-batch fermentation with fully U-^{13}C-labelled substrates. Furthermore, some authors have used feedback control strategies based on the off-gas analysis (mainly RQ = % CO_2/% O_2) to reach high cell density fermentations of *S. cerevisiae* (O'Connor et al., 1992; Shang et al., 2006) or improve production of polydroxyalkanoates by *R. eutropha* (Pederson & Srienc, 2004). Nevertheless, the off-gas analysis, mainly CO_2 production rate in LAB, would be a measurement of the consequence of generally affected cell membranes, but morphological analysis would provide information on the single-cell level. To date, no scientific work taking population heterogeneity as control parameter and applied to LAB has been found.

Interestingly, BioSense Solutions Aps (Farum, Denmark) developed the oCelloScope instrument, a compacted morphology investigation device, just a few years ago. This technology has successfully been applied to crystallization processes monitoring as well as to microbial and cancer research, conducted on micro titer plates. Recently, the equipment was successfully applied in yeast for analysis of the budding index (Pontius, 2019) and lately, to investigate the effect of decreasing the cultivation pH during *L. acidophilus* growth by means of cell size distribution (Narayana et al., 2020). These bacteria are also LAB and in the order of magnitude of the *S. thermophilus* cocci chains, so that the oCelloScope could potentially also be used to study morphological changes throughout LAB cultures in the future.

5.1.3. Application of PBM in Industrial LAB Production (RQ3)

Bacteria have developed an impressive ability to survive and propagate in highly diverse and changing environments by evolving phenotypic heterogeneity, thus ensuring that a subpopulation is well prepared for future environmental changes. In fact, the selection environment changes and favours different phenotypes at different growth times (De Jong et al., 2011). Furthermore, most microbial communities consist of a genetically diverse assembly of different organisms and the level of genetic diversity plays an important part in community properties and functions. However, biological diversity also arises at a lower level of biological organization, between genetically identical cells that reside in the same microenvironment. Cell surrounding environments are characterized by microscale chemical and physical gradients, both temporal and spatial, and microorganisms continuously adjust their phenotypes in response to these gradients (Ackermann, 2015). Depending on the environment and selective pressures, particular strategies ranging from purely deterministic mechanisms to those that exploit the randomness intrinsic to many cellular and molecular processes (Van Boxtel et al., 2017) have been developed. In this context, the cell size for a particular bacterial species typically falls within a narrow distribution at a steady growth condition, but the size of a single bacterium can even vary substantially across growth conditions. (Cesar & Huang, 2017) reviewed how rod-shaped bacteria adjust their size with changes in growth rate, by means of nutrient, mechanical and genetic factors, and concluded that the cell size is clearly a readout of physiological parameters such as growth rate. This is why, morphological changes as stress responses to potential industrial gradients (mainly pH in the production of starter cultures) affecting the growth rate were investigated in this work. Different microorganisms modify their size as an influence of extracellular pH-gradients (see Scientific Background), but LAB are specially adapted to those changes, specially toward acidic environments (Papadimitriou et al., 2016). (Wang, He, et al., 2018) just recently performed a deep metabolomics and morphologic analysis after *L. pantarum* were opposed to acid and alkali stress. For instance, based on

microscopic analysis, the morphology of the bacteria became thickset and the thickness of their cell walls decreased under high pH values. Their findings also demonstrate that energy metabolism was affected under different pH environments. Additionally, the authors observed an influence on the amino-acids metabolism, especially on those amino acids that are related to pH-homeostasis mechanisms (i.e. lysine, aspartic acid, arginine, proline and glutamic acid). Nevertheless, no studies about morphological changes of *S. thermophilus* under oscillating pH values are available and their influence on the cell division cycle is still not completely elucidated (see Scientific Background). In summary, alkali environments resulted in increased chain lengths, while at an acidic pH a trend toward shorter chains was detected (**Figure 31** and **Figure 45**) when the cocci chain length distribution was compared to optimal conditions. These observations served to develop the PBM presented in 4.3.2, but a deeper investigation toward understanding the elongation/separation events during growth under certain pH-gradients should be performed. For instance, in the ODEs of the model (Eq. 12-16), the growth rate was included in the event rates (conversion of the morphologies) as well as in the own growth of a particular population (i.e. $\mu \cdot C_i$ for i = 1c, 2c, 3c, 4c and 5+c). The idea behind was to separate the exact moment of elongation into another population or of separaton into two populations from the actual growth or cell division of each population. Without the individual growth terms (i.e. $\mu \cdot C_i$), only the initial populations would play a role in the conversion scheme (**Figure 54**), but actually each population also grows over time and contributes to the overall biomass production. Therefore, $X = C_{1c} + C_{2c} + C_{3c} + C_{4c} + C_{5+c}$, $\mu \cdot X = \mu \cdot (C_{1c} + C_{2c} + C_{3c} + C_{4c} + C_{5+c})$ and $r_X = r_{1c} + r_{2c} + r_{3c} + r_{4c} + r_{5+c}$. In this study, the growth within each coccus was assumed to be the same, although this is an assumption for model simplification. No literature reports any observation of the growth in single cocci of *S. thermophilus*. In this context, an isolation and growth observation in single cocci would need to be performed, for example, using microfluidic devices coupled to improved microscopic analysis. The morphological changes of a single chain should be monitored over time under pre-defined pH conditions, in order to investigate the elongation/separation events undergone in different pH environments. Platforms similar to (Fomina et al., 2016) should be employed, so as to ensure spatiotemporal pH control in such constrained volumes.

(Fernandes et al., 2013) compared experimental with mathematical dynamics of *S. cerevisiae* size and cycle position distributions, in response to the substrate consumption observed during batch cultivations. The good agreement between the proposed multi-scale model (a PBM coupled to an unstructured model) and experimental data, indicated that a mechanistic model is a suitable tool for describing the microbial population dynamics in a bioreactor. Thus, a mechanistic (Spann, Roca, et al., 2018) coupled to a population balance model was suggested in this work in order to understand the development of heterogeneous populations during *S. thermophilus* fermentation under different pH-gradients (Paper V). The evolution of the considered populations was successfully predicted at variable pH-oscillating conditions (see Paper V). In case of an overestimation of the population of 5+ cocci chain lengths by the simulation, most likely separation not only at one site, but multiple sites within the chain happens at the same time. Since the mismatch in the prediction occurs under mild stress conditions, it is assumed that separation mechanisms, as response to unfavourbale growth conditions, follow different patterns than under stronger environmental perturbations. Further separation events could be considered in the model, but this would lead to an impact on the sensitivity of individual parameters, and probably to a large equation set that is not required under most of the cultivation conditions, and subsequently to overdetermination. The main purpose of the PBM developed in this work was to simulate population heterogeneity under ideal growth conditions as well as under pH-

gradients, as they occur during *S. thermophilus* production in the large scale (rather emulated in Multi-CSDR experiments, as discussed below). Since the mass accumulation, that is the volumetric growth rate, was regarded as separate event within a coccus as pre-requisite for elongation events to form longer cocci chains, it was included as a term in the right side of the population balance equation. This is in contrast to proposed models of granulation and aggregation in PBMs as they are applied e.g. in wastewater treatment (Nopens et al., 2015). Other PBMs are applied to describe the volumetric growth rate by growth rates of individual cells. Then the right term of the PBM describes cell growth ("birth term") and divison ("death term"). Following this terminology, the volumetric cell growth represents, together with the elongation events, the birth term in case of cocci chain formation, and cocci separation the death term. The left side of the equation represents the cocci chain length distribution as a result of the individual concentration of cocci chains. The inversion of the sign of the growth rate means that the elongation rate in the birth term is the residual amount of events that are not originated due to the growth of the culture. That means they are time decoupled and thus represent elongation as prolonged separation event or terminated separation. The aim of this decoupling of PBM dynamics describing terms from growth events is to describe solely what is recognized as growth disturbance due to environmental growth conditions and the resulting stress response of the organism. Nevertheless, the different events are rated differently as an elongation, although regarded as a disturbance in general, is classified in natural and non-natural elongation to distinguish between small process disturbance with no or only small impact on the overall process performance, and heavy disturbances. This further classification can support any event recognition, with which, if the cocci chain length distribution will be available, the elongation and separation patterns can be chosen and the remaining growth rate can be estimated. The choice of the state of elongation and separation will support any identification of suitable and unsuitable growth conditions. If a full distribution of the cocci chain lengths is available, the identifiability of the corresponding growth rate shall be high. The application of such a methodology has to include a sensitivity analysis at a larger data set that goes beyond the present study.

What is more, all model predictions were based on arbitrary model parameters (event rate constants k^{NE}, k^{LAE}, k^{HAE}, k^{S} and $k^{S,5+c}$), which have never been described before in literature and cannot be experimentally confirmed without performing single-cell morphology investigations varying media pH. Firstly, a statistical analysis (i.e. standard deviation, 95 % confidence interval, coefficient of variation) of these parameters should be performed to see the variability of the model prediction. Furthermore, sensibility as well as uncertainty analysis should also be considered before using model-based predictions to improve the industrial process: if all the parameters of the original publication describing μ would also be considered in the parameter estimation, the model would end up with a large parameter set. In this context, (Anane, López C, et al., 2019) recently published an algorithm to determine the presence of non-identifiable parameters in models with high output uncertainty, by exploring the numerical properties of the sensitivity matrix. Additionally, the framework proposes a regularization technique, in conjunction with Monte Carlo Analysis. This methodology, applied to a macro-kinetic growth model describing *E. coli* fed-batch cultivations (Anane et al., 2017), resulted in a reduction in the uncertainty of model outputs from a maximum CV% of 748 % to 5 % after regularization as well as a 15-fold improvement in the accuracy of model predictions for two independent validation datasets.

Already some years ago, constraint-based modeling of genome-scale metabolic networks gained significant interest, also for LAB (Pastink et al., 2008) and even specifically for *S. thermophilus* (Pastink

et al., 2009). These models only act at the metabolic level so far, and hence, they miss much biology and the corresponding relevant constraints that are needed to explain many adaptive phenomena relevant for LAB, like population heterogeneity. The main limitation relies on the fact that stoichiometric models predict yields (not always related to cell activity), while, in most experimental setups and in nature, growth rate is more important for fitness and correlates with metabolic activity (Bachmann et al., 2017). The same authors introduced the new concept of protein pool trade-off or resource allocation perspective, i.e. the idea that cellular resources are limited and, hence, provide constraints on the functioning of cells. At the end, trade-offs exist in a microorganism between the synthesis of proteins for different metabolic pathways: proteins invested in growth cannot be invested into stress resistance or alternative nutrient uptake systems, for instance. This perspective has been very powerful in explaining many aspects of metabolic regulation, at least in model organisms such as *E. coli* (Schmidt et al., 2016) and *S. cerevisiae* (Keren et al., 2016), and may therefore also be true for LAB (Teusink et al., 2011) and included in the model-based prediction of their growth. Considering the utilization of different resources in case of longer chains (savings by intercellular exchange of protons, ions and other molecules to save energy) might lead to an even better understanding of the reason for cellular dynamics, including the formation of chains and the evolution of population heterogeneity and optimal cell states depending on the environmental growth conditions.

5.2. Scale down Model for pH-Gradients Appearing in Large scale LAB Processes

In large scale production of LAB, cells are presumably subjected to pH-gradients. These possibly result in inhomogeneous growth conditions within the fermenter and can affect cell yield. In this work, different scale down approaches at the laboratory were applied to analyze the effects of these heterogeneities on *S. thermophilus* growth and morphology:

a) One STR with intermittent acid and base pulses experienced by the whole cell population (**Figure 28** and **Figure 29**).

b) Single STR with pH shifts, experienced by the whole population (**Figure 31**).

c) Two- or even three- comparted STRs with 50 % or about 6 % of the volume, respectively, in the base addition vessel (**Figure 34** and **Figure 36**, respectively).

d) One STR connected to one or two PFRs with a working volume of 10 or 20 % of the whole population, which is either confronted with base or with acid pulses in the respective PFR modules (**Figure 42**).

With them, it was possible to simulate a wide range of pH-gradients/stress conditions that LAB may encounter in the production scale (several m^3). But which scale down design is the best option? The one that better simulates the hydrodynamics and cell responses in the industrial fermenter? This is one of the most typical questions in every scale down approach, the answer depends on on the knowledge of conditions in the large scale, which are usually neither measured nor known. Unfortunately, most of the information from large scale cultivation was also not available from the industrial partner in this study. Nevertheless, it was possible to compare some parameters across scales, like the cocci chain length distribution and the growth rate. Scale down conditions were then changed until the large scale performance was obtained.

5.2.1. Single- or Multi-compartment models? (RQ4)

With the experience acquired throughout the application of the scale down strategies described above, each of the lab simulator can be applied to simulate industrial scale pH-gradients, depending on the aim of the investigation. For example, long pH shifts can be induced in a one-compartment bioreactor, so that the whole cell population is subjected to the stress at the same time, thus monitoring cell response throughout a relatively long response time. This can be compared with short pulses to a culture, in which only a portion of cells is subject to unfavourable growth conditions. If the response behaviour differs, segregation of the whole culture in scale down is sensitive. This was observed for the re-assimilation of by-products, which were accumulated under unfavourable growth conditions in *C. glutamicum* cultivations: if these were consumed by other cells in the compartment with favourable growth conditions, the accumulation had nearly no effect (Käß et al., 2014). In case of LAB, however, a changed secretion of any by-products due to pH-gradient formation is hardly observable. It is assumed that differences of the responses of LAB between Single- and Multi-compartment scale down experiments are small, as also seen at the experimental results of this study. The impact on sequences and magnitudes of pH-gradients seem to be larger. If intercellular proton transport from cells with an adjusted pH_i to cells that just passed a zone of high pH will happen, then a distinctly different response pattern would be seen in Multi-compartment reactors. The adjustment of the cytoplasmic pH of many LAB species to the pH of their environment has long been observed (Kashket, 1987). One of the detrimental survival strategies of LAB is the adjustment of the pH_i to the environment rather than keeping a stable pH_i by increasing the gradient (Papadimitriou et al., 2016). Hence, after a base pulse toward all cells at the same time, the adjustment of the pH_i would require a larger amount of protons penetrating into the cells. Although a higher concentration of free protons will be available at a lower pH, it can be changed if the adsorption of protons by cells are large. This effect would be smaller if a portion of cells which remained longer at favourable growth conditions, would produce higher amounts of lactic acid and act as proton donor. (A similar condition in opposite direction would appear from an acid pulse toward a favourable growth condition.) This effect can be visible especially if cells circulate rapidly between a basic and an acidic environment, where “recreated” cells recently grown under favourable conditions would act as an additional proton source or sink. This might be also one reason for different outcomes if Single- or Multi-compartment systems are compared in this study, although the pH perturbations, in particular the frequencies, were not exactly the same among the different scale down designs, which as such originate in different results.

Beside the questions of compartments, the frequencies that are applied, have a big impact on the outcome. Just recently, (Wang, Chu, et al., 2019) revealed gross differences between single and repeated glucose pulses induced during *P. chrysogenum* fed-batch fermentations, which suggests that single pulse studies have limited value for understanding of metabolic responses in large scale bioreactors. Instead, intermittent feeding should be favored. In this work, a notably different effect on biomass productivity was observed when relatively long pH shifts (see **Figure 31**) or intermittent pH pulses (see **Figure 28**) were induced during *S. thermophilus* fermentation: intermittent high pH values (DpH = +1.0) resulted in a 40 % biomass productivity loss (**Figure 30**), while an ammonia pulse to increase the optimal pH until 8.0 was needed to accomplish a similar decreased performance (**Figure 32**). On the contrary, if the objective consists of simulating a specific zone of the large scale bioreactor prone to encompass concentration gradients, Multi-compartment scale down models are more suitable. When connecting several STRs, this is achieved by maintaining the liquid volumes constant between vessels, which is a challenging task if gravimetrical control is not available and the liquid

height is controlled by pumping through the connecting tubes (foam formation). If a STR is connected to one or more PFRs, this limitation is overcome and, generally, a 10 % (in each PFR) of the population is under inhomogenous conditions. A further advantage of this setup is that sampling ports along the height of the PFR allow the time resolution of the cellular response to the pulses induced. In scale down cultivations described in this work, the volume of the PFR was always a 10 % of the STR, sampling was only performed from the well-mixed STR and a residence time in the PFR was set to 2 min with the slowest pump rate.

Finally, the magnitude of pH-gradients has the greatest sensitivity on the results. Experimental conditions in this study induced pH-oscillations ranging from +2.0 and +2.5/-1.0 during Two- and Three-CSDR fermentations (**Figure 42**). In a recent publication, (Olughu, Nienow, et al., 2019) induced pH-gradients in a STR-PFR Two-CSDR strategy: residence times of 1, 2 and 5 min in the PFR were setup, but maintaining a constant frequency of cell entrance rate and thus subjecting a 10.5 %, 21 % and 52.5 % of the *C. glutamicum* population to the induced gradients, respectively. With this strategy, the authors induced pH-gradients in the range from 6.2 to 7.6 along the PFR (pH control = 7.0). The intermittent pH pulses in this publication cannot be compared with the ones induced in this thesis, because LAB are the microorganisms that lower the most the media pH, thus ending up with relatively higher basic excursions. Scale down results showed a decreased cadaverine (product) production of 26 %, 49 % and 59 % with increasing residence times, respectively, compared to the control cultivation. Furthermore, 3.1-fold more CO_2 than in the control was produced with t = 5 min, but no biomass productivity losses were observed. Nevertheless, the population of viable-but-non-culturable cells increased with the magnitude of fermentation gradients. The authors finally concluded that, the higher the ΔpH the more energy was used by cells to maintain a constant pH_i, reducing the amount of ATP for other cellular functions (e.g. cell division). They also stated that pH homoeostasis is controlled by the dynamic influx and efflux of ions across the cytoplasmic membrane, thus fluctuating cells' membrane potential as a response to the external pH oscillations. As previously stated, most LAB maintain a gradient to the environment rather than a stable pH_i, which has several, yet not clarified impacts on the response patterns to environmental pH-gradients. During *L. rhamnosus* scale down cultivations (STR-PFR) with pH shifts up to 0.88 units, four stress related genes were identified: *groEL*, *hrcA* and *atpA* (Wallenius et al., 2011). Among them, the latter translates to a subunit of a proton transporter, responsible for pH_i homeostasis. The expression of this gene was induced the most when there was the highest pH upshift (i.e. under basic conditions). This is considered to compensate for the reduced proton motive force at high external pH (Maurer et al., 2005). In further scale down studies published by the same authors and using the same LAB, the expression of another four stress related genes (*fat*, *hrcA*, *groEL* and *pstS*, in this case) for heat shock, phosphate uptake and control of cellular fatty acid composition correlated with a certain amplitude and frequency of the oscillations, i.e. ΔpH_{max} = 1.0 (+0.5;-0.5) (Wallenius et al., 2012).

(Enfors et al., 2001a) reported a response time for *E. coli* <14 s (first port of the PFR), detected by measurement of mRNA levels of genes expressed in a stress-dependent environment. This stress response of cells repeatedly exposed to pulses of high glucose concentration and an increasing degree of oxygen limitation relaxed in the STR, because bacteria were a mean residence time of 10 min in the glucose limited and oxygen sufficient zone (half life of mRNA of a few minutes). In this work, a residence time of 120 s in the PFR during *S. thermophilus* fermentation in a Two-CSDR with ammonia fed at the bottom of the PFR (pH_{max} = 7.5; ΔpH = +1.5), while controlling the pH in the STR, resulted in a lower STY and a retardation of cell division as well as metabolic activity (**Figure 43** and **Figure 44** A, B

and **Table 9**). Based on quantification of the pH-gradients encountered by these LAB in a 700 L pilot scale bioreactor (Paper III; pH_{max} = 6.3; ΔpH = +0.3), the pH oscillating conditions induced during Multi-CSDR experiments might be exaggerated. Nevertheless, without the exact knowledge of hydrodynamics and detailed process as well as vessel descriptions in the industrial scale (tens of m^3), a conclusion cannot be drawn. This is why, a scale down approach, relatively easy to implement and generally applicable to any bioprocess, is suggested in this work: firstly, process performance should be determined in the production scale with all PAT tools available to measure the most relevant CPPs, CQAs and KPIs. Then, different scale down approaches (Single-, Multi-CSDR, etc.) would be screened in the lab, by means of the same PAT tools, and only the setup providing the most similar process performance to the one measured in the large scale would be selected. This methodology considerably differs from (Haringa et al., 2016), since the authors suggest to develop a CFD model for each bioreactor and a metabolic model for each microorganism to end up with rather inflexible Euler-Lagrange method, difficult to be implemented across scales and bioprocesses. (Anane, Sawatzki, et al., 2019) also propose a different downscaling approach, in which, firstly, a mechanistic model is developed and the parameter estimation is performed against cultivations under optimal conditions. Then, a new parameter estimation is carried out to fit the experimental data to certain induced and assumed oscillating conditions, thus ending a up also with a rather specific scale down model for the bioprocess studied. In this work, rather the methodology of an iterative scale up and scale down approach, where knowledge is gained from the large scale and mimicked in the small scale, is proposed (Neubauer & Junne, 2016). A lack of resolution and measurement methods could be surely partly replaced by model approaches for a better description of the conditions in the large scale (like the PBM proposed in Paper V of this work), but should be accompanied by proven data similarity involving the single-cell physiology and morphology across scales (Delvigne et al., 2018).

It is worth mentioning, that scale down experiments in 1, 2 and 10 L bioreactors were performed at a tip speed of 200, 300 and 400 rpm, respectively, while the cultivation in the pilot scale 700 L fermenter was performed at 132 rpm (Paper III). The effect of mechanical shear stress on the chain length distribution in *S. thermophilus* cultures or other LAB have not been studied so far, but might be relevant, specially when the cocci chain elongation/separation are investigated and define cell size distribution, taken as pH-stress indicator as well as scale up&down criterion in this work. It is assumed, however, that the similar order of magnitude does not have a huge effect as a comparison between stirred and shaken systems would eventually have. Already more than two decades ago, (Hewitt et al., 1998) concluded that there were no detectable changes in off-gas analysis or optical density during continuous *E. coli* fermentations run at 400 and 1,200 rpm stirring speed. Moreover, cell size remained unchanged and cells presented intact membranes under all studied mechanical stress conditions, except after 7 h at the maximum tip speed, when the outer polysaccharide layer on the cell was stripped away. In case of *S. thermophilus*, similar or even higher shear forces have to be applied to achieve a remarkable impact on the chain length (Jaros et al., 2018). The authors observed that just an energy input of 2.50 $kJ \cdot mL^{-1}$ lead to a substantial increase in the portion of smaller cocci chain lengths, which is some orders of magnitudes higher than what is usually achieved at rpms between 400 and 800 in a STR (Devi & Kumar, 2017).

One of the major limitations of scale down experiments is the inability to sample cells at the right physiological state in a multi-compartment or pulse-based system (Van Gulik et al., 2013). Accurate sampling within the gradient field of scale down bioreactors is essential to capture the responses of cells to the specific stresses being investigated. The introduction of static mixers and spatial sampling

points along the length of the PFR module in multi-compartment scale down bioreactors is a good example for improving sampling possibilities in this setup (Junne et al., 2011). Another improvement to connect scale down studies and systems biology research to understand the intracellular regulation patterns at stressfull cultivation conditions are automated rapid sampling devices, which enable to capture the immediate response of the cells to fast perturbations as e.g. the BioScope (van Gulik, 2010), a microtube that can be operated similarly to a plug flow module of a scale down bioreactor. It was applied to mimic some stress induction zones, such as oxygen depletion with residence times of up to 70 seconds, during which the culture was exposed to oxygen limiting conditions (De Mey et al., 2010). This device and other rapid sampling techniques for general bioreactors (Schädel & Franco-Lara, 2009) allowed the elucidation of in vivo kinetic responses of cells to large scale heterogeneities (Lara et al., 2009; Visser et al., 2002). The application for pH gradients would be possible as well.

The rapid sampling also enables the analysis of intracellular metabolite pools by metabolomics techniques, which can be used to detect cellular responses that are not observable in the extracellular space. In this context, (Carnicer et al., 2012) used quantitative metabolomics to study the effect of pO_2 gradients on free amino acid pools in *P. pastoris* expressing a recombinant protein. Their results show that oxygen limitation leads to a rapid build-up of intracellular free amino acid pools, which results in low recombinant protein production rates. Moreover, advanced proteomics and gene expression analysis has enabled complete proteome-wide evaluation of the effects of concentration gradients induced in *E. coli* scale down experiments, as reported elsewhere (Brognaux et al., 2014; Lara et al., 2009; Lara, Leal, et al., 2006; Simen et al., 2017). The application of such omics techniques (metabolomics, transcriptomics, proteomics), could also enable the detection of up- and down-regulation of certain genes under stressful cultivation conditions in LAB scale down bioreactors, with the associated elucidation of molecular level response to oscillations. The rapid flow-through sampling device with embedded cold quenching developed by (Lameiras et al., 2015) for *A. niger* chemostat cultures is an example that would be suitable for incorporation into multi-compartment scale down bioreactors. Stringent response (SR), in many organisms mediated by Guanosine-tetra or -penta phosphate (p)ppGpp and sigma factors, is a highly conserved bacterial stress response originally defined as a response to amino acid starvation, but nowadays recognized a response for a wide range of environmental stress conditions (Potrykus & Cashel, 2008). In fact, the SR induces large scale transcriptional alterations that ultimately lead to a physiological shift to a non-growth state of some LAB (Papadimitriou et al., 2016) and could be of potential interest as targets for further investigations at pH-stress responses.

5.2.2. Advantages of Considering Individual Cells (RQ5)

Genetically identical bacteria are known to exhibit single-cell heterogeneity under controlled laboratory conditions (Rainey & Kerr, 2010). These heterogeneous traits include macromorphologies, such as cell size, as well as biochemical properties, such as protein and mRNA content (Heyse et al., 2019). Cells can be partitioned into clusters of cells with similar traits, called phenotypes. The variation in phenotypes within sympatric isogenic populations is referred to as the phenotypic heterogeneity (Ackermann, 2015). In principle, a heterogeneous gene expression appears to be disadvantageous, as it may reduce the mean fitness of the population under the prevailing environmental conditions (Fraser & Kærn, 2009). Therefore, maintaining a homogenous cell population and avoiding phenotypic heterogeneity during cell growth should lead to final biomass (product) consistency, accompanied by enhanced bioprocess reproducibility (Delvigne et al., 2014), thus enabling the potential

implementation of (model-based) control strategies in the industrial production of LAB starter cultures. Nevertheless, how organisms adjust their cell cycle dynamics to compensate for changes in environmental conditions is an important unanswered question in bacterial physiology. A cell using binary fission for reproduction passes through three stages during its cell cycle: a stage from cell birth to initiation of replication, a DNA replication phase and a period of cell division. (Lieder et al., 2016) presented a detailed analysis of durations of *P. putida* cell cycle phases, investigating their dynamics under environmental stress conditions with flow cytometry. Furthermore, since the Raman spectrum of a single cell is a combination of the spectra of all compounds cells consist of (e.g., proteins, nucleic acids, fatty acids, etc.), the signal intensity at every wavenumber is the result of all compounds that produce a signal at this wavenumber. (Teng et al., 2016) proposed a single-cell-level biochemical fingerprinting approach named “ramanome” to rapidly and quantitatively detect and characterize stress responses of *E. coli* cellular population. In general, different methods for monitoring the intensity of population heterogeneity have been described elsewhere (Delvigne et al., 2015) and shall be considered in early stage scale up&down of LAB cultivations. Scale down should therefore not be seen isolated from developments in sensor and monitoring technologies.

If the premise of this work is correct, base addition during LAB fermentation could compromise culture performance due to the potential impact of pH-gradients in large scale bioreactors. Multi-position base addition could be a solution, even guided with additional multi-position pH measurements along the height of industrial scale fermenters, but implementation is still demanding and no reports of practical implementation are available.. (Hoshan et al., 2019) recently assessed the feasibility of utilizing control of sparge gas composition as part of the pH control loop in CHO fed-batch cultures. The effectiveness of the proposed pH control strategy was successfully transferred from 250 mL to 200 L scale. Nevertheless, the high acidification activities of LAB compared to mammalian cells would probably hinder the application of this approach to large scale starter culture production.

If other gradients than pH shall be considered during LAB batch cultivations, the dissolved CO_2 concentration can be regarded as critical. Most LAB, as experienced in the preparation of experiments of this thesis, require distinct dissolved CO_2 concentrations to avoid lag phases or reduced growth. This is hardly achievable from a certain scale on. CO2 is known from being involved in early stages of cell division and, therefore, oscillating CO2 concentrations in industrial scale LAB production may lead to lower process performances, compared to lab experiments. This might be especially crucial for non-sparged cultivations like typical LAB fermentations as hardly no control of such a parameter is then feasible.

6. Conclusions

In this work, at-line electrooptical measurements of cell polarizability and size with automated sampling and sample preparation were successfully applied to LAB *L. plantarum* and *S. thermophilus* in Paper I and II, respectively. In fact, the AP level is suggested as an early indicator of nutrient limitation and growth imbalance after results presented in this study, thus potentially becoming a new CQA in the industrial production of starter cultures. Furthermore, the polarizability is proposed as novel scale up and down criterion to transfer process performance across scales and therefore being an alternative or supplement to established on-line measurements (e.g. pH + offgas). Nevertheless, this device will only become a standard PAT tool in the industry if further studies are performed in order to elucidate the impact of relatively flexible cocci chains to the orientation of *S. thermophilus* to an applied electrical field. With this, the reliability of the electrooptical measurements and acceptance in the industrial production of LAB would be improved.

The hydrodynamics as well as pH-gradients encountered by *S. thermophilus* in a 700 L pilot scale fermenter were characterized, resulting in a minor influence on biomass productivity and mild pH oscillations (pH = 5.9 – 6.3 throughout the height of the vessel). This CFD study (Paper III) poses the bases for using this strategy to characterize fluid dynamics in larger industrially relevant bioreactors. A possibility to avoid such pH-gradients, apart from increasing stirring speed with a concomitant increase on the power input, would be to include multi-position ammonia addition with multi-position pH monitoring along the industrial fermenter, which would also need additional investment.

Additionally, Single- (Paper V) as well as Multi-CSDR (Paper IV) were used to simulate pH-gradients during *S. thermophilus* fermentations in the lab. The latter approach, in which a 10-20 % of the cell population is subjected to the induced gradients, was applied for the first time in LAB and was also the most suitable scale down methodology to induce pH-gradients. Nevertheless, the pH oscillations applied possibly exceeded the actual uneven distribution of the pH in the production vessel, but this could only be confirmed by properly characterizing the large scale bioreactor with appropriate PAT tools. Such approaches would allow an iterative scale up and scale down approach, where knowledge is gained from the large scale and mimicked in the small scale, using the suitable PAT toolbox. Shifts of the pH value performed in Single-CSDR affected biomass productivity and cell morphology to an unrealistic extend because the whole population was exposed to even ΔpH = 2.5.

Microscopic analysis of morphological changes of LAB enabled the consideration of population heterogeneity throughout the vast majority of experiments performed in this work. Interestingly, a tendency toward extenden cocci chains was observed under alkali conditions, while shorter chain were normally detected at low pH. A mechanistic model describing bacterial growth dynamics, together with population balance modeling based on the knowledge acquired in this work, enabled the prediction of the cocci chain length distribution under the different pH conditions applied in this study (optimal growth conditions and Single- as well as Multi-CSD experiments). This model, if coupled to ISM techniques, would allow the implementation of model-based bioprocess control strategies in the industrial production of starter cultures, moving from a QbT to a QbD/QbC mentality. More generally, it consists of a step toward a paradigm change in the study and description of cell cultivations, where average cell behaviors observed experimentally now would be interpreted as a potential joint result of various co-existing single-cell behaviors, rather than a unique response common to all bacteria in the fermentation.

7. Outlook

The application of new PAT tools in the industrial LAB production looks quite challenging, since the mentality of "we have been doing this during more than 25 years and we made profit, so why should we suddenly change now?" is spread over the vast majority of industrial bioprocesses. The real challenge for a researcher working for a company is to find the benefit for the industrial plant, typically relying on off-line analyses that had been carried out over years, of applying novel and not already established methods. The potential of electrooptical measurements of cell polarizability is that it could be used as CQA across scales and maybe one day used as soft-sensor or feedback-control to ensure process consistency and product quality. Nevertheless, a generational change is needed for the long-term implementation of such a PAT tool, with some, still open, important questions (e.g. reliability of determination of flexible bacteria).

For a successfully integrated scale up in a company, the utmost importance is the proper technology-transfer from the laboratory to industrial scale. The task includes the elucidation of crucial information to be transferred from Research and Development to pilot-production and for development of the existing process to the production in industrial scale. Sensors, like the ones developed by Freesense ApS in Denmark, to characterize gradients (pH, temperature and lately pO_2) in industrial fermenters are already commercially available. The service includes the development of a CFD/compartment model so that the company can guess the mixing time, compartmentalization, residence time in compartments, etc., but the price is still really expensive nowadays. In terms of scale down methodologies simulating the conditions in the large scale, a tendency toward using miniaturized HTS systems (e.g. Eppendorf DASGIP®, ambr15, ambr250, 2mag) using kLa/OTR/OUR/RQ as scale down parameters in aerobic microorganisms from the vast majority of industries is clear. For anaerobic cultures, those parallel mini-bioreactor systems are typically also used in bioprocess development to screen for the optimal growth conditions. In history, this has been performed attaining at macroscopically measured variables (biomass, metabolites, etc.), but actually cell populations are rarely homogenous communities. The notion of phenotypic heterogeneity has changed how we look at microbial populations. Microbial cells are individuals that differ from each other in terms of their behaviour and their properties, and this individuality is based on a number of molecular mechanisms that generate phenotypic differences between cells even in the absence of genetic and environmental variation. In this context, morphological changes provide direct information about cells' physiological state and, if measured in-line, population distribution may serve as control parameter of future bioprocesses. ISM technologies have been developed for algae (>10 μm) and yeast (5-10 μm) in recent years, but their application in bacteria is still limited by image resolution of such small cells (0.5-5 μm).

A tangible interest of bioprocessing industries toward development of digital twins to accelerate bioprocess characterization as well as validation has also been observed in recent years. The widely proposed Euler-Lagrange methods (CFD + metabolic models) are characterized by a high computational demand, by being rather inflexible and, therefore, not widely applicable to variable bioprocesses. Relatively easy mechanistic models, coupled to compartment models (with notably less computational demand than CFD ones), have recently been successfully used as tools for risk-based on-line monitoring of LAB cultivations. Such approaches, if coupled to prediction of certain population dynamics, would provide a soft-sensor accounting for population heterogeneity, thus improving process understanding as well as design.

8. Theses

1. Cell polarizability may become a new CQA in the industrial production of LAB, serving as early indicator of nutrient limitation and growth imbalance.

2. The at-line electrooptical determination of the AP and mean cell size with automated sampling and sample preparation provides similar and complimentary information on cell viability than flow cytometry, but faster and with less effort, thus minimizing human error.

3. Special attention should be put in the electrooptical measurement of flexible chains.

4. The pH-gradients encountered during cultivation of *S. thermophilus* in a 700 L pilot scale fermenter were not influencing growth performance, but 10-100 times larger bioreactors in the industry should be characterized prior to assuming absence of pH oscillating conditions.

5. Oscillating pH conditions induced in different scale down setups lead to reduced growth rate and yielded biomass productivity loss.

6. Multi-compartment scale down simulators (preferably STR-PFR approaches) are describing more realistically industrially relevant pH-gradients, where a certain cell population is subjected to pulse-based alkali addition.

7. The cocci chain length distribution is a feasible scale down parameter to consider population heterogeneity in scale up&down of *S. thermophilus* fermentation.

8. Under optimal growth conditions, diplococcic chains are predominant, while at basic pH values, the cocci chain length distribution increases and at lower pH, the cell size decreases.

9. Mechanistic modeling of macroscopic variables as well as population heterogeneity, if coupled to hydrodynamics simulation and ISM techniques, can be relevant to develop a digital twin in LAB starter culture production.

10. Mechanistic models of biological systems may be highly unreliable in their predictions and should therefore be subjected to appropriate reliability tests.

9. References

A. Angersbach, V. Bunin, O. I. (2006). Electro-Optical Analysis of Bacterial Cells. In *Molecular and Colloidal Electro-optics* (pp. 307–325).

Abbasiliasi, S., Tan, J. S., Tengku Ibrahim, T. A., Bashokouh, F., Ramakrishnan, N. R., Mustafa, S., & Ariff, A. B. (2017). Fermentation factors influencing the production of bacteriocins by lactic acid bacteria: A review. *RSC Advances*, *7*(47), 29395–29420. https://doi.org/10.1039/c6ra24579j

Abbott, D. A., Suir, E., Van Maris, A. J. A., & Pronk, J. T. (2008). Physiological and transcriptional responses to high concentrations of lactic acid in anaerobic chemostat cultures of Saccharomyces cerevisiae. *Applied and Environmental Microbiology*, *74*(18), 5759–5768. https://doi.org/10.1128/AEM.01030-08

Aboka, F. O., van Winden, W. A., Reginald, M. M., van Gulik, W. M., van de Berg, M., Oudshoom, A., & Heijnen, J. J. (2012). Identification of informative metabolic responses using a minibioreactor: a small step change in the glucose supply rate creates a large metabolic response in Saccharomyces cerevisiae. *Yeast*, *29*(3-4), 95–110. https://doi.org/10.1002/yea.2892

Aboka, F. O., Yang, H., de Jonge, L. P., Kerste, R., van Winden, W. A., van Gulik, W. M., … Heijnen, J. J. (2006). Characterization of an Experimental Miniature Bioreactor for Cellular Perturbation Studies. *Biotechnology and Bioengineering*, *95*(6), 1032–1042. https://doi.org/10.1002/bit.21003

Ackermann, M. (2015). A functional perspective on phenotypic heterogeneity in microorganisms. *Nature Reviews Microbiology*, *13*(8), 497–508. https://doi.org/10.1038/nrmicro3491

Adamberg, K., Kask, S., Laht, T. M., & Paalme, T. (2003). The effect of temperature and pH on the growth of lactic acid bacteria: A pH-auxostat study. *International Journal of Food Microbiology*, *85*(1-2), 171–183. https://doi.org/10.1016/S0168-1605(02)00537-8

Åkerberg, C., Hofvendahl, K., Hahn-Hägerdal, B., & Zacchi, G. (1998). Modelling the influence of pH, temperature, glucose and lactic acid concentrations on the kinetics of lactic acid production by Lactococcus lactis ssp. lactis ATCC 19435 in whole-wheat flour. *Applied Microbiology and Biotechnology*, *49*(6), 682–690. https://doi.org/10.1007/s002530051232

Alvarez, H. M., Silva, R. A., Cesari, A. C., Zamit, A. L., Peressutti, S. R., Reichelt, R., … Steinbüchel, A. (2004). Physiological and morphological responses of the soil bacterium Rhodococcus opacus strain PD630 to water stress. *FEMS Microbiology Ecology*, *50*(2), 75–86. https://doi.org/10.1016/j.femsec.2004.06.002

Amanullah, A., Mcfarlane, C. M., Emery, A. N., & Nienow, A. W. (2001). Scale-Down Model to Simulate Spatial pH Variations in Large-Scale Bioreactors.

Ambriz-Aviña, V., Contreras-Garduño, J. A., & Pedraza-Reyes, M. (2014). Applications of Flow Cytometry to Characterize Bacterial Physiological Responses. *BioMed Research International*, *2014*. https://doi.org/10.1155/2014/461941

Amrane, A., & Prigent, Y. (1999). Differentiation of pH and free lactic acid effects on the various growth and production phases of Lactobacillus helveticus. *Journal of Chemical Technology and*

Biotechnology, *74*(1), 33–40. https://doi.org/10.1002/(SICI)1097-4660(199901)74:1<33::AID-JCTB994>3.0.CO;2-K

Anane, E., García, Á. C., Haby, B., Hans, S., Krausch, N., Krewinkel, M., … Cruz Bournazou, M. N. (2019). *A model-based framework for parallel scale-down fed-batch cultivations in mini-bioreactors for accelerated phenotyping*. *Biotechnology and Bioengineering*. https://doi.org/10.1002/bit.27116

Anane, E., López C, D. C., Barz, T., Sin, G., Gernaey, K. V., Neubauer, P., & Cruz Bournazou, M. N. (2019). Output uncertainty of dynamic growth models: Effect of uncertain parameter estimates on model reliability. *Biochemical Engineering Journal*, *150*(February), 107247. https://doi.org/10.1016/j.bej.2019.107247

Anane, E., López C, D. C., Neubauer, P., & Cruz Bournazou, M. N. (2017). Modelling overflow metabolism in Escherichia coli by acetate cycling. *Biochemical Engineering Journal*, *125*, 23–30. https://doi.org/10.1016/j.bej.2017.05.013

Anane, E., Sawatzki, A., Neubauer, P., & Cruz-Bournazou, M. N. (2019). Modelling concentration gradients in fed-batch cultivations of E. coli – toward the flexible design of scale-down experiments. *Journal of Chemical Technology and Biotechnology*, *94*(2), 516–526. https://doi.org/10.1002/jctb.5798

Aon, J. C., Tecson, R. C., & Loladze, V. (2018). Saccharomyces cerevisiae morphological changes and cytokinesis arrest elicited by hypoxia during scale-up for production of therapeutic recombinant proteins. *Microbial Cell Factories*, *17*(1), 1–15. https://doi.org/10.1186/s12934-018-1044-2

Azargoshasb, H., Mousavi, S. M., Jamialahmadi, O., Shojaosadati, S. A., & Mousavi, S. B. (2016). Experiments and a three-phase computational fluid dynamics (CFD) simulation coupled with population balance equations of a stirred tank bioreactor for high cell density cultivation. *Canadian Journal of Chemical Engineering*, *94*(1), 20–32. https://doi.org/10.1002/cjce.22352

Azizan, K. A., Ressom, H. W., Mendoza, E. R., & Baharum, S. N. (2017). 13C based proteinogenic amino acid (PAA) and metabolic flux ratio analysis of Lactococcus lactis reveals changes in pentose phosphate (PP) pathway in response to agitation and temperature related stresses. *PeerJ*, *2017*(7). https://doi.org/10.7717/peerj.3451

Bach, C., Yang, J., Larsson, H., Stocks, S. M., Gernaey, K. V., Albaek, M. O., & Krühne, U. (2017). Evaluation of mixing and mass transfer in a stirred pilot scale bioreactor utilizing CFD. *Chemical Engineering Science*, *171*, 19–26. https://doi.org/10.1016/j.ces.2017.05.001

Bachmann, H., Molenaar, D., Branco Dos Santos, F., & Teusink, B. (2017). Experimental evolution and the adjustment of metabolic strategies in lactic acid bacteria. *FEMS Microbiology Reviews*, *41*(1), S201–S219. https://doi.org/10.1093/femsre/fux024

Back, A., Rossignol, T., Krier, F., Nicaud, J. M., & Dhulster, P. (2016). High - throughput fermentation screening for the yeast Yarrowia lipolytica with real - time monitoring of biomass and lipid production. *Microbial Cell Factories*, 1–12. https://doi.org/10.1186/s12934-016-0546-z

Baert, J., Delepierre, A., Telek, S., Fickers, P., Toye, D., Delamotte, A., … Delvigne, F. (2016). Microbial population heterogeneity versus bioreactor heterogeneity: evaluation of Redox Sensor Green as an exogenous metabolic biosensor. *Engineering in Life Sciences*, *16*(7), 643–651.

https://doi.org/10.1002/elsc.201500149

Baert, J., Kinet, R., Brognaux, A., Delepierre, A., Telek, S., Sørensen, S. J., … Delvigne, F. (2015). Phenotypic variability in bioprocessing conditions can be tracked on the basis of on-line flow cytometry and fits to a scaling law. *Biotechnology Journal*, *10*(8), 1316–1325. https://doi.org/10.1002/biot.201400537

Baez, A., Flores, N., Bolívar, F., & Ramírez, O. T. (2009). Metabolic and transcriptional response of recombinant Escherichia coli to elevated dissolved carbon dioxide concentrations. *Biotechnology and Bioengineering*, *104*(1), 102–110. https://doi.org/10.1002/bit.22379

Baez, A., Flores, N., Bolívar, F., & Ramírez, O. T. (2011). Simulation of dissolved CO 2 gradients in a scale-down system: A metabolic and transcriptional study of recombinant Escherichia coli. *Biotechnology Journal*, *6*(8), 959–967. https://doi.org/10.1002/biot.201000407

Baez, A., & Shiloach, J. (2014). Effect of elevated oxygen concentration on bacteria, yeasts, and cells propagated for production of biological compounds. *Microbial Cell Factories*, *13*(1), 1–7. https://doi.org/10.1186/s12934-014-0181-5

Bannari, R., Bannari, A., Vermette, P., & Proulx, P. (2012). A model for cellulase production from Trichoderma reesei in an airlift reactor. *Biotechnology and Bioengineering*, *109*(8), 2025–2038. https://doi.org/10.1002/bit.24473

Belini, V. L., Wiedemann, P., & Suhr, H. (2013). In situ microscopy: A perspective for industrial bioethanol production monitoring. *Journal of Microbiological Methods*, *93*(3), 224–232. https://doi.org/10.1016/j.mimet.2013.03.009

Bensch, G., Rüger, M., Wassermann, M., Weinholz, S., Reichl, U., & Cordes, C. (2014). Flow cytometric viability assessment of lactic acid bacteria starter cultures produced by fluidized bed drying. *Applied Microbiology and Biotechnology*, *98*(11), 4897–4909. https://doi.org/10.1007/s00253-014-5592-z

Beutel, S., & Henkel, S. (2011). In situ sensor techniques in modern bioprocess monitoring. *Applied Microbiology and Biotechnology*, *91*(6), 1493–1505. https://doi.org/10.1007/s00253-011-3470-5

Binder, D., Drepper, T., Jaeger, K. E., Delvigne, F., Wiechert, W., Kohlheyer, D., & Grünberger, A. (2017). Homogenizing bacterial cell factories: Analysis and engineering of phenotypic heterogeneity. *Metabolic Engineering*, *42*(March), 145–156. https://doi.org/10.1016/j.ymben.2017.06.009

Binder, D., Probst, C., Grünberger, A., Hilgers, F., Loeschcke, A., Jaeger, K. E., … Drepper, T. (2016). Comparative single-cell analysis of different E. Coli expression systems during microfluidic cultivation. *PLoS ONE*, *11*(8), 1–19. https://doi.org/10.1371/journal.pone.0160711

Blombach, B., Buchholz, J., Busche, T., Kalinowski, J., & Takors, R. (2013). Impact of different CO2/HCO3- levels on metabolism and regulation in Corynebacterium glutamicum. *Journal of Biotechnology*, *168*(4), 331–340. https://doi.org/10.1016/j.jbiotec.2013.10.005

Bluma, A., Höpfner, T., Lindner, P., Rehbock, C., Beutel, S., Riechers, D., … Scheper, T. (2010). In-situ imaging sensors for bioprocess monitoring: State of the art. *Analytical and Bioanalytical Chemistry*, *398*(6), 2429–2438. https://doi.org/10.1007/s00216-010-4181-y

Bockisch, A., Biering, J., Päßler, S., Vonau, W., Junne, S., & Neubauer, P. (2014). In Situ Investigation of the Liquid Phase in Industrial Yeast Fermentations with Mobile Multiparameter Sensors. *Chemie Ingenieur Technik*, *86*(9), 1582–1582. https://doi.org/10.1002/cite.201450231

Bockisch, A., Kielhorn, E., Neubauer, P., & Junne, S. (2019). Process analytical technologies to monitor the liquid phase of anaerobic cultures. *Process Biochemistry*, *76*, 1–10. https://doi.org/10.1016/j.procbio.2018.10.005

Bouchedja, D. N., Danthine, S., Kar, T., Fickers, P., Sassi, H., Boudjellal, A., … Delvigne, F. (2018). pH level has a strong impact on population dynamics of the yeast Yarrowia lipolytica and oil micro-droplets in multiphasic bioreactor. *FEMS Microbiology Letters*, *365*(16), 1–10. https://doi.org/10.1093/femsle/fny173

Bracewell, D. G., Gernaey, K. V, Glassey, J., Hass, V. C., Heinzle, E., Mandenius, C. F., … Titchener-Hooker, N. (2010). Education and training for measurement, monitoring, modeling & control (M3C) in biochemical engineering: Workshop report and recommendation. *Biotechnology Journal*, *5*(4), 359–367. https://doi.org/10.1093/biostatistics/manuscript-acf-v5

Brand, E., Junne, S., Anane, E., Cruz-Bournazou, M. N., & Neubauer, P. (2018). Importance of the cultivation history for the response of Escherichia coli to oscillations in scale-down experiments. *Bioprocess and Biosystems Engineering*, *41*(9), 1305–1313. https://doi.org/10.1007/s00449-018-1958-4

Brognaux, A., Francis, F., Twizere, J. C., Thonart, P., & Delvigne, F. (2014). Scale-down effect on the extracellular proteome of Escherichia coli: Correlation with membrane permeability and modulation according to substrate heterogeneities. *Bioprocess and Biosystems Engineering*, *37*(8), 1469–1485. https://doi.org/10.1007/s00449-013-1119-8

Brognaux, A., Han, S., Sørensen, S. J., Lebeau, F., Thonart, P., & Delvigne, F. (2013). A low-cost, multiplexable, automated flow cytometry procedure for the characterization of microbial stress dynamics in bioreactors. *Microbial Cell Factories*, *12*(1), 1–14. https://doi.org/10.1186/1475-2859-12-100

Brooijmans, R. J. W., De Vos, W. M., & Hugenholtz, J. (2009). Lactobacillus plantarum WCFS1 electron transport chains. *Applied and Environmental Microbiology*, *75*(11), 3580–3585. https://doi.org/10.1128/AEM.00147-09

Brunner, M., Braun, P., Doppler, P., Posch, C., Behrens, D., Herwig, C., & Fricke, J. (2017). The impact of pH inhomogeneities on CHO cell physiology and fed-batch process performance – two-compartment scale-down modelling and intracellular pH excursion. *Biotechnology Journal*, *12*(7), 1–13. https://doi.org/10.1002/biot.201600633

Brunner, M., Doppler, P., Klein, T., Herwig, C., & Fricke, J. (2018). Elevated pCO 2 affects the lactate metabolic shift in CHO cell culture processes. *Engineering in Life Sciences*, *18*(3), 204–214. https://doi.org/10.1002/elsc.201700131

Buchholz, J., Graf, M., Freund, A., Busche, T., Kalinowski, J., Blombach, B., & Takors, R. (2014). CO 2 /HCO 3− perturbations of simulated large scale gradients in a scale-down device cause fast transcriptional responses in Corynebacterium glutamicum. *Applied Microbiology and*

Biotechnology, *98*(20), 8563–8572. https://doi.org/10.1007/s00253-014-6014-y

Bunin, V. D. (2002). Electrooptical analysis of a suspension of cells and its structures. In *Encyclopedia of surface and colloid science* (pp. 2032–2043). NY, USA: M. Dekker Publ.

Bunin, V. D., Ignatov, O. V., Guliy, O. I., Zaitseva, I. S., O'Neil, D., & Ivnitski, D. (2004). Electrooptical analysis of the Escherichia coli-phage interaction. *Analytical Biochemistry*, *328*(2), 181–186. https://doi.org/10.1016/j.ab.2004.02.015

Bylund, F., Collet, E., Enfors, S. O., & Larsson, G. (1998). Substrate gradient formation in the large-scale bioreactor lowers cell yield and increases by-product formation. *Bioprocess Engineering*, *18*(3), 171–180. https://doi.org/10.1007/s004490050427

Camisard, V., Brienne, J. P., Baussart, H., Hammann, J., & Suhr, H. (2002). Inline characterization of cell concentration and cell volume in agitated bioreactors using in situ microscopy: Application to volume variation induced by osmotic stress. *Biotechnology and Bioengineering*, *78*(1), 73–80. https://doi.org/10.1002/bit.10178

Carlquist, M., Fernandes, R. L., Helmark, S., Heins, A. L., Lundin, L., Sørensen, S. J., … Lantz, A. E. (2012). Physiological heterogeneities in microbial populations and implications for physical stress tolerance. *Microbial Cell Factories*, *11*, 1–13. https://doi.org/10.1186/1475-2859-11-94

Carnicer, M., ten Pierick, A., van Dam, J., Heijnen, J. J., Albiol, J., van Gulik, W., & Ferrer, P. (2012). Quantitative metabolomics analysis of amino acid metabolism in recombinant Pichia pastoris under different oxygen availability conditions. *Microbial Cell Factories*, *11*(1), 83. https://doi.org/10.1186/1475-2859-11-83

Carr, F. J., Chill, D., & Maida, N. (2002). The lactic acid bacteria: A literature survey. *Critical Reviews in Microbiology*, *28*(4), 281–370. https://doi.org/10.1080/1040-840291046759

Carrondo, M. J. T., Alves, P. M., Carinhas, N., Glassey, J., Hesse, F., Merten, O. W., … Mandenius, C. F. (2012). How can measurement, monitoring, modeling and control advance cell culture in industrial biotechnology? *Biotechnology Journal*, *7*(12), 1522–1529. https://doi.org/10.1002/biot.201200226

Caspeta, L., Flores, N., Pérez, N. O., Bolívar, F., & Ramírez, O. T. (2009). The effect of heating rate on escherichia coli metabolism, physiological stress, transcriptional response, and production of temperature-induced recombinant protein: A scale-down study. *Biotechnology and Bioengineering*, *102*(2), 468–482. https://doi.org/10.1002/bit.22084

Cesar, S., & Huang, K. C. (2017). Thinking big: the tunability of bacterial cell size. *FEMS Microbiology Reviews*, *41*(5), 672–678. https://doi.org/10.1093/femsre/fux026

Chalmers, J. J. (2015). Mixing, aeration and cell damage, 30+ years later: What we learned, how it affected the cell culture industry and what we would like to know more about. *Current Opinion in Chemical Engineering*, *10*, 94–102. https://doi.org/10.1016/j.coche.2015.09.005

Chapot-Chartier, M. P., & Kulakauskas, S. (2014). Cell wall structure and function in lactic acid bacteria. *Microbial Cell Factories*, *13*(Suppl 1), 1–23. https://doi.org/10.1186/1475-2859-13-S1-S9

Chassagnole, C., Noisommit-Rizzi, N., Schmid, J. W., Mauch, K., & Reuss, M. (2002). Dynamic modeling

of the central carbon metabolism of Escherichia coli. *Biotechnology and Bioengineering*, *79*(1), 53–73. https://doi.org/10.1002/bit.10288

Cheung, C. K. L., Leksawasdi, N., & Doran, P. M. (2018). Bioreactor scale-down studies of suspended plant cell cultures. *AIChE Journal*, *64*(12), 4281–4288. https://doi.org/10.1002/aic.16415

Conrady, M., Lemoine, A., Limberg, M. H., Oldiges, M., Neubauer, P., & Junne, S. (2019). Carboxylic acid consumption and production by Corynebacterium glutamicum. *Biotechnology Progress*, *35*(3). https://doi.org/10.1002/btpr.2804

Cortés, J. T., Flores, N., Bolívar, F., Lara, A. R., & Ramírez, O. T. (2016). Physiological effects of pH gradients on Escherichia coli during plasmid DNA production. *Biotechnology and Bioengineering*, *113*(3), 598–611. https://doi.org/10.1002/bit.25817

Cram, L. S. (2003). Flow cytometry, an overview. *Methods in Cell Science*, *24*, 1–9.

Craven, S., Whelan, J., & Glennon, B. (2014). Glucose concentration control of a fed-batch mammalian cell bioprocess using a nonlinear model predictive controller. *Journal of Process Control*, *24*(4), 344–357. https://doi.org/10.1016/j.jprocont.2014.02.007

Croop, B., Zhang, C., Lim, Y., Gelfand, R. M., & Han, K. Y. (2019). Recent advancement of light-based single-molecule approaches for studying biomolecules. *Wiley Interdisciplinary Reviews: Systems Biology and Medicine*, *11*(4), 1–12. https://doi.org/10.1002/wsbm.1445

Cunin, R., Glansdorff, N., Piérard, A., & Stalon, V. (1986). Biosynthesis and metabolism of arginine in bacteria. *Microbiological Reviews*, *50*(3), 314–352. Retrieved from http://www.ncbi.nlm.nih.gov/pubmed/3534538

Davey, H. M., & Hexley, P. (2011). Red but not dead? Membranes of stressed Saccharomyces cerevisiae are permeable to propidium iodide. *Environmental Microbiology*, *13*(1), 163–171. https://doi.org/10.1111/j.1462-2920.2010.02317.x

Davey, H. M., & Kell, D. B. (1996). Flow cytometry and cell sorting of heterogeneous microbial populations: the importance of single-cell analyses. *Microbiological Reviews*, *60*(4), 641–696. https://doi.org/10.1016/j.mimet.2004.10.020

Davey, H. M., & Winson, M. K. (2003). Using flow cytometry to quantify microbial heterogeneity. *Current Issues in Molecular Biology*, *5*(1), 9–15.

De Jong, I. G., Haccou, P., & Kuipers, O. P. (2011). Bet hedging or not? A guide to proper classification of microbial survival strategies. *BioEssays*, *33*(3), 215–223. https://doi.org/10.1002/bies.201000127

de Jonge, L., Buijs, N. A. A., Heijnen, J. J., van Gulik, W. M., Abate, A., & Wahl, S. A. (2014). Flux response of glycolysis and storage metabolism during rapid feast/famine conditions in Penicillium chrysogenum using dynamic 13C labeling. *Biotechnology Journal*, *9*(3), 372–385. https://doi.org/10.1002/biot.201200260

de Jonge, L. P., Buijs, N. A. A., ten Pierick, A., Deshmukh, A., Zhao, Z., Kiel, J. A. K. W., … van Gulik, W. M. (2011). Scale-down of penicillin production in Penicillium chrysogenum. *Biotechnology Journal*, *6*(8), 944–958. https://doi.org/10.1002/biot.201000409

De Mey, M., Taymaz-Nikerel, H., Baart, G., Waegeman, H., Maertens, J., Heijnen, J. J., & van Gulik, W. M. (2010). Catching prompt metabolite dynamics in Escherichia coli with the BioScope at oxygen rich conditions. *Metabolic Engineering*, *12*(5), 477–487. https://doi.org/10.1016/j.ymben.2010.04.003

Delvigne, F., Baert, J., Gofflot, S., Lejeune, A., Telek, S., Johanson, T., & Lantz, A. E. (2015). Dynamic single-cell analysis of Saccharomyces cerevisiae under process perturbation: Comparison of different methods for monitoring the intensity of population heterogeneity. *Journal of Chemical Technology and Biotechnology*, *90*(2), 314–323. https://doi.org/10.1002/jctb.4430

Delvigne, F., Baert, J., Sassi, H., Fickers, P., Grünberger, A., & Dusny, C. (2017). Taking control over microbial populations: Current approaches for exploiting biological noise in bioprocesses. *Biotechnology Journal*, *12*(7), 1–17. https://doi.org/10.1002/biot.201600549

Delvigne, F., Boxus, M., Ingels, S., & Thonart, P. (2009). Bioreactor mixing efficiency modulates the activity of a prpoS::GFP reporter gene in E. coli. *Microbial Cell Factories*, *8*, 1–17. https://doi.org/10.1186/1475-2859-8-15

Delvigne, F., Brognaux, A., Francis, F., Twizere, J. C., Gorret, N., Sorensen, S. J., & Thonart, P. (2011). Green fluorescent protein (GFP) leakage from microbial biosensors provides useful information for the evaluation of the scale-down effect. *Biotechnology Journal*, *6*(8), 968–978. https://doi.org/10.1002/biot.201000410

Delvigne, F., Destain, J., & Thonart, P. (2005). Bioreactor hydrodynamic effect on Escherichia coli physiology: Experimental results and stochastic simulations. *Bioprocess and Biosystems Engineering*, *28*(2), 131–137. https://doi.org/10.1007/s00449-005-0018-z

Delvigne, F., Destain, J., & Thonart, P. (2006). A methodology for the design of scale-down bioreactors by the use of mixing and circulation stochastic models. *Biochemical Engineering Journal*, *28*(3), 256–268. https://doi.org/10.1016/j.bej.2005.11.009

Delvigne, F., Ingels, S., & Thonart, P. (2010). Evaluation of a set of E. coli reporter strains as physiological tracer for estimating bioreactor hydrodynamic efficiency. *Process Biochemistry*, *45*(11), 1769–1778. https://doi.org/10.1016/j.procbio.2010.02.022

Delvigne, F., & Noorman, H. (2017). Scale-up/Scale-down of microbial bioprocesses: a modern light on an old issue. *Microbial Biotechnology*, *10*(4), 685–687. https://doi.org/10.1111/1751-7915.12732

Delvigne, F., Takors, R., Mudde, R., van Gulik, W., & Noorman, H. (2017). Bioprocess scale-up/down as integrative enabling technology: from fluid mechanics to systems biology and beyond. *Microbial Biotechnology*, *10*(5), 1267–1274. https://doi.org/10.1111/1751-7915.12803

Delvigne, F., Zacchetti, B., Fickers, P., Fifani, B., Roulling, F., Lefebvre, C., … Junne, S. (2018). Improving control in microbial cell factories: from single-cell to large-scale bioproduction. *FEMS Microbiology Letters*, *365*(22), 1–34. https://doi.org/10.1093/femsle/fny236

Delvigne, F., Zune, Q., Lara, A. R., Al-Soud, W., & Sørensen, S. J. (2014). Metabolic variability in bioprocessing: Implications of microbial phenotypic heterogeneity. *Trends in Biotechnology*, *32*(12), 608–616. https://doi.org/10.1016/j.tibtech.2014.10.002

Demling, P., Westerwalbesloh, C., Noack, S., Wiechert, W., & Kohlheyer, D. (2018). Quantitative

measurements in single-cell analysis: toward scalability in microbial bioprocess development. *Current Opinion in Biotechnology*, *54*, 121–127. https://doi.org/10.1016/j.copbio.2018.01.024

Devi, T. T., & Kumar, B. (2017). Mass transfer and power characteristics of stirred tank with Rushton and curved blade impeller. *Engineering Science and Technology, an International Journal*, *20*(2), 730–737. https://doi.org/10.1016/j.jestch.2016.11.005

Diaz, M., Herrero, M., Garcia, L. A., & Quiros, C. (2010). Application of flow cytometry to industrial microbial bioprocesses. *Biochemical Engineering Journal*, *48*(3), 385–407. https://doi.org/10.1016/j.bej.2009.07.013

Díaz, M., Herrero, M., García, L. A., & Quirós, C. (2010). Application of flow cytometry to industrial microbial bioprocesses. *Biochemical Engineering Journal*, *48*(3), 385–407. https://doi.org/10.1016/j.bej.2009.07.013

Dreher, T., Husemann, U., Adams, T., de Wilde, D., & Greller, G. (2014). Design space definition for a stirred single-use bioreactor family from 50 to 2000 L scale. *Engineering in Life Sciences*, *14*(3), 304–310. https://doi.org/10.1002/elsc.201300067

Eggeling, L., & Bott, M. (2015). A giant market and a powerful metabolism: l-lysine provided by Corynebacterium glutamicum. *Applied Microbiology and Biotechnology*, *99*(8), 3387–3394. https://doi.org/10.1007/s00253-015-6508-2

Ehgartner, D., Herwig, C., & Fricke, J. (2017). Morphological analysis of the filamentous fungus Penicillium chrysogenum using flow cytometry—the fast alternative to microscopic image analysis. *Applied Microbiology and Biotechnology*, *101*(20), 7675–7688. https://doi.org/10.1007/s00253-017-8475-2

Eigenstetter, G., & Takors, R. (2017). Dynamic modeling reveals a three-step response of Saccharomyces cerevisiae to high CO2levels accompanied by increasing ATP demands. *FEMS Yeast Research*, *17*(1), 1–11. https://doi.org/10.1093/femsyr/fox008

Elqotbi, M., Vlaev, S. D., Montastruc, L., & Nikov, I. (2013). CFD modelling of two-phase stirred bioreaction systems by segregated solution of the Euler-Euler model. *Computers and Chemical Engineering*, *48*, 113–120. https://doi.org/10.1016/j.compchemeng.2012.08.005

Emmerich, J., Tang, Q., Wang, Y., Neubauer, P., Junne, S., & Maaß, S. (2019). Optical inline analysis and monitoring of particle size and shape distributions for multiple applications: Scientific and industrial relevance. *Chinese Journal of Chemical Engineering*, *27*(2), 257–277. https://doi.org/10.1016/j.cjche.2018.11.011

Enfors, S. O., Jahic, M., Rozkov, a., Xu, B., Hecker, M., Jürgen, B., … Manelius, Å. (2001a). Physiological responses to mixing in large scale bioreactors. *Journal of Biotechnology*, *85*(2), 175–185. https://doi.org/10.1016/S0168-1656(00)00365-5

Enfors, S. O., Jahic, M., Rozkov, A., Xu, B., Hecker, M., Jürgen, B., … Manelius, Å. (2001b). Physiological responses to mixing in large scale bioreactors. *Journal of Biotechnology*, *85*(2), 175–185. https://doi.org/10.1016/S0168-1656(00)00365-5

Even, S., Lindley, N. D., Loubière, P., & Cocaign-Bousquet, M. (2002). Dynamic response of catabolic pathways to autoacidification in Lactococcus lactis: Transcript profiling and stability in relation to

metabolic and energetic constraints. *Molecular Microbiology*, *45*(4), 1143–1152. https://doi.org/10.1046/j.1365-2958.2002.03086.x

Faassen, S. M., & Hitzmann, B. (2015). Fluorescence spectroscopy and chemometric modeling for bioprocess monitoring. *Sensors (Switzerland)*, *15*(5), 10271–10291. https://doi.org/10.3390/s150510271

Farzan, P., & Ierapetritou, M. G. (2017). Integrated modeling to capture the interaction of physiology and fluid dynamics in biopharmaceutical bioreactors. *Computers and Chemical Engineering*, *97*, 271–282. https://doi.org/10.1016/j.compchemeng.2016.11.037

Farzan, P., & Ierapetritou, M. G. (2018). A framework for the development of integrated and computationally feasible models of large-scale mammalian cell bioreactors. *Processes*, *6*(7). https://doi.org/10.3390/pr6070082

Fenster, K., Freeburg, B., Hollard, C., Wong, C., Laursen, R. R., & Ouwehand, A. C. (2019). The production and delivery of probiotics: A review of a practical approach. *Microorganisms*, *7*(3), 1–17. https://doi.org/10.3390/microorganisms7030083

Fernandes, R. L., Carlquist, M., Lundin, L., Heins, A. L., Dutta, A., Sørensen, S. J., … Gernaey, K. V. (2013). Cell mass and cell cycle dynamics of an asynchronous budding yeast population: Experimental observations, flow cytometry data analysis, and multi-scale modeling. *Biotechnology and Bioengineering*, *110*(3), 812–826. https://doi.org/10.1002/bit.24749

Flickinger, M. C., & Nienow, A. W. (2010). Scale-Up, Stirred Tank Reactors. *Encyclopedia of Industrial Biotechnology*, 1–14. https://doi.org/10.1002/9780470054581.eib535

Fomina, N., Johnson, C. A., Maruniak, A., Bahrampour, S., Lang, C., Davis, R. W., … Ahmad, H. (2016). An electrochemical platform for localized pH control on demand. *Lab on a Chip*, *16*(12), 2236–2244. https://doi.org/10.1039/c6lc00421k

Fonseca, F., Cenard, S., & Passot, S. (2014). Freeze-Drying of Lactic Acid Bacteria. *Methods in Molecular Biology*, 477–488. https://doi.org/10.1007/978-1-4939-2193-5_24

Formenti, L. R., Nørregaard, A., Bolic, A., Hernandez, D. Q., Hagemann, T., Heins, A. L., … Gernaey, K. V. (2014). Challenges in industrial fermentation technology research. *Biotechnology Journal*, *9*(6), 727–738. https://doi.org/10.1002/biot.201300236

Fozo, E. M., & Quivey Jr., R. G. (2004). Synthesis of cyclopropane fatty acids in Lactobacillus helveticus and Lactobacillus sanfranciscensis and their cellular fatty acids chan. *Applied and Environmental Microbiology*, *70*(2), 929–936. https://doi.org/10.1128/AEM.70.2.929

Fragoso-Jiménez, J. C., Baert, J., Nguyen, T. M., Liu, W., Sassi, H., Goormaghtigh, F., … Gosset, G. (2019). Growth-dependent recombinant product formation kinetics can be reproduced through engineering of glucose transport and is prone to phenotypic heterogeneity. *Microbial Cell Factories*. https://doi.org/10.1186/s12934-019-1073-5

Fraser, D., & Kærn, M. (2009). A chance at survival: Gene expression noise and phenotypic diversification strategies. *Molecular Microbiology*, *71*(6), 1333–1340. https://doi.org/10.1111/j.1365-2958.2009.06605.x

Fujita, M., Iwahori, K., Tatsuta, S., & Yamakawa, K. (1994). Analysis of pellet formation of Aspergillus niger based on shear stress. *Journal of Fermentation and Bioengineering*, *78*(5), 368–373. https://doi.org/10.1016/0922-338X(94)90282-8

Gao, Y., Ray, S., Dai, S., Ivanov, A. R., Abu-Absi, N. R., Lewis, A. M., … Karger, B. L. (2016). Combined metabolomics and proteomics reveals hypoxia as a cause of lower productivity on scale-up to a 5000-Liter CHO Bioprocess. *Biotechnology Journal*, *11*(9), 1190–1200. https://doi.org/10.1002/biot.201600030

Garcia-Ochoa, F., & Gomez, E. (2009). Bioreactor scale-up and oxygen transfer rate in microbial processes: An overview. *Biotechnology Advances*, *27*(2), 153–176. https://doi.org/10.1016/j.biotechadv.2008.10.006

George, S., Larsson, G., & Enfors, S. O. (1993). A scale-down two-compartment reactor with controlled substrate oscillations: Metabolic response of Saccharomyces cerevisiae. *Bioprocess Engineering*, *9*, 249–257. https://doi.org/10.1007/BF01061530

George, S., Larsson, G., Olsson, K., & Enfors, S. O. (1998). Comparison of the Baker's yeast process performance in laboratory and production scale. *Bioprocess Engineering*, *18*, 135–142. https://doi.org/10.1007/s004490050423

Ginovart, M., Carbó, R., Blanco, M., & Portell, X. (2018). Digital image analysis of yeast single cells growing in two different oxygen concentrations to analyze the population growth and to assist individual-based modeling. *Frontiers in Microbiology*, *8*(JAN). https://doi.org/10.3389/fmicb.2017.02628

Glassey, J., Gernaey, K. V, Clemens, C., Schulz, T. W., Oliveira, R., Striedner, G., & Mandenius, C. F. (2011). Process Analytical Technology (PAT) for biopharmaceuticals. *Biotechnology Journal*, *6*(4), 369–377. https://doi.org/10.1002/biot.201000356

Gomes, J., Chopda, V. R., & Rathore, A. S. (2015). Integrating systems analysis and control for implementing process analytical technology in bioprocess development. *Journal of Chemical Technology and Biotechnology*, *90*(4), 583–589. https://doi.org/10.1002/jctb.4591

Gonçalves, L. M. D., Ramos, A., Almeida, J. S., Xavier, A. M. R. B., & Carrondo, M. J. T. (1997). Elucidation of the mechanism of lactic acid growth inhibition and production in batch cultures of Lactobacillus rhamnosus. *Applied Microbiology and Biotechnology*, *48*(3), 346–350. https://doi.org/10.1007/s002530051060

Gonzalez, M. E., & Barrett, D. M. (2010). Thermal, high pressure, and electric field processing effects on plant cell membrane integrity and relevance to fruit and vegetable quality. *Journal of Food Science*, *75*(7). https://doi.org/10.1111/j.1750-3841.2010.01763.x

González-Cabaleiro, R., Mitchell, A. M., Smith, W., Wipat, A., & Ofiteru, I. D. (2017). Heterogeneity in pure microbial systems: Experimental measurements and modeling. *Frontiers in Microbiology*, *8*(SEP), 1–8. https://doi.org/10.3389/fmicb.2017.01813

Gradov, D. V., Han, M., Tervasmäki, P., Latva-Kokko, M., Vaittinen, J., Pihlajamäki, A., & Koiranen, T. (2018). Numerical Simulation of Biomass Growth in OKTOP®9000 Reactor at Industrial Scale. *Industrial and Engineering Chemistry Research*, *57*(40), 13300–13311.

https://doi.org/10.1021/acs.iecr.8b02765

Graf, M., Zieringer, J., Haas, T., Nieß, A., Blombach, B., & Takors, R. (2018). Physiological response of Corynebacterium glutamicum to increasingly nutrient-rich growth conditions. *Frontiers in Microbiology*, *9*(AUG), 1–15. https://doi.org/10.3389/fmicb.2018.02058

Grimm, L. H., Kelly, S., Völkerding, I. I., Krull, R., & Hempel, D. C. (2005). Influence of mechanical stress and surface interaction on the aggregation of Aspergillus niger conidia. *Biotechnology and Bioengineering*, *92*(7), 879–888. https://doi.org/10.1002/bit.20666

Griswold, A., Chen, Y. M., Snyder, J. A., & Burne, R. A. (2004). Characterization of the Arginine Deiminase Operon of Streptococcus rattus FA-1. *Applied and Environmental Microbiology*, *70*(3), 1321–1327. https://doi.org/10.1128/AEM.70.3.1321

Grote, J., Krysciak, D., & Streit, W. R. (2015). Phenotypic heterogeneity, a phenomenon that may explain why quorum sensing does not always result in truly homogenous cell behavior. *Applied and Environmental Microbiology*, *81*(16), 5280–5289. https://doi.org/10.1128/AEM.00900-15

Grünberger, A., Probst, C., Helfrich, S., Nanda, A., Stute, B., Wiechert, W., … Kohlheyer, D. (2015). Spatiotemporal microbial single-cell analysis using a high-throughput microfluidics cultivation platform. *Cytometry Part A*, *87*(12), 1101–1115. https://doi.org/10.1002/cyto.a.22779

Grünberger, A., Wiechert, W., & Kohlheyer, D. (2014). Single-cell microfluidics: Opportunity for bioprocess development. *Current Opinion in Biotechnology*, *29*(1), 15–23. https://doi.org/10.1016/j.copbio.2014.02.008

Gschwend, K., Beyeler, W., & Fiechter, A. (1983). Detection of reactor nonhomogeneities by measuring culture fluorescence. *Biotechnology and Bioengineering*, *25*(11), 2789–2793. https://doi.org/10.1002/bit.260251121

Guan, N., Li, J., Shin, H. dong, Du, G., Chen, J., & Liu, L. (2017). Microbial response to environmental stresses: from fundamental mechanisms to practical applications. *Applied Microbiology and Biotechnology*, *101*(10), 3991–4008. https://doi.org/10.1007/s00253-017-8264-y

Guchte, M. van de, & Serror, P. (2002). Stress responses in lactic acid bacteria. *Antonie Van …*, 187–216. https://doi.org/10.1023/A:1020631532202

Guerra, A., von Stosch, M., & Glassey, J. (2019). Toward biotherapeutic product real-time quality monitoring. *Critical Reviews in Biotechnology*, *39*(3), 289–305. https://doi.org/10.1080/07388551.2018.1524362

Guez, J. S., Cassar, J. P., Wartelle, F., Dhulster, P., & Suhr, H. (2004). Real time in situ microscopy for animal cell-concentration monitoring during high density culture in bioreactor. *Journal of Biotechnology*, *111*(3), 335–343. https://doi.org/10.1016/j.jbiotec.2004.04.028

Hakkaart, X., Liu, Y., Hulst, M., el Masoudi, A., Peuscher, E., Pronk, J., … Daran-Lapujade, P. (2019). Physiological responses of Saccharomyces cerevisiae to industrially relevant conditions: slow growth, low pH and high CO2 levels. *Biotechnology & Bioengineering*, 1–29. https://doi.org/10.1002/bit.27210

Hansen, G., Johansen, C. L., Marten, G., Wilmes, J., Jespersen, L., & Arneborg, N. (2016). Influence of

extracellular pH on growth, viability, cell size, acidification activity, and intracellular pH of Lactococcus lactis in batch fermentations. *Applied Microbiology and Biotechnology*, *100*(13), 5965–5976. https://doi.org/10.1007/s00253-016-7454-3

Hardy, N., Augier, F., Nienow, A. W., Béal, C., & Ben Chaabane, F. (2017). Scale-up agitation criteria for Trichoderma reesei fermentation. *Chemical Engineering Science*, *172*, 158–168. https://doi.org/10.1016/j.ces.2017.06.034

Haringa, C., Deshmukh, A. T., Mudde, R. F., & Noorman, H. J. (2017). Euler-Lagrange analysis toward representative down-scaling of a 22 m3 aerobic S. cerevisiae fermentation. *Chemical Engineering Science*, *170*, 653–669. https://doi.org/10.1016/j.ces.2017.01.014

Haringa, C., Mudde, R. F., & Noorman, H. J. (2018). From industrial fermentor to CFD-guided downscaling: what have we learned? *Biochemical Engineering Journal*, *140*, 57–71. https://doi.org/10.1016/j.bej.2018.09.001

Haringa, C., Noorman, H. J., & Mudde, R. F. (2017). Lagrangian modeling of hydrodynamic–kinetic interactions in (bio)chemical reactors: Practical implementation and setup guidelines. *Chemical Engineering Science*, *157*, 159–168. https://doi.org/10.1016/j.ces.2016.07.031

Haringa, C., Tang, W., Deshmukh, A. T., Xia, J., Reuss, M., Heijnen, J. J., … Noorman, H. J. (2016). Euler-Lagrange computational fluid dynamics for (bio)reactor scale down: An analysis of organism lifelines. *Engineering in Life Sciences*, *16*(7), 652–663. https://doi.org/10.1002/elsc.201600061

Haringa, C., Tang, W., Wang, G., Deshmukh, A. T., van Winden, W. A., Chu, J., … Noorman, H. J. (2018). Computational fluid dynamics simulation of an industrial P. chrysogenum fermentation with a coupled 9-pool metabolic model: Toward rational scale-down and design optimization. *Chemical Engineering Science*, *175*, 12–24. https://doi.org/10.1016/j.ces.2017.09.020

Hashimoto, M., Nozoe, T., Nakaoka, H., Okura, R., Akiyoshi, S., Kaneko, K., … Wakamoto, Y. (2016). Noise-driven growth rate gain in clonal cellular populations. *Proceedings of the National Academy of Sciences of the United States of America*, *113*(12), 3151–3156. https://doi.org/10.1073/pnas.1519412113

Havlik, I., Reardon, K. F., Ünal, M., Lindner, P., Prediger, A., Babitzky, A., … Scheper, T. (2013). Monitoring of microalgal cultivations with on-line, flow-through microscopy. *Algal Research*, *2*(3), 253–257. https://doi.org/10.1016/j.algal.2013.04.001

Heins, A. L., Lencastre Fernandes, R., Gernaey, K. V., & Lantz, A. E. (2015). Experimental and in silico investigation of population heterogeneity in continuous Sachharomyces cerevisiae scale-down fermentation in a two-compartment setup. *Journal of Chemical Technology and Biotechnology*, *90*(2), 324–340. https://doi.org/10.1002/jctb.4532

Heins, A. L., Lundin, L., Nunes, I., Gernaey, K. V., Sørensen, S. J., & Lantz, A. E. (2019). The effect of acetate on population heterogeneity in different cellular characteristics of Escherichia coli in aerobic batch cultures. *Biotechnology Progress*, *35*(3). https://doi.org/10.1002/btpr.2796

Heins, A. L., & Weuster-Botz, D. (2018). Population heterogeneity in microbial bioprocesses: origin, analysis, mechanisms, and future perspectives. *Bioprocess and Biosystems Engineering*, *41*(7), 889–916. https://doi.org/10.1007/s00449-018-1922-3

Heins, A.-L., Johanson, T., Han, S., Lundin, L., Carlquist, M., Gernaey, K. V., … Eliasson Lantz, A. (2019). Quantitative Flow Cytometry to Understand Population Heterogeneity in Response to Changes in Substrate Availability in Escherichia coli and Saccharomyces cerevisiae Chemostats. *Frontiers in Bioengineering and Biotechnology*, *7*. https://doi.org/10.3389/fbioe.2019.00187

Henson, M. A. (2003). Dynamic modeling of microbial cell populations. *Current Opinion in Biotechnology*, *14*(5), 460–467. https://doi.org/10.1016/S0958-1669(03)00104-6

Henson, M. A., Müller, D., & Reuss, M. (2002). Cell population modelling of yeast glycolytic oscillations. *Biochemical Journal*, *368*(2), 433–446. https://doi.org/10.1042/BJ20021051

Hetényi, K., Németh, Á., & Sevella, B. (2011). Role of pH-regulation in lactic acid fermentation: Second steps in a process improvement. *Chemical Engineering and Processing: Process Intensification*, *50*(3), 293–299. https://doi.org/10.1016/j.cep.2011.01.008

Heunis, T., Deane, S., Smit, S., & Dicks, L. M. T. (2014). Proteomic profiling of the acid stress response in lactobacillus plantarum 423. *Journal of Proteome Research*, *13*(9), 4028–4039.

Hewitt, C. J., Boon, L. A., McFarlane, C. M., & Nienow, A. W. (1998). The Use of Flow Cytometry to Study the Impact of Fluid Mechanical Stress on Escherichia coli W3110 During Continuous Cultivation in an Agitated Bioreactor. *Biotechnology & Bioengineering*, *59*(5), 612–620. https://doi.org/10.1002/(sici)10970290(19980905)59:5<612::aidbit12>3.0.co;2-b

Hewitt, C. J., Caron, G. N. Von, Axelsson, B., McFarlane, C. M., & Nienow, A. W. (2000). Studies related to the scale-up of high-cell-density E. coli fed-batch fermentations using multiparameter flow cytometry: Effect of a changing microenvironment with respect to glucose and dissolved oxygen concentration. *Biotechnology and Bioengineering*, *70*(4), 381–390. https://doi.org/10.1002/1097-0290(20001120)70:4<381::AID-BIT3>3.0.CO;2-0

Hewitt, C. J., & Nebe-Von-Caron, G. (2001). An industrial application of multiparameter flow cytometry: Assessment of cell physiological state and its application to the study of microbial fermentations. *Cytometry*, *44*(May 2000), 179–187. https://doi.org/10.1002/1097-0320(20010701)44:3<179::AID-CYTO1110>3.0.CO;2-D

Hewitt, C. J., & Nebe-von-Caron, G. (2004). The Application of multi-parameter flow cytometry to monitor individual microbial cell physiological state. *Advances in Biochemical Engineering/Biotechnology*, *89*, 197–223. https://doi.org/10.1007/b93997

Hewitt, C. J., & Nebe-Von-Caron, G. (2004). The application of multi-parameter flow cytometry to monitor individual microbial cell physiological state. *Advances in Biochemical Engineering/biotechnology*, *89*, 197–223. https://doi.org/10.1007/b93997

Hewitt, C. J., & Nienow, A. W. (2007). The Scale-Up of Microbial Batch and Fed-Batch Fermentation Processes. *Advances in Applied Microbiology*, *62*(07), 105–135. https://doi.org/10.1016/S0065-2164(07)62005-X

Hewitt, C. J., Onyeaka, H., Lewis, G., Taylor, I. W., & Nienow, A. W. (2006). A comparison of high cell density fed-batch fermentations involving both induced and non-induced recombinant Escherichia coli under well-mixed small-scale and simulated poorly mixed large-scale conditions. *Biotechnology and Bioengineering*, *96*(3), 495–505. https://doi.org/10.1002/bit.21127

Heyse, J., Buysschaert, B., Props, R., Rubbens, P., Skirtach, A. G., Waegeman, W., & Boon, N. (2019). Coculturing bacteria leads to reduced phenotypic heterogeneities. *Applied and Environmental Microbiology*, *85*(8), 1–13. https://doi.org/10.1128/AEM.02814-18

Hoshan, L., Jiang, R., Moroney, J., Bui, A., Zhang, X., Hang, T. C., & Xu, S. (2019). Effective bioreactor pH control using only sparging gases. *Biotechnology Progress*, *35*(1). https://doi.org/10.1002/btpr.2743

Hossein Nezhad, M., Stenzel, D., & Britz, M. (2010). Effect of growth at low pH on the cell surface properties of a typical strain of Lactobacillus casei group. *Iranian Journal of Microbiology*, *2*(3), 147–154. Retrieved from http://www.pubmedcentral.nih.gov/articlerender.fcgi?artid=3279780&tool=pmcentrez&rendertype=abstract

Hosseini Nezhad, M., Hussain, M. A., & Britz, M. L. (2015). Stress Responses in Probiotic Lactobacillus casei. *Critical Reviews in Food Science and Nutrition*, *55*(6), 740–749. https://doi.org/10.1080/10408398.2012.675601

Hussain, M. A., Hosseini Nezhad, M., Sheng, Y., & Amoafo, O. (2013). Proteomics and the stressful life of lactobacilli. *FEMS Microbiology Letters*, *349*(1), 1–8. https://doi.org/10.1111/1574-6968.12274

Hutkins, R. W., & Nannen, N. L. (1993). pH Homeostasis in Lactic Acid Bacteria. *Journal of Dairy Science*, *76*(8), 2354–2365. https://doi.org/10.3168/jds.s0022-0302(93)77573-6

Huys, G. R., & Raes, J. (2018). Go with the flow or solitary confinement: a look inside the single-cell toolbox for isolation of rare and uncultured microbes. *Current Opinion in Microbiology*, *44*, 1–8. https://doi.org/10.1016/j.mib.2018.05.002

Jaros, D., Mende, S., Häffele, F., Nachtigall, C., Nirschl, H., & Rohm, H. (2018). Shear treatment of starter culture medium improves separation behavior of Streptococcus thermophilus cells. *Engineering in Life Sciences*, *18*(1), 62–69. https://doi.org/10.1002/elsc.201700121

Jiang, R., Chen, H., & Xu, S. (2018). pH excursions impact CHO cell culture performance and antibody N-linked glycosylation. *Bioprocess and Biosystems Engineering*, *41*(12), 1731–1741. https://doi.org/10.1007/s00449-018-1996-y

Jin, J., Qin, Q., Guo, H., Liu, S., Ge, S., Zhang, H., … Ren, F. (2015). Effect of pre-stressing on the acid-stress response in Bifidobacterium revealed using proteomic and physiological approaches. *PLoS ONE*, *10*(2), 1–14. https://doi.org/10.1371/journal.pone.0117702

Joux, F., & Lebaron, P. (2000). Use of fluorescent probes to assess physiological functions of bacteria at single-cell level. *Microbes and Infection*, *2*(12), 1523–1535. https://doi.org/10.1016/S1286-4579(00)01307-1

Jung, S. K. (2019). A Review of Image Analysis in Biochemical Engineering. *Biotechnology and Bioprocess Engineering*, *24*(1), 65–75. https://doi.org/10.1007/s12257-018-0372-8

Junker, B. H. (2004). Scale-up methodologies for Escherichia coli and yeast fermentation processes. *Journal of Bioscience and Bioengineering*, *97*(6), 347–364. https://doi.org/10.1016/S1389-1723(04)70218-2

Junne, S., Cruz-Bournazou, M. N., Angersbach, A., & Götz, P. (2010). Electrooptical monitoring of cell polarizability and cell size in aerobic Escherichia coli batch cultivations. *J Ind Microbiol Biotechnol*, *37*(9), 935–942.

Junne, S., Klein, E., Angersbach, A., & Götz, P. (2008). Electrooptical Measurements for Monitoring Metabolite Fluxes in Acetone–Butanol–Ethanol Fermentations. *Biotechnology & Bioengineering*, *99*(4), 862–869.

Junne, S., Klingner, A., Kabisch, J., Schweder, T., & Neubauer, P. (2011). A two-compartment bioreactor system made of commercial parts for bioprocess scale-down studies: Impact of oscillations on Bacillus subtilis fed-batch cultivations. *Biotechnology Journal*, *6*(8), 1009–1017. https://doi.org/10.1002/biot.201100293

Kaboré, A. K., Delaunay, S., Blanchard, F., Guedon, E., Fick, M., & Olmos, E. (2019). Study and modeling of fluctuating dissolved oxygen concentration impact on Corynebacterium glutamicum growth in a scale-down bioreactor. *Process Biochemistry*, *77*, 8–17. https://doi.org/10.1016/j.procbio.2018.10.016

Kaboré, A. K., Olmos, E., Blanchard, F., Fick, M., Delaunay, S., & Guedon, E. (2015). Impact of gas-liquid mass transfer on organic acids production by Corynebacterium glutamicum in unbaffled shake flasks. *Biochemical Engineering Journal*, *101*, 237–247. https://doi.org/10.1016/j.bej.2015.06.003

Kaboré, A. K., Olmos, E., Fick, M., Blanchard, F., Guedon, E., & Delaunay, S. (2017). Aerobiosis–anaerobiosis transition has a significant impact on organic acid production by Corynebacterium glutamicum. *Process Biochemistry*, *52*, 10–21. https://doi.org/10.1016/j.procbio.2016.10.007

Kar, T., Delvigne, F., Masson, M., Destain, J., & Thonart, P. (2008). Investigation of the effect of different extracellular factors on the lipase production by Yarrowia lipolityca on the basis of a scale-down approach. *Journal of Industrial Microbiology and Biotechnology*, *35*(9), 1053–1059. https://doi.org/10.1007/s10295-008-0382-1

Kar, T., Destain, J., Thonart, P., & Delvigne, F. (2012). Scale-down assessment of the sensitivity of Yarrowia lipolytica to oxygen transfer and foam management in bioreactors: Investigation of the underlying physiological mechanisms. *Journal of Industrial Microbiology and Biotechnology*, *39*(2), 337–346. https://doi.org/10.1007/s10295-011-1030-8

Kashket, E. R. (1987). Bioenergetics of lactic acid bacteria: cytoplasmic pH and osmotolerance. *FEMS Microbiology Letters*, *46*(3), 233–244. https://doi.org/10.1016/0378-1097(87)90110-8

Käß, F., Hariskos, I., Michel, A., Brandt, H. J., Spann, R., Junne, S., … Oldiges, M. (2013). Assessment of robustness against dissolved oxygen/substrate oscillations for C. glutamicum DM1933 in two-compartment bioreactor. *Bioprocess and Biosystems Engineering*, *37*(6), 1151–1162. https://doi.org/10.1007/s00449-013-1086-0

Käß, F., Junne, S., Neubauer, P., Wiechert, W., & Oldiges, M. (2014). Process inhomogeneity leads to rapid side product turnover in cultivation of Corynebacterium glutamicum. *Microbial Cell Factories*, *13*(1), 6. https://doi.org/10.1186/1475-2859-13-6

Keren, L., Hausser, J., Lotan-Pompan, M., Vainberg Slutskin, I., Alisar, H., Kaminski, S., … Segal, E. (2016).

Massively Parallel Interrogation of the Effects of Gene Expression Levels on Fitness. *Cell*, *166*(5), 1282–1294.e18. https://doi.org/10.1016/j.cell.2016.07.024

Kielhorn, E., Sachse, S., Moench-Tegeder, M., Naegele, H. J., Haelsig, C., Oechsner, H., … Junne, S. (2015). Multiposition Sensor Technology and Lance-Based Sampling for Improved Monitoring of the Liquid Phase in Biogas Processes. *Energy and Fuels*, *29*(7), 4038–4045. https://doi.org/10.1021/ef502816c

Kleerebezemab, M., Hols, P., & Hugenholtz, J. (2000). Lactic acid bacteria as a cell factory: Rerouting of carbon metabolism in Lactococcus lactis by metabolic engineering. *Enzyme and Microbial Technology*, *26*(9-10), 840–848. https://doi.org/10.1016/S0141-0229(00)00180-0

Koepff, J., Sachs, C. C., Wiechert, W., Kohlheyer, D., Nöh, K., Oldiges, M., & Grünberger, A. (2018). Germination and growth analysis of Streptomyces lividans at the single-cell level under varying medium compositions. *Frontiers in Microbiology*, *9*(NOV), 1–10. https://doi.org/10.3389/fmicb.2018.02680

Kostov, G. ., Lyubenova, V., Shopska, V., Petelkov, I., Ivanov, K., Iliev, V. ., … Ignatova, M. (2015). SOFTWARE SENSORS FOR MONITORING THE BIOMASS CONCENTRATION AND THE KINETICS OF CONTINUOUS BEER FERMENTATION WITH IMMOBILIZED CELLS. *COMPTES RENDUS DE L ACADEMIE BULGARE DES SCIENCES*, *68*(11), 1439–1448.

Kuschel, M., Siebler, F., & Takors, R. (2017). Lagrangian Trajectories to Predict the Formation of Population Heterogeneity in Large-Scale Bioreactors. *Bioengineering*, *4*(4), 27. https://doi.org/10.3390/bioengineering4020027

Kwak, S. K., & Kim, J. H. (2017). Statistical data preparation: Management of missing values and outliers. *Korean Journal of Anesthesiology*, *70*(4), 407–411. https://doi.org/10.4097/kjae.2017.70.4.407

Lameiras, F., Heijnen, J. J., & van Gulik, W. M. (2015). Development of tools for quantitative intracellular metabolomics of Aspergillus niger chemostat cultures. *Metabolomics*, *11*(5), 1253–1264. https://doi.org/10.1007/s11306-015-0781-z

Lange, J., Münch, E., Müller, J., Busche, T., Kalinowski, J., Takors, R., & Blombach, B. (2018). Deciphering the adaptation of corynebacterium glutamicum in transition from aerobiosis via microaerobiosis to anaerobiosis. *Genes*, *9*(6). https://doi.org/10.3390/genes9060297

Langheinrich, C., & Nienow, A. W. (1999). Control of pH in large-scale, free suspension animal cell bioreactors: Alkali addition and pH excursions. *Biotechnology and Bioengineering*, *66*(3), 171–179. Retrieved from http://ejournals.ebsco.com/direct.asp?ArticleID=VKL29T08GMPN6WL8AHQ1

Lapin, A., Müller, D., & Reuss, M. (2004). Dynamic behavior of microbial populations in stirred bioreactors simulated with Euler-Lagrange methods: Traveling along the lifelines of single cells. *Industrial and Engineering Chemistry Research*, *43*(16), 4647–4656.

Lapin, A., Schmid, J., & Reuss, M. (2006). Modeling the dynamics of E. coli populations in the three-dimensional turbulent field of a stirred-tank bioreactor-A structured-segregated approach. *Chemical Engineering Science*, *61*(14), 4783–4797. https://doi.org/10.1016/j.ces.2006.03.003

Lara, A. R., Galindo, E., Ramírez, O. T., & Palomares, L. a. (2006). Living with heterogeneities in bioreactors: understanding the effects of environmental gradients on cells. *Molecular Biotechnology*, *34*(3), 355–381. https://doi.org/10.1385/MB:34:3:355

Lara, A. R., Leal, L., Flores, N., Gosset, G., Bolívar, F., & Ramírez, O. T. (2006). Transcriptional and metabolic response of recombinant Escherichia coli to spatial dissolved oxygen tension gradients simulated in a scale-down system. *Biotechnology and Bioengineering*, *93*(2), 372–385. https://doi.org/10.1002/bit.20704

Lara, A. R., Taymaz-Nikerel, H., Mashego, M. R., Van Gulik, W. M., Heijnen, J. J., Ramírez, O. T., & Van Winden, W. A. (2009). Fast dynamic response of the fermentative metabolism of Escherichia coli to aerobic and anaerobic glucose pulses. *Biotechnology and Bioengineering*, *104*(6), 1153–1161. https://doi.org/10.1002/bit.22503

Larsson, G., Törnkvist, M., Ståhl Wernersson, E., Trägårdh, C., Noorman, H., & Enfors, S. O. (1996). Substrate gradients in bioreactors: Origin and consequences. *Bioprocess Engineering*, *14*, 281–289. https://doi.org/10.1007/s004490050218

Lattermann, C., & Büchs, J. (2015). Microscale and miniscale fermentation and screening. *Current Opinion in Biotechnology*, *35*, 1–6. https://doi.org/10.1016/j.copbio.2014.12.005

Lauterbach, T., Lenk, F., Walther, T., Int, T. U. D., Grösel, M., Lenk, S., … Peters, A. (2017). Sens-o-Spheres – Mobile , miniaturisierte Sensorplattform für die ortsungebundene Prozessmessung in Reaktionsgefäßen, 89–93. https://doi.org/10.5162/13dss2017/2.6

Layec, S., Gérard, J., Legué, V., Chapot-Chartier, M. P., Courtin, P., Borges, F., … Leblond-Bourget, N. (2009). The CHAP domain of Cse functions as an endopeptidase that acts at mature septa to promote Streptococcus thermophilus cell separation. *Molecular Microbiology*, *71*(5), 1205–1217. https://doi.org/10.1111/j.1365-2958.2009.06595.x

Lee, J. H., Kim, J., Park, J.-H., Heo, W. Do, & Lee, G. M. (2019). Analysis of Golgi pH in CHO cells using ratiometric pH-sensitive fluorescent proteins. *Biotechnology & Bioengineering*, 1–30. https://doi.org/10.1002/bit.26920

Lemoine, A., Delvigne, F., Bockisch, A., Neubauer, P., & Junne, S. (2017). Tools for the determination of population heterogeneity caused by inhomogeneous cultivation conditions. *Journal of Biotechnology*, *251*, 84–93. https://doi.org/10.1016/j.jbiotec.2017.03.020

Lemoine, A., Limberg, M. H., Kästner, S., Oldiges, M., Neubauer, P., & Junne, S. (2016). Performance loss of *Corynebacterium glutamicum* cultivations under scale-down conditions using complex media. *Engineering in Life Sciences*, 1–13. https://doi.org/10.1002/elsc.201500144

Lemoine, A., Maya Martnez-Iturralde, N., Spann, R., Neubauer, P., & Junne, S. (2015). Response of Corynebacterium glutamicum exposed to oscillating cultivation conditions in a two- and a novel three-compartment scale-down bioreactor. *Biotechnology and Bioengineering*, *112*(6), 1220–1231. https://doi.org/10.1002/bit.25543

Lencastre Fernandes, R., Nierychlo, M., Lundin, L., Pedersen, A. E., Puentes Tellez, P. E., Dutta, A., … Gernaey, K. V. (2011). Experimental methods and modeling techniques for description of cell population heterogeneity. *Biotechnology Advances*, *29*(6), 575–599.

https://doi.org/10.1016/j.biotechadv.2011.03.007

LeThanh, H., Neubauer, P., & Hoffmann, F. (2005). The small heat-shock proteins IbpA and IpbB reduce the stress load of recombinant Escherichia coli and delay degradation of inclusion bodies. *Microbial Cell Factories*, *4*, 1–12. https://doi.org/10.1186/1475-2859-4-6

Li, C., Shu, W., Wang, S., Liu, P., Zhuang, Y., Zhang, S., & Xia, J. (2018). Dynamic metabolic response of Aspergillus niger to glucose perturbation: evidence of regulatory mechanism for reduced glucoamylase production. *Journal of Biotechnology*, *287*, 28–40. https://doi.org/10.1016/j.jbiotec.2018.08.005

Li, D., Li, Z., & Gao, Z. (2019). Quadrature-based moment methods for the population balance equation: An algorithm review. *Chinese Journal of Chemical Engineering*, *27*(3), 483–500. https://doi.org/10.1016/j.cjche.2018.11.028

Li, J., Jaitzig, J., Lu, P., Süssmuth, R. D., & Neubauer, P. (2015). Scale-up bioprocess development for production of the antibiotic valinomycin in Escherichia coli based on consistent fed-batch cultivations. *Microbial Cell Factories*, *14*(1), 1–13. https://doi.org/10.1186/s12934-015-0272-y

Li, Q., Tang, F., Huo, X., Huang, X., Zhang, Y., Wang, X., & Zhang, X. (2019). Native State Single-Cell Printing System and Analysis for Matrix Effects. *Analytical Chemistry*, *91*(13), 8115–8122. https://doi.org/10.1021/acs.analchem.9b00344

Lieder, S., Jahn, M., Koepff, J., Müller, S., & Takors, R. (2016). Environmental stress speeds up DNA replication in Pseudomonas putida in chemostat cultivations. *Biotechnology Journal*, *11*(1), 155–163. https://doi.org/10.1002/biot.201500059

Limberg, M. H., Joachim, M., Klein, B., Wiechert, W., & Oldiges, M. (2017). pH fluctuations imperil the robustness of C. glutamicum to short term oxygen limitation. *Journal of Biotechnology*, *259*, 248–260. https://doi.org/10.1016/j.jbiotec.2017.08.018

Limberg, M. H., Pooth, V., Wiechert, W., & Oldiges, M. (2016). Plug flow versus stirred tank reactor flow characteristics in two-compartment scale-down bioreactor: Setup-specific influence on the metabolic phenotype and bioprocess performance of Corynebacterium glutamicum. *Engineering in Life Sciences*, *16*(7), 610–619. https://doi.org/10.1002/elsc.201500142

Limberg, M. H., Schulte, J., Aryani, T., Mahr, R., Baumgart, M., Bott, M., … Oldiges, M. (2017). Metabolic profile of 1,5-diaminopentane producing Corynebacterium glutamicum under scale-down conditions: Blueprint for robustness to bioreactor inhomogeneities. *Biotechnology and Bioengineering*, *114*(3), 560–575. https://doi.org/10.1002/bit.26184

Lin, H. Y., Mathiszik, B., Xu, B., Enfors, S. O., & Neubauer, P. (2001). Determination of the maximum specific uptake capacities for glucose and oxygen in glucose-limited fed-batch cultivations of Escherichia coli. *Biotechnology and Bioengineering*, *73*(5), 347–357. https://doi.org/10.1002/bit.1068

Lin, H. Y., & Neubauer, P. (2000). Influence of controlled glucose oscillations on a fed-batch process of recombinant Escherichia coli. *J Biotechnol*, *79*(1), 27–37.

Lindemann, D., Westerwalbesloh, C., Kohlheyer, D., Grünberger, A., & Von Lieres, E. (2019). Microbial single-cell growth response at defined carbon limiting conditions. *RSC Advances*, *9*(25), 14040–

14050. https://doi.org/10.1039/c9ra02454a

Liu, X. T., Hou, C. L., Zhang, J., Zeng, X. F., & Qiao, S. Y. (2014). Fermentation conditions influence the fatty acid composition of the membranes of Lactobacillus reuteri I5007 and its survival following freeze-drying. *Letters in Applied Microbiology*, *59*(4), 398–403. https://doi.org/10.1111/lam.12292

Liu, Y., Dong, Y., Chen, Y. Y. M., & Burne, R. A. (2008). Environmental and growth phase regulation of the Streptococcus gordonii arginine deiminase genes. *Applied and Environmental Microbiology*, *74*(16), 5023–5030. https://doi.org/10.1128/AEM.00556-08

Löffler, M., Simen, J. D., Jäger, G., Schäferhoff, K., Freund, A., & Takors, R. (2016). Engineering E. coli for large-scale production – Strategies considering ATP expenses and transcriptional responses. *Metabolic Engineering*, *38*, 73–85. https://doi.org/10.1016/j.ymben.2016.06.008

Löffler, M., Simen, J. D., Müller, J., Jäger, G., Laghrami, S., Schäferhoff, K., … Takors, R. (2017). Switching between nitrogen and glucose limitation: Unraveling transcriptional dynamics in Escherichia coli. *Journal of Biotechnology*, *258*, 2–12. https://doi.org/10.1016/j.jbiotec.2017.04.011

Looser, V., Hammes, F., Keller, M., Berney, M., Kovar, K., & Egli, T. (2005). Flow-cytometric detection of changes in the physiological state of E. coli expressing a heterologous membrane protein during carbon-limited fedbatch cultivation. *Biotechnology and Bioengineering*, *92*(1), 69–78. https://doi.org/10.1002/bit.20575

Luttmann, R., Bracewell, D. G., Cornelissen, G., Gernaey, K. V., Glassey, J., Hass, V. C., … Mandenius, C. F. (2012). Soft sensors in bioprocessing: A status report and recommendations. *Biotechnology Journal*, *7*(8), 1040–1048. https://doi.org/10.1002/biot.201100506

Lyubenova, V., Junne, S., Ignatova, M., & Neubauer, P. (2013). Software sensor design considering oscillating conditions as present in industrial scale fed-batch cultivations. *Biotechnology and Bioengineering*, *110*(7), 1945–1955. https://doi.org/10.1002/bit.24870

Ma, Y., & Marquis, R. E. (1997). Thermophysiology of Streptococcus mutans and related lactic-acid bacteria. *Antonie van Leeuwenhoek, International Journal of General and Molecular Microbiology*, *72*(2), 91–100. https://doi.org/10.1023/A:1000290426248

Manfredini, R., Cavallera, V., Marini, L., & Donati, G. (1983). Mixing and oxygen transfer in conventional stirred fermentors. *Biotechnology and Bioengineering*, *25*(12), 3115–3131. https://doi.org/10.1002/bit.260251224

Mañas, P., & Mackey, B. M. (2004). Morphological and Physiological Changes Induced by High Hydrostatic Pressure in Exponential- and Stationary-Phase Cells of Escherichia coli: Relationship with Cell Death. *Applied and Environmental Microbiology*, *70*(3), 1545–1554. https://doi.org/10.1128/AEM.70.3.1545-1554.2004

Marbà-Ardébol, A. M., Bockisch, A., Neubauer, P., & Junne, S. (2018). Sterol synthesis and cell size distribution under oscillatory growth conditions in Saccharomyces cerevisiae scale-down cultivations. *Yeast*, *35*(2), 213–223. https://doi.org/10.1002/yea.3281

Marbà-Ardébol, A. M., Emmerich, J., Muthig, M., Neubauer, P., & Junne, S. (2018). Real-time monitoring of the budding index in Saccharomyces cerevisiae batch cultivations with in situ

microscopy. *Microbial Cell Factories*, *17*(1), 1–12. https://doi.org/10.1186/s12934-018-0922-y

Marbà-Ardébol, A. M., Emmerich, J., Muthig, M., Neubauer, P., & Junne, S. (2019). In Situ Microscopy for Real-time Determination of Single-cell Morphology in Bioprocesses. *Journal of Visualized Experiments : JoVE*, (154), 1–9. https://doi.org/10.3791/57823

Marbà-Ardébol, A. M., Emmerich, J., Neubauer, P., & Junne, S. (2017). Single-cell-based monitoring of fatty acid accumulation in Crypthecodinium cohnii with three-dimensional holographic and in situ microscopy. *Process Biochemistry*, *52*, 223–232. https://doi.org/10.1016/j.procbio.2016.11.003

Marba-Ardebol, A. M., Turon, X., Neubauer, P., & Junne, S. (2016). Application of flow cytometry analysis to elucidate the impact of scale-down conditions in Escherichia coli cultivations. *Afinidad*, *73*(573), 7–15. Retrieved from http://www.raco.cat/index.php/afinidad/article/view/308400

Marquard, D., Enders, A., Roth, G., Rinas, U., Scheper, T., & Lindner, P. (2016). In situ microscopy for online monitoring of cell concentration in Pichia pastoris cultivations. *Journal of Biotechnology*, *234*, 90–98. https://doi.org/10.1016/j.jbiotec.2016.07.024

Marquard, D., Schneider-Barthold, C., Düsterloh, S., Scheper, T., & Lindner, P. (2017). Online monitoring of cell concentration in high cell density Escherichia coli cultivations using in situ Microscopy. *Journal of Biotechnology*, *259*, 83–85. https://doi.org/10.1016/j.jbiotec.2017.08.003

Marquis, R. E., Bender, G. R., Murray, D. R., & Wong, A. (1987). Arginine deiminase system and bacterial adaptation to acid environments. *Applied and Environmental Microbiology*, *53*(1), 198–200.

Mashego, M. R., van Gulik, W. M., Vinke, J. L., Visser, D., & Heijnen, J. J. (2006). In vivo kinetics with rapid perturbation experiments in Saccharomyces cerevisiae using a second-generation BioScope. *Metabolic Engineering*, *8*(4), 370–383. https://doi.org/10.1016/j.ymben.2006.02.002

Maurer, L. M., Yohannes, E., Bondurant, S. S., Radmacher, M., & Slonczewski, J. L. (2005). pH regulates genes for flagellar motility, catabolism, and oxidative stress in Escherichia coli K-12. *Journal of Bacteriology*, *187*(1), 304–319. https://doi.org/10.1128/JB.187.1.304-319.2005

McClure, D. D., Kavanagh, J. M., Fletcher, D. F., & Barton, G. W. (2016). Characterizing bubble column bioreactor performance using computational fluid dynamics. *Chemical Engineering Science*, *144*, 58–74. https://doi.org/10.1016/j.ces.2016.01.016

Mercade, M., Lindley, N. D., & Loubière, P. (2000). Metabolism of *Lactococcus lactis* subsp. *cremoris* MG1363 in acid stress conditions. *International Journal of Food Microbiology*, *55*(1-3), 161–165.

Mohamed Al-Rubeai, A. N. E. (1995). *Flow Cytometry Applications in Cell Culture*.

Möller, J., Bhat, K., Riecken, K., Pörtner, R., Zeng, A., & Jandt, U. (2019). Process-induced cell cycle oscillations in CHO cultures: online monitoring and model-based investigation. *Biotechnology and Bioengineering*, *49*(0), 0–1. https://doi.org/10.1002/bit.27124

Morchain, J., Gabelle, J. C., & Cockx, A. (2012). Coupling of Biokinetic and Population Balance Models to Account for Biological Heterogeneity in Bioreactors. *AlChe Journal*, *59*(2), 369–379. https://doi.org/10.1002/aic.13820

Morchain, J., Gabelle, J. C., & Cockx, A. (2014). A Coupled Population Balance Model and CFD Approach for the Simulation of Mixing Issues in Lab-Scale and Industrial Bioreactors. *AICHE Journal*, *60*(1),

27–40. https://doi.org/10.1002/aic

Müller, L., Klar, A., & Schneider, F. (2019). A numerical comparison of the method of moments for the population balance equation. *Mathematics and Computers in Simulation*, *165*(xxxx), 26–55. https://doi.org/10.1016/j.matcom.2019.02.020

Müller, S., Harms, H., & Bley, T. (2010). Origin and analysis of microbial population heterogeneity in bioprocesses. *Current Opinion in Biotechnology*, *21*(1), 100–113. https://doi.org/10.1016/j.copbio.2010.01.002

Murphy, M. G., & Condon, S. (1984). Correlation of oxygen utilization and peroxide accumulation in Lactobacillus plantarum. *Archives of Microbiology*, *138*, 44–48.

Mustafi, N., Grünberger, A., Mahr, R., Helfrich, S., Nöh, K., Blombach, B., … Frunzke, J. (2014). Application of a genetically encoded biosensor for live cell imaging of L-valine production in pyruvate dehydrogenase complex-deficient Corynebacterium glutamicum strains. *PLoS ONE*, *9*(1). https://doi.org/10.1371/journal.pone.0085731

Nagpal, R., Kumar, A., Kumar, M., Behare, P. V., Jain, S., & Yadav, H. (2012). Probiotics, their health benefits and applications for developing healthier foods: A review. *FEMS Microbiology Letters*, *334*(1), 1–15. https://doi.org/10.1111/j.1574-6968.2012.02593.x

Namdev, P. K., Thompson, B. G., & Gray, M. R. (1992). Effect of feed zone in fed-batch fermentations of Saccharomyces cerevisiae. *Biotechnology and Bioengineering*, *40*(2), 235–246. https://doi.org/10.1002/bit.260400207

Nannen, N. L., & Hutkins, R. W. (1991). Proton-Translocating Adenosine Triphosphatase Activity in Lactic Acid Bacterial. *Journal of Dairy Science*, *74*(3), 747–751. https://doi.org/10.3168/jds.s0022-0302(91)78220-9

Narayana, S. K., Mallick, S., & Siegumfeldt, H. (2020). Bacterial Flow Cytometry and Imaging as Potential Process Monitoring Tools for Industrial Biotechnology. *MDPI Fermentation*, *6*(10), 1–15.

Narayanan, H., Sokolov, M., Morbidelli, M., & Butté, A. (2019). A new generation of predictive models: The added value of hybrid models for manufacturing processes of therapeutic proteins. *Biotechnology and Bioengineering*, *116*(10), 2540–2549. https://doi.org/10.1002/bit.27097

Nasution, N., van Gulik, W. M., Kleijn, R. J., van Winden, W. A., Proell, A., & Heijnen, J. J. (2006). Measurement of Intracellular Metabolites of Primary Metabolism and Adenine Nucleotides in Chemostat Cultivated Penicillium chrysogenum. *Biotechnology & Bioengineering*, *94*(1), 159–166. https://doi.org/10.1002/bit.20842

Nasution, U., van Gulik, W. M., Proell, A., van Winden, W. A., & Heijnen, J. J. (2006). Generating short-term kinetic responses of primary metabolism of Penicillium chrysogenum through glucose perturbation in the bioscope mini reactor. *Metabolic Engineering*, *8*(5), 395–405. https://doi.org/10.1016/j.ymben.2006.04.002

Neubauer, P., Åhman, M., Törnkvist, M., Larsson, G., & Enfors, S. O. (1995). Response of guanosine tetraphosphate to glucose fluctuations in fed-batch cultivations of Escherichia coli. *Journal of Biotechnology*, *43*(3), 195–204. https://doi.org/10.1016/0168-1656(95)00130-1

Neubauer, P., & Junne, S. (2010). Scale-down simulators for metabolic analysis of large-scale bioprocesses. *Current Opinion in Biotechnology*, *21*(1), 114–121. https://doi.org/10.1016/j.copbio.2010.02.001

Neubauer, P., & Junne, S. (2016). Scale-Up and Scale-Down Methodologies for Bioreactors. In K. F. (Linköping U. Mandenius (Ed.), *Bioreactors* (First, pp. 323–354). Germany: Wiley-VCH Verlag GmbH & Co. KGaA. https://doi.org/10.1002/9783527683369.ch11

Neumeyer, A., Hübschmann, T., Müller, S., & Frunzke, J. (2013). Monitoring of population dynamics of Corynebacterium glutamicum by multiparameter flow cytometry. *Microbial Biotechnology*, *6*(2), 157–167. https://doi.org/10.1111/1751-7915.12018

Nezhad, M. H., Knight, M., & Britz, M. L. (2012). Evidence of changes in cell surface proteins during growth of Lactobacillus casei under acidic conditions. *Food Science and Biotechnology*, *21*(1), 253–260. https://doi.org/10.1007/s10068-012-0033-1

Nienow, A. W. (2006). Reactor engineering in large scale animal cell culture. *Cytotechnology*, *50*(1-3), 9–33. https://doi.org/10.1007/s10616-006-9005-8

Nienow, A. W. (2014). Re “Development of a scale-down model of hydrodynamic stress to study the performance of an industrial CHO cell line under simulated production scale bioreactor conditions” [Sieck, J.B., Cordes, T., Budach, W.E., Rhiel, M.H., Suemeghy, Z., Leist, C., Vill. *Journal of Biotechnology*, *171*(1), 82–84. https://doi.org/10.1016/j.jbiotec.2013.12.002

Nienow, A. W., Nordkvist, M., & Boulton, C. A. (2011). Scale-down/scale-up studies leading to improved commercial beer fermentation. *Biotechnology Journal*, *6*(8), 911–925. https://doi.org/10.1002/biot.201000414

Nienow, A. W., Scott, W. H., Hewitt, C. J., Thomas, C. R., Lewis, G., Amanullah, A., … Meier, S. J. (2013). Scale-down studies for assessing the impact of different stress parameters on growth and product quality during animal cell culture. *Chemical Engineering Research and Design*, *91*(11), 2265–2274. https://doi.org/10.1016/j.cherd.2013.04.002

Nieß, A., Failmezger, J., Kuschel, M., Siemann-Herzberg, M., & Takors, R. (2017). Experimentally Validated Model Enables Debottlenecking of in Vitro Protein Synthesis and Identifies a Control Shift under in Vivo Conditions. *ACS Synthetic Biology*, *6*(10), 1913–1921. https://doi.org/10.1021/acssynbio.7b00117

Nieß, A., Löffler, M., Simen, J. D., & Takors, R. (2017). Repetitive short-term stimuli imposed in poor mixing zones induce long-term adaptation of E. coli cultures in large-scale bioreactors: Experimental evidence and mathematical model. *Frontiers in Microbiology*, *8*(JUN), 1–9. https://doi.org/10.3389/fmicb.2017.01195

Noorman, H. (2011). An industrial perspective on bioreactor scale-down: What we can learn from combined large-scale bioprocess and model fluid studies. *Biotechnology Journal*, *6*, 934–943. https://doi.org/10.1002/biot.201000406

Nopens, I., Torfs, E., Ducoste, J., Vanrolleghem, P. A., & Gernaey, K. V. (2015). Population balance models: A useful complementary modelling framework for future WWTP modelling. *Water Science and Technology*, *71*(2), 159–167. https://doi.org/10.2166/wst.2014.500

Nørregaard, A., Bach, C., Krühne, U., Borgbjerg, U., & Gernaey, K. V. (2019). Hypothesis-driven compartment model for stirred bioreactors utilizing computational fluid dynamics and multiple pH sensors. *Chemical Engineering Journal*, *356*, 161–169. https://doi.org/10.1016/j.cej.2018.08.191

Nyanga-Koumou, A. P., Ouoba, L. I. I., Kobawila, S. C., & Louembe, D. (2012). Response mechanisms of lactic acid bacteria to alkaline environments: A review. *Critical Reviews in Microbiology*, *38*(3), 185–190. https://doi.org/10.3109/1040841X.2011.640978

O'Connor, G. M., Sanchez-Riera, F., & Cooney, C. L. (1992). Design and evalution of control strategies for high cell density fermentations. *Biotechnology and Bioengineering*, *39*(3), 293–304. https://doi.org/10.1002/bit.260390307

Ogonah, O. W., Polizzi, K. M., & Bracewell, D. G. (2017). Cell free protein synthesis: a viable option for stratified medicines manufacturing? *Current Opinion in Chemical Engineering*, *18*, 77–83. https://doi.org/10.1016/j.coche.2017.10.003

Olughu, W., Deepika, G., Hewitt, C., & Rielly, C. (2019). Insight into the large-scale upstream fermentation environment using scaled-down models. *Journal of Chemical Technology and Biotechnology*, *94*(3), 647–657. https://doi.org/10.1002/jctb.5804

Olughu, W., Nienow, A., Hewitt, C., & Rielly, C. (2019). Scale-down studies for the scale-up of a recombinant Corynebacterium glutamicum fed-batch fermentation: loss of homogeneity leads to lower levels of cadaverine production . *Journal of Chemical Technology & Biotechnology*. https://doi.org/10.1002/jctb.6248

Onyeaka, H., Nienow, A. W., & Hewitt, C. J. (2003). Further Studies Related to the Scale-up of High Cell Density Escherichia coli Fed-Batch Fermentations: The Additional Effect of a Changing Microenvironment When Using Aqueous Ammonia to Control pH. *Biotechnology and Bioengineering*, *84*(4), 474–484. https://doi.org/10.1002/bit.10805

Oosterhuis, N. M. G., Kossen, N. W. F., Olivier, A. P. C., & Schenk, E. S. (1985). Scale-down and optimization studies of the gluconic acid fermentation by Gluconobacter oxydans. *Biotechnology and Bioengineering*, *27*(5), 711–720. https://doi.org/10.1002/bit.260270521

Osman, J. J., Birch, J., & Varley, J. (2002). The response of GS-NS0 myeloma cells to single and multiple pH perturbations. *Biotechnology and Bioengineering*, *79*(4), 398–407. https://doi.org/10.1002/bit.10198

Otto, F. (1990). DAPI Staining of Fixed Cells for High-Resolution Flow Cytometly of Nuclear DNA. *Methods in Cell Biology*, *33*, 105–110.

Ou, F., McGoverin, C., Swift, S., & Vanholsbeeck, F. (2017). Absolute bacterial cell enumeration using flow cytometry. *Journal of Applied Microbiology*, *132*(2), 464–477. https://doi.org/10.1111/jam.13508

Ou, F., McGoverin, C., Swift, S., & Vanholsbeeck, F. (2019). Near real-time enumeration of live and dead bacteria using a fibre-based spectroscopic device. *Scientific Reports*, *9*(1), 1–10. https://doi.org/10.1038/s41598-019-41221-1

Palomares, L. A., & Ramírez, O. T. (2009). Bioreactor Scale-Up. *Encyclopedia of Industrial*

Biotechnology, 1–20. https://doi.org/10.1002/9780470054581.eib143

Panckow, R. P., Reinecke, L., Cuellar, M. C., & Maa, S. (2017). Photo-Optical In-Situ Measurement of Drop Size Distributions: Applications in Research and Industry. *Oil and Gas Science and Technology*, *72*(3). https://doi.org/10.2516/ogst/2017009

Papadimitriou, K., Alegría, Á., Bron, P. A., De Angelis, M., Gobbetti, M., Kleerebezem, M., … Kok, J. (2016). Stress Physiology of Lactic Acid Bacteria. *Microbiology and Molecular Biology Reviews*, *80*(3), 837–890. https://doi.org/10.1128/MMBR.00076-15.Address

Papapostolou, A., Karasavvas, E., & Chatzidoukas, C. (2019). Oxygen mass transfer limitations set the performance boundaries of microbial PHA production processes – A model-based problem investigation supporting scale-up studies. *Biochemical Engineering Journal*, *148*(December 2018), 224–238. https://doi.org/10.1016/j.bej.2019.04.024

Passot, S., Gautier, J., Jamme, F., Cenard, S., Dumas, P., & Fonseca, F. (2015). Understanding the cryotolerance of lactic acid bacteria using combined synchrotron infrared and fluorescence microscopies. *Analyst*, *140*(17), 5920–5928. https://doi.org/10.1039/c5an00654f

Pastink, M. I., Sieuwerts, S., de Bok, F. A. M., Janssen, P. W. M., Teusink, B., van Hylckama Vlieg, J. E. T., & Hugenholtz, J. (2008). Genomics and high-throughput screening approaches for optimal flavour production in dairy fermentation. *International Dairy Journal*, *18*(8), 781–789. https://doi.org/10.1016/j.idairyj.2007.07.006

Pastink, M. I., Teusink, B., Hols, P., Visser, S., De Vos, W. M., & Hugenholtz, J. (2009). Genome-scale model of Streptococcus thermophilus LMG18311 for metabolic comparison of lactic acid bacteria. *Applied and Environmental Microbiology*, *75*(11), 3627–3633. https://doi.org/10.1128/AEM.00138-09

Paul, K., Rajamanickam, V., & Herwig, C. (2019). Model-based optimization of temperature and pH shift to increase volumetric productivity of a Chinese hamster ovary fed-batch process. *Journal of Bioscience and Bioengineering*, *128*(6), 710–715. https://doi.org/10.1016/j.jbiosc.2019.06.004

Pederson, E. N., & Srienc, F. (2004). Mass spectrometry feedback control for synthesis of polyhydroxyalkanoate granule microstructures in Ralstonia eutropha. *Macromolecular Bioscience*, *4*(3), 243–254. https://doi.org/10.1002/mabi.200300137

Petersen, T. R. N. J. L. V. (2018). FERMSENSE 3D - Data-based tank mapping service for the Bioprocess industry. Retrieved from https://www.freesense.dk/sites/default/files/Fermsense 3D 4P19.pdf

Philip, P., Meier, K., Kern, D., Goldmanns, J., Stockmeier, F., Bähr, C., & Büchs, J. (2017). Systematic evaluation of characteristics of the membrane-based fed-batch shake flask. *Microbial Cell Factories*, *16*(1), 1–17. https://doi.org/10.1186/s12934-017-0741-6

Pigou, M., & Morchain, J. (2015). Investigating the interactions between physical and biological heterogeneities in bioreactors using compartment, population balance and metabolic models. *Chemical Engineering Science*, *126*, 267–282. https://doi.org/10.1016/j.ces.2014.11.035

Pigou, M., Morchain, J., Fede, P., Penet, M. I., & Laronze, G. (2017). An assessment of methods of moments for the simulation of population dynamics in large-scale bioreactors. *Chemical Engineering Science*, *171*, 218–232. https://doi.org/10.1016/j.ces.2017.05.026

Pigou, M., Morchain, J., Fede, P., Penet, M. I., & Laronze, G. (2018). New developments of the Extended Quadrature Method of Moments to solve Population Balance Equations. *Journal of Computational Physics*, *365*, 243–268. https://doi.org/10.1016/j.jcp.2018.03.027

Pontius, K. (2019). *Monitoring of Bioprocesses. Opportunities and challenges: Opportunities and Challenges*. Technical University of Denmark.

Poolman, B., Driessen, A. J. M., & Konings, W. N. (1987). Regulation of solute transport in streptococci by external and internal pH values. *Microbiological Reviews*, *51*(4), 498–508.

Pörtner, R., Platas Barradas, O., Frahm, B., & Hass, V. C. (2016). *Advanced Process and Control Strategies for Bioreactors*. *Current Developments in Biotechnology and Bioengineering: Bioprocesses, Bioreactors and Controls*. Elsevier B.V. https://doi.org/10.1016/B978-0-444-63663-8.00016-1

Posch, A. E., Herwig, C., & Spadiut, O. (2013). Science-based bioprocess design for filamentous fungi. *Trends in Biotechnology*, *31*(1), 37–44. https://doi.org/10.1016/j.tibtech.2012.10.008

Potrykus, K., & Cashel, M. (2008). (p)ppGpp: Still Magical? *Annual Review of Microbiology*, *62*(1), 35–51. https://doi.org/10.1146/annurev.micro.62.081307.162903

Presser, K. A., Ratkowsky, D. A., & Ross, T. (1997). Modelling the Growth Rate of Escherichia coli as a Function of pH and Lactic Acid Concentration. *Applied and Environmental Microbiology*, *63*(6), 2355–2360.

Quivey Jr., R. G., Faustoferri, R., Monahan, K., & Marquis, R. (2000). Shifts in membrane fatty acid associated with acid adaptation of Streptococcus mutans. *FEMS Microbiology Letters*, *189*, 89–92.

Rainey, P. B., & Kerr, B. (2010). Cheats as first propagules: A new hypothesis for the evolution of individuality during the transition from single cells to multicellularity. *BioEssays*, *32*(10), 872–880. https://doi.org/10.1002/bies.201000039

Ramkrishna, D. (2000). *Population Balances Theory and Applications to Particulate Systems in Engineering*. San Diego, CA, USA: Academic Press.

Ramkrishna, D., & Singh, M. R. (2014). Population Balance Modeling: Current Status and Future Prospects. *Annual Review of Chemical and Biomolecular Engineering*, *5*(1), 123–146. https://doi.org/10.1146/annurev-chembioeng-060713-040241

Ramos, C. L., Thorsen, L., Ryssel, M., Nielsen, D. S., Siegumfeldt, H., Schwan, R. F., & Jespersen, L. (2014). Effect of the gastrointestinal environment on pH homeostasis of Lactobacillus plantarum and Lactobacillus brevis cells as measured by real-time fluorescence ratio-imaging microscopy. *Research in Microbiology*, *165*(3), 215–225. https://doi.org/10.1016/j.resmic.2014.02.005

Randek, J., & Mandenius, C. F. (2018). On-line soft sensing in upstream bioprocessing. *Critical Reviews in Biotechnology*, *38*(1), 106–121. https://doi.org/10.1080/07388551.2017.1312271

Raschmanová, H., Zamora, I., Borčinová, M., Meier, P., Weninger, A., Mächler, D., … Kovar, K. (2019). Single-cell approach to monitor the unfolded protein response during biotechnological processes with Pichia pastoris. *Frontiers in Microbiology*, *10*(FEB).

https://doi.org/10.3389/fmicb.2019.00335

Rathore, A. S., Bhambure, R., & Ghare, V. (2010). Process analytical technology (PAT) for biopharmaceutical products. *Analytical and Bioanalytical Chemistry*, *398*(1), 137–154. https://doi.org/10.1007/s00216-010-3781-x

Rault, A., Bouix, M., & Béal, C. (2009). Fermentation pH influences the physiological-state dynamics of Lactobacillus bulgaricus CFL1 during pH-controlled culture. *Applied and Environmental Microbiology*, *75*(13), 4374–4381. https://doi.org/10.1128/AEM.02725-08

Ren, Y., Ji, Y., Teng, L., & Zhang, H. (2017). Using Raman spectroscopy and chemometrics to identify the growth phase of Lactobacillus casei Zhang during batch culture at the single-cell level. *Microbial Cell Factories*, *16*(1), 1–10. https://doi.org/10.1186/s12934-017-0849-8

Revilla-Guarinos, A., Alcántara, C., Rozès, N., Voigt, B., & Zúñiga, M. (2014). Characterization of the response to low pH of Lactobacillus casei ΔRR12, a mutant strain with low D-alanylation activity and sensitivity to low pH. *Journal of Applied Microbiology*, *116*(5), 1250–1261. https://doi.org/10.1111/jam.12442

Rhee, S. K., & Pack, M. Y. (1980). Effect of environmental pH on fermentation balance of Lactobacillus bulgaricus. *Journal of Bacteriology*, *144*(1), 217–221.

Richard, L., Guillouet, S. E., & Uribelarrea, J. L. (2014). Quantification of the transient and long-term response of Saccharomyces cerevisiae to carbon dioxide stresses of various intensities. *Process Biochemistry*, *49*(11), 1808–1818. https://doi.org/10.1016/j.procbio.2014.07.020

Robertson, J., McGoverin, C., Vanholsbeeck, F., & Swift, S. (2019). Optimisation of the protocol for the liVE/DEAD®BacLightTM bacterial viability kit for rapid determination of bacterial load. *Frontiers in Microbiology*, *10*(APR), 1–13. https://doi.org/10.3389/fmicb.2019.00801

Robitaille, J., Chen, J., & Jolicoeur, M. (2015). A single dynamic metabolic model can describe mAb producing CHO cell batch and fed-batch cultures on different culture media. *PLoS ONE*, *10*(9). https://doi.org/10.1371/journal.pone.0136815

Román, R., Farràs, M., Camps, M., Martínez-Monge, I., Comas, P., Martínez-Espelt, M., … Cairó, J. J. (2018). Effect of continuous feeding of CO2 and pH in cell concentration and product titers in hIFNγ producing HEK293 cells: Induced metabolic shift for concomitant consumption of glucose and lactate. *Journal of Biotechnology*, *287*, 68–73. https://doi.org/10.1016/j.jbiotec.2018.10.005

Rosseburg, A., Fitschen, J., Wutz, J., Wucherpfennig, T., & Schlüter, M. (2018). Hydrodynamic inhomogeneities in large scale stirred tanks – Influence on mixing time. *Chemical Engineering Science*, *188*, 208–220. https://doi.org/10.1016/j.ces.2018.05.008

Ruiz-Herrera, J., & Sentandreu, R. (2002). Different effectors of dimorphism in Yarrowia lipolytica. *Archives of Microbiology*, *178*(6), 477–483. https://doi.org/10.1007/s00203-002-0478-3

Sachs, C. C., Koepff, J., Wiechert, W., Grünberger, A., & Nöh, K. (2019). mycelyso – high-throughput analysis of Streptomyces mycelium live cell imaging data. *BMC Bioinformatics*, *20*(1), 1–7. https://doi.org/10.1186/s12859-019-3004-1

Sanchez-Gonzalez, Y., Cameleyre, X., Molina-Jouve, C., Goma, G., & Alfenore, S. (2009). Dynamic

microbial response under ethanol stress to monitor Saccharomyces cerevisiae activity in different initial physiological states. *Bioprocess and Biosystems Engineering*, *32*(4), 459–466. https://doi.org/10.1007/s00449-008-0265-x

Sandner, V., Pybus, L. P., McCreath, G., & Glassey, J. (2019). Scale-Down Model Development in ambr systems: An Industrial Perspective. *Biotechnology Journal*, *14*(4), 1–30. https://doi.org/10.1002/biot.201700766

Sandoval-Basurto, E. A., Gosset, G., Bolivar, F., & Ramírez, O. T. (2005). Culture of Escherichia coli under dissolved oxygen gradients simulated in a two-compartment scale-down system: Metabolic response and production of recombinant protein. *Biotechnology and Bioengineering*, *89*(4), 453–463. https://doi.org/10.1002/bit.20383

Sassi, H., Nguyen, T. M., Telek, S., Gosset, G., Grünberger, A., & Delvigne, F. (2019). Segregostat: a novel concept to control phenotypic diversification dynamics on the example of Gram-negative bacteria. *Microbial Biotechnology*, *12*(5), 1064–1075. https://doi.org/10.1111/1751-7915.13442

Sawatari, Y., & Yokota, A. (2007). Diversity and mechanisms of alkali tolerance in lactobacilli. *Applied and Environmental Microbiology*, *73*(12), 3909–3915. https://doi.org/10.1128/AEM.02834-06

Schädel, F., & Franco-Lara, E. (2009). Rapid sampling devices for metabolic engineering applications. *Applied Microbiology and Biotechnology*, *83*(2), 199–208. https://doi.org/10.1007/s00253-009-1976-x

Schaepe, S., Levisauskas, D., Simutis, R., & Lübbert, A. (2014). Data-based optimization of protein production processes. *Biotechnology Letters*, *36*(5), 929–935. https://doi.org/10.1007/s10529-013-1448-3

Schilling, B. M., Pfefferle, W., Bachmann, B., Leuchtenberger, W., & Deckwer, W. D. (1999). A special reactor design for investigations of mixing time effects in a scaled-down industrial L-lysine fed-batch fermentation process. *Biotechnology and Bioengineering*, *64*(5), 599–606. https://doi.org/10.1002/(SICI)1097-0290(19990905)64:5<599::AID-BIT10>3.0.CO;2-C

Schirmer, C., Blaschczok, K., Husemann, U., Leupold, M., Zahnow, C., Rupprecht, J., … Eibl, D. (2017). Standardized Qualification of Stirred Bioreactors for Microbial Biopharmaceutical Production Processes. *Chemie-Ingenieur-Technik*, *89*(12), 1766–1772. https://doi.org/10.1002/cite.201700039

Schmalzriedt, S., Jenne, M., Mauch, K., & Reuss, M. (2003). Integration of physiology and fluid dynamics. *Advances in Biochemical Engineering/biotechnology*, *80*, 19–68.

Schmidt, A., Kochanowski, K., Vedelaar, S., Ahrné, E., Volkmer, B., Callipo, L., … Heinemann, M. (2016). The quantitative and condition-dependent Escherichia coli proteome. *Nature Biotechnology*, *34*(1), 104–110. https://doi.org/10.1038/nbt.3418

Schmitz, J., Noll, T., & Grünberger, A. (2019). Heterogeneity Studies of Mammalian Cells for Bioproduction: From Tools to Application. *Trends in Biotechnology*, *37*(6), 645–660. https://doi.org/10.1016/j.tibtech.2018.11.007

Schoug, Å., Fischer, J., Heipieper, H. J., Schnürer, J., & Håkansson, S. (2008). Impact of fermentation pH and temperature on freeze-drying survival and membrane lipid composition of Lactobacillus

coryniformis Si3. *Journal of Industrial Microbiology and Biotechnology*, *35*(3), 175–181. https://doi.org/10.1007/s10295-007-0281-x

Schweder, T., Krüger, E., Xu, B., Jürgen, B., Blomsten, G., Enfors, S. O., & Hecker, M. (1999). Monitoring of genes that respond to process-related stress in large- scale bioprocesses. *Biotechnology and Bioengineering*, *65*(2), 151–159. https://doi.org/10.1002/(SICI)1097-0290(19991020)65:2<151::AID-BIT4>3.0.CO;2-V

Sedewitz, B., Schleifer, K. H., & Gotz, F. (1984). Physiological role of pyruvate oxidase in the aerobic metabolism of Lactobacillus plantarum. *Journal of Bacteriology*, *160*(1), 462–465.

Shang, F., Wen, S., Wang, X., & Tan, T. (2006). High-cell-density fermentation for ergosterol production by Saccharomyces cerevisiae. *Journal of Bioscience and Bioengineering*, *101*(1), 38–41. https://doi.org/10.1263/jbb.101.38

Shapiro, H. M., & Nebe-von-Caron, G. (2004). Multiparameter flow cytometry of bacteria. *Methods in Molecular Biology (Clifton, N.J.)*, *263*, 33–44. https://doi.org/10.1385/1-59259-773-4:033

Shi, H., Colavin, A., Bigos, M., Tropini, C., Monds, R. D., & Huang, K. C. (2017). Deep Phenotypic Mapping of Bacterial Cytoskeletal Mutants Reveals Physiological Robustness to Cell Size. *Current Biology*, *27*(22), 3419–3429.e4. https://doi.org/10.1016/j.cub.2017.09.065

Shi, L., Günther, S., Hübschmann, T., Wick, L. Y., Harms, H., & Müller, S. (2007). Limits of propidium iodide as a cell viability indicator for environmental bacteria. *Cytometry Part A*, *71*(8), 592–598. https://doi.org/10.1002/cyto.a.20402

Shu, G., Zhang, B., Hui, Y., Chen, H., & Wan, H. (2017). Optimization of cryoprotectants for Streptococcus thermophilus during freeze-drying using Box-Behnken experimental design of response surface methodology. *Emirates Journal of Food and Agriculture*, *29*(4), 256–263. https://doi.org/10.9755/ejfa.2016-07-960

Siebler, F., Lapin, A., Hermann, M., & Takors, R. (2019). The impact of CO gradients on C. ljungdahlii in a 125 m3 bubble column: Mass transfer, circulation time and lifeline analysis. *Chemical Engineering Science*, *207*, 410–423. https://doi.org/10.1016/j.ces.2019.06.018

Sieck, J. B., Budach, W. E., Suemeghy, Z., Leist, C., Villiger, T. K., Morbidelli, M., & Soos, M. (2014). Adaptation for survival: Phenotype and transcriptome response of CHO cells to elevated stress induced by agitation and sparging. *Journal of Biotechnology*, *189*, 94–103. https://doi.org/10.1016/j.jbiotec.2014.08.042

Siegumfeldt, H., Rechinger, K. B., & Jakobsen, M. (2000). Dynamic changes of intracellular pH in individual lactic acid bacterium cells in response to a rapid drop in extracellular pH. *Applied and Environmental Microbiology*, *66*(6), 2330–2335. https://doi.org/10.1128/AEM.66.6.2330-2335.2000

Simen, J. D., Löffler, M., Jäger, G., Schäferhoff, K., Freund, A., Matthes, J., … Broicher, A. (2017). Transcriptional response of Escherichia coli to ammonia and glucose fluctuations. *Microbial Biotechnology*, *10*(4), 858–872. https://doi.org/10.1111/1751-7915.12713

Simutis, R., & Lübbert, A. (2015). Bioreactor control improves bioprocess performance. *Biotechnology Journal*, *10*(8), 1115–1130. https://doi.org/10.1002/biot.201500016

Soini, J., Falschlehner, C., Liedert, C., Bernhardt, J., Vuoristo, J., & Neubauer, P. (2008). Norvaline is accumulated after a down-shift of oxygen in Escherichia coli W3110. *Microbial Cell Factories*, *7*, 1–14. https://doi.org/10.1186/1475-2859-7-30

Soini, J., Ukkonen, K., & Neubauer, P. (2011). Accumulation of amino acids deriving from pyruvate in <i>Escherichia coli</i> W3110 during fed-batch cultivation in a two-compartment scale-down bioreactor. *Advances in Bioscience and Biotechnology*, *02*(05), 336–339. https://doi.org/10.4236/abb.2011.25049

Sommeregger, W., Sissolak, B., Kandra, K., von Stosch, M., Mayer, M., & Striedner, G. (2017). Quality by control: Toward model predictive control of mammalian cell culture bioprocesses. *Biotechnology Journal*, *12*(7), 1–7. https://doi.org/10.1002/biot.201600546

Spadiut, O., Rittmann, S., Dietzsch, C., & Herwig, C. (2013). Dynamic process conditions in bioprocess development. *Engineering in Life Sciences*, *13*(1), 88–101. https://doi.org/10.1002/elsc.201200026

Spann, R., Gernaey, K. V., & Sin, G. (2019). A compartment model for risk-based monitoring of lactic acid bacteria cultivations. *Biochemical Engineering Journal*, *151*(January), 107293. https://doi.org/10.1016/j.bej.2019.107293

Spann, R., Lantz, A. E., Roca, C., Gernaey, K. V., & Sin, G. (2018). Model-based process development for a continuous lactic acid bacteria fermentation. *Computer Aided Chemical Engineering*, *43*, 1601–1606. https://doi.org/10.1016/B978-0-444-64235-6.50279-5

Spann, R., Roca, C., Kold, D., Eliasson Lantz, A., Gernaey, K. V., & Sin, G. (2018). A probabilistic model-based soft sensor to monitor lactic acid bacteria fermentations. *Biochemical Engineering Journal*, *135*, 49–60. https://doi.org/10.1016/j.bej.2018.03.016

Spann, R., Roca, C., Kold, D., Lantz, A. E., Gernaey, K. V., & Sin, G. (2017). *A Consistent Methodology Based Parameter Estimation for a Lactic Acid Bacteria Fermentation Model*. *Computer Aided Chemical Engineering* (Vol. 40). Elsevier Masson SAS. https://doi.org/10.1016/B978-0-444-63965-3.50372-X

Suhr, H., & Herkommer, A. M. (2015). In situ microscopy using adjustment-free optics . *Journal of Biomedical Optics*, *20*(11), 116007. https://doi.org/10.1117/1.jbo.20.11.116007

Sunya, S., Bideaux, C., Molina-Jouve, C., & Gorret, N. (2013). Short-term dynamic behavior of Escherichia coli in response to successive glucose pulses on glucose-limited chemostat cultures. *Journal of Biotechnology*, *164*(4), 531–542. https://doi.org/10.1016/j.jbiotec.2013.01.014

Sweere, A. P. J., Janse, L., & Kossen, N. W. F. (1988). Experimental Simulation of Oxygen Profiles and Their Influence on Baker's yeast production: 2. Two-Fermentor System, *586*, 579–586.

Sweere, A. P. J., Luyben, K. C. A. M., & Kossen, N. W. F. (1987). Regime analysis and scale-down: Tools to investigate the performance of bioreactors. *Enzyme and Microbial Technology*, *9*(7), 386–398. https://doi.org/10.1016/0141-0229(87)90133-5

Syed, Q. A., Buffa, M., Guamis, B. V., & Saldo, J. (2016). Factors Affecting Bacterial Inactivation during High Hydrostatic Pressure Processing of Foods: A Review. *Critical Reviews in Food Science and Nutrition*, *56*(3), 474–483. https://doi.org/10.1080/10408398.2013.779570

Szabo, R., & Štofaníková, V. (2002). Presence of organic sources of nitrogen is critical for filament formation and pH-dependent morphogenesis in Yarrowia lipolytica. *FEMS Microbiology Letters*, *206*(1), 45–50. https://doi.org/10.1016/S0378-1097(01)00505-5

Taimur Khan, M. M., Pyle, B. H., & Camper, A. K. (2010). Specific and rapid enumeration of viable but nonculturable and viable-culturable gram-negative bacteria by using flow cytometry. *Applied and Environmental Microbiology*, *76*(15), 5088–5096. https://doi.org/10.1128/AEM.02932-09

Tajsoleiman, T., Mears, L., Krühne, U., Gernaey, K. V., & Cornelissen, S. (2019). An Industrial Perspective on Scale-Down Challenges Using Miniaturized Bioreactors. *Trends in Biotechnology*, *37*(7), 697–706. https://doi.org/10.1016/j.tibtech.2019.01.002

Tajsoleiman, T., Spann, R., Bach, C., Gernaey, K. V., Huusom, J. K., & Krühne, U. (2019). A CFD based automatic method for compartment model development. *Computers and Chemical Engineering*, *123*, 236–245. https://doi.org/10.1016/j.compchemeng.2018.12.015

Takors, R. (2012). Scale-up of microbial processes: Impacts, tools and open questions. *Journal of Biotechnology*, *160*(1-2), 3–9. https://doi.org/10.1016/j.jbiotec.2011.12.010

Takors, R., Kopf, M., Mampel, J., Bluemke, W., Blombach, B., Eikmanns, B., … Dürre, P. (2018). Using gas mixtures of CO, CO 2 and H 2 as microbial substrates: the do's and don'ts of successful technology transfer from laboratory to production scale. *Microbial Biotechnology*, *11*(4), 606–625. https://doi.org/10.1111/1751-7915.13270

Tang, W., Deshmukh, A. T., Haringa, C., Wang, G., van Gulik, W., van Winden, W., … Noorman, H. J. (2017). *A 9-pool metabolic structured kinetic model describing days to seconds dynamics of growth and product formation by Penicillium chrysogenum*. *Biotechnology and Bioengineering* (Vol. 114). https://doi.org/10.1002/bit.26294

Taymaz-Nikerel, H., van Gulik, W. M., & Heijnen, J. J. (2011). Escherichia coli responds with a rapid and large change in growth rate upon a shift from glucose-limited to glucose-excess conditions. *Metabolic Engineering*, *13*(3), 307–318. https://doi.org/10.1016/j.ymben.2011.03.003

Teng, L., Wang, X., Wang, X., Gou, H., Ren, L., Wang, T., … Xu, J. (2016). Label-free, rapid and quantitative phenotyping of stress response in E. coli via ramanome. *Scientific Reports*, *6*. https://doi.org/10.1038/srep34359

Teusink, B., Bachmann, H., & Molenaar, D. (2011). Systems biology of lactic acid bacteria: A critical review. *Microbial Cell Factories*, *10*(SUPPL. 1), 1–17. https://doi.org/10.1186/1475-2859-10-S1-S11

Theron, C. W., Berrios, J., Delvigne, F., & Fickers, P. (2018). Integrating metabolic modeling and population heterogeneity analysis into optimizing recombinant protein production by Komagataella (Pichia) pastoris. *Applied Microbiology and Biotechnology*, *102*(1), 63–80. https://doi.org/10.1007/s00253-017-8612-y

Tissot, S., Farhat, M., Hacker, D. L., Anderlei, T., Kühner, M., Comninellis, C., & Wurm, F. (2010). Determination of a scale-up factor from mixing time studies in orbitally shaken bioreactors. *Biochemical Engineering Journal*, *52*(2-3), 181–186. https://doi.org/10.1016/j.bej.2010.08.005

Torres, N. V., Riol-Cimas, J. M., Wolschek, M., & Kubicek, C. P. (1996). Glucose transport by Aspergillus

niger: The low-affinity carrier is only formed during growth on high glucose concentrations. *Applied Microbiology and Biotechnology*, *44*(6), 790–794. https://doi.org/10.1007/s002530050634

Tsao, E. I., Bohn, M. A., Omstead, D. R., Munster, M. J., & Numsuwan, V. (1992). Effects of heat shock on the production of human erythropoietin from recombinant CHO cells. *Biotechnology and Bioengineering*, *40*(10), 1190–1196. https://doi.org/10.1002/bit.260401008

Turner, K. W., & Thomas, T. D. (1975). Uncoupling of growth and acid production in lactic streptococci. *New Zealand Journal of Dairy Science and Technology*, *10*, 162–167.

Ukkonen, K., Veijola, J., Vasala, A., & Neubauer, P. (2013). Effect of culture medium, host strain and oxygen transfer on recombinant Fab antibody fragment yield and leakage to medium in shaken E. coli cultures. *Microbial Cell Factories*, *12*(1), 1–14. https://doi.org/10.1186/1475-2859-12-73

Van Boxtel, C., Van Heerden, J. H., Nordholt, N., Schmidt, P., & Bruggeman, F. J. (2017). Taking chances and making mistakes: Non-genetic phenotypic heterogeneity and its consequences for surviving in dynamic environments. *Journal of the Royal Society Interface*, *14*(132). https://doi.org/10.1098/rsif.2017.0141

van Gulik, W. M. (2010). Fast sampling for quantitative microbial metabolomics. *Current Opinion in Biotechnology*, *21*(1), 27–34. https://doi.org/10.1016/j.copbio.2010.01.008

Van Gulik, W. M., Canelas, A. B., Seifar, R. M., & Heijnen, J. J. (2013). The Sampling and Sample Preparation Problem in Microbial Metabolomics. *Metabolomics in Practice: Successful Strategies to Generate and Analyze Metabolic Data*, 1–19. https://doi.org/10.1002/9783527655861.ch1

Vasdekis, A. E., Alanazi, H., Silverman, A. M., Williams, C. J., Canul, A. J., Cliff, J. B., … Stephanopoulos, G. (2019). Eliciting the impacts of cellular noise on metabolic trade-offs by quantitative mass imaging. *Nature Communications*, *10*(1). https://doi.org/10.1038/s41467-019-08717-w

Veiter, L., Rajamanickam, V., & Herwig, C. (2018). The filamentous fungal pellet—relationship between morphology and productivity. *Applied Microbiology and Biotechnology*, *102*(7), 2997–3006. https://doi.org/10.1007/s00253-018-8818-7

Villiger, T. K., Neunstoecklin, B., Karst, D. J., Lucas, E., Stettler, M., Broly, H., … Soos, M. (2018). Experimental and CFD physical characterization of animal cell bioreactors: From micro- to production scale. *Biochemical Engineering Journal*, *131*, 84–94. https://doi.org/10.1016/j.bej.2017.12.004

Visser, D., Van Zuylen, G. A., Van Dam, J. C., Eman, M. R., Pröll, A., Ras, C., … Heijnen, J. J. (2004). Analysis of in vivo kinetics of glycolysis in aerobic Saccharomyces cerevisiae by application of glucose and ethanol pulses. *Biotechnology and Bioengineering*, *88*(2), 157–167. https://doi.org/10.1002/bit.20235

Visser, D., Van Zuylen, G. A., Van Dam, J. C., Oudshoorn, A., Eman, M. R., Ras, C., … Heijnen, J. J. (2002). Rapid sampling for analysis of in vivo kinetics using the BioScope: A system for continuous-pulse experiments. *Biotechnology and Bioengineering*, *79*(6), 674–681. https://doi.org/10.1002/bit.10328

Vrábel, P., Van Der Lans, R. G. J. M., Luyben, K. C. A. M., Boon, L., & Nienow, A. W. (2000). Mixing in

large-scale vessels stirred with multiple radial or radial and axial up-pumping impellers: Modelling and measurements. *Chemical Engineering Science*, *55*(23), 5881–5896. https://doi.org/10.1016/S0009-2509(00)00175-5

Waldherr, S. (2018). Estimation methods for heterogeneous cell population models in systems biology. *Journal of the Royal Society, Interface*, *15*(147). https://doi.org/10.1098/rsif.2018.0530

Wallenius, J., Barth, D., & Eerikäinen, T. (2012). The effects of pH oscillation on Lactobacillus rhamnosus batch cultivation. *Applied Microbiology and Biotechnology*, *95*(5), 1265–1273. https://doi.org/10.1007/s00253-012-3946-y

Wallenius, J., Uuksulainen, T., & Scale-down, L. Á. T. Á. (2011). The effect of temperature and pH gradients on Lactobacillus rhamnosus gene expression of stress-related genes, 1169–1176. https://doi.org/10.1007/s00449-011-0568-1

Wang, C., Chen, Y., Zhou, H., Li, X., & Tan, Z. (2019). Adaptation mechanisms of Rhodococcus sp. CNS16 under different temperature gradients. *Chemosphere*. https://doi.org/10.1016/j.chemosphere.2019.124571

Wang, G., Chu, J., Noorman, H., Xia, J., Tang, W., Zhuang, Y., & Zhang, S. (2014). Prelude to rational scale-up of penicillin production: A scale-down study. *Applied Microbiology and Biotechnology*, *98*(6), 2359–2369. https://doi.org/10.1007/s00253-013-5497-2

Wang, G., Chu, J., Zhuang, Y., van Gulik, W., & Noorman, H. (2019). A dynamic model-based preparation of uniformly- 13 C-labeled internal standards facilitates quantitative metabolomics analysis of Penicillium chrysogenum. *Journal of Biotechnology*, *299*, 21–31. https://doi.org/10.1016/j.jbiotec.2019.04.021

Wang, G., Tang, W., Xia, J., Chu, J., Noorman, H., & van Gulik, W. M. (2015). Integration of microbial kinetics and fluid dynamics toward model-driven scale-up of industrial bioprocesses. *Engineering in Life Sciences*, *15*(1), 20–29. https://doi.org/10.1002/elsc.201400172

Wang, G., Wang, X., Wang, T., Gulik, W., Noorman, H. J., Zhuang, Y., … Zhang, S. (2019). Comparative fluxome and metabolome analysis of formate as an auxiliary substrate for penicillin production under glucose-limited cultivation of Penicillium chrysogenum . *Biotechnology Journal*, *1900009*, 1900009. https://doi.org/10.1002/biot.201900009

Wang, G., Zhao, J., Haringa, C., Tang, W., Xia, J., Chu, J., … Noorman, H. J. (2018). Comparative performance of different scale-down simulators of substrate gradients in Penicillium chrysogenum cultures: the need of a biological systems response analysis. *Microbial Biotechnology*, *11*(3), 486–497. https://doi.org/10.1111/1751-7915.13046

Wang, G., Zhao, J., Wang, X., Wang, T., Zhuang, Y., Chu, J., … Noorman, H. J. (2019). *Quantitative metabolomics and metabolic flux analysis reveal impact of altered trehalose metabolism on metabolic phenotypes of Penicillium chrysogenum in aerobic glucose-limited chemostats*. *Biochemical Engineering Journal*. Elsevier B.V. https://doi.org/10.1016/j.bej.2019.03.006

Wang, K., Yu, S., & Peng, W. (2019). *A novel moment method using the log skew normal distribution for particle coagulation*. *Journal of Aerosol Science* (Vol. 134). Elsevier Ltd. https://doi.org/10.1016/j.jaerosci.2019.04.013

Wang, S., Liu, P., Shu, W., Li, C., Li, H., Liu, S., … Noorman, H. (2019). Dynamic response of Aspergillus niger to single pulses of glucose with high and low concentrations. *Bioresources and Bioprocessing*, *6*(1). https://doi.org/10.1186/s40643-019-0251-y

Wang, T., & Dunlop, M. J. (2019). Controlling and exploiting cell-to-cell variation in metabolic engineering. *Current Opinion in Biotechnology*, *57*, 10–16. https://doi.org/10.1016/j.copbio.2018.08.013

Wang, W., He, J., Pan, D., Wu, Z., Guo, Y., Zeng, X., & Lian, L. (2018). Metabolomics analysis of Lactobacillus plantarum ATCC 14917 adhesion activity under initial acid and alkali stress. *PLoS ONE*, *13*(5), 1–16. https://doi.org/10.1371/journal.pone.0196231

Wehrs, M., Tanjore, D., Eng, T., Lievense, J., Pray, T. R., & Mukhopadhyay, A. (2019). Engineering Robust Production Microbes for Large-Scale Cultivation. *Trends in Microbiology*, *27*(6), 524–537. https://doi.org/10.1016/j.tim.2019.01.006

Wei, X. chen, Tang, L., & Lu, Y. hua. (2017). Dissolved oxygen control strategy for improvement of TL1-1 production in submerged fermentation by Daldinia eschscholzii. *Bioresources and Bioprocessing*, *4*(1), 1–9. https://doi.org/10.1186/s40643-016-0134-4

Wilkinson, D. J. (2009). Stochastic modelling for quantitative description of heterogeneous biological systems. *Nature Reviews Genetics*, *10*(2), 122–133. https://doi.org/10.1038/nrg2509

Wittmann, C., & Liao, J. C. (2016). *Industrial Biotechnology: Products and Processes*. (C. Wittmann & J. C. Liao, Eds.). Wiley-VCH Verlag GmbH & Co. KGaA. https://doi.org/10.1002/9783527807833

Wright, M. R., Bach, C., Gernaey, K. V., & Krühne, U. (2018). Investigation of the effect of uncertain growth kinetics on a CFD based model for the growth of S. cerevisiae in an industrial bioreactor. *Chemical Engineering Research and Design*, *140*, 12–22. https://doi.org/10.1016/j.cherd.2018.09.040

Wu, L., Schipper, D., Kresnowati, P., Proell, A. M., Ras, C., & Heijnen, J. J. (2006). Short-Term Metabolome Dynamics and Carbon, Electron, and ATP Balances in Chemostat-Grown. *Society*, *72*(5), 3566–3577. https://doi.org/10.1128/AEM.72.5.3566

Wu, L., Wang, S., Song, Y., Wang, X., & Yan, X. (2016). Applications and challenges for single-bacteria analysis by flow cytometry. *Science China Chemistry*, *59*(1), 30–39. https://doi.org/10.1007/s11426-015-5518-3

Xia, J., Wang, G., Lin, J., Wang, Y., Chu, J., Zhuang, Y., & Zhang, S. (2016). Advances and practices of bioprocess scale-up. *Advances in Biochemical Engineering/Biotechnology*, *152*, 137–151. https://doi.org/10.1007/10_2014_293

Xu, B., Jahic, M., Blomsten, G., & Enfors, S. O. (1999). Glucose overflow metabolism and mixed-acid fermentation in aerobic large-scale fed-batch processes with Escherichia coli. *Applied Microbiology and Biotechnology*, *51*(5), 564–571. https://doi.org/10.1007/s002530051433

Xu, S., Hoshan, L., Jiang, R., Gupta, B., Brodean, E., O'Neil, K., … Chen, H. (2017). A practical approach in bioreactor scale-up and process transfer using a combination of constant P/V and vvm as the criterion. *Biotechnology Progress*, *33*(4), 1146–1159. https://doi.org/10.1002/btpr.2489

Xu, S., Jiang, R., Mueller, R., Hoesli, N., Kretz, T., Bowers, J., & Chen, H. (2018). Probing lactate metabolism variations in large-scale bioreactors. *Biotechnology Progress*, *34*(3), 756–766. https://doi.org/10.1002/btpr.2620

Yamamori, T., & Yura, T. (1980). Temperature-induced synthesis of specific proteins in Escherichia coli: Evidence for transcriptional control. *Journal of Bacteriology*, *142*(3), 843–851.

Yang, K., Zhu, Y., Qi, Y., Zhang, T., Liu, M., Zhang, J., … Zhang, G. (2019). Analysis of proteomic responses of freeze-dried Oenococcus oeni to access the molecular mechanism of acid acclimation on cell freeze-drying resistance. *Food Chemistry*, *285*, 441–449. https://doi.org/10.1016/j.foodchem.2019.01.120

Yang, Y., Xia, J., Li, J., Chu, J., Li, L., Wang, Y., … Zhang, S. (2012). A novel impeller configuration to improve fungal physiology performance and energy conservation for cephalosporin C production. *Journal of Biotechnology*, *161*(3), 250–256. https://doi.org/10.1016/j.jbiotec.2012.07.007

Yu, T., & Chen, Y. (2019). Effects of elevated carbon dioxide on environmental microbes and its mechanisms: A review. *Science of the Total Environment*, *655*, 865–879. https://doi.org/10.1016/j.scitotenv.2018.11.301

Zacchetti, B., Wösten, H. A. B., & Claessen, D. (2018). Multiscale heterogeneity in filamentous microbes. *Biotechnology Advances*, *36*(8), 2138–2149. https://doi.org/10.1016/j.biotechadv.2018.10.002

Zare, F., Boye, J. I., Orsat, V., Champagne, C., & Simpson, B. K. (2011). Microbial, physical and sensory properties of yogurt supplemented with lentil flour. *Food Research International*, *44*(8), 2482–2488. https://doi.org/10.1016/j.foodres.2011.01.002

Zare, F., Champagne, C. P., Simpson, B. K., Orsat, V., & Boye, J. I. (2012). Effect of the addition of pulse ingredients to milk on acid production by probiotic and yoghurt starter cultures. *LWT - Food Science and Technology*, *45*(2), 155–160. https://doi.org/10.1016/j.lwt.2011.08.012

Zaunmüller, T., Eichert, M., Richter, H., & Unden, G. (2006). Variations in the energy metabolism of biotechnologically relevant heterofermentative lactic acid bacteria during growth on sugars and organic acids. *Applied Microbiology and Biotechnology*, *72*(3), 421–429. https://doi.org/10.1007/s00253-006-0514-3

Zhou, Y., Han, L. R., He, H. W., Sang, B., Yu, D. L., Feng, J. T., & Zhang, X. (2018). Effects of agitation, aeration and temperature on production of a novel glycoprotein gp-1 by streptomyces kanasenisi zx01 and scale-up based on volumetric oxygen transfer coefficient. *Molecules*, *23*(1), 1–14. https://doi.org/10.3390/molecules23010125

Zhu, L., Han, W., Song, B., & Wang, Z. (2018). Characterizing the fluid dynamics in the flow fields of cylindrical orbitally shaken bioreactors with different geometry sizes. *Engineering in Life Sciences*, *18*(8), 570–578. https://doi.org/10.1002/elsc.201700170

Ziegler, A., Schock-Kusch, D., Bopp, D., Dounia, S., Rädle, M., & Stahl, U. (2015). Single bacteria movement tracking by online microscopy - A proof of concept study. *PLoS ONE*, *10*(4), 1–17. https://doi.org/10.1371/journal.pone.0122531

Zieringer, J., & Takors, R. (2018). In Silico Prediction of Large-Scale Microbial Production Performance:

Constraints for Getting Proper Data-Driven Models. *Computational and Structural Biotechnology Journal*, *16*, 246–256. https://doi.org/10.1016/j.csbj.2018.06.002

Zou, X., Xia, J. Y., Chu, J., Zhuang, Y. P., & Zhang, S. L. (2012). Real-time fluid dynamics investigation and physiological response for erythromycin fermentation scale-up from 50 L to 132 m 3 fermenter. *Bioprocess and Biosystems Engineering*, *35*(5), 789–800. https://doi.org/10.1007/s00449-011-0659-z

Publications

I

1st Paper

frontiers in Bioengineering and Biotechnology

ORIGINAL RESEARCH
published: 04 December 2018
doi: 10.3389/fbioe.2018.00188

Electrooptical Determination of Polarizability for On-Line Viability and Vitality Quantification of *Lactobacillus plantarum* Cultures

Klaus Pellicer-Alborch[1], *Alexander Angersbach*[2], *Peter Neubauer*[1] *and Stefan Junne*[1]*

[1] *Chair of Bioprocess Engineering, Department of Biotechnology, Technische Universität Berlin, Berlin, Germany,*
[2] *EloSystems GbR, Berlin, Germany*

The rapid assessment of cell viability is crucial for process optimization, e.g., during media selection, determination of optimal environmental growth conditions and for quality control. In the present study, the cells' electric anisotropy of polarizability (AP) as well as the mean cell length in *Lactobacillus plantarum* batch and fed-batch fermentations were monitored with electrooptical measurements coupled to fully automated sample preparation. It was examined, whether this measurement can be related to the cells' metabolic activity, and thus represents a suitable process analytical technology. It is demonstrated that the AP is an early indicator to distinguish between suitable and unsuitable growth conditions in case of a poor energy regeneration or cell membrane defects in *L. plantarum* batch and fed-batch cultivations. It was shown that the applied method allowed the monitoring of physiological and morphological changes of cells in various growth phases in response to a low pH-value, substrate concentration changes, temperature alterations, exposure to air and nutrient limitation. An optimal range for growth in batch mode was achieved, if the AP remained above $25{\cdot}10^{-28}$ F·m^2 and the mean cell length at ~2.5 μm. It was further investigated, in which way the AP develops after freeze-drying of samples, which were taken in different cultivation phases. It was found that the AP increased most rapidly in resuspended samples from the retardation and late stationary phases, while samples from the early stationary phase recovered slowly. Electrooptical measurements provide valuable information about the physiologic and morphologic state of *L. plantarum* cells, e.g., when applied as starter cultures or as probiotic compounds.

Keywords: probiotics, polarizability, *Lactobacillus plantarum*, viability analysis, freeze–drying, cell length quantification, lactic acid bacteria, process analytical technology

OPEN ACCESS

Edited by:
Joseph Boudrant, Centre National de la Recherche Scientifique (CNRS), France

Reviewed by:
Ana M. R. B. Xavier, University of Aveiro, Portugal
Antonio Marzocchella, Università degli Studi di Napoli Federico II, Italy

***Correspondence:**
Stefan Junne
stefan.junne@tu-berlin.de

Specialty section:
This article was submitted to Process and Industrial Biotechnology, a section of the journal Frontiers in Bioengineering and Biotechnology

Received: *03 August 2018*
Accepted: *19 November 2018*
Published: *04 December 2018*

Citation:
Pellicer-Alborch K, Angersbach A, Neubauer P and Junne S (2018) Electrooptical Determination of Polarizability for On-Line Viability and Vitality Quantification of Lactobacillus plantarum Cultures. Front. Bioeng. Biotechnol. 6:188. doi: 10.3389/fbioe.2018.00188

INTRODUCTION

Lactic acid bacteria are applied for food preservation, but more importantly for yogurt and probiotics production. *Lactobacillus plantarum* plays a key role as cholesterol-lowering milk additive, which likely increases the immune responses, exert antimutagenic and anticarcinogenic activities and protect against gastrointestinal diseases, as summarized in numerous scientific review articles, e.g., (Nagpal et al., 2012; Kolaček et al., 2017). Several tools were introduced to monitor

physiologic key parameters in *L. plantarum* cultivations like multi-parameter flow cytometry (Arnold et al., 2002; Schenk et al., 2008; Bensch et al., 2014; Tropcheva et al., 2015), quantitative real-time PCR, e.g., (Clementschitsch et al., 2005; Davis, 2014; Sohier et al., 2014; Pega et al., 2016; Emerson et al., 2017), and viable cell counting for viability analysis (Savini et al., 2010; Perdana et al., 2012; Glušac et al., 2015). Although all these systems provide information on the metabolic state and physiology of the cell, they require manual *off-line* sample pre-treatment. The necessity of sample pre-treatment might be the reason for the lack of correlation between results of flow cytometry and colony forming units of *Lactobacillus* sp. (Léonard et al., 2016). The electrooptical analysis of the anisotropy of polarizability (AP), in contrast, represents a fully automated method that has been developed to monitor the viability of rod-shaped microorganisms, since they orientate under the effect of an electrical field. This orientation is measured by the change of extinction from two orthogonal light sources. The extinction decreases in the direction of orientation and increases in the orthogonal direction in comparison to a chaotic orientation. The time, which is needed for re-orientation depends directly on the cells' polarizability (Bunin, 2002). This principle is combined with a continuous and automated sampling and sample preparation (i.e., cell suspension filtration, adjustment of cell concentration and of conductivity) coupled to a flow cell (Angersbach et al., 2006a,b; Junne et al., 2008). The method provides a spectrum of the AP, since various frequencies (kHz to MHz) can be applied in one measurement.

The cell polarizability, if determined electrooptically, is mainly evoked by the Maxwell-Wagner polarization. It relies on the accumulation of electric charge at the interface between two media of different electrophysical properties (Zhivkov and Gyurova, 2008; Gyurova and Zhivkov, 2009). The interface of the cytoplasm and the cell wall is the main origin of this cell polarizability in case of bacteria. The intracellular ion balance is changing during the course of a cultivation due to substrate consumption and product formation, eventual inhibitor accumulation and an unsuitable pH-value, among others. This has an impact on the Maxwell-Wagner polarizability.

The authors have described the electrooptical monitoring of (i) the switch from the acidogenic to the solventogenic phase in *Clostridium acetobutylicum* cells (Junne et al., 2008), and (ii) the development of the polarizability in *Escherichia coli* batch cultivations (Junne et al., 2010). The slope of polarizability vs. the frequency made it possible to differentiate between phases of dominating acid or dominating solvent production in *C. acetobutylicum* cultures. Metabolite fluxes as determined from *off-line* concentration measurements correlated well with the course of the polarizability. A strong relation between the development of the polarizability and the specific acetate synthesis rate in *E. coli* experiments was observed.

The aim of the present study is the investigation of the time course of polarizability of *L. plantarum* ATCC 2014 in batch and fed-batch fermentations in complex, industrially relevant medium and at certain disturbances like a low pH-value, substrate pulse and temperature alterations. The ability to identify and predict certain cultivation stages based on the AP is investigated, with a special emphasis put on lactate synthesis and carbon source consumption. The main question is whether fermentation phases with active cells with high metabolic turnover rates can be distinguished from weak cells with low energy generation capabilities by means of the electrooptical analysis. Additionally, the development of the AP during the regeneration (cultivation) of freeze-dried cells as starter cultures is investigated. The AP showed distinct differences, samples taken from the retardation and late stationary phase had a higher AP soon after they were resuspended, and finally had a higher growth rate. The AP is thus a meaningful parameter to identify suitable harvesting stages prior to freeze-drying for the further use as a probiotic compound.

MATERIALS AND METHODS

Bacterial Strain and Media

The strain *L. plantarum* ATCC 2014 was used throughout this study. In all batch and fed-batch cultivation experiments, a 50% standard MRS medium (Carl Roth, Karlsruhe, Germany) was used, containing (per liter): 10 g glucose, 5 g peptone, 4 g beef extract, 2 g yeast extract, 0.5 g Tween 80, 1 g K_2HPO_4, 2.5 g sodium acetate, 1 g ammonium citrate, 0.1 g $MgSO_4$, 0.025 g $MnSO_4$. Media in pre-cultures were twice as concentrated. Two milliliter of antifoam 204 (Sigma-Aldrich Chemie GmbH, Steinheim, Germany) were added to reduce foam formation in the stirred bioreactor experiments.

Cultivation Conditions

Five hundered microliter of *L. plantarum* cell suspension from a cryostock were used to inoculate 50 mL of pre-culture and grown at 34°C overnight without agitation. Eight milliliter of this pre-culture were used to inoculate 200 mL cultivations in an EloFerm bioreactor (EloSystems, Berlin, Germany) when it reached a pH-value between 3.6 and 3.8 and an optical density (OD_{600}) between 4.2 and 5.2. Fifty milliliter of pre-culture were used for inoculation in case of 2 L cultivations in a KLF 2000 bioreactor (Bioengineering, Wald, Switzerland).

The pH-value was controlled at 5.8 by the addition of 1 M and 7.5 M NaOH solution in the batch and fed-batch bioreactor cultivations, respectively. The temperature was maintained at 34°C. The culture was gently stirred at 150 rpm during the initial batch phase. The liquid was sparged with nitrogen at a rate of 0.03 vvm and stirred with 200 rpm in the subsequent fed-batch phase. Continuous feeding of a solution, which contained 50% (v/v) of MRS medium and 50% (v/v) of a 440 g L^{-1} dextrose solution was started after the glucose of the batch phase was consumed. The feed reservoir was weighted to ensure appropriate feeding. A feed rate of 0.24 L h^{-1} was applied during the first fed-batch phase, while it was doubled during the second fed-batch phase. The oxygen (if there was any) and carbon dioxide content were quantified with the exhaust gas analyzer All-in-One (BlueSens, Herten, Germany).

Concentration Analysis

Optical density at 620 nm was monitored with a photometer EloCheck (EloSystems, Berlin, Germany) in a flow cell connected to a reactor bypass with an optical depth of 2.2 mm for every

15 s. The biomass concentration was additionally determined *off-line* with appropriately diluted samples at 600 nm in an Ultraspec 2100 *pro* UV/Visible spectrophotometer (Biochrom, Cambridge, UK).

The amount of cells per mL, c_n, was calculated following eq. 1 under consideration of the cell length as determined with the electrooptical measurement and as calibrated with captures of *L. plantarum* cultures under the microscope:

$$c_n = (3.1 \cdot OD_{600} / l_c^{1.33}) \cdot 10^9$$

l_c represents the mean cell length.

Metabolite analysis (i.e., glucose and lactate) and amino acid quantification was conducted with HPLC analysis as described previously (Lemoine et al., 2015).

The dried cell weight (DCW) was determined as follows: 1 mL of *L. plantarum* samples were centrifuged at 15,000 rpm and 4°C for 10 min, washed with 1 mL of 0.9% (w/w) NaCl and centrifuged again. The supernatant was discarded, whilst the pellet was dried in an oven at 70°C for 24 h. The amount of the residual biomass was determined gravimetrically.

In case of freeze-drying experiments, samples were taken after 4, 6, 8, and 21 h of a 200 mL bioreactor cultivation. Twenty milliliter of sample broth was centrifuged at 8,000 rpm and 4°C for 15 min. The supernatant was discarded and the wet sample was transferred to round bottom flasks. These were stored at −20°C for 1 day and then lyophilized with a LyoQuest lyophilizer (Telstar® Life Science solutions, Terrassa, Spain) until dryness at 0.9 mbar and −50°C. The different samples were suspended individually in 50% MRS and allowed to grow at 34°C in shake flasks with gentle mixing.

Determination of Cell Polarizability and Cell Length

A fully automated, commercialized sampling and analysis unit EloTrace (EloSystems, Berlin, Germany) was used to monitor the AP and cell length in a sampling interval of 15 min. Cells were separated from the culture broth by filtration through a cellulose filter of a pore size of 0.45 µm (Sartorius, Göttingen, Germany). The cell concentrate was diluted with distilled water of a conductivity of 5 $\mu S \cdot cm^{-1}$ to a final optical density of $OD_{600} = 0.1 \pm 5\%$ prior to the electrooptical measurement. The AP was acquired in a measurement chamber at four different frequencies: 210, 400, 900, and 2,100 kHz. Detailed principles of the method were described elsewhere (Bunin, 2002). All AP values contain a scaling factor of $5 \cdot 10^{-31}$ $F \cdot m^2$ for easier readability and comparison with other literature sources. The system was calibrated by microscopic analysis in order to correlate orientation and relaxation characteristics to the cell length.

Data Fitting and Visualization

Data of OD_{600} measurements, which were obtained every 15 min or of DCW, which was measured every hour in triplicates, was fitted with the smoothing spline function in the curve fitting toolbox of MATLAB R2013b (The MathWorks, Natick, MA). The growth rate was then calculated for each time interval with the slope of the curve with logarithmic (ln) linearization of the OD_{600} or biomass time course. All data plots were created with SigmaPlot version 11.0 (Systat Software, San José, CA).

Statistical Analysis

Data were expressed as mean standard deviation (SD) between duplicates for the description of reproducibility. Biological replicates were performed as fermentations under identical conditions.

RESULTS AND DISCUSSION

Statistical Analysis of the Electrooptical Measurement

The aim of this study is the investigation of the suitability of electrooptical polarizability measurements to determine uncomfortable growth conditions and potential losses of cell viability and metabolic activity. Therefore, the technical reproducibility of the measurement and the biological reproducibility of the physiology of the culture were determined. The biological reproducibility of the polarizability, measured in samples of two fermentations, which were performed under

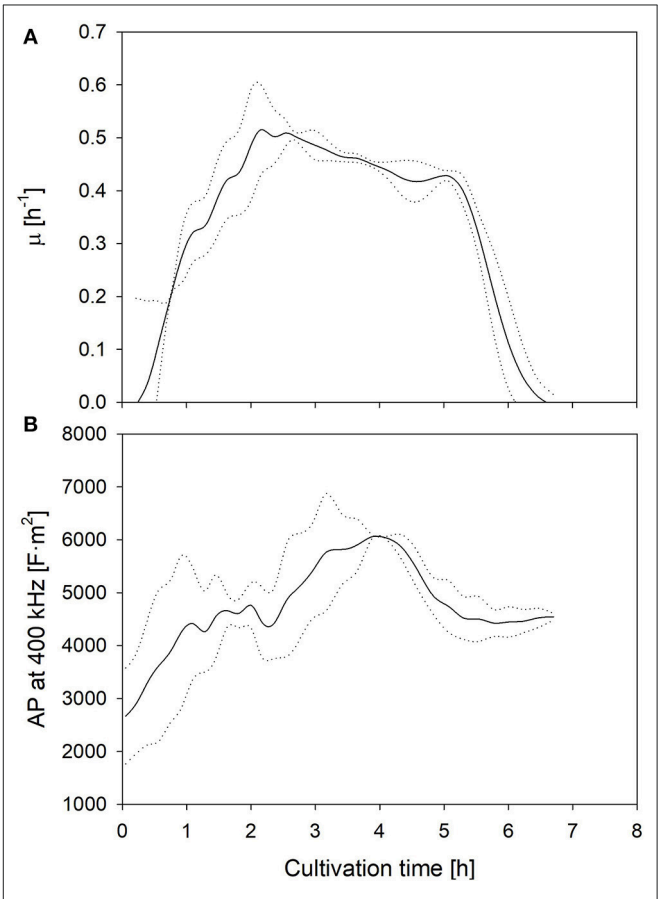

FIGURE 1 | Mean growth rate **(A)** as well as AP level at 400 kHz **(B)** development during fermentations under optimum (standard) conditions. Dotted lines represent the limits of the standard deviations between two biological replicates.

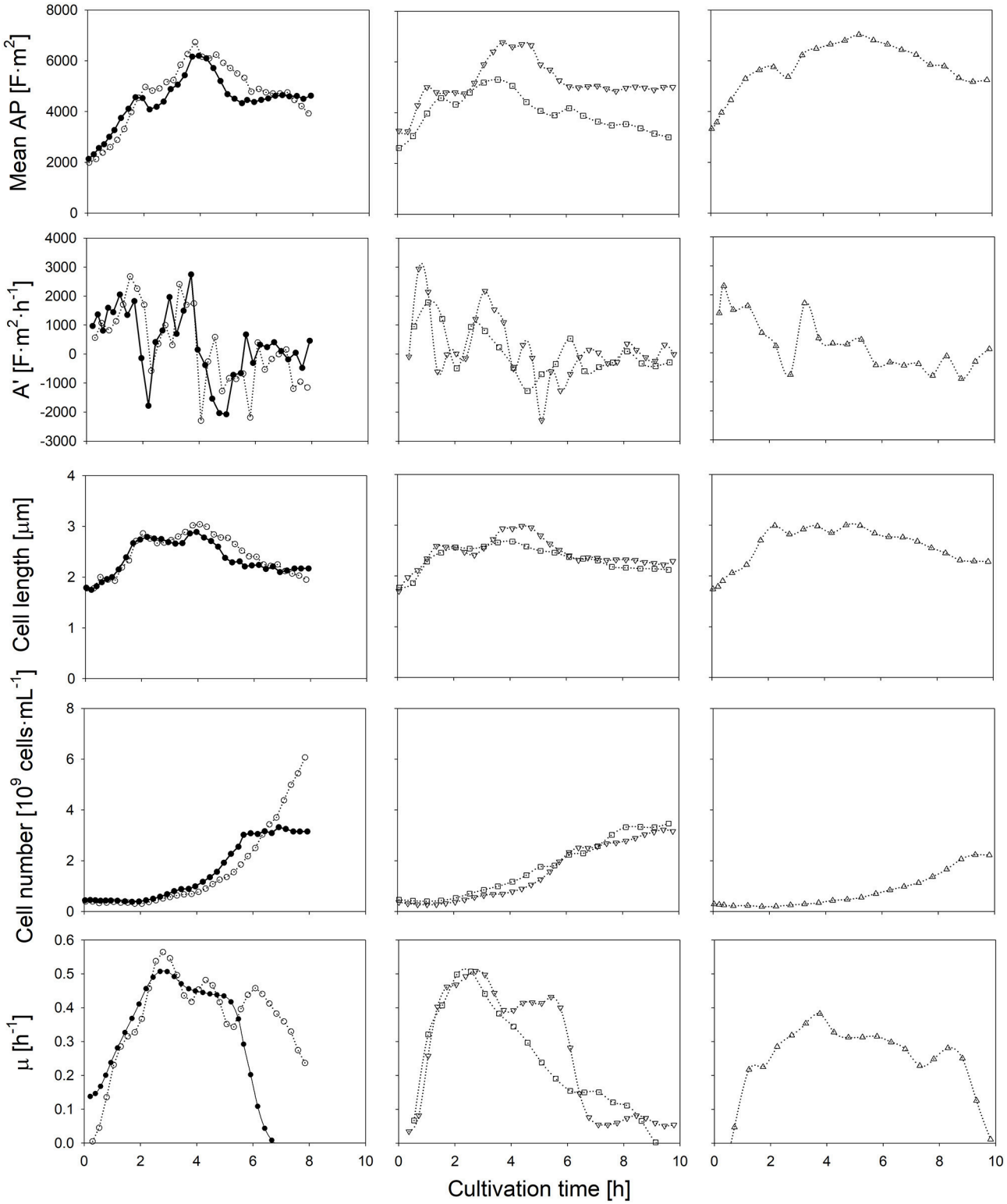

FIGURE 2 | Time course of the mean anisotropy of polarizability (AP), its first derivate, cell length, the amount of cells and the specific growth rate throughout six *L. plantarum* batch cultivations: at standard conditions (•), with additionally 1% of glucose in the medium (○), without pH control (□), with aeration (▽) and at a reduced temperature of 25°C (△). Error bars depicting the technical error of the polarizability measurement have not been represented, thus enabling the comparison between cultivation conditions.

optimal growth conditions, is summarized in **Figure 1**. The mean specific growth rate and the AP at 400 kHz are shown together with the upper and lower limits of the standard deviation (SD). The values expressed a large deviance during the first hour due to a wider spread of the AP of pre-cultures at the harvest time, but the growth rate and AP profiles developed very similar afterwards. The duplicate measurements of the AP of the same samples yielded a deviance of 5% or lower at all samples. This encouraged further investigation whether different cultivation conditions will lead to a distinct change of the AP, and whether this change can be correlated with growth and lactic acid formation.

Effects of Altered Cultivation Conditions on the AP and Cell Length

Firstly, in order to elucidate the impact of carbon availability, the initial amount of glucose was doubled in comparison to the control experiment, while it is assumed that the supply of ions and other essential nutrients remain unlimited (as observed from the growth rate). Secondly, fermentations w/o pH control were performed to investigate the influence of acidic conditions on the AP. Moreover, since the presence of oxygen may have an impact on the proton motive force in *Lactobacilli*, and thus the cells' polarizability, the nitrogen-sparged cultivation was compared to an aerated cultivation, in which a sparging rate of 1 vvm of air was applied. Finally, the impact of a lower cultivation temperature of 25°C, and thus a lower metabolic activity, on the AP was investigated (**Figure 2**).

If the initial glucose concentration was higher, the same AP profile was obtained at the beginning of the cultivation. The maximum growth rate was achieved when the AP reached about 5,000 F·m^2. The AP decreased earlier if lower amounts of glucose were available. In both cases, the drop of the AP below the threshold value occurred within the same order and time as the growth rate declined during the course of the cultivation. As the specific lactate production was rather similar, the change of the AP cannot be attributed to lactate accumulation. Most likely, the earlier onset of substrate limitation at a lower initial glucose concentration was the reason for the changed AP profiles. The growth rate does not develop in parallel to the cell number in the beginning of the cultivations, as growth measured with optical density and gravimetrical biomass determination relies on the increase of the cell length.

If the pH-value was not controlled, a sudden drop of the AP was observed after 3 h. The external pH reached a value of 4.5 at that time (**Figure S2**). Such a low pH value is regarded as unfavorable, as growth reduction occurs in such an acidic environment (Giraud et al., 1991; van de Guchte et al., 2002). Indeed, a growth reduction was observed about 30 min later. While the pH-value in the medium decreased further to a value of 3.6, the AP declined continuously (**Figure S2**). A low internal pH value has an impact on the cell viability (Valli et al., 2006) as it reduces the internal proton motive force. It is known that such an effect changes the transmembrane potential, mainly due to a change of the internal Maxwell-Wagner polarizability (Gyurova and Zhivkov, 2009). Transmission electron microscopy analysis revealed evidence of structural distortions of the cell surface of *L. casei* at pH-values of 4.0 (Hossein Nezhad et al., 2010). Such changes would surely affect the AP as the bi-electric layer of cells is weakened by the structural changes of the cell wall. Additionally, the non-dissociated form of lactic acid ($pK_a = 3.86$) is present at higher concentrations under acidic conditions. A passive transport by diffusion into the cell increases the lactic acid stress in bacteria (Hansen et al., 2016). In this case, cells use their energy mainly to shield them against this stress in order to maintain homeostasis rather than growth.

In contrast to a low pH-value, air sparging retarded growth only slightly and had no negative impact on the cells' physiological state. The time course of the AP and mean cell length was rather the same as in the control cultivation. It was observed earlier that the presence of heme and NADH as electron donor supports a fully active respiratory chain and the evolvement of a sufficient transmembrane potential in *L. lactis* and in other lactic acid bacteria (Brooijmans et al., 2007; Lechardeur et al., 2011). In case cells grow on heme, oxygen consumption is conducted with membrane vesicles. In that case, proton release is conducted by the respiratory chain rather than by H^+-ATPases (Blank et al., 2001; Pedersen et al., 2012). Due to the complex components in the industrial medium as it was used in this study, heme and NADH shall be present in excess at least at the onset of the batch cultivation, thus aerobic respiration

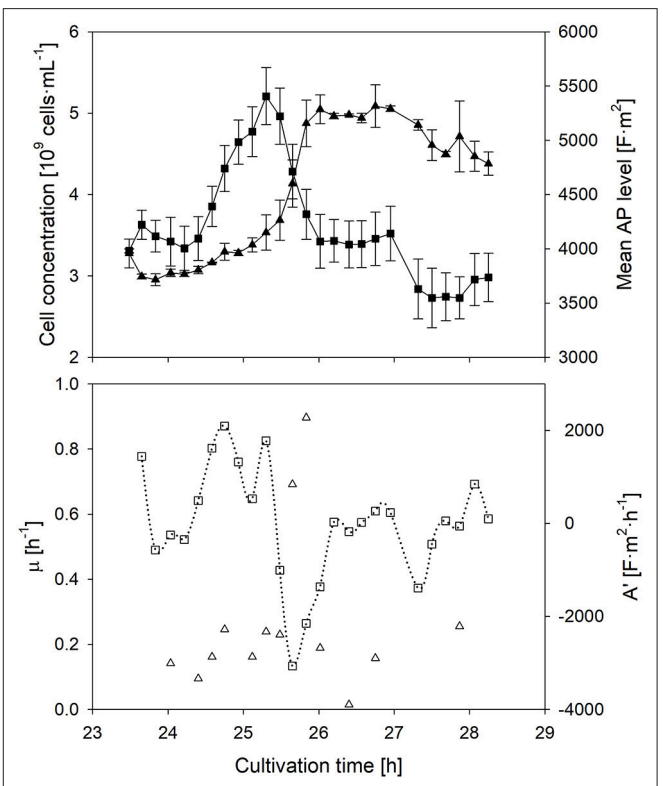

FIGURE 3 | Time course of the mean anisotropy of polarizability (■), its first derivative (□), cell concentration (▲) and specific growth rate (△) after a sudden substrate pulse after cells suffered 17 h of starvation. Error bars represent the technical reproducibility of EloTrace with two biological replicates.

was eventually activated. It was found that aerobic respiration at sufficient nutrient availability is even beneficial for the energetic household regeneration of *L. plantarum* (Guidone et al., 2013) despite to some common views. The AP, however, was obviously not altered although the proton motive force might have been affected.

Finally, at a lower fermentation temperature, the rate of chemical reactions is naturally lower, which yields a reduced specific growth rate and lower final cell number, as also observed for other lactic acid bacteria (Cheigh et al., 2002). The highest mean cell length among all experiments, however, is observed during a lower cultivation temperature. If the lower temperature reduces turnover rates in late reaction steps of the metabolism more profoundly than the substrate uptake, an intracellular accumulation of intermediates will occur. This leads usually to larger cell lengths due to a higher osmotic pressure inside the cell (Junne et al., 2010; Pilizota and Shaevitz, 2014). The temperature shift however did not alter the physiological conditions of cells notably. In this case, the consideration of both, the AP and cell length, can provide suitable information about conditions, in which a high growth rate can be achieved.

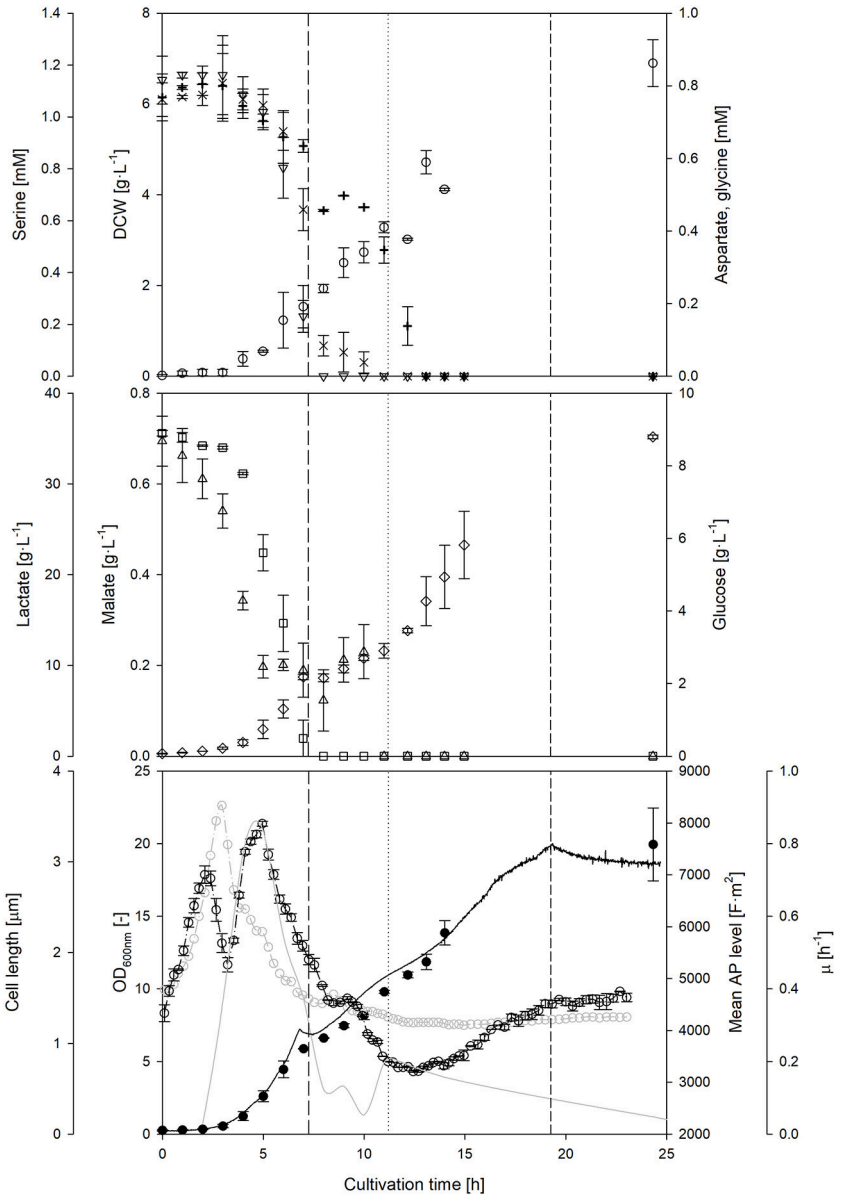

FIGURE 4 | Course of *on-line* and *off-line* cultivation parameters, as well as main metabolites and amino acids throughout a *L. plantarum* fed-batch cultivation under standard conditions. *Off-line* monitoring of DCW (○), aspartate (×), serine (▽), glycine (+), glucose (□), lactate (◇) and malate (△) concentrations over time. *At-line* optical density (–●–), cell length (–○–), mean polarizability (-– · ○ · –-) and growth rate (——) measurements. During the fed-batch phase, the feed start (— — — —), doubling of feed rate (.....) and feed stop (-------) are highlighted with vertical lines. Error bars denote standard deviation of two biological replicates.

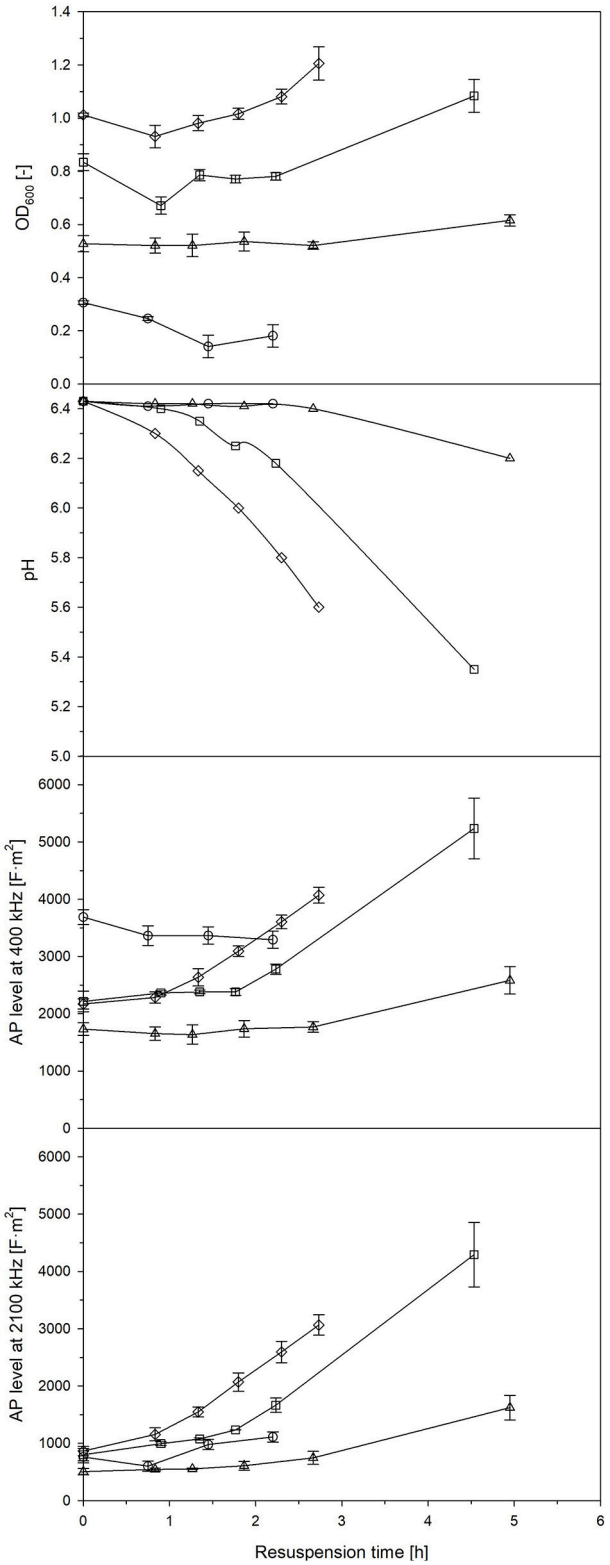

FIGURE 5 | OD_{600}, pH and AP level at a frequency of 400 kHz and 1,200 kHz of formerly freeze-dried and resuspended *L. plantarum* culture broth in 50% MRS media collected after 4 h (○), 6 h (□), 8 h (△) and 21 h of batch cultivation (◇). Error bars: Mean ± SD ($n = 2$).

The *at-line* monitoring of the AP enabled the identification of suitable cultivation conditions for all cases: an optimal range of the AP and cell length can be assumed, in which the cell reaches an optimal physiologic and morphologic state, that is an AP of above 4,500 (that is $22.5 \cdot 10^{-28}$ F·m^2 if the scaling factor $5 \cdot 10^{-31}$ is considered) at 400 kHz and a cell length of about 2.5 µm. Growth was always high during periods, in which the AP and cell length stayed above these thresholds. Both, the AP level at 400 kHz and the cell length showed a certain correlation with the specific growth rate (**Figure S1**). Since the AP changed earlier than growth rates, the correlation between it and growth values is not very strong. Nevertheless, the AP measurement is suitable to act as an early indicator for growth state changes. The AP and cell length allow the identification of different growth phases among all batch experiments: (i) an acceleration phase, during which the AP and the cell length increase rapidly as cells exhibit an increased metabolic activity; (ii) a log phase, during which the AP and cell length reach maximum values in parallel to the growth rate; (iii) a deceleration phase, in which the AP decreases as the cell lenght does while the growth rate steadily declines, and (iv) a stationary phase, during which bacterial growth is retarded and the AP and cell length remain almost constant.

The individual cells' AP depends on the transmembrane potential, and thus the ionic transport from the outside to the inside of the cell, which is related to the metabolic activity; this phenomenon has been described in literature (Geise et al., 2014). In order to prove the dependency between the metabolic activity and the AP, and to investigate the response time of the AP to a changed nutrient supply, a sudden glucose pulse addition in the stationary phase was performed (**Figure 3**). The glucose pulse led to an immediate response of growth. In this case, the AP is supposed to increase immediately as well. Indeed this is the case.

The response time of the AP to a situation, in which the activity of cells declines again while the added substrate is depleting, was investigated as well. In this case, the AP declined at the same time when nutrient limitation was reached after the pulse. The decline of the AP started ∼30 min earlier than the decline of the growth rate. This observation after nutrient depletion seems to be conserved among all batch experiments of this study.

Response of AP to Variable Feed Rates

In non-aerated cultivations, the decrease of byproduct formation, mainly carboxylic acids, can be a reason to conduct a nutrient-limited fed-batch cultivation. Since cells have a reduced substrate uptake due to the limited availability of a main nutrient component, mainly the carbohydrate source, a reduced accumulation of intermediates inside the cell occur, thus restricting byproduct formation to the necessity to regenerate the energy household.

The course of the AP was observed during a prolonged nutrient-limited growth phase (**Figure 4**). During a first fed-batch phase, the mean cell length remained almost constant, whereas the AP decreased. Due to the constant feed, substrate availability per cell is declining during this time, while the specific growth rate is reduced in parallel. Nevertheless, once the feed rate was doubled, a clear increase of the AP level was

observed. These results confirm that the AP depends on the nutrient availability under nutrient-limited conditions, however, the dependencies were not as clear as in the batch phase. The second feed phase showed a rather decoupled development of the AP and the growth rate: in contrast to previous observations, the AP still increased when growth declined. Cells seemed to recover from the previous nutrient limitation through accumulation of intracellular components and restoration of cellular structures independently of growth. AP analyses under alternating nutrient-limited fed-batch conditions rather provide information whether feeding conditions are suitable to maintain or restore cellular structures rather than a direct correlation to metabolic activity. The AP remained rather stable after the feeding had stopped. It seems that the AP is hardly affected after nutrient depletion once cells adapted to nutrient limitation for a certain time before. This is an important observation if cells shall be kept for a longer time w/o nutrient supply: the time that is needed for adaptation might be observable with the AP measurement.

In order to explain some of the behavior of the AP during nutrient limiting growth conditions, the availability of other sources beside carbohydrates and carboxylic acids were investigated. A depletion of three amino acids was detected during the feed phases: firstly, serine and afterwards aspartate, and finally glycine. A sudden drop of the AP level seemed to occur at the same time when aspartate became strongly limited after 9–10 h of cultivation. Bacterial cells have a different preference, which amino acid they consume in dependence of the growth phase (Wolfe, 2005). It is assumed that the depletion of preferred amino acids in the medium will likely influence the AP, as cells either have to consume other amino acids or at least to synthesize the corresponding amino acids by themselves. This usually also changes intracellular fluxes and the energetic household. The AP might serve as an early indicator for amino acid depletion in the complex medium, however, this hypothesis requires further investigation.

Streptococcus thermophilus is used as proteolytic lactic acid bacteria in order to provide proteases to secondary microorganisms (Wu et al., 2015). For this purpose, lactic acid bacteria are usually dried, e.g., freeze-dried, and revitalized prior to use. The development of the AP after a longer phase of starvation was described in the previous section. Now, the behavior of the AP of *L. plantarum* after revitalization (resuspension) of a freeze-dried cell pellet was observed. Samples were taken at different phases of a batch cultivation (**Figure S3**): (i) during the growth phase, (ii) at strong retardation/growth cessation, (iii) in the early stationary phase 2 h after growth cessation, and (iv) in the late stationary phase 13 h later. Growth behavior varied, while the most profound growth was seen at samples taken at strong retardation/growth cessation and from the late stationary phase. These were also samples with the highest and fastest increase of AP after revitalization (**Figure 5**). If measurements at 400 kHz were compared with measurements at 2,100 kHz, a faster and more profound increase was seen at the latter frequency. It seems that a high frequency, in this case, is more suitable to distinguish between the different states of revitalization, e.g., the reconstitution of ion transport and functional cell structures. It was found that freeze-resistant cells had a high content of CH_3 groups from lipid chains, cell proteins in an α-helix secondary structure and charged polymers, such as teichoic and lipoteichoic acids in *L. bulgaricus* (Passot et al., 2015). Certain options of drying cause membrane damages, which leads to high cell death (Bensch et al., 2014). Interestingly, the lactic acid production did not correlate well with the OD_{600}, typical activity measurements based on lactic acid synthesis would have led to other results than growth and AP measurements, as the pH in samples taken at growth cessation decreased faster (that is a higher lactic acid synthesis) during revitalization than in samples taken from the late stationary phase.

CONCLUSION

The *at-line* monitoring of the AP coupled to automated sample preparation enabled the identification of unfavorable cultivation conditions in *L. plantarum* batch and fed-batch fermentations. Different growth phases were identified throughout all experiments by means of electrooptical measurements. In contrast to many other studies with aerobic and anaerobic bacteria, *L. plantarum's* AP responded significantly to substrate pulses and insufficient substrate supply, and other unfavorable cultivation conditions. During fed-batch, the adaptation to nutrient-limitation is monitored with electrooptical measurements, thus providing a suitable parameter for optimization, as during revitalization after drying. The results support the hypothesis that an intact bielectric layer on the cells' surface yields a higher AP. Active cells with high metabolic turnover rates and energy generation were well distinguishable from weak cells with low regeneration capabilities, although the frequency matters for the distinguishability. In summary, the electrooptical monitoring represents a promising analytical tool, if conducted automatically as performed in this study, e.g., for the achievement of suitable production and conservation methods of *L. plantarum* and eventually other lactic acid bacteria.

AUTHOR CONTRIBUTIONS

KP-A conducted the experiments, collected data and wrote the manuscript. AA supported the electrooptical measurements and the preparation of the manuscript. PN supported supervision and the preparation of the manuscript. SJ supervised the work and the manuscript preparation.

ACKNOWLEDGMENTS

This project has received funding from the European Union's Horizon 2020 research and innovation program under the Marie Skłodowska-Curie actions grant agreement No. 643056 (project Biorapid). The authors gratefully acknowledge this financial support.

SUPPLEMENTARY MATERIAL

The Supplementary Material for this article can be found online at: https://www.frontiersin.org/articles/10.3389/fbioe.2018.00188/full#supplementary-material

REFERENCES

Angersbach, A., Bunin, V. D., and Ignatov, O. V. (2006a). "Electro-optical analysis of bacterial cells," in *Molecular and Colloidal Electrooptics*, ed S. Stoilov (New York, NY: M. Dekker Publ.), 86–112.

Angersbach, A., Ignatov, O., and Bunin, V. (2006b). "Electro-optical analysis of bacterial cells," in *Molecular and Colloidal Electro-Optics*, eds S. P. Stoylov and M. V. Stoimenova (Boca Raton, FL: CRC Press).

Arnold, S. A., Gaensakoo, R., Harvey, L. M., and McNeil, B. (2002). Use of at-line and *in-situ* near-infrared spectroscopy to monitor biomass in an industrial fed-batch *Escherichia coli* process. *Biotech. Bioeng.* 80, 405–413. doi: 10.1002/bit.10383

Bensch, G., Rüger, M., Wassermann, M., Weinholz, S., Reichl, U., and Cordes, C. (2014). Flow cytometric viability assessment of lactic acid bacteria starter cultures produced by fluidized bed drying. *App. Microbiol. Biotechnol.* 98, 4897–4909. doi: 10.1007/s00253-014-5592-z

Blank, L. M., Koebmann, B. J., Michelsen, O., Nielsen, L., K., and Jensen, P., R. (2001). Hemin reconstitutes proton extrusion in an H^+-ATPase-negative mutant of *Lactococcus lactis*. *J. Bacteriol.* 183, 6707–6709. doi: 10.1128/JB.183.22.6707-6709.2001

Brooijmans, R. J., Poolman, B., Schuurman-Wolters, G. K., de Vos, W. M., and Hugenholtz, J. (2007). Generation of a membrane potential by *Lactococcus lactis* through aerobic electron transport. *J. Bacteriol.* 189, 5203–5209. doi: 10.1128/JB.00361-07

Bunin, V. D. (2002). "Electrooptical analysis of a suspension of cells and its structures," in *Encyclopedia of Surface and Colloid Science*, ed M. Dekker (New York, NY: M. Dekker Publ.), 2032–2043.

Cheigh, C. I., Choi, H. J., Park, H., Kim, S. B., Kook, M. C., Kim, T. S., et al. (2002). Influence of growth conditions on the production of a nisin-like bacteriocin by *Lactococcus lactis* subsp. lactis A164 isolated from kimchi. *J. Biotechnol.* 95, 225–235. doi: 10.1016/S0168-1656(02)00010-X

Clementschitsch, F. j., Kern, J., Pötschacher, F., and Bayer, K. (2005). Sensor combination and chemometric modelling for improved process monitoring in recombinant *E. coli fed-batch cultivations. J. Biotechnol.* 120, 183–196. doi: 10.1016/j.jbiotec.2005.05.030

Davis, C. (2014). Enumeration of probiotic strains: review of culture-dependent and alternative techniques to quantify viable bacteria. *J. Microbiol. Meth.* 103, 9–17. doi: 10.1016/j.mimet.2014.04.012

Emerson, J. B., Adams, R. I., Román, C. M. B., Brooks, B., Coil, D. A., Dahlhausen, K., et al. (2017). Schrödinger's microbes: Tools for distinguishing the living from the dead in microbial ecosystems. *Microbiome* 5:86. doi: 10.1186/s40168-017-0285-3

Geise, G. M., Cassady, H. J., Paul, D., R., Logan, B. E., and Hickner, M. A. (2014). Specific ion effects on membrane potential and the permselectivity of ion exchange membranes. *Phys. Chem. Chem. Phys.* 16, 21673–21681. doi: 10.1039/C4CP03076A

Giraud, E., Lelong, B., and Raimbault, M. (1991). Influence of pH and initial lactate concentration on the growth of *Lactobacillus plantarum*. *App. Microbiol. Biotechnol.* 36, 96–99. doi: 10.1007/BF00164706

Glušac, J., Stijepić, M., Durdević-Milošević, D., Milanović, S., Kanurić, K., and Vukić, V. (2015). Growth and viability of *Lactobacillus delbrueckii* subsp. bulgaricus and Streptococcus thermophilus in traditional yoghurt enriched by honey and whey protein concentrate. *Iran. J. Vet. Re.* 16, 249–254.

Guidone, A., Ianniello, R. G., Ricciardi, A., Zotta, T., and Parente, E. (2013). Aerobic metabolism and oxidative stress tolerance in the *Lactobacillus plantarum* group. *W. J. Microbiol. Biotechnol.* 29, 1713–1722. doi: 10.1007/s11274-013-1334-0

Gyurova, A. Y., and Zhivkov, A. M. (2009). Influence of the medium electrolyte concentration on the electric polarizability of bacteria *Escherichia coli* in presence of ethanol. *Colloids Surf. B. Biointer.* 74, 23–27. doi: 10.1016/j.colsurfb.2009.06.017

Hansen, G., Johansen, C. L., Marten, G., Wilmes, J., Jespersen, L., and Arneborg, N. (2016). Influence of extracellular pH on growth, viability, cell size, acidification activity, and intracellular pH of *Lactococcus lactis* in batch fermentations. *App. Microbiol. Biotechnol.* 100, 5965–5976. doi: 10.1007/s00253-016-7454-3

Hossein Nezhad, M., Stenzel, D., and Britz, M. (2010). Effect of growth at low pH on the cell surface properties of a typical strain of *Lactobacillus casei* group. *Iran. J. Microbiol.* 2, 147–154.

Junne, S., Klein, E., Angersbach, A., and Goetz, P. (2008). Electrooptical measurements for monitoring metabolite fluxes in acetone–butanol–ethanol fermentations. *Biotechnol. Bioeng.* 99, 862–869. doi: 10.1002/bit.21639

Junne, S., Nicolas Cruz-Bournazou, M., Angersbach, A., and Götz, P. (2010). Electrooptical monitoring of cell polarizability and cell size in aerobic *Escherichia coli* batch cultivations. *J. Ind. Microbiol. Biotechnol.* 37, 935–942. doi: 10.1007/s10295-010-0742-5

Kolaček, Ã. S., Hojsak, I., Canani, R. B., Guarino, A., Indrio, F., Orel, R., et al. (2017). Commercial probiotic products: a call for improved quality control. A position paper by the ESPGHAN working group for probiotics and prebiotics. *J. Pediatr. Gastroenterol. Nutr.* 65, 117–124. doi: 10.1097/MPG.0000000000001603

Lechardeur, D., Cesselin, B., Fernandez, A., Lamberet, G., Garrigues, C., Pedersen, M., et al. (2011). Using heme as an energy boost for lactic acid bacteria. *Curr. Op. Biotechnol.* 22, 143–149. doi: 10.1016/j.copbio.2010.12.001

Lemoine, A., Maya Martínez-Iturralde, N., Spann, R., Neubauer, P., and Junne, S. (2015). Response of *Corynebacterium glutamicum* exposed to oscillating cultivation conditions in a two- and a novel three-compartment scale-down bioreactor. *Biotechnol. Bioeng.* 112, 1220–1231. doi: 10.1002/bit.25543

Léonard, L., Bouarab Chibane, L., Ouled Bouhedda, B., Degraeve, P., and Oulahal, N. (2016). Recent advances on multi-parameter flow cytometry to characterize antimicrobial treatments. *Front. Microbiol.* 7:1225. doi: 10.3389/fmicb.2016.01225

Nagpal, R., Kumar, A., Kumar, M., Behare, P., V., Jain, S., and Yadav, H. (2012). Probiotics, their health benefits and applications for developing healthier foods: a review. *FEMS Microbiol. Lett.* 334, 1–15. doi: 10.1111/j.1574-6968.2012.02593.x

Passot, S., Gautier, J., Jamme, F., Cenard, S., Dumas, P., and Fonseca, F. (2015). Understanding the cryotolerance of lactic acid bacteria using combined synchrotron infrared and fluorescence microscopies. *Analyst.* 140, 5920–5928. doi: 10.1039/C5AN00654F

Pedersen, M. B., Gaudu, P., Lechardeur, D., Petit, M. A., and Gruss, A. (2012). Aerobic respiration metabolism in lactic acid bacteria and uses in biotechnology. *Ann. Rev. Food Sci. Technol.* 3, 37–58. doi: 10.1146/annurev-food-022811-101255

Pega, J., Rizzo, S., Pérez, C., Rossetti, L., Díaz, G., Ruzal, S., et al. (2016). Effect of the addition of phytosterols and tocopherols on *Streptococcus thermophilus* robustness during industrial manufacture and ripening of a functional cheese as evaluated by qPCR and RT-qPCR. *Intern. J. Food Microbiol.* 232, 117–125. doi: 10.1016/j.ijfoodmicro.2016.06.003

Perdana, J., Bereschenko, L., Roghair, M., Fox, M. B., Boom, R., M., Kleerebezem, M., et al. (2012). Novel method for enumeration of viable *Lactobacillus plantarum* WCFS1 cells after single-droplet drying. *App. Environ. Microbiol.* 78, 8082–8088. doi: 10.1128/AEM.02063-12

Pilizota, T., and Shaevitz, J. W. (2014). Origins of *Escherichia coli* growth rate and cell shape changes at high external osmolality. *Biophys. J.* 107, 1962–1969. doi: 10.1016/j.bpj.2014.08.025

Savini, M., Cecchini, C., Verdenelli, M. C., Silvi, S., Orpianesi, C., and Cresci, A. (2010). Pilot-scale production and viability analysis of freeze-dried probiotic bacteria using different protective agents. *Nutrients* 2, 330–339. doi: 10.3390/nu2030330

Schenk, J., Viscasillas, C., Marison, I. W., and von Stockar, U. (2008). On-line monitoring of nine different batch cultures of *E. coli* by mid-infrared spectroscopy, using a single spectra library for calibration. *J. Biotechnol.* 134, 93–102. doi: 10.1016/j.jbiotec.2007.12.014

Sohier, D., Pavan, S., Riou, A., Combrisson, J., and Postollec, F. (2014). Evolution of microbiological analytical methods for dairy industry needs. *Front. Microbiol.* 5:16. doi: 10.3389/fmicb.2014.00016

Tropcheva, R., Lesev, N., Danova, S., Stoitsova, S., and Kaloyanova, S. (2015). Novel cyanine dyes and homodimeric styryl dyes as fluorescent probes for assessment of lactic acid bacteria cell viability. *J. Photochem. Photobiol. B Biology* 143, 120–129. doi: 10.1016/j.jphotobiol.2015.01.002

Valli, M., Sauer, M., Branduardi, P., Borth, N., Porro, D., and Mattanovich, D. (2006). Improvement of lactic acid production in *Saccharomyces cerevisiae* by cell sorting for high intracellular pH. *App. Environ. Microbiol.* 72, 5492–5499. doi: 10.1128/AEM.00683-06

van de Guchte, M., Serror, P., Chervaux, C., Smokvina, T., Ehrlich, S. D., and Maguin, E. (2002). Stress responses in lactic acid bacteria. *Antonie Van Leeuwenhoek* 82, 187–216. doi: 10.1023/A:1020631532202

Wolfe, A. J. (2005). The acetate switch. *Microbiol. Mol. Biol. Rev*. 69, 12–50. doi: 10.1128/MMBR.69.1.12-50.2005

Wu, Q., Law, Y. S., and Shah, N. P. (2015). Dairy *Streptococcus thermophilus* improves cell viability of *Lactobacillus brevis* NPS-QW-145 and its γ-aminobutyric acid biosynthesis ability in milk. *Sci. Rep*. 5:12885. doi: 10.1038/srep12885

Zhivkov, A. M., and Gyurova, A. Y. (2008). High frequency electric polarizability of bacteria *E. coli*: dependence on the medium ionic strength. *Colloids Surf. B. Biointerfaces* 66, 201–205. doi: 10.1016/j.colsurfb.2008.06.007

Conflict of Interest Statement: The authors declare that the research was conducted in the absence of any commercial or financial relationships that could be construed as a potential conflict of interest.

II

2nd Paper

Mechanistic model validation and electrooptical monitoring of *Streptococcus thermophilus* growth in lactose-limited acceleration stat (A-stat) fermentations

KLAUS PELLICER-ALBORCH[1], ROBERT SPANN[2], GÜRKAN SIN[2], KRIST V. GERNAEY[2], PETER NEUBAUER[1], STEFAN JUNNE[1*]

[1] Chair of Bioprocess Engineering, Department of Biotechnology, Technische Universität Berlin, Ackerstrasse 76 ACK 24, 13355 Berlin, Germany

[2]Process and Systems Engineering Center (PROSYS), Department of Chemical and Biochemical Engineering, Technical University of Denmark, Søltofts Plads Building 227 DK - 2800 Kgs. Lyngby, Denmark

Phone: +49 30 31472527

Fax: +49 30 31427577

e-mail: stefan.junne@tu-berlin.de

Keywords: Accelerostat; S. thermophilus; mechanistic model; polarizability; specific growth rate; cell viability; lactic acid bacteria

Abstract

Strain characterization is one of the first steps in bioprocess development, especially in those industries where the product is the biomass itself. Lactic acid bacteria (LAB) are a clear example thereof, since they are sold as starter cultures for the yogurt, cheese as well as probiotics production. In this work, a *Streptococcus thermophilus* strain from an industrially relevant company in the food market was characterized in terms of maximum specific growth rate (μ_{max}). Among all cultivation strategies available for such a purpose, the accelerostat (A-stat) mode was selected, so as to steadily change the dilution rate (which equals to the growth rate, μ, in this setup) within a single experiment, but avoiding the long stabilization phases typically encountered throughout automated stepwise change of μ in a chemostat culture. Furthermore, the anisotropy of polarizability (AP) at different frequencies as well as the cocci chain length were monitored at-line by means of electrooptical measurements with an industrially available device with automated sampling and sample preparation. These parameters, coupled to established off-line analyses of the cultivation broth (i.e. OD, DCW, C-source, etc.), enabled the identification of a μ_{max} of 1.3-1.4 h^{-1} and a wash-out point at 1.9 h^{-1} for the strain investigated. Additionally, the critical quality attributes (CQAs) during this fermentation mode were successfully simulated with a mechanistic biokinetic model trained exclusively with batch experiments. The at-line polarizability determination would allow the transition from a quality by testing (QbT) to a quality by design (QbD) approach, where the AP would serve as biomass activity and cell viability indicator, not measured so far during the process, but which could then be maintained in between certain boundaries by feedback control strategies. Finally, the in-silico prediction of CQAs during LAB continuous fermentations would also enable product quality by control (QbC) and improve downstream processing (DSP) planning and personnel scheduling.

Introduction

An accurate definition and understanding of the physiological state of cells is a key milestone in bioprocess development and scale up (or down), especially when using recombinant protein-producing microorganisms (Peebo and Neubauer 2018). Additionally, this is also essential for a complete description and successful reproduction of their phenotypes *in silico* (Abt, Barz et al. 2018). The physiological state of microorganisms fundamentally depends on a wide range of environmental parameters (e.g. pH, temperature, nutrient as well as O_2 availability, etc.) and a combination thereof, thus leading to an infinite combination of their values. In this regard, only the steady-state analysis enables the unequivocal definition of the physiological state of cells by providing a one-to-one correspondence between defined environmental conditions and biochemical processes derived thereof (Adamberg, Valgepea et al. 2015). This can be achieved by application of continuous cultivation methods (e.g. chemostats), which allows the study of cells at strictly defined physiological steady states with unchanging concentrations of intra- and extracellular molecules. Over decades, chemostats have been widely used for various applications and have been reviewed previously elsewhere (Bull 2010). Nevertheless, in the high-throughput era, analyzing steady-state metabolism at various environmental conditions within one experiment is preferred. This can be fulfilled by automated stepwise control of environmental parameters in a chemostat culture, but these experiments are very time-consuming due to the need to stabilize the culture after each step change, making them also prone to the emergence of unwanted mutations (Gresham and Hong 2014). Both issues can be circumvented by using pseudo steady-state cultivation methods, which enable the continuous change of one or several environmental parameters within a single experiment without the need of long stabilization phases after each change: cells are formally in a quasi-steady state, since the cell culture is moving

75 continuously from one steady state to another one (Adamberg, Valgepea et al. 2015). The
76 most used method among pseudo steady-states is the accelerostat (A-stat), mainly because
77 it enables the study of the effects and dynamics of one of the most important physiological
78 parameters on cell metabolism, the specific growth rate (μ). The experiment typically
79 starts with a batch phase, followed by stabilization of the culture at a fixed specific growth
80 rate (i.e. chemostat) to obtain an initial steady state. Subsequently, the dilution rate (D),
81 which equals to the specific growth rate (μ), is increased with a constant speed at a certain
82 slope ($D(t) = D(t_0) + a \cdot t$). Under such cultivation conditions, every time point represents
83 a physiological state of the microorganisms at the corresponding steady state. The A-stat
84 produces higher resolution data (possibility to monitor bacterial growth in real time to
85 study cell physiology in a large variety of specific growth rates, i.e. each sampling point
86 equals to a snapshot at that specific D, μ) and is much more time- and resource-efficient
87 (reduction of experiment's duration) compared with common chemostat approaches. The
88 cultivation strategy presented here has been applied to several microorganisms (Erm,
89 Adamberg et al. 2014, Adamberg, Valgepea et al. 2015, Gabardo, Pereira et al. 2015,
90 Glauche, Glazyrina et al. 2017), including lactic acid bacteria (LAB), but never to
91 characterize a *Streptococcus thermophilus* strain (Adamberg, Lahtvee et al. 2009,
92 Lahtvee, Valgepea et al. 2009, Lahtvee, Adamberg et al. 2011, Adamberg, Seiman et al.
93 2012).

94 Throughout such continuous experiments, the efficient quantification of bioprocess
95 parameters is of high importance for strain characterization and process development.
96 Apart from the usual off-line analyses (OD_{600}, concentration of biomass and relevant
97 metabolites, etc.), real-time measurements (pH, temperature, base addition, etc.) are also
98 relevant, since they enable the investigator to make a change in the process sooner, if
99 necessary (Wechselberger, Seifert et al. 2010). Cell concentration is definitely the most

relevant parameter during LAB production to be sold as starter cultures, but cellular activity is also relevant. In this context, electrooptical measurements coupled to automated sampling and sample preparation (Angersbach, Bunin et al. 2006) allow the at-line determination of cells' polarizability and size, thus providing information about the actual metabolic state as well as morphology of different microorganisms (Junne, Klein et al. 2008, Junne, Nicolas Cruz-Bournazou et al. 2010). The authors already applied this technology to batch as well as fed-batch LAB cultures (Pellicer-Alborch, Angersbach et al. 2018), but the application of this approach during continuous LAB cultivations has not yet been investigated.

In recent years, the *in silico* prediction of cell biomass and key metabolites using mechanistic models has been well investigated in bioprocesses subjected to environmental oscillatory conditions (Anane, Neubauer et al. 2017, Kroll, Hofer et al. 2017, Mears, Stocks et al. 2017, Anane, García et al. 2019, Anane, Sawatzki et al. 2019, Shirahata, Diab et al. 2019). Such modeling techniques have even been applied to the specific *S. thermophilus* strain used in this work (Spann, Glibstrup et al. 2018, Spann, Gernaey et al. 2019). Here we tried to predict the biomass, critical process parameters (CPPs; e.g. pH) as well as critical quality attributes (CQAs; e.g. lactose, lactic acid and galactose concentrations) during *S. thermophilus* A-stat continuous cultivations based on a parameter estimation performed with batch experiments (Spann, Roca et al. 2018) for the first time.

121 *Materials and methods*

122 *Bacterial strain and media*

123 The strain of *S. thermophilus* was provided by Chr. Hansen A/S (Hoersholm, Denmark)
124 and used throughout the whole study. In all cultivation experiments, a self-established De
125 Ma, Rogosa and Sharpe (MRS) medium was used, containing (per litre): 20 g lactose, 10
126 g peptone, 12 g yeast extract, 2 g K_2HPO_4, 5 g sodium acetate anhydrous, 2 g di-
127 ammonium hydrogencitrate, 0.2 g $MgSO_4 \cdot 7H_2O$ and 0.05 g $MnSO_4 \cdot H_2O$. All media
128 components were purchased by the company (Chr. Hansen A/S, Hoersholm, Denmark).

129 *Cultivation conditions*

130 For all experiments, 300 mL EloFerm glass bioreactors (EloSystems GmbH, Berlin,
131 Germany) equipped with a magnetic stirring flea and a pH probe (EasyFerm Bio VP 225,
132 Hamilton Robotics, Reno, NV) were used. Firstly, the empty assembled bioreactors were
133 sterilized in an autoclave at 121 ºC for 20 minutes. After temperature decrease, the
134 sterilized media was introduced into the bioreactor (C-source separated from the rest of
135 media components). Importantly, the pH of the media was adjusted at pH 6 with H_2SO_4
136 20 % v/v (Carl Roth, Karlsruhe, Germany) prior to sterilization. The bioreactors were
137 then inoculated (0.1 % v/v) directly with the cry stock (Chr. Hansen A/S, Hoersholm,
138 Denmark). The fermentation temperature was kept at 40 °C, while gassing the headspace
139 with nitrogen, and the pH was controlled at pH 6 with addition of NH_3 5 % (v/v) (Carl
140 Roth, Karlsruhe, Germany) throughout the fermentations.

141 *Analysis*

142 Optical density at 620 nm was monitored with a photometer EloCheck (EloSystems
143 GmbH, Berlin, Germany) in a flow cell connected to a reactor bypass with an optical
144 depth of 2.2 mm for every 15 sec. The amount of cells per mL, c_n, was determined

following Eq. 1 under consideration of the cell size as determined with the electrooptical measurement and as calibrated with manual cell counts:

$$c_n = (3.1 \cdot OD_{600} / l_c^{1.33}) \cdot 10^9 \quad (1)$$

where l_c represents the mean cell length.

Cell growth was additionally monitored off-line with appropriately diluted samples at a wavelength of 600 nm (OD_{600}) with an Ultraspec 2100 *pro* UV/Visible spectrophotometer (Amersham Biosciences, Amersham, UK). For dry cell weight (DCW) determination, 2 mL of cell suspension were pipetted into a previously dried and weighted 2 mL Eppendorf tube. Samples were then centrifuged at 4 ºC and 15,000 rpm for 10 minutes. The supernatant was discarded, whilst the cell pellet was washed with 1 mL of NaCl 0.9 % (w/w) solution. After a second step of centrifugation, the Eppendorf tube containing the washed cells was dried at 75 ºC for 24 hours and weighted again. The DCW was then calculated as the difference between the tube with sample and its tare. Samples for extracellular metabolite and free amino acid concentration were filtered through a membrane filter with a pore size of 0.8 μm (Carl Roth, Karlsruhe, Germany) directly at the sampling port of the bioreactor. The filtrate was transferred to a 1.5 mL Eppendorf tube and immediately stored at -80 ºC.

Determination of cell polarizability and cell length

A fully automated sampling and analysis unit EloTrace (EloSystems GmbH, Berlin, Germany) was used to monitor the AP and cell length in one of the two bioreactors with a sampling interval of 15 min. Cells were separated from the culture broth by filtration through a cellulose filter of a pore size of 0.45 μm (Sartorius, Göttingen, Germany). The cell concentrate was diluted with distilled water of a conductivity of 5 $\mu S \cdot cm^{-1}$ to a final optical density of OD_{600} = 0.1 +/- 5 % prior to the electrooptical measurement. The AP

was acquired in a measurement chamber at four different frequencies: 210, 400, 900 and 2,100 kHz. Detailed principles of the method were described elsewhere (Bunin 2002). All AP values contain a scaling factor of $5 \cdot 10^{-31}$ F · m² for easier readability and comparison with other literature sources. The system was calibrated by microscopic analysis in order to correlate orientation and relaxation characteristics to the cell length.

Quantification of metabolites

Extracellular organic acids and sugars were quantified with an Agilent 1200 HPLC system (Agilent Technologies, Santa Clara, USA) equipped with a refractive index detector (RID) and a HyperRez™ XP Carbohydrate H^+ column (300x7.7 mm, 8 µm) (Fisher Scientific, Schwerte, Germany) using 5 mM H_2SO_4 at a flow rate of 0.5 mL·min^{-1} and a temperature of 65 ºC. Prior to analysis the samples were thawed on ice and diluted ¼ with H_2O to a final volume of 200 µL. Subsequently, the HPLC vials (VWR, Radnor, USA) were prepared with a 200 µL micro-insert (VWR, Radnor, USA) and the diluted samples were transferred into the vials. Amino acid quantification was conducted with HPLC analysis as described previously (Lemoine, Martínez-Iturralde et al. 2015).

Microscopic image analysis

1 mL sample was taken directly from the bioreactor into a 1.5 mL Eppendorf tube and 10 µL were pipetted on a microscopic slide (VWR chemicals, Radnor, USA). The slide was then covered with a cover glass of thickness No. 1.5 (VWR chemicals, Radnor, USA) and placed under the microscope (CN-hFT, Hertel & Reuss, Kassel, Germany) with 100x oil immersion objective. The images were taken with a digital camera (Canon Power Shot G1X, Canon, Tokio, Japan) with 4-times magnification.

Data fitting and visualization

In order to calculate rates, off-line data was fitted to a Smoothing Spline with the fitting toolbox of MATLAB R2013b (The MathWorks, Natick, MA). Concentrations were then

obtained every desired interval of time. All data plots were created with SigmaPlot version 11.0 (Systat Software, San José, CA).

Statistical analysis

Data were expressed as mean standard deviation (SD) for the description of reproducibility. Biological replicates were performed as fermentations under identical conditions. The coefficient of variation (CV%) was then calculated using Eq. 2:

$$CV\% = \frac{SD}{Mean} \cdot 100 \tag{2}$$

Biokinetic model and pH simulation

An unstructured kinetic model for *S. thermophilus* developed by (Spann, Roca et al. 2018) was used, which described the lactose consumption, biomass growth and lactic acid synthesis. Effects of the lag-time, substrate limitation and inhibition, pH and lactate inhibition were considered in the growth function. Additionally, a simplified version of the Luedeking-Piret equation was applied to describe the lactic acid synthesis. More details on the model development can be found in the original publication, but the most relevant equations are:

$$\left(1 + Y_{gal}\right) \cdot lactose \xrightarrow{q_X} biomass + Y_{gal} \cdot galactose \tag{3}$$

$$\left(1 + Y_{gal}\right) \cdot lactose \xrightarrow{q_P} lactic\ acid + Y_{gal} \cdot galactose \tag{4}$$

$$q_X = \mu_{max} \cdot \left(1 - e^{-t/t_{lag}}\right) \cdot \frac{C_S}{C_S + K_s + \frac{C_S^2}{K_I}} \cdot e^{-\left(\frac{\left(pH_{opt} - pH\right)^2}{\sigma^2}\right)} \cdot \frac{1}{1 + e^{K_{P,La}\left(C_P - \frac{K_{La}}{1 + e^{K_{P,pH1} \cdot \left(pH - K_{P,pH2}\right)}}\right)}} \cdot C_X \tag{5}$$

$$q_P = \alpha \cdot q_X \tag{6}$$

where q_X and q_P are the volumetric growth and lactic acid production rates, respectively. Lactose (C_S), biomass (C_X), and lactic acid (C_P) were listed as additional variables, and

their rate equations were defined as expressions in the CFX expression language. Initial concentrations were $C_{S,t=0} = 20\ g\ L^{-1}$, $C_{X,t=0} = 0.025\ g\ L^{-1}$, and $C_{P,t=0} = 0\ g\ L^{-1}$. The kinetic parameters as listed in Table 1 were derived from a parameter estimation, which was based on 2 L lab-scale fermentations with the aforementioned medium at 300 rpm (two 6-blade Rushton turbines with a diameter = 53 mm) and 40 °C at different pH values (in the range of 5.5 – 7.0) and initial lactose concentrations (20 and 70 g L^{-1}) (Spann, Roca et al. 2018). It is worth mentioning when evaluating the model that the supplemented yeast extract contains ca. 6 g L^{-1} carbon, which is not included in the model. However, this is only partially taken up by the cells and the dynamic model accounts for it by under predicting the galactose concentration. Importantly, the pH value was kept at pH 6 during the whole simulation, since it was also maintained at this value throughout the fermentations. The model was implemented and solved in MATLAB® (The MathWorks®, Natick, MA) using the ode15s solver.

Table 1.

Symbol	Description	Value
K_I	Substrate inhibition parameter	164 g L^{-1}
K_S	Substrate limitation parameter	0.79 g L^{-1}
K_{La}	Lactate inhibition parameter	19.8 g L^{-1}
$K_{P,La}$	2nd lactate inhibition parameter	0.24 L g^{-1}
$K_{P,pH1}$	LA inhibition pH parameter	20
$K_{P,pH2}$	2nd LA inhibition pH parameter	7
pH_{opt}	Optimal pH in the pH function	6.39
t_{lag}	Lag-time coefficient	1 h
Y_{gal}	Galactose yield	0.69 g g^{-1}
α	Growth related production coefficient of lactic acid	5.19 g g^{-1}
μ_{max}	Maximum specific growth rate	2.06 h^{-1}
σ	Spread parameter in the pH function	1.42

227 *Results and discussion*

228 LAB are used as starter cultures in the yogurt production from milk, thus being used to
229 grow on lactose (equivalent to a molecule of glucose and one of galactose). Once this C-
230 source is incorporated into the cell through the lactose permease (LacS), it is cleaved by
231 a β-galactosidase and split into glucose and galactose intracellularly (Sørensen, Curic-
232 Bawden et al. 2016). The former is used by the *S. thermophilus* strain to generate biomass
233 through glycolysis and lactic acid fermentation, while the latter is, in principle, not
234 consumed and therefore excreted into the media.

235 Generally, bacteria can either spend the energy acquired from sugar for cell division and
236 increase of biomass or for maintenance and enhancement of cells' metabolic activity
237 (Olughu, Nienow et al. 2019), in principle related to their polarizability under the action
238 of an electrical field of a certain frequency. Therefore, there is typically a trade-off
239 between growth and intracellular biochemical reactions for adaptation mechanisms,
240 which depends basically on (i) growth phase, (ii) changing media components'
241 concentrations (specially, the C-source and byproducts) and (iii) extracellular
242 environmental factors (e.g. pH, osmotic stress, temperature, etc.).

243

244 *The A-stat fermentation with S. thermophilus*

245 The idea behind an A-stat strategy was the characterization of the strain in terms of
246 maximum specific growth rate: the culture reaches a point, when it cannot keep up with
247 the rising D, resulting in the so called wash-out, where cells can no longer consume the
248 amount of C-source introduced and this starts to accumulate extracellularly, in parallel
249 with a decrease of the cells' as well as byproduct/s' concentrations inside the fermenter,
250 which are "washed-out" from the bioreactor. Accelerostat experiments with a *S.*
251 *thermophilus* strain from Chr. Hansen A/S (Hoersholm, Denmark) were performed in

duplicates. The cultivations began with a batch phase, followed by chemostats at a dilution rate of initially 0.3 h^{-1} and then 0.1 h^{-1} for ca. 50 h each. Subsequently, the accelerostat was started with an acceleration rate of the feed of 0.005 h^{-2}. Later on, the acceleration rate was increased stepwise to 0.008 h^{-2} (Figure 1).

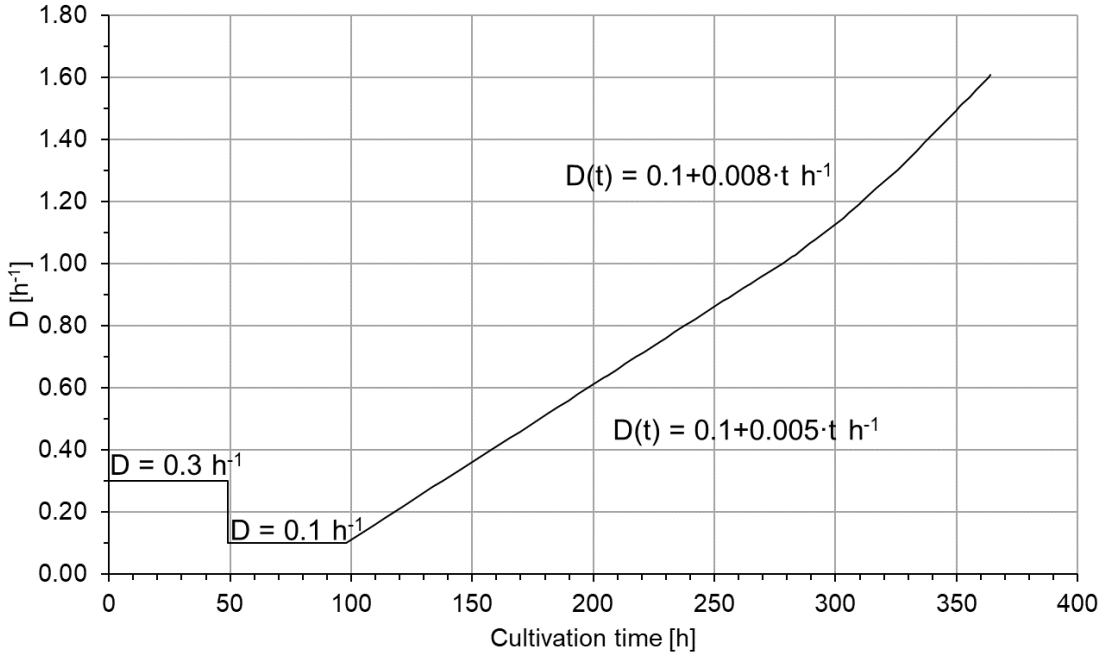

Figure 1. Dilution rate throughout duplicates of a *S. thermophilus* continuous cultivation. The cultivation started with a batch phase (data not shown), followed by two chemostat and an accelerostat phases.

The batch phases were started with 20 g·L^{-1} lactose, which was steadily being consumed, while biomass and OD_{600} were increasing, in parallel with the lactic acid and galactose concentrations measured in supernatant samples (data not shown). The first chemostats (D = 0.3 h^{-1}) were initiated once the on-line OD_{600} stabilized (DCW = 1.0 ± 0.02 g·L^{-1}) and the lactose concentration in both bioreactors was 12.2 ± 1.12 g·L^{-1} (lactic acid and galactose = 4.4 ± 0.36 g·L^{-1} 4.7 ± 0.32 g·L^{-1}, respectively) after about 7.5 hours of inoculation. This initial dilution rate was maintained for 10 reactor volumes to ensure a

steady-state in both fermenters: DCW = 1.8 ± 0.12 $g \cdot L^{-1}$, lactose = 0.3 ± 0.23 $g \cdot L^{-1}$, lactic acid = 7.8 ± 0.92 $g \cdot L^{-1}$ and galactose = 6.6 ± 0.49 $g \cdot L^{-1}$. At this point, the second chemostats (D = 0.1 h^{-1}) were started and maintained for 5 reactor volumes accomplishing a second steady-state in the two bioreactors: DCW = 1.6 ± 0.02 $g \cdot L^{-1}$, lactose = 0.2 ± 0.10 $g \cdot L^{-1}$, lactic acid = 9.4 ± 0.05 $g \cdot L^{-1}$ and galactose = 5.5 ± 0.62 $g \cdot L^{-1}$. The alteration in amino acid specific consumption rates with decreasing available C-source might be a consequence of a metabolic redistribution, with a higher proportion of amino acids being used as biosynthetic precursors. Almost no changes over time were detected for the vast majority of amino acids during chemostat experiments using complex media, but serine was depleted and alanine started to accumulate extracellularly shortly before the second chemostat cultures were started (data not shown). This was a clear indication of an influence of the C:N ratio on cell metabolism once the C-source started to be completely consumed. On the one hand, serine can generally be used either for biosynthesis or for conversion to pyruvate, so that under C-source limitation, increased conversion of serine to pyruvate to maintain the high ATP demand may be encountered. Additionally, serine is converted to glycine when the β–carbon atom of serine is transferred to tetrahydrofolate, whose derivatives serve as donors of one-carbon units in a variety of biosynthesis pathways (Meiser, Tumanov et al. 2016). Thus, the difference seen in the secretion of serine may have a background in the need for one-carbon units (Fernandez-de-Cossio-Diaz, Leon et al. 2017). What is more, as reported for mammalian cell culture, serine depletion in the medium can have negative impacts including increased asparagine consumption, alanine production, lactate production, and ammonium generation (Ritacco, Wu et al. 2018). On the other hand, high glycolytic flux (assumed when the continuous cultures were started) results in large accumulation of pyruvate that might not be processed, thus leading to production of large amounts of alanine, apart from lactate

(Torres, Berrios et al. 2019). Also, it is worth mentioning, that before the chemostat cultures were running, already a considerable amount of NH_3 had been introduced in the fermenters to compensate for the high lactic acid production rate of *S. thermophilus*. In fact, under high broth ammonium concentrations, a shift towards alanine transamination reaction has been reported elsewhere (Pan, Streefland et al. 2017): it consists in the conversion of pyruvate and ammonia to alanine, consuming one reducing agent. Because transamination reactions are readily reversible, alanine can be easily formed and thus has close links to metabolic pathways. This observation also highlights the influence of carbon source on amino acid metabolism and the flexibility of LAB to handle intracellular ammonia. Regrettably, no data on ammonia concentration in the bioreactors was available during the experiments, so these hypotheses cannot be confirmed. Moreover, deeper investigations on the metabolic fluxes around pyruvate during LAB cultures should be essential for future work.

From then on, the dilution rate was steadily increased over time in both vessels. At the beginning of the A-stat experiment (i.e. steady increase of D/μ over time), lactose was measured in residual concentrations (Figure 2), while lactic acid concentration, OD_{600} and DCW remained almost unchanged as the continuous cultivations evolved over time (as well as over D or μ). These observations, together with the fact that all analyzed aminoacids, succinate as well as acetate were comparably neither consumed nor produced throughout the fermentations, confirmed the quasi-steady state metabolism of the bacteria inside both bioreactors.

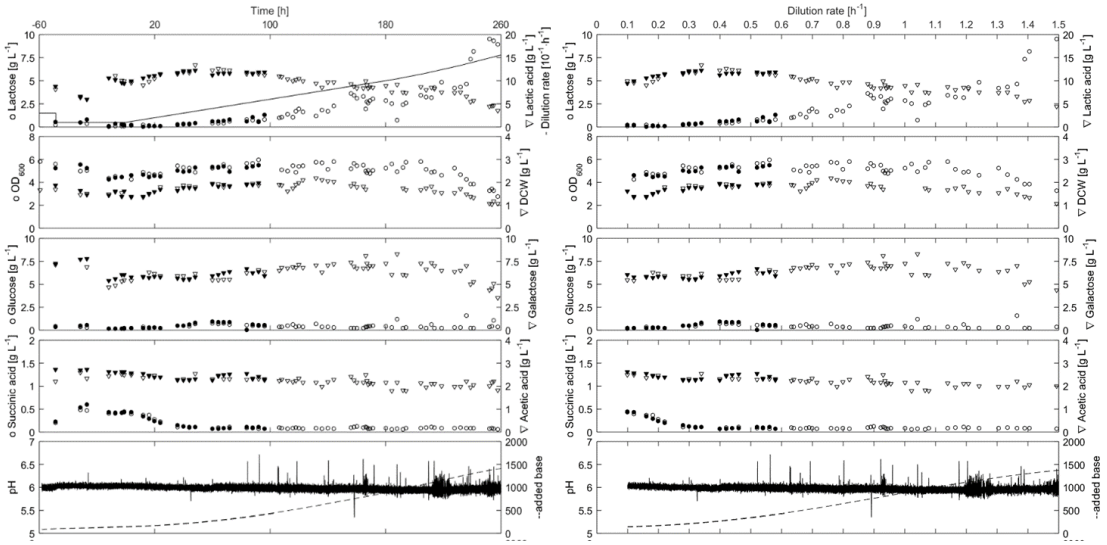

314

315 Figure 2. CPPs monitored throughout two (filled and unfilled symbols) A-stat cultivations
316 of *S. thermophilus* both, over time (left) as well as over the dilution rate (right). Off-line
317 analyses of OD_{600}, DCW and metabolites performed with HPLC are represented by
318 symbols, while in-line measurement of pH as well as at-line determination of base
319 addition, cell size and polarizability at 400 kHz are plotted with lines.

320

321 Just before D = 0.6 h^{-1} (i.e. about 100 h of experiment), feeding was interrupted due to a
322 mechanical error, thus influencing the whole cell metabolism: surprisingly, the galactose
323 (which is in principle not metabolized by this *S. thermophilus* strain, as commented
324 before) was depleted and lactic acid, OD_{600} and DCW values had increased just in the
325 next measuring point after the incident (data not shown). This is irrelevant for the actual
326 work, but indicated that the LAB had been adapting to limiting lactose concentration and
327 galactose excess in the media throughout the whole experiment (i.e. batch, two
328 chemostats and A-stat), so that once the preferred C-source lactose ceased to be
329 introduced, cells consumed the next C-source available (i.e. galactose). Sequencing of the
330 bacteria at that point and comparison with the inoculated biomass would have elucidated
331 and confirmed the genomic mutations undergone during the long continuous cultivation

towards using galactose also as substrate, but was not done in this work. For that reason, from then on, off-line data related to this replicate was no longer plotted in the graphs. Around D = 0.6 - 0.7 h^{-1}, the lactose started to accumulate extracellularly, but lactic acid, OD_{600} and DCW still remained statistically constant over time as well as D. It was first at D = 1.3 h^{-1} where the lactose concentration notably increased and the fermentation product, OD_{600} as well as DCW decreased in parallel notably, thus indicating a clear wash-out. This maximum specific growth rate was in accordance with analysis of the Lineweaver–Burk plot (Figure S1), resulting in a μ_{max} of 1.3 h^{-1} and a K_S of 0.9 $g \cdot L^{-1}$.

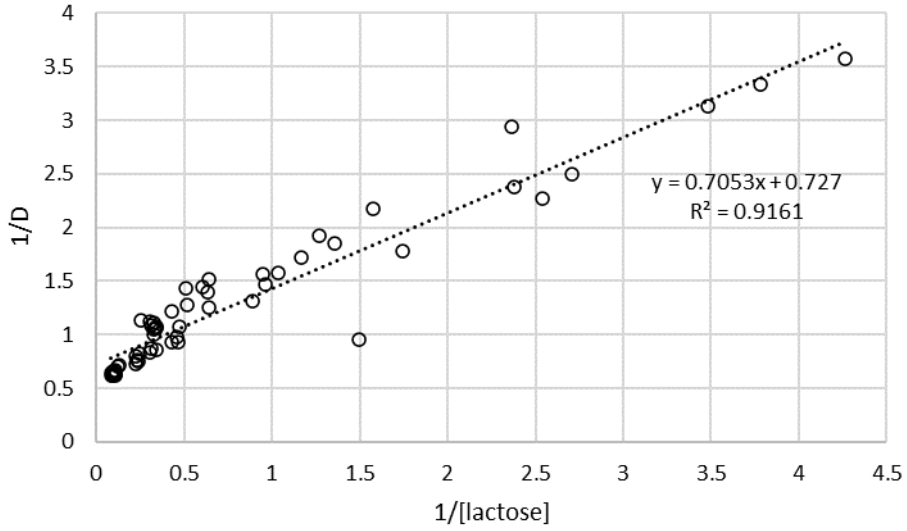

Figure S1. Lineweaver–Burk plot during the *S. thermophilus* A-stat fermentation.

The electrooptical measurement during continuous cultivations

Electrooptical measurements of cells' polarizability and size were measured at-line with the EloTrace device (EloSystems GmbH, Berlin, Germany) once enough bacteria were detected in the bioreactor (i.e. ≈ OD 0.5). This was just two hours before the continuous cultures were initiated, where a high cell division rate was analyzed and therefore *S. thermophilus* polarizability was steadily decreasing. An AP level at 400 kHz of around

3,000 (x5·10^{-31}) F·m^2 and a mean cell size of 3.0 μm were measured just at the end of the batch phase. These are similar values than those obtained after exponential growth of *L. plantarum* cultures under optimal growth conditions in the same fermenters (Pellicer-Alborch, Angersbach et al. 2018): polarizability and length of 4,500 F·m^2 and 2.0 μm, respectively. Differences in the AP level were expected since different microorganisms grown in variable media (even C-sources) will present distinct polarizability under the effect of an electrical field (Angersbach, Ignatov et al. 2006). More than the exact value, the relevant observation is the profile of the AP level over cultivation time after inoculation (Junne, Klein et al. 2008, Junne, Nicolas Cruz-Bournazou et al. 2010). Moreover, since *S. thermophilus* build cocci chains of variable length and *L. plantarum* are rod-shaped bacteria, it was not surprising that the former presented a higher mean cell size.

During the first seven hours of connection of the feed (D = 0.3 h^{-1}) the culture exhibited a steadily increasing polarizability as well as size, with almost no growth, thus adapting to the new environmental conditions and showing an active metabolism taking nutrients up for future biomass production (data not shown). Once cell division was started again (consumption of the remaining lactose in the media), the mean AP at 400 kHz dropped even below values before starting the chemostat phase. Importantly, the change of dilution rate (to D = 0.1 h^{-1}) was also performed when stable culture polarizability as well as morphology were detected by means of at-line electrooptical measurements. Interestingly, *S. thermophilus* also presented an adaptation phase with the new feeding rate showing again an increased mean AP level and cell size, of similar magnitudes (≈ 2,000 x5·10^{-31} F·m^2 and ≈ 2 μm, respectively) respect the previous steady-state reached. From D = 0.1 h^{-1} the dilution rate was firstly increased linearly over time (i.e. start of the accelerostat) when, once again, a stable AP level and cell size were observed. Just after

increasing slightly the feeding rate (slope = 0.005 h^{-2}), an increase in cells' polarizability as well as size was already detected (Figure 3), thus showing an active metabolism after more than 100 hours of experiment. During the A-stat experiment, the mean cell size (if the washing steps are ignored) as well as the AP level at 400 kHz measured at-line electrooptically were steadily increasing, reaching their maxima during the detected region of D between 0.9 and 1.3 h^{-1} (Figure 3). What is more, morphology changes were verified under the microscope, detecting the longest cocci chains around D = 0.8 h^{-1}.

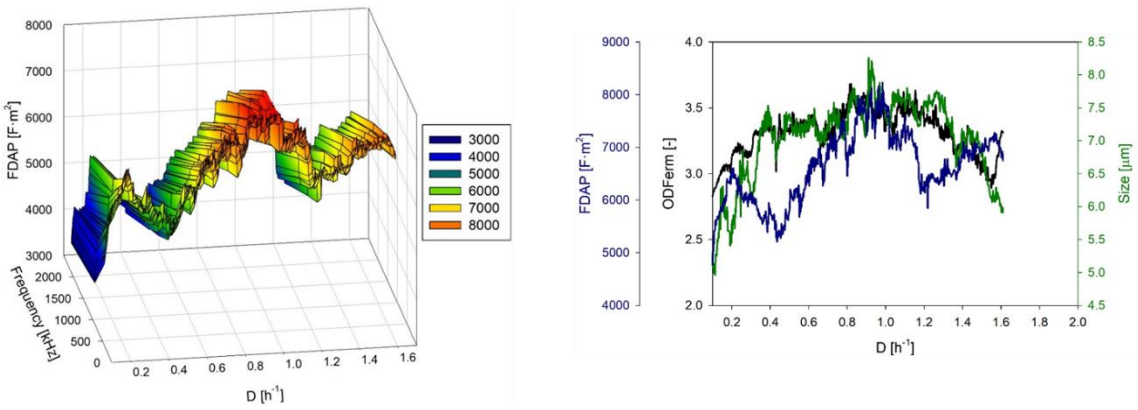

Figure 3. At-line electrooptical measurement of cell polarizability and size during a *S. thermophilus* A-stat fermentation. AP development over D at different frequencies (left) and comparison with on-line measurement of OD (black line right) with EloFerm (EloSystems GmbH, Berlin, Germany). AP level at 400 kHz (blue line right) and cell size (green line right).

The electrooptical polarizability shows a good agreement with the development of the metabolic activity as depicted in Figure S2.

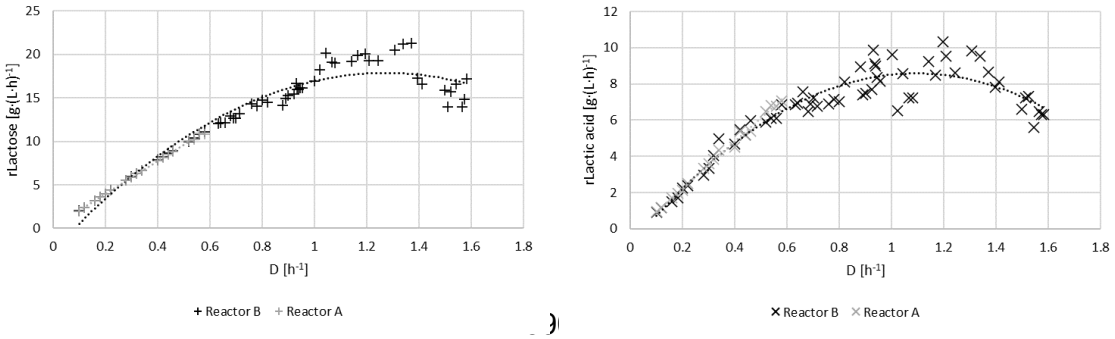

389

391 Figure S2. Lactose consumption rate and lactic acid production rate over D.

392

393 The cell division in *S. thermophilus* occurs in successive parallel planes perpendicular to
394 their axis (Zapun, Vernet et al. 2008) leading to diplococcal daughter cells connected
395 through their septa (Layec, Gérard et al. 2009). At the very late step of cell division, the
396 septum formed is cleaved and converted into the new pole of each daughter cell by the
397 action of cell wall hydrolases (Chapot-Chartier and Kulakauskas 2014). Nevertheless, at
398 high growth rates, a second round of cell division may start before closure of the septum,
399 therefore longer chains might be detectable. In fact, these bacteria growing at their μ_{max}
400 showed the longest chain length, which steadily decreased afterwards because of cell
401 division cessation and the action of peptidoglycan hydrolases (PGH) in cleaving septa.
402 This is the first time that electrooptical measurements are applied to *S. thermophilus*
403 bacteria, which form chains of variable cocci length, as described before. This
404 morphologic characteristic may provide the cells a certain flexibility and adaptability
405 (Fischetti 2016) under the action of an electrical field. Since the EloTrace device has been
406 applied to rigid and normally rod-shaped bacteria until now (Junne, Klein et al. 2008,
407 Junne, Nicolas Cruz-Bournazou et al. 2010, Pellicer-Alborch, Angersbach et al. 2018),
408 the complete understanding of the electrooptical measurement of flexible cocci chains
409 may be really challenging. Therefore, the morphologic changes throughout the

experiment were always confirmed with microscopic analyses and further investigation of this parameter should be carried out for such microorganisms.

It is worth mentioning, that a certain correlation between the polarizability and the yield biomass/substrate ($Y_{X/S}$) during the continuous cultivation of *S. thermophilus* was found: the higher the AP level at 400 kHz, the higher the $Y_{X/S}$ (Figure S3). In general, the higher the metabolic activity (in this case, taking substrate up for biomass production) the greater the cell polarizability.

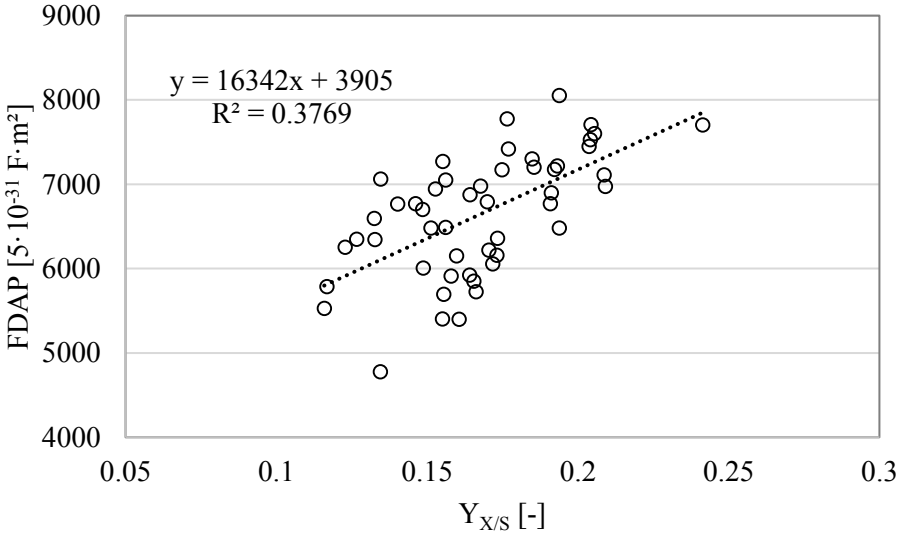

Figure S3. Linear correlation between the AP level at 400 kHz and the yield biomass/substrate ($Y_{X/S}$) throughout the A-stat experiment.

Finally, it should be noted that a daily equipment maintenance (i.e. system washing and filter renovation) was necessary for the correct operation of the EloTrace device and a subsequent reliable measurement of cell polarizability (Figure S2). The main objective of the equipment before the electrooptical measurement takes place is to ensure an OD of ≈ 0.1, thus ensuring the analysis of more or less the same number of cells (assuming no noticeable variations on their mean size during growth, which is not completely true in

this experiment set up), independently from the biomass concentration (i.e. OD) in the fermenter. This is partly achieved by reducing the conductivity of the sample suspension with several washing steps using deionized water, but the filter inevitably gets partially clogged and rests of salts (especially when using complex media to cultivate) remain in the filter, thus increasing the conductivity of the next washed sample (Figure S2). This is the main reason why at least a daily maintenance of the device is crucial, particularly for such a long experiment (more than two weeks). Taking this into account, plotting the electrooptical measurements throughout the whole A-stat cultivation ignoring the several washing steps has been challenging, but dividing the AP level at a certain frequency by the OD in the measuring chamber (ODEloCell) has helped (Figure S4). Apart from detecting some issues with the device at lower dilution rates, it was confirmed, that the maximum *S. thermophilus* polarizability was accomplished around D = 0.8-1.0 h^{-1}.

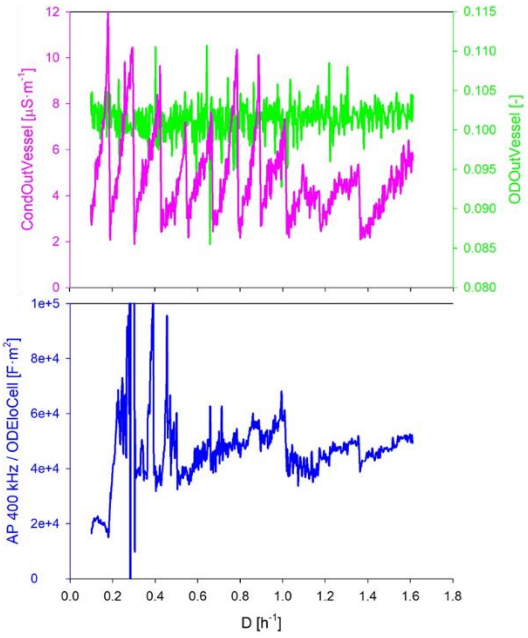

Figure S4. Conductivity (CondOutVessel, pink) and OD (ODOutVessel, green) before entering the polarizability measuring chamber of the EloTrace device throughout the A-stat fermentation. AP level at 400 kHz divided by the OD in the measuring chamber (ODEloCell) over D (blue).

These results confirm the evidence that the AP measurement could be used as an early indicator for growth retardation (Pellicer-Alborch, Angersbach et al. 2018), since it decreased earlier than the other key indicators (i.e. DCW, OD, lactic acid, galactose, etc). What is more, the automated sampling and sample preparation of the measuring device would enable its use as an at-line tool, thus allowing to change process parameters to avoid unfavourable cultivation conditions.

The mechanistic modeling of A-stat cultivations

The mechanistic model described here has already been used recently to successfully monitor batch *S. thermophilus* fermentations (Spann, Roca et al. 2018), to predict pH-gradients in a 700 L pilot scale fermenter, when coupled to computational fluid dynamic (CFD) studies (Spann, Glibstrup et al. 2018), and to develop a soft sensor for on-line risk-based monitoring of the same process, if coupled to a compartment model (Spann, Gernaey et al. 2019). Moreover, it was even applied to estimate the optimal dilution rate as well as substrate concentration in the feed in order to maximize biomass concentration, while minimizing the waste of substrate during a continuous fermentation in a 50 m^3 bioreactor (Spann, Lantz et al. 2018). The novelty in this work was that the model was trained with batch fermentations, but accurately predicted the A-stat evolution over time and dilution rate (Figure 4). What is more, the modelled rates of biomass production (r_X in g $X \cdot (L \cdot h)^{-1}$) as well as substrate consumption (r_S in g $S \cdot (L \cdot h)^{-1}$) were also in agreement with the experimentally calculated values with off-line analyses (Figure S5). Based on experimental and modelling results, the maximum specific growth rate for this *S. thermophilus* strain was concluded to be 1.3-1.4 h^{-1} with a wash out point at D = 1.9 h^{-1}.

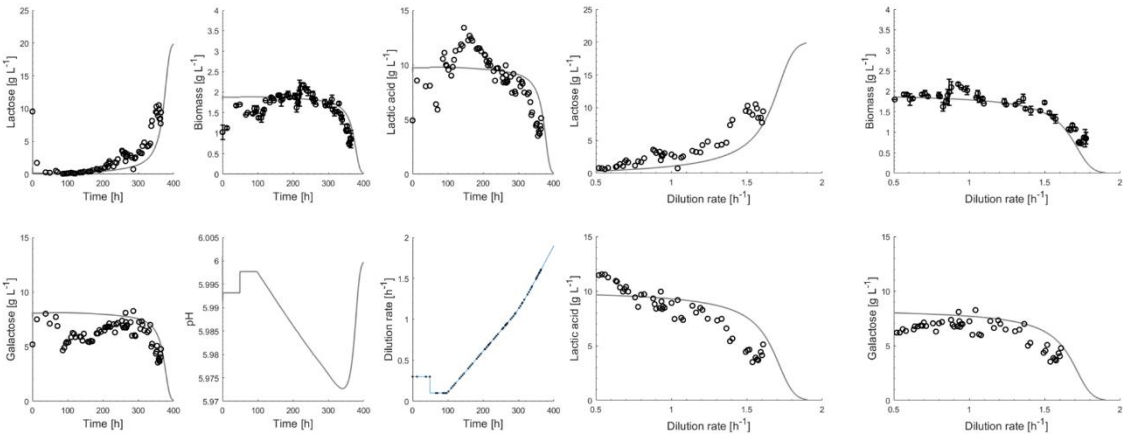

Figure 4. Experimental (dots) and modelled (lines) CPPs (pH, D) as well as CQAs (biomass, lactose, lactic acid and galactose concentrations) over time (left) and over dilution rate (D) during the A-stat experiment. Error bars: Mean ± SD (n = 2).

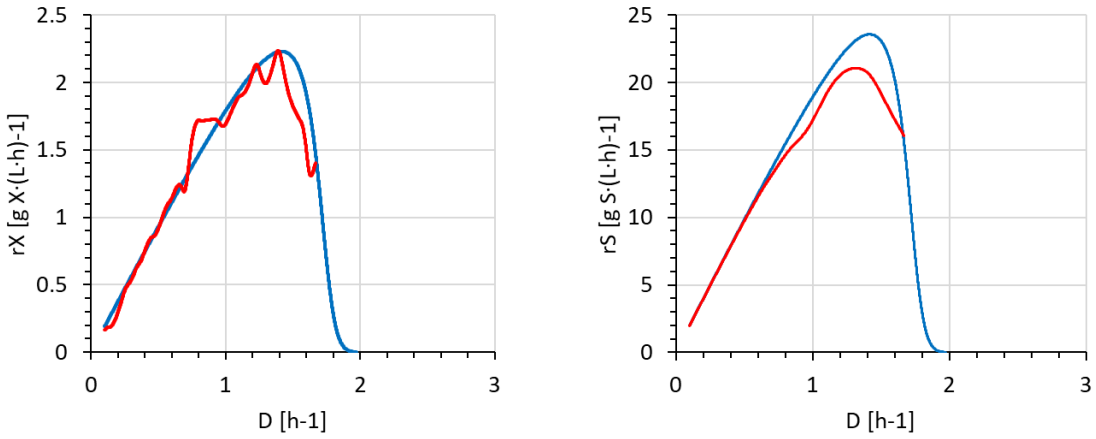

Figure S5. Experimental (red) and modelled (blue) rates of biomass production (r_X) and substrate consumption (r_S) over the dilution rate of the A-stat experiment.

(Gonzalez, Tebbani et al. 2016) recently predicted continuous fermentations, but of *Lactobacillus coryniformis* and performed their parameter estimation already with continuous experiments. Additionally, these authors defined the growth rate as a function of only the limiting substrate and the inhibitory product, while here the effect of the lag

481 time, the pH and the inhibition of substrate were also considered. What is more, after
482 training the model presented in this work with batch fermentations performed even with
483 a different initial lactose concentration (65 $g \cdot L^{-1}$ for parameter estimation vs. 20 $g \cdot L^{-1}$ in
484 the A-stat experiment), the critical process parameters (CPPs, e.g. pH, D) and critical
485 quality attributes (CQAs, e.g. biomass, lactose, lactic acid and galactose concentrations)
486 were still successfully predicted. Furthermore, sensitivity and identifiability analysis were
487 conducted to find an identifiable parameter subset for regression (Sin and Gernaey 2016).
488 Once this was completed, the confidence intervals of the estimated parameters were
489 derived from a linear approximation method using the Jacobian matrix of the parameter
490 estimation (Sin, Meyer et al. 2010). Finally, (Gonzalez, Tebbani et al. 2016) do not
491 mention anything about closing the carbon balance, but they also used a complex media
492 for the cultivation. In this work, a Z compound was included in the mixed weak acid/base
493 model to account for amino acids and further unknown C-sources in the fermentation
494 broth.

495

Conclusion

In this work, the maximum specific growth rate (μ_{max}) of *S. thermophilus* was successfully characterized through continuous A-stat fermentations, obtaining a μ_{max} = 1.3-1.4 h^{-1}, which is in accordance with previous studies performed by the same authors. Additionally, an automated sampling and sample preparation device for electrooptical measurements of cell polarizability and size was applied for the first time in LAB continuous cultivations, by performing daily equipment cleaning. What is more, the at-line AP level at a certain frequency correlated with key bacterial growth indicators and the automated mean cell size was in accordance with microscopic analysis of the cocci chains. These at-line determined culture parameters supported the results obtained with typical off-line measurements (namely, OD, DCW, HPLC-analyses, etc.). Finally, a mechanistic model calibrated with batch experiments successfully and reliably predicted key performance indicators (like biomass, lactose, lactic acid and galactose concentrations over time), suggesting the possibility to implement a model-based control strategy in continuous LAB production and validating the original in-silico simulation.

It was demonstrated that the electrooptical measurement of cell polarizability in LAB cultures may be of special interest for future improvement of the current QbT strategy established in the industrial scale manufacturing of starter cultures. The consideration of a new CQA (namely bacterial ionic activity under the application of a certain electrical field or even the mean chain length) is suggested, which could be measured at-line, thus allowing the move towards a QbD or QbC approach. This could be accomplished by e.g. ensuring these new CQAs by changing the CPPs (like stirring speed or base addition rate) during the production process in the industry, thus improving process reproducibility and product consistency.

Acknowledgments

This project has received funding from the European Union's Horizon 2020 research and innovation program under the Marie Skłodowska-Curie actions grant agreement No. 643056 (project Biorapid). The authors gratefully acknowledge this financial support and the contribution of Dr. Christophe Roca, Dr. Anders Clausen as well as Dr. David Kold from Chr. Hansen A/S by providing their knowledge and expertise, media and the strain for all experiments. The authors finally thank Peter Unger, Adriana Mora Barrabés, Julia Scharre, Manon Weiske and Lena Jack for their help during scale-down experiments.

Conflict of interest

All authors declare no competing interests.

References

Abt, V., T. Barz, N. Cruz, C. Herwig, P. Kroll, J. Möller, R. Pörtner and R. Schenkendorf (2018). "Model-based tools for optimal experiments in bioprocess engineering." Current opinion in chemical engineering **22**: 244-252.

Adamberg, K., P.-J. Lahtvee, K. Valgepea, K. Abner and R. Vilu (2009). "Quasi steady state growth of Lactococcus lactis in glucose-limited acceleration stat (A-stat) cultures." Antonie van Leeuwenhoek **95**(3): 219-226.

Adamberg, K., A. Seiman and R. Vilu (2012). "Increased biomass yield of Lactococcus lactis by reduced overconsumption of amino acids and increased catalytic activities of enzymes." PloS one **7**(10): e48223.

Adamberg, K., K. Valgepea and R. Vilu (2015). "Advanced continuous cultivation methods for systems microbiology." Microbiology **161**(9): 1707-1719.

Anane, E., Á. C. García, B. Haby, S. Hans, N. Krausch, M. Krewinkel, P. Hauptmann, P. Neubauer and M. N. Cruz‐Bournazou (2019). "Model‐based framework for parallel scale down fed‐batch cultivations in mini‐bioreactors for accelerated phenotyping." Biotechnology and bioengineering.

Anane, E., P. Neubauer and M. N. C. Bournazou (2017). "Modelling overflow metabolism in Escherichia coli by acetate cycling." Biochemical Engineering Journal **125**: 23-30.

Anane, E., A. Sawatzki, P. Neubauer and M. N. Cruz‐Bournazou (2019). "Modelling concentration gradients in fed‐batch cultivations of E. coli–towards the flexible design of scale‐down experiments." Journal of Chemical Technology & Biotechnology **94**(2): 516-526.

Angersbach, A., V. D. Bunin and O. V. Ignatov (2006). Electro-optical analysis of bacterial cells. Molecular and colloidal electrooptics. S. Stoilov. New York, M. Dekker Publ.**:** 86-112.

Angersbach, A., O. Ignatov and V. Bunin (2006). Electro-Optical Analysis of Bacterial Cells. Molecular and Colloidal Electro-optics, CRC Press.
Bull, A. T. (2010). "The renaissance of continuous culture in the post-genomics age." Journal of industrial microbiology & biotechnology **37**(10): 993-1021.
Bunin, V. D. (2002). Electrooptical analysis of a suspension of cells and its structures. Encyclopedia of surface and colloid science. New York, M. Dekker Publ.**:** 2032-2043.
Chapot-Chartier, M.-P. and S. Kulakauskas (2014). Cell wall structure and function in lactic acid bacteria. Microbial cell factories, BioMed Central.
Erm, S., K. Adamberg and R. Vilu (2014). "Multiplying steady-state culture in multi-reactor system." Bioprocess and biosystems engineering **37**(11): 2361-2370.
Fernandez-de-Cossio-Diaz, J., K. Leon and R. Mulet (2017). "Characterizing steady states of genome-scale metabolic networks in continuous cell cultures." PLoS computational biology **13**(11): e1005835.
Fischetti, V. A. (2016). M protein and other surface proteins on streptococci. Streptococcus pyogenes: Basic Biology to Clinical Manifestations [Internet], University of Oklahoma Health Sciences Center.
Gabardo, S., G. F. Pereira, R. Rech and M. A. Z. Ayub (2015). "The modeling of ethanol production by Kluyveromyces marxianus using whey as substrate in continuous A-Stat bioreactors." Journal of industrial microbiology & biotechnology **42**(9): 1243-1253.
Glauche, F., J. Glazyrina, M. N. Cruz Bournazou, G. Kiesewetter, F. Cuda, D. Goelling, A. Raab, C. Lang and P. Neubauer (2017). "Detection of growth rate‐dependent product formation in miniaturized parallel fed‐batch cultivations." Engineering in Life Sciences **17**(11): 1215-1220.
Gonzalez, K., S. Tebbani, F. Lopes, A. Thorigné, S. Givry, D. Dumur and D. Pareau (2016). "Modeling the continuous lactic acid production process from wheat flour." Applied microbiology and biotechnology **100**(1): 147-159.
Gresham, D. and J. Hong (2014). "The functional basis of adaptive evolution in chemostats." FEMS microbiology reviews **39**(1): 2-16.
Junne, S., E. Klein, A. Angersbach and P. Goetz (2008). "Electrooptical measurements for monitoring metabolite fluxes in acetone–butanol–ethanol fermentations." Biotechnology and Bioengineering **99**(4): 862-869.
Junne, S., M. Nicolas Cruz-Bournazou, A. Angersbach and P. Götz (2010). "Electrooptical monitoring of cell polarizability and cell size in aerobic Escherichia coli batch cultivations." Journal of Industrial Microbiology & Biotechnology **37**(9): 935-942.
Kroll, P., A. Hofer, I. V. Stelzer and C. Herwig (2017). "Workflow to set up substantial target-oriented mechanistic process models in bioprocess engineering." Process Biochemistry **62**: 24-36.
Lahtvee, P.-J., K. Adamberg, L. Arike, R. Nahku, K. Aller and R. Vilu (2011). "Multi-omics approach to study the growth efficiency and amino acid metabolism in Lactococcus lactis at various specific growth rates." Microbial cell factories **10**(1): 12.
Lahtvee, P.-J., K. Valgepea, R. Nahku, K. Abner, K. Adamberg and R. Vilu (2009). "Steady state growth space study of Lactococcus lactis in D-stat cultures." Antonie Van Leeuwenhoek **96**(4): 487.
Layec, S., J. Gérard, V. Legué, M. P. Chapot‐Chartier, P. Courtin, F. Borges, B. Decaris and N. Leblond‐Bourget (2009). "The CHAP domain of Cse functions as an endopeptidase that acts at mature septa to promote Streptococcus thermophilus cell separation." Molecular microbiology **71**(5): 1205-1217.
Lemoine, A., N. Martínez-Iturralde, R. Spann, P. Neubauer and S. Junne (2015). "Response of Corynebacterium glutamicum exposed to oscillating cultivation conditions in a two- and a novel three-compartment scale-down bioreactor." Biotechnol Bioeng **112**(6): 1220-1231.
Mears, L., S. M. Stocks, M. O. Albaek, G. Sin and K. V. Gernaey (2017). "Mechanistic fermentation models for process design, monitoring, and control." Trends in biotechnology **35**(10): 914-924.

Meiser, J., S. Tumanov, O. Maddocks, C. F. Labuschagne, D. Athineos, N. Van Den Broek, G. M. Mackay, E. Gottlieb, K. Blyth and K. Vousden (2016). "Serine one-carbon catabolism with formate overflow." Science advances **2**(10): e1601273.

Olughu, W., A. Nienow, C. Hewitt and C. Rielly (2019). "Scale‐down studies for the scale‐up of a recombinant Corynebacterium glutamicum fed‐batch fermentation: loss of homogeneity leads to lower levels of cadaverine production." Journal of Chemical Technology & Biotechnology.

Pan, X., M. Streefland, C. Dalm, R. H. Wijffels and D. E. Martens (2017). "Selection of chemically defined media for CHO cell fed-batch culture processes." Cytotechnology **69**(1): 39-56.

Peebo, K. and P. Neubauer (2018). "Application of continuous culture methods to recombinant protein production in microorganisms." Microorganisms **6**(3): 56.

Pellicer-Alborch, K., A. Angersbach, P. Neubauer and S. Junne (2018). "Electrooptical Determination of Polarizability for On-Line Viability and Vitality Quantification of Lactobacillus plantarum Cultures." Frontiers in bioengineering and biotechnology **6**: 188.

Ritacco, F. V., Y. Wu and A. Khetan (2018). "Cell culture media for recombinant protein expression in Chinese hamster ovary (CHO) cells: History, key components, and optimization strategies." Biotechnology progress **34**(6): 1407-1426.

Shirahata, H., S. Diab, H. Sugiyama and D. I. Gerogiorgis (2019). "Dynamic modelling, simulation and economic evaluation of two CHO cell-based production modes towards developing biopharmaceutical manufacturing processes." Chemical Engineering Research and Design **150**: 218-233.

Sin, G. and K. Gernaey (2016). "Data handling and parameter estimation." Experimental Methods in Wastewater Treatment: 201-234.

Sin, G., A. S. Meyer and K. V. Gernaey (2010). "Assessing reliability of cellulose hydrolysis models to support biofuel process design—Identifiability and uncertainty analysis." Computers & Chemical Engineering **34**(9): 1385-1392.

Sørensen, K. I., M. Curic-Bawden, M. P. Junge, T. Janzen and E. Johansen (2016). "Enhancing the sweetness of yoghurt through metabolic remodeling of carbohydrate metabolism in Streptococcus thermophilus and Lactobacillus delbrueckii subsp. bulgaricus." Appl. Environ. Microbiol. **82**(12): 3683-3692.

Spann, R., K. V. Gernaey and G. Sin (2019). "A compartment model for risk-based monitoring of lactic acid bacteria cultivations." Biochemical Engineering Journal **151**: 107293.

Spann, R., J. Glibstrup, K. Pellicer‐Alborch, S. Junne, P. Neubauer, C. Roca, D. Kold, A. E. Lantz, G. Sin and K. V. Gernaey (2018). "CFD predicted pH gradients in lactic acid bacteria cultivations." Biotechnology and bioengineering.

Spann, R., A. E. Lantz, C. Roca, K. V. Gernaey and G. Sin (2018). Model-based process development for a continuous lactic acid bacteria fermentation. Computer Aided Chemical Engineering, Elsevier. **43:** 1601-1606.

Spann, R., C. Roca, D. Kold, A. E. Lantz, K. V. Gernaey and G. Sin (2018). "A probabilistic model-based soft sensor to monitor lactic acid bacteria fermentations." Biochemical Engineering Journal **135**: 49-60.

Torres, M., J. Berrios, Y. Rigual, Y. Latorre, M. Vergara, A. J. Dickson and C. Altamirano (2019). "Metabolic flux analysis during galactose and lactate co-consumption reveals enhanced energy metabolism in continuous CHO cell cultures." Chemical Engineering Science **205**: 201-211.

Wechselberger, P., A. Seifert and C. Herwig (2010). "PAT method to gather bioprocess parameters in real-time using simple input variables and first principle relationships." Chemical Engineering Science **65**(21): 5734-5746.

Zapun, A., T. Vernet and M. G. Pinho (2008). "The different shapes of cocci." FEMS microbiology reviews **32**(2): 345-360.

III

3rd Paper

Received: 27 August 2018 | Accepted: 26 October 2018

DOI: 10.1002/bit.26868

ARTICLE

WILEY BIOTECHNOLOGY BIOENGINEERING

CFD predicted pH gradients in lactic acid bacteria cultivations

Robert Spann[1] | Jens Glibstrup[1] | Klaus Pellicer-Alborch[2] | Stefan Junne[2] | Peter Neubauer[2] | Christophe Roca[3] | David Kold[3] | Anna Eliasson Lantz[1] | Gürkan Sin[1] | Krist V. Gernaey[1] | Ulrich Krühne[1]

[1]Department of Chemical and Biochemical Engineering, Technical University of Denmark, Kgs., Lyngby, Denmark

[2]Department of Biotechnology, Chair of Bioprocess Engineering, Technische Universität Berlin, Berlin, Germany

[3]Chr. Hansen, Hoersholm, Denmark

Correspondence
Ulrich Krühne, Technical University of Denmark, Søltofts Plads Building 229, 2800 Kgs. Lyngby, Denmark.
Email: ulkr@kt.dtu.dk

Funding information
H2020, Grant/Award Number: 643056; European Union's Horizon 2020 Research and Innovation Program

Abstract

The formation of pH gradients in a 700 L batch fermentation of *Streptococcus thermophilus* was studied using multi-position pH measurements and computational fluid dynamics (CFD) modeling. To this end, a dynamic, kinetic model of *S. thermophilus* and a pH correlation were integrated into a validated one-phase CFD model, and a dynamic CFD simulation was performed. First, the fluid dynamics of the CFD model were validated with NaOH tracer pulse mixing experiments. Mixing experiments and simulations were performed whereas multiple pH sensors, which were placed vertically at different locations in the bioreactor, captured the response. A mixing time of about 46 s to reach 95% homogeneity was measured and predicted at an impeller speed of 242 rpm. The CFD simulation of the *S. thermophilus* fermentation captured the experimentally observed pH gradients between a pH of 5.9 and 6.3, which occurred during the exponential growth phase. A pH higher than 7 was predicted in the vicinity of the base solution inlet. Biomass growth, lactic acid production, and substrate consumption matched the experimental observations. Moreover, the biokinetic results obtained from the CFD simulation were similar to a single-compartment simulation, for which a homogeneous distribution of the pH was assumed. This indicates no influence of pH gradients on growth in the studied bioreactor. This study verified that the pH gradients during a fermentation in the pilot-scale bioreactor could be accurately predicted using a coupled simulation of a biokinetic and a CFD model. To support the understanding and optimization of industrial-scale processes, future biokinetic CFD studies need to assess multiple types of environmental gradients, like pH, substrate, and dissolved oxygen, especially at industrial scale.

KEYWORDS
computational fluid dynamics (CFD), dynamic simulation, heterogeneities, lactic acid bacteria (LAB) fermentation, pH gradients, transient CFD simulation

1 | INTRODUCTION

Heterogeneities of culture parameters like substrate concentrations, pH, and dissolved oxygen concentrations are regarded as mainly responsible for productivity loss in large-scale bioreactor cultivations. Transport limitations occur at large scale due to insufficient mixing, and cells are consequently exposed to fluctuating conditions. Non-limiting substrate concentrations in the range of 0.3–2 g L^{-1} are reported in feeding zones during fed-batch processes, whereas there are substrate-limited conditions further away from the feeding

position (Bylund, Collet, Enfors, & Larsson, 1998; Larsson et al., 1996). pH values might also be outside of physiological ranges next to acid or base addition points (Langheinrich & Nienow, 1999; Lara, Galindo, Ramírez, & Palomares, 2006). Mixing times of large-scale bioreactors for microbial cultures exceed 100 s to reach 95% homogeneity, and the circulation time of the cells, which is proportional to the mixing time, is consequently in the magnitude of 10 s and longer depending on the stirring conditions (Delvigne, Destain, & Thonart, 2006; Nagata, 1975). Cells might adapt to continuously changing environments whereas they move through the bioreactor. Biomass and product yield reduction are reported for several different strains and processes when a process is scaled up to large scale (Bylund et al., 1998; Enfors et al., 2001; George, Larsson, Olsson, & Enfors, 1998; Xu, Jahic, Blomsten, & Enfors, 1999). This is most likely related to heterogeneities, because microorganisms are exposed to fluctuating environmental conditions at large scale, which might affect the metabolic activity. pH gradients have shown an influence on the transcriptional response and enzyme activity in bacteria, and may therefore lead to decreased biomass growth and product formation as shown in scale-down studies (Amanullah, McFarlane, Emery, & Nienow, 2001; Cortés, Flores, Bolívar, Lara, & Ramírez, 2016; Onyeaka, Nienow, & Hewitt, 2003).

Computational fluid dynamic (CFD) modeling is capable of representing the fluid dynamic conditions in bioreactors. It was already applied for process optimization by improving the impeller configuration for an increased oxygen transfer rate (Yang et al., 2012; Zou, Xia, Chu, Zhuang, & Zhang, 2012). Moreover, biokinetic models are coupled with fluid dynamics to analyze environmental gradients during fermentations (Schmalzriedt, Jenne, Mauch, & Reuss, 2003; Wang et al., 2015). Either compartment models can be built and coupled with a biokinetic model or a biokinetic model is directly integrated into a CFD model. Compartment models, which are based on the knowledge about the fluid dynamics in the bioreactor obtained from CFD models, reduce the number of spatial elements and decrease the computational demand (Vrábel et al., 2001). If biokinetic models are directly integrated into CFD, both the Euler–Euler approach (Bannari, Bannari, Vermette, & Proulx, 2012; Elqotbi, Vlaev, Montastruc, & Nikov, 2013) and the Euler–Lagrange approach combined with a population balance model (Haringa et al., 2016; Lapin, Müller, & Reuss, 2004; Lapin, Schmid, & Reuss, 2006; Morchain, Gabelle, & Cockx, 2013) are commonly applied. The fluid is treated as a continuum in both approaches, but the biological phase is treated as a continuum in the Euler–Euler approach and as a discrete phase in the Euler–Lagrange approach. The latter allows tracking single cells there. So far, studies have mainly been focused on substrate and oxygen gradients in aerobic nutrient-limited fed-batch processes. Furthermore, their relevance is questionable because many of the aforementioned works use CFD models that were not experimentally validated for example, by comparing the model response to mixing experiment data. There is, therefore, a considerable lack of scientific literature focusing specifically on dynamic CFD simulations of biokinetic models integrated into validated CFD models with the intention to simulate the formation of pH gradients in pilot and large-scale bioreactors.

The objective of this study was to predict the pH gradients, which occur in a 700L bioreactor during a *Streptococcus thermophilus* fermentation, by coupling CFD and kinetic modeling in a CFD simulation. This tool, which combines fluid dynamics and microbial kinetics, will be used to study pH heterogeneities at pilot scale. To this end, first, a one-phase CFD model of a 700 L bioreactor for a *S. thermophilus* fermentation was set up. Tracer pulse experiments with a NaOH solution and multi-position pH monitoring validated the fluid dynamic model predictions of the bioreactor. Then a kinetic model describing the biomass growth, lactic acid synthesis, and lactose consumption of *S. thermophilus* was integrated into the validated CFD model to simulate a pH-controlled batch cultivation. An algebraic equation was applied to calculate the pH value based on the lactic acid and ammonia concentrations.

2 | MATERIALS AND METHODS

2.1 | Bioreactor geometry and settings

A stirred tank bioreactor (Chemap AG, Switzerland) equipped with three 6-blade Rushton turbines was used (Figure 1) and filled to a liquid height of H_L = 1.92 m, corresponding to a volume of 700 L, for both the mixing time experiment and the fermentation. The stirrer speed was 242 rpm (P/V = 0.79 kW m^{-3}) for the mixing time determination and 132 rpm (P/V = 0.13 kW m^{-3}) for the fermentation. The stirrer speed was measured with a testo 477 LED stroboscope (Testo SE & Co. KGaA, Germany). The Reynolds number (Re) was defined as:

$$Re = \frac{N \cdot D_i^2 \cdot \rho_{H_2O}}{\mu_{H_2O}} \quad (1)$$

where N represents the stirrer speed, D_i the impeller diameter, ρ the fluid density, and μ the dynamic viscosity of the fluid.

The power input (P) was calculated:

$$P = N_P \cdot \rho \cdot N^3 \cdot D_i^5 \quad (2)$$

where N_P is the power number. N_P was assumed to be 5.5 (Doran, 1995; Ruston, Costich, & Everett, 1950) for each Rushton turbine as Re > 105 (see the results section). The power input could unfortunately not be measured in the studied bioreactor.

2.2 | Mesh generation and simulation settings

The bioreactor geometry was designed in SolidWorks (Dassault Systèmes, France). The sparger ring, the gas inlet pipe, and a supporting structure, which holds the shaft, were omitted. The bioreactor consisted of a stationary tank domain and three rotating impeller domains. Only half of the bioreactor volume was modeled applying a rotational periodicity plane. Meshes with six-sided hexahedral elements were defined for both domains in ANSYS ICEM CFD 17.1 (ANSYS, Inc., US-PA). The stationary domain consisted of

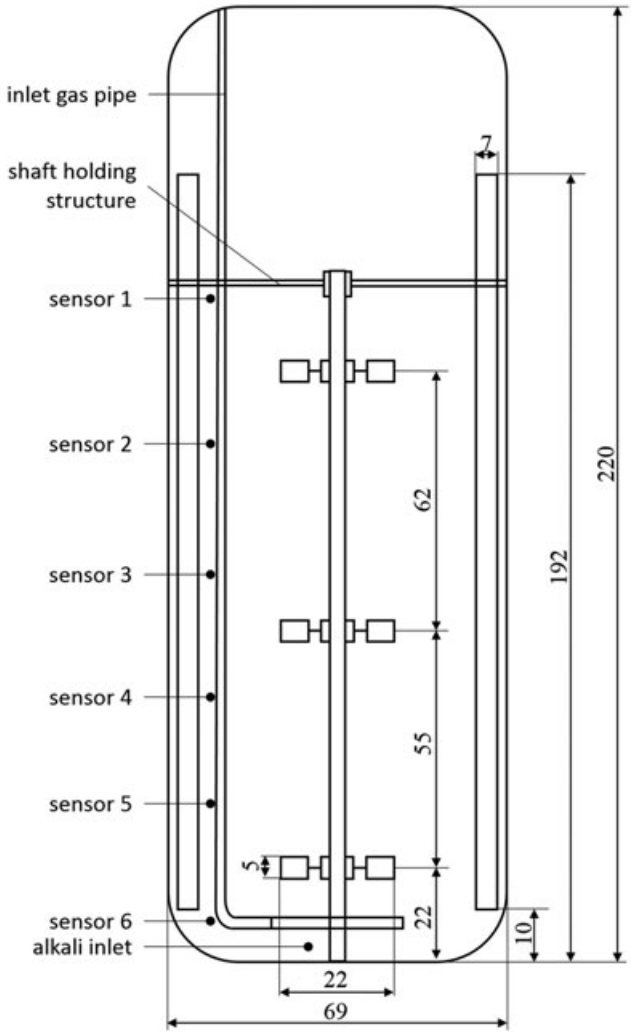

FIGURE 1 The geometry of the stirred tank bioreactor with dimensions in cm. The bioreactor is equipped with three 6-blade Rushton turbines and four baffles. Six monitoring points were positioned in the bioreactor. The reactor was filled up to 1.92 m liquid height both in the pulse experiment to determine the mixing time and in the fermentation

approximately 2,000 mesh elements per liter. Each rotating domain, with a height of $H_l = 0.075$ m and diameter $D_l = 0.32$ m, was defined with about 95,000 elements per liter. The complete mesh consisted of 1.6 million nodes. The interface between the rotating and stationary domains was defined as Frozen-Rotor interfaces. CFD simulations were performed in ANSYS CFX 17.1 with the k-ε turbulence model (the Supporting Information Material). The top boundary was assumed a flat surface with a free-slip wall. The liquid density was assumed to be $\rho = 997\,\mathrm{kgm^{-3}}$ and the dynamic viscosity $\mu = 8.9 \cdot 10^{-4}\,\mathrm{kgm^{-1}s^{-1}}$ in both the tracer pulse and fermentation simulation.

2.3 | Tracer pulse simulations

An additional variable was specified for the tracer pulse experiments in all domains with a diffusion coefficient $D_{tracer}=5.17 \cdot 10^{-9}\mathrm{m^2s^{-1}}$ corresponding to the characteristics of the tracer compound OH^- (Cents, Brilman, & Versteeg, 2005). Six monitoring points were located at different positions, which corresponded to the sensor positions (Figure 1). Vertical positions of the sensors were, with respect to the bottom of the bioreactor: 0.10 m, 0.35 m, 0.60 m, 0.95 m, 1.25 m, and 1.60 m. The horizontal distance to the bioreactor wall was 0.10 m. A transient (time-dependent velocity field) simulation was performed with a physical time scale of a step time of 0.1 s and a root mean square (RMS) residual target of 10^{-4}. The RMS is a measure to validate the convergence. The tracer pulse was simulated by starting the simulation with 1 mol of the tracer variable in a cylindrical volume with a height of 0.20 m and a width of 0.10 m, which was at the center at the top of the liquid phase.

2.4 | Tracer pulse experiments

The bioreactor was filled with tap water. A NaOH solution (27%, Novadan ApS, Denmark) was used as tracer substance for the pulse experiments. When dosing a pulse, 80 ml of NaOH was poured into the liquid at the center of the bioreactor within 1 s, from 0.30 m above the liquid level. Experiments were carried out at 35 °C within a pH range of 5.0–6.0 to ensure that the mixing time is measured without the interference of the slow reverse reaction of the carbonate dissociation (Einsele, 1976). The pH was reduced with H_3PO_4 (75%, Novadan ApS). The pulses were performed in three replicates. Six pH sensors (CPS471D, Endress+Hauser AG, Switzerland) mounted on a lance measured the pH at different positions every second. The positions were equivalent with the monitoring points in the tracer pulse simulation with the exception of the top placed sensor, which failed to record the data (Figure 1).

2.5 | Mixing time calculation

Mixing times were calculated after normalizing the pH measurements according to Paul, Atiemo-Obeng, and Kresta (2003):

$$\mathrm{pH}'_{i,\,\mathrm{exp}}(t) = \frac{\mathrm{pH}_{i,\mathrm{exp}}(t) - \mathrm{pH}_{i,\mathrm{exp}}(t\,=0)}{\mathrm{pH}_{i,\mathrm{exp}}(t\,=\infty) - \mathrm{pH}_{i,\mathrm{exp}}(t\,=0)} \tag{3}$$

where $\mathrm{pH}'_{i,\mathrm{exp}}$ is the normalized pH output of the i-th sensor in the experiment, $\mathrm{pH}_{i,\mathrm{exp}}$ is the experimental pH value measurement, and $\mathrm{pH}_{i,\mathrm{exp}}(t\,=\infty)$ are the average pH measurements measured between 4.5 and 5 min after the pulse. The normalized response of all sensors was plotted with the logarithmic squared deviation with respect to the normalized upper bound 1 to determine the mixing time:

$$\log D^2 = \log\left[\frac{1}{n}\cdot\sum_{i=1}^{n}\left(\mathrm{pH}'_{i,\,\mathrm{exp}}(t) - 1\right)^2\right] \tag{4}$$

where n is the number of sensors. $\log D^2 = -2.6$ when 95% homogeneity was achieved, $\log D^2 = -2$ and $\log D^2 = -1.65$ at 90% and 85% homogeneity, respectively. The simulated tracer pulse concentrations were normalized by Eq. (3), in which the pH values were replaced by the tracer concentrations.

2.6 | Streptococcus thermophilus fermentation and analysis

The batch fermentation of the homolactic *S. thermophilus* strain (provided by Chr. Hansen A/S, Hørsholm, Denmark) was carried out in the aforementioned 700 L stirred tank bioreactor at a stirring speed of 132 rpm, 40°C, and with N_2 headspace gassing. The pH was controlled by adding 24% (w/v) ammonia solution (NH_4OH) through a pipe, which was located 0.1 m above the bottom in the center of the vessel, to maintain pH = 6.0. The pH-value was measured by means of a sensor, which was located 0.3 m above the bottom of the bioreactor close to the reactor wall. The initial pH was 6.8. The medium contained 70 g L^{-1} lactose, 10 g L^{-1} casein hydrolysate, 12 g L^{-1} yeast extract, 11.5 mM K_2HPO_4, 36.6 mM sodium acetate, 8.2 mM trisodium citrate, 0.8 mM $MgSO_4$, and 0.3 mM $MnSO_4$. The pH was monitored every second at 4 of the 6 previously mentioned positions at heights of 0.10 m, 0.60 m, 1.25 m, and 1.60 m. Dry cell weight was determined from centrifuged, washed (with 0.9% NaCl), and dried (at 70°C for 24 hr) cell broth. Sugars and organic acids were quantified from filtered (0.2 µm) samples in an HPLC system (Dionex UltiMate 3000, Thermo Fisher Scientific, Waltham, MA) and a refractive index detector (ERC RefractoMax 520), with an Aminex® HPX-87H column (Bio-Rad Laboratories, Hercules, CA) using 5 mM H_2SO_4 at a flow rate of 0.6 ml min^{-1} at 50°C according to suppliers instructions.

2.7 | Biokinetic and ph simulation in the CFD model

An unstructured kinetic model of *S. thermophilus*, which described the lactose consumption, biomass growth, and lactic acid synthesis, was integrated into the CFD model (Eqs. (5-8)). Effects of the lag-time, substrate limitation, and inhibition (Haldane, 1930), pH (Willem schepers, Thibault, & Lacroix, 2002), and lactate inhibition (Aghababaie, Khanahmadi, & Beheshti, 2015) were considered in the growth function. A simplified version of the Luedeking–Piret equation (Luedeking & Piret, 1959) was applied to describe the lactic acid synthesis.

$$\left(1 + Y_{gal}\right) \cdot \text{lactose} \xrightarrow{q_X} \text{biomass} + Y_{gal} \cdot \text{galactose} \tag{5}$$

$$\left(1 + Y_{gal}\right) \cdot \text{lactose} \xrightarrow{q_P} \text{lactic acid} + Y_{gal} \cdot \text{galactose} \tag{6}$$

$$q_X = \mu_{max} \cdot \left(1 - e^{-t/t_{lag}}\right) \cdot \frac{C_S}{C_S + K_s + \frac{C_S^2}{K_I}} \cdot e^{-\left(\frac{(pH_{opt} - pH)^2}{\sigma^2}\right)} \cdot \frac{1}{1 + e^{K_{P,La}\left(C_P - \frac{K_{La}}{1 + e^{K_{P,pH1} \cdot (pH - K_{P,pH2})}}\right)}} \cdot C_X \tag{7}$$

$$q_P = \alpha \cdot q_X \tag{8}$$

where q_X and q_P are the volumetric growth and lactic acid production rates, respectively. Lactose (C_S), biomass (C_X), and lactic acid (C_P) were listed as additional variables, and their rate equations were defined as expressions in the CFX expression language. Initial concentrations were $C_{S,t=0} = 70 gL^{-1}$, $C_{X,t=0} = 0.025 gL^{-1}$, and $C_{P,t=0} = 0 gL^{-1}$. The kinetic parameters as listed in Table 1 were derived from a parameter estimation, which was based on 2 L lab-scale fermentations with the aforementioned medium at 300 rpm (two 6-blade Rushton turbines with a diameter = 53 mm) and 40°C at different pH values (in the range of 5.5–7.0) and initial lactose concentrations (20 and 70 g L^{-1}) (Spann et al., 2018). It must be considered in the evaluation of the model that the supplemented yeast extract contains ca. 6 g L^{-1} carbon, which is not included in the model. However, this is only partially taken up by the cells and the dynamic model accounts for it by under-predicting the galactose concentration. The biomass, lactic acid, and lactose concentrations, which are crucial in this study, are predicted accurately (Spann et al., 2018).

TABLE 1 Kinetic parameters of the integrated *S. thermophilus* model

Symbol	Description	Value
K_I	Substrate inhibition parameter	164 g L^{-1}
K_S	Substrate limitation parameter	0.79 g L^{-1}
K_{La}	Lactate inhibition parameter	21.1 g L^{-1}
$K_{P,La}$	2. lactate inhibition parameter	0.2 L g^{-1}
$K_{P,pH1}$	LA inhibition pH parameter	20
$K_{P,pH2}$	2. LA inhibition pH parameter	7
pH_{opt}	Optimal pH in the pH function	6.22
t_{lag}	Lag-time coefficient	0.38 hr
Y_{gal}	Galactose yield	0.63 g g^{-1}
α	Growth related production coefficient of lactic acid	5.59 g g^{-1}
μ_{max}	Maximum specific growth rate	2.16 hr^{-1}
σ	Spread parameter in the pH function	1.09

An algebraic linear correlation for the pH calculation based on the lactic acid and ammonia concentrations was obtained based on experiments performed at 2 L scale (the Supporting Information Material):

$$pH = -0.44 \cdot \left(C_P - 5.29 \cdot C_{NH_3}\right) + 7.00 \tag{9}$$

The dynamic simulation with a time step of 1 s and an RMS residual target of $1 \cdot 10^{-5}$ was carried out using a steady state result as initialization state. Continuity, momentum, and energy equations were derived from a steady state solution, and thus assumed constant. They were therefore not solved in the dynamic simulation to reduce the computational time. The impeller speed was set to 200 rpm for the steady state velocity profile in the fermentation simulation in contrast to 132 rpm in the experimental fermentation. This modification was necessary to represent the mixing behavior in the fermentation simulation (with a steady state velocity profile) as the predicted mixing times differed when applying a steady state or transient velocity profile (see the Results and the Discussion sections for further details). The pH

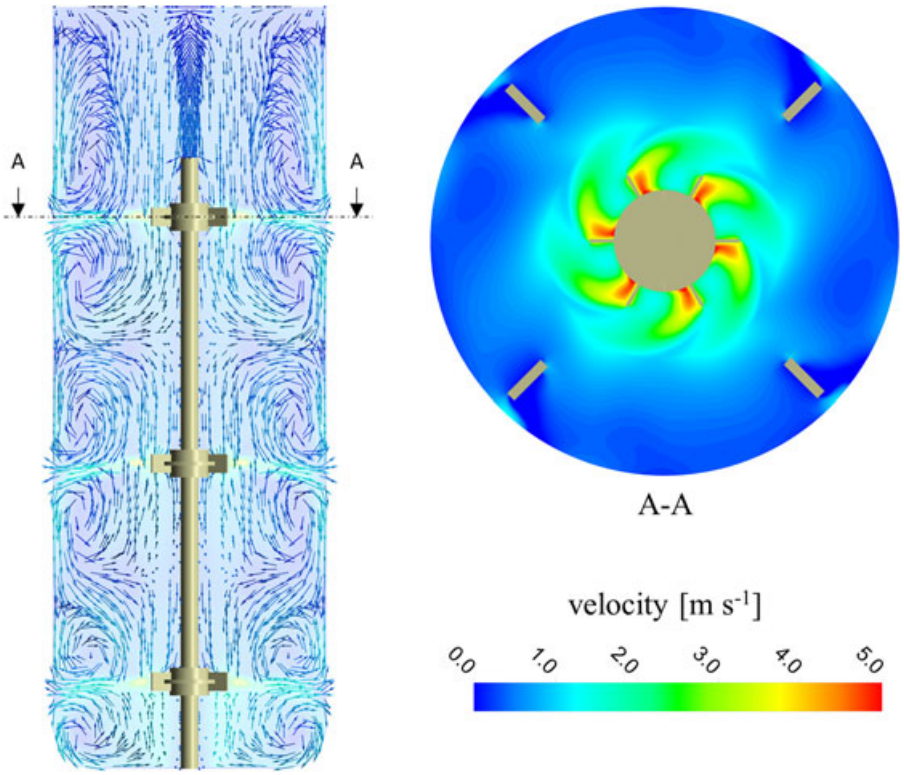

FIGURE 2 Steady state solution of the 700 L stirred tank bioreactor for a stirrer speed of 300 rpm. Left: velocity streamlines with velocity in stationary frame. Right: contour plot with the circumferential velocity in stationary frame [Color figure can be viewed at wileyonlinelibrary.com]

was controlled by adding ammonia at the same position as in the experiment. Control was conducted with a P-controller, which was using the step function:

$$NH_{3,add} = \text{step}(6 - \text{pH}) \cdot (6 - \text{pH}) \cdot 11900\ \text{gh}^{-1} \quad (10)$$

where the pH is calculated at the monitoring point 35 cm above the bottom of the bioreactor. The kinetic model was also implemented in MATLAB (The MathWorks, Natick, MA) and solved with the ode 15 s solver. There, the fermentation broth was modeled as a single compartment with a homogeneous distribution of the pH and all state variables, that is no gradients were considered.

3 | RESULTS

A one-phase CFD model of a 700 L bioreactor for *S. thermophilus* fermentation was set up and tracer pulse experiments with NaOH and multi-position pH monitoring validated the fluid dynamic model predictions. A kinetic model of *S. thermophilus* was integrated into the validated CFD model to predict pH gradients during the fermentation.

3.1 | The velocity profile of the bioreactor

A steady-state solution of the CFD model was initially obtained, which predicted the macroscopic flow profile of the bioreactor. It clearly revealed six recirculation loops, which were generated by the Rushton turbines (Figure 2). A turbulent flow regime was assumed because the Reynolds number was $2.2 \cdot 10^5$ at 242 rpm. The fluid velocity was highest behind the turbine blades, which turned with 2.8 m s^{-1} tip speed at 242 rpm. Low velocities were observed close to the bioreactor wall and especially around the baffles. The steady state solution converged with respect to the RMS values of the velocity components, while the velocities were unstable at the monitoring points. Further analysis revealed that the velocity profile of the bioreactor had a transient (time-dependent) nature (Supporting Information Movie 1). The four recirculation loops *between* the impellers were changing in size and moving up- and downwards. The tracer pulse simulation was therefore performed with a transient velocity field.

3.2 | Tracer pulse simulation and experiments

Fast radial and slower axial mixing were predicted in the tracer pulse simulations (Figure 3 and Supporting Information Movie 2). It took several seconds until the tracer passed to a subsequent recirculation loop after the simulated injection from the top. The monitoring points in the CFD model and pH sensors in the experiment were positioned in each anticipated recirculation loop to be able to follow the dynamic distribution of the tracer.

3.3 | The dynamic response at all sensor locations

The dynamic responses of the monitoring points during tracer pulse simulations were captured with the intention to understand the fluid flow dynamics when for example, an acid or a base

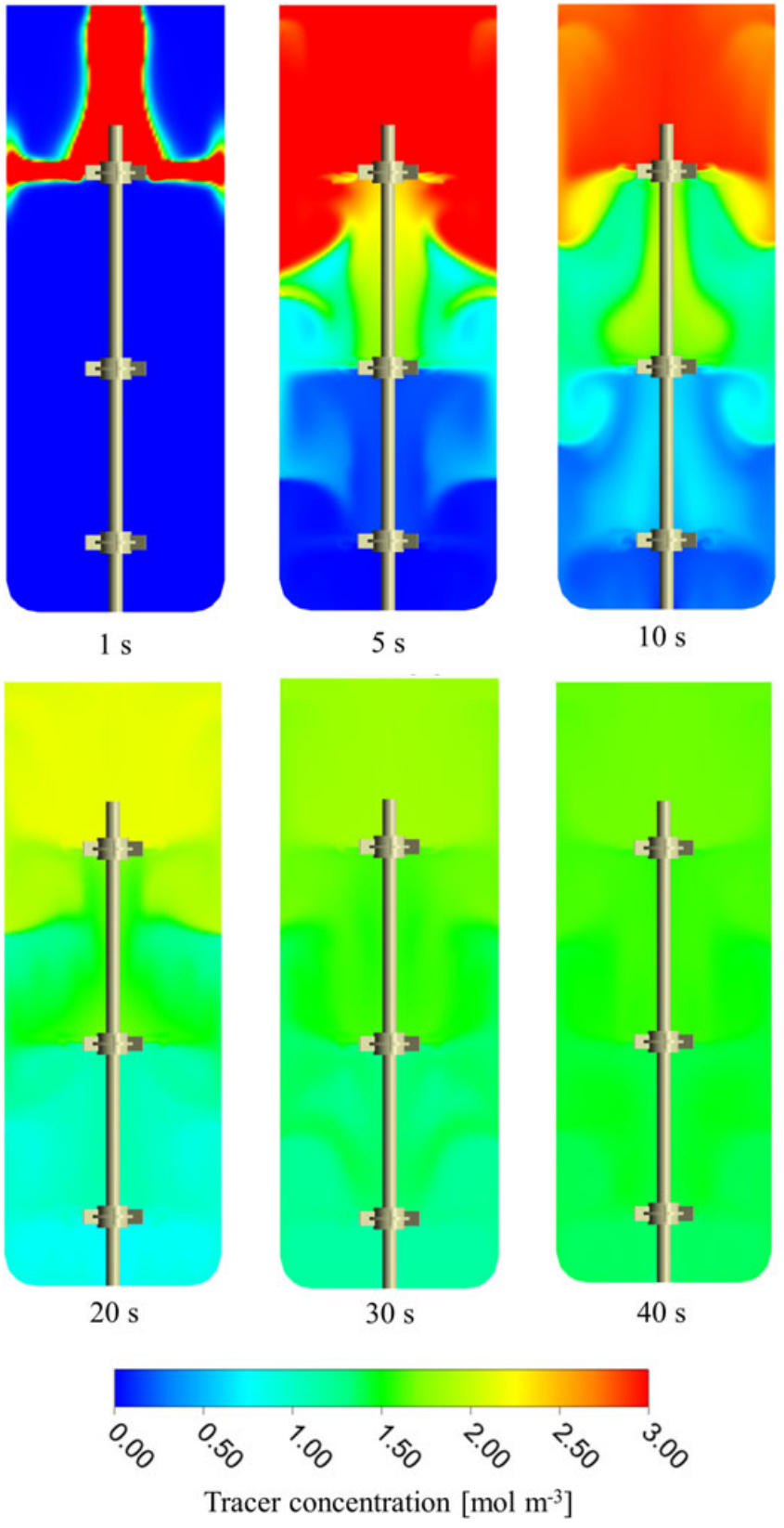

FIGURE 3 Concentration fields of the tracer during the transient simulation of the pulse in the 700 L stirred tank bioreactor at 242 rpm. The tracer was injected at 0 s at the top of the liquid phase and snapshots are taken at different time points [Color figure can be viewed at wileyonlinelibrary.com]

solution is added to regulate the pH value in a cultivation. The two monitoring locations 1 and 2 at the upper part of the liquid phase showed an overshooting response before they reached a stable value, whereas the other monitoring points 3–6, which were located farther away from the injection point, responded with sigmoid curves (Figure 4). To validate the tracer pulse simulations, these results were compared with the experimental measurements. Both the shapes and order of magnitude of the

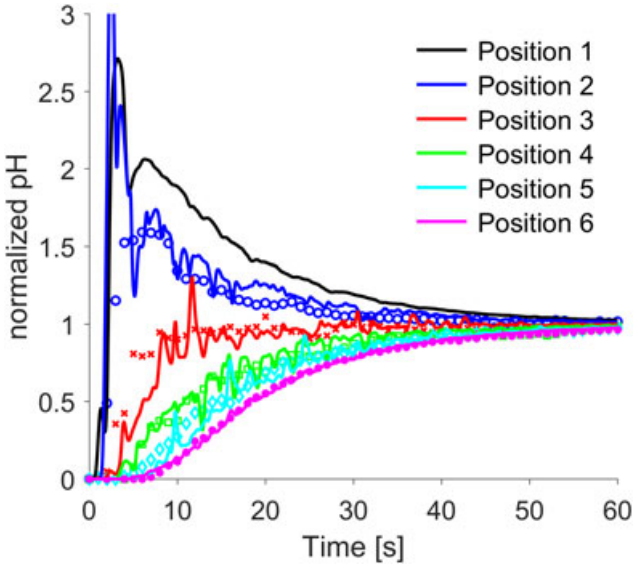

FIGURE 4 Normalized pH response of the five pH sensors (Position 2–6, as shown in Figure 1) in the pulse experiment and six monitoring points in the transient simulation performed at 242 rpm. Experimental values (symbols) and simulated values (solid lines). The pH showed an overshoot close to the injection point at the top of the bioreactor before it leveled out. The pH increased gradually at the lower positioned sensors and monitoring points [Color figure can be viewed at wileyonlinelibrary.com]

dynamic trends obtained from the predictions agreed with the measurements obtained at the different positions. Nevertheless, oscillations of the pH signal and the initial high overshoot of Sensor 2 predicted by the simulation were not captured by the measurements.

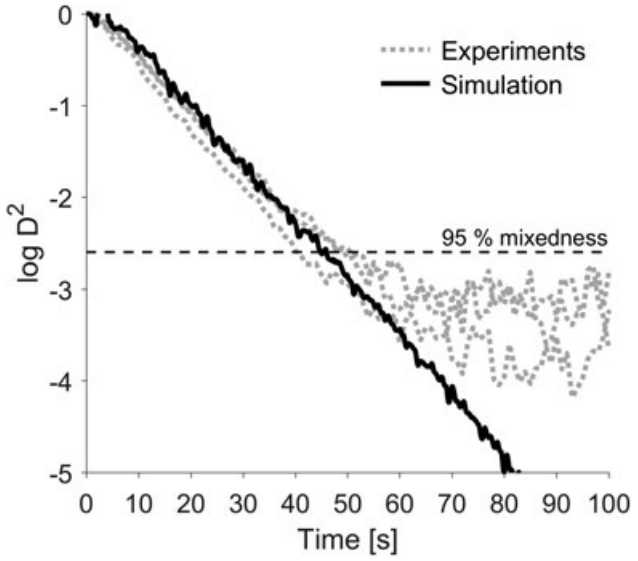

FIGURE 5 Logarithmic squared deviation of the pH values in the tracer pulse experiments and simulation considering all monitor points. Three tracer pulse experiments (dotted lines) and the CFD simulation (solid line) at 242 rpm are shown. 95% homogeneity was reached at log $D^2 = -2.6$. CFD: computational fluid dynamic

TABLE 2 Experimental and CFD predicted mixing times for different levels of homogeneity at 242 rpm ($P/V = 0.79$ kW m^{-3})

	Mixing time for the tracer pulses (s)	
Level of homo-geneity	Experiments	CFD simulation
85%	26 30 30	30
90%	32 36 35	36
95%	42 50 51	46

Note. CFD: computational fluid dynamic.

3.4 | Determination of the mixing time

To assess the progress of reaching homogeneity, the logarithmic squared deviation of all sensors was evaluated. All experimental curves followed the predicted trend until 95% homogeneity was achieved (Figure 5). The variance of the replicates increased for homogeneities higher than 95%. The predicted and measured mixing times at the levels of 85%, 90%, and 95% homogeneity matched very well (Table 2). 95% homogeneity was reached after about 46 s.

The dynamic response at all locations and the mixing time prediction gave considerable evidence that the fluid flow in the bioreactor was well described by the applied CFD model.

3.5 | Simulated and measured ph gradients in the *S. thermophilus* fermentation

As a next step, the CFD and biokinetic models were combined in a dynamic simulation to predict the pH gradients during the fermentation. Therefore, an unstructured nonsegregated kinetic model of *S. thermophilus* and a pH correlation were integrated into the validated CFD model. A dynamic simulation was performed with the purpose of predicting the pH gradients during the batch fermentation. A steady-state velocity profile was applied, which decreased the computational demand in contrast to solving the fluidic profile for the entire fermentation time. The mixing time at the fermentation conditions of 132 rpm was 85 s according to a tracer pulse simulation with a transient velocity profile. The impeller speed had to be set to 200 rpm in the fermentation simulation to represent the same mixing time with a steady state velocity profile (Supporting Information Figure S1). Expected biomass growth, substrate consumption, and lactic acid production profiles of a Monod type kinetic model were observed and in accordance with the measurements (Figure 6). A final biomass concentration of 6 g L^{-1} was reached after 5 hr when 34 g L^{-1} lactic acid seemed to inhibit growth completely. The observed biomass yield was similar to 2 L lab-scale experiments,

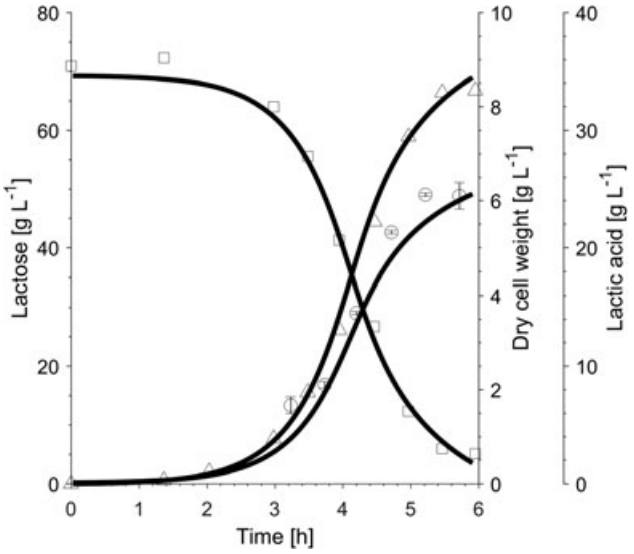

FIGURE 6 Dry cell weight, lactose, and lactic acid concentrations as measured and predicted in the *S. thermophilus* batch fermentation. The fermentation was carried out in the 700 L bioreactor at 132 rpm, 40°C, and the pH controlled at pH = 6. Dry cell weight (circles) with standard deviation, lactose (squares), lactic acid (triangles), and the CFD simulation result (solid line)

where instantaneous mixing was assumed (Supporting Information Figure S2). As the applied time step was crucial to solve the differential equations in the CFD model, a time step of 1 s was chosen. An increased time step led to larger deviations of the kinetic profiles (data not shown). The obtained kinetic results from the CFD simulation were very similar to the single-compartment simulation performed in MATLAB, in which a homogeneous distribution of the pH and all state variables was assumed (Supporting Information Figure S3). The pH predictions were in close agreement with the measurements in all locations (Figure 7). In the beginning of the fermentation, the pH dropped from 6.8 to the controlling pH value 6, when the pH controller started in both the simulation and experiment. A minimum pH of 5.9 was attained in the top zone of the bioreactor during the exponential growth phase. In the bottom zone, where ammonium hydroxide was added, pH values of up to 6.3 were measured and simulated at the sensor positions. Close to the base injection, pH values larger than 7 were predicted (Figure 8). As the applied pH correlation is only valid up to a pH of 7, a more accurate pH prediction was not possible in this case.

4 | DISCUSSION

To simulate the pH gradients of a *S. thermophilus* fermentation in a 700 L bioreactor, a one-phase CFD model was first validated and then coupled with a biokinetic model and a pH correlation. Multi-position pH monitoring in tracer pulse experiments validated the fluid dynamic model predictions of the one-phase CFD model. The CFD model predicted the mixing time of around 46 s to reach 95% homogeneity at an impeller speed of 242 rpm and forecasted the dynamic response of all sensors in the tracer pulse experiments. The dynamic simulation of the non-aerated *S. thermophilus* batch fermentation predicted both the biokinetic profiles and the pH gradients matching the experimental observations. Rather large pH gradients between pH values of 5.9 and higher than 7 were predicted in the bioreactor whereas the fermentation was controlled at pH 6.

The simulated flow profiles showed six recirculation loops generated by the three Rushton turbines consistent with literature data (Vrábel, Van der lans, Luyben, Boon, & Nienow, 2000). pH sensors and monitoring points were placed so that conditions in all

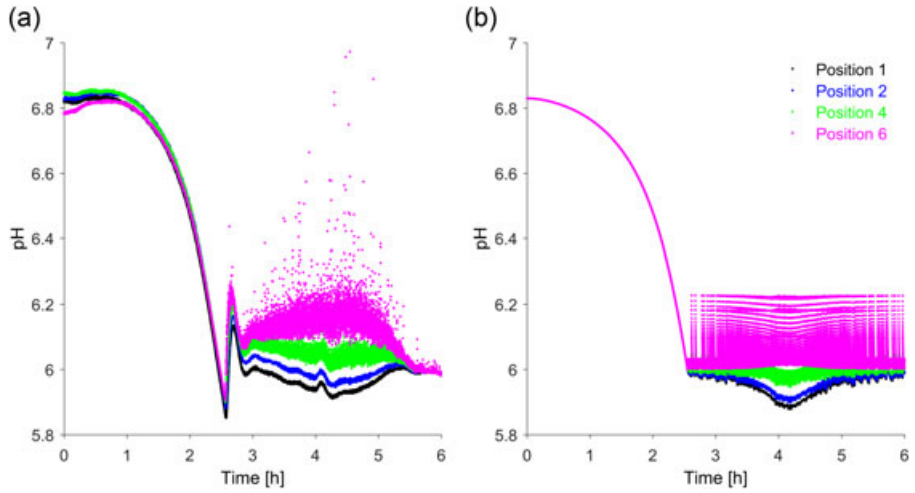

FIGURE 7 pH values measured and predicted every second at different positions during the *S. thermophilus* fermentation. Fermentation (a) and CFD simulation (b). In the beginning of the fermentation, the pH dropped from 6.8 to the controlling pH value 6, when the pH controller started. The pH was controlled at pH = 6 using the measurement of sensor 5 by adding NH_4OH at the bottom of the bioreactor. pH sensors and monitoring points were placed at position 1, 2, 4, and 6 in the bioreactor as shown in Figure 1. The pH dropped down to pH = 5.9 in the top zone of the bioreactor, whereas a maximum of around pH = 6.3 was measured and predicted at position 6 in the bottom zone of the bioreactor. CFD: computational fluid dynamic [Color figure can be viewed at wileyonlinelibrary.com]

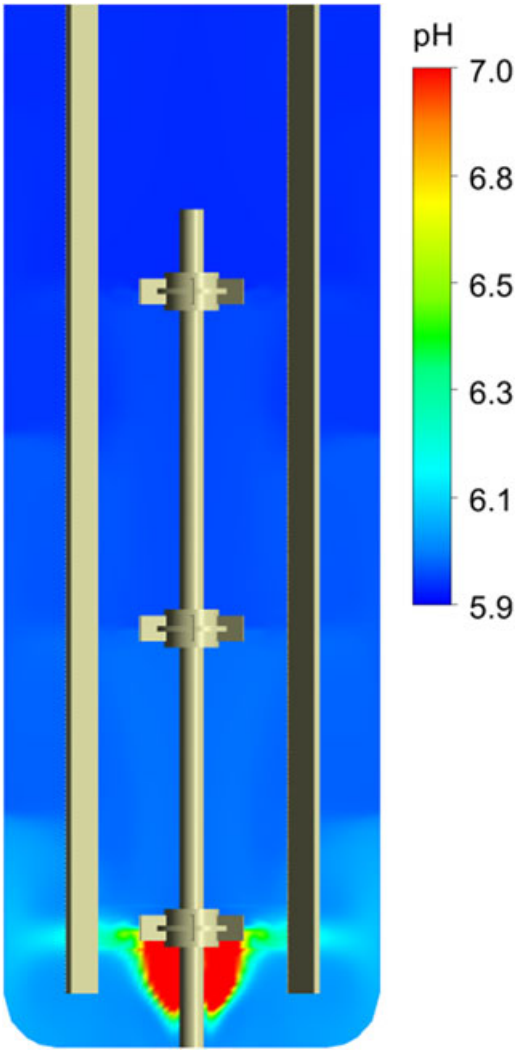

FIGURE 8 Simulated pH gradients during the *S. thermophilus* fermentation in the 700 L bioreactor after 4 hr 40 min of cultivation time. The pH was higher than 7 close to the alkali inlet at the bottom of the bioreactor and around 5.9 in the top zone of the bioreactor. As the applied pH correlation is only valid up to a pH of 7, a more accurate pH prediction was not possible [Color figure can be viewed at wileyonlinelibrary.com]

six recirculation loops were monitored in tracer pulse experiments and simulated accordingly. The dynamic pH response of the pH sensors was well represented by the simulated data. It is important to stress that the CFD model relied among other criteria on physical and chemical properties, empirical equations, and the mesh structure. Importantly, no parameter estimation/model calibration of the CFD model was performed to fit experimental data. However, the predicted oscillating behavior of the pH and the initial overshoot of Sensor 2 was not measured. This can likely be attributed to the response time of the applied ISFET pH sensors, which is in a range of 4–8 s to reach ± 0.02 of the final pH value in the relevant pH range. This response time was determined in own measurements and is in accordance with vendor specifications. Furthermore, there was a discrepancy between the predicted and measured homogeneity when 95% homogeneity was reached 60 s after the pulse, which could be caused by the fluctuating sensor output (±0.01), whereas the model asymptotically approaches 100% homogeneity.

It was shown that the recirculation loops were dynamically changing, and hence a transient velocity profile was required. Dynamic velocity changes that might have caused the dynamic behavior of the recirculation loops have been already observed for Rushton turbines (Hartmann, Derksen, & Van den akker, 2004; Nikiforaki, Montante, Lee, & Yianneskis, 2003). However, the velocities have not yet been experimentally validated for the studied system.

Both observed and simulated mixing times were consistent with results from Delvigne et al. (2006). They reported similar mixing times between 20 and 53 s to reach 85% homogeneity in stirred tank bioreactors with working volumes of 350, 1,200, and 1,800 L with a comparable power input to the present study. However, as no power input measurements were available for our 700 L bioreactor, the theoretical power input could not be validated in this study. With regard to the definition of mixing time in CFD simulations, Larsson (2015) concluded that there is no consistent definition so far. Instead, there exist several possibilities to determine the mixing time from observing the CFD system at one or several points, up to detecting the concentration on flat surface planes covering a larger area of the CFD system. In contrast to previous studies, which only used one position to calculate the mixing time, six points, which were distributed over the whole liquid phase, were used in this study to improve reproducibility and accuracy of the results. Overall, it should be noted that both the experimental setup as well as the way of treating and interpreting the data still lead to uncertainties. For example, the location of the top sensors and their monitoring points affects the accuracy of the measurements and predictions of the overshoot after the tracer pulse. A sensitivity analysis of the sensor locations in the simulation could support the assessment of the accuracy of the model. Up to now, this study has proven that the CFD model achieved a good prediction of the fluid dynamics in the bioreactor.

4.1 | Discussion of the results from the combined CFD and biokinetic model

Since heterogeneities at large scale affect the productivity of many chemical and biochemical processes, a tool to couple fluid dynamics and reaction kinetics is highly demanded. Dynamic simulations of biokinetic models integrated in the fluidic profile simulated by a CFD model can pave the way for an enhanced understanding of microbial behavior in large-scale bioreactors. Consequently, it is a basic requirement that the CFD simulation provides accurate results.

To achieve an affordable computational time for the biokinetic CFD simulation, a steady state velocity profile was required. The necessary manipulation of the stirrer speed (to 200 rpm) in the steady-state simulation was necessary because of the general transient fluid dynamics in the bioreactor as discussed above. It could also be considered to apply other turbulent models in the future. However, a tuning of the CFD model to fit the experimental data should be generally avoided, and the computational development might allow in

future using the transient velocity profile for the biokinetic CFD simulation within an acceptable time frame.

Due to the higher computational demand, while solving the differential equations in all nodes of the CFD model mesh (about 1.6 million nodes in this study), discretization errors are likely when selected time steps are inappropriate. The same issue occurs if RMS targets are too high. Applying a time step of 1 s resulted in a similar biological growth as observed in the experiment, while larger time steps led to larger deviations between measurements and predictions. This is most likely due to the accumulation of numerical errors. However, a smaller time step might have reduced numerical errors further, but will also increase the computational burden. The similarity between the single-compartment simulation – where completely mixed conditions were assumed – and the CFD simulation results might be caused by three reasons: (a) either the pH gradients had a very small effect on the culture performance in the present study, or (b) the biokinetic model was not sensitive to pH changes, or (c) the small differences arose from the aforementioned numerical errors in the CFD simulation due to the coarse time step.

pH gradients between 5.9 and 6.3 were predicted and observed between the top and the bottom zone of the bioreactor, respectively. A pH higher than 7 was predicted for the vicinity of the base solution inlet. Even though the pH measurements and predictions matched, the uncertainties in the applied pH correlation need to be considered. The fast production of lactic acid led to a small decrease of the pH at the top of the bioreactor, whereas the addition of ammonium hydroxide caused a pulse-wise increase of the pH at the bottom of the bioreactor. Langheinrich and Nienow (1999) reported pH gradients of 0.8 units due to alkali addition in an 8 m^3 reactor for mammalian cell cultures. pH gradients have a noticeable effect on productivity. Aghababaie et al. (2015) reported that the growth of *S. thermophilus* was reduced by 20% when cultivated 0.3 pH units away from the optimal pH conditions. However, cells are not constantly exposed to unfavorable environmental conditions while moving through a large-scale bioreactor. Cortés et al. (2016) and Amanullah et al. (2001) showed in two-compartment scale-down studies of *E. coli* and *B. subtilis*, in which they mimicked oscillating pH conditions up to a delta pH of 0.9, that growth was not statistically significantly affected. However, the organic acid metabolism changed, and *E. coli* responded on the transcriptional level to the alkaline stress. The extracellular pH affects the intracellular pH of lactic acid bacteria (Cachon, Antérieux, & Diviès, 1998; Hansen et al., 2016) and by this the enzymatic activity. *Lactobacillus* sp. maintains their intracellular pH with the energy consuming Na^+ (K^+)/H^+ antiporters (Sawatari & Yokota, 2007). The additional energy requirements could lead to altered culture performance in large-scale fermentations. The remaining open question is how fast the cells are affected by pH changes and how fast they adapt to them. In the immediate vicinity of the inlet for base addition, the cells are exposed to unfavorable pH values that might lead to viability loss (Hansen et al., 2016). Cells that are moving through the bioreactor and have suffered in an unfavorable environment before will not function in an optimal manner immediately, when they enter a more favorable zone, as they need to adapt to the new conditions again (Löffler et al., 2016; Nieß, Löffler, Simen, & Takors, 2017). Further studies like Vanrolleghem, Sin, and Gernaey (2004), who studied and modeled the dynamic response to substrate pulses in wastewater treatment plants, are required to understand the adaptation processes of microorganisms under oscillating conditions better. This knowledge about metabolic phenomena, for example, the dynamic response of growth to changing substrate availability, could then expand the biokinetic models coupled with CFD models (Delvigne & Noorman, 2017).

Coupling biokinetic and fluid dynamic modeling will open the way for the understanding and optimization of large-scale processes. To predict gradients at large scale is of utmost interest because measurements during fermentations at large scale are either very difficult or even impossible to perform due to the size of the bioreactors, the costs of a single fermentation run, and the GMP regulations at production sites. Scale-down systems (Oosterhuis, 1984) could be designed based on the CFD predictions, and mimic the gradients in lab-scale experiments (Lara et al., 2006; Neubauer & Junne, 2016). They allow to study the response mechanisms upon external oscillating conditions and can be integrated into the scale-up process (Neubauer et al., 2013). This will reduce the risk of failure when scaling up processes.

5 | CONCLUSION

The present study was designed to predict pH gradients in a 700 L lactic acid bacteria fermentation by applying a dynamic CFD simulation. It gave evidence that pH heterogeneities existed in the studied 700 L bioreactor. More important, it proved that pH gradients could be quantitatively predicted with the CFD simulation. pH gradients between 5.9 at the top and above 7 close to the alkali inlet at the bottom of the bioreactor were predicted. The high pH in the alkali inlet zone could cause cell damage and an undesired production loss in large-scale bioreactors. Therefore, the results could support the fine-tuning of the stirring rate when reaching the maximum growth rate to distribute the base faster. In summary, these findings suggest that coupling a biokinetic model and a fluid dynamic model is a very useful tool to predict gradients in bioreactors. However, to predict the effect on microorganisms growing under oscillating conditions was beyond the scope of this study. The validation of the applied CFD model with multi-position pH monitoring during mixing experiments is a promising outcome of this study, which should be performed in further CFD studies of bioprocesses as well. Future work should include multiple environmental gradients in the dynamic CFD simulations. Besides pH, also a substrate, oxygen, carbon dioxide, and temperature gradients are of high interest for batch, fed-batch, and continuous cultivations since most of them are regarded to contribute to productivity loss at large scale.

ACKNOWLEDGMENTS

This project has received funding from the European Union's Horizon 2020 Research and Innovation Program under the Marie Skłodowska-Curie grant agreement No 643056 (Biorapid project). The authors

would like to thank Jifeng Yang, Pinxiang Han, and Peter Nielsen for the support during this study. We are grateful to Chr. Hansen A/S for the cooperation.

CONFLICTS OF INTEREST

The authors declare that they have no conflicts of interest.

ORCID

Robert Spann http://orcid.org/0000-0003-1223-2805
Gürkan Sin http://orcid.org/0000-0003-0513-4502
Ulrich Krühne http://orcid.org/0000-0001-7774-7442

REFERENCES

Aghababaie, M., Khanahmadi, M., & Beheshti, M. (2015). Developing a detailed kinetic model for the production of yogurt starter bacteria in single strain cultures. *Food and Bioproducts Processing*, *94*, 657–667.

Amanullah, A., McFarlane, C. M., Emery, A. N., & Nienow, A. W. (2001). Scale-down model to simulate spatial pH variations in large-scale bioreactors. *Biotechnology and Bioengineering*, *73*, 390–399.

Bannari, R., Bannari, A., Vermette, P., & Proulx, P. (2012). A model for cellulase production from Trichoderma reesei in an airlift reactor. *Biotechnology and Bioengineering*, *109*, 2025–2038.

Bylund, F., Collet, E., Enfors, S. -O., & Larsson, G. (1998). Substrate gradient formation in the large-scale bioreactor lowers cell yield and increases by-product formation. *Bioprocess Engineering*, *18*, 171.

Cachon, R., Antérieux, P., & Diviès, C. (1998). The comparative behavior of Lactococcus lactis in free and immobilized culture processes. *Journal of Biotechnology*, *63*, 211–218.

Cents, A. H. G., Brilman, D. W. F., & Versteeg, G. F. (2005). CO2 absorption in carbonate/bicarbonate solutions: The Danckwerts-criterion revisited. *Chemical Engineering Science*, *60*, 5830–5835.

Cortés, J. T., Flores, N., Bolívar, F., Lara, A. R., & Ramírez, O. T. (2016). Physiological effects of pH gradients on *Escherichia coli* during plasmid DNA production. *Biotechnology and Bioengineering*, *113*, 598–611.

Delvigne, F., Destain, J., & Thonart, P. (2006). A methodology for the design of scale-down bioreactors by the use of mixing and circulation stochastic models. *Biochemical Engineering Journal*, *28*, 256–268.

Delvigne, F., & Noorman, H. (2017). Scale-up/Scale-down of microbial bioprocesses: A modern light on an old issue. *Microbial Biotechnology*, *10*, 685–687.

Doran, P. M. (1995). *Bioprocess engineering principles*. London, UK: Academic Press.

Einsele, A. (1976). Charakterisierung von bioreaktoren durch mischzeiten. *Chem. Rundschau*, *25*, 53–55.

Elqotbi, M., Vlaev, S. D., Montastruc, L., & Nikov, I. (2013). CFD modelling of two-phase stirred bioreaction systems by segregated solution of the Euler-Euler model. *Computing and Chemical Engineering*, *48*, 113–120. https://doi.org/10.1016%2Fj.compchemeng.2012.08.005

Enfors, S. O., Jahic, M., Rozkov, A., Xu, B., Hecker, M., Jürgen, B., … Manelius, Å. (2001). Physiological responses to mixing in large scale bioreactors. *Journal of Biotechnology*, *85*, 175–185.

George, S., Larsson, G., Olsson, K., & Enfors, S. -O. (1998). Comparison of the Baker's yeast process performance in laboratory and production scale. *Bioprocess Engineering*, *18*, 135–142.

Haldane, J. B. S. (1930). Enzymes. London, UK: Longmans, Green.

Hansen, G., Johansen, C. L., Marten, G., Wilmes, J., Jespersen, L., & Arneborg, N. (2016). Influence of extracellular pH on growth, viability, cell size, acidification activity, and intracellular pH of Lactococcus lactis in batch fermentations. *Applied Microbiology and Biotechnology*, *100*, 5965–5976.

Haringa, C., Tang, W., Deshmukh, A. T., Xia, J., Reuss, M., Heijnen, J. J., … Noorman, H. J. (2016). Euler-Lagrange computational fluid dynamics for (bio)reactor scale down: An analysis of organism lifelines. *Engineering in Life Sciences*, *16*, 652–663.

Hartmann, H., Derksen, J. J., & Van den akker, H. E. A. (2004). Macroinstability uncovered in a Rushton turbine stirred tank by means of LES. *AIChE Journal*, *50*, 2383–2393.

Langheinrich, C., & Nienow, A. W. (1999). Control of pH in large-scale, free suspension animal cell bioreactors: Alkali addition and pH excursions. *Biotechnology and Bioengineering*, *66*, 171–179.

Lapin, A., Müller, D., & Reuss, M. (2004). Dynamic behavior of microbial populations in stirred bioreactors simulated with Euler–Lagrange methods: Traveling along the lifelines of single cells. *Industrial & Engineering Chemistry Research*, *43*, 4647–4656.

Lapin, A., Schmid, J., & Reuss, M. (2006). Modeling the dynamics of *E. coli* populations in the three-dimensional turbulent field of a stirred-tank bioreactor-A structured-segregated approach. *Chemical Engineering Science*, *61*, 4783–4797.

Lara, A. R., Galindo, E., Ramírez, O. T., & Palomares, L. a (2006). Living with heterogeneities in bioreactors: Understanding the effects of environmental gradients on cells. *Molecular Biotechnology*, *34*, 355–381.

Larsson, G., Törnkvist, M., Wernersson, E., Trägårdh, C., Noorman, H., & Enfors, S. O. (1996). Substrate gradients in bioreactors: Origin and consequences. *Bioprocess Engineering*, *14*, 281–289.

Larsson, HK. 2015. Modelling of mass transfer phenomena in chemical and biochemical reactor systems using computational fluid dynamics. *PhD thesis, Tech. Univeristy Denmark*.

Luedeking, R., & Piret, E.L. (1959). Kinetic study of the lactic acid fermentation. Batch process at controlled pH. *Biotechnology and Bioengineering*, *67*, 636–644.

Löffler, M., Simen, J. D., Jäger, G., Schäferhoff, K., Freund, A., & Takors, R. (2016). Engineering *E. coli* for large-scale production – Strategies considering ATP expenses and transcriptional responses. *Metabolic Engineering*, *38*, 73–85.

Morchain, J., Gabelle, J. -C., & Cockx, A. (2013). Coupling of biokinetic and population balance models to account for biological heterogeneity in bioreactors. *AIChE Journal*, *59*, 369–379.

Nagata, S. (1975). *Mixing: Principles and application*. New York: Wiley

Neubauer, P., Cruz, N., Glauche, F., Junne, S., Knepper, A., & Raven, M. (2013). Consistent development of bioprocesses from microliter cultures to the industrial scale. *Engineering in Life Sciences*, *13*, 224–238.

Neubauer, P., & Junne, S. (2016). Scale-up and scale-down methodologies for bioreactors. In Mandenius, C. F. (Ed.), *Bioreactors: Design, Operation and Novel Applications* (pp. 323–354). Weinheim, Germany: Wiley-VCH Verlag GmbH & Co. KGaA

Nieß, A., Löffler, M., Simen, J. D., & Takors, R. (2017). Repetitive short-term stimuli imposed in poor mixing zones induce long-term adaptation of *E. coli* cultures in large-scale bioreactors: Experimental evidence and mathematical model. *Frontiers in Microbiology*, *8*, 1–9.

Nikiforaki, L., Montante, G., Lee, K. C., & Yianneskis, M. (2003). On the origin, frequency and magnitude of macro-instabilities of the flows in stirred vessels. *Chemical Engineering Science*, *58*, 2937–2949.

Onyeaka, H., Nienow, A. W., & Hewitt, C. J. (2003). Further studies related to the scale-up of high cell density *Escherichia coli* fed-batch fermentations: The additional effect of a changing microenvironment when using aqueous ammonia to control pH. *Biotechnology and Bioengineering*, *84*, 474–484.

Oosterhuis, N. 1984. Scale-up of bioreactors: a scale-down approach. *PhD thesis, Delft Univ. Technol*.

2003). Paul, E. L., Atiemo-Obeng, V. A., & Kresta, S. M. (Eds.), *Handbook of industrial mixing*. Hoboken, NJ, USA: John Wiley & Sons, Inc

Ruston, J. H., Costich, E. W., & Everett, H. J. (1950). Power characteristics of mixing impellers Part II. *Chemical Engineering Progress*, *46*, 467–476.

Sawatari, Y., & Yokota, A. (2007). Diversity and mechanisms of alkali tolerance in Lactobacilli. *Applied and Environmental Microbiology*, *73*, 3909–3915.

Schmalzriedt, S., Jenne, M., Mauch, K., & Reuss, M. (2003). Integration of physiology and fluid dynamics. In von Stockar, U., van der Wielen, L.A.M., Bruggink, A., Cabral, J.M.S., Enfors, S.-O., Fernandes, P., Jenne, M., Mauch, K., Prazeres, D.M.F., Reuss, M., Schmalzriedt, S., Stark, D., von Stockar, U., & Straathof,, A.J.J. (Eds.), *Process integration and biochemical engineering* (pp. 19–68). Berlin, Heidelberg: Springer Berlin Heidelberg. https://doi.org/10.1007/3-540-36782-9_2

Spann, R., Roca, C., Kold, D., Eliasson Lantz, A., Gernaey, K. V., & Sin, G. (2018). A probabilistic model-based soft sensor to monitor lactic acid bacteria fermentations. *Biochemical Engineering Journal*, *135*, 49–60.

Vanrolleghem, P. A., Sin, G., & Gernaey, K. V. (2004). Transient response of aerobic and anoxic activated sludge activities to sudden substrate concentration changes. *Biotechnology and Bioengineering*, *86*, 277–290.

Vrábel, P., Van der lans, R.G.J.M., Luyben, K.C.A.M., Boon, L., & Nienow, A. W. (2000). Mixing in large-scale vessels stirred with multiple radial or radial and axial up-pumping impellers: Modelling and measurements. *Chemical Engineering Science*, *55*, 5881–5896.

Vrábel, P., Van der lans, R. G. J. M., Van der schot, F. N., Luyben, K. C. A. M., Xu, B., & Enfors, S. O. (2001). CMA: Integration of fluid dynamics and microbial kinetics in modelling of large-scale fermentations. *Chemical Engineering Journal*, *84*, 463–474.

Wang, G., Tang, W., Xia, J., Chu, J., Noorman, H., & van Gulik, W. M. (2015). Integration of microbial kinetics and fluid dynamics toward model-driven scale-up of industrial bioprocesses. *Engineering in Life Sciences*, *15*, 20–29.

Willem schepers, A., Thibault, J., & Lacroix, C. (2002). Lactobacillus helveticus growth and lactic acid production during pH-controlled batch cultures in whey permeate/yeast extract medium. Part II: Kinetic modeling and model validation. *Enzyme and Microbial Technology*, *30*, 187–194.

Xu, B., Jahic, M., Blomsten, G., & Enfors, S. -O. (1999). Glucose overflow metabolism and mixed-acid fermentation in aerobic large-scale fed-batch processes with *Escherichia coli*. *Applied Microbiology and Biotechnology*, *51*, 564–571.

Yang, Y., Xia, J., Li, J., Chu, J., Li, L., Wang, Y., … Zhang, S. (2012). A novel impeller configuration to improve fungal physiology performance and energy conservation for cephalosporin C production. *Journal of Biotechnology*, *161*, 250–256.

Zou, X., Xia, J., Chu, J., Zhuang, Y., & Zhang, S. (2012). Real-time fluid dynamics investigation and physiological response for erythromycin fermentation scale-up from 50 L to 132 m3 fermenter. *Bioprocess and Biosystems Engineering*, *35*, 789–800.

SUPPORTING INFORMATION

Additional supporting information may be found online in the Supporting Information section at the end of the article.

How to cite this article: Spann R, Glibstrup J, Pellicer-Alborch K, et al. CFD predicted pH gradients in lactic acid bacteria cultivations. *Biotechnology and Bioengineering*. 2018;1–12. https://doi.org/10.1002/bit.26868

IV

4th Paper

Response of *Streptococcus thermophilus* exposed to pH gradients in Two- and Three-Compartment Scale-Down Cultivations

KLAUS PELLICER-ALBORCH[1], LUCAS KASPERSETZ[1], VERENA TIEDE[1], PETER NEUBAUER[1], STEFAN JUNNE[1*]

[1] Bioprocess Engineering, Department of Biotechnology, Technische Universität Berlin, Ackerstrasse 76 ACK 24, D-13355 Berlin, Germany

[*] Phone: +49 30 31472527

Fax: +49 30 31427577

e-mail: stefan.junne@tu-berlin.de

Abstract

Stress response of lactic acid bacteria (LAB) to oscillating pH-values, which appear through base addition in large scale pH-controlled batch fermentations, are scarcely investigated so far. In the present study, multi-compartment reactor experiments were applied for *Streptococcus thermophilus* fermentations to investigate the response to pH gradients in a scale-down approach.

Results show a reduced growth, substrate uptake and lactic acid product synthesis at pH gradients. It was observed that the distribution of the cocci chain length was altered during the course of batch fermentations in dependence on the magnitude of pH gradients in scale-down cultivations. A relation was found between the reduction of growth under stress conditions and the cocci chain length distribution: a high degree of cocci chain length heterogeneity is an indicator of unfavourable cultivation conditions. Such relations are probably due to a changed activity of peptidoglycan hydrolases that are involved in cell separation of several LAB. The cocci chain length distribution thus represents a sensitive parameter for the process performance, it is a suitable scale-down criterion at similar shear force regimes. Automated image analysis of the cocci chain length was then successfully applied to predict growth reduction at pH gradient-induced stress. The developed workflow can be used for process optimization and early detection of disturbances under consideration of population heterogeneity in LAB cultures.

Introduction

Lactic acid bacteria (LAB) are mainly used as starter cultures for the production of yogurt, cheese, probiotic applications, and food preservation, respectively. One of the LAB, which are frequently applied, is the gram-positive, round shaped, homofermentative and facultative anaerobic bacterium *Streptococcus thermophilus* [1]. It is non-pathogenic, generally recognised as safe (GRAS) and widely used in the food fermenting industry, e.g. in yogurt and cheese production [2]. It is the second most frequently used bacterium in the dairy industry [3]. If used in starter cultures in dairy products, *S. thermophilus* does not only metabolize lactose into lactic acid, but also ensures desired quality characteristics like viscosity, taste, acidity, water holding capacity [4] and increases the availability of bioactive compounds [3]. The ability to colonize the human gastrointestinal tract has attracted a broad interest in the past decades for the use as a probiotic compound [5]. Probiotic effects include, among others, an improved digestion of lactose [6], the stimulation of the intestinal immune system [7] and the prevention of diarrhoea [2, 8].

S. thermophilus cultures are produced in a m^3-scale in batch processes, under microaerobic or anaerobic conditions (i.e. if the reactor's head space is sparged with nitrogen to maintain a positive pressure to minimize contamination risks). The specific power input in such production scales is often insufficient to keep mixing times sufficiently low so that concentration gradients of additives occur [9]. Due to the usual operation of LAB cultivations in batch mode, the pH-value is among the most important parameters that imply a spatial distribution once base addition started for control [10]. It is known from other organisms that an oscillating pH-value as it appears in large scale, is sensitive for growth and the production profile in various organisms, leading to responses on a multi –omics level [11, 12]. Undesired stress responses were observed for LAB [13,

14], which might alter biomass productivity, cell-to-cell variation, and product quality under production conditions (e.g. final bacterial activity and viability at cell harvest).

In order to study the stress response of *S. thermophilus* cultures in an oscillating environment, Two- and Three-compartment reactor (Two- and Three-CR) scale-down cultivations were conducted, in which cells were opposed to pH gradients. Reactors were equipped with a 10 L stirred tank reactor (STR) and one or two plug-flow reactors (PFR). Such and other multi-compartment reactors have been applied frequently to study the impact of large scale effects on the cellular level. They allow to resolve the microbial response of the portion of cells, which is actually opposed to unfavorable growth conditions [15, 16]. In the applied concept, cells are in unfavourable growth conditions in the PFR module(s), while the major portion is grown under ideal conditions in the STR module at the same time.

In this study, the concentration of biomass and main metabolites and the cocci chain length distribution was investigated in *S. thermophilus* cultures to describe i) the impact of pH gradients of various magnitudes on the process performance in a multi-compartment scale-down bioreactor, ii) the consistency of stress responses across several scale-down experiments and iii) the suitability to detect a stress-related response on the macromorphologic level with automated imaging.

78 *Materials and methods*

79 *Bacterial strain and media*

80 A wildtype *S. thermophilus* strain as used in industrial scale production was provided by
81 Chr. Hansen A/S (Hoersholm, Denmark) [17] and applied throughout all experiments.
82 The De Ma, Rogosa and Sharpe (MRS) medium was used for all cultivations, containing
83 (per litre): 73.7 or 21.1 g lactose monohydrate, 10 g casein hydrolysate (Chr. Hansen A/S,
84 Hoersholm, Denmark), 12 g yeast extract, 2 g K_2HPO_4, 3 g sodium acetate anhydrous,
85 2.4 g tri-sodium citrate dihydrate, 0.2 g $MgSO_4 \cdot 7H_2O$ and 0.05 g $MnSO_4 \cdot H_2O$ (all
86 chemicals were purchased from Carl Roth, Karlsruhe, Germany, if not stated otherwise).
87 2 mL of antifoam 204 (Sigma-Aldrich Chemie, Steinheim, Germany) were added to
88 reduce foam formation in the stirred bioreactor experiments.

89 *Cultivation conditions*

90 For all experiments, a 15 L stirred tank bioreactor (Techfors-S, Infors AG, Bottmingen,
91 Switzerland) with 10 L of working volume, equipped with three Rushton turbine stirrers,
92 baffles, a cell density sensor (Dencytee, Hamilton Inc., Reno, CA), a pH probe (Polilyte
93 Plus ARC 120, Hamilton) and an exhaust gas analyzer All-in-One (BlueSens, Herten,
94 Germany) was used. Medium components were dissolved in 7.5 L of distilled water
95 except of lactose and added to the bioreactor for sterilization. Once the bioreactor
96 temperature reached 40 ºC, the separately autoclaved lactose solution (2.5 L) was added
97 to the reactor. The liquid was sparged with N_2 until the O_2 concentration in the off-gas
98 was below 0.1 % (v/v). Subsequently, CO_2 was sparged until a CO_2 concentration
99 between 1 and 3 % (v/v) was measured in the off-gas. 0.01 % (v/v) of the concentrated
100 inoculum (12 mL of direct inoculation material, provided by Chr. Hansen A/S and stored
101 at -80 ºC) was used to inoculate all bioreactor cultivations. 1 mL of thawed cell suspension
102 was diluted in 5 mL MRS medium without carbon sources to easily transfer the entire

inoculation volume into the reactor. The agitation speed was kept at 400 rpm and the temperature at 40 °C throughout all fermentations. The pH-value was controlled at pH 6.0 with 25 % NH_3 (v/v) (VWR International, Radnor, PA).

One or two PFR modules were connected to the STR via hose pumps. The pump rate was chosen so that the residence time was 120 s in each PFR. The total working volume of a PFR was 1.2 L or 1.8 L, if transfer parts are considered. Up to four pH probes (Polilyte Plus ARC 120, Hamilton) were installed at different heights of each PFR module in order to monitor pH gradients. The parts and features of the plug flow module were described in more detail elsewhere [18]. The base feed was directly connected via an inlet tube to the bottom of the PFR. In case of Three-CR cultivations (two PFRs), the same set up was used as in Two-CR cultivations with a second PFR module, which represented an acidified environment. 2h after the base was fed initially into one PFR module, the acid feed of 51% (v/v) H_3PO_4 was started pulse-wise at the other PFR to increase the pH stress. A continuous addition of acid would have let to an overall increase of base addition and finally relevant dilution of the culture. pH gradients as mimicked here were based on experimental observation in pilot and industrial scale, but represent an extension under the assumption of a “worst-case” scenario.

Analysis

Cell growth was monitored *off line* with appropriately diluted samples at a wavelength of 600 nm (OD600) with an Ultraspec 2100 *pro* UV/Visible spectrophotometer (Amersham Biosciences, Amersham, UK). For dry cell weight (DCW) determination, 2 mL of cell suspension were pipetted into a previously dried and weighted 2 mL Eppendorf tube. Samples were centrifuged at 4 ºC and 10,000 rpm for 10 min. The supernatant was discarded, whilst the cell pellet was washed with 1 mL of 0.9 % (w/w) NaCl solution. After a second step of centrifugation, the Eppendorf tube containing the washed cells was

128 dried at 75 ºC for 24 hours and weighted again. The DCW was then calculated as the
129 difference between the tube with and w/o sample. Samples for extracellular metabolite
130 and free amino acid concentration were filtered through a membrane filter with a pore
131 size of 0.8 μm (Carl Roth, Karlsruhe, Germany) directly at the sampling port of the
132 bioreactor. The filtrate was transferred to a 1.5 mL Eppendorf tube and immediately
133 stored at -80 ºC.
134 For the analysis of total main carbon metabolites and nucleotides, 4 mL of cell suspension
135 were rapidly harvested into a frozen syringe containing 1 mL of pre-cooled perchloric
136 acid with 0.5 gL^{-1} butanol as internal standard. The further treatment was described
137 elsewhere [19]. Briefly, the syringe containing the quenched cell suspension was shaken
138 on ice on a horizontal shaker for 15 min. Afterwards, the sample was transferred to a 50
139 mL falcon tube and 845 μL 5M K_2CO_3 were added for acid neutralization. The cell
140 fragments were finally separated with a membrane filter with a pore size of 0.8 μm (Carl
141 Roth, Karlsruhe, Germany) and the filtrate was stored directly at -80 ºC. All steps were
142 performed on ice, all plastic parts were pre-cooled prior to their use.
143

144 *Quantification of metabolites*

145 Quantification of free amino acids was conducted with an Agilent 1260 Infinity High
146 Performance Liquid Chromatography (HPLC) system (Agilent Technologies,
147 Waldbronn, Germany), equipped with an Agilent 1200 system fluorescence detector
148 (excitation and emission wavelengths of 340 and 450nm, respectively), a C18 Gemini®
149 column (5 µ, 100 Å, 150x4.6 mm) and a Security Guard™ precolumn (both columns
150 supplied by Phenomenex®, Aschaffenburg, Germany). For derivatization, ortho-
151 phthaldialdehyde was applied as described previously [20]. Separation was achieved
152 using a 40 mM NaH_2PO_4 (pH = 7.8) polar phase and a 45:45:10 MeOH:CH_3CN:H_2O
153 solution as nonpolar phase at a flow rate of 1 mL·min^{-1} and a temperature of 40 ºC.

154 Carboxylic acids and sugars were quantified with an Agilent 1200 HPLC system
155 equipped with a refractive index detector (RID) and a HyperRez™ XP Carbohydrate H^+
156 column (300x7.7 mm, 8 µm) (Fisher Scientific, Schwerte, Germany) operated with 5 mM
157 H_2SO_4 at a flow rate of 0.5 mL·min^{-1} and a temperature of 65 ºC.

158 *Microscopy image analysis*

159 1 µL of culture broth were pipetted on a microscopic slide with a cover glass and captured
160 with a light microscope (CN-hFT, Hertel & Reuss, Kassel, Germany) with a
161 magnification of 1,000. The captures were taken with a digital camera (Canon Power Shot
162 G1X, Canon, Tokio, Japan) with a four fold magnification. Images were stored as 8-bit
163 image TIFF files without compression with 256 possible shades of grey (2^8 combinations
164 in binary code). The median grey value of each image set was calculated using ImageJ
165 (version 2.0.0) for background quantification. Afterwards, the background pixels were
166 subtracted from each image (segmentation) [21]. The software Cell Profiler (version
167 2.1.0) was applied to identify cocci chains of *S. thermophilus*, to segment them into
168 individual cocci and to measure the maximal axis length and area.

169 *Data fitting and visualization*

170 In order to calculate uptake and release rates, concentration data were fitted with a
171 smoothing spline function of the curve fitting toolbox from MATLAB R2013b (The
172 MathWorks, Natick, MA). All data plots were made with SigmaPlot version 11.0 (Systat
173 Software, San José, CA).

174 *Statistical analysis*

175 Data were expressed as mean standard deviation (SD) for the description of
176 reproducibility. Biological replicates were performed as fermentations under identical
177 conditions. The coefficient of variation (CV%) was then calculated using Equation 1:

178 $$CV\% = \frac{SD}{Mean} \cdot 100 \quad (1)$$

179

Results and discussion

This study aimed to investigate the stress response of *S. thermophilus* to oscillating pH-values in scale-down batch cultivation experiments. The addition of concentrated pH control agents, e.g. NH_4OH, has a strong impact on the local pH-value and the process performance in many microbial cultivations. If ammonia was used as pH control additive, a negative effect on *E. coli* cell growth and viability was observed when the mean circulation time increased to over 100 s in an environment with pH-gradients of 0.3 or higher [22]. Therefore, in this study, a single-CR LAB cultivation in a STR was compared with cultivations in two different scale-down reactor designs (Figure 1). The Two-CR consisted of an STR that was connected to a plug-flow reactor (PFR 1), into which base was added in the front part. The Three-CR consisted of the STR, PFR 1 and an additional PFR module, into which acid was regularly added to mimic zones in the reactor, which are far away from the spot of base addition, and in which a low pH-value occurs due to the excretion of lactic acid from bacteria (PFR 2).

The pH-value was monitored at the bottom and top of each PFR module. The pH-value remained uncontrolled until it reached a value of 6.0 during the first hours of cultivation. Then pH control was switched on, which led to pulse-wise increased pH-values in PFR 1 (Figure 2). Maximum pH-values of 8.2 were achieved. Acidic pulses where induced manually in PFR 2 of the Three-CR experiments 2 hours after pH control had started. This led to minimum pH-values of about 4.2. As initial lactose concentrations, 20 $g \cdot L^{-1}$ were applied in first experiments, while 70 $g \cdot L^{-1}$ initial lactose concentrations were applied during Three-CR fermentations. This increased the time of pH control, and thus the amount of pH pulses (Figure 2). At the same time, the effect of a higher overall lactic acid production was examined. The residence time of cells were set to 120 s in each PFR module. This time was selected based on assumptions of the power input, but without the

exact knowledge of conditions in the industrial scale bioreactor (e.g. mixing and circulation times). The authors recently published a study, which described mixing in the same process in a pilot scale fermenter of 700 L [17]. A mixing time of 45 seconds (the time to achieve 95 % of homogeneity) was determined, while a pH gradient of 0.4 was measured (from 5.9 in the upper zone to 6.3 in the lower part of the bioreactor at base addition). Nevertheless, the volume of the production scale, in which the process is conducted, is hundred times larger. The specific power input, which is applied there, leads to increased mixing times and most likely also higher pH-gradients. Under the assumption of geometrical similarity between the pilot and industrial scale (height to diameter ratio), the length of the flow pattern is 4.6 times greater. In order to maintain the mixing time, the fluid velocity in industrial scale would have to be 4.6 times higher [23], which would require a 20-fold increase in the specific power input (P/V) as it is proportional to the square of the fluid velocity v^2. Under the assumption of the available power at industrial scale, an increase in mixing time by a factor of two or more is assumed, which led to the chosen scale-down set up with residences times of 120 s in each PFR module.

Growth and main carbon metabolism

The pH gradients, as induced in the Two-CR cultivations, did not alter the final biomass concentration (Figure 3A), the same biomass yield was obtained as under gradient-free conditions (Table 1). Nevertheless, as observed at the specific growth (μ), lactose uptake (q_S) and lactate production (q_P) rates (Figure 3A), cell division and metabolic activity was considerably retarded under scale-down conditions, a lower maximum growth rate was achieved (μ = 0.95 vs. 1.5 h^{-1}; q_S = 6.8 vs. 10 g lactose·(g DCW·h)$^{-1}$; and q_P = 3 vs. 5 g lactate·(g DCW·h)$^{-1}$). While all substrate was consumed, a lower yield of lactate was determined in Two-CR cultivations (Figure 4B). One reason for a lower extracellular

lactic acid concentration might be a changed chemical equilibrium between the dissociated and non-dissociated form inside the cells. The portion of the dissociated form of lactic acid, which does not cross the cytoplasmic membrane by simple diffusion, is increased at a high pH-value [24]. Under these conditions, less lactic acid might have been excreted. A higher intracellular concentration of lactate has usually a negative effect on the cells' viability and metabolic activity. If cells cope with a high pH-value and intracellular lactate accumulation is fostered, several mechanisms are activated, which facilitate survival and growth of LAB under alkaline conditions [25]. They include an increase of the activity of (i) the ATP-driven potassium extrusion and the potassium-proton antiport system, (ii) the sodium-proton antiport system, (iii) the proton-translocating adenosine triphosphatase (ATPase), support (iv) of the formation of transmembrane proton gradients (ΔpH), and (v) the adaptation of protein synthesis, respectively. Thus, LAB are able to maintain a homeostatic cytoplasmic or intracellular pH (pH_i) during short and small changes of the environmental pH-value, typically at a neutral or near neutral value, when the external pH varies. This requires additional resources of carbon, amino acids and energy. Then these mechanisms demand for resources, which are not available for the synthesis of byproducts like lactic acid.

In contrast to the Two-CR fermentations, a considerable reduction of biomass formation was measured in the Three-CR experiments (Figure 3B, Table 1). Different growth rates prior to the onset of base addition originate from different start points of pH-value oscillations, which does not matter if response patterns are in the focus of research as it is the case here.

The experiments were performed with a higher concentration of lactose so that lactic acid inhibition occurred at about 30 $g \cdot L^{-1}$ [26], which led to unconsumed lactose. The pH-value in the main fermenter was not allowed to drop below 5.2 prior to the onset of base

addition so that growth inhibiting conditions were avoided [27]. Hence, any inhibiting effect was directly caused by a high lactic acid concentration. If lactic acid is accumulated in the medium, less lactic acid can pass from the inside to the outside of a cell due to a low gradient. As consequence, the pH_i decreases while lactic acid dissociates inside the cell [28]. It is commonly accepted in literature, that both, the dissociated and non-dissociated forms of lactic acid can inhibit growth of LAB [27, 29]. While [30, 31] stated that the non-dissociated form of lactic acid was the main inhibitory compound for growth of *Lactobacillus helveticus* and of *Lactococcus lactis*, respectively, a loss of cell viability and membrane integrity by high lactate concentrations was examined in *Lactobacillus bulgaricus* cultures [32]. The authors concluded that the higher the lactate concentration, the higher the cellular mortality (which was more than one order of magnitude higher in cultures conducted at a higher pH-value). They observed that the dissociated form accumulated more profoundly in fermentations, which were controlled at pH 6, than at pH 5, which is in accordance to the chemical equilibrium. It was concluded that the non-dissociated form of lactic acid is not solely responsible for growth inhibition and stated that the total acid concentration has to be considered [33]. In fact, if 100 $g \cdot L^{-1}$ of initial lactose concentration was applied at *S. thermophilus* fermentations under optimal conditions, no increase of biomass concentration was achieved in comparison to 70 $g \cdot L^{-1}$ of initial lactose concentrations, which underlines the complete inhibition of lactic acid in these cases: 10.5 % less lactose was consumed and 29 % less lactic acid was produced during Three-CR (Figure 4C). Right after the phosphoric acid feed was connected to the second PFR, the substrate consumption and product formation were drastically affected compared to Single-CR cultivations. Interestingly, glucose tend to accumulate extracellularly once the acid pulses were applied (Figure 4D). The substrate consumption

rate (q_S) was about 21.9 g lactose·h^{-1} in Single-CR experiments and only 11.6 g lactose·h^{-1} in Three-CR cultivations (spec. values are depicted in Figure 3B).

Enzymes, which are involved in the carbohydrate metabolism of LAB possess a rather neutral pH optimum [32], and may thus have a decreased activity under pH stress [34]. If one of the first steps in glycolysis, like the phosphorylation of glucose to glucose-6-phosphate by hexokinases, is not conducted efficiently, glucose penetrates back into the medium [35]. This is one reason why starvation response was observed under acid stress as a result of a reduced activity of the sugar uptake [36]. A lower specific glucose uptake rate was reported for LAB at a low pH-value [37]. In this case, less energy is available for a cell. Additionally, the aforementioned adaptation mechanisms to pH stress consume energy: up-regulation of a gene, which codes for proton pumps was observed under oscillating pH-values and temperatures [38]. Such proton pumps like the F_0-F_1-ATPase expulse protons out of the cell at the expense of ATP to maintain the pH_i [36, 39]. The LacS permease activity, which mediates the exchange of extracellular lactose with intracellular galactose, may also be affected under pH stress [40]. Other studies demonstrated that even small deviations from the optimal pH-value have an effect on biomass productivity during *S. thermophilus* batch fermentations [41]. The authors concluded that *S. thermophilus* is sensitive to variation of the pH-value, optimal growth is achieved between 6.5 and 7.5. Interestingly, the authors investigated the influence of fermentation temperatures and pH-values on the co-cultivation of *S. thermophilus* and *L. bulgaricus* [42]. A pH-value, which was 0.8 units below the optimum during fermentations at 38 ºC led to a biomass production loss by 35 % in case of *S. thermophilus*.

Strong effects on growth and side metabolite production were seen in *S. thermophilus* scale-down cultivations with oscillating pH-values. A reduction of metabolic activity can

304 be recognized by the amount of base, which was added to compensate for lactic acid
305 release. The time course of the extracellular and total concentration of metabolites showed
306 a similar trend at all experiments (Figure S1). Hence, any determination of intracellular
307 concentrations is hardly possible, most probably due to the considerable high extracellular
308 concentrations, which makes the quantification of the volumetric portion of intracellular
309 concentrations in suspension samples hardly feasible. In case of the time courses of amino
310 acid concentrations, no remarkable differences between Single-CR and scale-down
311 experiments were measured (Figure S2).

312 *Population heterogeneity*

313 In order to investigate, whether and when the homogeneity among the population is
314 affected by pH gradients, the cocci chain length distribution was monitored with light
315 microscopy and automated cell recognition tools [43] in Two- and Three-CR
316 experiments.

317 The diplococcal morphology was found to be the dominant cocci chain length in *S.*
318 *thermophilus* cultivations, whenever they were conducted under optimal conditions
319 (Figure 5). As described by [44], the cell division in LAB occurs in successive parallel
320 planes perpendicular to their axis. This leads to diplococcal daughter cells, which are
321 connected through their septa [45, 46]. Then, at the very late step of cell division, the
322 septum is cleaved and converted into the new pole of each daughter cell by the action of
323 cell wall hydrolases, mostly peptidoglycan hydrolases (PGHs). A second round of cell
324 division may start before closure of the septum at high growth rates. Therefore, two or
325 even four cocci chains might be detectable. If cell division is disturbed, an increase of the
326 portion of unevenly distributed cocci chains of a length of one, three or five cocci shall
327 be observable. Indeed, base pulses, which were induced in Two-CR fermentations, shifted
328 the population distribution towards longer chains (Figure 5A). Finally, 5 or more cocci

chains were the dominant chain lengths, which were detectable under pH oscillating conditions, while such chain lengths were hardly detected under gradient-free growth. The cocci chain length distribution was broader under the pH stress induced in the Three-CR system (Figure 5B). A large portion of single cocci were observed beside longer chains of an uneven number of cocci. Already 1.5 hours after starting the pH control (that is after connecting the PFRs and inducing base pH shifts), a 22 % lower number of diplococcal cells and more than twice the amount of single cells were identified under Three-CR conditions in comparison to Single-CR cultivations.

A reasonable explanation for the increasing chain length under pH-gradients in a basic environment might be a decreased activity of the chain dispersing chromosome segregation protein CSE, the main PGH proposed for *S. thermophilus*. One study reported that a histidine-dependent amidohydrolase/peptidase (CHAP) domain, which mediates coccus division, is only active in a pH range between 4.0 and 4.5 *in vitro* [45]. Therefore, longer chains may be expected under alkaline conditions as daughter cells are not separated with the same intensity than at acidic conditions, however, the impact of gradients on the expression has not been observed. Moreover, the LysM binding domain of the CSE protein, which binds to peptidoglycans and plays a role in localization and substrate recognition, might be affected by the extracellular pH-value as well. The LysM domains in homologous PGHs in *Lactococcus lactis* differ in their isoelectric points [47]. The LysM domain of the CSE protein might be incapable of binding at high pH-values. Cation transport ATPases such as Na^+ (K^+)/H^+ antiporters, as they were described in Lactobacilli [48], can contribute to pH homeostasis, especially to alkaline tolerance. This might be another reason for a reduced growth and for an increased maintenance at high pH values.

353 The adaptation to acid stress is essential for the survival of LAB. While lactic acid
354 accumulation creates an unfavorable environment for many other bacteria [36, 49], the
355 adaptation to an acidic environment creates a growth advantage of LAB against potential
356 competing microbes. Another adaptation mechanism to acid stress is the production of
357 basic compounds, which can support alkalinization of the environment and cytoplasm, at
358 the expense of energy utilization. Ammonia-generating mechanisms described for
359 *Streptococcus sp.* include (i) the hydrolysis of urea by urease and (ii) the catabolism of
360 arginine via the arginine deiminase system (ADS) [50]. The latter mechanism has been
361 studied thoroughly [51, 52]. Nevertheless, they have not been investigated in LAB so far.

362 Finally, osmotic stress may also be considered, since more than 200 g of 25 % (v/v)
363 NH_4OH were added if 70 $g \cdot L^{-1}$ of initial lactose concentration was applied. After
364 induction of acid pulses with 51 % v/v H_3PO_4, an increase of the osmolality in the medium
365 is expected, which might also lead to intracellular water loss and cell shrinkage [53].
366 Bacterial membranes possess high water permeabilities, so that cellular hydration is
367 altered within seconds after an osmotic shift [54].

Conclusions and Outlook

Oscillating pH conditions were successfully simulated in Two- and Three-CR scale-down experiments. In summary, *S. thermophilus* responded with a reduced growth rate, a biomass productivity loss and increased population heterogeneity under the inhomogeneous cultivation conditions in scale-down experiments. These effects may be due to a combination of the physical, chemical as well as biological stress responses from LAB. Changes on cell morphology due to varying environmental conditions prove the potential of microscopy-based image analysis as process analytical technology (PAT). *In situ* image detection with automatic recognition methods for detection of morphological changes [9, 55], enable to gain real-time population heterogeneity data and develop process monitoring as well as control strategies. Additionally, the fast recognition of heterogeneities in time and space enables fast adaptations of the process towards favorable conditions to ensure a desired performance [56, 57].

It has been demonstrated, that the cocci chain length distribution could be used as scaling parameter of LAB production subjected to certain pH gradients during this study. A scale up or down would be successful, if a similar cocci chain length distribution would be obtained. Studies concerning the acidification activity (i.e. rate of decrease of pH in milk after a certain time) of biomass with different population heterogeneity (i.e. shorter or longer cocci chains), would give a better insight into the effect on product quality [28, 58]. Additionally, a better understanding of the industrial scale process and performance (e.g. computational fluid dynamics (CFD) studies as well as mixing and residence time calculations) is needed, in order to realistically mimic the conditions in lab scale simulators [17].

Acknowledgments

This project has received funding from the European Union's Horizon 2020 research and innovation program under the Marie Skłodowska-Curie actions grant agreement No. 643056 (project Biorapid). The authors gratefully acknowledge this financial support and the contribution of Dr. Christophe Roca, Dr. Anders Clausen as well as Dr. David Kold from Chr. Hansen A/S by providing their knowledge and expertise, media and the strain for all experiments. The authors finally thank Peter Unger, Adriana Mora Barrabés, Julia Scharre, Manon Weiske and Lena Jack for their help during scale-down experiments.

Conflict of interest

All authors declare no competing interests.

References

[1] Q. Wu, H.M. Tun, F.C.-C. Leung, N.P. Shah, Genomic insights into high exopolysaccharide-producing dairy starter bacterium Streptococcus thermophilus ASCC 1275, Scientific reports 4 (2014) 4974.
[2] D.M. Linares, T.F. O'Callaghan, P.M. O'Connor, R.P. Ross, C. Stanton, Streptococcus thermophilus APC151 strain is suitable for the manufacture of naturally GABA-enriched bioactive yogurt, Frontiers in microbiology 7 (2016) 1876.
[3] X. Lecomte, V. Gagnaire, S. Lortal, A. Dary, M. Genay, Streptococcus thermophilus, an emerging and promising tool for heterologous expression: advantages and future trends, Food microbiology 53 (2016) 2-9.
[4] Z. Sun, X. Chen, J. Wang, W. Zhao, Y. Shao, L. Wu, Z. Zhou, T. Sun, L. Wang, H. Meng, Complete genome sequence of Streptococcus thermophilus strain ND03, Journal of bacteriology 193(3) (2011) 793-794.
[5] Y. Cui, T. Xu, X. Qu, T. Hu, X. Jiang, C. Zhao, New Insights into various production characteristics of Streptococcus thermophilus strains, International journal of molecular sciences 17(10) (2016) 1701.
[6] F. Guarner, G. Perdigon, G. Corthier, S. Salminen, B. Koletzko, L. Morelli, Should yoghurt cultures be considered probiotic?, British Journal of Nutrition 93(6) (2005) 783-786.
[7] Y.-F. Hong, Y.-D. Lee, J.-Y. Park, B. Jeon, D. Jagdish, S. Jang, D.K. Chung, H. Kim, Immune regulatory effect of newly isolated Lactobacillus delbrueckii from Indian traditional yogurt, J. Microbiol. Biotechnol 25(8) (2015) 1321-1323.
[8] R.S. Beniwal, V.C. Arena, L. Thomas, S. Narla, T.F. Imperiale, R.A. Chaudhry, U.A. Ahmad, A randomized trial of yogurt for prevention of antibiotic-associated diarrhea, Digestive diseases and sciences 48(10) (2003) 2077-2082.

[9] A. Lemoine, F. Delvigne, A. Bockisch, P. Neubauer, S. Junne, Tools for the determination of population heterogeneity caused by inhomogeneous cultivation conditions, Journal of biotechnology 251 (2017) 84-93.
[10] A. Amanullah, C. McFarlane, A. Emery, A. Nienow, Scale‐down model to simulate spatial pH variations in large‐scale bioreactors, Biotechnology and bioengineering 73(5) (2001) 390-399.
[11] J.T. Cortés, N. Flores, F. Bolívar, A.R. Lara, O.T. Ramírez, Physiological effects of pH gradients on Escherichia coli during plasmid DNA production, Biotechnology and bioengineering 113(3) (2016) 598-611.
[12] M.H. Limberg, M. Joachim, B. Klein, W. Wiechert, M. Oldiges, pH fluctuations imperil the robustness of C. glutamicum to short term oxygen limitation, Journal of biotechnology 259 (2017) 248-260.
[13] M. Hosseini Nezhad, M.A. Hussain, M.L. Britz, Stress responses in probiotic Lactobacillus casei, Critical reviews in food science and nutrition 55(6) (2015) 740-749.
[14] F. Delvigne, Q. Zune, A.R. Lara, W. Al-Soud, S.J. Sørensen, Metabolic variability in bioprocessing: implications of microbial phenotypic heterogeneity, Trends in Biotechnology 32(12) (2014) 608-616.
[15] P. Neubauer, S. Junne, Scale-down simulators for metabolic analysis of large-scale bioprocesses, Current opinion in biotechnology 21(1) (2010) 114-121.
[16] R. Takors, Scale-up of microbial processes: impacts, tools and open questions, Journal of biotechnology 160(1-2) (2012) 3-9.
[17] R. Spann, J. Glibstrup, K. Pellicer‐Alborch, S. Junne, P. Neubauer, C. Roca, D. Kold, A.E. Lantz, G. Sin, K.V. Gernaey, CFD predicted pH gradients in lactic acid bacteria cultivations, Biotechnology and bioengineering 116(4) (2019) 769-780.
[18] S. Junne, A. Klingner, J. Kabisch, T. Schweder, P. Neubauer, A two-compartment bioreactor system made of commercial parts for bioprocess scale-down studies: impact of oscillations on Bacillus subtilis fed-batch cultivations, Biotechnol J 6(8) (2011) 1009-17.
[19] U. Theobald, W. Mailinger, M. Baltes, M. Rizzi, M. Reuss, In vivo analysis of metabolic dynamics in Saccharomyces cerevisiae: I. Experimental observations, Biotechnology and bioengineering 55(2) (1997) 305-316.
[20] J.O. Krömer, O. Sorgenfrei, K. Klopprogge, E. Heinzle, C. Wittmann, In-depth profiling of lysine-producing Corynebacterium glutamicum by combined analysis of the transcriptome, metabolome, and fluxome, Journal of bacteriology 186(6) (2004) 1769-1784.
[21] Q. Wu, F. Merchant, K. Castleman, Microscope image processing, Elsevier2010.
[22] H. Onyeaka, A.W. Nienow, C.J. Hewitt, Further studies related to the scale‐up of high cell density Escherichia coli fed‐batch fermentations: the additional effect of a changing microenvironment when using aqueous ammonia to control pH, Biotechnology and bioengineering 84(4) (2003) 474-484.
[23] P.M. Doran, Bioprocess engineering principles, Elsevier1995.
[24] A. Revilla‐Guarinos, C. Alcantara, N. Rozes, B. Voigt, M. Zúñiga, Characterization of the response to low pH of L actobacillus casei Δ RR 12, a mutant strain with low D‐alanylation activity and sensitivity to low pH, Journal of applied microbiology 116(5) (2014) 1250-1261.
[25] A.P. Nyanga-Koumou, L.I.I. Ouoba, S.C. Kobawila, D. Louembe, Response mechanisms of lactic acid bacteria to alkaline environments: a review, Critical reviews in microbiology 38(3) (2012) 185-190.
[26] R. Spann, C. Roca, D. Kold, A.E. Lantz, K.V. Gernaey, G. Sin, A probabilistic model-based soft sensor to monitor lactic acid bacteria fermentations, Biochem Eng J 135 (2018) 49-60.
[27] K. Hetényi, Á. Németh, B. Sevella, Role of pH-regulation in lactic acid fermentation: Second steps in a process improvement, Chemical Engineering and Processing: Process Intensification 50(3) (2011) 293-299.

[28] G. Hansen, C.L. Johansen, G. Marten, J. Wilmes, L. Jespersen, N. Arneborg, Influence of extracellular pH on growth, viability, cell size, acidification activity, and intracellular pH of Lactococcus lactis in batch fermentations, Applied microbiology and biotechnology 100(13) (2016) 5965-5976.
[29] C. Åkerberg, K. Hofvendahl, G. Zacchi, B. Hahn-Hägerdal, Modelling the influence of pH, temperature, glucose and lactic acid concentrations on the kinetics of lactic acid production by Lactococcus lactis ssp. lactis ATCC 19435 in whole-wheat flour, Applied microbiology and biotechnology 49(6) (1998) 682-690.
[30] A. Amrane, Y. Prigent, Differentiation of pH and free lactic acid effects on the various growth and production phases of Lactobacillus helveticus, Journal of Chemical Technology & Biotechnology: International Research in Process, Environmental & Clean Technology 74(1) (1999) 33-40.
[31] S. Even, N.D. Lindley, P. Loubière, M. Cocaign‐Bousquet, Dynamic response of catabolic pathways to autoacidification in Lactococcus lactis: transcript profiling and stability in relation to metabolic and energetic constraints, Molecular microbiology 45(4) (2002) 1143-1152.
[32] A. Rault, M. Bouix, C. Béal, Fermentation pH influences the physiological-state dynamics of Lactobacillus bulgaricus CFL1 during pH-controlled culture, Applied and environmental microbiology 75(13) (2009) 4374-4381.
[33] L. Gonçalves, A. Ramos, J. Almeida, A. Xavier, M. Carrondo, Elucidation of the mechanism of lactic acid growth inhibition and production in batch cultures of Lactobacillus rhamnosus, Applied Microbiology and Biotechnology 48(3) (1997) 346-350.
[34] J. Jin, Q. Qin, H. Guo, S. Liu, S. Ge, H. Zhang, J. Cui, F. Ren, Effect of pre-stressing on the acid-stress response in Bifidobacterium revealed using proteomic and physiological approaches, PloS one 10(2) (2015) e0117702.
[35] W. Müller-Esterl, Glykolyse–Prototyp eines Stoffwechselwegs, Biochemie, Springer2018, pp. 597-606.
[36] K. Papadimitriou, Á. Alegría, P.A. Bron, M. De Angelis, M. Gobbetti, M. Kleerebezem, J.A. Lemos, D.M. Linares, P. Ross, C. Stanton, Stress physiology of lactic acid bacteria, Microbiology and Molecular Biology Reviews 80(3) (2016) 837-890.
[37] A.Z. Andersen, A.L. Carvalho, A.R. Neves, H. Santos, U. Kummer, L.F. Olsen, The metabolic pH response in Lactococcus lactis: an integrative experimental and modelling approach, Computational biology and chemistry 33(1) (2009) 71-83.
[38] J. Wallenius, T. Uuksulainen, K. Salonen, J. Rautio, T. Eerikäinen, The effect of temperature and pH gradients on Lactobacillus rhamnosus gene expression of stress-related genes, Bioprocess and biosystems engineering 34(9) (2011) 1169.
[39] C.L. Ramos, L. Thorsen, M. Ryssel, D.S. Nielsen, H. Siegumfeldt, R.F. Schwan, L. Jespersen, Effect of the gastrointestinal environment on pH homeostasis of Lactobacillus plantarum and Lactobacillus brevis cells as measured by real-time fluorescence ratio-imaging microscopy, Research in microbiology 165(3) (2014) 215-225.
[40] K.I. Sørensen, M. Curic-Bawden, M.P. Junge, T. Janzen, E. Johansen, Enhancing the sweetness of yoghurt through metabolic remodeling of carbohydrate metabolism in Streptococcus thermophilus and Lactobacillus delbrueckii subsp. bulgaricus, Applied and environmental microbiology (2016) AEM. 00462-16.
[41] M. Aghababaie, M. Khanahmadi, M. Beheshti, Developing a detailed kinetic model for the production of yogurt starter bacteria in single strain cultures, Food and Bioproducts Processing 94 (2015) 657-667.
[42] M. Aghababaie, M. Khanahmadi, M. Beheshti, Developing a kinetic model for co-culture of yogurt starter bacteria growth in pH controlled batch fermentation, Journal of Food Engineering 166 (2015) 72-79.
[43] M.-O. Baradez, D. Marshall, The use of multidimensional image-based analysis to accurately monitor cell growth in 3D bioreactor culture, PLoS One 6(10) (2011) e26104.
[44] A. Zapun, T. Vernet, M.G. Pinho, The different shapes of cocci, FEMS microbiology reviews 32(2) (2008) 345-360.

[45] S. Layec, J. Gérard, V. Legué, M.P. Chapot‐Chartier, P. Courtin, F. Borges, B. Decaris, N. Leblond‐Bourget, The CHAP domain of Cse functions as an endopeptidase that acts at mature septa to promote Streptococcus thermophilus cell separation, Molecular microbiology 71(5) (2009) 1205-1217.
[46] M.-P. Chapot-Chartier, S. Kulakauskas, Cell wall structure and function in lactic acid bacteria, Microbial cell factories, BioMed Central, 2014, p. S9.
[47] G. Buist, A. Steen, J. Kok, O.P. Kuipers, LysM, a widely distributed protein motif for binding to (peptido) glycans, Molecular microbiology 68(4) (2008) 838-847.
[48] Y. Sawatari, A. Yokota, Diversity and mechanisms of alkali tolerance in lactobacilli, Applied and environmental microbiology 73(12) (2007) 3909-3915.
[49] M. van de Guchte, P. Serror, C. Chervaux, T. Smokvina, S.D. Ehrlich, E. Maguin, Stress responses in lactic acid bacteria, Antonie Van Leeuwenhoek 82(1-4) (2002) 187-216.
[50] Y.-L. Liu, M. Nascimento, R.A. Burne, Progress toward understanding the contribution of alkali generation in dental biofilms to inhibition of dental caries, International journal of oral science 4(3) (2012) 135.
[51] Y. Liu, Y. Dong, Y.-Y.M. Chen, R.A. Burne, Environmental and growth phase regulation of the Streptococcus gordonii arginine deiminase genes, Applied and environmental microbiology 74(16) (2008) 5023-5030.
[52] A. Griswold, Y.-Y.M. Chen, J.A. Snyder, R.A. Burne, Characterization of the arginine deiminase operon of Streptococcus rattus FA-1, Applied and environmental microbiology 70(3) (2004) 1321-1327.
[53] I.R. Booth, M.D. Edwards, S. Black, U. Schumann, S. Miller, Mechanosensitive channels in bacteria: signs of closure?, Nature Reviews Microbiology 5(6) (2007) 431.
[54] J.M. Wood, Bacterial osmoregulation: a paradigm for the study of cellular homeostasis, Annual review of microbiology 65 (2011) 215-238.
[55] A.-M. Marbà-Ardébol, J. Emmerich, P. Neubauer, S. Junne, Single-cell-based monitoring of fatty acid accumulation in Crypthecodinium cohnii with three-dimensional holographic and in situ microscopy, Process Biochemistry 52 (2017) 223-232.
[56] S. Müller, H. Harms, T. Bley, Origin and analysis of microbial population heterogeneity in bioprocesses, Current opinion in biotechnology 21(1) (2010) 100-113.
[57] R. González-Cabaleiro, A.M. Mitchell, W. Smith, A. Wipat, I.D. Ofiţeru, Heterogeneity in pure microbial systems: experimental measurements and modeling, Frontiers in microbiology 8 (2017) 1813.
[58] D. Dandoy, C. Fremaux, M.H. de Frahan, P. Horvath, P. Boyaval, P. Hols, L. Fontaine, The fast milk acidifying phenotype of Streptococcus thermophilus can be acquired by natural transformation of the genomic island encoding the cell-envelope proteinase PrtS, Microbial cell factories, BioMed Central, 2011, p. S21.

577 *Tables*

578 Table 1. Mean value, in brackets: standard deviation (SD) of biological duplicates (n = 2)
579 and coefficient of variation (CV%), of the final biomass concentration in g L^{-1}, the
580 biomass yield ($Y_{X/S}$), lactate yield ($Y_{P/S}$) and biomass-specific lactate yield ($Y_{P/X}$) in
581 Single-CR (STR), Two- and Three-CR experiments with 20 or 70 g·L^{-1} of initial lactose
582 concentration.

Lactose conc.		STR	Two-CR	Three-CR
20 g·L^{-1}	Final biomass conc. [g L^{-1}]	1.94 (0.03 / 1.57)	2.05 (0.04 / 1.69)	
	$Y_{X/S}$	0.095 (0.000 / 0.479)	0.095 (0.002 / 1.66)	
	$Y_{P/S}$	0.616 (0.059 / 9.60)	0.485 (0.015 / 3.08)	
	$Y_{P/X}$	6.50 (0.66 / 10.08)	5.13 (0.24 / 4.74)	
70 g·L^{-1}	Final biomass conc. [g L^{-1}]	5.43 (0.01 / 0.20)		4.41 (0.20 / 4.61)
	$Y_{X/S}$	0.075 (0.001 / 1.11)		0.076 (0.001 / 1.25)
	$Y_{P/S}$	0.383 (0.014 / 3.56)		0.317 (0.006 / 1.75)
	$Y_{P/X}$	5.14 (0.13 / 2.46)		4.18 (0.02 / 0.50)

583
584
585
586
587
588
589
590
591

Figure legend

Figure 1. Single-compartment reactor (Single-CR, A) and scale-down simulators used during this work. Two-compartment reactor (Two-CR, B) and Three-compartment reactor (Three-CR, C) set up.

Figure 2. Development of the pH-value in different compartments of the scale-down experiments. The pH-value in the STR (black) describes the experimental set up, in which pH control was started once the pH-value dropped below 6.0. pH-values as induced in the PFR during Two-CR fermentations (A), measured with two probes located at the top and bottom of the PFR module (blue and red, respectively), ranged from 5.6 to 8.2. In Three-CR cultivations (B), pH values ranged between 4.7 and 9.4, pH pulses on top and bottom of PFR 1 (blue and red), and on top and bottom of PFR 2 (dark blue and dark red).

Figure 3. DCW development throughout Single-CR (filled circles), Two-CR (empty circles, A) and Three-CR (empty circles, C) experiments. Error bars: Mean ± SD (n=2). Online optical density (OD, solid line in A and C), growth rate (μ,dashed line in A and C), specific lactose consumption rate (q_S, dotted line in B and D) and specific lactic acid production rate (q_P, dashed-dotted-dotted line in B and D) during Single-CR (black), Two-CR (grey, A and B) and Three-CR (grey, C and D) fermentations. The vertical dashed line indicates the start of pH control and connection of PFR 1 in scale-down experiments (Two-CR in A and B, and Three-CR in C and D), while the vertical dotted line designates the start of manual acidic pulses at the bottom of PFR 2 (Three-CR in C and D).

Figure 4. Lactose (triangles upward), lactic acid (squares), glucose (diamonds) and galactose (triangles downward) concentration course throughout Single-CR (filled symbols in A and B with 20 $g \cdot L^{-1}$, and in C and D with 70 $g \cdot L^{-1}$ initial lactose

616 concentration), Two-CR (A and B with empty symbols) and Three-CR (C and D with
617 empty symbols) experiments.

618 **Figure 5.** Cocci chain length distribution during Single-CR (black bars), Two-CR (grey
619 and crossed bars) and Three-CR (grey and vertical-lined bars) fermentations.

620

621 **Figure S1.** Total (filled symbols) and intracellular (empty symbols) lactose (triangles
622 upward), lactic acid (squares), glucose (diamonds) and galactose (triangles downward)
623 concentration throughout Single-CR (A and B) and Three-CR (C and D) experiments.

624

Figure 1

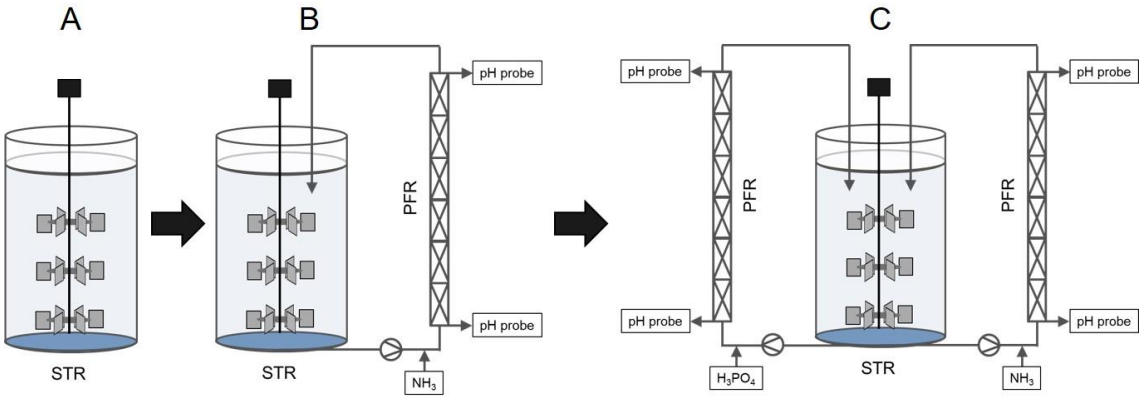

Figure 1. Single-compartment reactor (Single-CR, A) and scale-down simulators used during this work. Two-compartment reactor (Two-CR, B) and Three-compartment reactor (Three-CR, C) set up.

631 Figure 2

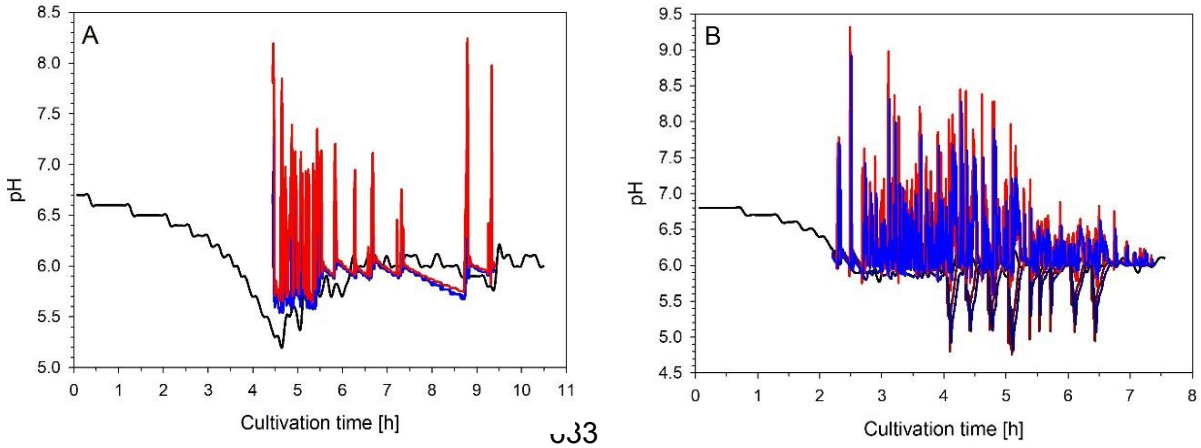

633

632

634 Figure 2. Development of the pH-value in different compartments of the scale-down
635 experiments. The pH-value in the STR (black) describes the experimental set up, in which
636 pH control was started once the pH-value dropped below 6.0. pH-values as induced in the
637 PFR during Two-CR fermentations (A), measured with two probes located at the top and
638 bottom of the PFR module (blue and red, respectively), ranged from 5.6 to 8.2. In Three-
639 CR cultivations (B), pH values ranged between 4.7 and 9.4, pH pulses on top and bottom
640 of PFR 1 (blue and red), and on top and bottom of PFR 2 (dark blue and dark red).

641

642 Figure 3

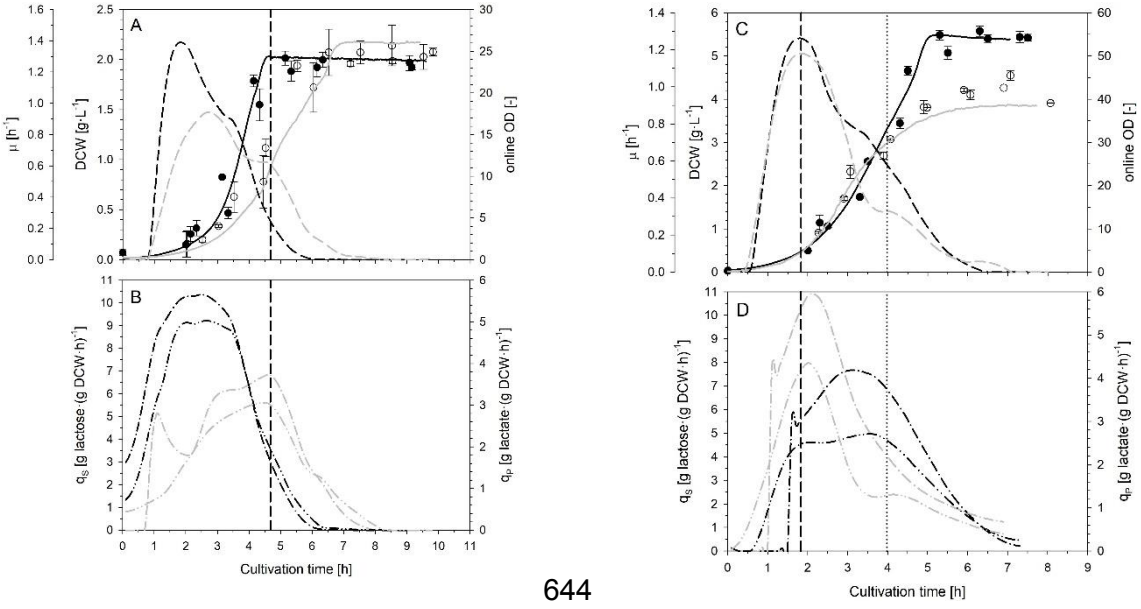

643 644

645 Figure 3. DCW development throughout Single-CR (filled circles), Two-CR (empty
646 circles, A) and Three-CR (empty circles, C) experiments. Error bars: Mean ± SD (n=2).
647 Online optical density (OD, solid line in A and C), growth rate (□,dashed line in A and
648 C), specific lactose consumption rate (qS, dashed-dotted line in B and D) and specific
649 lactic acid production rate (qP, dashed-dotted-dotted line in B and D) during Single-CR
650 (black), Two-CR (grey, A and B) and Three-CR (grey, C and D) fermentations. The
651 vertical dashed line indicates the start of pH control and connection of PFR 1 in scale-
652 down experiments (Two-CR in A and B, and Three-CR in C and D), while the vertical
653 dotted line designates the start of manual acidic pulses at the bottom of PFR 2 (Three-CR
654 in C and D).

655 Figure 4

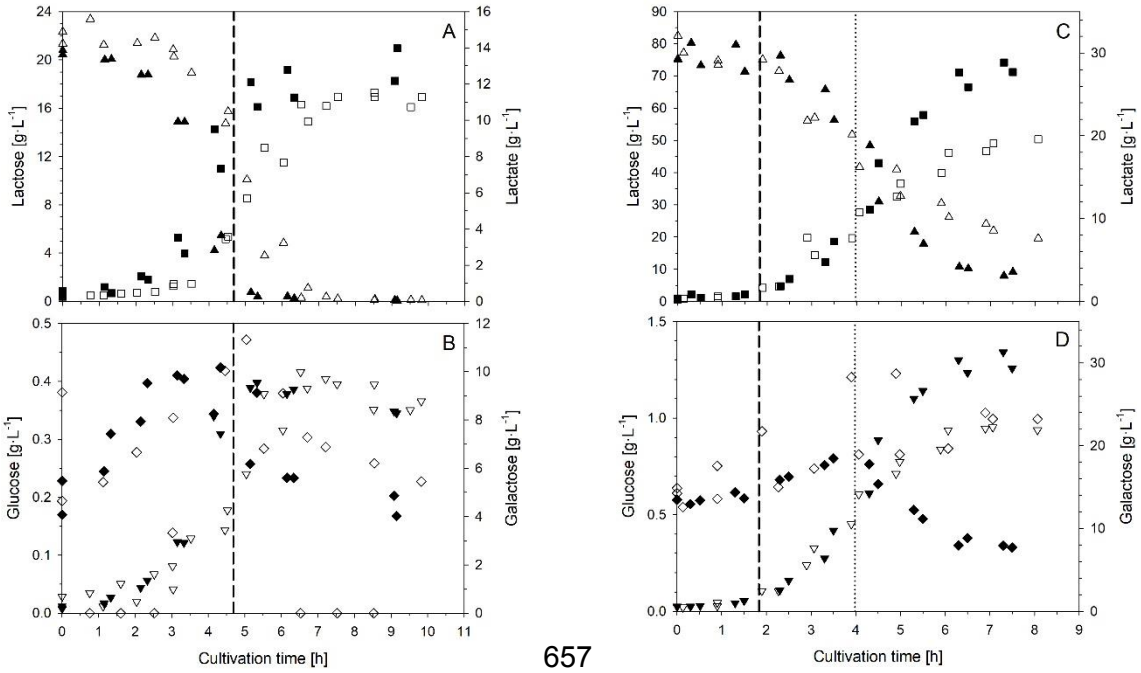

656 657

658 Figure 4. Lactose (triangles upward), lactic acid (squares), glucose (diamonds) and
659 galactose (triangles downward) concentration course throughout Single-CR (filled
660 symbols in A and B with 20 $g \cdot L^{-1}$, and in C and D with 70 $g \cdot L^{-1}$ initial lactose
661 concentration), Two-CR (A and B with empty symbols) and Three-CR (C and D with
662 empty symbols) experiments.

663

664

665 Figure 5

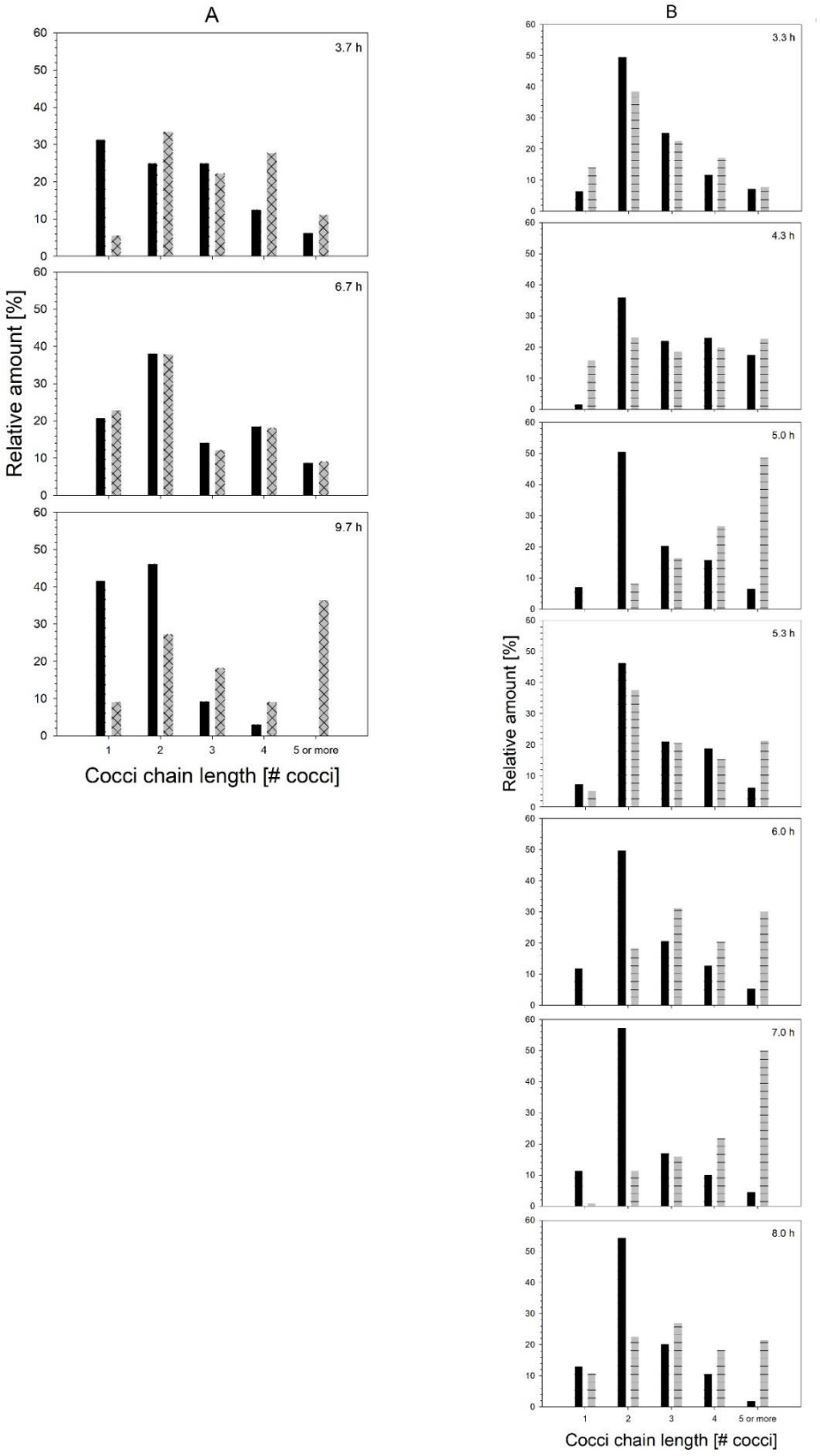

Figure 5. Cocci chain length distribution during Single-CR (black bars), Two-CR (grey and crossed bars) and Three-CR (grey and vertical-lined bars) fermentations.

679 Figure S1

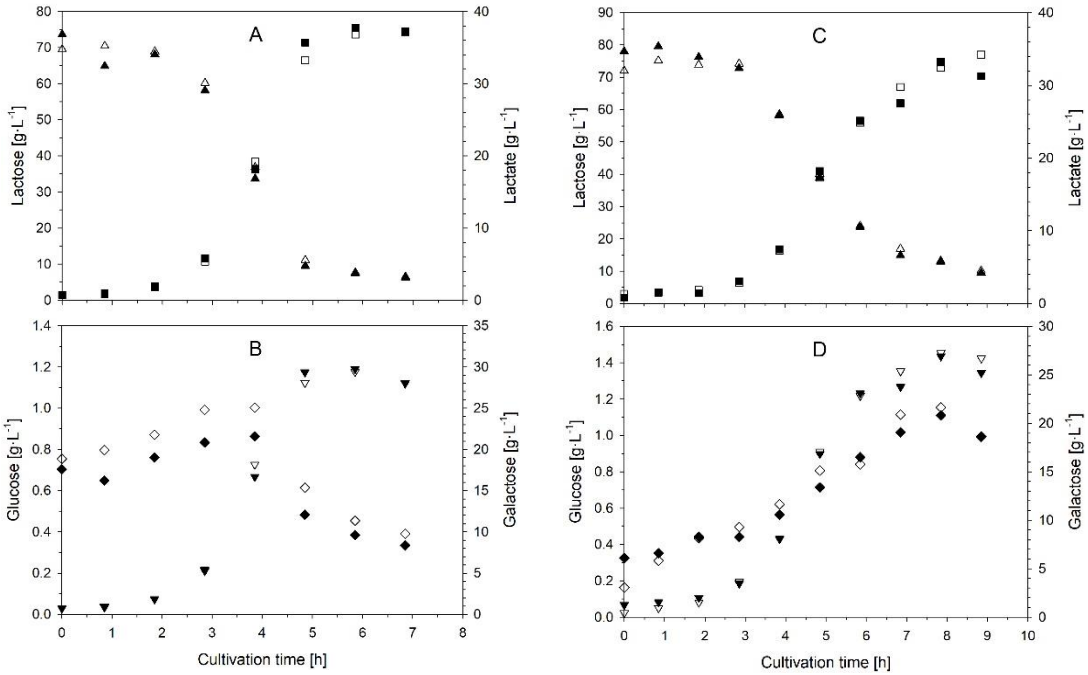

680

681 **Figure S1.** Total (filled symbols) and intracellular (empty symbols) lactose (triangles
682 upward), lactic acid (squares), glucose (diamonds) and galactose (triangles downward)
683 concentration throughout Single-CR (A and B) and Three-CR (C and D) experiments.

684

685

686

687

688

689

690

691

692

693

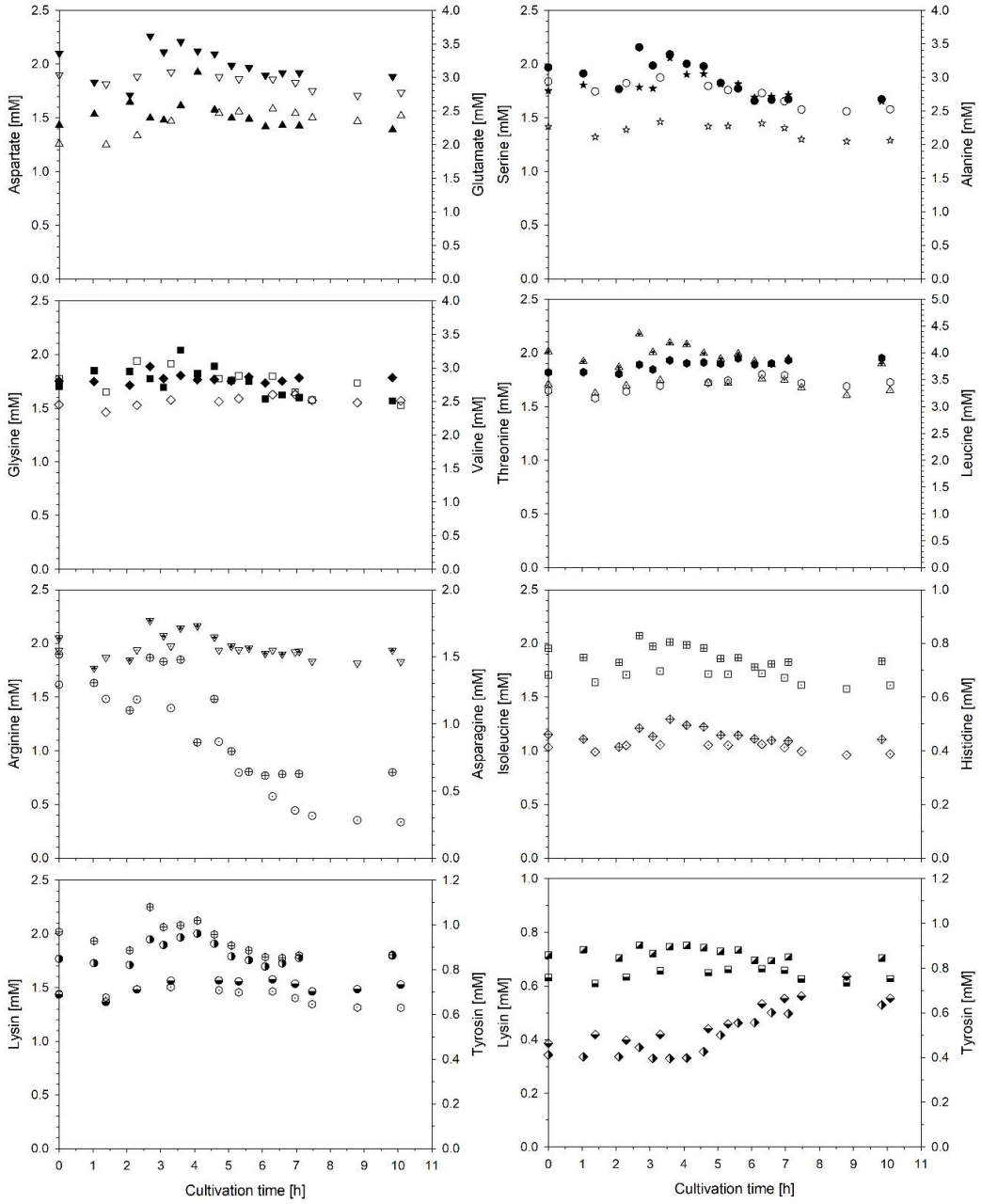

Figure S2: Development of amino acids (concentrations in mM) throughout Single-CR (filled, crossed and right filled symbols) and Two-CR (empty, dotted and bottom filled symbols) fermentations. Aspartate (upper triangles), Glutamate (downer triangles), Serine (stars), Alanine (circles), Glycine (squares), Valine (diamonds), Threonine (hexagons), Leucine (marked upper triangles), Arginine (marked lower triangles), Asparagine (marked circles), Isoleucine (marked squares), Histidine (marked diamonds), Lysin (marked hexagons), Tyrosin (semi-filled circles), Methionine (semi-filled squares) and Tryptophan (semi-filled diamonds).

V

5th Paper

Population Balance Modelling of *Streptococcus thermophilus* Based on the Cocci Chain Length Distribution for Optimization of Starter Cultures Production

KLAUS PELLICER-ALBORCH[1], ROBERT SPANN[2], FRANCESCO CRISTINO FALCO[2], PEDRAM RAMIN[2], KRIST V. GERNAEY[2], PETER NEUBAUER[1], STEFAN JUNNE[1*]

[1] Chair of Bioprocess Engineering, Department of Biotechnology, Technische Universität Berlin, Ackerstrasse 76 ACK 24, 13355 Berlin, Germany

[2]Process and Systems Engineering Center (PROSYS), Department of Chemical and Biochemical Engineering, Technical University of Denmark, Søltofts Plads Building 227 DK - 2800 Kgs. Lyngby, Denmark

Phone: +49 30 31472527

Fax: +49 30 31427577

e-mail: stefan.junne@tu-berlin.de

Keywords: bioprocess scale-down; pH gradients; population heterogeneity; single-cell size distribution; *S. thermophilus*; lactic acid bacteria; population models

Abstract

In the industrial production of starter cultures, lactic acid bacteria (LAB) are cultivated in batch bioreactors with pH control to ensure the highest yield possible, unaffordable with the natural acidification rates of theses microorganisms. Taking into account the extended mixing times and limitations in the power input, the appearance of pH gradients along the height of the fermenter is almost inevitable. Furthermore, the recent tendency towards development of dynamic growth models for bioprocesses has also attracted the interest of companies in the Food & Feed industry. Unlike chemical systems, there is no well-established thermodynamic law to define the equilibrium between liquid and biotic phases in biological processes. The authors recently applied multi-compartment scale-down approaches (STR-PFR and PFR-STR-PFR) to simulate the mentioned oscillating conditions in the lab, concluding the existence of a relationship between the reduction of growth activity and the cocci chain length distribution. In this work, these results were confirmed with single-compartment (STR) pulse feeding experiments and both scale-down strategies were compared, by means of biomass productivity as well as population heterogeneity. The nature and intensity of bioreactions are sensitive to operating conditions because the complex network of an intracellular reaction responds to external stimuli. From a modeling point of view, the most relevant difficulty is the fact that both the liquid and biotic phase mutually influence each other. This is why, apart from already predictable macroscopic variables in *Streptococcus thermophilus* fermentation, certain population classes were modeled, based on microscopic analysis of bacterial morphology under different experimental setups, inducing variable pH gradients. The cocci chain length distribution under optimal as well as scale-down conditions were successfully simulated, but parameter identifiability and model uncertainty should be performed in the future to improve output reliability.

50 *Introduction*

51 Nowadays, the *in silico* prediction of cell biomass is well investigated in bioprocesses
52 subjected to environmental oscillatory conditions (Anane, Neubauer et al. 2017, Spann,
53 Roca et al. 2018). Nevertheless, by viewing microbial populations as a homogenous
54 culture of identical cells, cell-to-cell variations and their effects on microbial population
55 dynamics are not considered. It has been proved that environmental and stochastic factors
56 lead to phenotypic heterogeneities in bioprocesses, but the impact on process performance
57 remains poorly understood (Delvigne and Goffin 2014). Moreover, the underlying
58 mechanisms are in very few cases integrated in the development of new bioprocess
59 control strategies (Müller, Harms et al. 2010), thus motivating the development of
60 experimental and mathematical models that account for cell heterogeneities (Lemoine,
61 Delvigne et al. 2017). In general, as described by (Heins and Weuster-Botz 2018),
62 population heterogeneity can be divided in two major classes: intrinsic and extrinsic. The
63 first one originates from the stochastic nature of gene expression including biochemical
64 reactions leading to anabolism and catabolism of macromolecules and their activation and
65 repression. Opposite to the extrinsic heterogeneity, the intrinsic one is not affected by
66 changing environmental conditions in a bioreactor, like gradients in substrate, pH,
67 temperature and oxygen. The second one is linked to the metabolic state of the cell and
68 variations in the amounts of intracellular compounds, e.g. copy number of regulatory
69 proteins and transcription factors, lead to stochastic growth rate fluctuations (Delvigne,
70 Zune et al. 2014).

71 The authors recently published the response of *Streptococcus thermophilus* fermentations
72 to certain pH gradients induced in scale-down bioreactors (Paper IV). Two-compartment
73 (Two-CR) and Three-compartment reactors (Three-CR), composed of a stirred tank
74 reactor (STR) connected to one or two plug flow rectors (PFR), respectively, were used

75 to induce different pH oscillations. During these experiments, a certain part of the
76 population (typically a 10 % in each PFR) was subjected to changing environmental
77 conditions, while keeping the rest (90 or 80 % in Two- and Three-CR experiments,
78 respectively) under optimal, well-mixed conditions. In this study, the authors compare
79 these results with experiments in single-compartment bioreactors (Single-CR), by means
80 of cell size or cocci chain length distribution. In this setup, a 100 % of the population
81 suffered the pH gradients induced during fermentations under pH control at different pH
82 values. When developing modeling approaches for bioprocess scale up, treating the biotic
83 phase as a population of variable physiological states is of central importance (Morchain
84 2017) and this is why cell-to-cell morphologic variations, apart from common
85 macroscopic variables (e.g. C-source or byproduct concentrations), under the different
86 scale-down conditions were considered. In fact, all data sets were used to develop a
87 population model (PM) for the *S. thermophilus* process, which aims at predicting the
88 population heterogeneity based on the pH value and pH gradients measured in the
89 bioreactor.

90 The evolution of population subsets in response to induced stresses during scale-down
91 investigations has been taken into account in recent years (Gernaey and Gani 2010,
92 Delvigne, Takors et al. 2017). On the one hand, in multi-compartment scale-down
93 experiments, only a fraction of the culture is exposed to the stress inducing agent at any
94 given time. This fraction is determined by the ratio of the STR to PFR volumes (Wang,
95 Zhao et al. 2018), representing the PFR typically a 10 % of the total bioreactor volume,
96 as mentioned before. On the other hand, in single-compartment pulse-based systems, the
97 response of the culture to the induced oscillating conditions is synchronized, without the
98 existence of population subsets. Nevertheless, within the response time of the pulses, the
99 evolution of the population in response to the stresses represents a special type of

100 population heterogeneity that can be followed with advanced process analytical
101 technology (PAT), such as high-resolution online microscopy (Marbà-Ardébol,
102 Emmerich et al. 2018) or automated flow cytometry (Delvigne and Goffin 2014). The
103 two recent reviews by (González-Cabaleiro, Mitchell et al. 2017) and (Delvigne, Baert et
104 al. 2017) give important bases of the mathematical formulations to describe microbial
105 populations and the tools available to measure/analyze the existence of sub-groups.

106 (Zamamiri, Zhang et al. 2002) highlighted that a drawback of PM is, besides solving the
107 resulting partial differential integral equations, the determination of population
108 parameters. In order to improve the fundamental understanding on microbial population
109 dynamics, methods, which provide information about the physiological state of the single
110 cell, are required. In this work, cell morphology was selected as physiological
111 characteristic of “healthy” and “stressed” bacteria.

112 *Materials and methods*

113 *Bacterial strain and media*

114 The strain of *S. thermophilus* was provided by Chr. Hansen A/S (Hoersholm, Denmark)
115 and used throughout the whole study. In all Single-CR cultivation experiments, a self-
116 established De Ma, Rogosa and Sharpe (MRS) medium was used, containing (per litre):
117 73.7 g lactose monohydrate (Carl Roth, Karlsruhe, Germany), 10 g casein hydrolysate
118 (Chr. Hansen A/S, Hoersholm, Denmark), 12 g yeast extract (Chr. Hansen A/S,
119 Hoersholm, Denmark), 2 g K_2HPO_4 (Carl Roth, Karlsruhe, Germany), 3 g sodium acetate
120 anhydrous (Carl Roth, Karlsruhe, Germany), 2.4 g tri-sodium citrate dihydrate (Carl Roth,
121 Karlsruhe, Germany), 0.2 g $MgSO_4 \cdot 7H_2O$ (Carl Roth, Karlsruhe, Germany) and 0.05 g
122 $MnSO_4 \cdot H_2O$ (Carl Roth, Karlsruhe, Germany).

123 *Cultivation conditions*

124 For all experiments, a 1 L stirred tank glass bioreactor (Multifors, Infors HT, Bottmingen,
125 Switzerland) equipped with two Rushton turbine impellers, baffles, a pH probe
126 (EasyFerm, Hamilton, Darmstadt, Germany) and an exhaust gas analyzer All-in-One
127 (BlueSens, Gas Sensor GmbH, Herten, Germany) was used. Firstly, the bioreactor was
128 assembled, then the medium components without lactose and dissolved in 0.7 L distilled
129 water were added. The amount of lactose was dissolved in 0.3 L of distilled water and
130 transferred to a 0.5 L bottle. The filled reactor was connected to an empty glass bottle as
131 well as to the lactose bottle via hose pumps. The whole system was sterilized in an
132 autoclave at 121 ºC for 20 minutes. After sterilization and temperature decrease, the
133 whole lactose solution was pumped into the reactor and the empty flask was filled with
134 NH_3 25 % (v/v) (VWR Chemicals, Radnor, USA). The liquid was then sparged with N_2
135 until the O_2 concentration detected in the outgas analyzer was below 0.1 %. Subsequently,
136 a pulse of CO_2 was given until a CO_2 concentration of 1-3 % was detected in the outgas

analysis. 0.01 % v/v of the concentrated inoculum (12 mL direct inoculation material (DIM), stored at -80 ºC and provided by Chr. Hansen A/S, Hoersholm, Denmark) was used to inoculate all bioreactors. The tube was thawed on ice and 100 µL of cells were suspended in 1 mL MRS medium without carbon source to ease the transfer of the entire inoculation volume. After inoculation under sterile conditions through a septum, the agitation speed was kept at 200 rpm and the temperature at 40 °C throughout all fermentations. The pH control was set at pH 6, after the pH dropped below that value for the first time, using 25 % NH_3 (v/v) (VWR chemicals, Radnor, USA). At the same moment, a feeding profile was started (see Supplementary material). Basic pH shifts were induced by pulse-based feeding of this base, whilst the pH diminished via natural acidification of the bacteria. The feeding profile was implemented into the bioprocess platform eve® (Infors HT, Bottmingen, Switzerland) as an individual feeding profile. The profile included the setpoints for the desired ΔpH, which are summarized in Table 1. In order to achieve a faster increase of the pH during a pulse, an output setpoint was included, which was 0.2 pH units higher than the actual maximum pH value desired.

Table 1. Summary of pulse-feeding scale-down experiments with different pH gradients (ΔpH). NH_3 25 % v/v was introduced by the controller until the upper pH setpoint was reached. The culture broth was then allowed to decrease the pH due to lactic acid production until the lower pH setpoint was accomplished. For more information see Figure 4 and Supplementary material.

ΔpH	pH_{max}	pH_{min}	Pulses
0 (optimal conditions)	6.0	6.0	0
1.5	7.0	5.5	5
1.8	7.3	5.5	4
2.0	7.0	5.0	2
2.5	8.0	5.5	2

Analysis

Cell growth was monitored off line with appropriately diluted samples at a wavelength of 600 nm (OD600) with an Ultraspec 2100 *pro* UV/Visible spectrophotometer (Amersham Biosciences, Amersham, UK). For dry cell weight (DCW) determination, 2 mL of cell suspension were pipetted into a previously dried and weighted 2 mL Eppendorf tube. Samples were centrifuged at 4 ºC and 15,000 rpm for 10 minutes. The supernatant was discarded, whilst the cell pellet was washed with 1 mL of 0.9 % (w/w) NaCl solution. After a second step of centrifugation, the Eppendorf tube containing the washed cells was dried at 75 ºC for 24 hours and weighted again. The DCW was then calculated as the difference between the tube with sample and its tare. Samples for extracellular metabolite and free amino acid concentration were filtered through a membrane filter with a pore size of 0.8 μm (Carl Roth, Karlsruhe, Germany) directly at the sampling port of the bioreactor. The filtrate was transferred to a 1.5 mL Eppendorf tube and immediately stored at -80 ºC.

Quantification of metabolites

Extracellular organic acids and sugars were quantified with an Agilent 1200 HPLC system (Agilent Technologies, Santa Clara, USA) equipped with a refractive index detector (RID) and a HyperRez^{TM} XP Carbohydrate H^+ column (300x7.7 mm, 8 μm) (Fisher Scientific, Schwerte, Germany) using 5 mM H_2SO_4 at a flow rate of 0.5 mL·min^{-1} and a temperature of 65 ºC. Prior to analysis the samples were thawed on ice and diluted

¼ with H_2O to a final volume of 200 µL. Subsequently, the HPLC vials (VWR, Radnor, USA) were prepared with a 200 µL micro-insert (VWR, Radnor, USA) and the diluted samples were transferred into the vials.

Microscopic-based image analysis

1 mL sample was taken directly from the bioreactor into a 1.5 mL Eppendorf tube and 10 µL were pipetted on a microscopic slide (VWR chemicals, Radnor, USA). The slide was then covered with a cover glass of thickness No. 1.5 (VWR chemicals, Radnor, USA) and placed under the microscope (CN-hFT, Hertel & Reuss, Kassel, Germany) with 100x oil immersion objective. The images were taken with a digital camera (Canon Power Shot G1X, Canon, Tokyo, Japan) with 4-times magnification. Images were stored as TIFF without compression as 8-bit images with 256 possible shades of grey (2^8 combinations in binary code). The median grey value of each image set was calculated using ImageJ (ImageJ version 2.0.0), which was used to quantify the background. Afterwards, the background pixels were subtracted from each image (step also called segmentation) within a set (Wu, Merchant et al. 2010). The Cell Profiler software (Cell Profiler version 2.1.0) was implemented to identify the cocci chains of *S. thermophilus*, to segment them into individual cocci and to measure the maximal axis length and area. Finally, the chain length distribution throughout the cultivation time was calculated. More information regarding the image processing with ImageJ can be found in (Sage, Prodanov et al. 2012) and further information concerning the cell identification with Cell Profiler can be found in (Carpenter, Jones et al. 2006).

Data fitting and visualization

In order to calculate rates, data were fitted to a Smoothing Spline with the fitting toolbox of MATLAB R2013b (The MathWorks, Natick, MA). Concentrations were then obtained

every desired interval of time. All data plots were created with SigmaPlot version 11.0 (Systat Software, San José, CA).

Statistical analysis

Data were expressed as mean standard deviation (SD) for the description of reproducibility. Biological replicates were performed as fermentations under identical conditions. The coefficient of variation (CV%) was then calculated using Equation 1:

$$CV\% = \frac{SD}{Mean} \cdot 100 \quad (1)$$

Population model

The dynamic biokinetic model of (Spann, Roca et al. 2018) was used as the basis for the PM. This model originally described the evolution of state variables such as biomass, lactose, and lactic acid throughout the *S. thermophilus* fermentation. Importantly, the biomass growth rate was modelled as a function depending on the lag-time (f_{lag}), lactose inhibition and limitation (f_S), lactate inhibition (f_P), and the pH (f_{pH}) (Eq. 1). It is worth mentioning, that the lactose consumption is the sum of the biomass growth and the lactic acid synthesis rate, considering the complete secretion of galactose, since the studied strain metabolizes only glucose and secretes galactose under the present cultivation conditions. The model was implemented and solved in MATLAB® (The MathWorks®, Natick, MA) using the solver ode15s and discarding the mixed weak acid/base model of the original publication, since the pH value at each available timepoint is used as input variable for the model.

$$\frac{dX}{dt} = \mu = \mu_{max} \cdot f_{lag} \cdot f_S \cdot f_P \cdot f_{pH} \cdot f_{pHmin} \cdot X =$$

$$= \mu_{max} \cdot \left(1 - e^{-\frac{t}{t_{lag}}}\right) \cdot \left(\frac{S}{S+K_S+\frac{S^2}{K_I}}\right) \cdot \left(\frac{1}{1+e^{K_P \cdot (P-K_{P1})}}\right) \cdot \left(e^{-\left(\frac{\left(pH_{opt}-pH\right)^2}{\sigma_{pH}^2}\right)}\right) \cdot \left(1 - \frac{10^{pH_{min}}}{10^{pH}}\right) \cdot X \quad (1)$$

In this study, the population heterogeneity is assessed by means of different morphologies of the lactic acid bacteria (LAB) under certain pH gradients. As explained in more detail afterwards, rates of conversion (elongation or separation) between bacteria of different morphologies (namely "natural" and "abnormal" cells) are suggested. Furthermore, three model assumptions are contemplated: (i) every coccus has the same size (i.e. volume, shape, circularity, etc.), as observed under the microscope, (ii) there is either one elongation or separation event at a time and (iii) the elongation as well as separation rates are affected by the pH gradients (ΔpH) faced. The event rates are defined by Eq. 2-6.

$$r^{NE,1c} = k^{NE} \cdot \mu \cdot C_{1c} \quad (2)$$

$$r^{LAE,i} = k^{LAE} \cdot \mu \cdot C_i \qquad i \in 2c \text{ and } 3c \quad (3)$$

$$r^{HAE,j} = k^{HAE} \cdot \mu \cdot C_j \qquad j \in 2c, 3c \text{ and } 4c \quad (4)$$

$$r^{S,k} = k^{S} \cdot \mu \cdot C_k \qquad k \in 2c, 3c \text{ and } 4c \quad (5)$$

$$r^{S,5+c} = k^{S,5+c} \cdot \mu \cdot C_{5+c} \quad (6)$$

where "NE" accounts for "natural elongation", "LAE" accounts for "light abnormal elongation" (i.e. event where a chain elongates simultaneously from both opposed poles), "HAE" accounts for "heavy abnormal elongation" (i.e. event where only one of the extremes of the cell elongates) and "S" accounts for "separation". Moreover, 1c, 2c, 3c, 4c and 5^+c stand for 1-, 2-, 3-, 4- and 5 or more cocci chains, respectively. What is more, 1c and 2c chains were considered "natural" cell sizes, while 3c, 4c and 5^+c chains were assessed as "abnormal" morphologies, based on observations under the microscope when *S. thermophilus* were subjected to variable pH-gradients.

The variation of a population with a certain morphology over time depends on (i) the conversion of other cells to this chain length, (ii) its own evolution to the other morphologies and (iii) its own growth during the process. With this, the ordinary differential equations (ODEs) are defined for the system (Eq. 7-11), where the growth rate is calculated based on Eq. 1 from (Spann, Roca et al. 2018). Importantly, here solely the conversion rates constants (k^{NE}, k^{LAE}, k^{HAE}, k^{S} and $k^{S,5+c}$) are considered as parameters to be estimated, while the rest of parameters are taken from the original publication. Since each initial data set (i.e. fermentation) possesses a different lag phase, the experimental data was normalized prior to be used as input for the model. Additionally, the pH value is the only input variable, as commented before, since it is measured during the process or experiment. This means, that the model simulates the state variables at each pH value available from the online sensor (every 1 or 5 minutes in single- or multi-compartment scale-down experiments, respectively).

$$\frac{dC_{1c}}{dt} = r^{S,2c} + \frac{1}{3}\cdot r^{S,3c} + \frac{1}{4}\cdot r^{S,4c} + \frac{1}{5}\cdot r^{S,5+c} - r^{NE,1c} + \mu \cdot C_{1c} \quad (7)$$

$$\frac{dC_{2c}}{dt} = \frac{2}{3}\cdot r^{S,3c} + r^{S,4c} + \frac{2}{5}\cdot r^{S,5+c} - r^{S,2c} + r^{NE,1c} - r^{LAE,2c} - r^{HAE,2c} + \mu \cdot C_{2c} \quad (8)$$

$$\frac{dC_{3c}}{dt} = \frac{3}{4}\cdot r^{S,4c} + \frac{3}{5}\cdot r^{S,5+c} - r^{S,3c} + r^{HAE,2c} - r^{LAE,3c} - r^{HAE,3c} + \mu \cdot C_{3c} \quad (9)$$

$$\frac{dC_{4c}}{dt} = \frac{4}{5}\cdot r^{S,5+c} - 2r^{S,4c} + r^{LAE,2c} + r^{HAE,3c} - r^{HAE,4c} + \mu \cdot C_{4c} \quad (10)$$

$$\frac{dC_{5+c}}{dt} = -2r^{S,5+c} + r^{LAE,3c} + r^{HAE,4c} + \mu \cdot C_{5+c} \quad (11)$$

Summarizing, the population model has five parameters to be estimated (k^{NE}, k^{LAE}, k^{HAE}, k^{S} and $k^{S,5+c}$) and needs the pH value as input variable.

Parameter estimation

The parameter estimation was performed to fit the experimental cell size distribution (i.e. 1-, 2-, 3-, 4- and 5 or more cocci throughout the experiment or data set) using the methodology from (Sin and Gernaey 2016), as described in (Spann, Roca et al. 2017).

The parameter estimation was conducted in MATLAB R2013b (The MathWorks, Natick, MA) with the nonlinear least-squares solver (lsqnonlin). In the objective function, the weighted error of the model predictions was calculated for the five populations (namely 1c, 2c, 3c, 4c and 5^{+}c) at all measured time points i (Eq. 12). The residuals vector then contained the weighted error vectors of the five states j.

$$Error_i = \left| \frac{\hat{y}_i - y_{measured,i}}{w_j} \right| \quad (12)$$

where w_j is the maximum value of each specific component. Furthermore, the uncertainty of the estimated parameters was quantified with the relative error (RE) between the standard deviation of the parameter estimate with respect to the estimated mean value (Eq. 13).

$$RE_i = \frac{\sigma_{\hat{\theta}_i}}{\hat{\theta}_i} \quad (13)$$

Initial conditions

If not otherwise stated, the initial conditions were taken from (Spann, Roca et al. 2018). Importantly, all the parameters of the mixed weak acid/base model were discarded, because the pH was measured in-line and used as an input variable for the model. The initial lactose concentration was calculated as the mean value between the HPLC results of the first two data points of each experiment. Since all cultivations were normalized by their lag-phase a t_{lag} of 0.38 h for all model predictions was taken. The minimum pH value needed to ensure cell growth (pH_{min}) was 4.8, which was experimentally calculated after carrying out a fermentation without pH control (Figure S1). Finally, the initial parameter values for completing Eq. 1 were taken from the original publication, while the initial parameter estimates for the PM were calculated as one third of the sum of their correspondent lower and upper value (see Table S1).

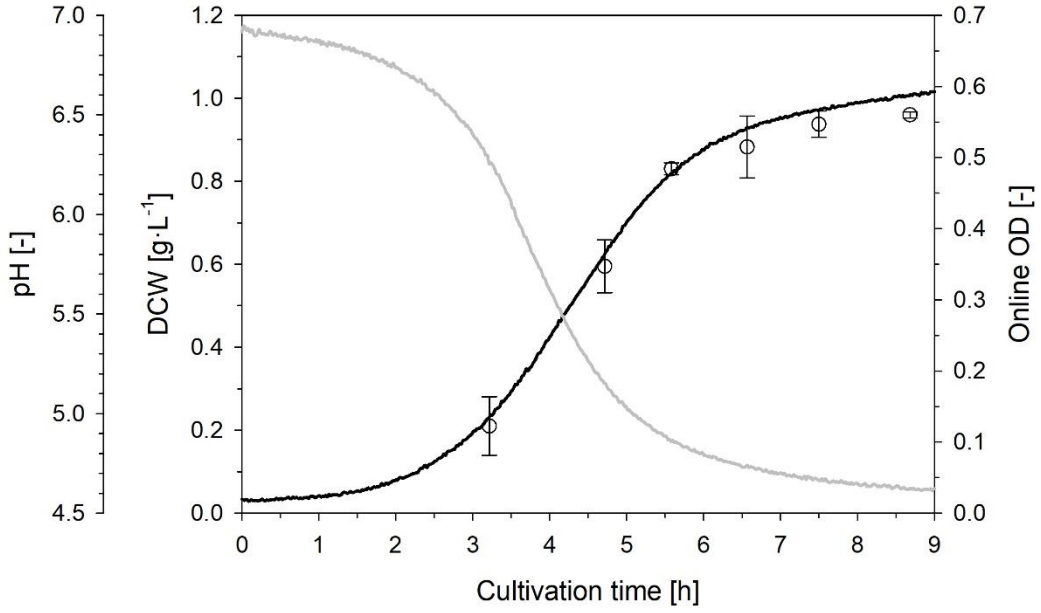

Figure S1. Evolution of the biomass (empty dots), online OD (black line) and pH (grey line) throughout a *S. thermophilus* fermentation without pH control. Error bars: Mean ± SD (n = 2).

Table S1. Initial parameter estimates for the population model, based on expert knowledge.

Kinetic parameter	Initial value	Lower bound	Upper bound
k^{NE}	333.3	0.00001	1000
k^{LAE}	66.7	0.00001	200
k^{HAE}	133.3	0.00001	400
k^{S}	333.3	0.00001	1000
$k^{S,5+c}$	133.3	0.00001	400

Assessment of the model fit

The goodness of fit for the model prediction in the model validation procedure was assessed with the root mean sum of squared errors (RMSSE) and calculated with Eq. 14.

$$RMSSE = \sqrt{\frac{1}{n}\sum_{i}^{n}\left(y_{measured,i} - \hat{y}_i\right)^2} \quad (14)$$

317 *Results and discussion*

318 *Pulse-feeding scale-down simulators*

319 In this study, biological duplicates of Single-CR cultivations with variable pH gradients
320 (namely ΔpH 1.5, 1.8, 2.0 and 2.5) were compared with fermentations under optimal
321 conditions (i.e ΔpH = 0). The pH development throughout these experiments is
322 summarized in Figure 1. The culture broth was allowed to reach pH 6 due to high lactic
323 acid production and the base feeding profile (see Supplementary material) was then
324 started. Basic pulses were induced with NH_3 25 % v/v addition, while acid stress was
325 accomplished by letting the bacteria decrease the pH through own lactic acid production.
326 In contrast with (Paper IV), in this work the basic excursions were performed through a
327 programmed feeding profile to reach the desired alkaline pH value. Once this was
328 accomplished, the media pH was allowed to decrease until the desired acidic pH value
329 through natural lactic acid production from the LAB, when a new ammonia pulse started
330 (Figure 1). Therefore, as seen in the pH development during the different experiments, *S.*
331 *thermophilus* was exposed to less than 6 pH perturbations when the smallest ΔpH was
332 induced (Table 1), while in the real industrial pH control scenario, alkali additions are
333 notably more frequent (Spann, Glibstrup et al. 2018) and, in fact, (Paper IV) aimed at
334 resembling. These are two completely different scenarios, which induced different stress
335 responses as well as yield losses in other microorganisms (Cortés, Flores et al. 2016,
336 Brunner, Braun et al. 2017), but were never studied in LAB. In the current industrial
337 process, only base is introduced to compensate the metabolic lactic acid synthesis of *S.*
338 *thermophilus* and thus, no manual acid pulses were induced during Single-CR scale-down
339 experiments. On the contrary, throughout the scale-down fermentations carried out by
340 (Paper IV), acid pulses with phosphoric acid were induced when using the Three-CR
341 approach. Importantly, when compensating base pulses with the addition of an acid,

342 cellular responses to increased osmolarity may arise (Osman, Birch et al. 2002) and this
343 was another reason why acid pulses were avoided in this study.

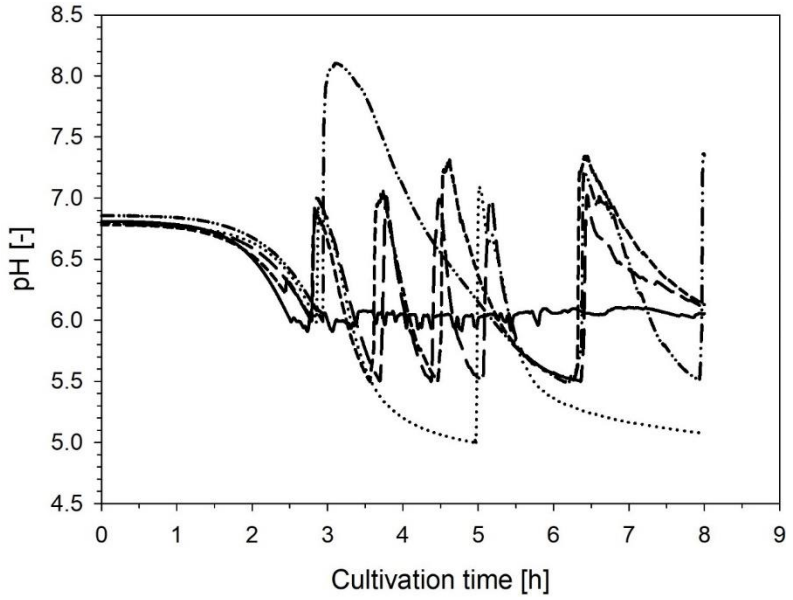

344

345 Figure 1. Evolution of the pH value during Single-CR experiments with pH gradients
346 (ΔpH) of 0 (solid line), 1.5 (long dashed line), 1.8 (short dashed line), 2.0 (dotted line)
347 and 2.5 (dashed-dotted-dotted line).

348

349 *Growth, main carbon metabolism and cocci chain length distribution*

350 The influence of different pH shifts on *S. thermophilus* 1 L batch fermentations in Single-
351 CR scale-down bioreactors with pulse-based feeding of ammonia was assessed by means
352 of biomass growth (Figure 2), main carbon metabolites (Figure 3) and cocci chain length
353 distribution (Figure 4). The results are then compared with multi-compartment scale-
354 down studies performed previously (Paper IV).

355 Under standard conditions, the stationary phase was entered after 6-7 h reaching a final
356 DCW of 6.4 $g \cdot L^{-1}$. This is in accordance with fermentations carried out with the same
357 inoculum and initial lactose concentration in the 10 L scale (Paper IV). Moreover, the
358 higher the ΔpH, the higher the biomass productivity loss, i.e. the lower the final DCW

(Figure 2A), resulting in a 48.5 % biomass loss in the worst-case scenario with a ΔpH of 2.5. Importantly, in Single-CR systems, these pH gradients are experienced by the whole cell population (100 %), while a certain percentage of the biomass is really subjected to oscillating environmental conditions in the large scale, scenario better simulated in multi-compartment systems, where 10 or 20 % of the bacteria are under an induced stressed during Two- or Three-CR setups, respectively (Paper IV). This is why it was expected that the pH shifts induced in this work promote higher biomass productivity losses than multi-compartment experiments. Furthermore, the maximum growth rate (μ_{max} = 1.2 h^{-1}) under optimal conditions (Figure 2B) was also in accordance with the same experiments in the 10 L scale, published before. Interestingly, the first pH gradients induced (i.e. ΔpH = 1.5), were affecting the maximum growth rate value but not the slope of decrease of the growth rate over time. From ΔpH = 1.8 on, the higher the pH gradient, the more pronounced the decline of the growth rate. It is worth mentioning, that small growth increases were detected in experiments with ΔpH = 2.0 as well as 2.5, which correspond to the timepoints where base pulses occurred or the pH value was next to the optimal point. These observations support the hypothesis made by (Paper IV), that *S. thermophilus* growth is more sensible to an acidic environment than to higher pH values. This is mainly due to stress responses from the LAB to an increasing amount of extracellular non-dissociated lactic acid at low pH, which try to maintain the intracellular pH (pH_i) at the expense of ATP (Ramos, Thorsen et al. 2014, Papadimitriou, Alegría et al. 2016).

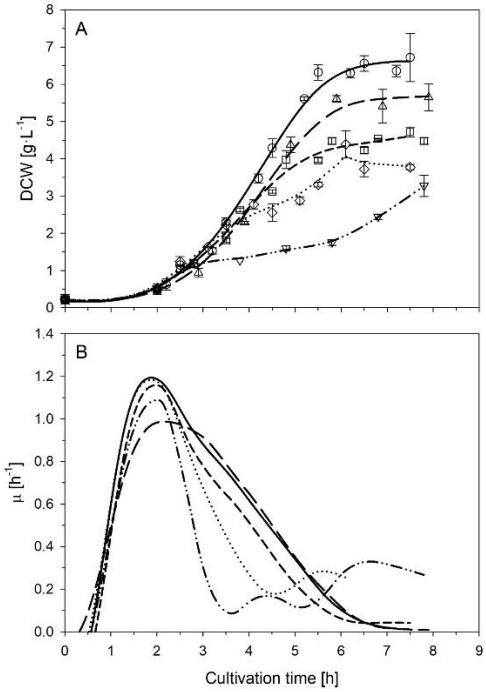

Figure 2. Development of the biomass (A) and the growth rate (B) throughout pulse-feeding scale-down experiments in biological duplicates with a ΔpH of 0 (open circles and solid lines), 1.5 (open triangles up and long dashed lines), 1.8 (open squares and short dashed lines), 2.0 (open diamonds and dotted lines) and 2.5 (open triangles down and dashed-dotted-dotted lines). Error bars: Mean ± SD (n = 3).

Regarding the development of metabolites over time (Figure 3), the fermentation under standard conditions showed a constantly decreasing lactose concentration, but without a depletion of the carbon source (Figure 3A). This is also in accordance with previous experiments (Paper IV), where the main nutrient is not completely consumed even under optimal conditions because of by-product accumulation (i.e. high lactic acid concentration in the media). Moreover, the higher the pH shift, the more lactose remained unconsumed in the medium at the end of the fermentation. Galactose and lactate accumulated almost on parallel, with more lactate production as well as a higher galactose

excretion with a lower pH gradient (Figure 3B and 3D, respectively). Importantly, glucose accumulated under strong ΔpH, when compared to the glucose concentration over time throughout fermentations under optimal conditions (Figure 3C). Under standard conditions (i.e. ΔpH = 0) and for ΔpH = 1.5, the glucose concentration was incorporated again after 4-5 h of cultivation, whereas for a higher ΔpH, it rather increased. That resulted in an accumulation of glucose in the medium up to 1.8 $g \cdot L^{-1}$ for ΔpH = 1.8 and even 5.2 $g \cdot L^{-1}$ for ΔpH = 2.5, which indicates an influence of oscillating pH on the glycolysis. This observation was already commented in the previous publication (Paper IV) and here the effect of pH gradients on the glycolytic pathway was confirm, probably on the first step of phosphorylation of the glucose moiety (Jin, Qin et al. 2015).

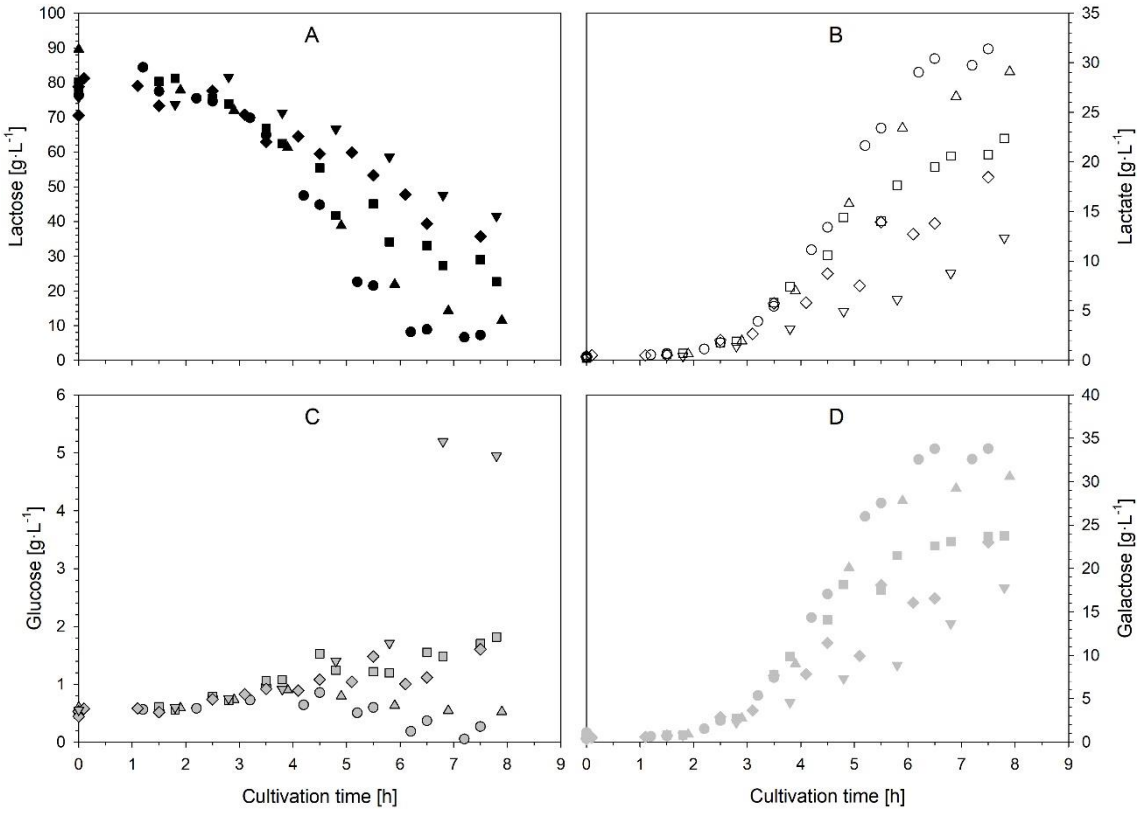

Figure 3. Metabolites' development during Single-CR experiments under different pH gradients: 0 (circles), 1.5 (triangles up), 1.8 (squares), 2.0 (diamonds) and 2.5 (triangles down). Lactose (A, black filled symbols), lactate (B, empty symbols), glucose (C, grey

409 filled and black edged symbols) and galactose (D, grey filled and edged symbols)
410 concentrations over time.

411

412 Under standard conditions with a controlled pH, the cocci chain length distribution was
413 more homogenous compared to oscillating conditions (Figure 4). As seen in Figure 4F,
414 diplococcic chains represented the major part from the population towards the end of the
415 fermentations, whilst long chains (i.e. of 5 or more cocci, 5^{+}c) disappeared almost
416 completely after 6 h of experiment. Initially longer chains (3 and 4 cocci chains, 3c and
417 4c, respectively) evolved to single- (1c) and two- (2c) cocci chains, possibly because of
418 a higher activity of the endopeptidase enzyme responsible for cell separation in *S.*
419 *thermophilus* (Layec, Gérard et al. 2009). Under oscillating pH conditions, a broader
420 distribution of the cocci chain length with longer chains becoming more relevant was
421 observed (Figure 4A-E). As an example, after the first base pulse in the cultivations with
422 ΔpH = 1.5 (Figure S2-A), the population consisted of mainly longer chains with 48 % of
423 the biomass with five or more cocci (5^{+}c) and a reduction in diplococcic chains (2c)
424 compared to conditions with the pH controlled at 6 (Figure 4F). The second pulse led to
425 a distribution with two (2c), three (3c) and four cocci (4c), where they represented about
426 80 % of the population. The next sample was taken before the fourth base pulse, when
427 the broth pH was 5.6. At that timepoint, an increase of single cocci (1c) up to 21 % was
428 observed. While single cocci (1c) and diplococcic chains (2c) decreased half an hour later,
429 especially chains of four (4c) and larger cocci (5^{+}c) increased up to 20 % and 40 %,
430 respectively, at a pH of 6. Further samples were all taken at pH 6 or higher, showing the
431 predominance of longer chains of four and longer cocci chains. In summary, high pH
432 pulses resulted in rather longer chains, while at a lower pH a trend towards smaller chains
433 was detected (Figure S2). This is in accordance with previous results with multi-

compartment scale-down experiments (Paper IV). More precisely, the amount of single cocci (1c) as well as chains of five or more cocci (5^{+}c) seemed to be good indicators of the influence of pH shifts, when compared to optimal conditions.

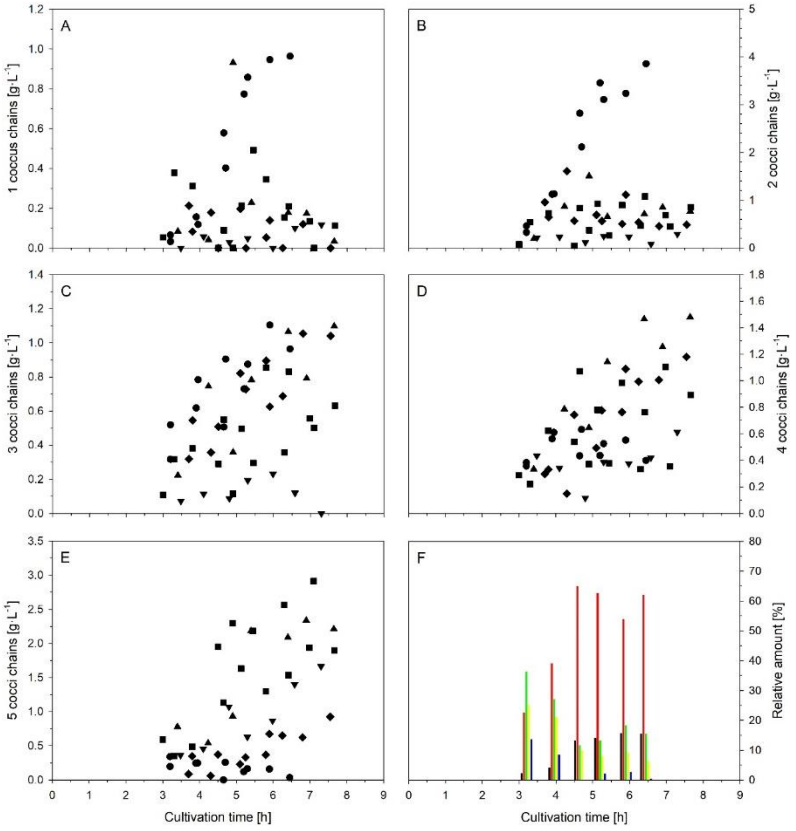

Figure 4. Cell size distribution evolution during Single-CR experiments under different pH gradients (A-E): 0 (circles), 1.5 (triangles up), 1.8 (squares), 2.0 (diamonds) and 2.5 (triangles down). The amount of cocci per chain (in $g \cdot L^{-1}$) were calculated from the cocci chain length distribution (F, example for $\Delta pH = 0$) and the biomass at the same timepoint. Relative amount of one coccus (black bars), two (red bars), three (green bars), four (yellow bars) and five or more (blue bars) cocci chains over time. For information regarding the experiments with induced pH gradients, see Figure S2.

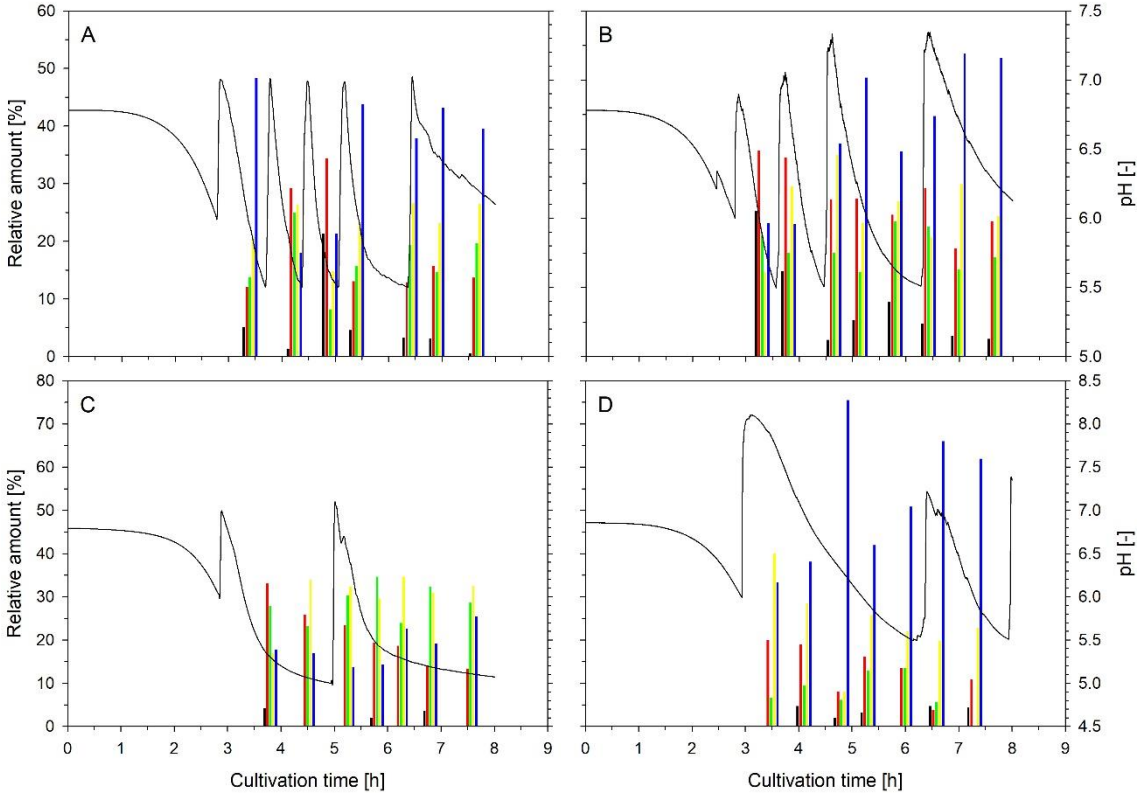

Figure S2. Development of the pH (solid black line) and the cocci chain length distribution (vertical colored bars) throughout Single-CR scale-down fermentations with ΔpH = 1.5 (A), 1.8 (B), 2.0 (C) and 2.5 (D). Relative amount of one coccus (black bars), two (red bars), three (green bars), four (yellow bars) and five or more (blue bars) cocci chains.

Population modeling

(Spann, Roca et al. 2018) originally used the mixed weak acid/base model to predict the pH development during a fermentation, but it is one of the few critical process parameters (CPP) available during the industrial scale process and therefore it was suggested to use it as input variable. In contrast to (Spann, Roca et al. 2018), the PM developed here needed to be able to model the state variables in strong acidic conditions. This is why an additional term in the calculation of the growth rate (Eq. 1) was included, which depends

459 on the minimum pH value needed for the cells to grow (f_{pHmin}). This additional parameter
460 was experimentally calculated by performing a fermentation without pH control and
461 identifying the pH value at which growth ceased (Figure S1). The term included in the
462 original calculation of μ represents a logarithmic decay towards acidic environments (Eq.
463 15).

464 $$f_{pHmin} = 1 - \frac{10^{pHmin}}{10^{pH}} \quad (15)$$

465 Moreover, a new parameter estimation from the original parameter set was not necessary,
466 since the same strain, with the same media components were used and because only
467 cultivations where the macroscopic variables were accurately fitted (RMSSE < 0.6 $g \cdot L^{-1}$
468 for biomass) were used for the parameter estimation in the PM.

469 Based on previous results (Paper IV) and experiments performed in this work, the cell
470 morphology of *S. thermophilus* was differentiated between "natural" and "abnormal"
471 cocci chain lengths. Here, on the one hand, two- as well as four-cocci chains were
472 suggested as "natural" morphologies, which are the most relevant cell sizes detected
473 under optimal growth conditions. On the other hand, one-, three-, five-cocci and longer
474 chains were proposed as "abnormal" cell sizes, which predominate when the culture broth
475 is subjected to variable pH oscillating environments. What is more, based on the cell
476 division process of these LAB, chains are continuously being elongated and separated
477 during growth and therefore also a discretization between "natural" as well as "abnormal"
478 events (i.e. elongation and separation) needs to be taken into account. With all these
479 hypotheses, a scheme summarizing the rates of conversion between the different
480 morphologies of the whole population considered was proposed (Figure 5).

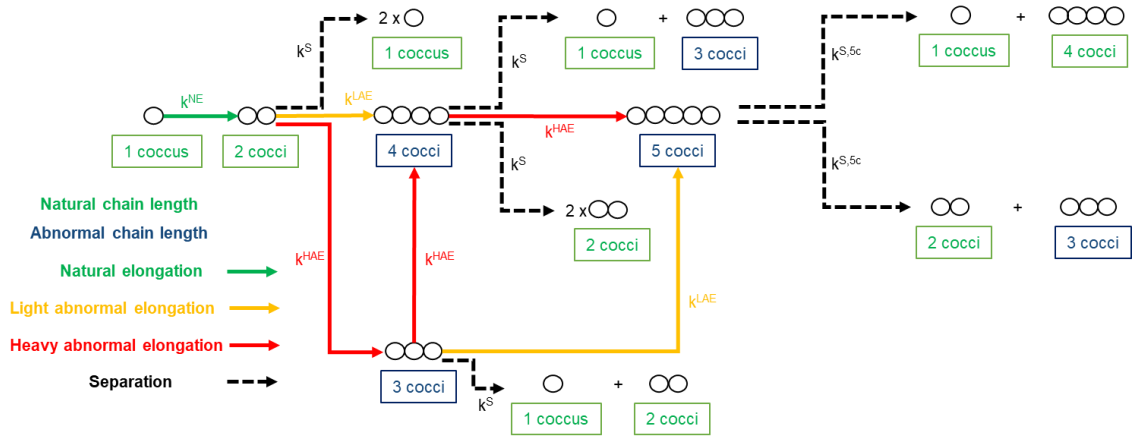

Figure 5. Scheme of the *S. thermophilus* populations considered in the PM based on authors' observations during fermentations under optimal as well as oscillating pH conditions. One, two- and four-cocci chains are considered "natural" morphologies (in green), while three- and five-cocci or more chains are regarded as "abnormal" cell sizes (in blue). Additionally, separation (S, dashed black lines) was considered to be equal among populations, except for the longest cocci chains (S,5c). The elongation term was separated into "natural" (NE), "light abnormal" (LAE) and "heavy abnormal" events (HAE) depicted with green, orange and red arrows, respectively.

The PM parameters (namely, k^{NE}, k^{LAE}, k^{HAE}, k^{S} and $k^{S,5+c}$) were estimated in order to fit the experimental cell size distribution (i.e. 1-, 2-, 3-, 4- and 5 or more cocci) throughout cultivations under optimal pH conditions in 1 L (this study) and 10 L (Paper IV) as well as under single- (this work) or multi-compartment (Paper IV) scale-down experiments with pH oscillating environments. On the one hand, the initial conditions for the carbon metabolism were taken from the original publication (Spann, Roca et al. 2018), with a t_{lag} of 0.38 h and using the measured pH as input variable. On the other hand, the initial values for the PM parameters were taken as one third of the difference between their maximum

499 and minimum values (Table S1), because these rate constants are arbitrary and no
500 literature was available to compare or discuss their absolute values.

501 The cocci chain length distribution during the vast majority of data sets selected were
502 successfully predicted with the population model developed (see Figure 6 as an example
503 of a Single-CR scale-down simulation). Moreover, lactose consumption as well as
504 biomass and lactic acid production, together with galactose accumulation (i.e. off-line
505 determined metabolites of the central carbon metabolism) were also accurately simulated
506 (Figure 7). Interestingly, despite the fact that the measured oscillating pH during scale-
507 down experiments was used as input variable for the model predictions, a relatively good
508 model fit was still obtained. In this context, it is worth mentioning that there was limited
509 microscopic data available from Two-CR scale-down experiments (Paper IV) and
510 therefore were not included in the simulations. Furthermore, the central carbon
511 metabolism of Single-CR fermentations with base pulses with $\Delta pH > 1.8$ was affected to
512 such an extent (i.e. RMSSE > 0.6 $g \cdot L^{-1}$ for biomass), that the original parameter set for
513 the description of the macroscopic variables should be changed. This is why, these data
514 sets were also discarded in this study. An important observation is, that all population
515 developments over time were supposed to follow an exponential growth, which also
516 limits the modelling capabilities and sets relevant constraints. Since the experimental
517 population concentrations were calculated from the corresponding biomass divided into
518 the different proportions of cocci chain morphologies considered (i.e. 1c, 2c, 3c, 4c and
519 5c+), this correlation type was assumed. One way in which degradation of certain
520 populations could be taken mathematically into account, would be incorporating a decay
521 term in the ODEs (i.e. the population rates). To decide whether this additional “death”
522 term should also be exponential or not shall be deeply investigated in the future.

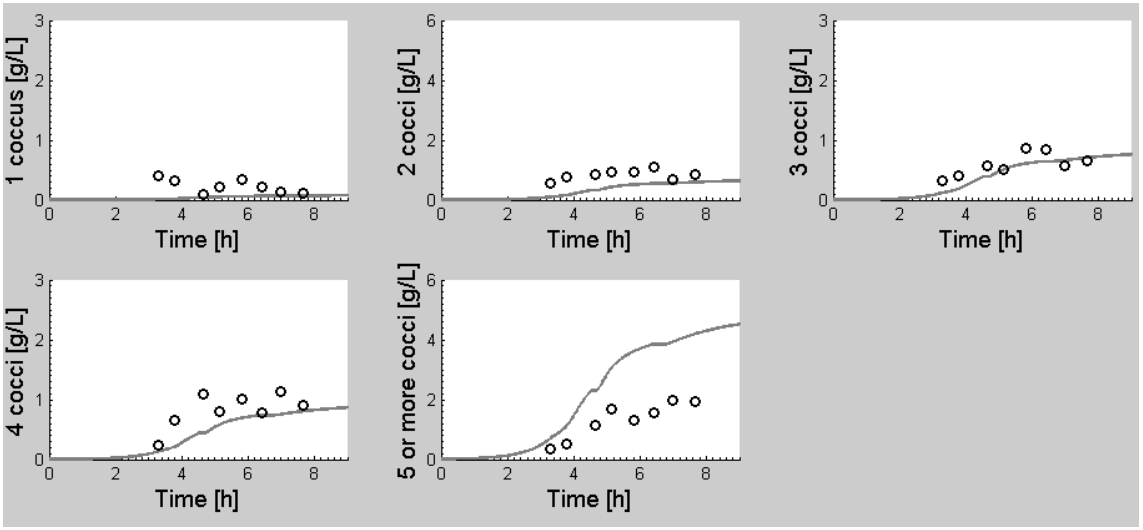

523

524 Figure 6. Experimental (empty circles) and predicted (lines) of population heterogeneity
525 (namely 1-, 2-, 3-, 4- and 5- or more cocci chains) throughout a *S. thermophilus*
526 cultivation where a ΔpH = 1.8 (+1.3;-0.5) was induced in a 1 L STR with 70 $g \cdot L^{-1}$ initial
527 C-source concentration, with ammonia pulses.

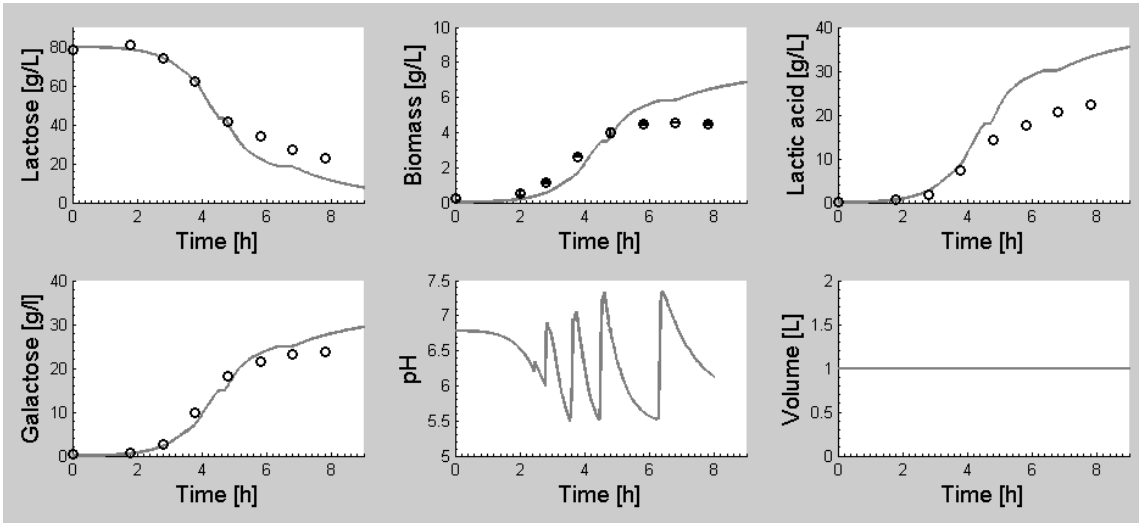

528

529 Figure 7. Experimental (empty circles) and predicted (lines) values of macroscopic
530 variables (namely lactose, biomass, lactic acid and galactose concentrations as well as
531 pH) throughout cultivation where a ΔpH = 1.8 (+1.3;-0.5) was induced in a 1 L STR with
532 70 $g \cdot L^{-1}$ initial C-source concentration, with ammonia pulses.

533

534 Importantly, the same kinetic constants for the PM enabled the acceptable prediction of
535 all variables under optimal growth conditions as well as when pH-gradients were induced,
536 during both, single- and multi-compartment scale-down experiments, at least in
537 duplicates (Table 2). Firstly, both separation constants (i.e. k^{S} and $k^{S,\ 5c+}$) in 1 L STR
538 fermentations were double as high as in 10 L STR experiments. Moreover, the k^{LAE} was
539 four times lower in the smaller fermenters. These two observations were initially
540 attributed to the belief that an increased local shear stress was probably encountered by
541 bacteria in the smallest bioreactor, because the 1 L vessel was agitated at half of the tip
542 speed of the ten times larger fermenter (200 and 400 rpm, respectively). Nevertheless,
543 taking into account the stirrer diameter and based on calculations of the Reynolds number
544 as well as the power input per unit volume (P/V) in both vessels (Table S2), the
545 hydrodynamic stress (τ) in the 1 L bioreactor was apparently only a 26 % of that of the
546 10 L one (Sieck, Budach et al. 2014). Maybe the 2x factor between the natural elongation
547 term in both scales would rather explain the differences observed in subsequent event
548 rates, leading to a combination of factors. The response of varying hydrodynamic stress
549 has been typically studied in mammalian cell culture (Chalmers 2015), where the
550 microorganisms are generally more shear sensitive than bacteria. (Sieck, Budach et al.
551 2014) found a characteristic local minimum in CHO cell viability after stress induction,
552 followed by viability recovery. Moreover, transcriptome analysis revealed adaptation
553 mechanisms identifying a certain fingerprint, but cellular metabolism, productivity and
554 product quality were not significantly affected by shear stress. Additionally, sparging
555 stress is also normally included in such studies, where in LAB would be irrelevant
556 because only nitrogen is sparged in the head space to maintain a sterile positive pressure
557 inside the bioreactor. Importantly, k^{HAE} took its minimum value without pH gradients (in
558 both, 1 L as well as 10 L STR), becoming a potential indicator of unfavourable growth

559 environments. The rate of natural elongation (k^{NE}) was generally high, mainly because 1c
560 chains were hardly detected under the microscope in all cultivation conditions: the natural
561 cell division of *S. thermophilus* occurs in successive parallel planes perpendicular to their
562 axis leading to diplococcal daughter cells (Zapun, Vernet et al. 2008). Both, k^{S} and $k^{S, 5c+}$,
563 were lower and k^{HAE} was noticeably higher in both, Single-CR as well as Multi-CR scale-
564 down experiments than under optimal STR conditions. As explained before, separation is
565 considered as an indicator for optimal growth (Chapot-Chartier and Kulakauskas 2014),
566 which is definitely hindered under pH-oscillating conditions (see Figure 2). What is more,
567 the heavy abnormal elongation term relates to unfavourable bacterial division, where only
568 one of the extremes of the cell elongates, which in fact was detected under scale-down
569 conditions (Figure 4). Finally, k^{LAE} was almost not affected under Three-CR scale-down
570 experiments, but considerably influenced when base pulses were induced in Single-CR
571 fermentations. Furthermore, k^{HAE} was slightly higher in 1 L Single-CR than 10 L Multi-
572 CR oscillating cultivations. Both observations emphasize the different percentage of cell
573 population subjected to the induced gradients: in Single-CR experiments the whole
574 biomass (i.e. 100 % of cells) suffered from changing pH conditions, while a maximum of
575 20 % of the bacteria were in contact with pH-gradients in Three-CR fermentations
576 (Neubauer and Junne 2010, Lemoine, Delvigne et al. 2017), and therefore less impacted
577 on the cell division cycle.

578

579 Table 2. Final biomass (i.e. DCW) and maximum pH gradient induced under optimal (1
580 L and 10 L STR) as well as scale-down (Three-CR and Single-CR) cultivation conditions.
581 Estimated kinetic parameters (k^{NE}, k^{LAE}, k^{HAE}, k^{S} and $k^{S,5+c}$) from the PM after prediction
582 of duplicates or triplicates of the different fermentation conditions.

Experiment (replicates)	*Experimental*		*Population model*				
	DCW_{end}	**DpH_{max}**	**k^{NE}**	**k^{LAE}**	**k^{S}**	**k^{HAE}**	**$k^{S,5c+}$**
STR,10L (n = 2)	5.4	+0;-0	1000.0	8.4	23.3	0.0	43.1
3CSDR,10L (n = 2)	4.3	+2.0;-1.3	1000.0	5.6	9.2	288.2	31.9
STR,1L (n = 2)	6.3	+0;-0	514.3	1.9	48.3	0.0	84.8
1CSDR,1L (n = 3)	5.7	+1.3;-0.5	736.6	36.8	49.4	372.4	16.4

583

584 Table S2. Reynold number (Re), power input to unit volume (P/V), mixing time (t_m) and
585 hydrodynamic stress (τ) for STR of 1 and 10 L with impeller diameters of 3.7 and 6.6 cm,
586 respectively, and stirred at 200 and 400 rpm, respectively.

Bioreactor	**Re [-]**	**P/V [kg/(m·s^3)]**	**t_m [s]**	**τ [kg/(m·s^2)]**
STR,10L	$4 \cdot 10^4$	186	8	0.35
STR,1L	$7 \cdot 10^3$	12	9	0.09

587

588

589 The arbitrary model parameters (i.e. event rate constants k^{NE}, k^{LAE}, k^{HAE}, k^{S} and $k^{S,5+c}$)
590 for the PM allowed to successfully predict population heterogeneity as well as main
591 metabolites during *S. thermophilus* fermentations with and without variable pH-
592 oscillating conditions. Nevertheless, one current limitation is that those parameters have
593 never been described before in literature and cannot be experimentally confirmed without
594 performing additional single-cell morphology investigations varying media pH to fully
595 elucidate the cell cycle of these LAB. In this work, the validation of the mechanistic
596 model was claimed by presenting the outputs of the model showing a good agreement
597 with experimental data, within a certain experimental range (i.e. pH oscillations).
598 Therefore, the reliability of the parameter estimates was not considered, thus,
599 theoretically, although only having defined five rates, an infinite combination thereof
600 could show the same fit (i.e. a non-identifiable parameter set was used). In future studies,
601 (i) the structural and practical identifiability of the PM parameters will be tested, as well

602 as (ii) the uncertainty of parameter estimates after fitting and (iii) the propagation of this
603 uncertainty on model outputs (Raue, Kreutz et al. 2009). In this context, an algorithm to
604 determine the presence of non-identifiable parameters in models with high output
605 uncertainty was recently published (Anane, Barz et al. 2019). The authors propose to
606 explore the numerical properties of the sensitivity matrix and a regularization technique,
607 in conjunction with Monte Carlo Analysis. This methodology, applied to a macro-kinetic
608 growth model describing *E. coli* fed-batch cultivations (Anane, Neubauer et al. 2017),
609 resulted in a reduction in the uncertainty of model outputs from a maximum CV% of
610 748 % to 5 % after regularization as well as a 15-fold improvement in the accuracy of
611 model predictions for two independent validation datasets. Such an approach could
612 clearly improve the reliability of the current prediction of *S. thermophilus* population
613 heterogeneity under certain pH gradients presented in this work.

614 *Conclusion*

615 Pulse-feeding of ammonia in Single-CR *S. thermophilus* fermentations induced alkaline
616 gradients until pH 8.0 (i.e. ΔpH = +2.0), while the pH was allowed to decrease until pH
617 5.0 (i.e. ΔpH = -1.0) through acidification due to metabolic lactic acid production from
618 the LAB. These pH oscillations were rather shifts, compared to the pulses induced in
619 Multi-CR experiments of the previous publication. The smallest pH shift performed in
620 this work (ΔpH = 1.5: +1.0;-0.5) yielded already more than a 10 % biomass productivity
621 loss, while no statistical difference on final DCW was obtained under Two-CR scale-
622 down cultivations, compared to gradient free fermentations. This emphasizes the fact that
623 the whole cell population was subjected to the oscillations in the Single-CR system, thus
624 being more influenced by them than bacteria in the Multi-CR setup. Furthermore, a
625 tendency towards chain length elongation under basic environments and towards shorter
626 chains at lower pH values than the optimum was detected in this work, which could not
627 be elucidated in past Three-CR experiments with acid and basic pH pulses. Finally, an
628 already published mechanistic model describing *S. thermophilus* growth (i.e. biomass and
629 lactic acid production, in parallel with lactose consumption and galactose accumulation)
630 was extended to simulate key populations identified in cultivations with and without pH
631 oscillating conditions (Single- as well as Multi-CR). The population model successfully
632 predicted population heterogeneity, by means of morphological differences, under
633 different pH gradients, but model reliability should be improved through analyzing
634 parameter identifiability as well as uncertainty. This in-silico growth and cell division
635 representation, if coupled to advanced in-situ microscopy as well as image recognition
636 techniques, would allow the implementation of a soft-sensor or model-based process
637 control strategies in the industrial production of starter cultures for the Food & Feed
638 industry to ensure product quality and improve process understanding.

Acknowledgments

This project has received funding from the European Union's Horizon 2020 research and innovation program under the Marie Skłodowska-Curie actions grant agreement No. 643056 (project Biorapid). The authors gratefully acknowledge this financial support and the help of Lucas Kaspersetz during the Single-CR scale-down experiments. The authors also thank Dr. Christophe Roca, Dr. Anders Clausen as well as Dr. David Kold from Chr. Hansen A/S for shipping the media and strain for the experiments, but also for their knowledge and expertise provided.

Conflict of interest

All authors declare no competing interests.

References

Anane, E., T. Barz, G. Sin, K. V. Gernaey, P. Neubauer and M. N. C. Bournazou (2019). "Output uncertainty of dynamic growth models: effect of uncertain parameter estimates on model reliability." Biochemical Engineering Journal: 107247.

Anane, E., P. Neubauer and M. N. C. Bournazou (2017). "Modelling overflow metabolism in Escherichia coli by acetate cycling." Biochemical Engineering Journal **125**: 23-30.

Brunner, M., P. Braun, P. Doppler, C. Posch, D. Behrens, C. Herwig and J. Fricke (2017). "The impact of pH inhomogeneities on CHO cell physiology and fed‐batch process performance–two‐compartment scale‐down modelling and intracellular pH excursion." Biotechnology journal **12**(7): 1600633.

Carpenter, A. E., T. R. Jones, M. R. Lamprecht, C. Clarke, I. H. Kang, O. Friman, D. A. Guertin, J. H. Chang, R. A. Lindquist and J. Moffat (2006). "CellProfiler: image analysis software for identifying and quantifying cell phenotypes." Genome biology **7**(10): R100.

Cortés, J. T., N. Flores, F. Bolívar, A. R. Lara and O. T. Ramírez (2016). "Physiological effects of pH gradients on Escherichia coli during plasmid DNA production." Biotechnology and bioengineering **113**(3): 598-611.

Chalmers, J. J. (2015). "Mixing, aeration and cell damage, 30+ years later: what we learned, how it affected the cell culture industry and what we would like to know more about." Current Opinion in Chemical Engineering **10**: 94-102.

Chapot-Chartier, M.-P. and S. Kulakauskas (2014). Cell wall structure and function in lactic acid bacteria. Microbial cell factories, Springer.

Delvigne, F., J. Baert, H. Sassi, P. Fickers, A. Grünberger and C. Dusny (2017). "Taking control over microbial populations: Current approaches for exploiting biological noise in bioprocesses." Biotechnology journal **12**(7): 1600549.

675 Delvigne, F. and P. Goffin (2014). "Microbial heterogeneity affects bioprocess
676 robustness: Dynamic single‐cell analysis contributes to understanding of microbial
677 populations." Biotechnology journal **9**(1): 61-72.
678 Delvigne, F., R. Takors, R. Mudde, W. van Gulik and H. Noorman (2017). "Bioprocess
679 scale‐up/down as integrative enabling technology: from fluid mechanics to systems
680 biology and beyond." Microbial biotechnology **10**(5): 1267-1274.
681 Delvigne, F., Q. Zune, A. R. Lara, W. Al-Soud and S. J. Sørensen (2014). "Metabolic
682 variability in bioprocessing: implications of microbial phenotypic heterogeneity." Trends
683 in Biotechnology **32**(12): 608-616.
684 Gernaey, K. V. and R. Gani (2010). "A model-based systems approach to
685 pharmaceutical product-process design and analysis." Chemical Engineering Science
686 **65**(21): 5757-5769.
687 González-Cabaleiro, R., A. M. Mitchell, W. Smith, A. Wipat and I. D. Ofiţeru (2017).
688 "Heterogeneity in pure microbial systems: experimental measurements and modeling."
689 Frontiers in microbiology **8**: 1813.
690 Heins, A.-L. and D. Weuster-Botz (2018). "Population heterogeneity in microbial
691 bioprocesses: origin, analysis, mechanisms, and future perspectives." Bioprocess and
692 biosystems engineering: 1-28.
693 Jin, J., Q. Qin, H. Guo, S. Liu, S. Ge, H. Zhang, J. Cui and F. Ren (2015). "Effect of pre-
694 stressing on the acid-stress response in Bifidobacterium revealed using proteomic and
695 physiological approaches." PloS one **10**(2): e0117702.
696 Layec, S., J. Gérard, V. Legué, M. P. Chapot‐Chartier, P. Courtin, F. Borges, B. Decaris
697 and N. Leblond‐Bourget (2009). "The CHAP domain of Cse functions as an
698 endopeptidase that acts at mature septa to promote Streptococcus thermophilus cell
699 separation." Molecular microbiology **71**(5): 1205-1217.
700 Lemoine, A., F. Delvigne, A. Bockisch, P. Neubauer and S. Junne (2017). "Tools for the
701 determination of population heterogeneity caused by inhomogeneous cultivation
702 conditions." Journal of biotechnology **251**: 84-93.
703 Marbà-Ardébol, A.-M., J. Emmerich, M. Muthig, P. Neubauer and S. Junne (2018). "Real-
704 time monitoring of the budding index in Saccharomyces cerevisiae batch cultivations with
705 in situ microscopy." Microbial cell factories **17**(1): 73.
706 Morchain, J. (2017). Numerical tools for scaling up bioreactors. Current Developments
707 in Biotechnology and Bioengineering, Elsevier**:** 495-523.
708 Müller, S., H. Harms and T. Bley (2010). "Origin and analysis of microbial population
709 heterogeneity in bioprocesses." Current opinion in biotechnology **21**(1): 100-113.
710 Neubauer, P. and S. Junne (2010). "Scale-down simulators for metabolic analysis of
711 large-scale bioprocesses." Current opinion in biotechnology **21**(1): 114-121.
712 Osman, J. J., J. Birch and J. Varley (2002). "The response of GS‐NS0 myeloma cells
713 to single and multiple pH perturbations." Biotechnology and bioengineering **79**(4): 398-
714 407.
715 Papadimitriou, K., Á. Alegría, P. A. Bron, M. De Angelis, M. Gobbetti, M. Kleerebezem,
716 J. A. Lemos, D. M. Linares, P. Ross and C. Stanton (2016). "Stress physiology of lactic
717 acid bacteria." Microbiology and Molecular Biology Reviews **80**(3): 837-890.
718 Ramos, C. L., L. Thorsen, M. Ryssel, D. S. Nielsen, H. Siegumfeldt, R. F. Schwan and
719 L. Jespersen (2014). "Effect of the gastrointestinal environment on pH homeostasis of
720 Lactobacillus plantarum and Lactobacillus brevis cells as measured by real-time
721 fluorescence ratio-imaging microscopy." Research in microbiology **165**(3): 215-225.
722 Raue, A., C. Kreutz, T. Maiwald, J. Bachmann, M. Schilling, U. Klingmüller and J. Timmer
723 (2009). "Structural and practical identifiability analysis of partially observed dynamical
724 models by exploiting the profile likelihood." Bioinformatics **25**(15): 1923-1929.
725 Sage, D., D. Prodanov, J.-Y. Tinevez and J. Schindelin (2012). MIJ: making
726 interoperability between ImageJ and Matlab possible. ImageJ User & Developer
727 Conference.

728 Sieck, J. B., W. E. Budach, Z. Suemeghy, C. Leist, T. K. Villiger, M. Morbidelli and M.
729 Soos (2014). "Adaptation for survival: phenotype and transcriptome response of CHO
730 cells to elevated stress induced by agitation and sparging." Journal of biotechnology **189**:
731 94-103.
732 Sin, G. and K. Gernaey (2016). "Data Handling and parameter estimation." Experimental
733 Methods in Wastewater Treatment: 201-234.
734 Spann, R., J. Glibstrup, K. Pellicer‐Alborch, S. Junne, P. Neubauer, C. Roca, D. Kold,
735 A. E. Lantz, G. Sin and K. V. Gernaey (2018). "CFD predicted pH gradients in lactic acid
736 bacteria cultivations." Biotechnology and bioengineering.
737 Spann, R., C. Roca, D. Kold, A. E. Lantz, K. V. Gernaey and G. Sin (2017). A Consistent
738 Methodology Based Parameter Estimation for a Lactic Acid Bacteria Fermentation
739 Model. Computer Aided Chemical Engineering, Elsevier. **40:** 2221-2226.
740 Spann, R., C. Roca, D. Kold, A. E. Lantz, K. V. Gernaey and G. Sin (2018). "A
741 probabilistic model-based soft sensor to monitor lactic acid bacteria fermentations."
742 Biochemical Engineering Journal **135**: 49-60.
743 Wang, G., J. Zhao, C. Haringa, W. Tang, J. Xia, J. Chu, Y. Zhuang, S. Zhang, A. T.
744 Deshmukh and W. van Gulik (2018). "Comparative performance of different scale‐down
745 simulators of substrate gradients in Penicillium chrysogenum cultures: the need of a
746 biological systems response analysis." Microbial biotechnology **11**(3): 486-497.
747 Wu, Q., F. Merchant and K. Castleman (2010). Microscope image processing, Elsevier.
748 Zamamiri, A. M., Y. Zhang, M. A. Henson and M. A. Hjortsø (2002). "Dynamics analysis
749 of an age distribution model of oscillating yeast cultures." Chemical engineering science
750 **57**(12): 2169-2181.
751 Zapun, A., T. Vernet and M. G. Pinho (2008). "The different shapes of cocci." FEMS
752 microbiology reviews **32**(2): 345-360.
753

Supplementary material

In order to induce the desired pulse-based feeding profile, an individual feeding profile was implemented into the bioprocess platform software eve® (Infors HT, Bottmingen, Switzerland).

```
 if(double.IsNaN(process["pHPhase"]))
{
        process["pHPhase"] = 0;
}
var pHPhase = process["pHPhase"];
if (pHPhase < 1)
{
        output.Setpoint = output.Value;
        if (output.Value <= 6)
        {
                process["pHPhase"] = 1;
        }
}
else if (pHPhase < 2)
{
        output.Setpoint = //Enter value;
        if(output.Value >=//Enter value)
        {
                process["pHPhase"] = 2;
        }
}
else if (pHPhase < 3)
{
        output.Setpoint = output.Value;
        if(output.Value <=//Enter value)
        {
                process["pHPhase"] = 3;
        }
}
```

```
787     else if (pHPhase < 4)
788     {
789             output.Setpoint =//Enter value;
790             if(output.Value >=//Enter value)
791             {
792                     process["pHPhase"] = 2;
793             }
794     }
795
```

Appendix

i. Flow cytometry analysis

a. Staining protocol TU Berlin

Preparation of Phosphate Buffered Saline (PBS):

a) For 1L of solution weigh the following components:
   - 8.00 g NaCl (M = 58.44 $g \cdot L^{-1}$),
   - 0.20 g KCl (M = 74.56 $g \cdot L^{-1}$),
   - 1.44 g $Na_2HPO_4 * 2H_2O$ (M = 177.99 $g \cdot L^{-1}$),
   - 0.24 g KH_2PO_4 (M = 136.09 $g \cdot L^{-1}$).

b) Add 800 ml $H_2O_{dest.}$

c) Adjust to pH 7.2 using HCl or NaOH

d) Fill volume up to 1 L with $H_2O_{dest.}$

e) Filter the solution with a pore size of 0.2 μm (discard the first fraction of about 10 ml in order to avoid impurities caused by the filter material).

Before analysis in the flow cytometer:

a) Activate the "Acquisition Mode" and wait until the laser is heated up (488 nm: ≈37 ºC; 405 nm & 635 nm: ≈ 25 ºC). Check it by clicking "View", "Hardware Monitor" and "Lasers and detectors".

b) Calibrate with calibration solution automatically by bar code recognition: the calibration solution contains beads of 2 and 3 μm in order to enable the adjustment of the voltage settings. Particles of 3 μm are stained with multiple fluorescent dyes to comprise the emission spectra of commonly used fluorochromes. Beads are excited between 400 nm and 650 nm to yield emission in all fluorescent channels.

c) The following laser and filter set is available at MACSQuant® (**Figure 57**):

V1: DAPI (DNA: 451 nm), V2: DAPI (RNA: 500 nm), B1: Box, Rh123; B3: PI

Optical specification of MACSQuant® Analyzer

Excitation	Channel	Filters	Detection range [nm]
405 nm	V1	450/50	425 - 475
	V2*	525/50	500 - 550
488 nm	B1	525/50	500 - 550
	B2	585/40	565 - 605
	B3	655 (LP) +(730 LP DM)	655 - 730
	B4	750 (LP)	750 -
635 nm	R1	655 (LP) +(730 LP DM)	655 - 730
	R2	750 (LP)	750 -
488 nm	FSC/SSC	488/10	

*MQ10 Only

Figure 57. Available lasers and filters at MACSQuant® Analyser.

Settings at MACSQuant® for Measurement:

Channel	Scaling	voltage	Trigger	Experiment settings
SSC	Log 3		2.0	Cell concentration ≈ 10^6 cells·mL^{-1}
FSC	Log 3		8.0	Stop after 100.000 events
B1	h Log			Medium flow rate
B2	h Log			Mixing
B3	h Log			60 µl uptake volume
B4	h Log			180 µl total volume (for mixing)

Concentrations of staining solutions:

	BOX	PI	DAPI
Stock solution (storage at -20 ºC)	0.5 mg·mL^{-1} DMSO	1.6 mg·mL^{-1} H_2O	10 mg·mL^{-1} H_20
Working solution (storage at 4 ºC)	6.5 µg·mL^{-1} PBS	12.8 µg·mL^{-1} PBS	270 µg·mL^{-1} PBS
Final concentration in samples	0.5 µg·mL^{-1} PBS	1 µg·mL^{-1} PBS	20 µg·mL^{-1} PBS

Samples / Analysis frequency:

	BOX	PI	DAPI
Time Points	7	7	7
Replicates	3	3	3
Total stained samples each dye	21	21	21
Positive controls 3-5 times per cultivation day (double estimation)	6	6	6
Total (samples + positive)	27 each dye		

Staining solutions = working solutions (stored in the dark at 4°C, maximal for a week):

a) Calculation of volumes:

	Vol./sample [μL]	Total Vol. needed [μL]	Vol. Prepared [μL]
Box	15	405	1000
PI	15	405	1000
DAPI	15	405	1000

b) Pipetting scheme for preparation of working dilutions:

Final concentration in sample	Dilution grade	Volume from dye stock solution	Volume PBS	Total vol. prepared
Box: 0.5 μg·ml^{-1}	1:75 → end: 1:1000	13 μL from 0.5 mg·ml^{-1}	987 μL	1 ml
PI: 1 μg·ml^{-1}	1:120 → end: 1:1600	8 μL from 1.6 mg·ml^{-1}	992 μL	1 ml
DAPI: 20 μg·ml^{-1}	1:37.5 → end: 1:500	27 μL from 10.0 mg·ml^{-1}	973 μL	1 ml

Sample Preparation:

a) Harvesting of cells:

- Harvest 1 ml of sample as fast as possible from bioreactor.
- After sampling, store the sample immediately on ice and continue immediately with the following steps.
- Frequency of sampling: once right before batch, then every hour during the batch cultivation (although two and possibly three samples will be taken during the lag phase, they will be used in order to check whether the settings of the last experiment are still adequate).

b) Washing of cells (should take maximal 2 minutes):

- Filter the 1 ml samples with vacuum filtration using a filter pore size of 0.2 μm (make sure the vacuum pump is properly soaking the liquid).
- Wash the cells with 5 ml filtered PBS (rinsing the filter 5 times with 1 ml PBS).
- Dissolve the cells stuck on the filter in 5 ml filtered PBS in a 15 ml falcon tube by gentle shaking for 30 seconds.
- Dilute in PBS until obtaining a cell concentration of around $1 \cdot 10^6$ cells·mL^{-1} (OD ≈ 0.06).

Staining conditions:

a) 185 µl of the diluted sample are mixed with 15 µl of each working solution in Eppendorf tubes and incubated in dark (see **Table 10**).

b) For negative controls (i.e. unstained cells): 200 µl of the diluted sample are transferred into each tube

Table 10. Staining conditions for *Streptococcus* sp. cells.

	Culture volume [µL]	**Dye working solution volume [µL]**	**Temperature [ºC]**	**Staining time [min]**
Box	185	15	RT	4
PI	185	15	4	2
DAPI	185	15	37	30

Positive controls:

a) Frequency of sampling: after the start of the batch phase, in the log phase and shortly before the end of the fermentation.

b) They are treated as normal samples until the step of dissolving the cells in PBS after washing and diluting to $1 \cdot 10^6$ cells·ml^{-1}.

c) Each dye is applied in double estimation, this means 6 positive controls at each time point for 3 dyes.

d) After washing the two Eppendorf tubes are put in the thermo block at 80 ºC for one hour.

Negative controls:

a) Frequency of sampling: after the start of the batch phase, in the log phase and shortly before the end of the fermentation.

b) They are also treated as normal samples until the step of dissolving the cells in PBS after washing and diluting to $1 \cdot 10^6$ cells·ml^{-1}.

c) The negative controls correspond to non-stained cells, so the diluted sample on ice is directly analyzed.

Cleaning of the MACSQuant® after use (with 2% Sodium-Hypochlorite solution)

Extra cleaning between samples might be necessary from time to time in order to ensure the cleaning of all components from microorganisms and debris.

1) Fill an Eppendorf tube with 2 % filtered **s**odium-hypochlorite solution
2) Introduce the experiment settings as indicated in **Figure A1**:
   - Rack: single tube rack
   - Flow rate: high
   - No mixing of the sample
   - Uptake volume: maximal (450µL)
   - Sample volume: maximal volume of the filled Eppendorf tube (1.5mL)
3) Put the tube in the rack for single tubes and start like a normal measurement
4) Repeat the steps 1-3 until most dots are disappeared / Nearly no particles are passing the lasers! Check this in the different channel displays!

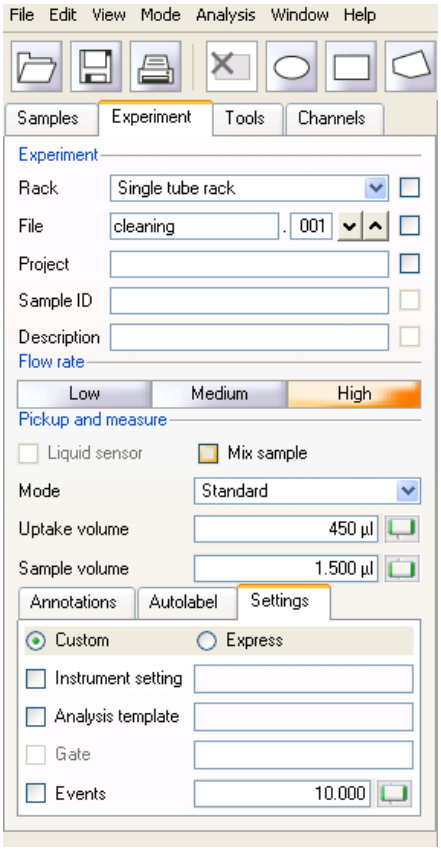

Figure A1. Settings for cleaning.

These steps do not replace the final cleaning procedure with the Chill-5-Rack at the end of the measurements / at the end of the day.

For more information about the use of the MACSQuant and the software MACSQuantify use the printed manuals next to the flow cytometer or have a look in the digital versions:

1) Instrument:
   https://www.google.de/url?sa=t&rct=j&q=&esrc=s&source=web&cd=3&cad=rja&uact=8&ved=0CDoQFjACahUKEwjvzYzZn9PIAhWiv3IKHfJJB98&url=https%3A%2F%2Fwww.miltenyibiotec.com%2F~%2Fmedia%2FImages%2FProducts%2FImport%2F0008000%2FIM0008005.ashx%3Fforce%3D1&usg=AFQjCNHeUOCz5GvpescfFwJ2nR-EZfSwBA&sig2=xReJMmRf6Iu5mbEjMBSO0w

2) Software:

https://www.google.de/url?sa=t&rct=j&q=&esrc=s&source=web&cd=4&cad=rja&uact=8&ved=0CEEQFjADahUKEwjvzYzZn9PIAhWiv3IKHfJJB98&url=http%3A%2F%2Fwww.miltenyibiotec.com%2F~%2Fmedia%2FImages%2FProducts%2FImport%2F0010100%2FIM0010172.ashx%3Fforce%3D1&usg=AFQjCNEll3-1omQlBOsrle8xecl6m-znxQ&sig2=vacvxsX-UUwjAvPu2fzKyQ

b. Staining protocol Chr. Hansen A/S

For flow cytometric analysis at the industrial partner, a BD Accuri™ C6 Plus device (BD Biosciences-SG, Allschwil, Switzerland) was used:

a) For staining *S. thermophilus* cells, SYBR Green (Sigma-Aldrich, Søborg, Denmark) was used:
   - ✓ The solution of the manufacturer was firstly diluted 250x in a 1.5 mL Eppendorf tube.
   - ✓ 5 µL of this working solution were mixed with 195 µL of sample in every experiment to end up with a 10,000x dilution of the original concentration.

b) For staining permeabilized bacteria, PI (Sigma-Aldrich, Søborg, Denmark) was used:
   - ✓ Stock solution: 10 mg of dye were dissolved in 1 mL PBS buffer (10 mg/mL PI)
   - ✓ Intermediate solution: 50 µL were dissolved in another 1 mL PBS buffer (0.5 mg/mL PI)
   - ✓ Final concentration in every sample: 0.0128 mg/mL PI

For more information about the use of the BD Accuri™ C6 Software use the digital brochure: https://www.bdbiosciences.com/documents/BD_Accuri_C6_Software_User_Guide.pdf

c. Verification dyes used in TU Berlin

For flow cytometric analysis in TU Berlin, DAPI and PI were used to stain all cells and the permeabilized bacteria, respectively. **Figure 58** shows that a gate differentiating the stained from the unstained samples could be drawn in both cases. Importantly, the positive control for PI (i.e. killing the bacteria at 80 ºC for ten minutes) successfully resulted in the shift of the whole population (all cells dead, permeabilized) to the PI gate defined.

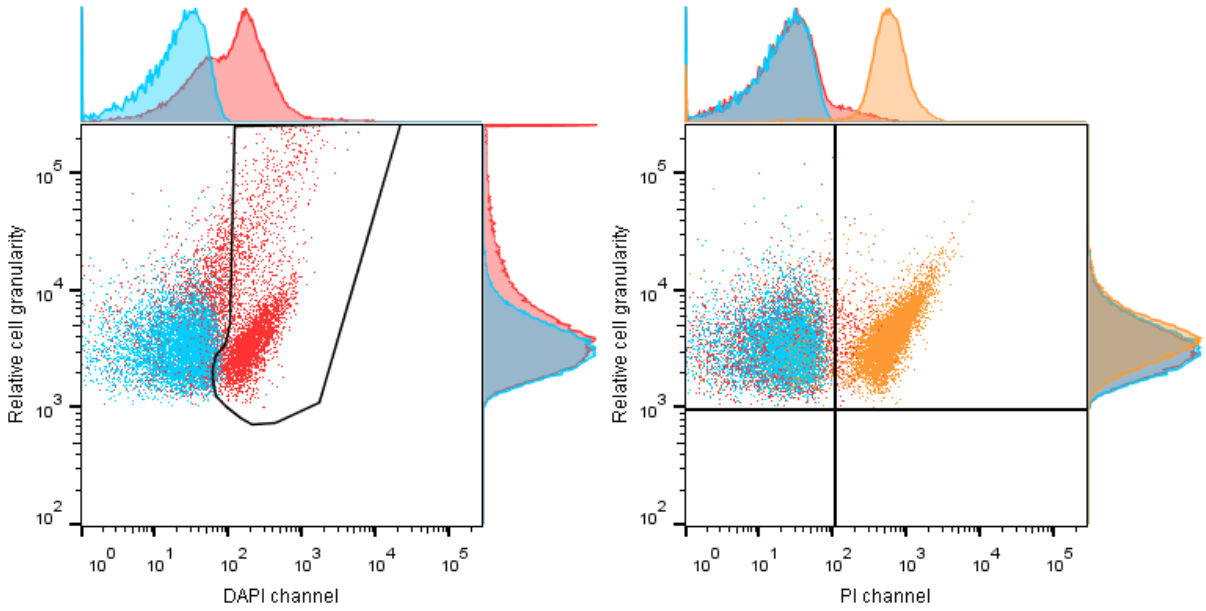

Figure 58. Flow cytometry analysis of unstained *S. thermophilus* samples (blue), a DAPI-stained sample (left red), a PI-stained sample (right red) and a sample incubated at 80 ºC for ten minutes (positive control for PI - right orange). The gate to identify the cells corresponds to the area defined with the black line in the DAPI channel, while the dead/permeabilized bacteria were quantified with the upper right quadrant of the PI channel.

Furthermore, the reproducibility of both staining procedures was also investigated (**Figure 59.** Triplicates (red, blue and orange) of *S. thermophilus* samples stained with DAPI (left) and PI (right).), resulting in an acceptable deviation between three stained samples for both dyes.

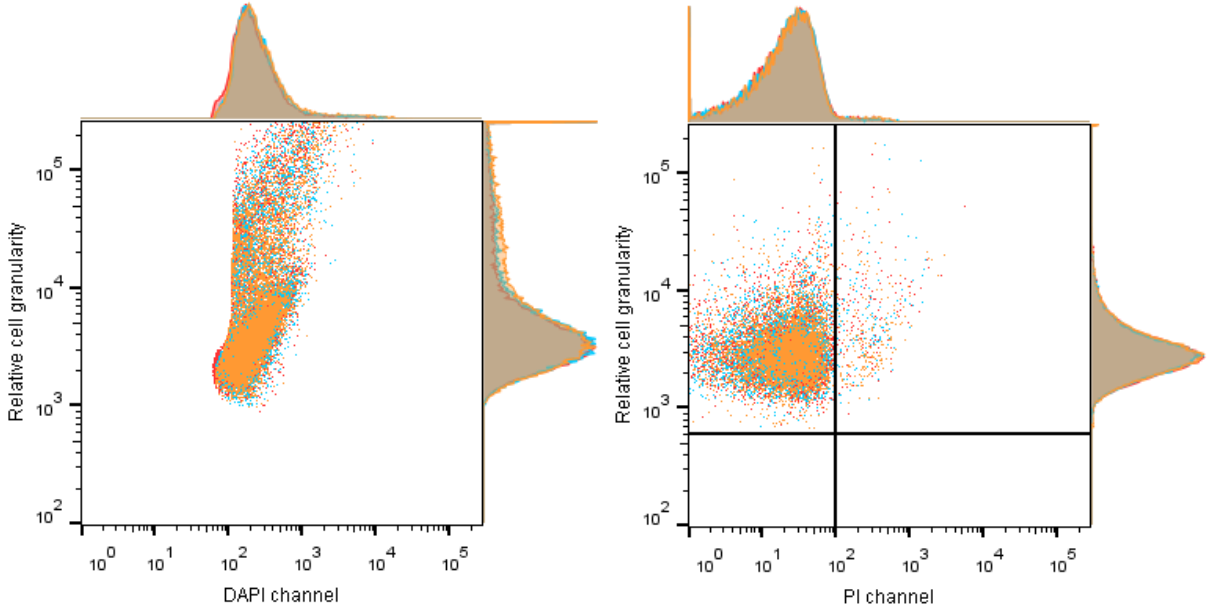

Figure 59. Triplicates (red, blue and orange) of *S. thermophilus* samples stained with DAPI (left) and PI (right).

d. Verification dyes used in Chr. Hansen A/S

For flow cytometric analysis in Chr. Hansen A/S, SYBR® Green and PI were used to stain all cells and the permeabilized bacteria, respectively. **Figure 60** shows that a gate differentiating the stained from the unstained samples could be drawn in both cases. Importantly, the positive control for PI (i.e. killing the bacteria at 80 ºC for ten minutes) successfully resulted in the shift of the whole population (all cells dead, permeabilized) to the PI gate defined.

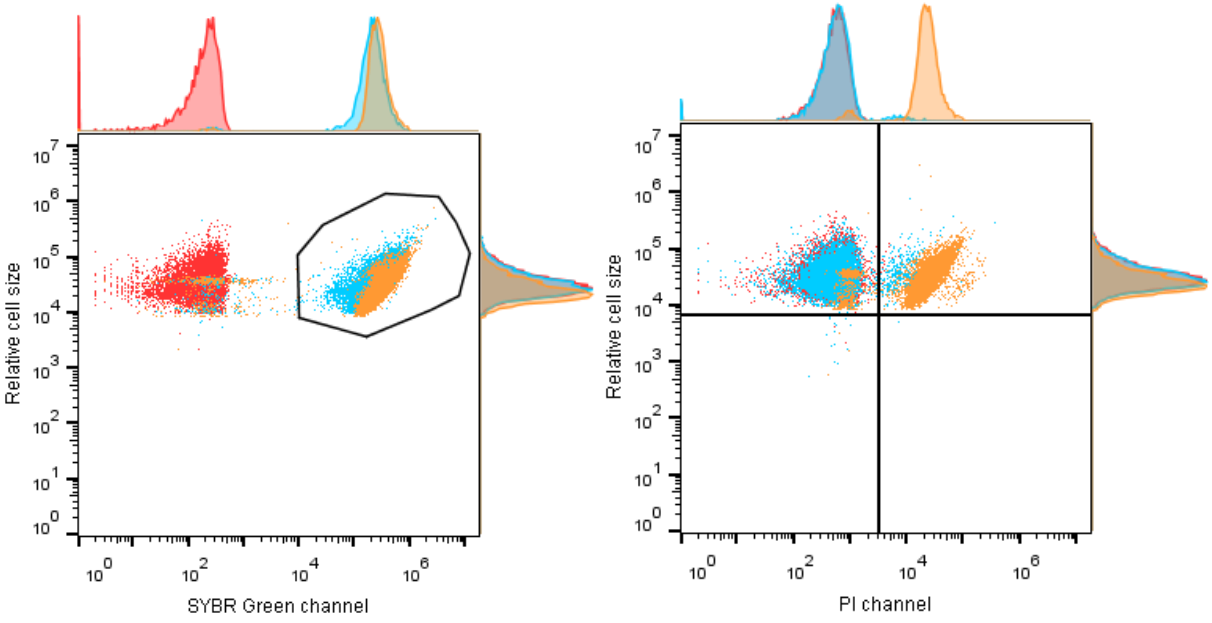

Figure 60. Flow cytometry analysis of unstained *S. thermophilus* samples (red), a SYBR Green-stained sample (left blue), a PI-stained sample (right blue) and a sample incubated at 80 ºC for ten minutes (positive control for PI - orange). The gate to identify the cells corresponds to the area defined with the black line in the SYBR Green channel, while the dead/permeabilized bacteria were quantified with the upper right quadrant of the PI channel.

ii. CellProfiler pipeline for quantification of microscopic pictures

In order to ease the quantification of microscopic pictures taken throughout the different fermentations carried out in this work, a free and open source software was used, which also allowed to avoid the human error included in the manual cell size and cocci amount per chain counting. A pipeline was developed in the CellProfiler software (http://www.cellprofiler.org), consisting of the following modules:

a) Microscopic images (100x magnification using immersion oil) were first pre-processed applying the "Invert" operation in the "ImageMath" module to invert intensities and obtain a foreground lighter than the background. During the entire work, different microscopes at different locations (e. g. TU Berlin, Chr. Hansen A/S, DTU) were used. Therefore, for each individual experiment analyzed, the function "Multiply the first image by" was slightly modified until a clear differentiation between the cocci chains and the background was obtained.

b) Chains were then automatically identified using the "IdentifyPrimaryObjects" module setting the "Manual threshold" globally to 0.001. Object clumping and object separation were distinguished by "Intensity", with a "Size of smoothing filter" of 10. Depending on the microscope, the magnification and/or the zooming used when the pictures were taken, the minimum and maximum "Typical diameter of objects, in pixel units" were modified.

c) Similarly, cocci were identified automatically using the same module, but this time setting the threshold globally through the "Otsu (two classes)" method. Object clumping and object separation were distinguished by "Shape", in this case. Again, the minimum and maximum "Typical diameter of objects, in pixel units" were modified, typically cocci being a 10 % of the size of the chains.

d) Then, the "RelateObjects" module was used to associate "Child objects" (i.e. cocci) with "Parent objects" (i.e. chains).

e) To visualise the identification of chains and cocci, the "OverlayOutlines" module was used, outlining the chains in yellow and the cocci in red and overlaiding them on pre-processed images.

f) The "SaveImages" module was used to save the identification results.

g) The number of cocci per chain was finally calculated for each chain with the "MeasureObjectSizeShape" module and exported to an Excel spreadsheet with the "ExportToSpreadsheet" module.

List of all publications:

I. **Pellicer-Alborch, K.**, Angersbach, A., Neubauer, P., Junne S. *Electrooptical Determination of Polarizability for On-Line Viability and Vitality Quantification of Lactobacillus plantarum Cultures*. Front. Bioeng. Biotechnol. 2018; 6:188. DOI: 10.3389/fbioe.2018.00188

II. **Pellicer-Alborch, K.**, Spann, R., Sin, G., Gernaey, K. V., Neubauer, P., Junne, S. *Mechanistic model validation and electrooptical monitoring of Streptococcus thermophilus growth in lactose-limited acceleration stat (A-stat) fermentations*. In preparation.

III. Spann, R., Glibstrup, J., **Pellicer-Alborch, K.**, Junne, S., Neubauer, P., Roca, C., Kold, D., Lantz, A. E., Sin, G., Gernaey, K. V., Krühne, U. *CFD predicted pH gradients in lactic acid bacteria cultivations*. Biotechnol. Bioeng. 2018; 1-12. DOI: 10.1002/bit.26868

IV. **Pellicer-Alborch, K.**, Kaspersetz, L., Paulick, K., Neubauer, P., Junne, S. *Response of Streptococcus thermophilus exposed to pH gradients in Two- and Three-Compartment Scale down Cultivations*. Submitted in MDPI, Bioengineering. (2020)

V. **Pellicer-Alborch, K.**, Spann, R., Cristino-Falco, F., Ramin, P., Gernaey, K. V., Neubauer, P., Junne, S. *Population Balance Modelling of Streptococcus thermophilus based on the Cocci Chain Length Distribution for Optimization of Starter Cultures Production*. In preparation.

VI. Kögler, M. (eq.), **Pellicer-Alborch, K.** (eq.), Paul, A., Viitala, T., Bunker, A., Junne, S., Neubauer, P. Surface-enhanced Raman spectroscopy (SERS) and Time-Gated (TG-SERS) Raman-spectroscopy as advanced process analytical tools for monitoring of lactic acid bacteria fermentations in complex media. In preparation.

VII. **Pellicer-Alborch, K.**, Zavadni, I., Stosch, H., Angersbach, A., Götz, P., Neubauer, P., Junne, S. Elelectrooptical Monitoring of Cell Polarizability in *Escherichia coli* Batch, Fed-Batch and Continuous Cultivations. In preparation

VIII. Gómez-Camacho. C. E., **Pellicer-Alborch, K.**, Bockisch, A., Neubauer, P., Junne, S., Ruggeri, B. Insights into the black-box of biohydrogen production: electro-optical techniques to monitor the physiological state. In preparation.

Recent doctoral theses at Bioprocess Engineering, TU Berlin:

1. Ángel Córcoles García (2019) Molecular genetic approaches to decrease mis-incorporation of non-canonical branched chain amino acids into a recombinant protein in *Escherichia coli*
2. Moonsung Cho (2019) Suspension of a point-mass-loaded filament in non-uniform flows: the ballooning flight of spiders
3. Sarah Kamel (2019) Enzymatic synthesis of α-D-pentosefuranose-1-phosphate
4. Heba Yehia Mohamed (2019) Chemoenzymatic synthesis of nucleoside analogs as potential medicinal agents
5. Funda C. Ertem (2019) Life cycle assessment and modeling approaches as a combined evaluation tool for sustainable control strategies at biogas plants
6. Emmanuel Anane (2019) Model based strategies for scale-down studies in fed-batch cultivation of *Escherichia coli* expressing protein
7. Ekaterina Osmekhina (2018) Quantitative approach for detection of RNA and proteins by sandwich hybridization technology
8. Elvis Legala (2018) Reconstruction of the lanthipeptide ruminococcin-A biosynthesis machinery in Escherichia coli and structural characterization
9. Anika Bockisch (2018) Mobile multi-parameter measurements for the dynamic analysis of gradients in brewing vessels
10. Juan Antonio Arzate (2018) Modeling and simulation of biogas production based on anaerobic digestion of energy crops and manure
11. Anna Maria Marbá (2018) Monitoring of the single-cell morphology for the evaluation of microbial eukaryotic bioprocesses
12. Martin Kögler (2018) Advanced Raman spectroscopy for bioprocess monitoring
13. Anja Lemoine (2017) Impact of oscillations in substrate and oxygen availability on *Corynebacterium glutamicum* cultivations
14. Basant El Kady (2017) Application of the enzyme controlled glucose feeding for the production of recombinant proteins. Starter cultures and autoinduction
15. Julia Glazyrina (2017) Endophytes as source of polypeptide and polyketide antibiotics fengycin and bacillaene. Process development for fengycin production
16. Florian Glauche (2017) Platform technologies for automated bioprocess development
17. Eva Brand (2017) Growth rate dependent impact of oscillating conditions on *Escherichia coli* physiology
18. Christian Reitz (2017) Impacts of oscillating cultivation conditions on the quality of recombinant inclusion bodies in *Escherichia coli*

Full copies of the theses are available at https://depositonce.tu-berlin.de/.